THE STRUCTURAL BEHAVIOUR OF TIMBER JOINTS MADE WITH FULLY OVERLAPPING NAILS

by

Alexander Porteous

BSc(Hons), MSc(Eng), DIC, CEng, MIStructE, FICE, DipIStructE.

DECLARATION

No portion of the work referred to in this thesis has been submitted in support of an application for another degree or qualification in this or any other University or institute of learning.

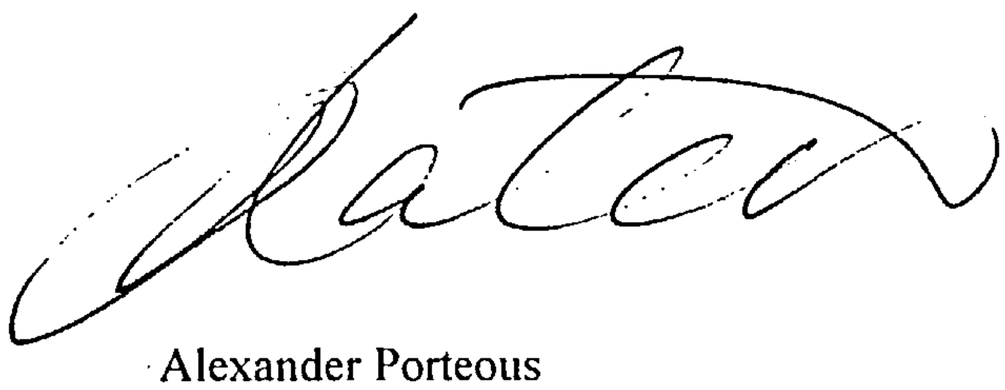

Alexander Porteous

SYNOPSIS

Title: THE STRUCTURAL BEHAVIOUR OF TIMBER JOINTS MADE WITH FULLY OVERLAPPING NAILS

Author: Alexander Porteous

An integrated programme of experimental and analytical work was carried out to evaluate the non-linear semi-rigid characteristics of timber connections using fully overlapping nails subjected to short duration lateral loading and moment. The investigation is part of a continuing programme of research at Napier University into the behaviour of timber joints using fully overlapping nails as the connecting mechanism.

The effects of the factors and material properties that influence the behaviour of nailed joints were addressed in a structured and controlled way allowing semi-empirical models to be developed for the lateral load behaviour of multi-nailed timber joints using steel and plywood gusset plates. A quality control procedure was established for the testing programme and consistent standards were applied to the preparation and testing work. The semi-empirical models that were developed included for the effect of timber density; gusset plate material effect; nail strength; number of nails; nail diameter; row spacing and the effect of the moisture content in the timber. They covered joints assembled with and without a gap between the timber and the gusset plates and for joints assembled with steel gusset plates, the effect of the predrill size used in the gusset plate was also investigated. The model results compared very well with the results from tests, accurately predicting the non-linear behaviour of the joints up to failure.

An extensive analytical and experimental study was carried out to investigate the moment-rotation behaviour of these types of joints. Two linear and four non-linear models were developed for each type of joint and the efficiencies of the models were compared to determine the one that best simulated the joint behaviour. The linear models consistently underestimated the capacity of the joint, giving conservative results. The best solutions were obtained by applying the torsion formula used for steel connections and incorporating the nail behaviour models developed for the non-linear lateral load joints. Account was taken of the non-linear behaviour of the connection and alternative models using fixed and moveable centres of rotation were developed. Very good comparisons were achieved between these models and the test results.

A detailed comparison was made between the behaviour of the joints using the lateral load-displacement models and Eurocode 5 (EC5) and it was concluded that EC5 rules did not accurately simulate the behaviour of this type of joint. It was concluded that the nail spacing rules in the code did not apply to fully overlapping nails. A limit state design method based on the principles used in EC5 has been developed from the models for the design of joints using fully overlapping nails and subjected to lateral loading or moment.

The semi-rigid behaviour of the joints was also investigated and it was concluded that to safely predict the response of structures assembled with fully overlapping nails, the semi-rigid behaviour must be included for in the analysis procedure. Rigidity factors, end fixing moment reduction factors and the secant rotational stiffness coefficients for the joints were derived. It was also shown that where the analysis was limited to the serviceability limit state, a modified elastic method of analysis could be used and where it was beyond this state a non-linear method of analysis was required.

ACKNOWLEDGEMENTS

I express my sincerest gratitude to Dr Abdy Kermani for his constant support, encouragement and advice throughout this research. Despite the inconvenience I must have caused, he always made himself available to discuss issues, offered constructive criticism and consistently gave clear and helpful guidance on the way to proceed.

My gratitude is also given to the technical team in the School of the Built Environment for the assistance and never failing support during the experimental stage of the research. Particular thanks are given to Mr Alan Barber who at all times gave sound practical advice and ensured the test samples were immaculately prepared. Acknowledgements are also given to Mr William Laing and Mr John Callaghan who were also very supportive and helpful throughout the testing period. Thanks are also given to Mr Charlie Cope, chief technician.

Finally, I thank my wife, Margaret. Without her loving support, patience, encouragement and companionship I would never have completed this work. She has given up a lot to allow me to do this research and I sincerely thank her for giving me this opportunity. Thank you again Margaret.

CONTENTS

PUBLICATIONS

Porteous, A., and Kermani, A., August 2002, "Load-Displacement Characteristics of Multi-Nailed Timber Joints with Plywood Gussets", Proceedings of the 7th World Conference on Timber Engineering 2002 (WCTE-2002), Malaysia, Vol.2. pp.455-463.

1. INTRODUCTION

1.1 GENERAL

Sustainable; biodegradable; recyclable; renewable; green; non-toxic; ecological and environmentally friendly are becoming essential pre-requirements of construction materials in the twenty first century and a material which envelopes all of these factors, as well as also being very cost competitive, is timber.

Timber has been used as a construction material from earliest recorded times [1] and with the introduction of international initiatives directed at creating more sustainable construction practices; the implications of the Egan Report on the construction industry [2] and the added financial impact from the introduction of Landfill taxes [3], there is a reawakening of the environmental and financial benefits of the use of timber in construction.

It is a material that is used in all stages of the construction process but with greater emphasis now being placed in its use as the primary structural material for building, civil and structural engineering projects. A striking example of the use of timber is in the structure of the £43M development for the Sheffield Winter Garden [4] where it forms 20m high by 22m wide arches which support glass cladding forming a spectacular enclosure for housing exotic palms. There is also the more innovative use of timber in the form of gridshell structures where its flexibility, low torsional stiffness and need for only a relatively low-tech jointing requirement can provide an efficient and architecturally expressive way of covering space [181].

The predominant use of timber as a structural material in the UK is in timber frame housing where in addition to complying with the environmental and sustainable aspects of the construction process, it allows the designer much greater flexibility through all stages of the design procedure; lends itself to quality controlled offsite factory fabrication; is easily and quickly erected on site; provides good thermal insulation and is relatively lightweight, reducing the cost of foundations and the supporting structure. The opportunities for timber construction in medium rise timber framed buildings in the UK have also been recognised by Government. There has been a joint initiative by Government and the timber industry involving a full scale testing programme on a six storey standard timber platform frame to address structural strength and stiffness behaviour, including the requirement that such structures must fully satisfy the UK Building Regulations in regard to robustness in the event of an accident or due to misuse [5].

The weakest link in the behaviour of timber structures is the joint and it is a commonly said that a timber structure is primarily an assembly of joints separated by members. Joints are generally the most critical components and invariably govern the overall strength, serviceability and durability of any engineered timber structure.

Napier University has been investigating the behaviour of nailed timber joints in structures over several years. Research has been undertaken into appropriate methods of analysis for use with nailed joints and also how the joints influence the behaviour of structures [12, 94]. The research covered in this thesis has been undertaken to further the limit of understanding of the strength and stiffness behaviour of this type of joint and also provide information that may be of benefit to design engineers responsible for the safe and efficient use of use timber structures assembled with nailed joints.

1.2 RESEARCH OBJECTIVES

In this research, attention has been focussed on the strength and stiffness behaviour of nailed timber joints formed with steel gusset plates and with plywood gusset plates of varying thickness and subjected to short duration loading. To align with the results of previous research at Napier University, three member joints have been used with nails driven from each of the joint faces to act in single shear. The nails on each face were positioned so that they fully overlapped with nails driven from the opposite face for the thickness of the central timber member. Nails overlapping in this manner have been referred to as fully overlapping nails.

A structured research programme of experimental and analytical work was pursued and the core objectives of the research were as follows:

i) To undertake a review of the available research on laterally loaded and moment carrying nailed joints, including their semi-rigid behaviour, when subjected to short duration lateral loading.

ii) To develop appropriate experimental methods to study the translational, rotational and semi-rigid behaviour of the joints.

iii) To develop a quality control programme within which the experimental work would be undertaken.

iv) To develop mathematical/empirical models capable of simulating the lateral load-displacement and moment-displacement behaviour of multi-nailed timber joints.

v) To compare the behaviour of the mathematical/empirical lateral load-displacement models with the rules for joint design given in Eurocode 5 (EC5).

vi) To develop a limit state design method for multi-nailed joints subjected to a lateral load or a moment.

vii) To investigate the semi-rigid behaviour of multi-nailed joints, deriving the fixity factor relationship; the end fixing moment reduction factor; the secant rotational stiffness coefficient and

categorise the joints.

viii) To investigate the most appropriate method of analysis to be used for structures assembled with multi-nailed joints.

1.3 CONTENTS OF THE THESIS

The thesis is divided into eight chapters.

In Chapter 2, the literature relating to the behaviour of nailed joints is reviewed. The review covered the influence of material properties on nailed joints; the methods used for modelling the lateral load and moment behaviour of such joints and investigations into the semi-rigid behaviour of nailed joints. At the end of the chapter the key factors arising from the review have been identified for inclusion in the research programme.

Chapter 3 describes the experimental programme to be used to investigate the lateral load and moment behaviour of multi-nailed timber joints. The behaviour of fully overlapping nails is also addressed. Reference is also made to the quality control programme established for the work and the procedures used are given in Appendix A.

In Chapter 4, the semi-empirical modelling of the laterally loaded nailed joints is described. The analysis follows a structured approach in which the effect of each factor on joint behaviour is individually investigated. The results of the alternative models developed for joints with steel gusset plates and with plywood gusset plates are presented and compared with the experimental results.

In Chapter 5, semi-empirical modelling of the moment-slip behaviour of nailed joints has been presented. Alternative options for modelling moment behaviour are developed and reviewed to determine the most accurate method. The results of multi-nailed joint configurations using the selected method are compared with the experimental results. Tests are also done with double joints formed using common gusset plates and the results compared with the semi-empirical models.

Chapter 6 compares the semi-empirical models developed for lateral load-displacement with the rules in EC5. The mean property based models are converted to a characteristic value base and the background to EC5 is reviewed to establish a common basis for the comparison. The strength and stiffness characteristics of the models are compared with the code rules at the serviceability and ultimate limit states.

In Chapter 7, a design method is given for multi-nailed timber joints subjected to short duration lateral loading and short duration moment. The method is limit state based and aligns with the requirements of EC5. Any deviations from the code are given. The chapter also investigates the semi-rigid behaviour of

nailed joints, evaluating fixity factors, end fixing moment reduction factors and secant rotational stiffness coefficients. The behaviour of the nailed joints is categorised and guidance is given on the method of analysis to be used for structures assembled with these joints.

In Chapter 8, the conclusions are given with recommendations for future research.

2. LITERATURE REVIEW

2.1 INTRODUCTION

In this chapter a literature review has been carried out into the factors that affect the behaviour of nailed timber joints. The review has covered the effects of material properties; the methods that have been used to model the lateral load and moment behaviour of this type of joint; the semi-rigid behaviour of nailed joints and the significance of taking semi-rigid behaviour into account in the structural analysis of frames assembled with nailed joints.

A key objective of the review is to obtain an understanding of the analysis methodologies that have been used and to identify those factors that should be taken into account in the research programme.

2.2 GENERAL

The use of nails and timber as construction materials has been ongoing for hundreds, if not thousands of years. Evidence exists of iron, copper and bronze nails used by the ancient Egyptians, Greeks and Romans as connectors in building construction.

Prior to the 19th century, forged and hand-wrought nails were introduced for use in all kinds of buildings to provide for structural stability. The first nail-making machines were developed to cut and head nails, permitting the manufacture of nails of different lengths with different points and heads for appropriate use. With the development of automatic wire-nail production machinery in the middle of the 19th century, an era began which made the wire nail the most used fastener in timber construction. During the 20th century timber construction changed from being craftsman led, based on laid down working practices, to engineered solutions based on analysis of the forces and displacements the structure would be subjected to when in service. Because joints were the weakest link in timber structures this prompted the need to study the performance of nails and of nailed joints and the first fundamental research was undertaken by researchers in Germany in the 1930's.

Research into the strength and stiffness behaviour of nailed joints was progressed by empirical methods; classical elastic theory; ultimate strength theory and more recently by the finite element method. In all of these approaches it was recognised that joint behaviour was complex and lead to the investigation of the effects of material properties and of the other factors influencing joint behaviour.

2.3 MATERIAL FACTORS

2.3.1 Timber Density

Timber is a cellular material characterised by different values of the ratio of its cell wall thickness to

total cell diameter and as this ratio increases so does its density, strength and stiffness [1, 78]. The value of timber density across species is variable, varying by a factor of 10 from the lowest average value at 176kg/m^3 for Balsa to about 1230kg/m^3 for the densest hardwood [1]. Also, within a species a similar variation in density between the lowest and highest density value can be expected. Timber is hygroscopic, absorbing moisture from the atmosphere if it is dry and yielding moisture to the atmosphere when wet, and in so doing the density, and consequently strength and stiffness properties, have been found to vary. To provide a base-line for comparison purposes, in engineering analysis it has been common practice to use the specific gravity of the timber (the oven-dry mass to volume of timber at 12% moisture content) as the strength parameter, rather than density [7, 19, 71]. The effect of moisture content was then able to be addressed as a factor on its own merit. Basic density, which is the oven dry mass divided by the green condition volume, has also been used as the strength parameter [71, 83].

The strength and stiffness properties of timber have been directly correlated to timber density [158, 159] and from research into joint behaviour using empirical and elastic theory approaches it was found that joint strength and stiffness were linear functions of density. Such relationships have been established by Brock [18], Mack [6], Morris [9], Morris *et al* [83] and SaRibeiro [11] using empirical analysis approaches and by Keunzi [82], Wilkinson [19] and Norén [160] using elastic analysis methods.

With the plastic theory approach, the strength and stiffness behaviour has been found to be a function of the embedment strength of the timber and this is discussed in the following section.

2.3.2 Embedment Strength

The embedment strength of timber is one of the most important parameters influencing the load-carrying capacity of nailed joints. It is not a direct material property and is defined as the ultimate pressure per unit length of nail divided by the nail diameter. The first detailed investigation was carried out by Siimes *et al* [161] into the embedment strength of Finnish pine where it was found that it was a function of the density of the timber, the moisture content of the timber and the nail shape. The results were in agreement with similar research carried out using Nordic pine and spruce by Norén [160]. One of the first of many semi-empirical formulae developed for this function was prepared by Foschi *et al* [162], postulating the relationship to be:

$$f_e = \frac{1}{d_n}(p_o + 2p_1)(1 - e^{(-\frac{2c}{p_o})})$$

where f_e is the embedment strength in N/mm^2; d_n is the nail diameter in mm and c,p_o and p_1 were parameters developed from experimental data.

Alternative formulae were developed by many other researchers and one of the main reasons why there were varying results was the lack of a common standard for testing to determine the embedment function. In the 1980's Whale *et al* [41, 127] developed a standard procedure for embedment tests and from these produced semi-empirical relationships for the embedment equations in timber and timber based products and after minor adjustments their equations were incorporated into EC5 [11]. Also BS EN 383 [37], the testing procedure for embedment strength of timber structures with dowel type fasteners, was published in 1993 establishing a standard test procedure for future work.

In the Whale *et al* research, predrilling was used for all hardwood and no predrilling was used for softwood. Different equations were derived for embedment in hardwood and in softwood but it was concluded that the difference had been due to the effect of the predrilling [127] and was not a function of the timber species. The differences were subsequently adjusted in EC5 and the same equations were adopted for softwood and hardwood with the difference solely relating to the whether or not predrilling was being used. For plywood, only one equation was required and it was not a function of predrilling. The equations in Eurocode5 [11] for the characteristic embedment strength for timber with and without predrilled holes and for plywood are:

(i) Timber using nails up to 8mm in diameter:

with predrilled holes $f_{h.k} = 0.082(1-0.01d)\rho_k$; without predrilling $f_{h.k} = 0.082\rho_k d^{-0.3}$.

(ii) Plywood using nails with a head diameter of at least $2d$:

all conditions $f_{h.k} = 0.11\rho_k d^{-0.3}$

where $f_{h.k}$ is the characteristic embedment strength in N/mm^2; d is the nail diameter in mm and p_k is the characteristic material density in kg/m^3.

It will be noted from these equations that the embedment strength has also been shown to be a linear function of the timber density. However, as the joint ultimate strength equation is based on the square root of the embedment strength, when using an ultimate load approach the joint strength will be the square root of the timber density.

2.3.3 Moisture Content

As has been stated in section 2.3.1, timber is a hygroscopic material and its strength and stiffness properties are affected by the level of moisture and its rate of adjustment to achieve an equilibrium state. Increasing the moisture level produces lower strength properties and elastic property values until it reaches the fibre saturation level, beyond which there is no further effect on these properties [1, 78, 79]. Although the relationship between moisture content and timber properties has not been found to be linear [78] it has generally been assumed to vary linearly when the moisture content is between 8% and 20% [79]. The moisture content effect is dependent on the strength property and specific values have

been given in Table 2, page A4/16, STEP 1 [79] where the change per 1% variation in moisture content ranges from 0.5% to 5% depending on the property affected. EN 384 1995 [80] also gives strength adjustment factors which are generally lower than those in STEP 1. No information is given in these references for the effect of change in moisture content on the behaviour of joint strength.

Mack [6] developed his joint strength equation using green timber and from comparative tests using dry timber found the strength factor to be 1.39. This was considerably greater than the factor of 1.25 recommended by Pearson *et al* for Australian timbers [164]. Mack [71] also compared the joint strengths of green timber and timber at a moisture content of 12% and found for short-term lateral loading there was effectively no difference in the reduced load strength behaviour between these conditions. This was the condition where the joint load-displacement profile was obtained by dividing the test load profile by the load at the maximum slip limit. This finding was also supported by Morris [9].

Morris developed a relationship between joint strength and moisture content where $P = a(\delta)^b$, P being the joint load at deformation δ, a and b were constants of fit, and b was also a function of moisture content. For joints with plywood outer members it was found that $b = 0.806m_p^{-0.166}$ and for joints where all members were solid timber $b = 0.778m_p^{-0.092}$. In the relationship m_p was the percentage moisture content of the timber. With moisture content values between 12% and the fibre saturation level it is noted that the value of b is only marginally changed, however, the equation is only valid up to a slip of 0.25mm.

There has also been investigation into the effect of moisture content on embedment strength and relationships for Norwegian timbers were developed by Kuipers *et al* [165] incorporating the moisture content function $f_{e\omega} = f_e(\frac{26}{\omega + 14})$ where $f_{e\omega}$ is the embedment strength at moisture content ω %.

Moisture content has also been linked to duration of load effects. The higher the moisture content the more pronounced the duration of load effect will be [166] and this has been included for in the strength modification factors for service classes and load duration classes given in EC5 [11].

2.3.4 Nail Diameter

Nails of varying shape have been used in timber joints but the most widely used has been common wire nails having a plain shank of circular cross-section and only this type has been addressed in the research review.

From the research into the effect of nail diameter on joint strength the relationship has been found to be a power function of the form d^a, where d is the nail diameter and a is a constant. Also where joints

have been formed using gusset plate connections the gusset plate material has not been considered to be a factor which would cause the power function constant to vary.

In the research by Wikinson [81], based on the original theory put forward by Kuenzi [82], the nail diameter relationship was determined using classical elastic theory and found to be a function of $d^{1.75}$. Using a semi-empirical approach in which the nail diameter effect was determined from tests on three member joints with a pair of nails in single shear using three different nail diameters, Mack [6] also found that the function was $d^{1.75}$. This was also accepted as the nail function relationship by Morris and Gajjar [84] in their research into timber joints with plywood gussets. In Goh's research [12], which was also a semi-empirical approach, the nail diameter function was d^2, but this was based on an argued relationship rather than from the results of tests. In the work by SaRibiero *et al* [70] which was based on the load-displacement model developed by McLain [7], because of the form of model used the nail diameter function cannot be readily abstracted but from inspection will be a function less than d^2.

Using the plastic theory approach, from the ultimate limit state strength equations developed by Larsen [45] for a two member joint with a nail in single shear, Smith *et al* [54] showed that the joint strength equation could be written $P_y = 0.577 d^2 f_y^{0.5}$, where P_y is the joint strength, d is the nail diameter and f_y is the nail yield stress. In isolation this gave a nail strength function of d^2. From extensive nail bending tests by Whale *et al* [126], however, it was shown that the relationship between yield stress and nail diameter was $f_y = 50(16 - d)\,\mathrm{N/mm^2}$, and after inputting this relationship into the joint strength equation and performing a least squares linear regression analysis fit, the nail diameter function was reduced to $d^{1.65}$ for both softwoods and hardwoods. Subsequently, in developing the Eurocode5 [11] strength equations, the joint strength function was further modified and after abstracting all of the functions which have a nail diameter relationship, the nail diameter function can be shown to be $d^{1.65}$ for nails driven without predrilled holes and $d^{1.8}$ for nails driven with predrilled holes .

From the research the nail diameter function has been shown to vary depending on the analysis approach being used.

2.3.5 Nail Strength

In the elastic methods of analysis, as the nail was assumed to behave elastically, nail strength was not considered to be a relevant factor and was not taken into account [81]. The movement function adopted with classical theory related primarily to the behaviour of the foundation modulus (or embedment) of the timber.

With the empirical methods of analysis there has also only been a very limited investigation into the effect of nail strength. Mack [6] compared the effect of joints using nails of special high carbon with the behaviour of joints using common low carbon steels and found there was a factor of 1.21 difference

with the higher carbon nails. However, this finding was not taken further and Mack's empirical strength equation did not include a function for nail strength. Also, with such models, no work has been published on the behaviour of nail strength variation effects within low carbon nails

Nail strength has however been a factor in analyses using the ultimate strength approach where the failure mode of the joint involved yield failure of the nail. As the use of plastic theory became more common, it was realised that the codes in most countries were deficient regarding their specifications for the strength properties of nails for plastic design and attention was drawn to this by Ehlbeck [16]. The standard for nails in the UK, BS 1202 : Part 1 ; 1974 [23], only specified quality control on nail sizes, giving no strength criteria, and an in-depth investigation by Smith *et al* [126] was undertaken into the properties of UK nails. It was found that when taking into account the effect of strain hardening of the nail wire the nail yield strength could be expressed as $f_y = (950\text{-}50d_{nom}) \pm 150$ N/mm^2. This was subsequently modified to $f_y = 50(16\text{-}d)$ [41] and prior to the publication of EC5 [11] it was proposed that the nail wire strength should be taken to be the average of the nail tensile strength and the yield strength [68] and a minimum tensile strength value, $f_u = 600$N/mm^2, has been used in the code with the intention to further change by introducing a factor of $\frac{f_u}{600}$ to the nail strength equation[15].

After extensive testing in Germany the nail strength equation was adjusted to relate the yield moment to the tensile strength of the nail wire and its diameter [68] and, taking account of the intended change to the nail tensile strength, the equation for the characteristic value of smooth round wire nails to be included in EC5 [15] will be $M_{y,k} = \frac{f_y}{600} 180 d^{2.6}$, where $M_{y,k}$ is the yield moment in Nmm of a nail of diameter d mm.

2.3.6 Nail Length/Material Thickness

Material thickness, or more precisely, nail length, tends to be a factor which is important in the ultimate strength and elastic analysis approaches but does not often feature as a significant factor in the empirical methods. In the work by Mack [6] tests were done using two member joints comprising 25mm thick timbers; 38/38mm timbers and 25/50mm timbers with single 3.66mm diameter nails in single shear and showed that the variation in strength was only 4%. It was concluded that for the limited combination of timber sizes and nail lengths and diameters in Australian building practice, under normal circumstances, a factor for nail length was not required and none was included for in Mack's load-slip equations. The range of slenderness ratio λ (nail length divided by nail diameter) used in the testing programme was 6.9 to 22.9.

In the McLain [7] empirical formula member sizes were not varied and nails with a slenderness ratio of 5.7 were always used. That was subsequently modified by SaRibeiro *et al* [70] to include for the effect of variation in gusset plate thickness but because of the nature of the McLain model, the gusset plate

thickness factor was a complex function. Morris *et al* [83] also developed Mack's method to include for plywood gusset plates of varying thickness based on tests using nails in double shear with λ ranging from 17.9 to 22. It was shown that there was a relationship between gusset plate thickness and joint strength involving a combination of material density, the thickness of the timber and the plywood gusset plates. Hunt *et al* [25] also did tests on joints increasing the length of nail pointside penetration from 6 to 22 times the nail diameter and also tests where the thickness of plywood gusset plate was increased from 7.5mm to 20mm thick. It was shown that joint strength increased with increasing penetration and increasing gusset plate thickness. The semi-empirical equation developed by Goh [12] included a plywood gusset plate factor $\beta = 0.025\sigma_{\max,par}$, where $\sigma_{\max,par}$ is the compressive strength of the plywood and a steel factor $\beta = 1$ for steel gusset plates but they did not include for material thickness effects.

In the elastic theory approach nail length is a factor and the effect reduces as the nail gets longer. Wilkinson [81], has shown that when the foundation modulus function times the nail length is greater than 2, nail length will have no further effect.

With the ultimate load approach λ is a key factor in the determination of strength. Ehlbeck [16] summarises the results of early research done in Germany in 1935 into embedment strength, noting that the optimum λ for maximum embedment strengths was approximately 7. As λ reduced below 7 the embedment strength also reduced due to the timber splitting. Above 7 it reduced due to flexure of the nail and the tests ranged from a slenderness ratio of 4 to 17. Ehlbeck also stated that for embedment tests, λ should never exceed 4 as the deformation in the nail will influence the stress distribution and give an incorrect result. In the research into embedment strength by Smith *et al* [73] for EC5 [11] a slenderness ratio of 2 was used and in BS EN 383 : 1993 [37] the limit for λ has been set to lie within the range 1.5 to 4 times the nail diameter. For joints where λ exceeds about 7 Larsen [45] found that joint failure was in a ductile manner with a plastic hinge forming in the nails on either side of the interface between the joint members, conforming to what is referred to as a mode 3 failure in the European yield model [176]. This was also reported to be the case by Smith *et al* [54] and supported by Jorrison [47].

2.3.7 Grain Direction

The cells in timber run in a vertical direction and the general arrangement of the alignment of these cells is referred to as its grain. Timber has directional properties relative to the grain direction but exhibits no symmetry and is consequently referred to as an anisotropic material [78, 159, 167]. As a first approximation however, it is generally considered to be orthotropic and depending on the angle of loading relative to the grain the elastic properties will vary significantly over its orthogonal axes. With Beech timber, for example, the modulus of elasticity when loaded along the grain direction is over 12 times that obtained when loaded tangentially at right angles to the grain [1].

Because of the complex cellular nature of timber, a failure theory has still to be fully developed and approximations have to be made to determine behaviour when loading has been applied at an angle to the grain. Empirical methods have been used in such circumstances and the most commonly used is the formula developed by Hankinson [114], of the form:

$$n = \frac{pq}{p\sin^s \vartheta + q\cos^s \vartheta}$$

where n is the unit strength at an angle ϑ to the gain direction, p is the unit strength parallel to the grain, q is the unit strength perpendicular to the grain. There has been debate over the value to be used for s however experimental evidence appears to support $s = 2$ [78]. The expression has been applied frequently to timber, particularly for the case of compression in two directions.

The early work by Siimes *et al* [161], Larsen [45] and subsequent research by Girhammer *et al* [173] showed that for nailed joints the angle of load relative to the grain direction had little effect. Whale *et al* [41] found there was a slight indication that nailed softwood members were stronger when loaded perpendicular to the grain, whilst nailed hardwoods were stronger parallel to the grain. However the differences were relatively small and proposed that orientation effects were ignored for nailed joints. This finding was accepted and in EC5 [11] the embedment strength equation is the same for loading parallel and perpendicular to the grain with nailed joints. It is to be noted however that not all researchers agree with this finding. Hunt *et al* [25] found that embedment tests using Australian timbers gave test results perpendicular to the grain much less than those parallel to the grain. This was also stated to be the case by Bullen [20], again with Australian timbers.

The effect of direction of loading on plywood has also been investigated theoretically and by testing. Most classical failure theories were derived for homogeneous isotropic materials which were assumed to behave in a linear stress-strain manner up to failure. Because of orthotropic symmetry these theories require considerable modification to be applicable to composite materials such as plywood. The majority of work in this field has been done by Norris [168], with some later developments to the theory by Hollaway [170]. For plane stress conditions, using energy theory, Norris found the strength at the proportional limit when loaded at an angle ϑ to the grain to be:

$$\frac{1}{\sigma_{p\vartheta}^2} = \left(\frac{\cos^4 \vartheta}{\sigma_{p1}^2} + \left(\frac{1}{\sigma_{p12}^2} - \frac{1}{\sigma_{p1}\sigma_{p2}}\right)\sin^2 \vartheta \cos^2 \vartheta + \frac{\sin^4 \vartheta}{\sigma_{p2}}\right)$$

where $\sigma_{p\vartheta}$ is the stress at the proportional limit at an angle ϑ to the grain; σ_{p1} and σ_{p2} are the normal stresses in direction *1* and *2*; σ_{p12} is the shear stress at the proportional limit in the *1,2* plane.

Notwithstanding the theoretical approach, Whale *et al* [41] investigated the effect of nail forces on the grain direction of veneers in plywood by testing and found there was no significant difference between the contributions of parallel and perpendicular veneers and in EC5 [11] the embedment strength is taken to be the same irrespective of the veneer direction.

2.3.8 Number of Rows of Nails

In the early research the majority of testing was based on the use of single nail joints and the assumption was made that for a joint with n nails, the joint strength would be n times the load carrying capacity of the single nail. Most codes were based on this premise. [86, 87, 169].

Lantos [86] pointed out that the load distribution in a multi-fastener joint depended on the number of fasteners in a row; the stiffness of the members and the slip modulus of the joint. Because the slip modulus of a nailed joint is relatively low, this allowed for a reasonably even load distribution to develop under load and for a joint with 20 nails in a line Lantos showed the load reduction was only 5%. Consequently Lantos argued that a reduction factor was not required for nailed joints. Mack [6], however, did tests on lines of nails with 12 nails and found there was a load reduction of 6% but he argued that a load reduction factor was justified. McGowan [172] found with glue-laminated timber joints using hardened nails, with up to 4 rows of nails there was a linear increase in capacity and beyond that number the rate of increase in capacity fell away. Thomas *et al* [175] found for joints with up to 3 rows of nails the strength also increased linearly and introduced a factor of 0.9 for all joints with more than 3 rows. More recently, in the semi-empirical strength equation by Goh [12], joint strength is a given by:

$$F = \prod A N_n N_s S \beta (B(1 - e^{-0.75\delta}) - N_n \delta e^{-0.75\delta})$$

where N_n is the number of nails in the joint. In this equation the joint strength reduces as the number of nails is increased and it is also a function of the joint slip.

In EC5 [11] the current rules are based on joint strength being a multiple of the number of nails in the joint but amendments are proposed to incorporate a strength reduction factor for appropriate joint configurations [15]. A factor, n^{kef}, which will be used to multiply the number of rows of nails in the joint, will be included in the joint strength equation. In the function, n represents the number of nails in a single line lying in the direction of the applied load; k_{ef} is a power factor which is unity when the row spacing is $\geqslant 14d$ and less than unity when the row spacing is less than $14d$.

2.3.9 Predrilling for Nails

Predrilling is required in certain timbers to stop the timber from splitting and in the case of hardwoods, to allow the nail to be driven without buckling. Predrilling also allows the nail spacing to be reduced

whilst still allowing the timber to behave in a ductile manner.

Mack [6] found when using Australian hardwoods predrilling was always required and from tests on softwood using a drill 80% of the nail diameter, there was only a 1% increase in joint strength over joints formed without predrilling. Wilkinson [81] used a predill of 90% of the nail diameter and found that the 'elastic bearing constant', k_o, when loading parallel to the grain, was over 45% greater than when determined without predrilling. Wilkinson's strength equation [81] is a function of $k_o^{0.75}$ and on this basis results in a strength increase of 17%. Predrill sizes up to 100% of the nail size have been used [171].

Whale *et al* [41] did embedment tests on timber and on plywood without predrilling and also with predrilling using a predrill 80% of the nail diameter in accordance with the recommendations of BS 5268: Part2: 1984 [72]. Different equations were derived for embedment in softwood and in hardwood but it was concluded that the difference had been due to the effect of the predrilling [127] and the strength equations were solely related to density and nail diameter irrespective of timber species. Using timber joints without predrilling, the mean embedment strength was $0.09\rho(d)^{-0.36}$ and with predrilling it increased to $0.13\rho(d)^{-0.36}$, where the mean density is ρ and d is the nail diameter, resulting in a 44.4% increase in strength. For plywood tests, Whale *et al* [41] found the embedment strength to be $0.012(10-d)\rho$, and predrilling was not relevant.

After further development the Whale *et al* equations were slightly modified and incorporated into EC5 [11] as given in section 2.3.2.

2.3.10 Joint Friction

Friction in a joint comes in two forms. There is that arising where there is direct contact between the joint member interfaces at the assembly stage and there is the other arising when the joint is loaded and the joint members are drawn together when the nails are being deformed. The former is dependent on the contact pressure at assembly and the coefficient of friction between the mating faces. The latter occurs in the upper load transmission range and will ultimately be dependent on the withdrawal resistance of the nails in the joint. Where joints are assembled with a gap between the members the former type is not present but under loading the latter will invariably arise.

Aune *et al* [17] found for joints with steel gusset plates that the difference in the strength of joints where timber was or was not in contact with steel gusset plates was minimal. For joints with plywood gusset plates with a gap of 0.23mm and without a gap, Aune *et al* found there was an increase of 47% to 56% arising from total friction contact. Mack [6] found with dry timber joints and a gap of 0.71mm there was an increase of 35% arising from the total friction contact and when the gap was increased to 1.42mm there was no additional gain in strength.

It is not practical to control the pressure imposed between the contact faces of nailed joints, particularly if the joint is hand made, and invariably in service there will be some drying out of the timber/composites resulting in a gap arising between the joint interfaces. For these reasons the normal practice is to test joints with a gap [6, 7, 17, 83].

In the testing undertaken to validate the EC5 [11] strength equations, the joints were fabricated with small gaps between the joint members to provide a lower-bound estimate of strength and stiffness [53, 127]. Further, despite the requirement in the code that nails be driven to a depth such that the surface of the nail heads are flush with the timber surface, in these tests the nail heads were not fully driven home into the side members. Ehlbeck *et al* [68] confirmed that the ultimate strength equations used for joints in EC5 [11] excluded the friction effect arising from direct contact of the joint interfaces. The only friction factor included for in the code was the nail tension effect where a factor of 1.1 has generally been incorporated into the relevant strength equations. In Eurocode5 [15], however, the intention is to further enhance the nail tension effect relating it more directly to the withdrawal resistance of the nails in the joint.

2.4 SHORT DURATION LATERALLY LOADED NAILED JOINTS

2.4.1 Empirical Approach

The first empirical solution applied to the properties of solid timber was by Ivanov [69] in 1949 with the development of a non-linear load-slip relationship of the form:

$$s = a_1 F + a_2 F^2$$

where a_1 and a_2 are constants, s is the joint slip and F is the joint load. The method had very limited application and it was not until the 1960's and later that practical empirical methods were developed.

The first authoritative procedure deriving an empirical formula for short term lateral loading of a nailed joint and developed in an analytical manner from test data was by Mack [6]. Mack argued that the relationship between joint strength and slip was a function of the product of the effect of each variable that could influence behaviour and from tests confirmed there was no significant interaction between the variables. From single shear tests on three member joints using single nails Mack found that the yield load of a joint occurred at a slip of approximately 3.5mm and arbitrarily set the upper limit of validity of his empirical equation at 2.54mm. The yield load occurred at approximately 50 to 80% of the ultimate test load based on joints with an initial gap of 0.7mm, and the 2.54mm slip was above the design limit set by the national code. The method used a concept of reduced load, defined as the ratio of the load at displacement δ to the load at 2.54mm slip, from which, using logarithmic transformation and iteration, a displacement function for the joint was derived. After simplification Mack established an exponential relationship for joint behaviour for single shear, single nail joints of the form:

$$P = \prod A(d^a)(k_s)(b\delta + c)^d(1 - e^{f\delta})$$

where P is the load per single nail in single shear in the joint; d is the nail diameter; k_s is a species factor (which Mack later proved to be $0.27D$, where D is the oven dry density of the timber [71]); δ is the joint slip and A,a,b,c,d and f are constants of fit. Mack also showed from tests on joints with nails in double shear, the strength was two times the single shear strength equation.

Because the equation could not readily be inverted to express displacement in terms of load, Mack [71] developed another relationship, using the same format, for small joint displacements up to 0.5mm slip. This slip limit was chosen as it was close to the maximum slip of 0.4mm allowed at the basic working load in the Australian code [88]. Mack concluded that even at such low slips the load slip relationship could not be accurately represented by a straight line and developed the following power relationship:

$$P = 0.2d^{1.75}D\delta^{0.5}$$

Mack's approach to the development of empirical solutions has been widely used [9, 83, 174]. Using the reduced load approach, Morris [9] developed a load-slip relationship for joint behaviour but only up to a slip of 0.25mm. The expression was in the form of a power relationship, $F = As^B$, where F is the load per single nail in single shear in the joint; s is the joint slip and A and B are constants of fit. All of the development was undertaken using single species timber. Morris *et al* [83] also tested the validity of the Mack relation using UK timber and plywood of varying thickness. The joints were in double shear with plywood gussets. Morris *et al* [83] effectively validated the Mack [6,71] equations and developed a function to take account of the use of plywood gusset plates of varying thickness. The load slip equation for joints with a slip up to 2.5mm was of the form:

$$P = 455.6d^{1.75}\bar{G}(0.128\delta + 0.68)(1 - e^{-3\delta})^{0.8}$$

where $\bar{G}$ is a function of the specific gravity of the timber and plywood and the respective material thickness.

McLain [7] developed an empirical expression for joint load-slip from tests using several species of timber of the same thickness (50.8mm) with different materials for the joint gusset plates, but all 19mm thick. A single nail size, 3.33mm in diameter, was used in single shear and the load-displacement expression was of the form:

$$P = A\log(1 + B\Delta)$$

where Δ is the joint displacement and A and B are curve fitting empirical constants. The equation was

limited in application and was further developed by SaRibeiro *et al* [70] to take account of variations in gusset plate thickness and nail diameter. The expressions developed for the curve fitting empirical constants were:

$$A_{MC} = \beta_0 + \beta_1 SG + \beta_2 (SGt) + \beta_3 (SG^2 \phi)$$

$$B \quad = \beta_0 + \beta_1 \log(SG) + \beta_2 \log(t) + \beta_3 (SG^2 \phi)$$

where A_{MC} was a function of moisture content; the β values were constants; SG was the specific gravity of the timber; t was the thickness of the gusset plate and ϕ was the nail diameter.

More recently Goh [12] has developed a semi-empirical equation using single species timber and different types of gusset plate for joints using fully overlapping nails in single shear. The expression has been based on tests using multiple nailing configurations and the form of the load-displacement expression is given in section 2.3.8.

The benefit of the empirical expression is that with computers and modern software applications being readily available for use in design offices, as well as being able to determine joint strength at varying slips, the associated secant stiffness of the joint can also be readily obtained. Also, with this type of model the varying behaviour of the joint over the loading cycle is able to be included for in the analysis of the structure.

2.4.2 Elastic Theory Approach

The elastic theory approach uses the classical differential equation for the deflection curve of a beam supported on an elastic foundation, namely:

$$\frac{EId^4 y}{dx^4} = -ky$$

where E is the modulus of elasticity of the beam, I is its second moment of area; k is the foundation modulus and y is the deflection at point x on the beam. This approach has only been used on a limited basis.

The method was initially developed by Kuenzi [82], making E equal to the elastic modulus of the nail, I equal to the moment of inertia of the nail and k equal to the foundation modulus of the timber. The solution of the differential equation finally resulted in expressions involving a characteristic $\lambda = \sqrt{\frac{k}{4EI}}$ and produced a rather complex single shear load-slip equation which allowed the computation of joint deformation in an assumed elastic range up to the proportional limit of the joint. Keunzi's theory made

several arbitrary assumptions and this was later considerably improved by Wilkinson [81]. Wilkinson validated the key assumptions, simplified the equations by using the same species of timber in both members of the joint and developed a load-slip equation for smooth round nails in predrilled holes of the form:

$$P = 0.1667 E^{0.25} (k_0)^{0.75} d^{1.75} \delta$$

where E was the modulus of elasticity of the timber; k_0 was the elastic bearing constant and d was the nail diameter. The expression could also be adjusted to be used for joints with dissimilar members and this was carried out by Ehlbeck [68].

Noren [160] also used the classical elastic theory but presented his load-displacement expression in a different way. For members having different elastic bearing constants, the load-displacement relationship was:

$$P = \frac{K\delta}{4\lambda(\psi_1+\psi_2)}$$

where K is the foundation modulus and $((\psi_1 + \psi_2)$ is a function of the characteristic λ for each member, the member thickness and the joint configuration.

The elastic theory expressions are limited to the 'elastic limit' of load-slip behaviour, which had been taken to be of the order of 0.3mm. This was, slightly less than the 0.4mm design limit which had generally been used to determine the working load capacity of a nail in most permissible stress design codes at that time. However, the assumption of linear behaviour has in itself been the subject of dispute as the actual load-slip behaviour has invariably been shown to be a curve from the commencement of loading [6, 7, 12, 68, 83].

2.4.3 Ultimate Theory Approach

The first published research to provide clear guidance on the application of plastic theory to timber joint behaviour was by Johansen [43] in 1949. Plastic theory was very much in its infancy at that time, being developed from its application to steel structures. The basic concept of plastic behaviour in steel structures was put forward initially by Ewing [156] in 1899 in his text book on the strength of materials. Serious research into the use of the theory did not get underway until the early 1930's, started by Maier-Leibnitz [155] and followed by Baker *et al* [156] at Cambridge University. Researchers had been aware that elastic theory was deficient and could not address the behaviour of materials beyond the elastic limit and well before this period the need for the study of plastic behaviour had been appreciated by the Love [139], the well known elastician, who had written in 1892:

> "It is imperatively necessary that effects which cannot be calculated exactly should be taken into account in construction, and it is in this sense that elastic theory is at this time behind engineering practice."

Johansen developed strength equations based on the embedment strength of the joint materials and the yield moment of the dowel connector used. The equations assumed idealised conditions, and ignored the types of friction effects referred to in section 2.3.10.

Larsen [45] fully validated Johansen's approach for nailed joints by completing the outstanding analysis applied to tests which Johansen had done but had not managed to investigate. Larsen analysed the various failure modes which could arise and compared the results with the test behaviour. The types of failure ranged from embedment failure of the gusset plates; a combination of embedment failure and partial yield of the nails and finally embedment failure with full plastic failure of the nails. These failure modes formed the corner stones of the ultimate strength equations and were subsequently referred to as the European yield model [47, 54, 176].

Larsen [45] found from Johansen's tests that for a ratio of joint slip to nail diameter up to unity the joint behaviour followed the Mack [6] load-slip expression almost exactly. It was also found that the ultimate failure load occurred at a slip ranging from 1 to 1.5 but could extent up to 2 times the Mack slip limit of 2.54mm. The failure load expression for a two member single shear nailed joint, assuming embedment failure on both members, full plastic failure of the nail and ignoring the nail tension effect was:

$$P = s_H dl \sqrt{\frac{4\beta}{(1+\beta)} \frac{M_y}{s_H dl^2}}$$

where s_H is the embedment strength of member1; β is the ratio of the embedment strength of member 2 to member 1; d is the nail diameter; l is the nail penetration length in member 1 and M_y is the yield moment of the nail. Larsen [45] also investigated the increase in load in the joint due to the nail tension effect referred to in section 2.3.10 and found that normally the strength increase was about 20% higher than the theoretical capacity when the effect was ignored.

The Johansen equations were used by many researchers [17, 20, 54, 65] but in particular by Smith *et al* [126] and, as stated by Bullen [20], as a consequence of this work the ultimate load theory was adopted by the drafting panel of EC5 "Common Unified Rules for Timber Structures 1988". Since then the European yield model [47, 54, 176] has formed the basis of the design of joints in the European and Canadian codes with the US code also allowing the use of the model, where it is referred to as the load and resistance factor design method (LRFD) [176]. The Australian code is also investigating incorporating the method but currently retains the empirical approaches developed by Mack.

When the force in a nailed connection acts at an angle to the grain there is also the possibility of the timber splitting due to tension stresses being set up in the joint by the nail forces. If this occurs the joint will fail by brittle failure rather than in a ductile mode, which is the failure mode assumed by the EC5 strength equations. To check the splitting resistance of timber, linear elastic fracture mechanics theory was applied to the splitting behaviour of timber in the early 1990's [119]. At that time the research was principally associated with the evaluation of fracture properties of timber test specimens [118]. Since then a number of researchers have investigated the splitting behaviour of joints [119, 120, 121, 122] using this approach and recommendations for the design of joints subjected to splitting forces have been prepared for inclusion in EC5 [15].

The strength equations in the ultimate strength approach give no information on the stiffness behaviour of the joint. Ehlbeck *et al* [68] has stated that from the results of tests done in various testing laboratories the serviceability limit state slip was found to be $40\frac{d^{0.8}}{\rho_k}$ and $60\frac{d^{0.8}}{\rho_k}$ for nailed joints with and without predrilled holes respectively. Based on a serviceability limit state load of 40% of the failure load expression for the two member single shear nailed joint given above, the joint stiffness at the serviceability limit state has been given in EC5 [11] as $\frac{\rho_k^{1.5} d}{20}$ and $\frac{\rho_k^{1.5}}{25}$. These values have been in use since 1994 however more recent research has suggested these values require to be amended and revisions are being proposed in EC5 [15].

2.4.4 Finite Element Approach

The finite element approach is the most recent method to be used to analyse the behaviour of nailed joints. It is a method that gives analysts the opportunity to address the combined elastic and plastic behaviour of nailed joints using a mathematical approach which can be tailored to suit the requirements of the problem being investigated. As well as incorporate material non-linearity the method can also be modelled to include for large displacement theory. This can include for large displacement or rotation with small strain in which the stress-strain relation may be linear or non-linear. Alternatively it can address large displacement or rotations with large strains, and again the stress-strain relation may be linear or non-linear. It can also include for non-linear analysis involving changes in boundary conditions during motion. This situation is very relevant to the analysis of contact problems which arise in nailed joints when there is a loss of contact between the nail and the timber during the joint slip process.

The first important use of the finite element method of analysis for the investigation of joint behaviour was by Foschi [4] in 1974 using a non-linear one dimensional model for the prediction of the load-displacement relationship for single shear nailed timber joints with lateral loading. It was assumed that the nail was an ideal elastic-plastic material and that the load-deformation relationship for the

foundation, which was assumed to be discontinuous, was of the form developed by Mack [6].

This was followed by a more detailed elasto-plastic one dimensional model developed by Smith [163] using a cubic polynomial to describe the displacement of the nail. The analysis involved a comparison of results using small and large displacement solutions. Hunt *et al* [25] extended the Foschi [4] analysis and used a three point Gauss-Legendre integration technique based on the use of Legendre polynomials to solve the finite element equations. Chui *et al* [177] also used the Foschi approach and included for shear deformation in the nails; friction between the nail and the timber and for nail withdrawal effects. It was also modified to take large displacement theory into account.

One dimensional analysis cannot take shear performance into account accurately because the axial force in the nail cannot be accounted for and a two dimensional finite element method using small and large deflection theory has been used by Nishiyama *et al* [178] for the load-slip analysis of nailed timber joints. The nail was split into elements which were assumed to behave elastically and at the element junctions spring properties were used to simulate non-linear plastic behaviour. It was concluded that the large deflection theory approach should be used to obtain the more accurate result.

Commercially available software applications have been used for the analysis of nailed joint structures but not to a significant extent. As these applications become more user friendly it is to be anticipated that investigation of nail behaviour using the finite element method will be more readily adopted.

2.5 SHORT DURATION MOMENT-ROTATION OF NAILED JOINTS

Providing there is no buckling or yielding of the joint members, the transfer of moment through a nailed joint will be by the dowel action of the nails and the bearing of the nails on the timber and side members.

Ehlbeck [16] has stated that the conventional elastic torsion formula used in the design of steel joints can also be used for nailed joints. The torsion formula is $F_i = \frac{Mr_i}{\sum r_i^2}$, where F_i is the load on a nail with the distance r_i from the centroid of the nail group; M is the moment on the joint and $\sum r_i^2$ is the sum of the squares of the distance of each of the nails from the centroid of the nail group.

Morris [108, 109] used the formula when investigating the rotational rigidity of multi-nailed joints subjected to a moment. Perkins *et al* [179] also used the formula in the design of multi-nailed joints but noted that because of the non-linear behaviour of the nails, contrary to the assumption in the torsion formula, the force in each nail will not be a linear function of its distance from the centroid of the nail group. Perkins *et al* assumed a power empirical function for the relationship between nail force and joint slip, $F = As^B$, where F was the force in the extreme nail; s was the associated nail slip and A and

B were constants of fit. It was assumed that the centre of rotation remained fixed at the centriod of the nail group during rotation and that the slip in each nail was proportional to the ratio of the distance of the nail from the centroid to radius of the extreme nail position times the slip at that position. Using the relationship between slip and rotation, $s_i = \vartheta r_i$, the joint rotation was set out as a function of the joint moment and the nail radii as follows:

$$\vartheta = \left(\frac{M}{A\sum r_i^{(1+B)}}\right)^{B^{-1}}$$

where ϑ is the angular rotation of the joint in radians and r_i is the radius of the nail from the centroid of the nail group. Perkins *et al* found that the experimental curves were of the same form as the theoretical results but generally fell below them, indicating that a higher rotation existed at a given bending moment. This was attributed to inaccuracies in the values of the constants A and B used in the joint slip relationship.

Boult [84] investigated the moment behaviour of square symmetrical nailed patterns using steel gusset plates with the nailing configuration achieving a concentration of nails at the maximum distance from the centre of rotation. The joints were analysed assuming the centre of rotation was at the centroid of the nail group and used both the simple torsion formula approach and a two dimensional finite element commercial package called ADINA. It was found that the simple torsion analysis predicted nail forces that were over 47% higher than the finite element results which took into account nail slip and timber strain effects. Nailing pattern effects were also investigated, where extreme nails were removed to even out the effect of nail forces, but reached no clear conclusion on whether this would increase or reduce the moment capacity of the joint.

Kermani *et al* [92] showed that for joints tested under moments of up to 70% of the ultimate load, the centre of rotation remained fixed at the centroid of the nail group. Kermani [94] also used the elastic torsion equation incorporating the Perkins *et al* [179] approach to develop the moment resistance of nailed joints in a study of the semi-rigid behaviour of such joints in timber portal frames assuming a fixed centre of rotation. The load-slip relationship was based on the results of tests on 2 and 4 nail single shear joints, developing an exponential type curve. Kermani [94] idealised the non-linear load-slip behaviour of the joint into a series of piecewise linear relationships, changing the stiffness properties of the joint at each slip increment. The moment contribution of each nail in the joint at each increment was summated to obtain the full moment. A purpose designed computer program was developed for the analysis, and the solutions from the theoretical approach compared very favourably with the test results.

Bouchier et al [123] developed a modelling method for determining the moment behaviour of fasteners in timber using a finite element approach. The dowels were simulated in the model by simple springs

that incorporated contact properties. Load distribution in the dowels was, however, restricted to elastic behaviour using the initial slope of the non-linear curve of the dowel embedment relationship. The model is only of value for making comparative studies of the initial behaviour of a joint and for the effect of varying joint configurations. The load distribution of the dowels was compared with the results using the analytical method developed for moment transfer in joints given in STEP 1 [79] at the serviceability limit state. Because of the restriction placed on the dowel stiffness behaviour, the conclusions drawn from the method were limited. One of interest was that the centre of rotation of the joint remained at the centroid of the nail group.

Goh [12] developed two methods using the Perkins *et al* [179] approach, both incorporating his empirical load-displacement model referred to in section 2.3.1. One method was developed assuming a fixed centre of rotation at the centroid of the nailing configuration. The second used a variable centre of rotation approach, incorporating the method given by Hiria [134] for determining the movement of the centre of rotation of a joint when subjected to a moment. Both of his methods took into account the non-linear behaviour of the nail in the joint and both gave a good comparison with the results from moment tests. Various nailing configurations were used with both steel and plywood gusset plate joints and the variable centre approach gave the more accurate result.

Another method, also used by Goh [12], was the 'geometric approach' developed by Nowak *et al* [107] to predict the ultimate capacity of eccentrically loaded steel connections. The method was based on the behaviour of the joint fasteners and the geometry of the connection and used a truss analogy approach in which each fastener was modelled to be attached directly to the point of intersection of the load and the line through the centroid of the nailing group. The nail force acted along the direction of this line and was proportional to the distance of the nail from the intersection point. With these assumptions the method was not able to take into account the effect of nails lying on the same horizontal line as the geometric centre of the joint. Apart from the limitations of the method, Goh [12] found it did not give accurate results when compared with the results from moment tests.

2.6 SEMI-RIGID BEHAVIOUR OF NAILED JOINTS

When the joint in a structure is subjected to rotation, providing there is no relative movement between the joint members, each will rotate by the same amount. In this condition joints are referred to as rigid, giving maximum rotational stiffness to the structure. At the other extreme, where the members are connected such that no moment is able to be transferred between them, the joint is referred to as a pin joint. With timber structures, the traditional approach in analysis has been to assume joints are either rigid or pinned but the actual behaviour will fall somewhere between these extremes giving what is generally referred to as a semi-rigid joint.

Semi-rigid behaviour takes into account the stiffness of the joint and the majority of investigations into this effect have been carried out using steelwork connections. In nearly all of the work the assumption

has been made that only moment-rotation displacements need be considered and it has been accepted that the effects of shear force and axial deformations on the joint can be ignored [79, 94, 100, 101, 102].

Connection behaviour varies with the type of connection being used and several experimental studies have been done by researchers to establish moment-rotation stiffness relationships for different connection types. Several models have been developed representing linear, bilinear and trilinear relations [137, 146, 147] but, depending on the shape of the actual moment-rotation relationship of the joint, in some situations these models only give poor approximations. Polynomial models involving the use of curve fitting constants have also been developed, the best known of which was the model developed by Frye and Morris [148];

$$\vartheta_r = C_1(KM)^1 + C_2(KM)^3 + C_3(KM)^5$$

where K is a standardisation parameter dependent on the connection type and geometry and C_1, C_2 and C_3 are constants of fit. The main drawback with that model however, was that the nature of a polynomial was to peak and trough within a certain range resulting in areas with negative stiffness. Apart from giving incorrect stiffness values, such areas also cause numerical difficulties and instability in the analysis process if a tangent stiffness approach was being used.

Several power models have been developed and the one which represents the nonlinear moment-rotation behaviour of a variety of connections reasonably well has been the Ang and Morris model [149]. It is a four parameter power model which using a standardised constant dependent upon the connection type and will suit most curves, including moment-rotation curves that flatten out near final loadings.

Exponential power models have also been developed [12, 150, 151, 152]. The advantage of this type of curve has been that it did not suffer from the peak and trough and numerical instability problems associated with the polynomial models. The Kishi *et al* [151] model is a refinement of the Lui *et al* [150] model and is of the form:

$$M = \sum_{j=1}^{m} C_j(1 - e^{-|\vartheta_r|/2j\alpha}) + M_0 + \sum_{k=1}^{n} D_k(\vartheta_r - \vartheta_k)H[\vartheta_r - \vartheta_k]$$

where M_0 is the starting value of the connection moment to which the curve is fitted, α is a scaling factor, ϑ_k is the starting rotation of the curve, H[θ] is a step function and C_j and D_k are constants of fit. The benefit of this model is that as well as its stability, it is able to accommodate any sharp change in slope in the M-θ_r curve.

The semi-rigid behaviour of linear moment-rotation models has been investigated by Monforton *et al*

[137], Livesley [136], McGuire *et al* [138] using classical and matrix methods of analysis. Monforton *et al* [137] has shown that the end fixing moment taken by a semi-rigid joint in a frame will be less than the equivalent fully fixed rigid joint. The end fixing moment reduction factors were functions of the type of loading on the member and the member fixity factors, where Monforton *et al* defined the fixity factor as a function of the joint and member properties:

$$\gamma_i = \frac{L}{(L + 3EI\lambda_i)}$$

where γ_i is the fixity factor at end i of the member, L is the beam length, EI is the flexural stiffness of the member and $\lambda_i = \frac{\phi_i}{M_i}$, where ϕ_i is the rotation in the joint. For a pin joint, the fixity factor is zero, for a rigid joint it is unity and for a semi-rigid joint the factor will be some intermediate value. Goh [12] also showed how the fixity factor degrades with joint rotation when he developed the factors for alternative joint configurations using his non-linear moment-rotation model. The largest value of the fixity factor at the commencement of rotation reported by Goh for joints with steel gusset plates was 0.14 and for joints with plywood gusset plates was 0.05, both appearing to be rather low.

Kermani [76] also used the Monforton fixity factors (referred to by Kermani as rigidity factors) in the study of the semi-rigid behaviour of nailed plywood gusset plate knee joints in timber portal frames. The analysis was modelled in a series of linear steps, the stiffness matrix of the structure being updated at each step to take account of the effect of the change in value of the joint rigidity factors as the joints were deformed. Kermani used a single bay ridge portal frame timber structure and got a good comparison between the experimental results and the model. It was also shown that including for semi-rigidity in the joints had a very significant effect on structure behaviour. It was shown that if an assumed pinned apex joint possessed only 5% rigidity, the total deflection of the eaves and apex joints and also the magnitude of the moments induced at the eaves joints would decrease by 35%. At the other extreme, if an assumed fully rigid apex joint possessed only 50% rigidity instead of 100%, the total deflections at eaves and apex and also moments induced at eaves joints would be increased by only 5%.

The semi-rigid behaviour of timber trusses has also been investigated. Brynildsen *et al* [142] studied the non-linear semi-rigid behaviour of W-braced trusses with plywood gusset nailed joints. A power function was used for the load-slip relationship and because a flexibility coefficient approach rather than stiffness approach was to be used, the joint slip was expressed in terms of the load, ie $\delta = a(\frac{P}{n})^b$, where n was the number of nails and a and b were constants of fit. The semi-rigidity of each joint was simulated by a spring, as had been proposed by Porteous [141], and analyses were done taking constant b equal to unity (ie a linear joint flexibility), as well as a non-linear case where b was 2.655. The non-linear analysis used the Perkins *et al* [179] moment relationship and a step-wise loading approach

similar to that used by Kermani [76]. From the results, Brynildsen *et al* concluded that semi-rigid joint behaviour affected the moment distribution through the truss as well its deflection and the results compared favourably with the results of full scale tests. Also, it was found that linear flexibility in the joints up to the design load condition (ie a loading equivalent to the serviceability limit state load) gave results comparable with the non-linear analysis. It was concluded that the assumption of linear flexibility in joint behaviour up to the serviceability limit state load would be acceptable for design purposes.

Reardon [180] also investigated the semi-rigid behaviour of W-braced trusses including for the secondary effects of axial loads on member behaviour, but only considered the joints to be linearly semi-rigid. The effect of the gusset plates was included for by assuming they were inflexible elements between the adjacent semi-rigid joints. The results from the analysis compared well with the results of full scale tests and demonstrated that by assuming rigid rather than semi-rigid joint behaviour, deflections were underestimated by at least 25%, axial load effects were small and moments could increase by 10%. These results have been interpreted to apply only to the serviceability limit state condition.

2.7 SUMMARY

From the literature review it is clear that the behaviour and method of analysis of nailed joints is a function of many factors. Joint strength and stiffness will be influenced by the properties of the materials used and by the method of assembly of the joint. Results from the mathematical modelling of a structure using such joints will be influenced by how the joints are modelled and the method of structural analysis adopted. Taking account of the findings from the literature review, the major factors that will be included for in the research are summarised in the following paragraphs.

From the research joint strength has consistently been shown to be linearly related to the density of the timber in the joint. Although alternative timber species can be included for in the programme, by accepting this relationship the research can be progressed using only a single species of timber. As this will allow more of the research resource to be allocated to those factors that are known to have a variable effect on joint behaviour, the programme has been taken forward on this basis.

Moisture content of the timber has been shown to greatly influence material properties and the programme will be progressed such that the moisture content will be controlled or its effect will be taken into account in the modelling work. The most common environment used for the design of timber structures is the service class 1 condition, requiring that the average moisture content in most softwoods will not exceed 12% [11]. The objective will be to store the timber in a stable environment to try and achieve this condition and to develop a strength factor for the effect of change in moisture content where the variation is considered to be excessive.

The effect of nail diameter on joint strength has been shown to be a power function of the diameter but there is no consistency in the value of the power coefficient to be used. This factor will be investigated using 2.65mm 3.00mm and 3.35mm nominal diameter round wire nails. These nail sizes were used to suit the timber size available and to be able to correlate with the results of investigations by other researchers.

Nail strength is a key factor in the ultimate strength approach to joint behaviour and is also used in the finite element method. In the elastic method it is not required because of the limited joint displacements allowed. With the empirical approach, which generally involves the joint being displaced close to the ultimate limit state, only Mack [6] has made reference to it as a possible factor. Because of its significance in the ultimate strength approach and because the testing programme will test joints beyond the ultimate limit state load, this factor will be included for in the research programme.

The literature review has shown that the effect of varying the numbers of rows of nails in a joint was mixed but generally there was a reduction when more than three or four rows were used. There has however been little published research into the effect of varying the row spacing. Because this is considered to be an important factor, row spacing as well as row number effect will be included for in the programme.

The majority of the research work has been done using predrilled holes in the timber, primarily because this had been required to be able to drive the nail. As the density in the timber used in the programme will exceed 500kg/m^3, the limit set for predrilling in EC5 [15], all of the timber joints will be predrilled. Joint friction arising from the assembly process has a significant influence on joint strength and stiffness but the effect is variable. Because the force will be lost if shrinkage takes place in the joint, EC5 [11] ignores it and only includes for the nail tension effect. The factor is however considered to be significant and the programme will investigate the behaviour of joints with and without friction on assembly.

There are four main methods for modelling the behaviour of nailed joints. The elastic method is very restrictive in its application and as such is not suitable to meet the objectives of the programme. The ultimate load approach is appealing because of the direct link with EC5. However, as it will not provide information on the semi-rigid behaviour of a joint or establish a secant stiffness relationship that could be used for the assessment of joint slip, it is also considered to be unsuitable. The finite element method could be used but to achieve a satisfactory FE model considerable effort would be required to determine the elastic and plastic orthotropic properties of the materials and there would still be no guarantee of achieving accurate results. By a process of elimination it is concluded that the empirical method is the most appropriate analysis method to be used. It will envelope all of the design states up to the characteristic load; provides a stiffness relationship at all states of slip; will establish a relationship that can be developed to model moment behaviour and will allow the semi-rigid properties of the joint to be determined.

Semi-rigidity in joint behaviour has also been shown to significantly influence the stiffness and moment distribution behaviour of a structure. The semi-rigid behaviour of nailed joints will be investigated together with the joint fixity factor and the level of moment reduction to be expected from this type of joint. The secant rotational stiffness coefficient will also be investigated to classify the joint behaviour. Guidance will be given on the type of analysis that should be used with structures that incorporate nailed joints and include for this effect.

The research will also incorporate other factors not covered by the issues identified in the literature review and these will be explained when they arise in subsequent chapters.

3. MULTI-NAILED TIMBER JOINTS – LATERALLY LOADED SHEAR AND MOMENT TESTS

3.1 INTRODUCTION

The majority of published research into the behaviour of timber joints subjected to lateral loading using nails as the connector has been based on the use of single nails acting in single or double shear [6, 7, 8, 9]. The capacity of joints with multi-nails has been obtained by multiplying the single nail result by the number of nails in the joint. Indeed the current issue of BS5268 [10] "The Structural Use of Timber", is based on such an approach provided the number of nails in a line acting parallel to the line of the shear force on the joint is less than 10. Where the number of nails in the line is equal to or greater than 10, a reduction factor of 0.9 is applied. Also, in the current issue of EC5- "Design of Timber Structures" [11], providing minimum spacing criteria is met, the multi-nail joint capacity is determined by multiplying the single nail result by the number of nails in the joint.

From the literature review the performance of multi-nail joints with variations in connection configuration using overlapping nails, and in particular fully overlapping nails, does not appear to have been investigated to any depth in published data. This research programme has been structured to investigate the significant factors that influence the strength and stiffness behaviour of multi-nailed joints that use fully overlapping nails through the serviceability and ultimate limit states and up to failure of the joint.

The only published research into the use of fully overlapping nails appears to have been carried out at Napier University by Goh [12] who focussed on the effect of multi-nailed joints with nailing patterns of varying nail density. However, the work was based on the use of a 33.3mm module for nail spacing configurations and did not address minimum spacing criteria. From a review of the research it was decided that the investigation needed to be revisited and restructured using an approach that would systematically address the key factors affecting the strength and stiffness of such multi-nailed joints. In particular to include for the effects of variation in nail spacing and incorporate code recommendations for minimum spacing and distance criteria.

In line with international practice, all of the U.K. codes used for the design of the leading structural materials i.e. steel, concrete, geotechnics *et al*, [58,59,60], are based on a limit state design philosophy and rather than use BS 5268 [10], which is based on a permissible stress approach [61], it was decided that the limit state EC5 [11] code would be used as the reference document for the research programme.

During the research programme EC5 [11] has been revised and issued in draft form on three occasions [13, 14, 15] and it interesting to note that in these revisions the code has recognised that, among other factors, nail spacing is a significant factor in the design of multi-nail joints.

3.2 OVERLAPPING NAILS

In EC5 [11] a limitation is placed on the use of overlapping nails in that for a three member joint, if the distance (t_2 - l) as shown in Figure 3.1 is greater than four times the nail diameter, nails without predrilled holes driven from each side of the joint are allowed to overlap in the central member.

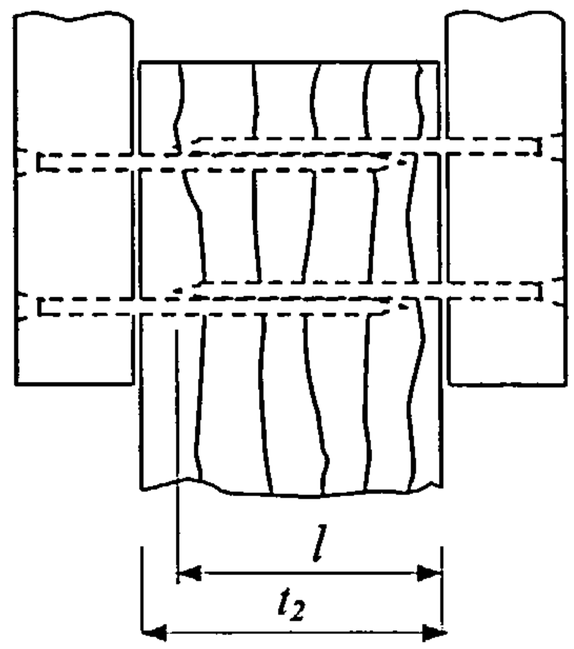

Figure 3.1 Overlapping Nails

The code limitation is ambiguous in regard to its application to joints which use overlapping nails with pre-drilled holes. As this research programme is based on the investigation of joints using nails which overlap for the full thickness of the central member in three member joints and used predrilled holes, the matter was referred to the EC5 drafting committee for clarification. After consideration, the drafting committee confirmed that providing predrilling was used, the code rules would apply to the use of nails overlapping for the full thickness of the central member. To distinguish nails formed in this manner from the overlapping nail definition used in the code, in this research such a configuration is referred to fully overlapping nails.

The splitting of timber members in a joint is related to the dimensions of the timber; the nail size; the locations of the nails in the timber and their positions relative to each other. Ehlbeck [16] states that splitting can be reduced or even eliminated by effective predrilling. However, as the maximum diameter of the predrill must be less than the nail diameter to ensure a fixing is achieved, the process of driving a nail into a predrilled hole must always set up splitting forces, however small, and these forces will be magnified when overlapping nails are used.

The magnitude of the splitting force when using overlapping nails in timber will vary depending on the direction of the nail overlap relative to the grain direction. Driving a nail into timber imposes stresses in the timber and the stress resultant (F) at right angles to the direction of the grain in the vicinity of the nail will tend to cause the timber to split along the grain direction. When a second nail is driven to overlap with the first, this imposes another set of splitting stresses. If the nails overlap in line with the grain direction the splitting force in the timber will be effectively doubled. If, however, they overlap at right angles to the grain direction, effectively overlapping adjacent growth rings, the splitting force will

be comparable to that set up by the single nail. This is shown diagrammatically in Figures 3.2A and 3.2B.

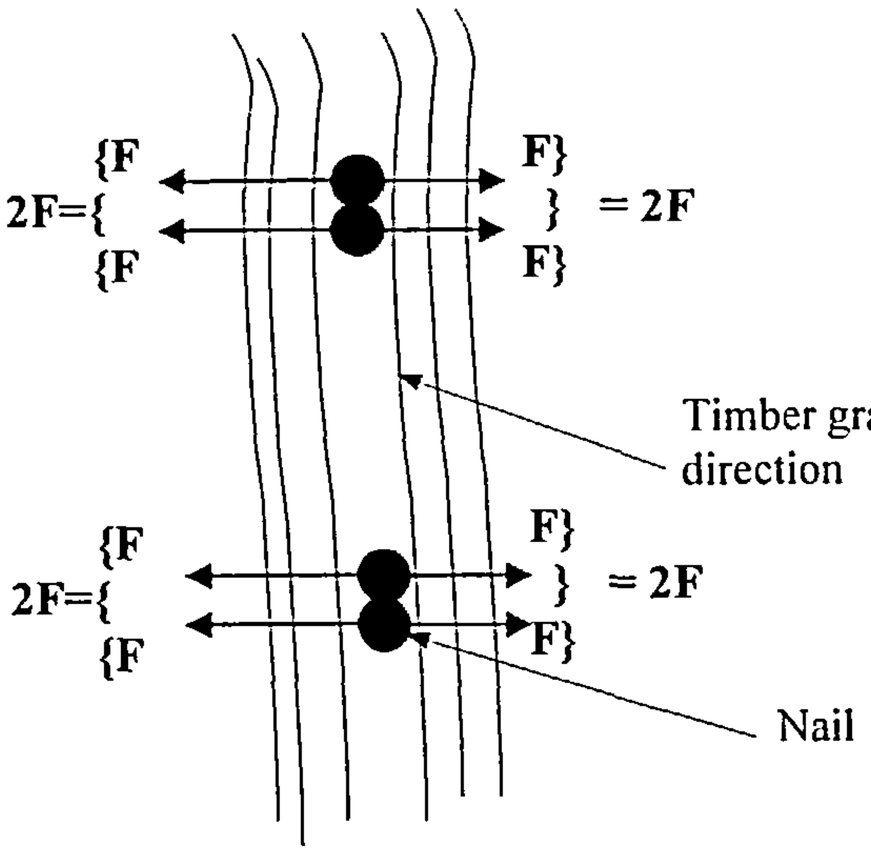

Figure 3.2A
Nails overlapping along the direction of the grain

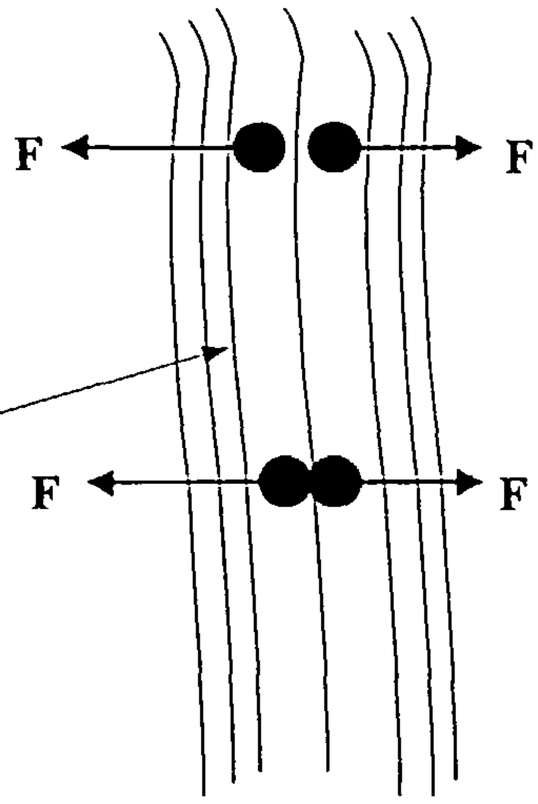

Figure 3.2B
Nails overlapping at right angles to the direction of the grain

The absolute value of the stress resultant will depend on the depth of penetration of each nail into the timber and on the spacing of the overlapping nails. The greatest force will arise when the nails are driven to overlap the full depth of the central member and the nail spacing is reduced to that distance at which the splitting resistance of the timber reaches its failure limit.

In Table 6.3.1.2 of EC5 [11] minimum nail spacing and distances are given for nails driven into timber with and without the use of predrilling. And as no reference is made in the code to any special conditions applying when overlapping nails are used, the criteria are also valid for overlapping nails. Based on the acceptance of fully overlapping nails by the code drafting committee, the testing programme was commenced on the understanding that the criteria would equally apply to the use of fully overlapping nails. The minimum recommendations given for use with predrilled holes were used to establish the nail spacing and distances for the steel gusset plate joint configurations, which was the first type of joint to be tested.

3.3 QUALITY CONTROL PROGRAMME

Prior to the commencement of the experimental programme, to standardise and control the testing activities, procedures were prepared for material selection; the test referencing system to be used and the test protocols to be followed. These were compiled into a quality control document providing the procedures and requirements to be followed throughout the testing period and are included under Appendix A.

3.4 EXPERIMENTAL PROGRAMME

3.4.1. General

The experimental programme was designed to examine the effects of nail diameter; nail strength; nail spacing; number of nails; joints with and without a gap between the gusset plates and the timber and the use of different gusset plate materials on joint strength and stiffness.

The joints comprised a timber member between either two steel or plywood gusset plates, connected by fully overlapping nails and were subjected to short duration direct shear or moment loading. The thickness of the gusset plates were:

i) 6 mm thick mild steel plate,
ii) 19 mm thick plywood
iii) 12 mm thick plywood
iv) 9 mm thick plywood

The joint configurations for the shear tests were in general based on the use of two lines of fully overlapping nails with varying numbers of rows of nails at different nail spacing. For the moment tests the joint configurations were based on nail patterns that used varying grid spacing, generally within a 100mm square grid but with variations outside the grid when using joints with plywood gussets.

When the testing programme was commenced no guidance was given in EC5 [11] or BS5268 Part 2 [10] as to the maximum tolerance permitted when forming predrilled holes in steel gussets and the criteria adopted was to select a size of predrill that would just allow the free fit of the nail point through the predrilled hole. During the early stage of the testing programme the first draft revision of EC5 was issued [13] requiring that steel gussets be predrilled using drills not greater than 1.1 times the nail diameter and the programme was changed to conform with the new criteria. The plywood and timber were predrilled using drill sizes in accordance with the requirements of EC5 [11].

Because of the number of tests to be undertaken, to minimise the effort and time required to prepare test samples, considerable thought was given to the joint set-up. In Goh's test set-up [12] for joints subjected to shear forces a bolt and packing detail had been fitted at the base of the joint. This was presumed to have been used to prevent gusset plate spread during testing and to improve the lateral stability of the joint. But it added considerable additional effort to the assembly process and required all plywood gussets to be predrilled.

To investigate the need for this detail a programme of preliminary tests was undertaken on joint configurations with and without a bolt fixing to compare behaviour. It was found that there was no tendency towards gusset plate spread or lateral instability in any of the tests and as there was also no

significant difference in the strength and the stiffness behaviour of the joints between the two set-ups, the testing programme was progressed without the use of packing pieces and bolts.

To reduce friction pick-up in the joint and obtain lower bound results from the tests, metal spacers were placed between the timber and the gusset plates when the joint was being assembled to form a gap. These were removed on the completion of the joint. Thicknesses of spacers ranging from 0.23mm to 0.8mm have been used by researchers [6, 7, 17, 20] and for this programme, taking account of the more limited shrinkage expected in joints in the United Kingdom, 0.2mm spacers were adopted. Tests were also carried out using joints assembled without the use of spacers.

3.4.2. Materials

The timber was cut from dressed British grown Douglas Fir, approximately 155mm by 45 mm solid planks. It was obtained from a local supplier and had been visually stress graded SS with a strength class of C18 in accordance with BS 4978 [182] under the TRADA quality assurance system.

The plywood was 19 mm thick 7-ply, 12 mm thick 5-ply and 9 mm thick 5-ply sheathing plywood formed using tropical hardwoods and dressed to nominal thicknesses of approximately 17 mm, 10 mm and 7mm respectively. It was imported from Indonesia and complied with the requirements of BSEN 314 [21] and BSEN 315 [22].

The joint connectors were 2.65, 3.00 and 3.35 mm nominal diameter common wire nails. They were plain shank, flat head and medium diamond point round bright wire nails in accordance with BS1202: Part1 1974 [23]. At the start of the programme nails manufactured by Rynail were used, however, because of the extent of testing, additional nails had to be obtained and only nails manufactured by Castlenail could be sourced. To limit the degree of variability in the programme the Rynail nails were used for the timber/steel gusset plate joint tests and Castlenail nails were used for the timber/plywood gusset plate tests. The nominal nails sizes used were:

2.65 mm diameter × 50mm long.
2.65 mm diameter × 60mm long.
3.00 mm diameter × 50mm long.
3.00 mm diameter × 60mm long.
3.35 mm diameter × 50mm long.
3.35 mm diameter × 60mm long.

The nails were checked for variations in diameter and length and it was found that the quality control of the length of the 2.65mm diameter Rynail nails was extremely poor and well outside the BS 1202 [23] requirement of ± 0.8mm. To maintain a control these nails were selected using a digital calliper. The

remaining 3.00 and 3.35mm diameter Rynail nails and all sizes of the Castlenail nails were within the code length criteria.

The nails were also checked for variation in diameter and both manufacturers were within the tolerance limit of ± 0.05 mm. In the analyses of all tests the actual nail sizes rather than the nominal sizes have been used and from control checks the average actual diameter of each nail size from each manufacturer was as given in Table 3.2.

Nominal Diameter (mm)	Rynail nails actual diameter (mm)	Castlenail nails actual diameter (mm)
2.65	2.66	2.66
3.00	3.01	3.01
3.35	3.36	3.33

Table 3.2 Nail supplier and nail diameters used in programme

The mild steel for the steel gusset plates was 6mm thick, Grade 43A, in accordance with BS EN 10 025 [24].

3.4.3. Test Sample and Assembly Procedure

A typical joint configuration used for the shear and the moment tests is shown in Figures 3.3 and 3.4 respectively.

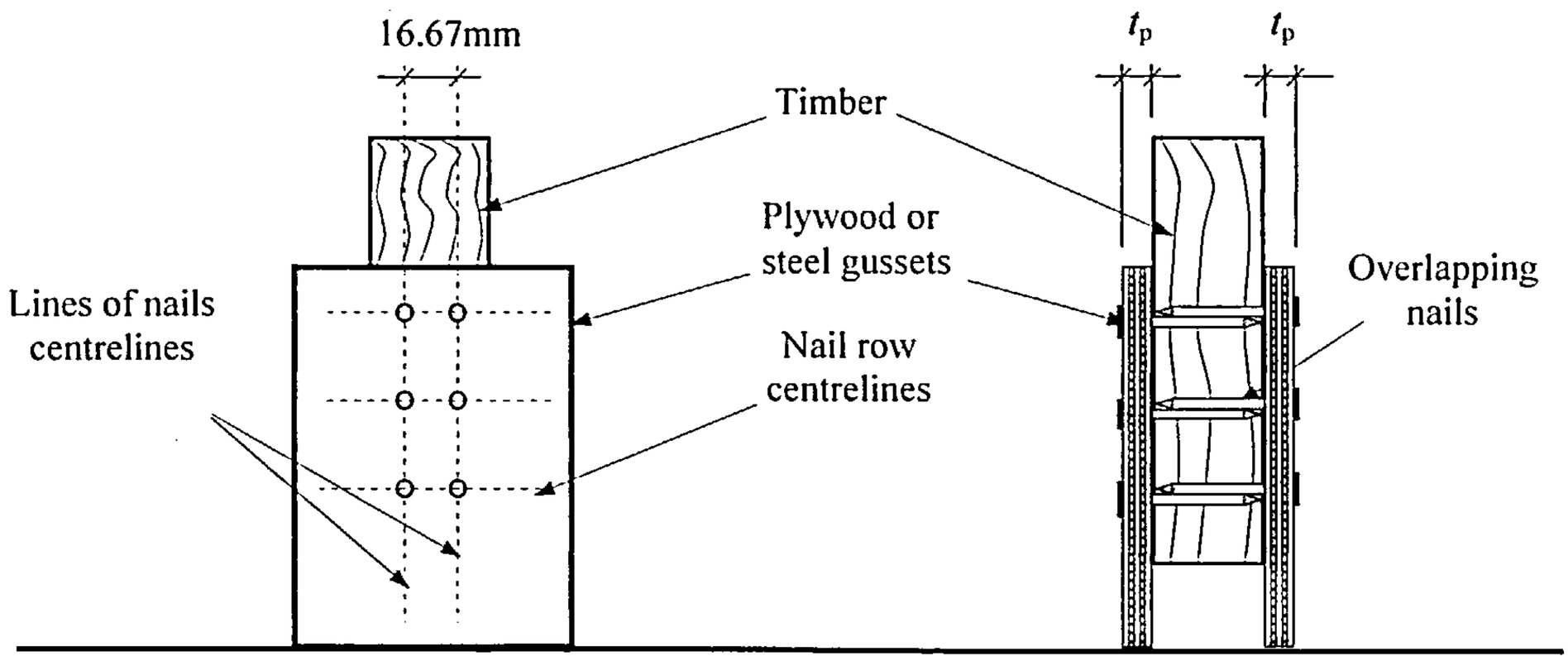

Figure 3.3 Typical shear joint configuration.

For the shear test joints the gusset plates were 125mm wide and varied in length to suit the number and spacing of rows of nails being used. The steel gusset plates ranged from 240mm up to 450mm long and

to minimise the overall number of plates required, the same plates were used for each of the five tests that were carried out for each joint configuration. They were also used for other spacing configurations tests. This meant that predrilled holes in steel gusset plates could be reused for at least 10 tests and in some cases up to 20 tests. The plywood gusset plates ranged from 145mm to 520mm in length and were predrilled using the same size of drill as was used for predrilling the timber in the joint. New plywood plates were used for each test. Tests were carried out using the three thicknesses of plywood.

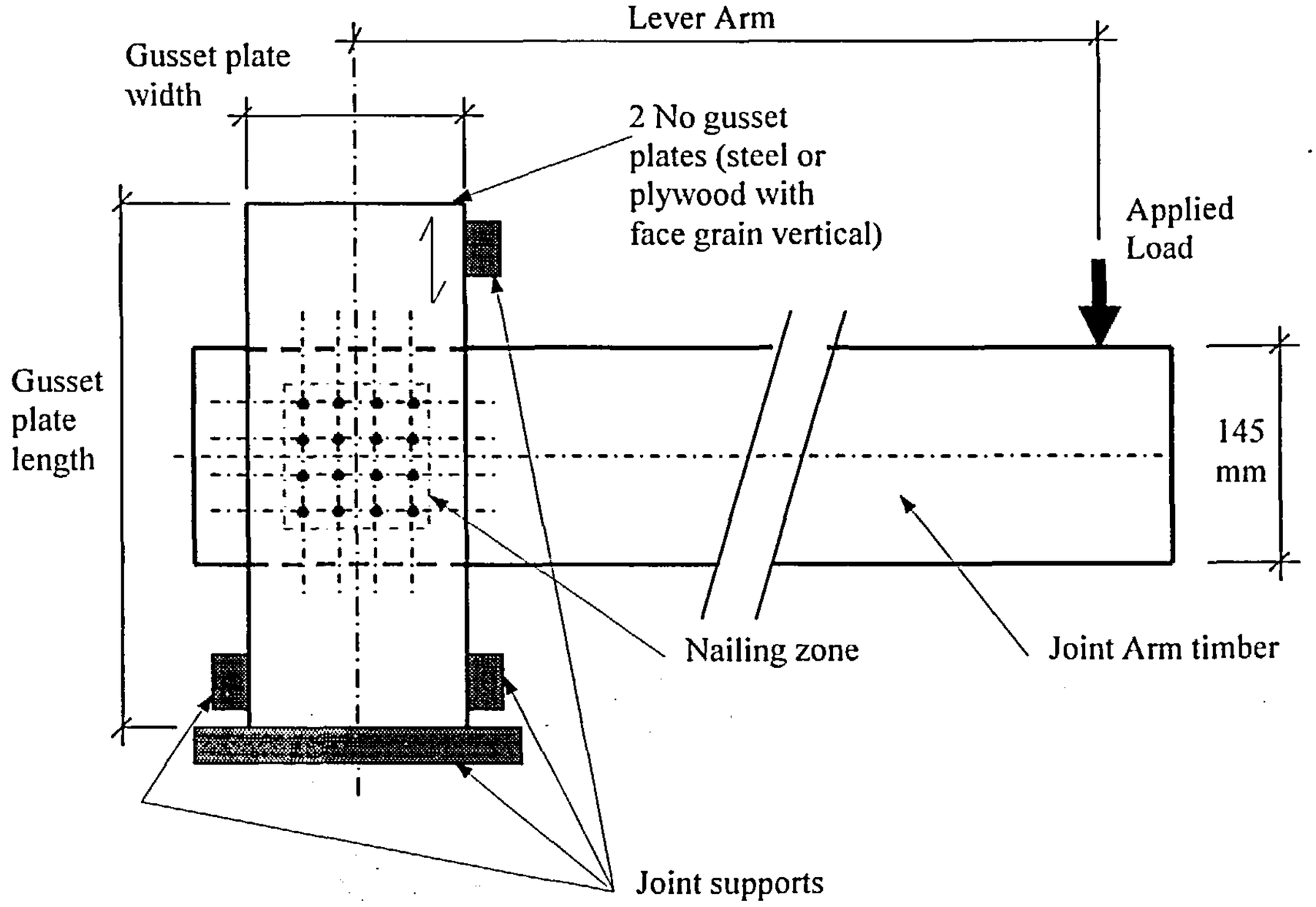

Figure 3.4 Typical moment joint configuration

For the moment tests the plywood gusset plates were all 400mm long and ranged in width from 150mm to 305mm to suit the joint configuration and again the three thicknesses of plywood were used. For the steel gusset plate moment tests only plates 400mm long by 140mm. wide were used.

Five tests were generally used to form a test set for each shear joint configuration. To minimise variations in the properties of the timber (and plywood) within a set, each test set was assembled using timber taken from the same plank and plywood taken from the same plywood sheet. For the moment tests the approach was to treat each test as a stand alone result, although average test results were also used, and the material selection and assembly procedure followed the framework used for the shear joints.

The material for each test was visually inspected and the selection criteria was that only timber that did not exhibit cracks, fissures, knots, fungal decay, excessive width of annual growth rings, resin pockets

and grain defects (including excessive grain slope) was used. For plywood only material with no visual defects (including missing areas of ply and plywood with wood filler used in the facing plies) was acceptable. Although dressed timber had been ordered, the smoothness of the plank faces varied significantly and to achieve a consistent standard of surface condition, the faces which mated with the gusset plates were lightly sanded in the power sander before joint assembly.

All of the timber and plywood was stored in the same area for a period in excess of twelve months prior to the commencement of testing and the environmental conditions in the area maintained the moisture content (m.c.) of the timber in the range 11% to 15.5% over the testing period for the timber/steel gusset joints and 12.5% to 14% over the testing period of the timber/plywood gusset joints. The moisture content readings of the plywood were consistently lower and ranged between 7.5% and 10.00%. This was due to the effect of the mass of the resin bonding. The moisture content of the timber ply in the plywood sheets was effectively the same as the moisture content of the timber. The materials were generally cut by the in-house technician staff the day the samples were to be tested. Joints were assembled in the testing laboratory at normal room temperature and tested within 10 minutes of fabrication. Moisture content checks taken immediately after testing confirmed that there had been negligible change from the mc of the materials at the time of assembly.

To minimise the risk of inaccuracies in assembly and to maintain a high level of consistency and quality control in the assembly procedure, the joints were fabricated using jigs. The jig set up to control the assembly of the moment joints with a partially assembled sample using steel gusset plates is shown in Figures 3.5.

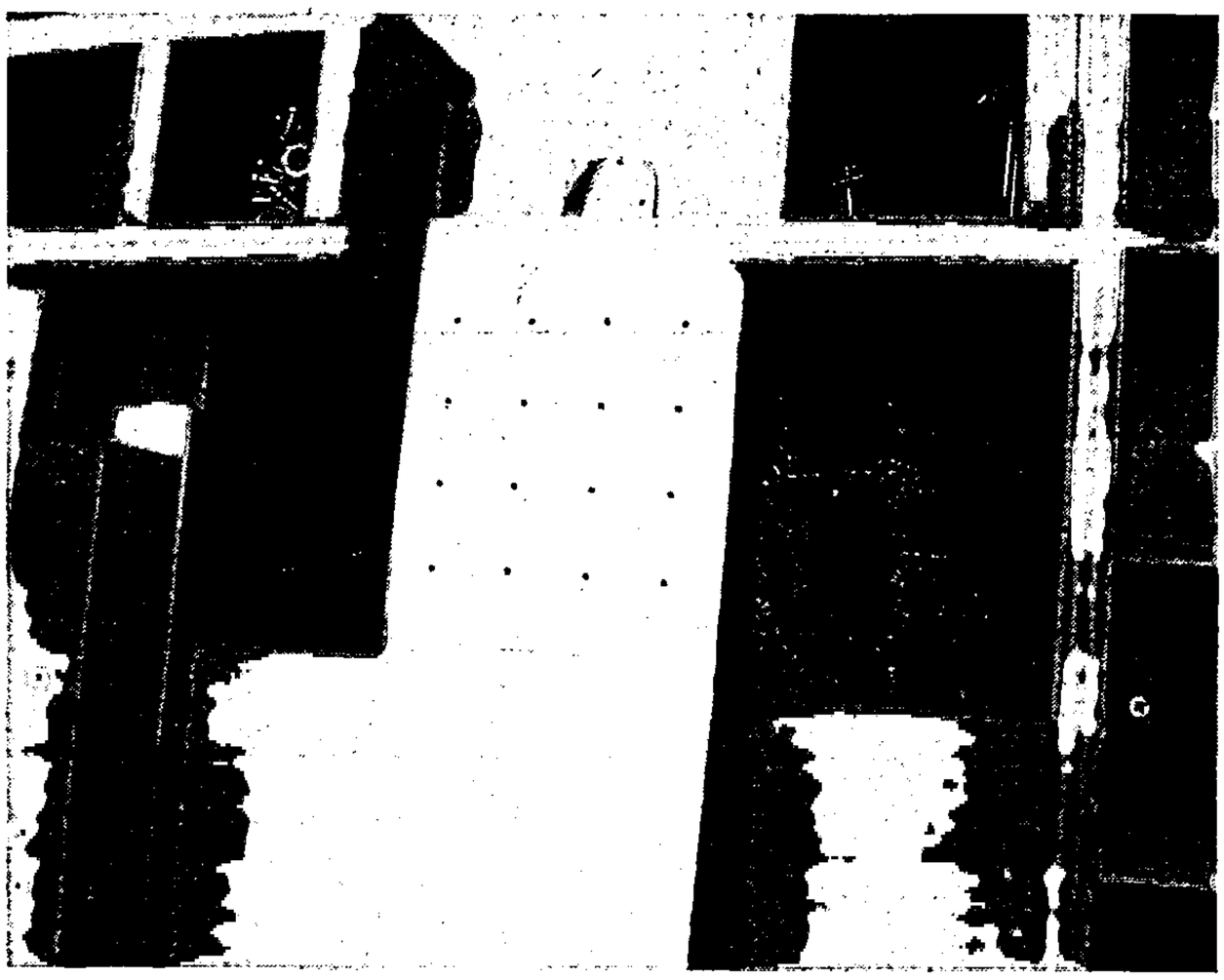

Figure 3.5 Jig for the assembly of moment joints

The joint assemblies complied with the principles set out in BS EN 1380:1999 "Timber structures-Test methods-Load bearing nailed joints" [26], but using fully overlapping rather than single nails for the connections. They also complied with the requirements of BS EN 26891 – "Timber Structures – Joints made with Mechanical Fasteners-General Principles for the Strength and Deformation Characteristics" [27] and with the guidance given in Section 8 of BS 5268 [10].

Moisture content tests were carried out in accordance with BS EN 322: 1993 "Wood-based panels – Determination of moisture content" [28] and material density was determined in accordance with ISO 3131:1975, "Wood – Determination of density for physical and mechanical tests" [29] and BS EN 323:1993 "Wood–based panels – Determination of density" [30].

The results of the above tests are given in Appendix B together with the results of additional tests that were required to provide data for analyses purposes.

3.4.4 Shear Test Joint Programme

3.4.4.1 Factors Investigated

A structured testing programme was set up to investigate those factors that were considered to be significant and could affect joint behaviour. The factors investigated were:

The effect of the direction of the nail overlap
The effect of the number of lines of nails in a joint
The effect of the lateral spacing of the nail lines
The effect of the predrill size used for the steel gusset plates
The effect of the nail diameter
The effect of the nail strength
The effect of the row spacing
The effect of the number of nails in the joint
The effect of the moisture content of the timber/plywood
The effect of the gusset plate material
The effect of a gap between the timber and the gusset plates

The experimental investigation into the above factors is discussed in the following paragraphs.

The effect of nail force relative to the grain direction of the timber was not included in the programme. This was because the results of testing by other researchers [16, 42] and codified recommendations [10, 11] have concluded that the difference in strength and stiffness for loading parallel and perpendicular to the grain is negligible when using nail connectors and can be ignored. Testing was based solely on set-ups where the joint loading was parallel to the direction of the timber grain in the joint. Tests were

however carried out using plywood gusset plates loaded along the direction of and at right angles to the face grain to confirm that plywood gusset plate grain direction was also a negligible factor. Apart from these tests, in all other test set-ups investigating the joint factors where plywood gusset plates were used, the face grain of the plywood always aligned with the direction of loading.

To investigate nail spacing effects, a 16.67mm spacing module was selected with the freedom to deviate from it to suit maximum and minimum spacing criteria. The joint nailing configurations and the associated joint reference used for the shear tests are shown in Appendix C and the number of pairs of fully overlapping nails used in each joint is given in brackets. An extensive range of nailing configurations was required to address all of the factors investigated. The number of nails used in the shear joints varied from a minimum of 4 (2 pairs of overlapping nails) to a maximum of 32 (16 pairs of overlapping nails).

The testing programme was commenced by investigating the effect of the direction of alignment of the nail overlap relative to the direction of the grain in the central timber member. The objective of these tests was to demonstrate that when using nails which fully overlapped, the direction of the alignment of the nail overlap relative to the grain direction would affect the internal forces set up in the joint. From these tests the alignment that imposed the greatest internal stress could be identified and used throughout the testing programme. This was investigated by using two sets of joints of the same configuration. In one set the nails overlapped in predrilled holes which aligned along the timber grain direction and in the other the predrilled holes were aligned at right angles to the timber grain direction. These formed the extreme positions and bound the intermediate alignments. The joints were assembled using steel gusset plates with two lines and two or more rows of overlapping nails and with nail spacing and timber end distances set at the minimum values given in Table 6.3.1.2 of EC5 [11].

Joints assembled with the nails overlapping along the direction of the timber grain either caused the timber to completely split or to show signs of splitting at the nail positions. Those with the nails overlapping at right angles to the grain direction did not split the timber and there were no visible signs of even small splits at the nail positions. These simple tests confirmed the expected behaviour as outlined in Figure 3.2. For the remainder of the programme only nails that overlapped in line with the direction of the grain in the timber were used.

The effect of the number of lines of nails was then studied to determine if this was a variable factor in joint behaviour. From tests on joints made with increasing numbers of lines of fully overlapping nails it was concluded that joint strength and stiffness were linear functions of the number of lines of nails in the joint. To minimise resources it was decided to adopt joints made with only two lines of nails at right angles to the grain direction as the testing module for the shear test programme. The module would be able to be adjusted to suit the variations in nail number, nails size and nail spacing to be investigated and the capacity of joints with greater numbers of lines would be obtained by multiplying the single line result by the number of lines in the joint.

Nail line spacing effect was also investigated. Joint nailing configurations BA and CO (4 nails) and BK and CR (12 nails) were used and from an analysis of the test results it was concluded that lateral spacing had no effect on strength and stiffness. From these tests a line spacing of 16.67mm was selected for the two line joints as the minimum practical spacing that would provide a stable framework for the multi-row joints to be investigated in the shear test programme.

Having established the direction of nail overlapping to be used for the test programme and that only two lines of nails would be used to form the basic joint module for all shear joints, the shear testing programme was able to be started.

The shear testing programme commenced using joints formed with steel gusset plates and connected by 2.65mm diameter fully overlapping nails. As no guidance was given in EC5 [11] or BS5262 Part 2 [10] on the maximum tolerance permitted in the predrilled holes in the steel gusset plates, the size of drill to be used was the one that would just allow a free fit of the point-side of the nail. A 3.2mm diameter drill was selected. During the early stage of the testing programme the first draft revision of EC5 was issued [13] requiring that thick steel gussets plates (i.e. steel plates with a thickness $\geq$ the nail diameter) had to be predrilled using drills with a hole tolerance less than 0.1 times the nail diameter. The drill size used in the testing programme was changed to a 2.8mm diameter drill for the 2.65mm diameter nails and 3.2mm and 3.5mm diameter drills were selected for the 3.00mm and 3.35mm diameter nails. The results of the tests using 2.65mm diameter nails with the gusset plates predrilled using 2.8mm and 3.2mm drills have however been compared to investigate the effect of predrill size in steel gusset plates on joint strength and stiffness behaviour.

For joints with steel gusset plates, only Rynail nails were used and for joints with plywood gusset plates, only Castlenail nails were used and to investigate the effect of the nail strength on joint strength and stiffness behaviour, strength tests were carried out on each of the manufacturer's three nail sizes.

Joints with multi-rows of nails were selected and tested using the three nail sizes. At the commencement of the programme the minimum nail spacing and distance criteria was that given in Table 6.3.1.2 of EC5 [11] but over the testing period the code was revised in draft form on three occasions and a summary of the relevant changes to the spacing and distance criteria is given in Table 3.3.

When the testing programme commenced the minimum spacing rule in Table 6.3.1.2 of EC5 [11] was that nail spacing parallel to the grain was 7 times the nail diameter and when steel gusset plates were used a spacing factor of 0.7 could also be applied giving a minimum spacing factor of 0.7×7×nail diameter (4.9×nail diameter). This was subsequently increased to 0.7×10×nail diameter and at the end of the testing programme it had reduced to 0.7×5×nail diameter (3.5×nail diameter).

Initially multi-row tests were formed using 2.65mm diameter nails with rows at 16.67mm centre to

centre and end distances in accordance with the requirements of Table 6.3.1.2. However when assembled on this basis the joints were failing either by splitting when they were being formed or at relatively low loads during the load test.

Spacing or distance	**Minimum distance using predrilled holes and based on nail diameter *d* being less than 6mm.**			
	EC5[11] Table 6.3.1.2	EC5[13] Table 8.2	EC5[14] Table 8.2	EC5[15] Table 8.2
Spacing // to grain	7*d*	7*d*	10*d*	5*d*
Spacing ⊥ to grain	4*d*	4*d*	4*d*	4*d*
Loaded end distance	12*d*	12*d*	12*d*	12*d*
Unloaded end distance	7*d*	7*d*	7*d*	7*d*
Loaded edge distance	7*d*	7*d*	7*d*	5*d*
Unloaded edge distance	3*d*	3*d*	3*d*	3*d*

Table 3.3 Revisions to table 8.2 in EC5

In EC5 [11] the load carrying capacity of a single fastener connection with dowel type connectors is based on yield theory, first described by Johansen [43], and subsequently validated by Larsen [45], Aune [44] and Hilson et al. [46]. The approach used is that failure occurs when the joint bedding material has reached its embedment strength and the connector has reached its yield strength resulting in the joint failing in a ductile mode. In this form of failure there is no sudden loss in joint strength or stiffness and the design rules for joint strength and stiffness in the code have been based on this premise. At failure the joint load is sustained as the joint continues to deform and the degree of ductility in the joint is the measure of the deformation in the joint at the ultimate deformation limit divided by the deformation at the elastic limit [62].

In the code the load carrying capacities of multi-connector joints are obtained by multiplying the capacity of the single connector by the number of effective connectors lying in the load direction. By complying with the minimum spacing and distance criteria and associated design rules in the code, ductile forms of joint failure should always occur. Failure in a brittle mode, such as splitting of the timber, with the consequent sudden loss of strength and stiffness is not addressed as, by compliance with the design rules, it should be prevented [47].

Despite the confirmation of the applicability of EC5 to joints formed with fully overlapping nails, this was not being supported by the brittle failure of the joints during assembly or when under test. It appeared that the minimum spacing and distance criteria in the code was based on the use of non-overlapping or overlapping nails but did not apply to the use of fully overlapping nails.

In earlier work it had been concluded that the use of fully overlapped nails aligned along the timber grain direction imposed up to two times the splitting force caused by a single nail. To take this increase in force into account it was decided that the end distances in the timber member in the joints should be increased to two times the minimum code requirement. From the earlier testing it had been concluded that lateral spacing of the nails was not a factor and the 16.67mm centre to centre minimum lateral spacing was retained. Testing using the 2.65mm diameter nails continued on this basis. For the subsequent joint tests using the 3.00mm and 3.35mm diameter nails the loaded and unloaded end distances for the timber were also based on two or more times the minimum distance criteria given in the code.

All three nails sizes were tested at two times the minimum code spacing in EC5 [15] and tests were also carried out at 16.67mm centre to centre with the 2.65mm and 3.00mm diameter nails. To address 'maximum' nail spacing effect, the row spacing was increased in increments to values which equalled and exceeded 4 times the minimum spacing value recommended in that code revision. The minimum, intermediate and maximum row spacing used in the tests with the three nail sizes are given in Table 3.4.

Nail diameter mm.	**Row spacing – mm.**							
2.65	16.67	19.00	25.00	33.33	38.00	50.00		
3.00	16.67	21.00	25.00	33.33	42.00	50.00	66.67	70.00
3.35	23.00	33.33	50.00	66.67	75.00	100.00		

Table 3.4 Nail spacing used with steel gusset plates

A similar testing programme was carried out on joints made with plywood gusset plates using 2 lines of overlapping nails at 16.67mm centre to centre. Row spacing was based on similar criteria to that adopted for joints with steel gussets but using the EC5 factor of 0.85 for plywood gusset plates. The minimum, intermediate and maximum row spacing used for these tests are given in Table 3.5.

As preliminary testing proved that the plywood was not susceptible to splitting, the loaded and unloaded end and edge distances for the plywood were sized to be greater than or equal to the minimum values recommended in EC5 [11]. The minimum distances used are given in Table 3.6.

Nail Diameter mm	Row spacing – mm			
2.65	23	33.33	50	66.67
3.00	26	33.33	66.67	75
3.35	28	50	66.67	83.3

Table 3.5 Nail spacing used with plywood gusset plates

From an analysis of the results of the testing programme, row spacing factors were developed for all nail sizes for steel gusset plate and plywood gusset plate joints.

Nail diameter mm	Minimum distance in the direction of load based on nail diameter d.	
	Loaded edge or end distance	Unloaded edge or end distance
2.65	7*d*	3*d*
3.00	7*d*	3*d*
3.35	7*d*	3*d*

Table 3.6 Minimum end and edge distances for plywood gusset plates

In both the steel gusset plate and plywood gusset plate joint tests the number of rows of nails was varied to investigate the effect. The numbers of rows used for each nail size with the steel gusset and plywood gusset joints are given in Table 3.7.

Nail diameter mm	Number of rows of fully overlapping nails with steel and plywood gusset plates					
2.65	Steel	1	2	3	4	5
	Plywood	1	3	4	5	7
3.00	Steel	1	3	4	5	6
	Plywood	1	3	4	5	7
3.35	Steel	1	3	4	5	7
	Plywood	1	3	4	5	6

Table 3.7 Numbers of rows of fully overlapping nails in joints with steel gusset plates and plywood gusset plates

Over the duration of the steel gusset plate joint tests the moisture content in the timber reduced from 15.5% to 11.00% and it was decided that the strength effect associated with this level of change should

be included for in the testing programme.

To investigate the effect a set of 8 tests using timber sections cut from contiguous pieces of a Douglas Fir plank was prepared and left in the timber store whilst an equivalent set of 8 timber pieces was stored in a laboratory area. Both sets were left for a period of seven weeks to allow the moisture content to stabilise. At the end of the period the samples in the timber store had an average moisture content of 14.32%. Those in the laboratory had an average moisture content of 10.14%. Joints were then assembled using nailing configuration CO and from the test results a relationship was developed between moisture content and joint strength.

In all of the above tests the joints were assembled with a gap between the timber and the gusset plates. To investigate friction effects, joints were also assembled with no gap between the timber and the gusset plates and a series of tests was carried out with joints using 2.65mm, 3.00mm and 3.35mm diameter nails, made with steel and with plywood gussets and using fully overlapping nails in varying nailing configurations.

To confirm that the direction of the face grain of the plywood gusset was not a factor that need be considered in the main testing programme, two sets of joints were tested using 19mm plywood gusset plates. One set had the face grain of the plywood parallel to the direction of loading and the other had the face grain at right angles to the loading direction. Both test sets used 3.35mm diameter nails and nailing configuration DB. From the average results the joints loaded perpendicular to the face grain were marginally stronger, by 2.9%, than those loaded parallel to the grain, and the coefficient of variation of the respective test sets were 0.015 and 0.094. The strength difference was considered to be within the margin of error to be expected in the testing programme and confirmed this was a factor that could be ignored in the programme.

3.4.4.2 Experimental Procedures

A typical set-up for the shear test joints is shown in Figure 3.6.

The joints were fitted with angle brackets for transducer readings. The transducers were strain gauge based and for joints formed using steel gusset plates, only transducers T1 were used. For joints with plywood gusset plates, transducers T1 and T2 were used. The transducers were linked to a data acquisition system, and details are given in Appendix D.

The brackets on the timber were secured in a position such that the transducer was reading the displacement of the timber just below the row of nails furthest from the testing machine loading head. This ensured the total displacement of the timber in the joint was being measured. The brackets fitted to the plywood gusset plates were located close to the joint base support to measure only the crushing in the bearing end of the plywood gussets, where they had been cut.

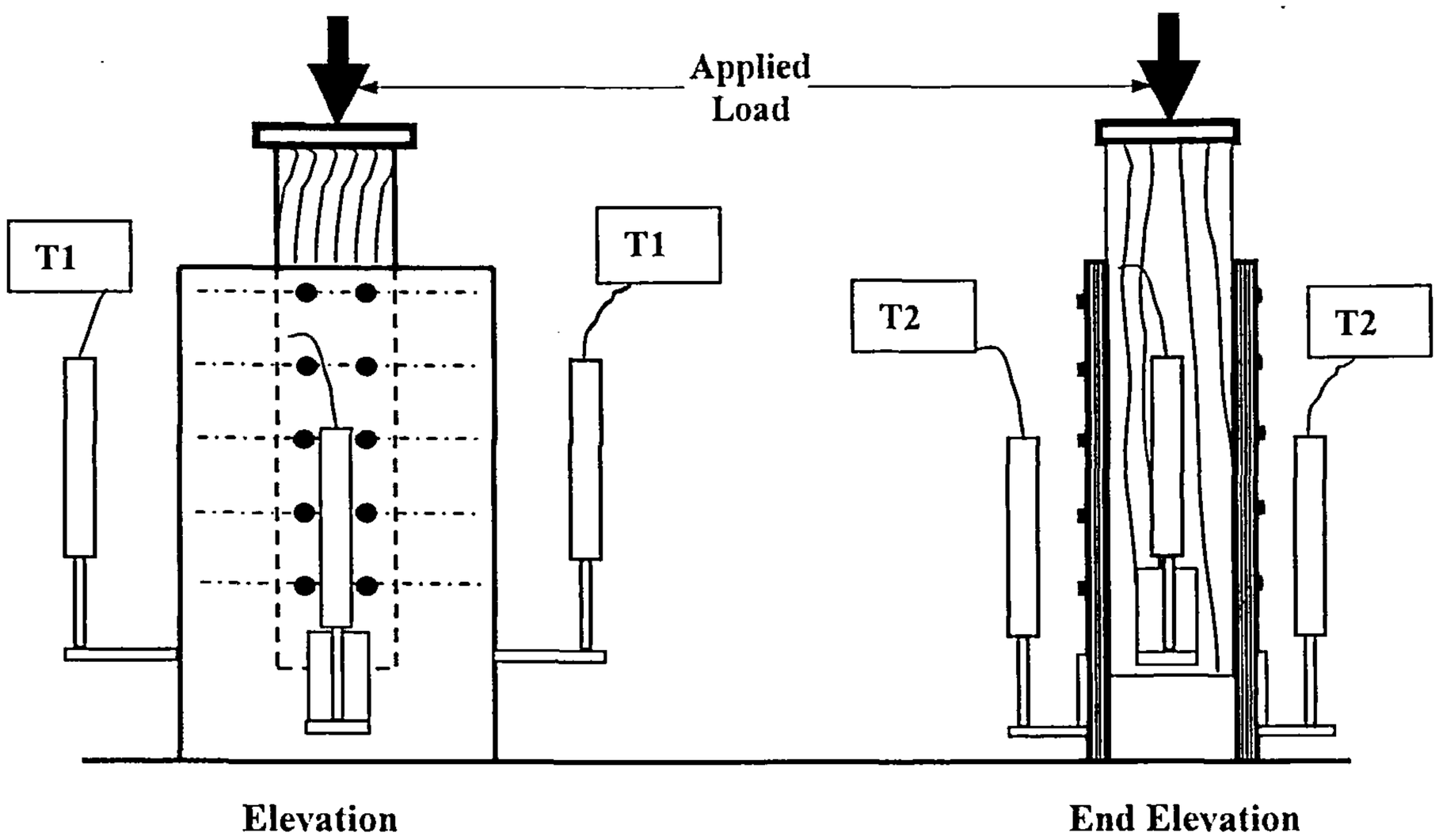

Figure 3.6 Typical shear test set-up

From preliminary tests it had been observed that the compression in the plywood gusset plates over the length of the joint was less than 0.1mm at maximum loading and it was considered this could be ignored. However the crushing effect at the bearing ends of the gussets where the plywood had been cut was in excess of 0.5mm under low loading and this order of movement had to be recorded and allowed for in the analysis. Also, to confirm that the test results were not sensitive to variations in the width of the plywood gussets, some tests were carried out using 44mm wide gusset plates rather than the 125mm width generally used in the programme. For the same nailing configuration it was found that the stiffness behaviour of these tests was almost exactly the same and it was concluded that the effect of the width of the gusset plate used in the tests could be ignored.

All tests were undertaken using a Schenck-Treblek RM Testing Machine fitted with a 50kN load cell which recorded the load on the joint. An example of a shear joint under test is shown in Figure 3.7.

The joint was centred in the rig and the transducers located so that respective pairs T1 and T2 (where used) were also at equal distances from the centre of the machine loading head. The machine load head was slowly lowered to make contact with a metal spreader block placed on top of the joint and any slight out of alignment between the loading head and the spreader block was taken up by inserting metal shims into the gap. Test loading complied in principle with the requirements of BS EN 26891 (1991) [27] and a monotonic loading profile as shown in Figure 3.8 was used.

Prior to commencing the testing programme, over 130 preliminary tests were undertaken on varying joint configurations to determine the rate of slip to be used and from an analysis of the slip rate of each test when the load was at 20% of the joint failure load, the average rate was found to be 0.34mm/minute. Incorporating the ± 25% variation allowed in BS EN 26891, a rate of slip of

0.4mm/minute was adopted as the rate to be used for all of the lateral load tests in the programme.

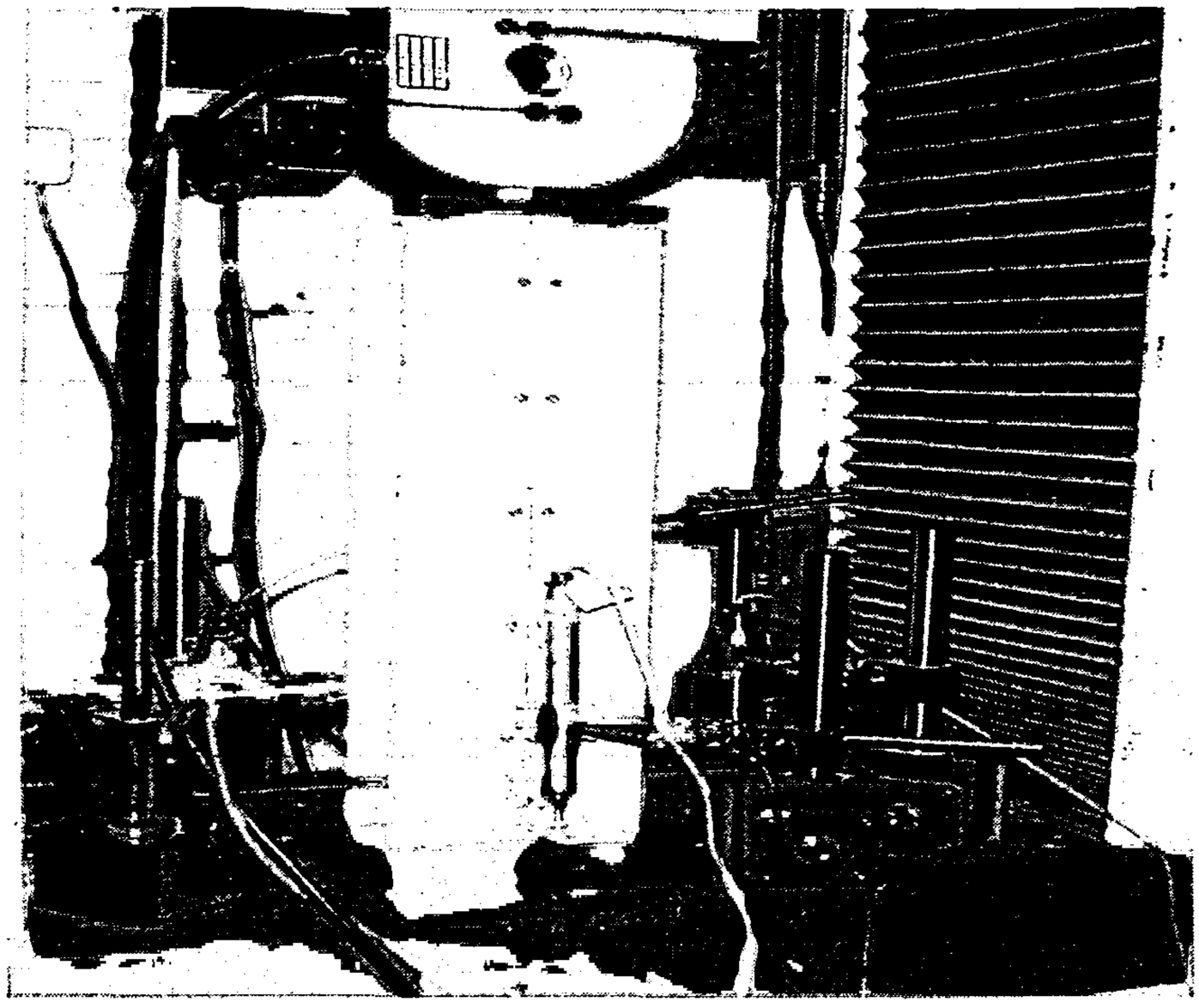

Figure 3.7 Test joint in shear

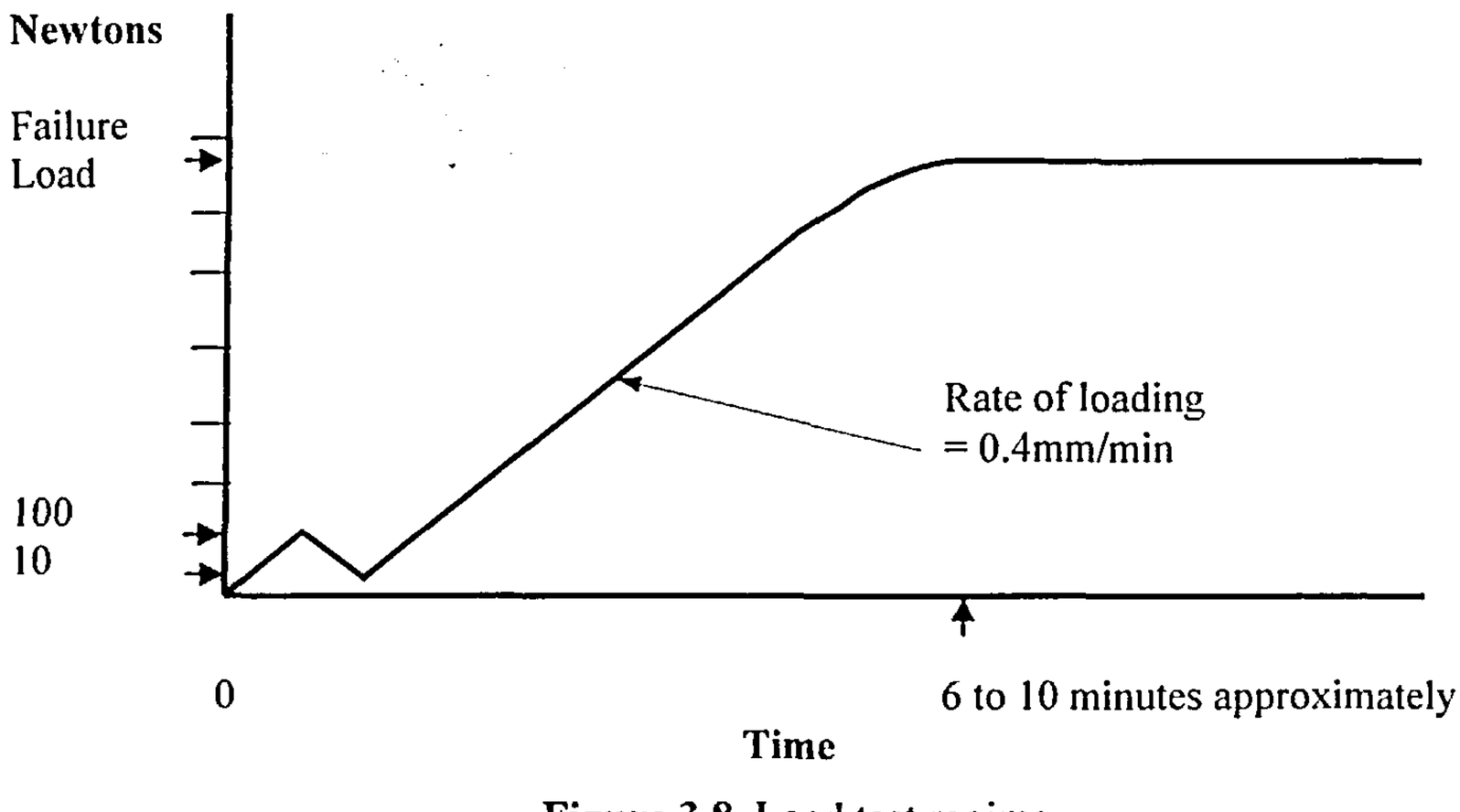

Figure 3.8 Load test regime

Using this rate of slip, the test load was applied up to 100N then reduced immediately at the same rate to 10N to bed the joint in. The joint was then reloaded at the same rate until the failure load was reached or until the joint slip was at least 4.5mm. As allowed in BS EN 26891, the preload cycle which would load the joint up to 40% of the estimated maximum failure load was omitted. Also, the periods of constant load were not incorporated as these were only relevant when using manually read dial gauges

as opposed to the high speed data logging devices used in the programme set-up [48].

The data from the load cell and transducers was collected using System 5000 [49], recording load and displacement values at one second intervals. The one second interval was selected as readings at quicker rates had been found to introduce spurious information which did not contribute to the accuracy of the processed results. Load and displacement data was collected on disc and downloaded to Microsoft Excel [50] for processing and subsequent analysis in conjunction with Mathcad 2001i [51] and Axum 6 [52].

In processing the data, the datum for load and displacement was taken as the start of the 10N reload cycle. Joint displacements were taken as the average of transducer readings T1 for joints with steel gusset plates and the average of (T1-T2) readings for joints with plywood gusset plates.

After each shear test the mode of failure was observed and recorded. Moisture content and density tests were then carried out using samples cut from the joint timber and the plywood gussets, where used.

3.4.5 Moment Test Programme

3.4.5.1 Factors Investigated

From the shear testing programme in section 3.4.4, semi-empirical relationships were developed for the load-displacement behaviour of multi-nail and single nail connections subjected to lateral loading. The objective of the moment testing programme was to investigate whether or not these relationships could be used to analyse the behaviour of joints formed with fully overlapping nails when subjected to a moment.

The extent of testing in the moment programme was considerably less than that used in the lateral load programme for two main reasons. Firstly, the main factors influencing joint behaviour using fully overlapping nails had already been addressed in the lateral load programme and as they were also applicable to the moment programme, did not have to be repeated. Secondly, to obtain sufficient data and achieve the required degree of confidence in the semi-empirical analysis of the lateral load programme, five tests had been used for each nailing configuration test set. This number of tests was not considered to be required in the moment testing programme. The main objective of the moment programme was to investigate whether or not the semi-empirical lateral load relationship could be applied to moment connections, not to develop a relationship from the results of the moment tests. In such circumstances it was considered that individual tests in addition to average results based on test sets could be used for comparison purposes.

The programme addressed:

The behaviour of joints made with steel and plywood gusset plates.
The behaviour of joints made with varying nail patterns.
The correction procedure required to convert vertical transducer readings to arc movements, taking account of the position of the transducers.
The effect of variation in the angle of the grain across the thickness of the timber sample.
The stiffness effect of gusset plates in multiple joint configurations.

Sections of planks were cut to the required length to suit the rig set-up used for testing and it was decided that a nailing grid of 33.33mm centre to centre would generally be adopted for the nailing configurations to be used. Some tests would be done using mixed patterns by varying the vertical and horizontal spacing and a summary of the nailing configurations used in the programme is given in Appendix C. The number of nails used in the moment joints varied from 4 to 70.

Because of the size and number of gusset plates required, for practical reasons the testing programme concentrated more on the use of plywood gusset plate joints rather than steel gusset plate joints. The steel gusset plate moment testing was primarily restricted to joints with nailing grid pattern RA, using 2.65mm, 3.00mm and 3.35mm diameter Rynail nails. For these joints the timber was selected such that the plane of the grain direction was more or less parallel with the face of the plank. For the plywood gusset plate moment tests, Castlenail nails were used and a variety of joint configurations were tested to investigate more fully the applicability of the lateral load formulae. Also, for these tests the timber was selected to be able to investigate the effect of variations in the plane of the grain direction across its width. All thicknesses of plywood were used and predrilling of the steel gusset plates and of the timber and plywood continued using the same drill sizes as had been used in the direct shear programme.

Although the direction of each nail force relative to the direction of the timber grain varies in a joint subjected to moment, there would still be a significant component of force acting along the grain direction and it was decided to continue to overlap the nails along the direction of the timber grain, as had been adopted in the lateral load testing programme.

In all of the joint set-ups the edge and end distances of the plywood equalled or exceeded the minimum distances given in Table 3.6. The edge distances for the timber also equalled or exceeded the minimum recommendations given in Table 3.3, with the end distance of the timber end closest to the joint being made equal to or greater than two times the recommended minimum loaded end distance.

The programme commenced using plywood gusset plate joints and a variety of joint configurations were used to investigate the applicability of the lateral load formula. The nail spacing used in the programme along the direction of the grain of the timber and at right angles to it is given in Table 3.8.

The numbers of rows of nails used in the joint configurations along the direction of the timber grain (vertical direction) and at right angles to it (horizontal direction) are given in Table 3.9.

Nail diameter mm	Nail spacing in the direction of the timber grain – V Nail spacing at right angles to the direction of the timber grain – H						
2.65	V	33.33	100	33.33	33.33	33.33	66.67
	H	33.3	33.33	50	133.33	200	200
3.00	V	33.33	16.67	16.67	66.67	33.33	
	H	33.33	33.33	200	200	50	
3.35	V	33.33	16.67	33.33			
	H	33.33	33.33	50			

Table 3.8 Nail spacing used with plywood gusset plate moment joints

For the steel gusset plate moment joints the nail spacing was restricted to 33.33mm centre to centre along and at right angles to the direction of the timber grain and in addition there was a variation where the spacing at right angles to the grain was increased to 100mm centre to centre.

Nail diameter mm	Number of rows of nails in the direction of the timber grain - N_V Number of rows of nails at right angles to the timber grain - N_H												
2.65	N_V	4	4	4	4	4	2	2					
	N_H	4	5	6	7	8	7	2					
3.00	N_V	4	4	4	4	7	7	6	3	1	7	4	5
	N_H	4	5	6	7	4	5	2	2	2	2	2	2
3.35	N_V	4	4	4	7	7							
	N_H	4	5	6	4	5							

Table 3.9 Number of rows and lines of nails with plywood gusset plate moment joints

In addition to single joint moment tests, combined moment joint configuration incorporating two joints assembled using 17mm thick plywood gussets plates with either 2.65mm diameter or 3.00mm diameter Castlenail nails, were also tested. The objective of these tests was to confirm that multiple joints would also be able to analysed using the single joint moment theory.

3.4.5.2 Experimental Procedures

Typical test set-ups for a single joint and a double joint are shown in Figures 3.9 and 3.10.

Because fully overlapping nails were used, the gusset plate nailing groups were offset relative to each other by at least the nail diameter. To investigate if this would have an effect on the joint behaviour tests were carried out using joints with pairs of transducers secured to each gusset plate and aligned vertically with the extreme nail positions on the respective plates. The tests showed that the displacement of the joint relative to each plate was effectively the same and it was decided to proceed

with the testing programme using only two transducers. Where possible, the transducers were positioned to align with the extreme nail line positions on one of the gusset plates and secured to that plate. Attaching the transducers to the gusset plate rather than the testing rig also ensured that direct measurements were being taken of the displacement of the timber relative to the gusset plate and there was no need to also have to monitor the rig movement. The transducers were generally aligned with the extreme nail line positions as the nails on these lines would include the most highly stressed nails in the joint and would be used to establish the joint rotation behaviour up to failure. Additional transducers were also used with joints where N_H exceeded 6 to investigate the occurrence of flexural movement of the timber over the length of the joint.

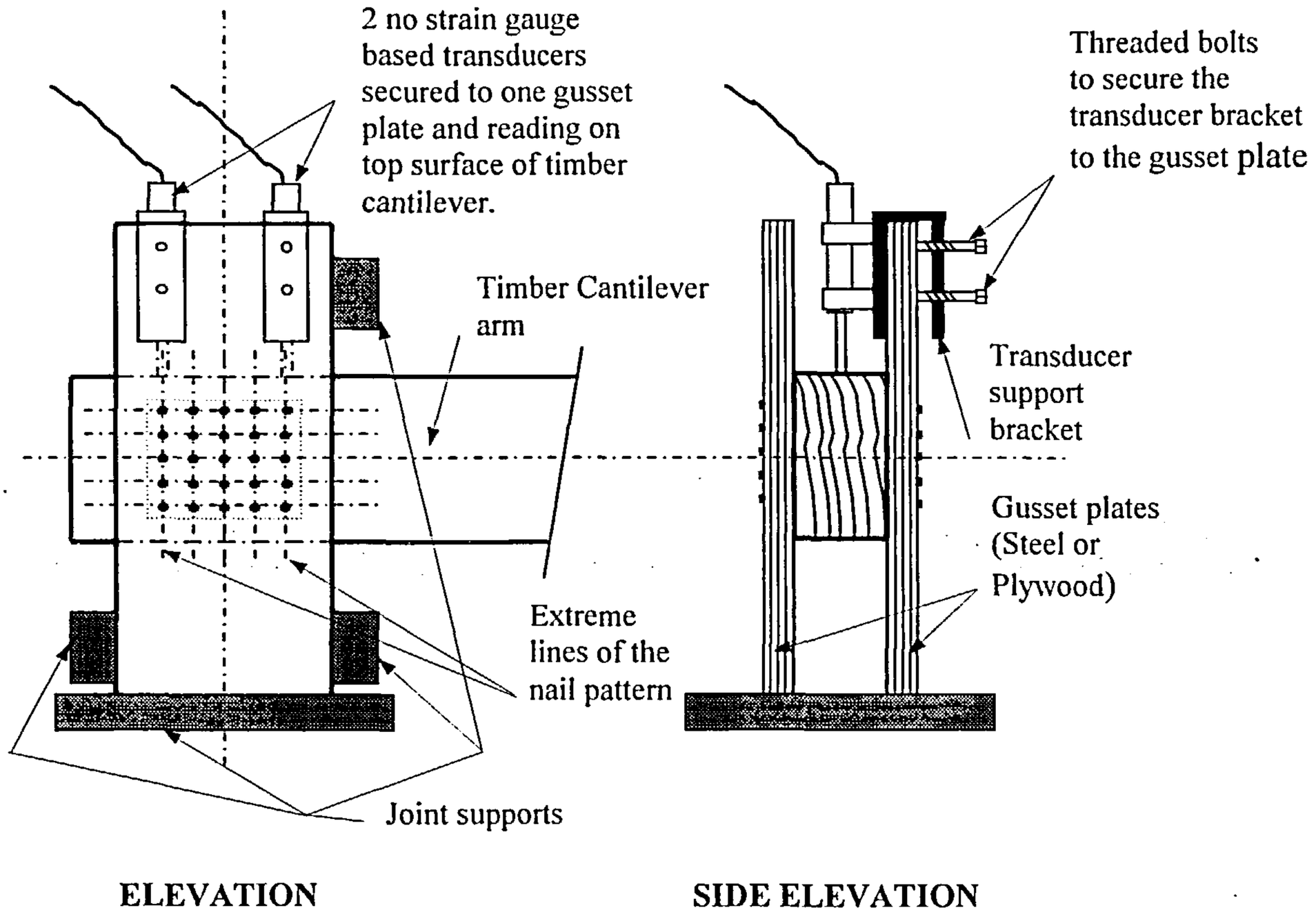

Figure 3.9 Typical single moment joint set-up

The gusset sizes were such that their combined stiffness in the joint well exceeded that of the nailing configurations and any flexural and shear movement across the top or bottom of the plates would be small and have a negligible effect on transducer alignment and transducer readings. The transducers were linked to the data acquisition system referred to in Appendix D.

All tests were undertaken using the Schenck-Treblek RM Testing Machine fitted with a 50kN load cell, which recorded the load being applied to the beam. A photograph of a moment joint under test is shown in Figure 3.11.

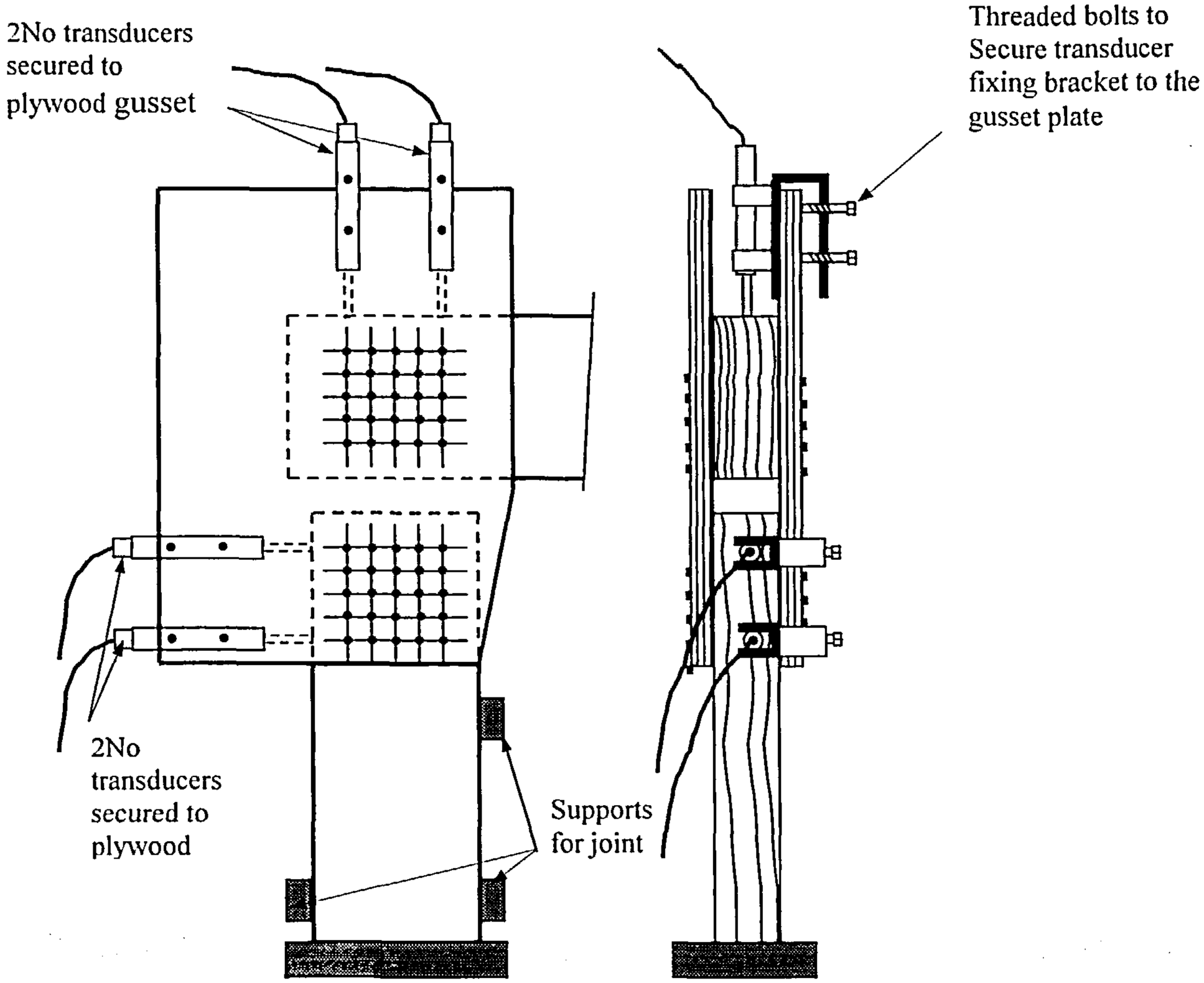

Figure 3.10 Typical double joint moment test set-up

The test rig was designed to allow the joint to be securely held in position without imposing internal stresses on the connections from the securing arrangement. The base of the joint was held by clamping each gusset plate in position using individual screwed connectors and at the top the gusset plates were again individually held using adjustable screwed supports. The joint was also supported laterally at the base using timber wedges. To minimise the shear force imposed on the joint during the loading process and to suit the varying sizes of the gusset plates, the rig was also able to be adjusted in position relative to the testing machine loading point.

Test loading complied in principle with the requirements of BS EN 26891 (1991) [27] and the monotonic loading profile used for the direct shear testing programme, shown in Figure 3.8, was applied. The loading rate on the beam was adjusted to suit the test joint nailing configuration. Because of the geometry of the joint and its set-up in the rig, during a test the nails are loaded at different rates with those furthest from the nail group centroid being subjected to the fastest rate. The speed of

movement of the machine loading head was adjusted for each joint configuration to achieve a slip rate of 0.4mm/minute in the nail at the greatest distance from the nail group centroid.

Figure 3.11 Moment joint using steel gusset plates under test

Load was applied up to 100N then reduced immediately at the same slip rate to 10N to bed the joint in. The joint was then reloaded at the same rate until the failure load was reached or until the slip in the nail at the furthest distance from the nail group centroid was at least 4.5mm.

For the double moment joints the same rig was used as for the single moment joints and a photograph of a double moment joint in the rig is shown in Figure 3.12.

The displacement of each joint was recorded using a pair of transducers, both pairs secured to the same gusset plate, and positioned close to the extreme nail line positions of the respective joints. The loading regime remained as that used for the single moment joint and the movement of the machine loading head for the test was based on the speed that would result in a maximum loading rate of 0.4mm/minute in the most extreme nail position in the combined joint.

For both joint types the data from the load cell and transducers was collected using System 5000 [49], recording machine load and transducer displacement values at one second intervals. Load and displacement data was collected, downloaded and processed as for the lateral load tests.

In processing the data the datum position for load and displacement readings was taken as the commencement of the 10N reload cycle and because the transducers positions were displaced from the

extreme nail locations and were not reading the actual movement of the most highly loaded nails, they had to be processed to take account of the geometry of the set-up and include for second order movement effects to obtain the extreme nail slip values. The analysis and processing procedure is covered in Chapter 5.

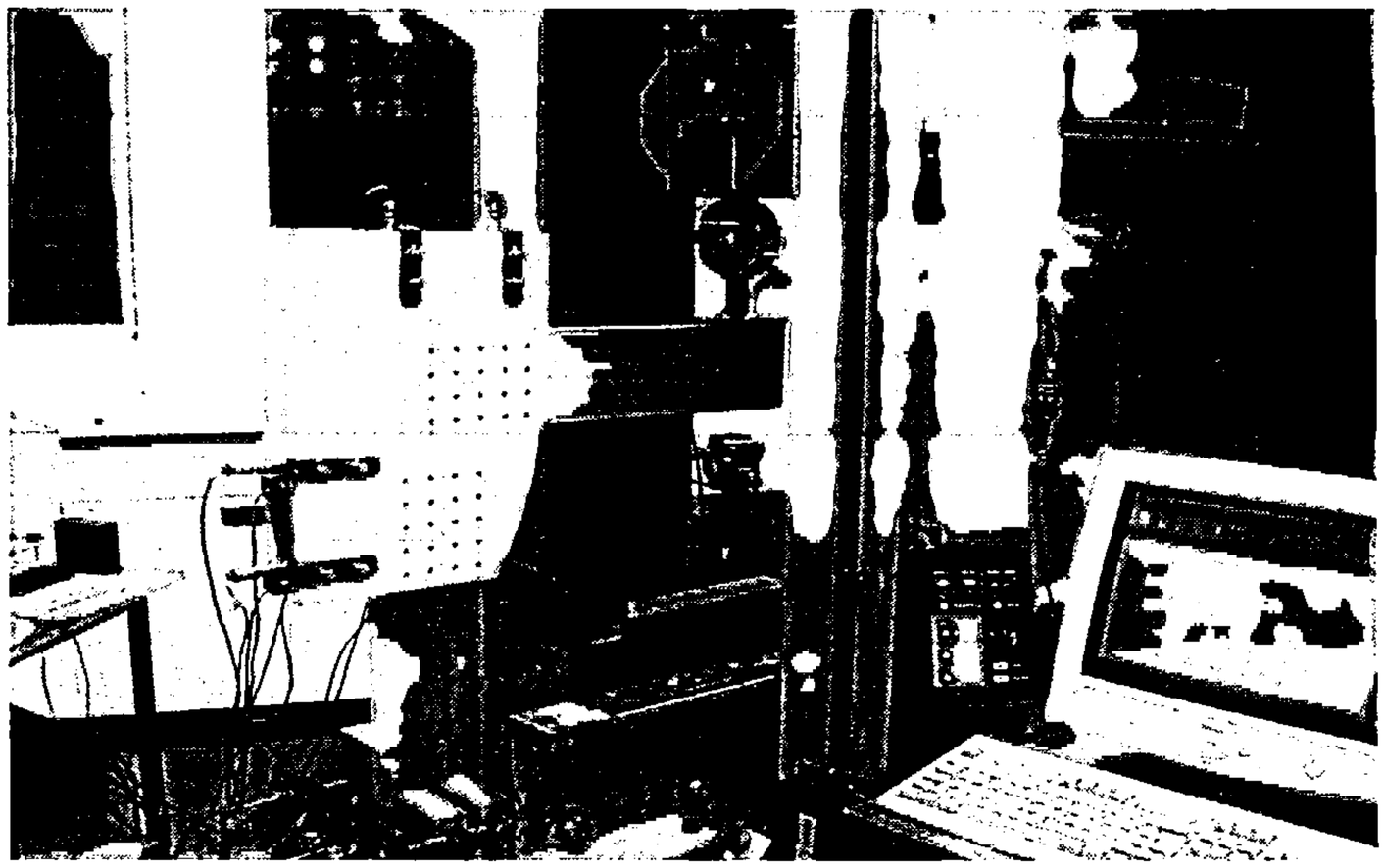

Figure 3.12 Double moment joint under test

After each moment test the mode of failure was observed and recorded and then moisture content and density tests were carried out using samples cut from the joint timber and the plywood gussets, where used.

3.5 OBSERVATIONS, DISCUSSION AND CONCLUSIONS

3.5.1 The Effect of the Direction of Nail Overlap

From the results of the testing programme it has been shown that when using nails which overlap for the full thickness of a timber member in a joint, the strength of the joint will vary depending on the direction of overlap of the nails relative to the direction of the timber grain. When the nail fully overlaps in the direction of the grain, the splitting force in the joint will be greater than when the nail is fully overlapped at right angles to the grain. In the former the splitting energy induced in the timber by each overlapping nail is focussed within the zone between adjacent growth rings and will effectively combine. In the latter the nail alignment will generally result in each overlapping nail being driven into separate growth ring zones and the splitting energy per zone will consequently be less.

To ensure a consistent approach was used throughout the testing programme it was decided to adopt the upper bound solution with the overlapping nails being driven so that the direction of the nail overlap was always aligned along the direction of the timber grain.

3.5.2 The Effect of the Number of Lines of Nails in a Joint

Tests were carried out on joints loaded along the direction of the timber grain with varying numbers of fully overlapping nails in a row at right angles to the grain direction. From these it was confirmed that joint strength was the multiple of the single line strength and the number of lines of nails in the joint. This agreed with the design rules given in most timber design codes [10, 11, 55, 56].

To minimise resources it was decided to adopt joints made with only two lines of nails at right angles to the grain direction as the testing module for the lateral load test programme. This would be able to be adjusted in length to suit the variations in nail number, nail diameter and row spacing to be investigated. The capacity of joints with greater numbers of lines would be obtained by multiplying the single line result by the number of lines used.

3.5.3 The Effect of the Lateral Spacing of Nail Lines

Joints with lines of nails at varying spacing were tested and it was concluded that the lateral spacing of the lines had no effect on joint capacity and a line spacing of 16.67mm was selected for the two line configuration to be used in the programme. This was the smallest practicable spacing that could be used for all of the shear joint configurations to be tested. It would also minimise timber resources. Also the size tied in well with the 33.33mm module that was to be used in the multi-row joints.

3.5.4 The Effect of a Gap between the Timber and the Gusset Plates

It was considered that the programme should address lower bound strength and stiffness properties in line with the approach used by Hilson *et al* [53] and spacers were used during the assembly of the joints to achieve a gap between the timber and the adjacent gusset plate faces to reduce the friction pick-up in the joint. The coefficient of friction in timber with smooth surfaces can, when loaded parallel to the grain, reach 0.3 [57] and the effect on joint stiffness if not strength, particularly at low loading, is significant.

Tests were also carried out with the gusset plates in direct contact with the timber to compare the behaviour of the respective joint types.

3.5.5 Observed Failure Modes

When a joint which has been formed using dowel connectors is loaded to failure it will fail in either a ductile or a brittle mode. The ductile mode is one in which the bedding material and connector fail by yielding with no sudden loss of joint strength or stiffness. In the brittle mode, failure occurs by material splitting, connectors shearing, shear plug failure or tension failure of reduced cross sections with sudden loss in strength and stiffness. In the European yield model [47] three ductile modes of failure are

postulated, referred to by Hilson *et al* [53] as Mode1, Mode2 and Mode3 failures.

> Mode 1 is where the connector remains rigid and the bedding material fails by yielding.
> Mode 2 is where there is a yield failure of the bedding material in conjunction with partial yielding of the dowel.
> Mode 3 is where the bedding material again fails by yielding and there is full plastic failure of the dowel.

The modes of failure when using overlapping nails in a three member joint, also giving the possible variation in the modes, are shown in Figure 3.13.

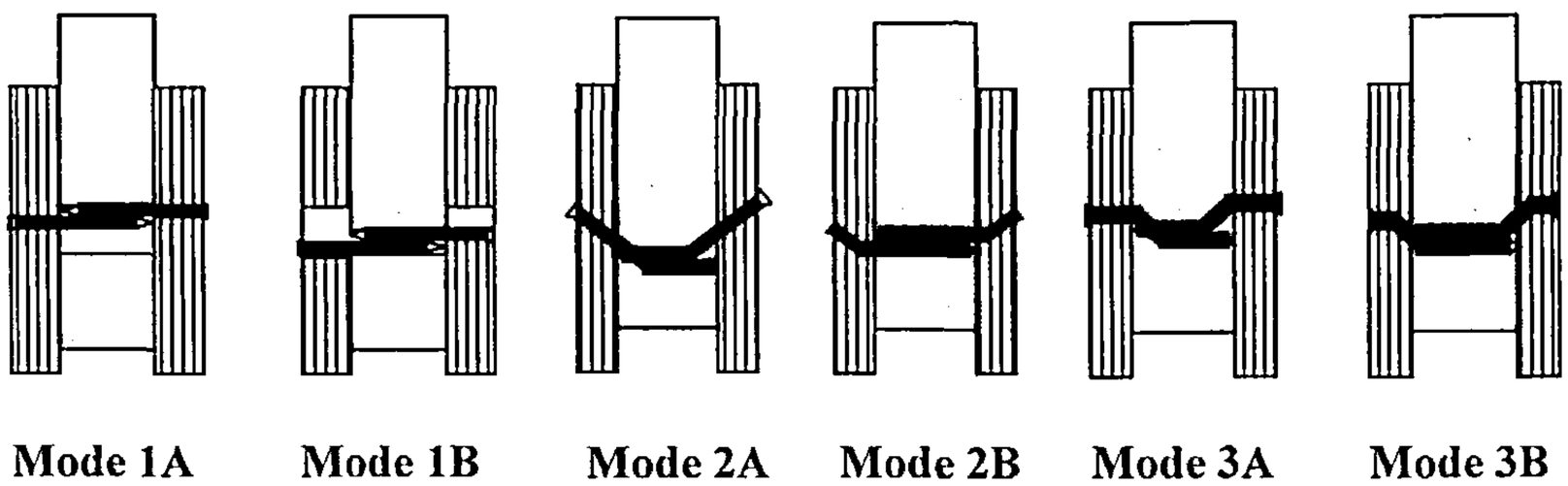

Figure 3.13 European yield model modes applied to three member joints with fully overlapping nails.

EC5 [15] is based on the European yield model modes of failures and the detailing requirements of the code are written to ensure that only ductile failures should occur [47]. In the testing programme however, brittle failures arose where nails failed in shear at the timber/gusset plate interface in steel gusset plate joints and where the timber split on assembly or under test with steel gusset plate and with plywood gusset plate joints. Splitting predominantly occurred during the early testing phase when the code criteria for nail spacing and distances were assumed to apply. When the loaded and unloaded end distance and nail spacing was changed to twice the code recommendations, the occurrence of splitting significantly reduced. An example of a brittle failure is shown in Figure 3.14 and a ductile failure is shown in Figure 3.15.

In the testing programme the types of failure which occurred were:

(a) Lateral load testing programme

Mode 2A

This type of failure only occurred in plywood gusset plate joints and arose with all three thicknesses of plywood. The plywood gusset plates failed in bearing as did a relatively small area of the timber. A plastic hinge formed in the nail in the timber at a distance of up to 6mm from the timber face. This was by far the most common type of failure in the programme.

Mode 3A

This type of failure occurred in joints with steel gusset plates. The nail head was effectively held rigid by the steel gusset plate and a plastic hinge formed in the nail at the steel gusset/timber interface. Also the timber yielded over a similar distance to that found in the Mode 2A failures and a second plastic hinge formed in the nail where it was rigidly held by the timber. This was the typical failure mode of the steel gusset joints.

Figure 3.14 Failure due to wood splitting

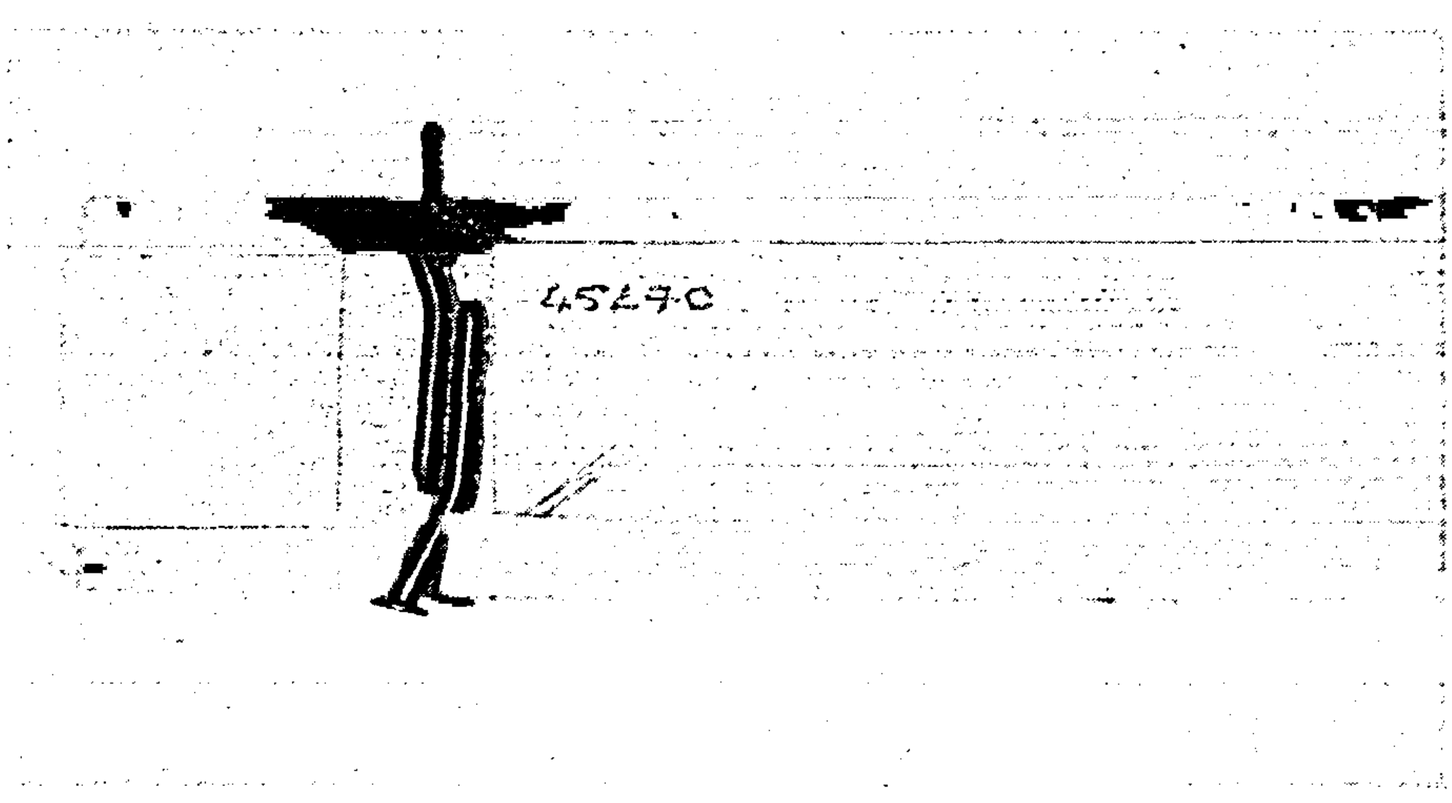

Figure 3.15 Failure due to timber/plywood/nail Yield

Mode 3B

This type of failure occurred in the plywood gusset plate joints when using 17mm thick plywood. The nail head side was held securely in the plywood and a plastic hinge formed in the nail within the thickness of the gusset. At the same time the plywood gusset plates failed by yielding. Again there was a limited area of yielding in the timber and a second plastic hinge formed in the nail where it was held rigidly in the timber.

Nail Head Shear

This only occurred in joints with steel gusset plates. The process of predrilling the steel gusset for the nail left a sharp edge in the gusset at the timber interface and during the joint loading process the nail was stressed onto and over this edge and on occasions the nail head sheared. This most commonly arose when using 3.35mm diameter nails but there was no clear pattern to the occurrence. The event occurred in 47 joint tests, which represented less than 4% of the steel gusset shear testing programme.

Timber Splitting

Splitting in the timber occurred with both steel gusset and plywood gusset plate joints. As stated earlier it was a relatively common occurrence at the start of the testing programme when the end distance was based on the criteria in Table 3.3. When the end distances were increased to two times the values in the Table the occurrence reduced. It has to be noted however that in the steel gusset plate test programme approximately 25% of the joints failed eventually by splitting of the timber and in the plywood gusset plate programme only 1% failed in this manner. With the steel gusset plates the predrill hole in the gusset acted as a rigid guide for the nail during driving, considerably increasing the nail stiffness. When overlapping with adjacent nails the increased rigidity caused small splits to arise in the timber and these eventually caused the joint to fail by splitting under load. This did not occur with the plywood gussets.

b) Moment testing programme

Timber Splitting

In the moment tests nails are subjected to forces at angles to the timber grain and failure by splitting of the timber due to a combination of the nail force at right angles to the grain and shear forces along the grain direction is to be expected. With the steel gusset plate moment joints, 50% failed in this manner and with the plywood gusset plate moment joint, less than 1% failed this way.

Mode 3A and 3B

Where failure was not by splitting, the majority of the moment joints failed in Mode 3A when using steel gusset plates and Mode 3B when using plywood gusset plates, in the manner described for the equivalent modes in the lateral load joints.

As all of the lateral load joint configurations in the testing programme complied with EC5 [15] criteria, it is surprising to note that a significant number of tests failed in a brittle manner rather than a ductile mode. The slenderness ratios for the nails in all of the tests exceeded 15, and for large slenderness ratios i.e. greater that 6-7, Mode 3 failures were expected to occur [45, 54]. The small percentage of timber splitting failures with plywood gusset plate joints can be argued to be statistically acceptable but for the steel gusset joints, where 50% of the failures were related to timber splitting and 4% where nail heads sheared, validates the comment by Jorrison [47] that notwithstanding full compliance with the requirements of EC5 brittle failures will occur. It is suggested that the detailing rules in the code need to be reviewed.

3.6 SUMMARY

This chapter has given details of the experimental work carried out to study the direct shear-displacement and moment rotation behaviour of multi-nailed timber joints assembled using steel and plywood gusset plates and connected using fully overlapping nails. It identifies the most critical direction of alignment of the nail overlap and this has been used throughout the testing programme. It is concluded that the EC5 minimum spacing and end distance rules applied to the timber have to be modified when using fully overlapping nails and two times the code values have been used.

Although the code rules are based on ductile failure modes, failure by splitting was found to be a common occurrence in the testing programme, suggesting that the minimum spacing and distance rules require to be fully reviewed.

4. SEMI-EMPIRICAL MODELLING OF LATERALLY LOADED SHEAR JOINTS

4.1 INTRODUCTION

In this chapter, the results of the tests on the laterally loaded shear joints described in Chapter 3 are presented and analysed. The factors influencing joint behaviour are investigated and semi-empirical expressions are developed to simulate the strength and stiffness behaviour of laterally loaded multi-nailed joints under short duration loading. Joints with steel gusset plates are addressed first, followed by the analysis of joints with plywood gusset plates.

The analysis commences with an investigation into the effect of the number of lines of nails in a joint and the nail line spacing. This was carried out to show that joint strength was a linear function of the number of lines of nails in the joint. It was also undertaken to substantiate the use of the 16.67mm spaced two line configurations generally adopted for the joints in the testing programme. The tests were carried out using 2.65mm diameter nails and steel gusset plates.

This is followed by an analysis of the effects of displacement function, moisture content, timber and plywood density, generic function, nail strength, nail diameter, number of rows of nails, row spacing and number of nails in the joint, using all nail diameters. These analyses give lower bound solutions for joints assembled with a gap between the gusset plates and the timber. Upper bound solutions have also been determined for joints assembled without gaps.

From these analyses expressions have been developed for the effect of each factor and semi-empirical relationships produced for the load-displacement behaviour of each type of joint. The results from the semi-empirical models are also compared with the test results.

4.2 GENERAL

4.2.1 The Effect of the Number of Lines of Nails in a Joint

In this research, in the shear testing programme a line of nails is defined as a run of nails along any line which lies in the direction of the applied load and a row of nails is a run of nails along any line at right angles to the direction of the applied load. This is shown diagrammatically in Figure 4.1.

Because of the difficulty in controlling out of alignment effects when using single line joints, it was decided that a two line joint configuration would generally be used. To confirm that joint strength was a multiple of the number of lines in the joints, at the commencement of the programme tests were conducted using timber joints with steel gusset plates having two, three and four lines of pairs of fully overlapping 2.65mm diameter, 50mm long Rynail nails, each line 33.33 mm apart. The nailing configurations used in these joints being M, ZG, and ZH respectively and the results of the tests,

presented as joint load divided by timber density plotted against the joint slip, are shown on Figures 4.2 to 4.4. The Figures also give the associated best fit curve based on a least squares linear regression analysis [42] using a fourth order polynomial fit.

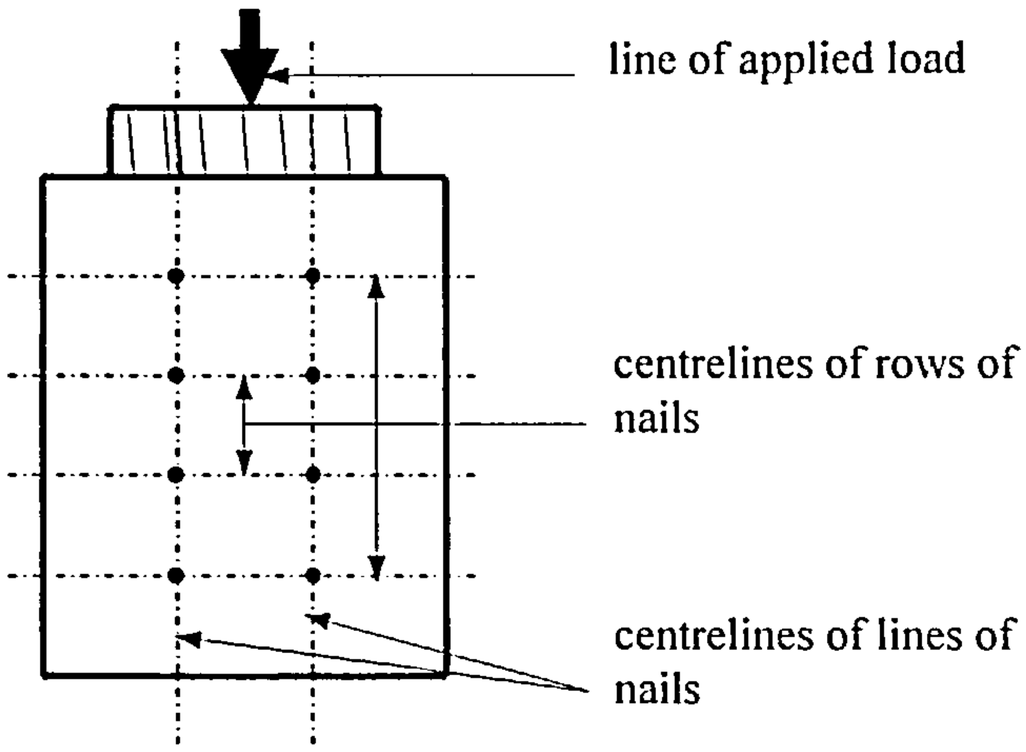

Figure 4.1 Lines and rows of nails in a loaded joint

A fourth order polynomial fit was used to obtain the best fit against the test data over the full range of joint slip and the coefficients of determination, R^2, which measure the proportion of total variation about the mean explained by the regression, come within the range 0.9836 to 0.9928.

To obtain the best fit between the curves, comparison has been made using multiples of the two line result, adjusting the multiplier for each case until the percentage mean deviation is zero. Percentage mean deviation (md%) is a statistical parameter such that if $P1_r$ is the experimental load at point 'r' on a graph that is being compared with another graph with a value $P2_r$ at the same point, and over the length of the graph there are n points, then:

$$md\% := \sum_{r=1}^{n} \frac{\left(P1_r - P2_r\right)}{P2_r \cdot n} \cdot 100$$

Using the average data from joints ZH and ZG and comparing with multiples of the average data from joint M, exact fits will be obtained by adjusting the multiplying factors until the percentage mean deviation is zero. For an exact fit the multiples should be 1.5 and 2 respectively. From the percentage mean deviation analysis, comparing M with ZH the multiple is 1.508 and comparing M with ZG it is 1.9901. Allowing for the effects of experimental error, using this statistical approach the results effectively show that there is a linear relationship between joint strength and the number of lines of nails in the joint.

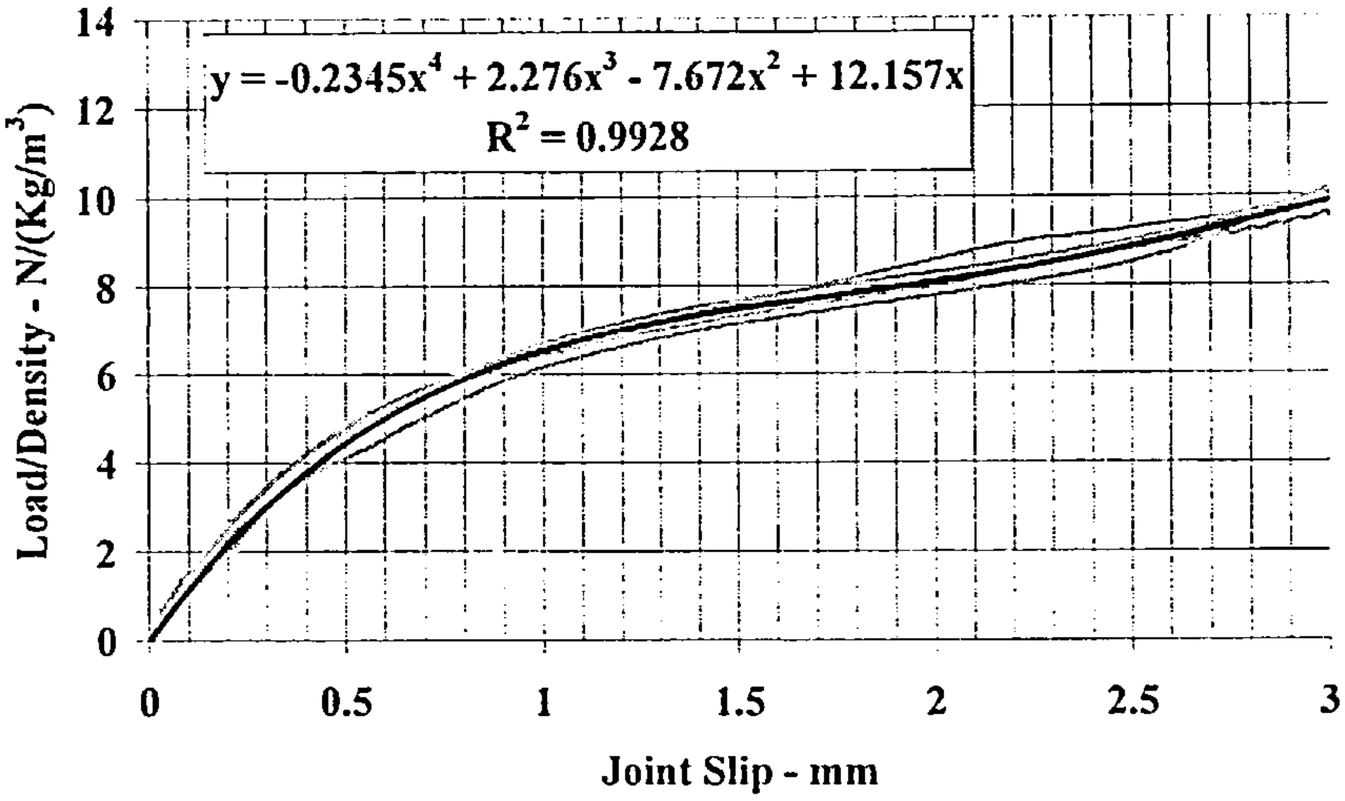

Figure 4.2 Two line joint M

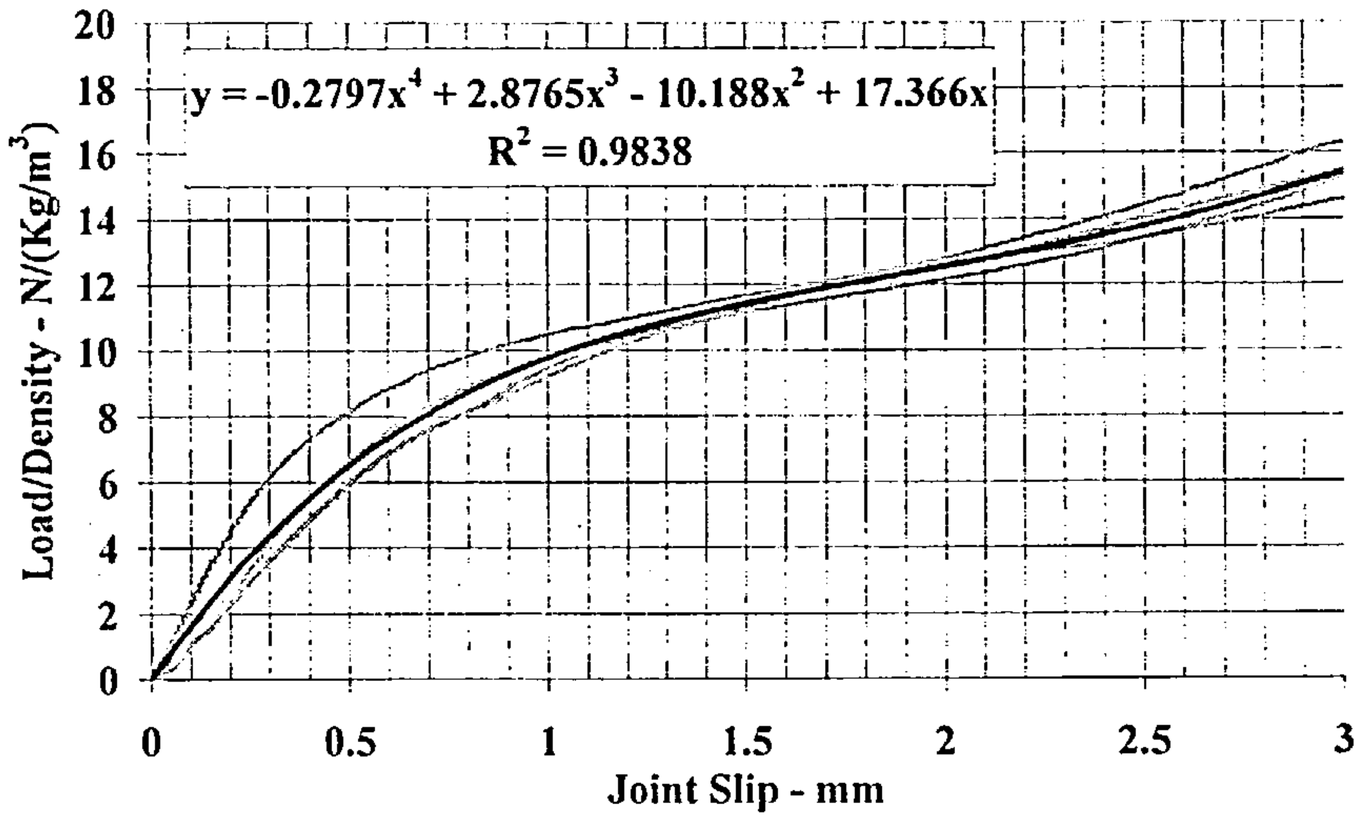

Figure 4.3 Three line joint ZG

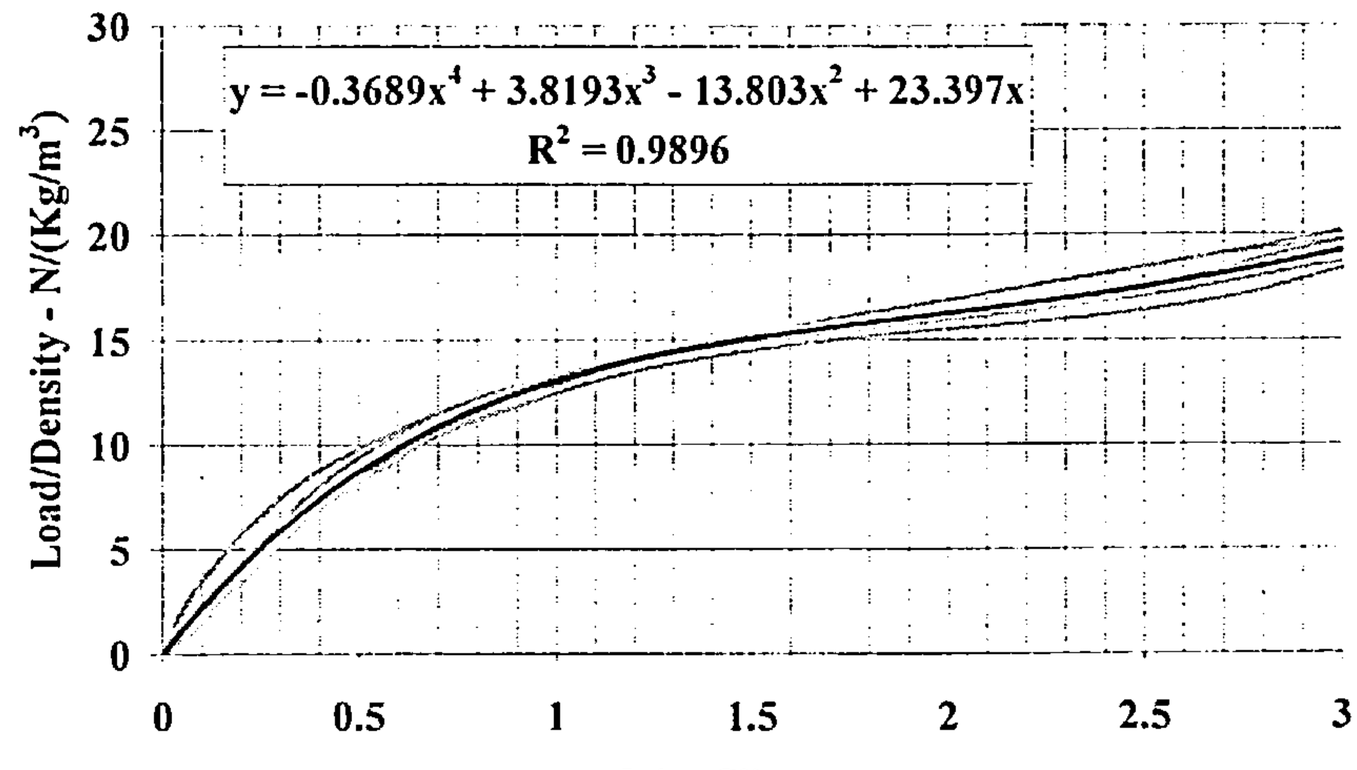

Figure 4.4 Four line joint ZH

The regression analysis best fit curves for joints M, ZH and ZG are shown on Figure 4.5. In addition the curves obtained by multiplying the graph for joint M by 1.5 and by 2 are superimposed and the close fit between the respective sets of graphs can be observed.

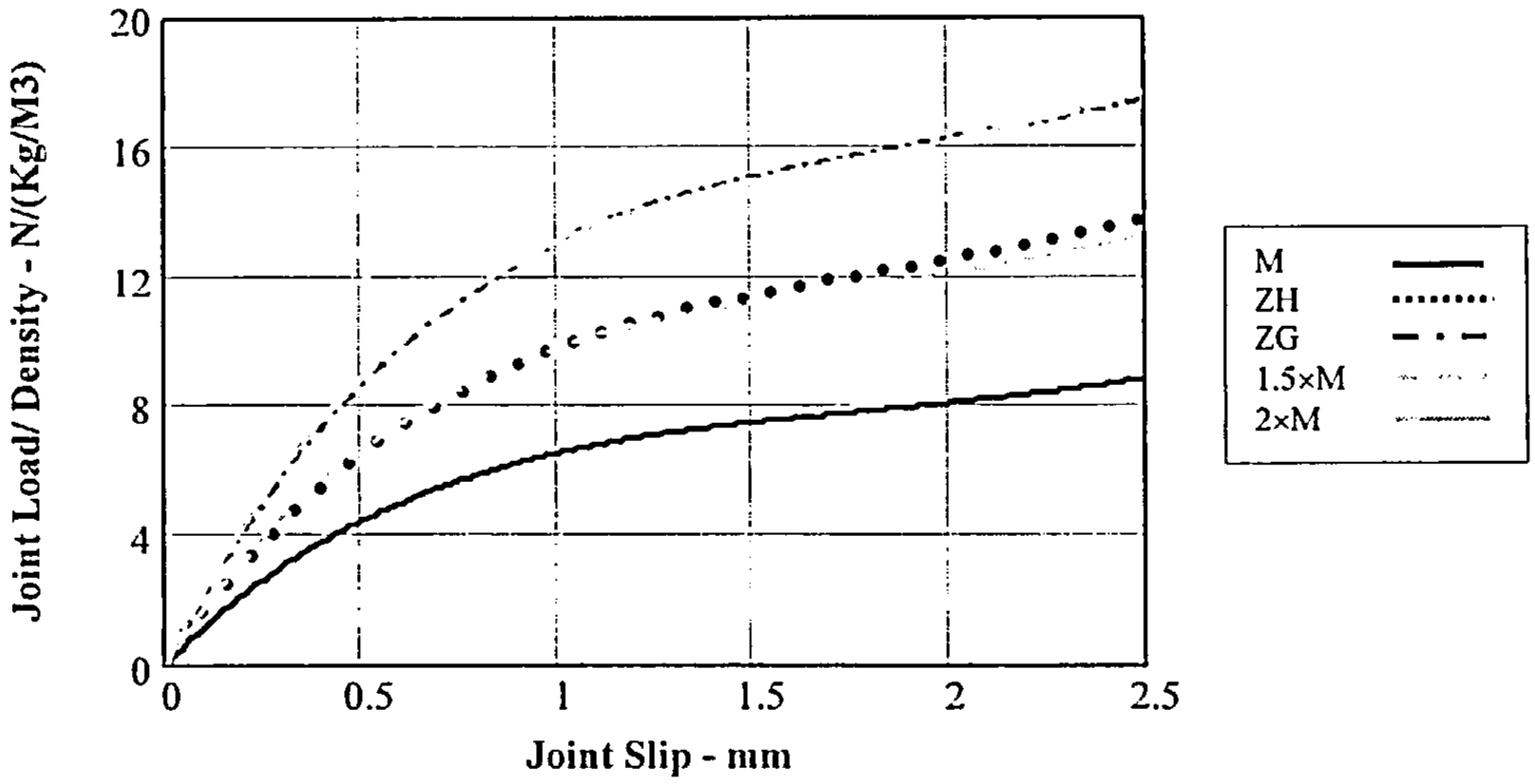

Figure 4.5 A comparison of the curves for joints M (2 lines), ZH (3 lines) and ZG (4 lines) with multiples of joint M.

The finding is in line with the approach used in timber design codes [10,11,55,56] where the strength of a joint along the direction of load is obtained by multiplying the strength of the single line of nails aligned in that direction by the number of lines of nails in the joint. The testing programme has been progressed on this basis.

4.2.2 The Effect of the Lateral Spacing of Lines of Nails in a Joint

To investigate the effect of nail line spacing, tests were carried out on joints formed with steel gusset plates connected by two lines of nails at different spacing. Two pairs of joint configurations were investigated; one using two lines of single row fully overlapping 2.65mm diameter nails at 6mm and 16.67mm centre to centre (joints BA and CO respectively); the second using two lines of three row joints also formed using fully overlapping 2.65mm diameter nails and the line spacing was again 6mm and 16.67mm centre to centre (joints BK and CR respectively). The results of the tests divided by the timber density were plotted against the joint slip and for each case the best fit curve based on a least squares linear regression analysis, again using a fourth order polynomial, was obtained. The coefficient of determination, R^2, of each set of tests was 0.98 to 0.9973 and an example of one of the best fit curves is given in Figure 4.6.

The curves obtained are compared in Figure 4.7 and using the percentage mean deviation approach referred to in section 4.2.1, the average of the fits gives a multiplication factor of 0.995. This is effectively unity, confirming that varying the nail line spacing has no effect on the joint strength and is not a factor that needs to be addressed in the joint behaviour.

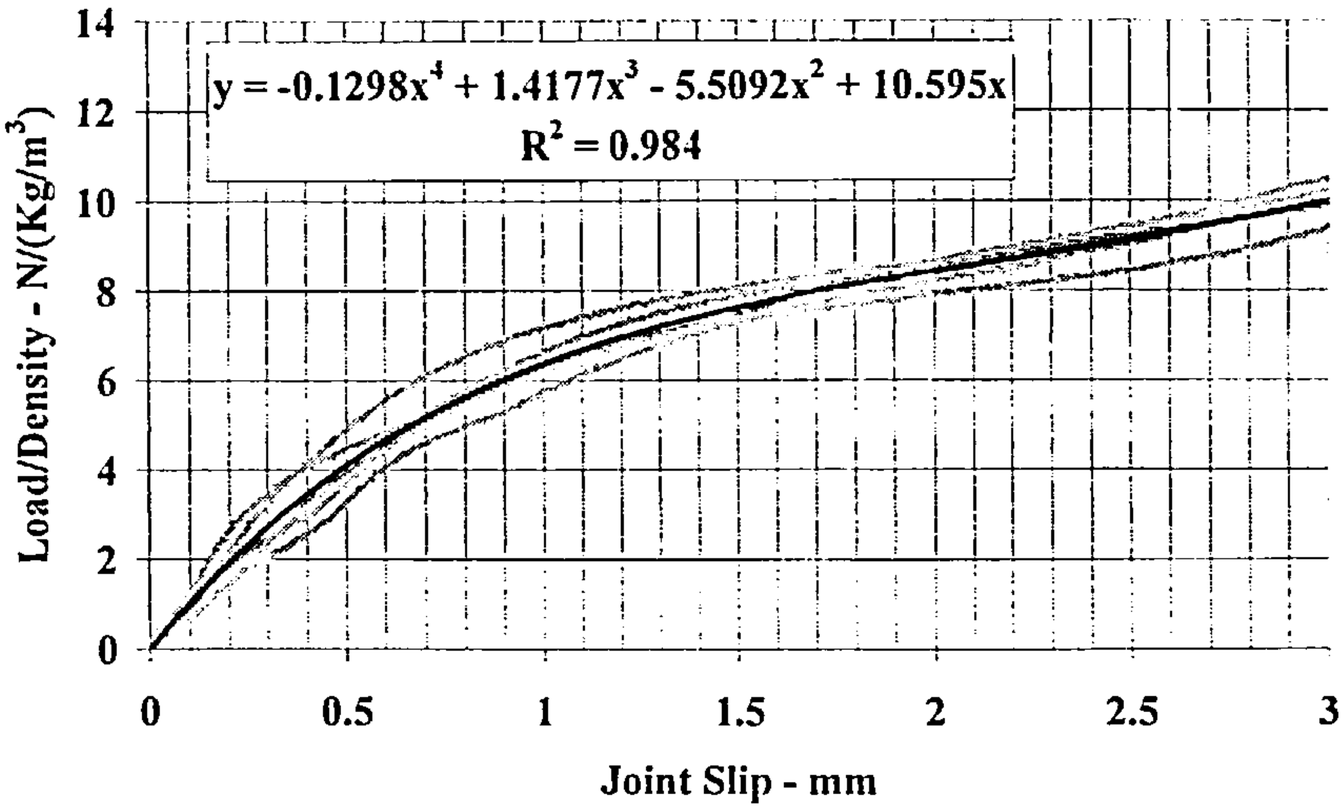

Figure 4.6 One row in two lines at 6mm centre to centre BA

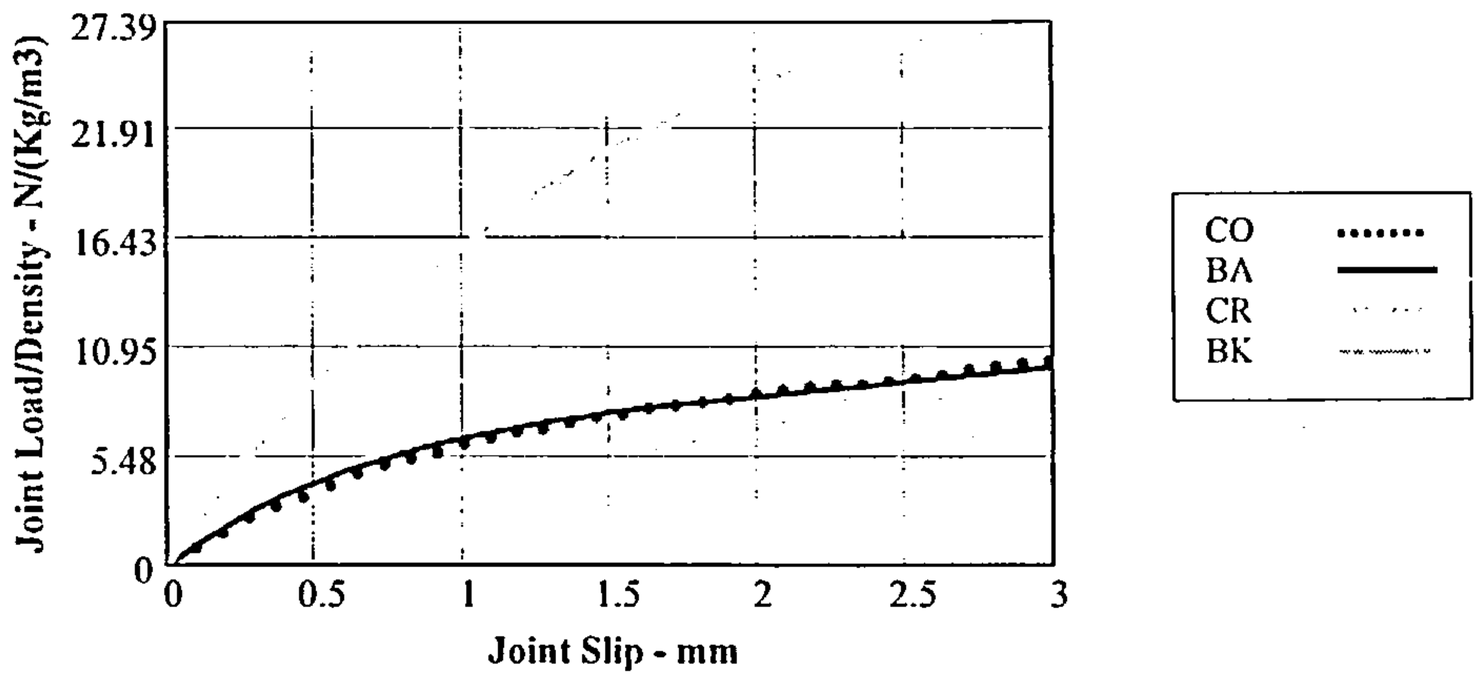

Figure 4.7 Comparison of joints CO~BA and CR~BK

It is to be noted the use of a 6mm spacing at right angles to the grain for nail lines formed using 2.65mm diameter nails is less than the 4*d* minimum spacing (perpendicular to the grain) recommended in EC5 [11]. This suggests that when using joints loaded in direct shear there may be some scope to reduce the 4*d* criteria if this was considered to be desirable.

To standardise on the joint set-up for the programme a line spacing of 16.67mm centre to centre has been used for all of the shear tests set-ups.

4.3 THE ANALYSIS PROCEDURE USED TO INVESTIGATE THE JOINT FACTORS

Most parts of the world have timber codes predicated on the limit states design (LSD) approach using ultimate load theory with a partial factor safety format and international practice is to move towards this format and away from the permissible stress design (PSD) approach. The PSD approach is based on an elastic design philosophy with load factors applied to obtain the failure load condition [11,55,56,63,64].

L.S.D has been used for the design of all of the major engineering materials for some considerable time now and is the methodology that will soon be used for timber design in the UK. However a consequence of the drive towards acceptance of this approach is that over the past 10 to 15 years research into joint behaviour has mainly been focussed on the behaviour of joints at the ultimate limit state. Only limited consideration has been given to investigations into overall joint behaviour, including behaviour at the serviceability limit state, which is effectively equivalent to the permissible stress condition in the PSD approach [44, 47, 65, 66, 67].

From the background work to the development of EC5[11], the European L.S.D. code, Ehlbeck *et al* [68] state that for nailed joints the slip at the serviceability limit state is equivalent to the slip at approximately 40% of the load carrying capacity of the connector and from the results of many tests available from various test laboratories, the slip at this limit has been estimated to be:

$$\delta_{inst} = 40d^{0.8} / \rho_k \qquad \text{....(1)}$$

where:

δ_{inst} = the instantaneous slip of a nailed joint at approximately 40% of the load carrying capacity (mm).

d = the nail diameter (mm).

ρ_k = the characteristic density of the joint timber (kg/m^3).

From equation (1) the nail slip is a function of the nail diameter and the timber density and for the three nails sizes used in the testing programme, adopting 400 kg/m^3 and 600kg/m^3 as approximate extreme values of the characteristic density of the timber, the slips at the serviceability limit state will be as given in Table 4.1.

Nail Diameter – d mm		**2.65**		**3.00**		**3.35**	
Timber Density - ρ_k kg/m^3		**400**	**600**	**400**	**600**	**400**	**600**
Nail slip at the Serviceability State – mm	**EC5[11]**	0.219	0.146	0.241	0.161	0.263	0.175
	EC5[15]	0.447	0.298	0.494	0.329	0.539	0.359

Table 4.1 Nail slip at the serviceability limit state based on EC5 [11] and EC5 [15]

EC5 has been revised in draft form on several occasions and in the latest revision [15] the characteristic load-carrying capacity of a nail has been increased, the serviceability limit state slip modulus has been reduced. Applying the proposed changes to equation (1), the slip at the serviceability limit state is now

approximately:

$$\delta_{inst} \approx 82d^{0.8} / \rho_k \qquad \text{....(2)}$$

The nail slip has increased by over 100% and the slip at the serviceability state based on this revision is also given in Table 4.1.

Using a 3.35mm diameter nail with timber having a characteristic density of 400kg/m^3, the slip is now 0.539mm compared to 0.263mm under EC5 [11]. Nail sizes range from 1.4mm to 8.00mm diameter [23] and if an 8.00mm diameter nail were to be used the corresponding slip would be 1.082mm compared to a value of 0.531mm under EC5 [11].

It is to be questioned that engineers are fully alert to the significance of the value of slip inherent in the code equations and the methodology used in this research programme has been one which will determine a load-displacement relationship based on an empirical approach. It will establish a failure limit for joint slip and load and also a level of slip at the serviceability limit that will be more or less standard for each size of nail and joint type. The slip will be more readily defined and able to be taken into account in the design process. In addition the empirical relationship will be able to be incorporated into any semi-rigid analyses of structural frames formed with joints of the type used in the programme.

From the literature review of the methodologies used by researchers into the development of load-displacement relationships for joints, [6, 7, 9, 12, 69, 70, 71] it was noted that Mack [6] concluded that the factors influencing joint strength and stiffness behaviour did not significantly interact. By combining the effects of the individual factors, a semi-empirical relationship for the overall joint behaviour could be developed.

This was a very important finding and based on this premise the analysis programme has been structured to investigate in turn each issue which affects joint behaviour under short term loading. Care has been taken to ensure that the effects of potentially interacting functions have been isolated before being taken into account.

From a review of the results of the joint tests it was noted that at 3.2mm slip, joints made with steel gusset plates were starting to show an increased frequency in the occurrence of brittle failure caused by timber splitting or nail heads being sheared off. Based on this finding, for all joints with steel gusset plates, the failure slip of the joint has been taken to be 3.2mm. Also, from the initial load-displacement curves of the test joints made with steel gusset plates, applying a factor of 40% to the joint load at the 3.2mm joint slip limit, the average joint slip was of the order of 0.44mm. It is to be noted that this is in line with the 0.4mm limit used in the BS 5268: Part2:1984 [72] for the permissible working load [73] approach and that adopted by other countries in their PSD codes [86, 87, 88].

On the understanding that there is no significant interaction between the factors that influence joint behaviour, the load-slip relationship of a joint can be set out as a function of the joint displacement, as well as of the variables that affect the joint, in the following form:

$$P = f_1(\delta), f_2(D), f_3(mc), f_4(d), f_5(f_u), f_6(k_g), f_7(r), f_8(S_p), f_9(l), f_{10}(v) \quad \ldots(3)$$

where

P	the load on the joint	$f_6(k_g)$	generic function
$f_1(\delta)$	the joint displacement function	$f_7(r)$	nail row function
$f_2(D)$	density function	$f_8(S_p)$	row spacing function
$f_3(mc)$	moisture content function	$f_9(l)$	nail line function
$f_4(d)$	nail diameter function	$f_{10}(v)$,	etc are functions of the remaining variables that effect the joint behaviour.
$f_5(f_u)$	nail strength function		

As the load-slip behaviour has been based on the use of short term loading, those factors affecting rheological characteristics are not relevant and have not been considered in this programme. The variables associated with functions $f_1(\delta)$ to $f_9(n)$ have been investigated and the load-displacement relationship to be developed will be:

$$P = f_1(\delta), f_2(D), f_3(mc), f_4(d), f_5(f_u), f_6(k_g), f_7(r), f_8(S_p), f_9(l) \quad \ldots(4)$$

Functions $f_1(\delta)$ to $f_9(l)$ have been determined for joints with steel gusset plates and for joints with plywood gusset plates and are discussed in this Chapter. Over the testing period for joints using plywood gusset plates the moisture content of the timber was between 12.5% and 14% and for such a small variation a moisture content function was not considered to be required and was not developed. For the steel gusset plate joints however, the timber moisture content ranged from 11% to 15.5% and a moisture content function has been developed for these joints. Expressions have also been developed for joints assembled with no gap between the timber and the gusset plates.

4.4 THE ANALYSIS OF STEEL GUSSET PLATE JOINTS FORMED WITH A GAP AND USING PREDRILLED HOLES LESS THAN 1.1 TIMES THE NAIL DIAMETER

4.4.1 The Joint Displacement Function ($f_1(\delta_v)$)

Because the joint functions do not significantly interact, equation (4) can be written:

$$P = f_1(\delta)\, K \quad \ldots(5)$$

where K is the product of $f_2(D), f_3(mc), f_4(d), f_5(f_u), f_6(k_g), f_7(r), f_8(S_p), f_9(l)$.

Rearranging, the joint displacement function can be rewritten $f_1(\delta) = P/K$, indicating that the joint displacement is $1/K$ times the load on the joint. If K is given the value of the load on the joint at the slip limit of 3.2mm, ($P_{3.2}$), the displacement function will equal unity and at any intermediate load, P_x, the displacement function, $f_1(\delta_x)$, at the associated slip, δ_x, will be:

$$f_1(\delta_x) = P_x/P_{3.2} \qquad \ldots(6)$$

where, adopting the same terminology used by Mack [6], $P_x/P_{3.2}$ is referred to as the reduced load. Over the range of $\delta_x = 0$ to 3.2mm the reduced load will define the displacement function of the joint.

Using the relationship in equation (6), dividing the load-slip graphs from the joint testing programme by the joint load at 3.2mm slip, the reduced load data can be fitted to a curve to form the displacement function. A typical set of load-slip graphs for a test set of joints using nailing configuration ED made with steel gusset plates and using 2.65mm, 3.00mm and 3.35mm diameter nails are shown on Figure 4.8. To allow for comparison between the test sets, each test result has been divided by the timber density of the test sample and has been presented as a load per unit density against joint slip.

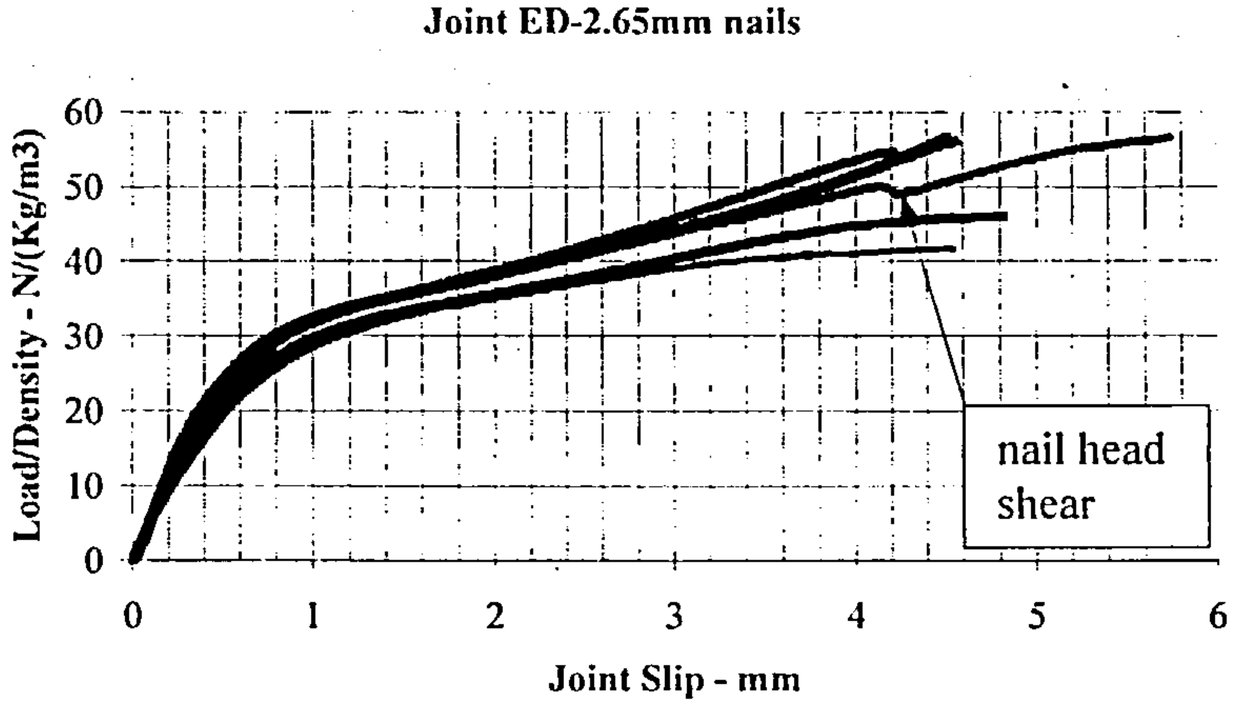

Figure 4.8 Load/density against joint slip for join configuration ED test sets using 2.65mm, 3.00mm, and 3.35mm diameter nails

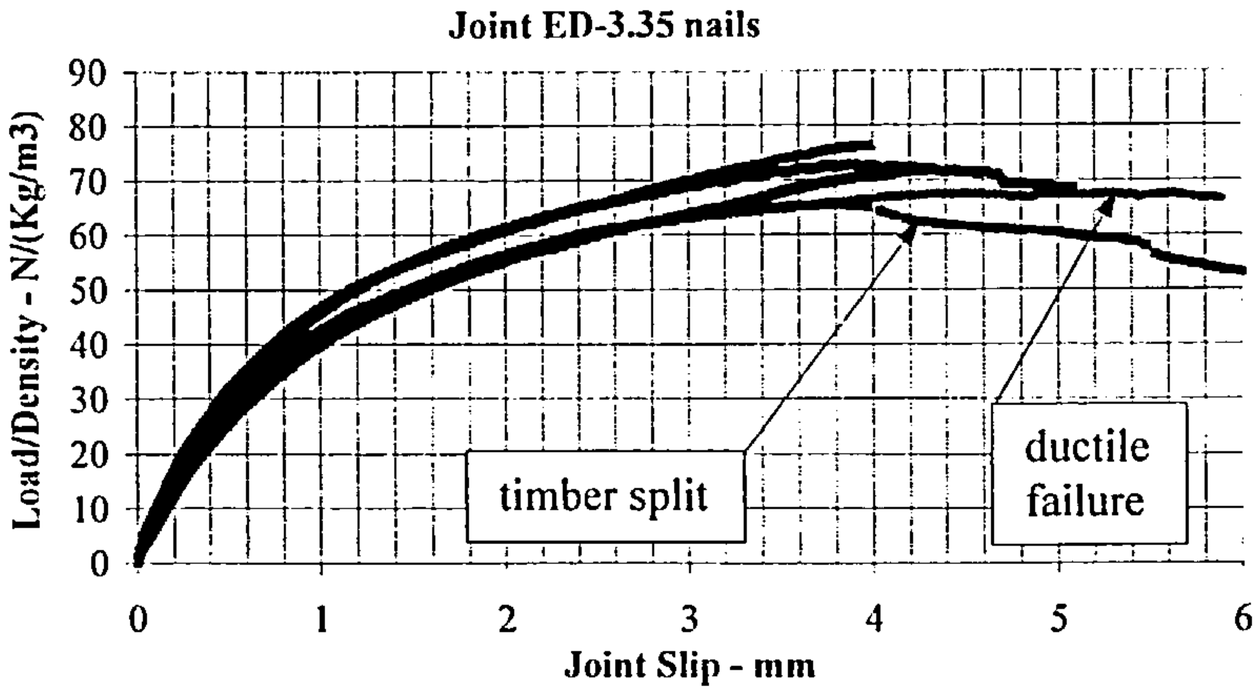

Figure 4.8 cont'd Load/density against joint slip for join configuration ED test sets using 2.65mm, 3.00mm, and 3.35mm diameter nails

It is of interest to note that the results of the test sets incorporate the four types of graph associated with the failure modes obtained from the joints tested with steel gusset plates. The types are:

1. Where a nail head sheared, the graph would suddenly exhibit a dip and as the load continued to be applied it would start to increase in slope again. This is shown on the 2.65mm diameter test set.

2. Where the timber split during the test the graph would fall away relatively suddenly, continuing to fall until the timber was completely split. This is clearly shown on the 3.35mm diameter test set.

3. The third type of graph is where the nails start to develop withdrawal resistance in the wood and in these instances when the slip was between 2.00mm and 3.50mm there is an inflection in the graph leading to an increase in slope as shown on the 3.00mm diameter test set.

4. The fourth type is where the joint failed in a ductile manner. The load increased gradually to a maximum load and then levelled off or marginally increased with slip as shown on the 3.35mm diameter test set.

To obtain the reduced load data for each test the graphs have been terminated at the 3.2mm slip limit and divided by the load at that slip as shown in Figure 4.9.

It is possible to obtain an accurate individual fit to each reduced load data curve using a least squares approach with polynomial equations of the 'nth' order. However, because of the number of variables involved in this type of equation, it does not lend itself for use in situations where a generic displacement function is required.

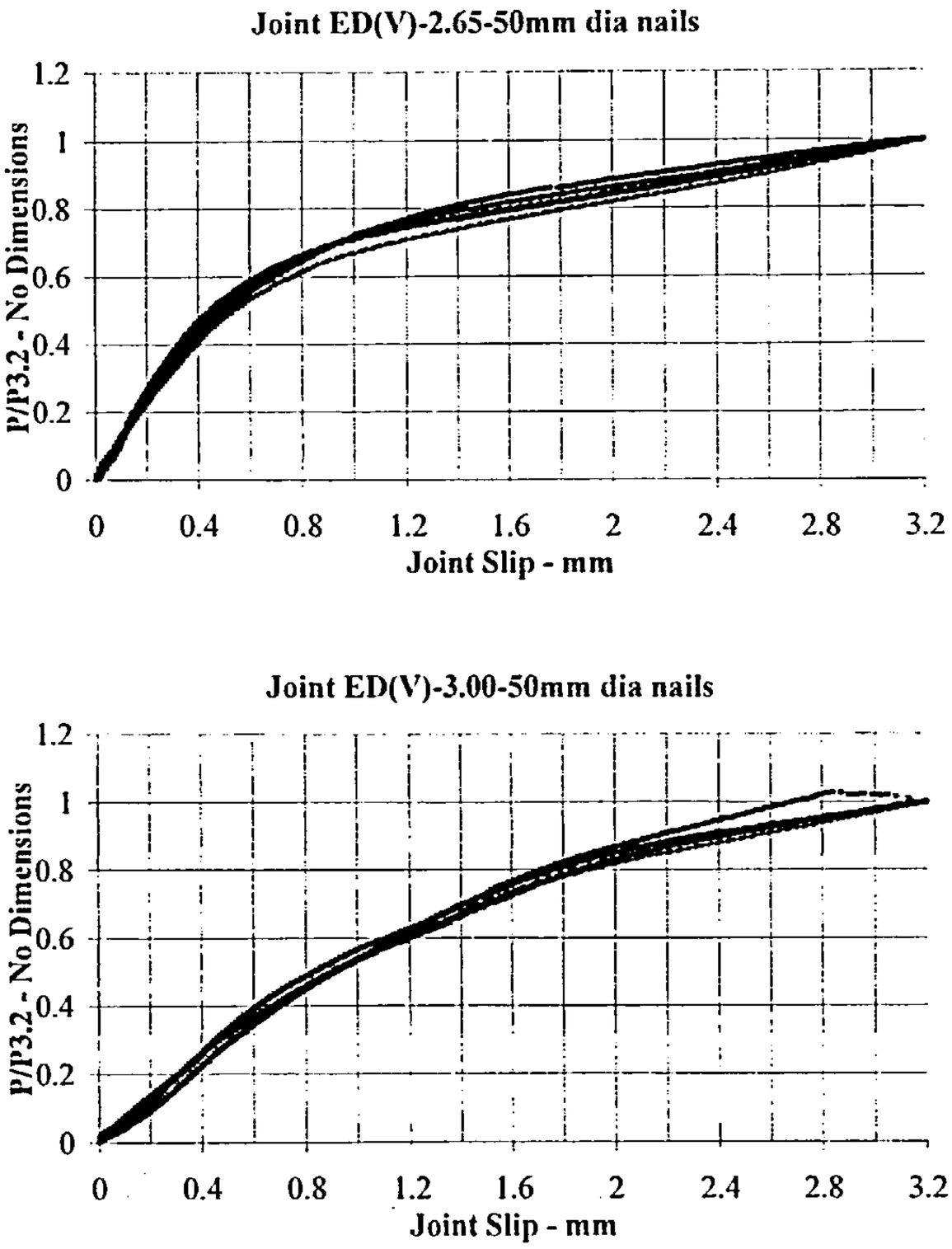

Figure 4.9 Reduced Load ($P_x/P_{3.2}$) against joint slip for joint configuration ED test sets using 2.65mm, 3.00mm, and 3.35mm diameter nails.

Many forms of displacement function have been developed from test results and used in load-displacement relationships for dowel type joints. The most notable being those developed by Mack [6], McLain [7], Foschi [8], Morris [9], Smith [74] and Kermani *et al* [75]. From trial fits using alternative functions, the one that gave the best fit to the test data is a function of the form previously used by Mack [6].

The function is a generalised four parameter non linear exponential equation as defined in equation (7) and shown in graphical form in Figure 4.10:

$$f_1(\delta_x) = (1 - e^{C\delta x/3.2})^D(A\,\delta_x/3.2 + B) \qquad \ldots(7)$$

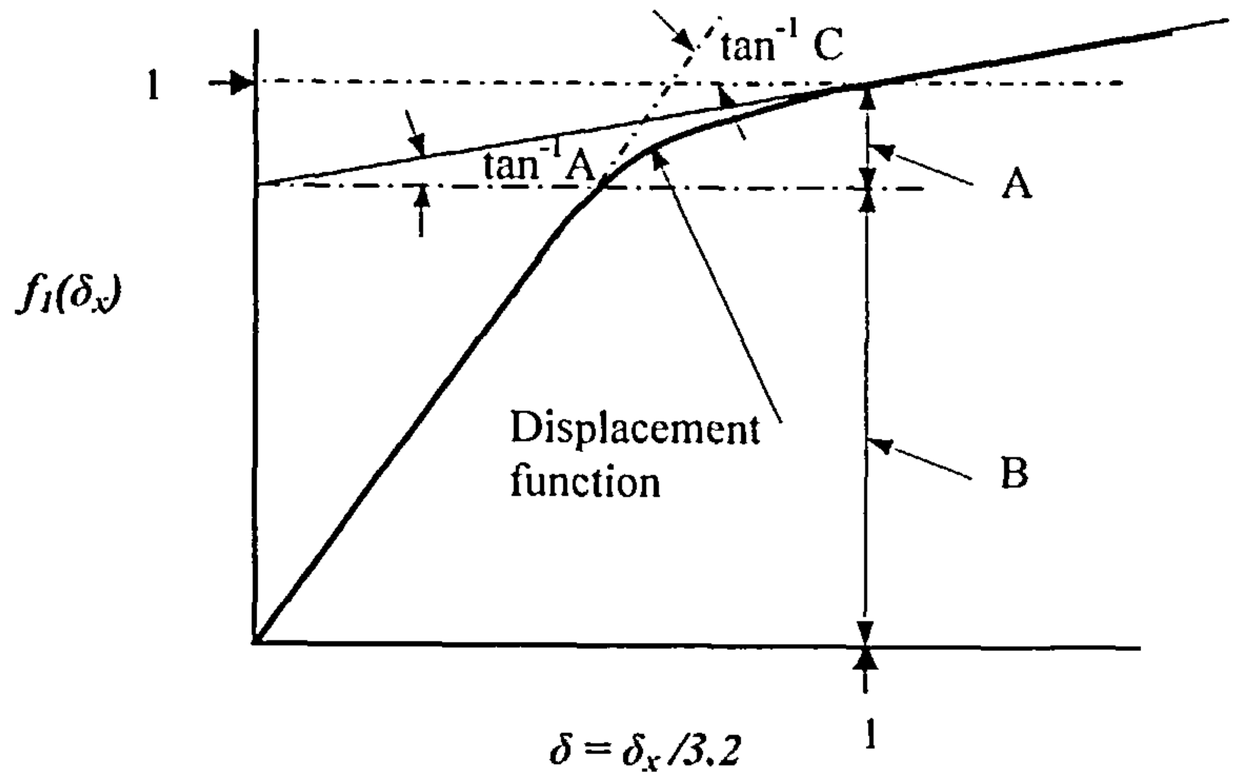

Figure 4.10 The graphical representation of Equation (7)

where

$f_1(\delta_x)$	=	the displacement function = $P/P_{3.2}$
δ	=	the joint displacement divided by the maximum slip (3.2mm)
δ_x	=	the joint displacement at load P_x
A	=	the stiffness of the tangential line with the displacement function at $\delta = 1$
B	=	the intercept of the tangent line with the displacement function.
C	=	the initial tangent stiffness of the displacement function.
D	=	a constant.

As the function $f_1(\delta_x)$ is unity at a slip of 3.2mm, (A + B) must be unity and if C is a sufficiently large negative number, $(1 - e^{C\delta x/3.2})^D$ will also be effectively unity.

To determine the constants A, B, C and D the reduced load graphs of a selection of the 2.65mm, 3.00mm and 3.35mm diameter joints tests were combined to form a data base for each nail size against which least squares non linear regression analysis fits using Mathcad [51] were performed. The data bases were also aggregated to enable a least squares non linear regression fit to be obtained for the combined nail sizes. The joint configurations selected for each nail size are given in Table 4.2 and five replicates were used for each test set: As the data for the Mathcad analysis was processed in Excel [50], the capacity of the software limited the maximum number of tests able to be included to approximately 135. This had no significant effect on the accuracy of the displacement functions obtained.

Tests set nominal nail diameter	Nail configurations used
2.65	CW; EB; EC; ED; EG; EF; RZJ; RZG.
3.00	ED; EF; EG; EJ; EH; EI; EK; RZJ.
3.35	ED; EF; EG; EH; EJ, EK, RZJ

Table 4.2 Joint nailing configurations used for test sets

Mathcad has a number of functions for performing least squares non linear regression and the one most suitable for use with non-linear equations is G*enfit*. The algorithm used is based on the Gauss Newton method [76] as modified by Levenberg-Marquardt [51]. The key concept underlying the technique is that a Taylor series expansion is used to express the non-linear equation in an approximately linear form, curtailing after the first derivatives. Initial estimates are given to the unknown constants and by applying least squares theory and iterating until the solutions converge, those constants which give the minimum error in the fit against the data are determined.

Least squares regression will generate the optimum values of constants A, B, C and D for each reduced load data base, however, because the data bases differ between the nail sizes, the values of the respective constants for each data base will also differ. To obtain equations which could be compared across the nail sizes, and also with the results from joints made with plywood gusset plates, pre-fixed values were assigned to A and B. From the analysis of a limited number of tests, values of 0.32 and 0.68 were assigned to A and B respectively and C and D were determined from the regression analysis. The displacement functions obtained are given in equations (8), (9), (10) and (11) and are also plotted against the associated reduced load data plots on Figures 4.11 and 4.12.

Nail Diameter	Displacement Function	
2.65mm	$f(\delta_x) = (1-e^{-1.905\delta x})^{0.801}(0.1\delta x + 0.68)$	....(8)
3.00mm	$f(\delta_x) = (1-e^{-1.676\delta x})^{1.2}(0.1\delta x + 0.68)$	....(9)
3.35mm	$f(\delta_x) = (1-e^{-1.865\delta x})^{0.904}(0.1\delta x + 0.68)$	....(10)
All diameters	$f(\delta_x) = (1-e^{-1.712\delta x})^{0926}(0.1\delta x + 0.68)$	....(11)

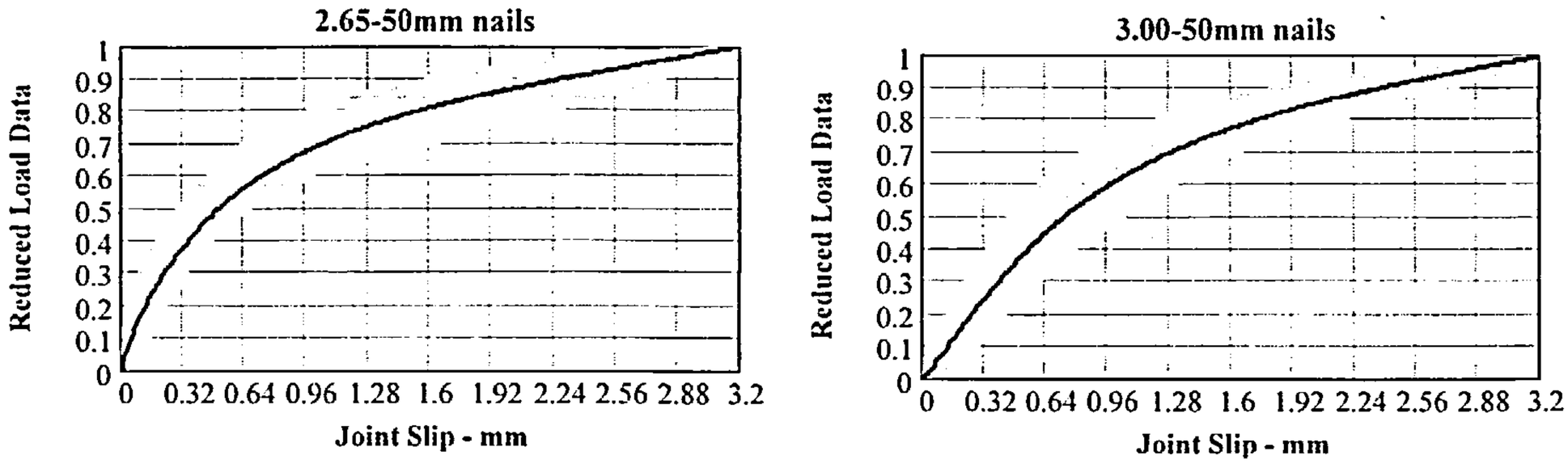

Figure 4.11 Regression graphs for 2.65mm, 3.00mm, and 3.35mm diameter nails

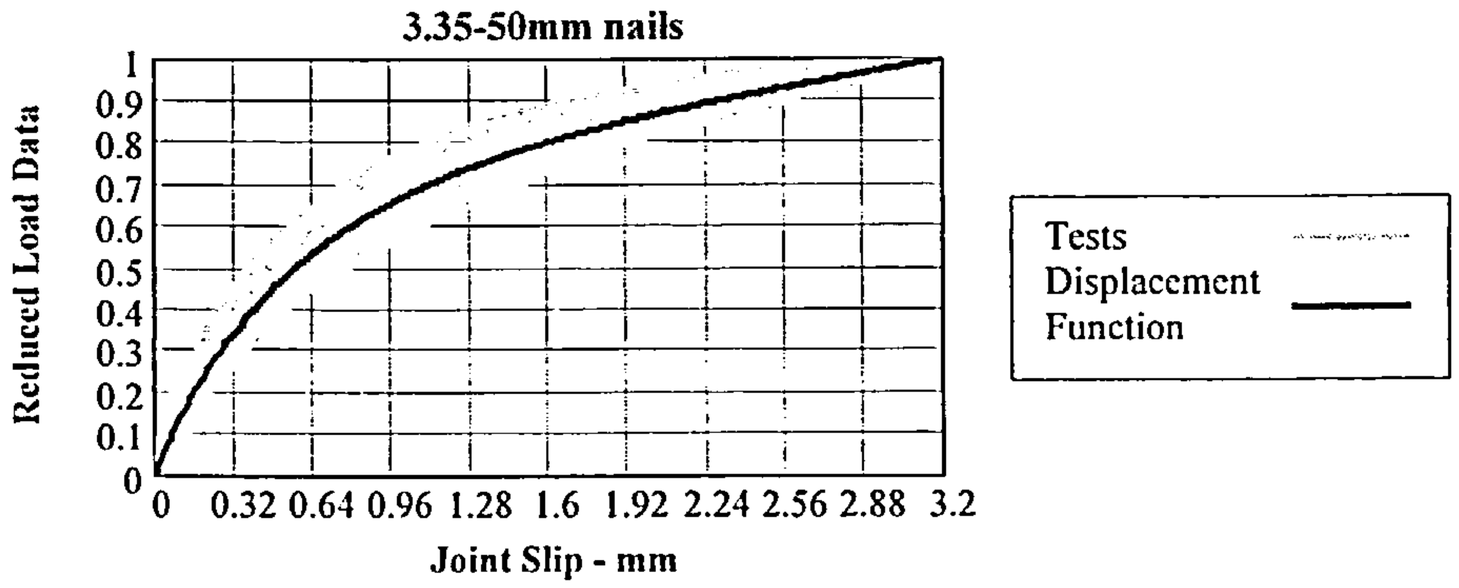

Figure 4.11 cont'd. Regression graphs for 2.65mm, 3.00mm, and 3.35mm diameter nails

To confirm that the use of pre-fixed values for A and B introduced no significant error to the equation a full regression fit was undertaken for each nail size and also for the combined data. The fits confirmed there had been no loss in accuracy. The result of the full regression fit against the combined data is given in equation (12) and the comparison with equation (11) is given in Figure 4.12. It is to be noted that the plots of the equations are effectively coincident and the graphs cannot be discriminated.

$$f(\delta_x) = (1-e^{-1.625\delta x})^{0.908}(0.096\delta x + 0.696) \qquad ...(12)$$

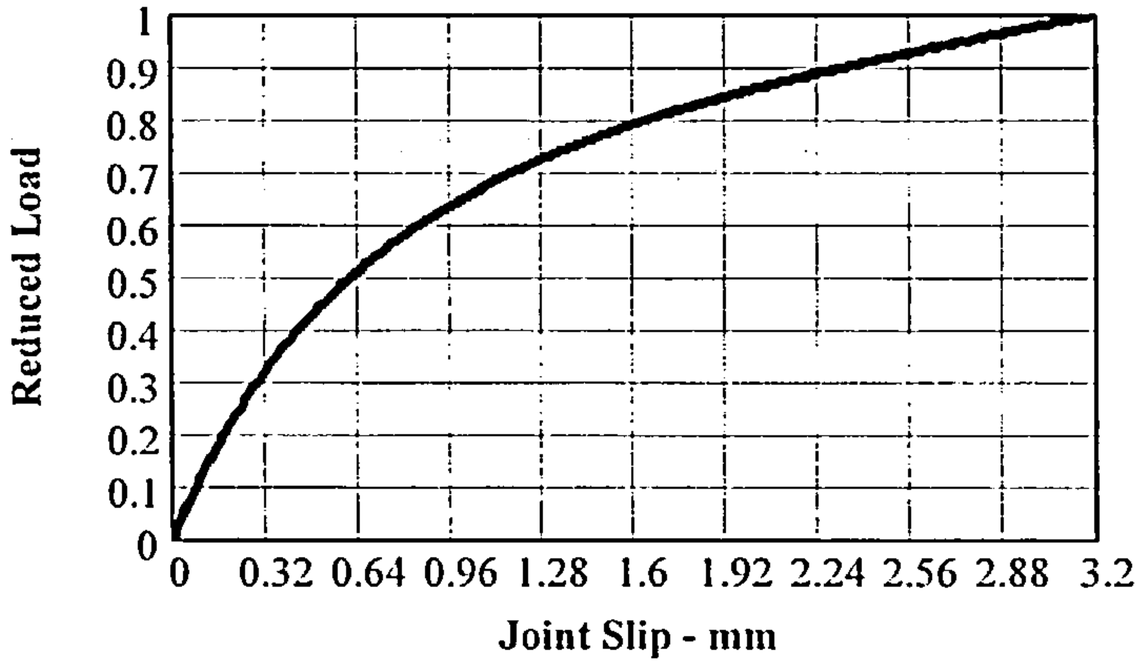

Figure 4.12 Regression graphs in equations (11) and (12) against the combined 2.65mm; 3.00mm and 3.35mm nail joint data.

It is to be noted that there is a significant spread of the reduced load data for each nail size and the coefficient of determination, R^2, for each fit is:

Nail Diameter	R^2 value	Nail Diameter	R^2 value
2.65mm	0.83	3.35mm	0.881
3.00mm	0.883	All diameters	0.873

A factor contributing to the spread of the data is that the same steel gusset plates were used for at least 5 tests and on occasions 20 tests and where the nail was bearing onto the plate at the plate-timber interface the predrilled holes were increasingly deformed with each subsequent test. This reduced the

degree of fixity of the nail, allowing the nail rotation to increase with each test and the stiffness of the load-slip graph to reduce.

The displacement functions in equations (8) to (11) are shown on Figure 4.13.

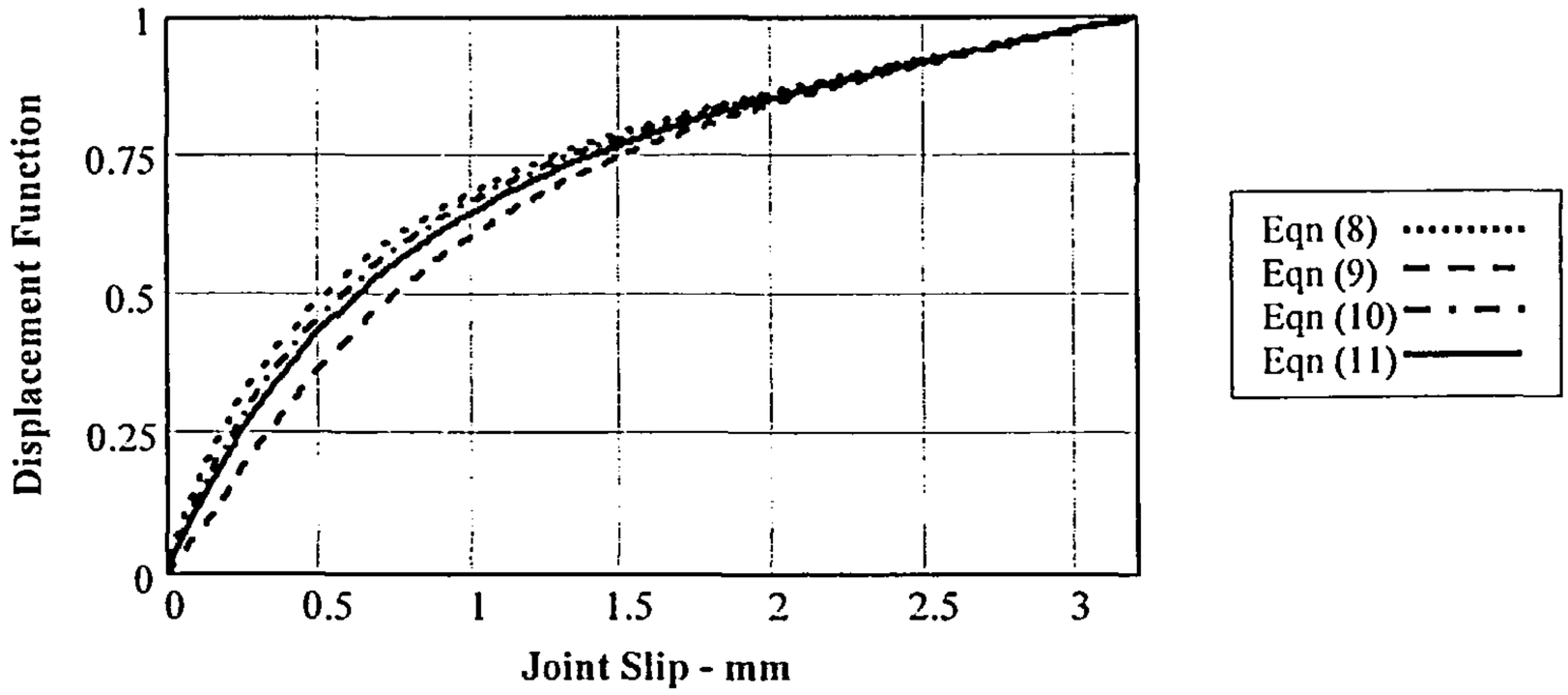

Figure 4.13 Displacement functions given in equations (8),(9),(10) and (11)

The displacement functions using 2.65mm and 3.35mm diameter nails are reasonably comparable and both exhibit much stiffer behaviour that the 3.00mm nail diameter displacement function. It had been expected that all graphs would be comparable in behaviour and the reduced stiffness of the 3.00mm diameter nails was not expected. There is no obvious reason why this should be the case and is likely to relate to factors associated with the frequency of use of the gusset plates; a reduced bearing resistance in the 3.00mm diameter nails and tolerance variations in the size of the predrilled holes.

The displacement functions derived by Mack [6], Kermani *et al* [75] and McLain [7] for joints using steel gusset plates are given in equations (13), (14) and (15) respectively and after reduction to unit values at the maximum slip, are compared with equation (11), the average displacement function for the three nail sizes, in Figure 4.14.

Because Mack's [6] function is only valid up to a slip limit of 2.54mm, equations (11) and (14) have been adjusted to equate to unity at that slip. Also, as the Kermani *et al* [75] function is a function of the number of nails in the joint, an average of 16 nails has been used in that equation to equate to the average number of nails used for the joints in the reduced load data base. In determining the coefficients for the McLain equation [7], a timber density of 600Kg/m^3 has been used.

$$fMack(\delta x) = (1-e^{-2.953\delta x})^{0.5}\,(0.193\delta x+0.51) \quad \ldots.(13)$$

$$fKermani(\delta x) = (83(1-e^{-0.75\delta x}) - 0.73N\delta x e^{-0.75\delta x}) \quad \ldots.(14)$$

$$fMcLain(\delta x) = 0.545\log(1+ 28.24\delta x) \quad \ldots.(15)$$

where x is the joint slip and N is the number of nails in the joint.

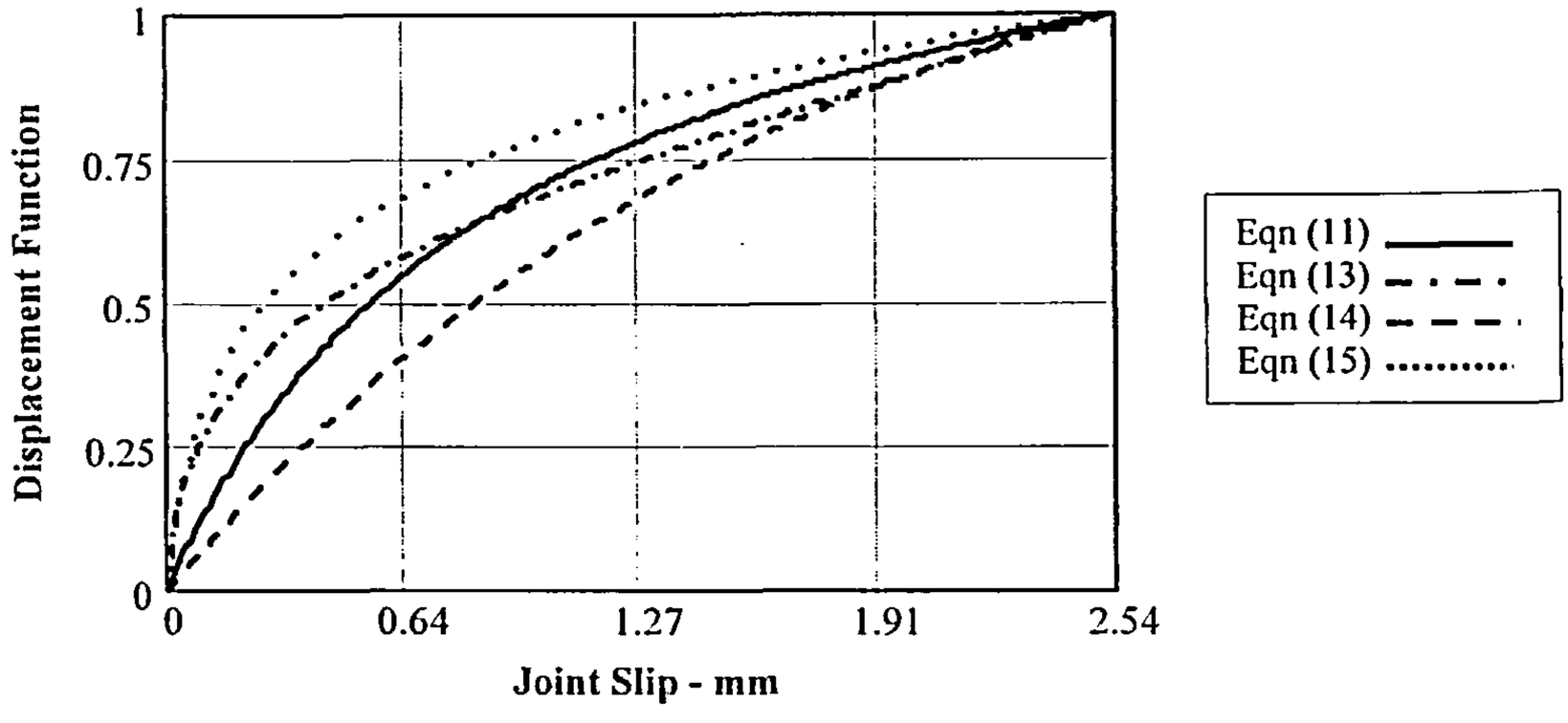

Figure 4.14 The average displacement function – eq'n (11); Mack's displacement function – eq'n (13); Kermani *et al* displacement function – eq'n (14); McLain's displacement function – eq'n (15)

The joint displacement function obtained from the test programme is considerably stiffer than the Kermani *et al* function over the full slip range and as the number of nails in the joint increases, the differences will increase even more. In regard to the Mack function, beyond 0.8mm slip the functions are reasonably comparable, varying by approximately 5% at most in strength. Less than 0.8mm slip. Mack's function is stiffer and stronger and at a slip of 0.4mm is approximately 20% greater in strength and stiffness. This difference is more than likely to be due to the fact that Mack's joints were formed without the use of spacers, resulting in a stiffer behaviour of the joint at the lower loads. In regard to the McLain equation, it has the strongest and stiffest profile of all of the functions but bears no resemblance to the behaviour of the joints in the test programme. It is however interesting to note that the test programme displacement function is approximately the average of all of the functions considered.

From the analysis, the displacement function to be used will be:

$$f_1(\delta_x) = (1\text{-}e^{-1.712\delta x})^{0926}(0.1\delta x + 0.68) \qquad \ldots.(16)$$

4.4.2 Density Function ($f_2(D)$)

From equations (4) and (16), at 3.2mm slip, $f_1(\delta_x) = 1$ and $P = P_{3.2}$, the following relationship will exist:

$$P_{3.2} = (1) f_2(D) f_3(mc) f_4(d) f_5(f_u) f_6(k_g) f_7(r) f_8(S_p) f_9(l) \qquad \ldots.(17)$$

To investigate the effect of the timber density on joint behaviour, the joint load at 3.2mm slip ($P_{3.2}$) was compared using sets of joints with differing values of density but having the same nailing configuration and the same nail diameter. This ensured that the effect of nail strength; nail diameter; number of nails;

nail row and spacing functions would be the same between the sets and would not influence the comparison. Also, to eliminate the effect of moisture content, only samples with comparable moisture contents were used. On this basis, for test sets 1 and 2, equation (17) can be written:

$$P1_{3.2} = f_2(D1)\, f_3(mc)\, f_4(d)\, f_5(f_u)\, f_6(k_g)\, f_7(r)\, f_8(S_p)\, f_9(l) \quad \text{.....(17a)}$$

$$P2_{3.2} = f_2(D2)\, f_3(mc)\, f_4(d)\, f_5(f_u)\, f_6(k_g)\, f_7(r)\, f_8(S_p)\, f_9(l) \quad \text{.....(17b)}$$

and dividing equation (17a) by (17b) the relationship becomes:

$$P1_{3.2}/P2_{3.2} = f_2(D1)/f_2(D2) \quad \text{....(18)}$$

A comparison of the average strength and density ratios of the 5 replicate test sets from the testing programme having the maximum difference in timber density, comparable moisture contents and using the same nailing configuration for each nail diameter is given in Table 4.3 to 4.5.

Joint Configuration	**Sample Reference**	**Density Kg/m^3**	**Moisture Content %**	**$P_{3.2}$ N**
EA	S24L/4A-6B	656.08	14.84	17801.81
EA	S25L/7A-9A	598.11	14.28	16408.5
	$f_2(D1)/f_2(D2)$	**1.0969**	**$P1_{3.2}/P2_{3.2}$**	**1.0849**
			% difference between ratios	**1.1%**

Table 4.3 Comparison of strength and density ratios - 2.65mm nail joints

Because a single species of timber was used in the programme, the variation in density was limited. However the tests enveloped a density change of approximately 34%, which was sufficient to assess the density effect and within the bounds of experimental error the result demonstrates that there is a linear relationship between joint strength and timber density. The percentage difference between the ratios of the timber densities and the joint strengths was 1.1% for the 2.35mm diameter nail set tests; 0.76% for the 3.00mm diameter nail set tests and 2.38% for the 3.35mm diameter nail set tests, and if adjustments were made to equate the effect of moisture content between each set, the results would be even closer

Joint Configuration	**Sample Reference**	**Density Kg/m^3**	**Moisture Content %**	**$P_{3.2}$ N**
EJ	S28L/11C-12C	486.67	14.05	17449.5
EJ	S29L/11A-12C	598.11	14.11	21413.69
	$f_2(D1)/f_2(D2)$	**0.8211**	**$P1_{3.2}/P2_{3.2}$**	**0.8149**
			% difference between ratios	**0.76%**

Table 4.4 Comparison of strength and density ratios - 3.00mm nail joints

Joint Configuration	Sample Reference	Density Kg/m^3	Moisture Content %	$P_{3.2}$ N
EG	S33L/9A-10B	632.28	14.18	43884.97
EG	S31L/3A-4C	472.66	13.92	33585.52
	$f_2(D1)/f_2(D2)$	1.3377	$P1_{3.2}/P2_{3.2}$	1.3067
			% difference between ratios	2.38%

Table 4.5 Comparison of strength and density ratios - 3.35mm nail joints

The linear relationship between density and joint strength agrees with the findings of other researchers McLain [7], Mack [71], Morris [77], Kermani *et al* [75] and the density function $f_2(D)$ to be used for timber joints with steel gussets connected by fully overlapping nails in single shear will be:

$$f_2(D) = Density \quad \ldots.(19)$$

4.4.3 Moisture Content Function ($f_3(mc)$)

As mentioned in Chapter 2, timber is a hydroscopic material and moisture content is an important factor influencing the load carrying capacity and stiffness behaviour of timber joints. Over the period of the testing programme the moisture content of the timber used in the joints made with steel gusset plates ranged from 11% to 15.5% and as this is a significant variation the effect of change in moisture content on the joint strength has been taken into account in the analysis.

Based on measurements of the strength of a set of closely matched specimens, each at a different moisture content, Bodig *et al* [78] have given an indication of how the moisture content alters the mechanical properties of Douglas Fir and their graph showing the relationship developed is given in Figure 4.15.

From the Figure, within the range 10% to 15%, the strength of the timber can be taken to be linearly related to the change in moisture content and over this range the increase in strength per 1% reduction in moisture content is approximately 5.9%. It is also to be noted that in STEP 1, section A4, Table 2, [79] the percentage increase in compression strength parallel to the grain for a 1% reduction in moisture content is 5%. In EN 384: 1995 [80], however, the increase in compression strength parallel to the grain is only 3% for a 1% decrease in moisture content.

The above recommendations vary by almost 100% and with a 4.5% variation in the moisture content in the testing programme, the difference between a factor of 3% and 5.9% would result in a strength variation of over 13%. This was considered to be too large to be ignored and strength tests were carried out to develop a programme specific moisture content factor.

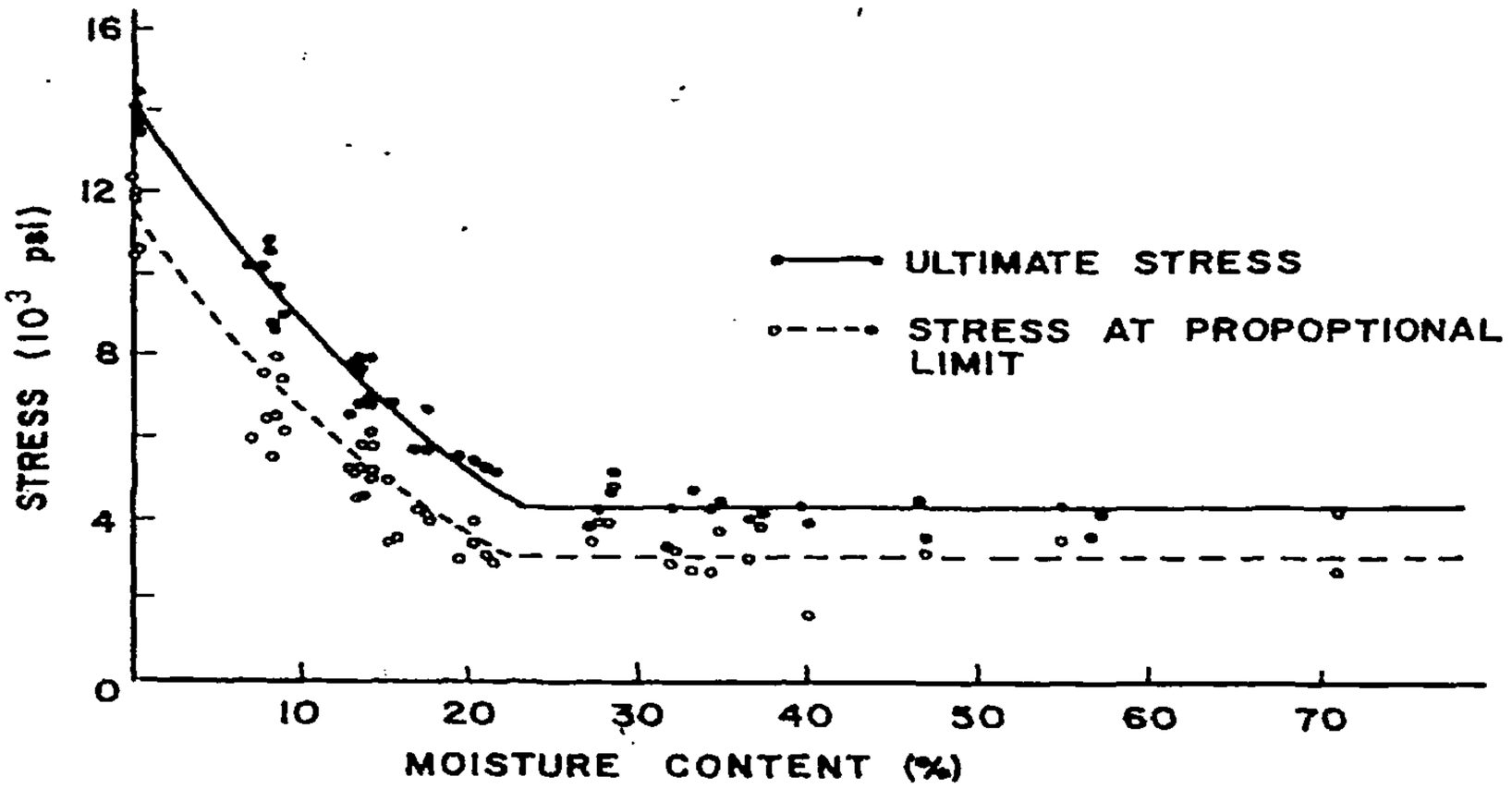

Figure 4.15 Relationship between compression parallel to the grain properties and moisture content of Douglas Fir [78]

Sixteen clear samples were cut from adjacent sections of a timber plank and eight were stored in the timber store area and the remaining eight in a laboratory for a period of seven weeks after which the average moisture content of the samples in the store area was 14.32% and in the laboratory area was 10.14%. Joints were then fabricated using steel gusset plates connected by 4 fully overlapping 3.35m diameter by 50mm long Rynail nails with nailing configuration CO and tested, all in one day. The average load displacement curve for each set of tests was obtained using least squares regression analysis and it was found that the strength of the joints made with the laboratory samples were 11.5% stronger than those made with the samples from the timber store area. Adopting a linear relationship between strength and moisture content and setting the strength of the samples with a moisture content of 14.32% at an arbitrary value of unity, the following equation was obtained for the joint strength factor:

$$y(mc) = -0.0275(mc) + 1.394 \qquad \text{.....(20)}$$

where $y(mc)$ is the strength factor of the timber at a moisture content of mc. Conversion of the strength of a joint using timber at any moisture content, mc, to the strength it would have with timber at a moisture content of 12% is achieved by multiplying the joint strength by the following moisture content factor:

$$f(mc) = y(12)/y(mc) \qquad \text{.....(21)}$$

Converting the strength of joints made with timber at 13% moisture content to the strength at a moisture content of 12%, from equation (20), y(13) = 1.0363 and y(12) = 1.0638 and inserting these values into equation (21) the moisture content factor becomes 1.0266. In other words the strength in the joint will increase by 2.66% for a 1% decrease in moisture content. This is more in line with the 3% change

recommended in EN 384: 1995 [80] rather than the 5% change given in STEP 1 [79]. To take account of the effect of moisture content on the joint strength in the analysis programme, the value of the joint load at 3.2mm slip ($P_{3.2}$) in all of the tests has been converted to the equivalent load at a 12% moisture content by multiplying $P_{3.2}$ by the moisture content factor, *f(mc),* based on the moisture content of the timber used in the joint. This results in the joint strength equation (4) being based on a moisture content of 12% and allows all of the joint functions to be derived on the same basis. When the generic equation has been developed, to obtain the strength at the moisture content of the timber used in the joint the equation will be divided by the moisture content factor *f(mc)*.

The moisture content function $f_3(mc)$ to be used for timber joints with steel gussets connected by fully overlapping nails to convert the strength equation from its base of 12% moisture content to a strength at any moisture content *mc* will be:

$$f_3(mc) = 1/f(mc) \qquad \text{.....(22)}$$

4.4.4 Nail Diameter Function ($f_4(d)$) and Nail Strength Function ($f_5(f_u)$)

With single row joints using two lines of fully overlapping nails, for each nail size the load displacement relationship per unit density at 3.2mm slip and at a moisture content of 12% given in equation (4) can be written as:

$$P_{3.2}\, y(12)/y(mc)/f_2(D) = f_4(d)\, f_5(f_u)\, f_6(k_g)\, f_7(r)\, f_8(S_p), f_9(l) \qquad \text{....(23)}$$

where

$P_{3.2}$	is the load in the joint at a slip of 3.2mm.
$y(12)/y(mc)$	is the factor to convert the joint strength to an equivalent strength at 12% moisture content.
$f_2(D)$	is the density of the timber in the joint
$f_7(r)$	is the row function and will be taken as unity for a single row of nails
$f_8(S_p)$	is the row spacing function and will also be taken as unity for a single row of nails
$f_9(l)$	is the number of lines of overlapping nails in the joint

the remaining functions $f_4(d)\, f_5(f_u)\, f_6(k_g)$ being unknowns to be evaluated.

From the joint test results, values for ($P_{3.2}\, y(12)/y(mc)$/Density) were obtained for joints with a single row of nails using nail configuration CO. Also the equivalent function was obtained from the analysis of multi-row joints with row spacing equal to or greater than 4×0.7×7 times the nail diameter by dividing the $P_{3.2}\, y(12)/y(mc)$/Density) result by the number of rows in the joint. There were minor differences between the single row and multi-row values and the average result for each nail size are given in Table 4.6.

The 'values' give the load per unit density per single row of nails at a moisture content of 12% and at a slip of 3.2mm slip using joint configuration CO.

Nominal nail diameter – mm	***$P_{3.2}y(12)/y(mc)$*/density/number of rows**
2.65	10.5298
3.00	12.5101
3.35	15.2004

Table 4.6 Value of $P_{3.2}y(12)/y(mc)$/density/number of rows for each nail test set

From equation (23), with $f_9(l) = 2$, (equating to the two lines of nails in the joint) the following equations can be established for the load taken by a pair of fully overlapping nails in single shear in a joint with steel gusset plates:

$$10.5298/2 = f_4(d_{2.65})\, f_5(f_{u2.65})\, f_6(k_g) \quad \text{....(24a)}$$

$$12.5110/2 = f_4(d_{3.00})\, f_5(f_{u3.00})\, f_6(k_g) \quad \text{....(24b)}$$

$$15.2004/2 = f_4(d_{3.35})\, f_5(f_{u3.35})\, f_6(k_g) \quad \text{....(24c)}$$

Equations (24a), (24b) and (24c) are functions of the nail diameter, nail strength and the generic function of the joint and by dividing by equation (24a) are reduced to functions of the nail diameter and nail strength only:

$$1 = f_4(d_{2.65}/d_{2.65})\, f_5(f_{u2.65}/f_{u2.65}) \quad \text{....(25a)}$$

$$1.4322 = f_4(d_{3.00}/d_{2.65})\, f_5(f_{u3.00}/f_{u2.65}) \quad \text{....(25b)}$$

$$1.4000 = f_4(d_{3.35}/d_{2.65})\, f_5(f_{u3.35}/f_{u2.65}) \quad \text{....(25c)}$$

When designing with steel, concrete, masonry etc., whether in elastic or plastic conditions, the strength equations are linear functions of the material strength. In accord with this a linear function has also been used for the nail strength function in the timber joint equation. On this basis the nail strength function becomes:

$$f_5(f_u) = f_u/f_{u2.65} \quad \text{...(26)}$$

where

f_u is the tensile strength of the nail size used in the joint

$f_{u2.65}$ is the tensile strength of the 2.65mm diameter nail

From tests on the Rynail nails the tensile strength of the wire in the 2.65, 3.00 and 3.35mm diameter, 50m long nails was 804, 769 and 829 N/mm^2 respectively, as reported in Appendix B. From equation (26) the nail strength functions for each nail size will be as given in Table 4.7.

Nail diameter – mm	Nail strength function $f_5(f_u)$
2.65	804/804
3.00	769/804
3.35	829/804

Table 4.7 Nail strength functions for the nails used in the steel gusset joints

By inserting the nails strength functions in equations (25a, 25b, 25c) the nail diameter function is obtained. Using the actual nail diameter sizes, 2.66mm, 3.01mm and 3.36mm as given in Chapter 3, performing a least squares linear regression fit and adopting a power function relationship, the nail diameter function $f_4(d)$ is:

$$f_4(d) = 0.2458\ (d)^{1.4468} \qquad \ldots.(27)$$

The coefficient of determination R^2 against the fit was 0.9827 and the regression plot against the data is shown in Figure 4.16.

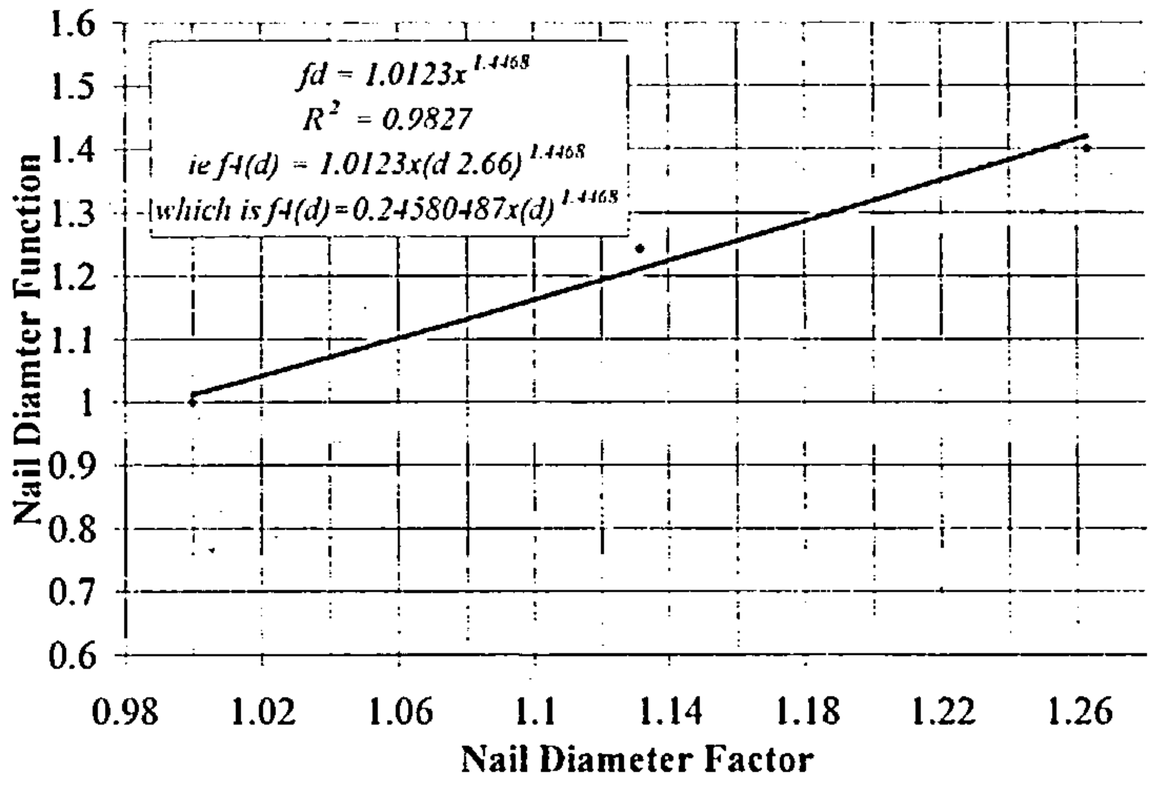

Figure 4.16 Nail diameter function regression fit

From the research by Wikinson [81], based on the original theory put forward by Kuenzi [82], the nail diameter function was a function of $d^{1.75}$, which is the same function developed by Mack [6] and also used by Morris and Gajjar [84]. In Goh's research [12] the function has been based on d^2. With the ultimate strength theories a function of $d^{1.65}$ was developed from Larsen's equations [45] by Smith *et al* [54] and in EC5 [15], for small nail diameters in predrilled holes, the function is $d^{1.8}$.

A comparison between the diameter function in equation (27) and the functions developed by Wilkinson [81] and EC5 [15] is given on Figure 4.17. As the nail diameter increases, equation (27) shows a much lower rate of increase than the other models and is 7.3% less than the Eurocode function at a nail diameter of 3.35mm. As the nail diameter gets smaller however, the function gets closer to the

others and will exceed these models when the diameter is less than 2.65mm. Only three nail sizes were used in the testing programme and the function can only be taken as valid for these nail sizes.

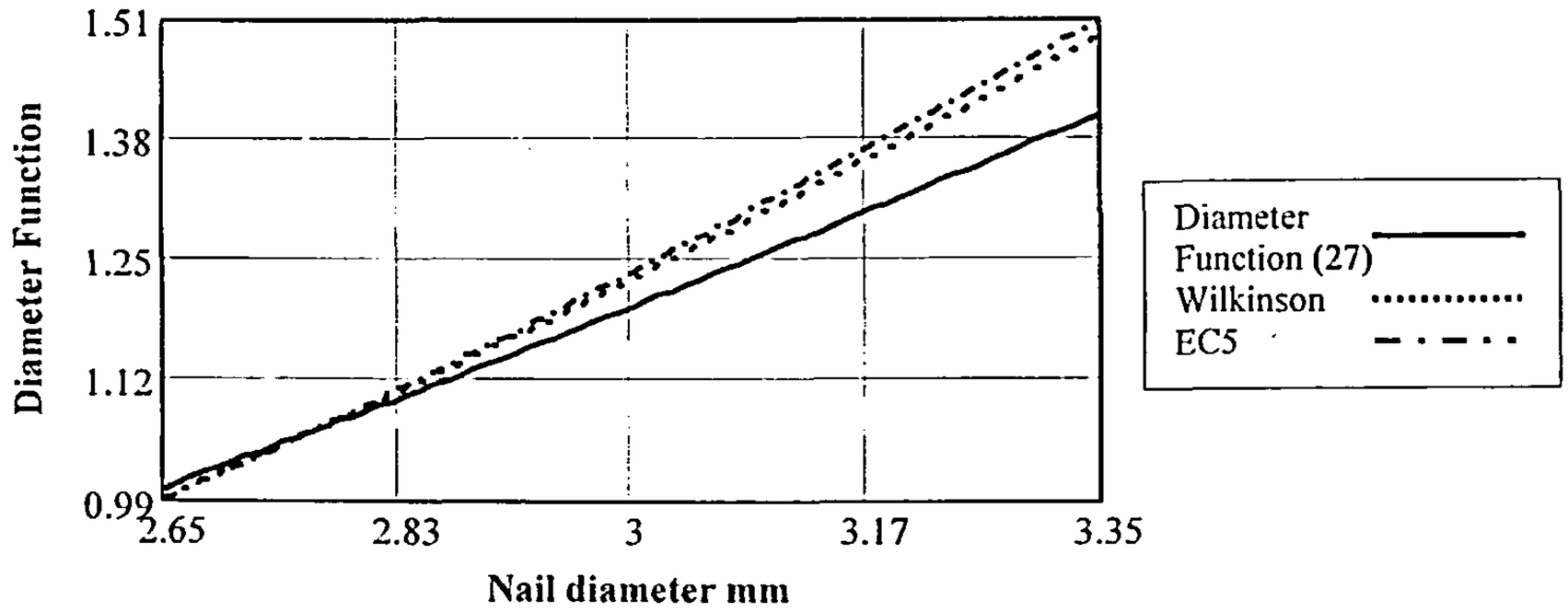

Figure 4.17 Comparison of equation (27) with the diameter functions used by Wilkinson [81]; and EC5 [15].

4.4.5 Generic Function ($f_6(k_g)$)

In Mack's original research [6], this function is referred to as the 'species factor', and was later defined by him as a multiple of the basic density of the timber (ie the oven dry mass per unit green volume) [71]. This gave the impression that the factor was solely a function of the density of the timber in the joint.

Such an interpretation of the function is considered to be incorrect and in this analysis the timber density function has been shown to be a factor in its own right and has been addressed in section 4.4.2. The species factor, or the 'generic function' as it is called in this analysis, is a separate function which is independent of the density of the material in the joint.

The generic function is the 'fit' function for the test set-up being used and takes into account those factors that are relevant to joint behaviour and have not been addressed in the individual functions $f_1(\delta)$ to $f_9(l)$. It will be relevant to all joints that are assembled in the same way as those that have been tested in the programme and if any changes are made, the value of the function will also change.

For example, the steel gusset joints in the testing programme have incorporated predrilling of the timber; have a gap between the timber and the steel gussets; have only used thick steel gusset plates predrilled by particular sizes of predrill. The generic function to be developed will apply to all joints with these characteristics. If, however, any of these factors are changed the generic function will be affected and must also be adjusted to take the effect of the change into account.

The relationship between the generic function $f_6(k_g)$ and the joint strength is given in equations (24a), (24b) and (24c) and inserting the nail strength functions given in Table 4.7 and the nail diameter function given in equation (27) into these equations, the following expressions are obtained:

$$10.5298/2 = (0.2458(2.66)^{1.4468})(804/804)\, f_6(k_g) \quad \text{....(28a)}$$

$$12.5110/2 = (0.2458(3.01)^{1.4468})(769/804)\, f_6(k_g) \quad \text{....(28b)}$$

$$15.2004/2 = (0.2458(3.36)^{1.4468})(829/804)\, f_6(k_g) \quad \text{....(28c)}$$

The generic function $(f_6(k_g))$ associated with each nail diameter can be readily obtained and the values are given in Table 4.8 for each nail diameter together with the average for all nail diameters.

Nail diameter – mm	Generic function
2.66	5.20091
3.01	5.40268
3.36	5.19311
Average for all nail diameters	**5.26557**

Table 4.8 The Generic function $(f_6(k_g))$ for steel gusset plate joints with a pair of fully overlapping nails

The function should be the same for all nail diameters and as the deviations from the average are +2.6% and -1.4%, this is considered to be an acceptable result. The generic function $(f_6(k_g))$ for steel gusset plate joints with a pair of fully overlapping nails is taken as the average value for all nail sizes - 5.26557.

4.4.6 Nail Row Function $(f_7(r))$

Some researchers [6, 12, 84, 172] have suggested there is a non linear relationship between joint strength and the number of rows~nails in a joint. As the numbers of rows~nails are increased the joint strength also increases but at a rate which is less than that obtained by multiplying the single nail strength by the number of nails in the joint.

To investigate this effect an analysis was carried out on the results of those test joints with a row spacing approximately equal to or greater than 4 times the minimum values recommended in EC5 [15]. As discussed in section 3.4.4.1, when using fully overlapping nails the minimum row spacing will be 2 times the minimum spacing recommendations given in EC5 and the upper limit of approximately 4 times the minimum spacing has been selected as the benchmark for the row function analysis. It is considered that any row spacing effect would be able to be ignored at and beyond this limit.

The row spacing criteria used for the selection of the joints to be analysed for each diameter has been chosen to try and align with the latest spacing criteria in EC5 [15]. Table 8.1 of the code gives an upper limit of *14d* and a lower limit of *5d* as the extremes for nails which do not fully overlap. As stated in the previous paragraph, a factor of 2 is applied to these limits and also applying the 0.7 coefficient given in

clause 8.3.1.4 of the code when using joints formed with steel gusset plates, the row spacing criteria used for the joint selection are given in Table 4.9.

Nail diameter mm	**Minimum spacing $0.7\times2\times5\times d$**	**Maximum spacing $0.7\times4\times7\times d$**	**Acceptable spacing for the nail row function analysis**
2.65	18.55	51.94	$\geq$50
3.00	24.5	59.00	$\geq$60
3.35	32.93	65.86	$\geq$ 66

Table 4.9 Criteria used for row spacing in the Row Function $(f_7(r))$ analysis

With multi-row joints using two lines of fully overlapping nails, for each nail size the load displacement relationship per unit density at 3.2mm slip and at a moisture content of 12% given in equation (23) will apply. Using joints with a row spacing equal to or greater than the criteria given in Table 4.9, the row spacing function $f_8(S_p)$ will be unity. Also, as all of the joints tested in the programme had 2 lines of nails, the nail line function $f_9(l)$ will be 2 and for each nail diameter equation (23) can be rewritten as:

$$P_{3.2}\, y(12)/y(mc)/f_2(D) = f_4(d) f_5(f_u) f_6(k_g) f_7 \times 1 \times 2 \qquad \ldots.(29)$$

For joints with a single row of nails (configuration CO), the row function will be taken as unity. Applying equation (29) to each nail diameter and dividing by the equation for joint configuration CO, functions $f_4(d)$ $f_5(f_u)$ $f_6(k_g)$ will be eliminated and the row function $f_7(r)$ for each nail diameter will be given as:

$$f_7(r)r = (P_{3.2} y(12)/y(mc)/f_2(D) \text{for multi-nail joint}) / (P_{3.2}\, y(12)/y(mc)/f_2(D) \text{ for joint CO}) \qquad \ldots.(30)$$

where r is the number of rows in the joint.

Equation (30) was evaluated for all multi-nail joints for each nail diameter compliant with the row spacing criteria given in Table 4.9 and the results are given in Table 4.10. A linear regression analysis was carried out on the data for each nail diameter and for the combined data and the latter is shown in Figure 4.18. The coefficient of determination R^2 exceeded 0.99 in all of the fits and the row function relationship for each nail diameter was:

2.65mm diameter nails	$f_7(r) = 0.9809 \times r$	.... (31a)
3.00mm diameter nails	$f_7(r) = 0.9743 \times r$	.... (31b)
3.35mm diameter nails	$f_7(r) = 1.0098 \times r$	.... (31c)
All nail diameters	$f_7(r) = 0.9932 \times r$	.... (31d)

2.65mm diameter config'n	Number of rows in joint	$f_7(r)\times r$	3.00mm diameter config'n	Number of rows in joint	$f_7(r)\times r$	3.35mm diameter config'n	Number of rows in joint	$f_7(r)\times r$
CO	1	1	CO	1	1	CO	1	1
EF	3	2.9269	EJ	3	2.93939	EJ	3	2.931986
RZJ	4	3.78403	EH	3	3.02633	EJ	3	3.001078
EG	5	4.69578	EJ	3	3.05408	EJ	3	3.00962
EG	5	5.22983	EH	3	3.25117	EJ	3	3.0491
			RZJ	4	3.83104	EH	3	3.05971
			EK	5	4.68470	EL	3	3.17687
			EI	5	4.77865	EI	5	4.90541
			EK	5	4.94713	EI	5	4.913565
			EK	5	5.03603	EK	5	4.95732
			EP	6	5.62166	EK	5	4.97386
						EK	5	5.00639
						EK	5	5.03142
						EI	5	5.07018
						EI	5	5.08274
						EK	5	5.091228
						EQ	7	7.3415

Table 4.10 Value of $f_7(r)\times r$ for each nail diameter and joint configuration

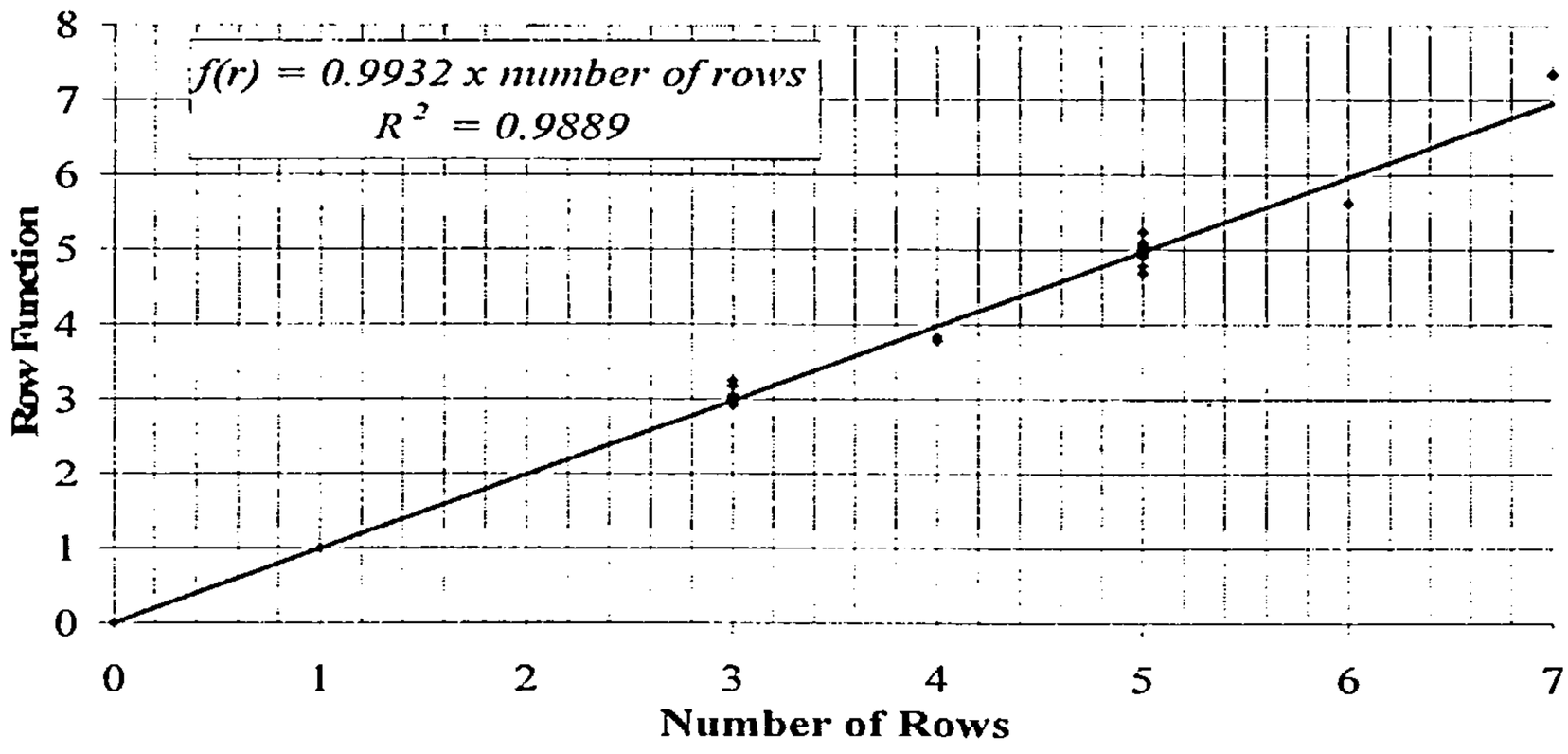

Figure 4.18 Linear regression fit of the Row Function Data in Table 4.8 for 2.65mm, 3.00mm and 3.35mm diameter nails

The row function coefficient for the full data fit is 0.9932, which is effectively unity, and the row function for all nail diameters used in the analysis is:

$$f_7(r) = 1 \times r \quad \ldots.(32)$$

It is to be noted that this disagrees with the finding by Nozynski [103] but is in line with the recommendations in EC5 [15] when using row spacing exceeding 2 times the minimum recommend spacing.

The maximum number of rows used in the testing programme at this spacing was 7 and further testing is required to confirm that the finding will also apply to joints with a greater number of rows.

4.4.7 Row Spacing Function ($f_8(Sp)$)

Although the analysis in section 4.4.6 focussed on a solution for the nail row function, the relationship was obtained using joints with row spacing equal to or exceeding $4\times0.7\times7\times d$, as summarised in Table 4.11.

It is seen that the row spacing used generally exceeded the spacing criteria and by up to 50% in the case of the 3.35mm diameter joints. On this basis the row function must also be considered to be a function of the row spacing and, as the row function has been shown to be unity in this range, the row spacing function for spacing equal to or greater than $4\times0.7\times7\times d$ must also be unity, ie:

$$f(Sp) = 1 \quad \ldots.(33)$$

2.66mm diameter-nailing conf'n	Row spacing in the joint ($4\times0.7\times7\times d$=52.14) mm	3.01mm diameter-nailing conf'n	Row spacing in the joint ($4\times0.7\times7\times d$=59) mm	3.36mm diameter-nailing conf'n	Row spacing in joint ($4\times0.7\times7\times d$=65.86) mm
EF	50	EJ	66.67	EJ	66.67
EG	50	RZJ	66.67	RZJ	66.67
RZJ	66.67	EK	66.67	EK	66.67
		EP	66.67	EQ	66.67
		EH	75	EH	75
		EI	75	EI	75
				EL	100

Table 4.11 The joint row spacing used in the row function analysis

To obtain the relationship for the row spacing function for joints with row spacing between the minimum recommended spacing of $0.7\times2\times5\times d$ up to the $0.7\times4\times7\times d$ limit, the joints in this range were analysed using a similar approach to that used in section 4.4.6. For joints in this range the row function

will be as given in equation (32) and as all of the joints tested in the programme had 2 lines of nails, the nail line function $(f_9(l))$ will again be 2. For each nail diameter, equation (23) can be rewritten as:

$$P_{3.2}\, y(12)/y(mc)/f_2(D) = f_4(d)\, f_5(f_u)\, f_6(k_g) \times (1 \times \mathrm{r}) \times f_8(S_p) \times 2 \qquad \ldots.(34)$$

For joints with a single row of nails (configuration CO), the row spacing function will be taken as unity. Applying equation (34) to each of the results of the joint tests for each nail diameter and dividing by the equation for joint configuration CO, functions $f_4(d)\, f_5(f_u)\, f_6(k_g)$ will be eliminated and the row spacing function $f_6(Sp)$ for each nail diameter will be given as:

$$f_8(Sp) = [(P_{3.2} y(12)/y(mc)/f_2(D) \text{for multi-nail joint})/r]/[(P_{3.2}\, y(12)/y(mc)/f_2(D) \text{ for joint CO}] \qquad \ldots.(35)$$

Equation (35) was evaluated for all multi-nail joints with joint spacing within the range being investigated for each nail diameter and the results are given in Table 4.12. The figure given in brackets for the single row nailing configuration, CO, is used solely to ensure the factor will equate to unity in the data fitting process.

Although joints with a row spacing at 16.67mm is just outside the lower limit for 2.65mm diameter nails, the data was incorporated to give a lower bound to the analysis. A plot of the data was carried out against *Sp/d* for each nail diameter and also for the combined data 'all nail diameter' case and the latter plot is shown in Figure 4.19.

2.65mm diameter -nailing conf'n	Row spacing	$f_8(S_p)$	3.00mm diameter -nailing conf'n	Row spacing	$f_8(Sp)$	3.35mm diameter -nailing conf'n	Row spacing	$f_8(Sp)$
CW	16.67	0.824798	EA	25	0.825531	ED	33.33	0.860199
CW	16.67	0.848831	EB	25	0.848156	ED	33.33	0.932287
CS	16.67	0.872284	ED	33.33	0.82939	EF	50	0.908232
EB	25	0.847486	ED	33.33	0.911396	EF	50	0.929154
ED	33.33	0.828818	RZI	33.33	0.915803	EG	50	0.948316
EC	33.33	0.845586	RZH	42	0.92472	EG	50	0.953271
ED	33.33	0.908487	EN	50	0.928478	EG	50	0.967801
EC	33.33	0.924615	EG	50	0.941668	CO	(65.856)	1
RZG	38	0.962093	EF	50	0.951366			
CO	(52.14)	1	CO	(58.996)	1			

Table 4.12 Value of $f_8(Sp)$ for each nail diameter and joint configuration for a row spacing between $0.7\times2\times5\times d$ and $0.7\times4\times7\times d$

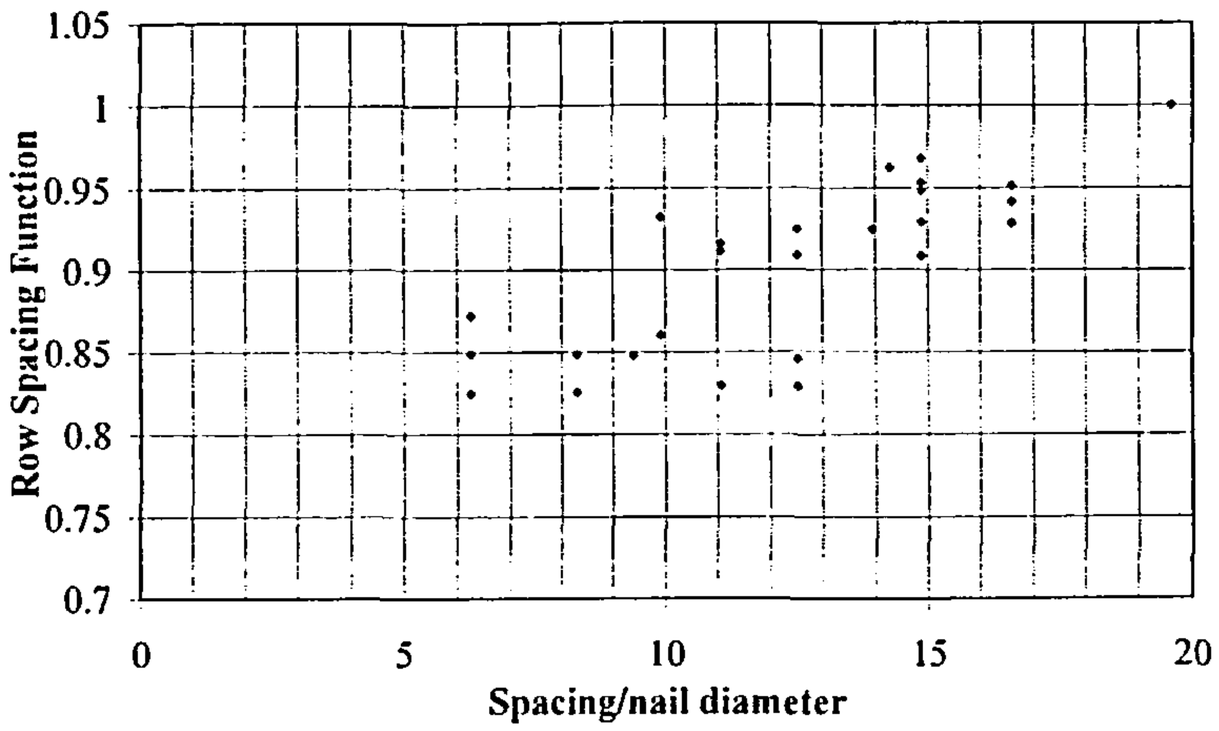

Figure 4.19 Plot of all nail diameter data against row spacing/nail diameter

It is observed that there is a high degree of variability in the data and the coefficient of determination R^2 based on a linear regression fit is 0.6891. However there is a clear trend of a reducing row spacing function as the value of row spacing/nail diameter reduces. A non-linear regression analysis was also carried out against numerous possible non linear functions to obtain the curve that gave the best fit and the optimum solution was found to be:

$$f(Sp) = 0.817392 + 0.0008758\,(Sp/d)^{1.7958} \qquad \ldots.(36)$$

Because of the variability of the data and noting that the maximum change in the value of the spacing function over the data range was only 17.5%, it was decided that a linear relationship would be equally acceptable and was easier to apply. On this basis, using joints with row spacing between $2\times0.7\times5\times d$ and $4\times0.7\times7\times d$, the row spacing function is:

$$f(Sp) = 0.7428 + 0.0132(Sp/d) \qquad \ldots.(37)$$

A comparison between equation (36) and (37) is given on Figure 4.20. It is noted that there is only a relatively small difference between the functions and equation (37) will be used.

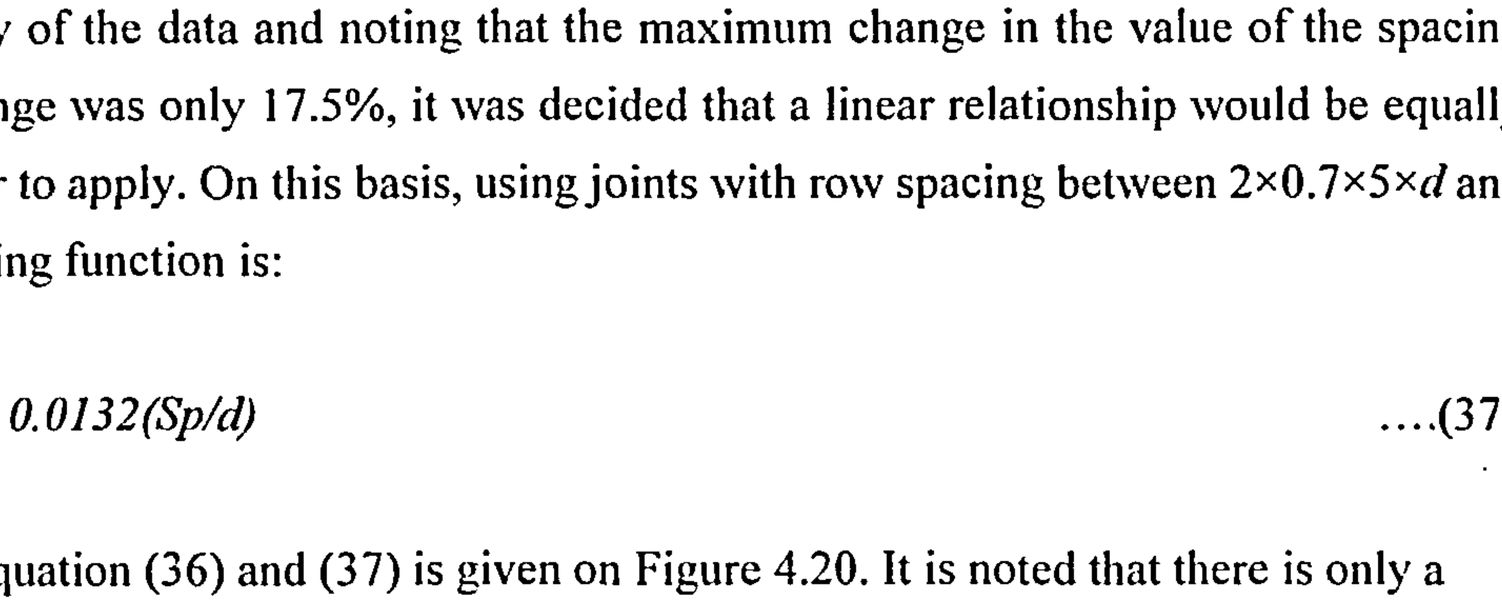

Figure 4.20 Comparison between equation (36) and (37)

Combining the relationships in equations (33) and (37), the row spacing function $f_8(Sp)$ relationship for a joint with steel gusset plates using fully overlapping nails in single shear is:

$$f_8(Sp) = 1 \qquad \text{when the row spacing exceeds } 0.7\times4\times7\times d$$

$$f_8(Sp) = 0.7428 + 0.0132(Sp/d) \qquad \text{when the row spacing is between } 0.7\times2\times5\times d \text{ and } 0.7\times4\times7\times d. \qquad \text{.....(38)}$$

A plot of the function is shown in Figure 4.21 together with the data up to 0.7×4×7×d superimposed.

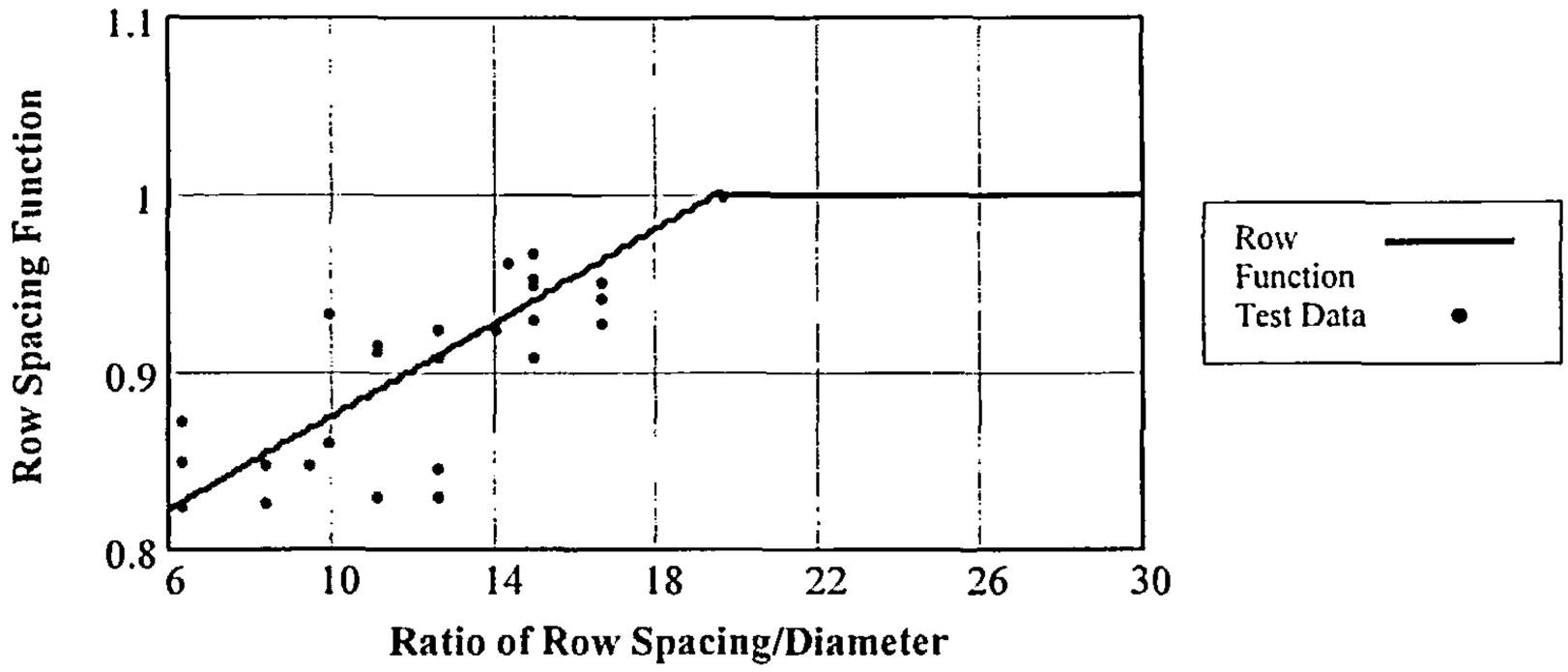

Figure 4.21 Nail Row Spacing Function for all nail diameters

From the testing programme, the graph is valid for a minimum row spacing of 16.67mm for 2.65mm diameter nails, which equates to a row spacing/diameter ratio of 6.29 for all nail sizes. The upper limit is a row spacing/diameter ratio of 19.6 for all nail sizes, above which the factor is unity. At the minimum row spacing/diameter ratio (Sp/d = 7) the function is 0.835. The greatest difference between the equation and the data is associated with a joint configuration using 2.65mm diameter nails where the function is approximately 9.4% greater than the test result. Otherwise the maximum difference is around ± 5%.

4.4.8 Nail Line Function ($f_9(l)$)

This function takes account of the effect of the number of lines in the joint. From the analyses in section 4.2.1 it has been shown that for joints with the same line configuration there is a linear relationship between joint strength and the number of lines of nails in the joint and on this basis the nail line function $f_9(l)$ will be:

$$f_9(l) = 1 \qquad \text{....(39)}$$

As all of the joints in the testing programme use lines having the same nailing configuration, this function will apply to all joints. If however a joint having lines of different nailing configuration is to be analysed, a joint specific function will have to be developed.

4.4.9 Semi-empirical Model for Laterally Loaded Steel Gusset Plate Joints formed with a Gap and using Predrilled Holes less that 1.1 times the Nail Diameter

The load-displacement relationship for the joint in terms of the joint functions is given in equation (4) and substituting the relationships developed in sections 4.4.4 to 4.4.8 for the individual functions, including for the discontinuity in the row spacing function, the load-displacement equation will be in two forms:

$$P\delta_x=(1-e^{-1.712\delta x})^{0926}(0.1\delta x+0.68)(Density)(1/f(mc))(0.2458(d)^{1.4468})(f_u/804)(5.26557)(r)(0.7428+0.0132Sp/d)n \quad \ldots(40a)$$

$$P\delta_x=(1-e^{-1.712\delta x})^{0926}(0.1\delta x+0.68)(Density)(1/f(mc))(0.2458(d)^{1.4468})(f_u/804)(5.26557)(r)(n) \quad \ldots(40b)$$

where equation (40a) is valid for nail row spacing between $0.7\times2\times5\times d$ and $0.7\times4\times7\times d$ and equation (40b) will apply when the spacing exceeds $0.7\times4\times7\times d$.

Rearranging and simplifying, equations (40a) and (40b) can be written:

i) for nail row spacing between $0.7\times2\times5\times d$ and $0.7\times4\times7\times d$:

$$P\delta_x = AD(d)^{1.4468}f_u r(0.7428+0.0132(Sp/d))n(1-e^{-1.712\delta x})^{0.926}(0.1\delta x + 0.68)/f(mc) \quad \ldots.(41a)$$

ii) for nail row spacing exceeding $0.7\times4\times7\times d$:

$$P\delta_x = AD(d)^{1.4468}f_u rn(1-e^{-1.712\delta x})^{0.926}(0.1\delta x + 0.68)/f(mc) \quad \ldots.(41b)$$

where:

$P_{\delta x}$ = load taken by the joint at displacement δx using predrilled holes in the steel gusset plates less than 1.1 times the nail diameter - N.

A = constant = 1.6098284×10^{-3}.

D = is the density of the timber in the joint. – kg/m^3.

d = nail diameter – mm.

f_u = strength of the nail wire - N/mm^2.

r = the number of rows of nails.

S_p/d = ratio of nail row spacing (mm) divided by nail diameter (mm).

n = the number of lines of nails

$f(mc)$ = the moisture content factor = $(-0.0275(12)+1.394)/(-0.0275(mc)+1.394)$ where mc is the moisture content (%) of the timber.

The semi-empirical model equations (41a) and (41b) apply to joints with thick steel gusset plates predrilled with holes for the nails less than 1.1 times the nail diameter; assembled with a nominal gap between the plates and the timber; connected by fully overlapping nails in predrilled holes in accordance with the requirements of EC5 [15]; with nail lines of the same configuration and with uniform row spacing, subjected to short duration lateral loading.

These equations are used in other Chapters in the Thesis and to reduce equation sizes they have been simplified by using the following constants in the relevant equation:

$$S_{GS} = AD(d)^{1.4468} f_u (0.7428+0.0132(Sp/d))/f(mc) \quad \text{....(41c)}$$

$$S_G = AD(d)^{1.4468} f_u /f(mc) \quad \text{....(41d)}$$

On this basis, equations (41a) and (41b) reduce to

i) for nail row spacing between $0.7\times2\times5\times d$ and $0.7\times4\times7\times d$:

$$P\delta_x = S_{GS}(1-e^{-1.712\delta x})^{0.926}(0.1\delta x + 0.68)rn \quad \text{....(41e)}$$

ii) for nail row spacing exceeding $0.7\times4\times7\times d$:

$$P\delta_x = S_G(1-e^{-1.712\delta x})^{0.926}(0.1\delta x + 0.68)rn \quad \text{....(41f)}$$

From the equations it is possible to determine the load-deformation characteristics of connections using a prescribed number of nails at a particular row spacing up to the joint failure slip limit of 3.2mm. Alternatively, for a prescribed displacement it is possible to determine and compare the load sustained by the joint for different nailing configurations.

4.4.10 Comparison of Semi-Empirical Model with Test Results

The model has been applied to the joint configurations used in the testing programme and typical examples of the results are compared at the 3.2mm upper slip limit in Tables 4.13 to 4.15. The model results have been based on the average properties of the test set and to obtain a direct comparison the test results have been adjusted to equate to the strength at the average moisture content using equation (21). This was based on the moisture content of the sample divided by the average moisture content of the set. The percentage difference between the model result and the test result is also given, with a negative sign indicating an underestimation and a positive sign indicating an overestimation by the model.

From the tables it can be seen that there is a reasonable good fit between the model and the average test results and over all of the tests, the average deviation of the model result from the tests sets is less than 1%.

The results of a few of the joint tests and the model have also been plotted together and are presented in Figures 4.22 to 4.24. The comparison is again based on the model using the average properties of the test sets but on this occasion no adjustment has been made to the test results to correct for the average moisture content effect referred to above. The adjustment only leads to a small change in the result and does not alter the nature of the comparison. An example with the adjustment carried out is given in Appendix F for comparison purposes.

In the figures the model result is represented by the solid line.

Nail conf'n-number of nails	Row spacing (mm)	Number of rows	Average timber density (kg/m^3)	Average mc (%)	Test load (N)	Model load (N)	% error
CO-4	-	1	594.50	13.65	5907.61	6077.71	+2.88
CS-8	16.67	4	557.39	13.69	19585.37	18765.85	-4.18
CW-20	16.67	5	606.75	14.71	24499.41	24830.24	+1.35
CW-20	16.67	5	543.52	13.72	23211.11	22855.05	-1.53
EA-12	25	3	598.11	14.28	16407.32	15606.18	-4.88
EB-20	25	5	605.49	14.66	25275.88	26056.26	-3.09
EC-12	33.33	3	661.13	14.71	16392.3	17859.96	+8.95
EC-12	33.33	3	611.45	14.48	16749.8	16623.54	-0.75
ED-20	33.33	5	636.51	14.63	27373.75	28721.87	+4.92
ED-20	33.33	5	615.08	14.47	27538.46	27878.09	+1.23
RZG-12	38	3	538.14	14.00	15509.19	15202.97	-1.97
EG-20	50	5	630.74	14.45	31192.96	31210.26	+0.06
EG-20	50	5	535.46	13.30	28485.13	27336.91	-4.03
EF-12	50	3	618.61	14.47	17868.25	18361.82	+2.76
RZJ-16	66.67	4	548.17	12.25	22126.83	23264.06	+5.14

Table 4.13 Sample comparison of laterally loaded joints using 2.66mm diameter nails of strength $804N/mm^2$ at a slip of 3.2mm

Nail conf'n-number of nails	Row spacing (mm)	number of rows	Average timber density (kg/m^3)	Average mc (%)	Test load (N)	Model load (N)	% error
CO-4	-	1	490.63	12.08	6204.05	5980.31	-3.61
EA-12	25	3	553.09	14.25	16138.61	16244.98	+0.66
EB-20	25	5	543.29	14.37	27086.11	26507.60	-2.14
ED-20	33.33	5	490.96	13.79	26063.00	25380.60	-2.62
RZI-16	33.33	4	533.46	13.30	22909.44	22355.28	-2.42
RZH-12	42	3	517.07	11.7	17939.74	17672.36	-1.49
EF-12	50	3	564.23	14.01	19097.91	18827.91	-1.41
EN-28	50	7	640.91	12.94	50144.42	51358.81	+2.42
EG-20	50	5	597.58	13.76	33600.48	33461.28	-0.41
EJ-12	66.67	3	592.73	14.11	21413.69	20534.19	-4.11
RZJ-16	66.67	4	520.17	11.38	24951.46	25821.55	+3.49
EK-20	66.67	5	510.09	13.30	28858.34	30104.66	+4.32
EP-24	66.67	6	645.44	13.89	43176.6	44989.61	+4.20
EH-12	75	3	583.39	14.35	21317.41	20077.94	-5.81
EH-12	75	3	561.77	15.31	18944.37	18822.81	-0.64
EI-20	75	5	568.49	15.12	31057.47	31917.21	+2.77

Table 4.14 Sample comparison of laterally loaded joints using 3.01mm diameter nails of strength $769N/mm^2$ at a slip of 3.2mm.

Nail conf'n-number of nails	Row spacing (mm)	Number of rows	Average timber density (kg/m^3)	Average mc (%)	Test load (N)	Model load (N)	% error
CO-4	-	1	614.58	13.68	9341.83	9076.16	-2.84
ED-20	33.33	5	606.71	13.55	38342.93	39218.75	+2.28
EF-12	50	3	564.27	13.25	24096.56	23716.52	-1.58
EG-20	50	5	600.67	14.03	40918.52	41200.26	+0.69
EG-20	50	5	550.14	13.11	38475.18	38684.25	+0.46
EJ-12	66.67	3	651.6	14.74	28084.00	28041.3	-0.15
EJ-12	66.67	3	632.67	14.33	27293.27	27537.36	+0.89
RZJ-16	66.67	4	500.00	11.66	33117.00	31149.18	-5.94
EK-20	66.67	5	646.59	15.07	45448.05	45950.19	+1.10
EK-20	66.67	5	560.10	14.22	40559.66	40754.17	+0.48
EQ-24	66.67	7	599.14	13.13	59789.15	62857.97	+5.13
EH-12	75	3	485.91	14.00	21782.39	21341.61	-2.02
EI-20	75	5	485.21	14.26	35294.58	35269.16	-0.07
EL-12	100	3	565.44	13.98	23859.6	24848.18	+4.14

Table 4.15 Sample comparison of laterally loaded joints using 3.36mm diameter nails of strength $829N/mm^2$ at a slip of 3.2mm.

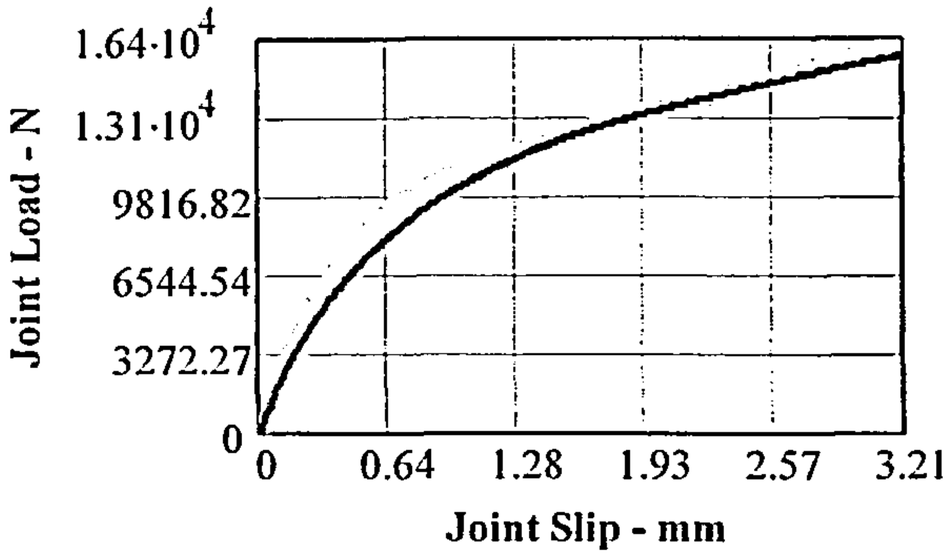

(a) Nailing Configuration 'EA'

(D = 598; mc = 14.28)

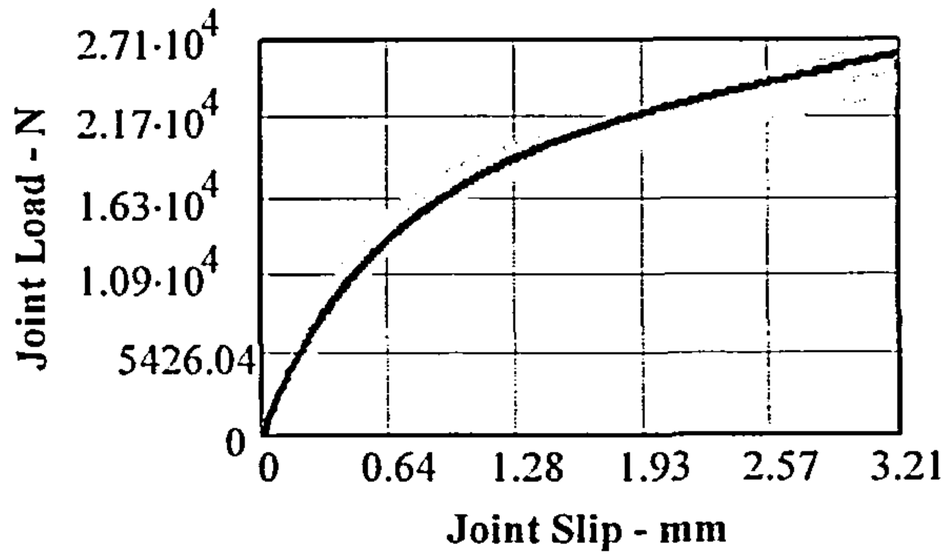

(b) Nailing Configuration 'EB'

(D = 605; mc = 14.66)

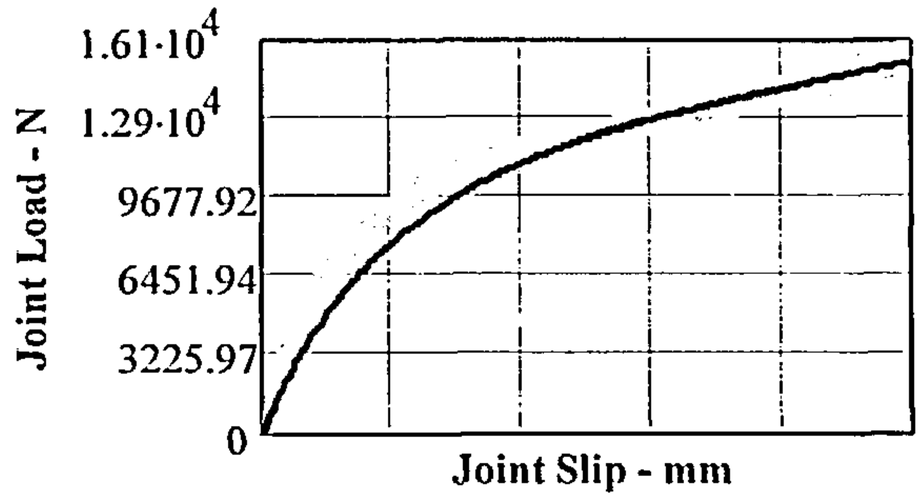

(c) Nailing Configuration 'RZG'

(D = 538; mc = 14.00)

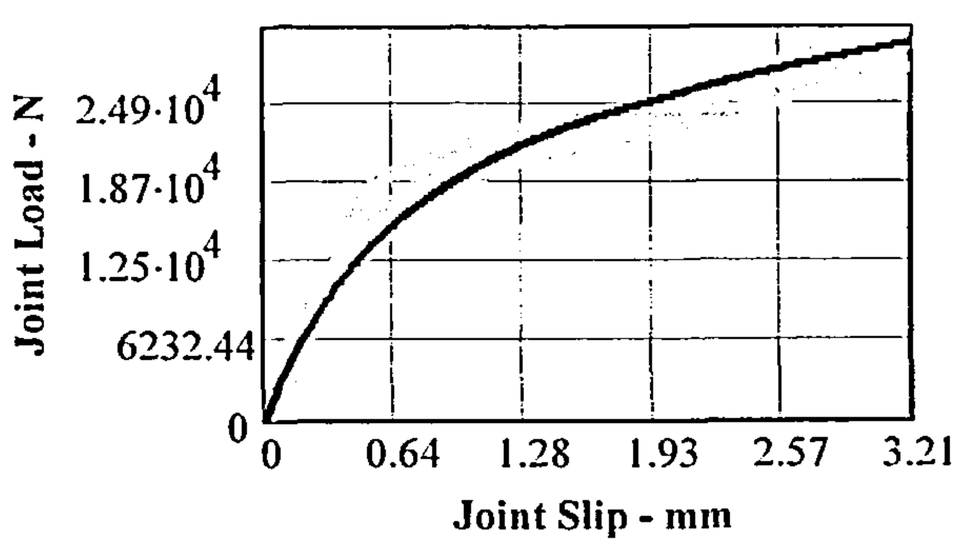

(d) Nailing Configuration 'EG'

(D = 604; mc = 14.45)

Figure 4.22 Load-deformation behaviour of timber joints made with fully overlapping 2.66mm diameter nails and 6mm thick steel gusset plates with 2.8mm diameter predrilled holes.

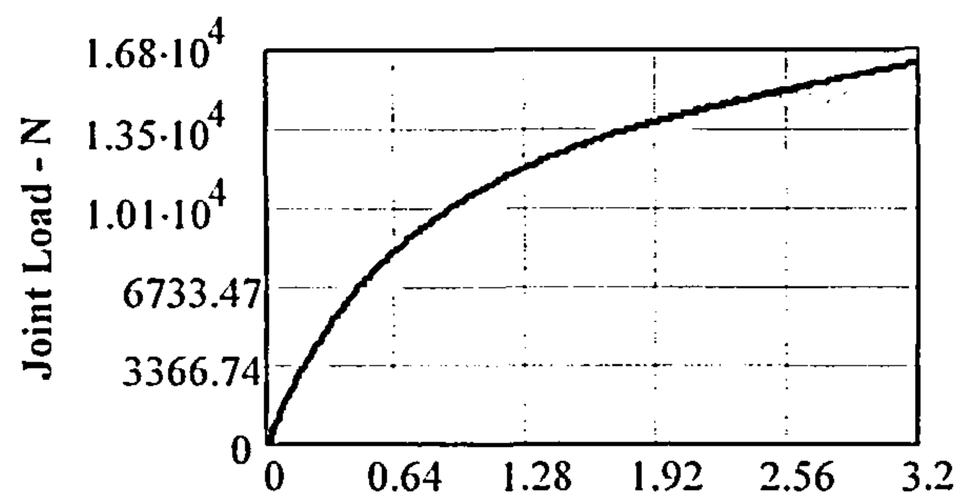

(e) Nailing Configuration 'EA'

(D = 553; mc = 14.25)

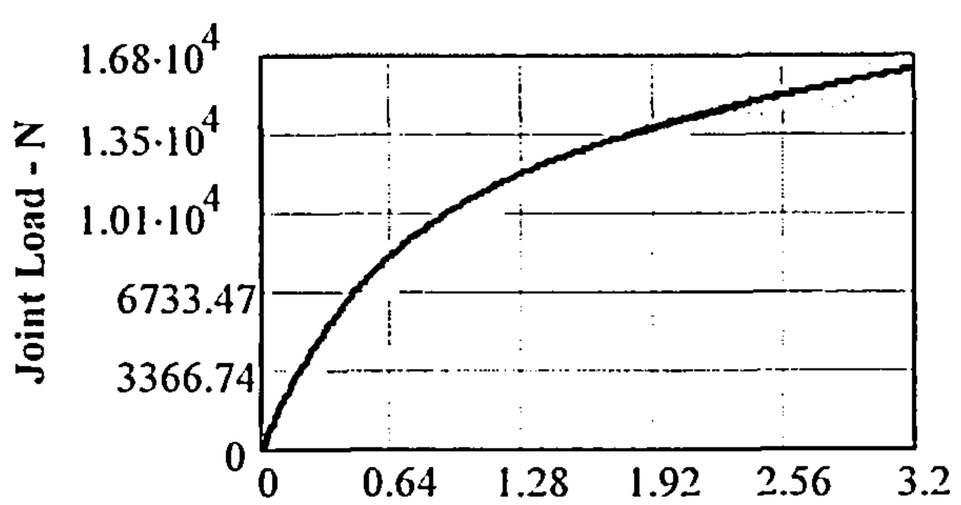

(f) Nailing Configuration 'EB'

(D = 543; mc = 14.37)

Figure 4.23 Load-Deformation behaviour of timber joints made with fully overlapping 3.01mm diameter nails and 6mm thick steel gusset plates with 2.8mm diameter predrilled holes.

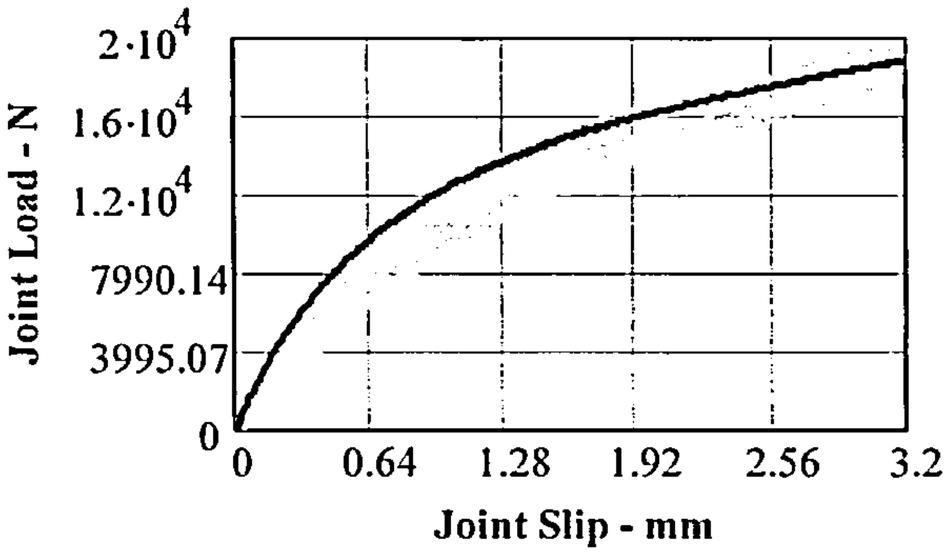

(g) Nailing Configuration 'EH'
(D = 562; mc = 15.31)

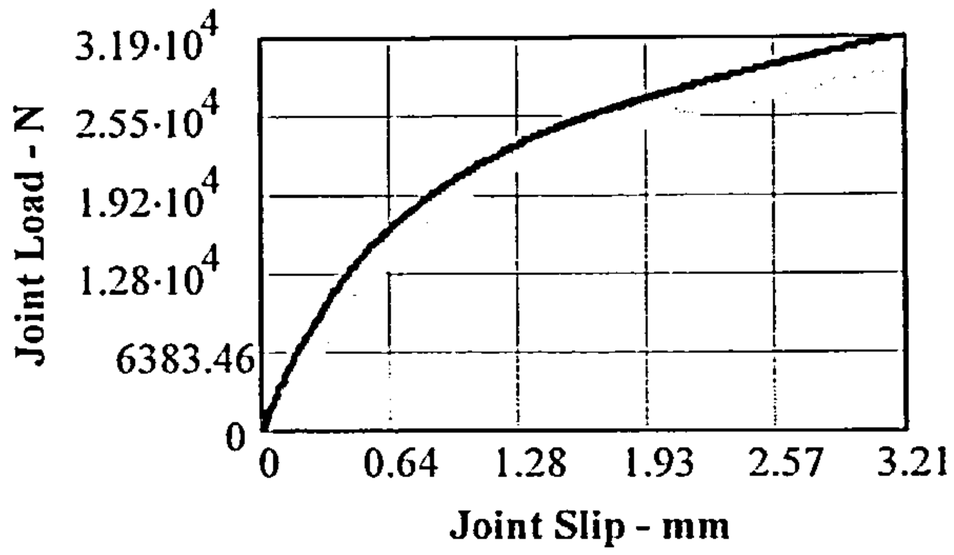

(h) Nailing Configuration 'EI'
(D = 568; mc = 15.12)

Figure 4.23 cont'd Load-Deformation behaviour of timber joints made with fully overlapping 3.01mm diameter nails and 6mm thick steel gusset plates with 2.8mm diameter predrilled holes.

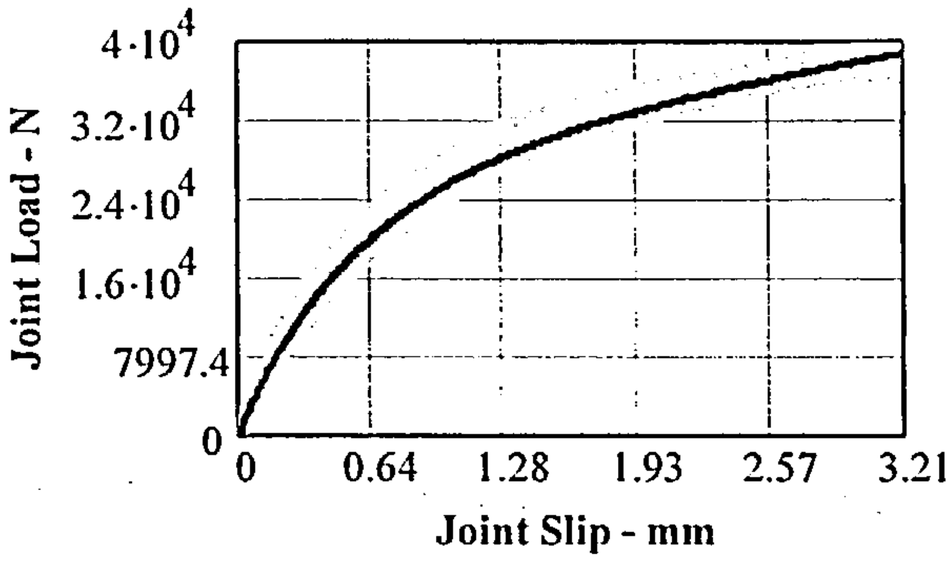

(i) Nailing Configuration 'EG'

(D = 550; mc = 13.11)

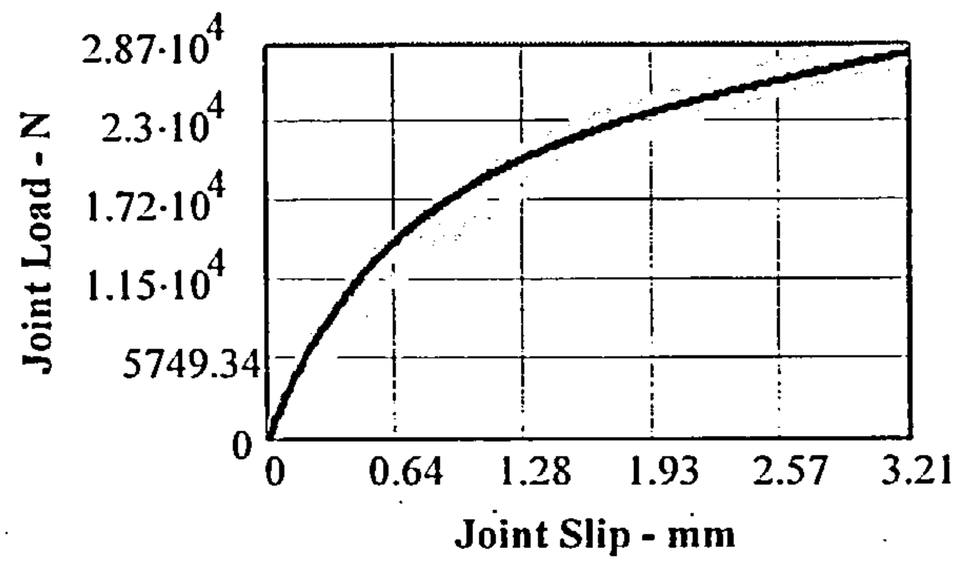

(j) Nailing Configuration 'EJ'

(D = 652; mc = 14.74)

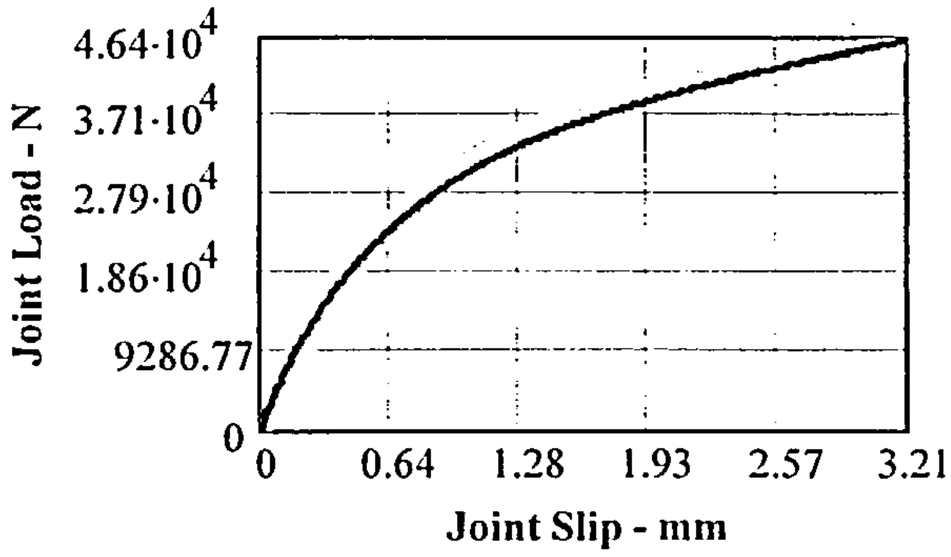

(k) Nailing Configuration 'EK'
(D = 647; mc = 15.07)

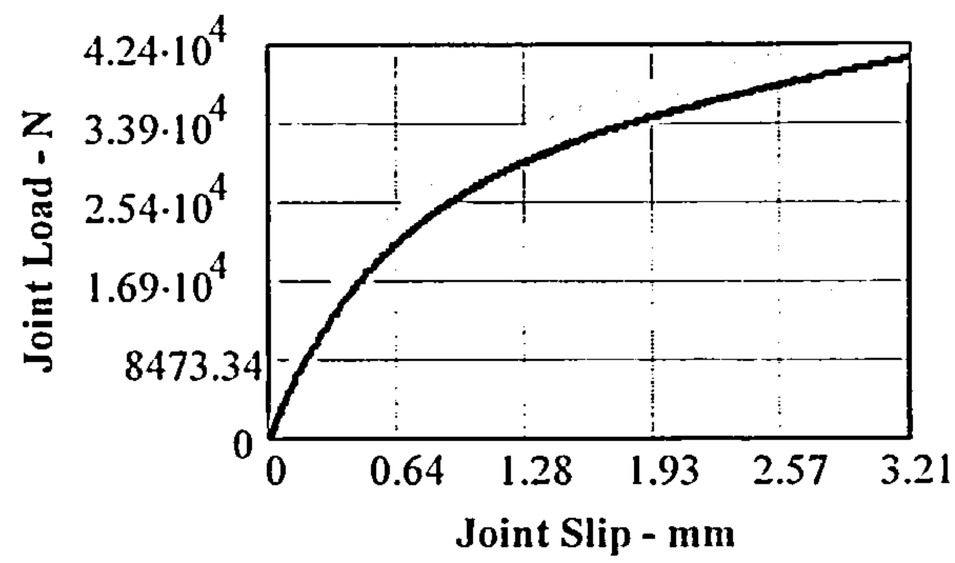

(l) Nailing Configuration 'EK'
(D = 560; mc = 14.22)

Figure 4.24 Load-deformation behaviour of timber joints made with fully overlapping 3.36mm diameter nails and 6mm thick steel gusset plates and 2.8mm diameter predrilled holes.

The results presented in Figure 4.22 are for joints assembled with 2.65mm diameter nails In all of the joints there was a reasonably good fit between the model and the average of the test results over the full length of the displacement curve. Up to 5 rows of nails have been used in the joints and the nail row

spacing has varied from the minimum to over two times the minimum value permitted for joints with fully overlapping nails, enveloping the extremes of the joint spacing effect. Apart from one instance, the model results have been within approximately ± 5% of the average test result at the $P_{3.2}$ limit. Also, at a load of approximately 40% of the $P_{3.2}$ load, which is equivalent to the load at the 'serviceability limit' of the joint, the model compares well with the test graphs, giving a good comparison with the joint strength and stiffness at that condition.

The model results in Figure 4.23 for the joints assembled with 3.00mm diameter nails fits well with the tests results at the 3.2mm slip however over the displacement curve there was a higher degree of variability in the test results and variation with the model curve. A significant amount of this was to be expected as the average displacement function used in the model had a stiffer/stronger profile than the actual displacement function derived from the 3.00mm diameter nail joint tests. However it must also be accepted that there was a higher degree of variability in the actual test results per test set than was to be expected from the behaviour of the other nail diameter tests and the reason for this is not clear. The same procedure was used for material selection and joint assembly for all the test sets and there is no single factor which can be identified to be specific to the 3.00mm diameter nailed joints that would account for this phenomenon. Up to 7 rows of nails have been used and the row spacing has again varied between the minimum and over two times the minimum values and again the model result has been within approximately ±5% of the average test result at the $P_{3.2}$ limit. At the serviceability load, however, the fit is not as good as that obtained with the other nail sizes and this is due to the use of the average displacement function. A better result will be obtained using the displacement function given in equation (9).

The results presented in Figure 4.24 are for the joints assembled with 3.36mm diameter nails and as with the 2.65mm diameter nails, a good fit has been obtained between the model and the average of the tests results over the full length of the displacement curves. Up to 7 rows of nails have been used in the joints and the spacing has again been varied from the minimum to over two times the minimum values and the model result is within approximately ± 5% of the average test result at the $P_{3.2}$ limit. At 40% of the $P_{3.2}$ load, the model graph compares extremely well with the average of the test graphs giving a very good comparison with the joint strength and stiffness at that condition.

4.5 THE ANALYSIS OF LATERALLY LOADED STEEL GUSSET PLATE JOINTS FORMED WITH A GAP AND USING PREDRILLED HOLES GREATER THAN 1.1 TIMES THE NAIL DIAMETER

At the time the testing programme was commenced no guidance was given in EC5 [11] or BS5262 Part 2 [10] as to the maximum tolerance permitted when forming predrilled holes in steel gussets and the criteria adopted was to use a predrill size that would just allow the free fit of the nail point through the predrilled hole. Trying various predrill sizes and ensuring there was no obstruction to the nail passing

through the steel gusset plate, a 3.2mm diameter predrill was selected for use with 2.65mm diameter nails. This resulted in a predrill size that was 1.2 times the nail diameter.

During the early stage of the testing programme, the first draft revision of EC5 was issued [13] introducing a requirement that to be able to develop the full strength of a joint with steel gussets, the size of the predrilled hole must not be greater than 1.1 times the nail diameter. At the time of receipt of the revised code the testing of joints with steel gussets connected by 2.65mm diameter fully overlapping nails was well in hand. Nevertheless it was felt that the code guidance should be complied with and the new criterion was adopted. The 3.2mm predrill was changed to a 2.8mm diameter predrill giving a predrilled hole approximately 1.05 times the nail size, and in accordance with clause 8.2.2 of EC5 [15], the plates could then be classified as thick plates. To compare the behaviour of the joints assembled with the different sizes of predrill, the reduced load data from the joints that used 3.2mm predrilled holes has been analysed using a least squares non linear regression fit. The displacement function for these joints is given in equation (42) and is shown against the reduced load data plot in Figure 4.25.

$$f_{3.2}(\delta_x) = (1-e^{-1805\delta x})^{1.51}(0.1\delta x + 0.68) \qquad \text{....(42)}$$

The displacement function using 2.8m diameter predrilled holes in the steel gussets is given in equation (8) and a comparison with equation (42) is given in Figure 4.26.

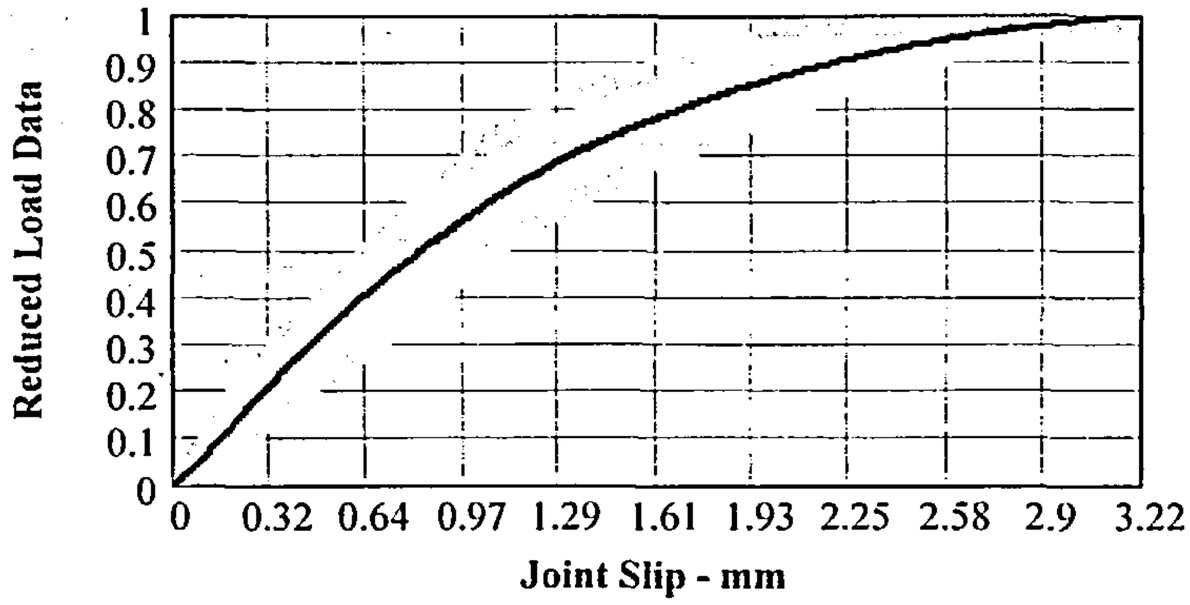

Figure 4.25 Regression graph of displacement function for 2.65mm diameter nails when used in joints made with steel gusset plates having 3.2mm predrill holes

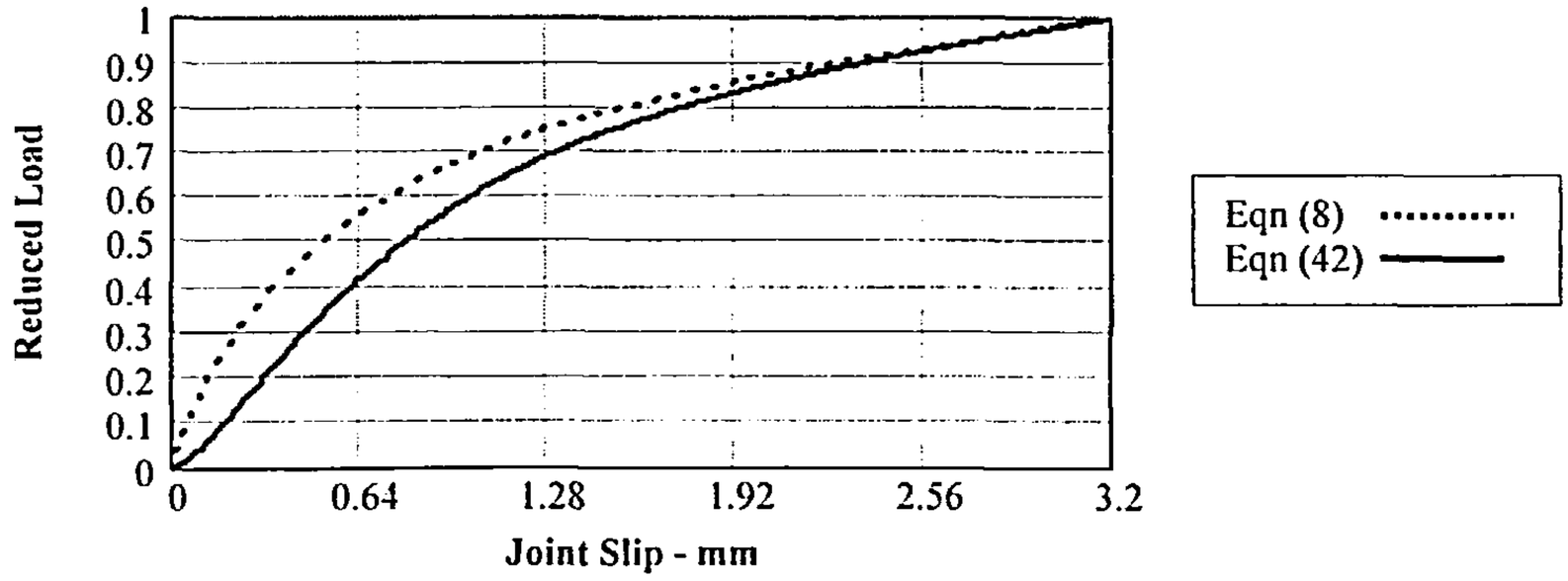

Figure 4.26 Comparison of the displacement functions for joints with plywood gusset plates having 2.8mm and 3.2mm predrilled holes.

The slight dip at the start of equation (42) is associated with the looseness of fit of the nail in the gusset plate and is in line with the behaviour of bolted joints where the bolts have an initial slip on taking up their tolerance gap or bedding into the rough surface of the predrilled hole [89, 90]. This behaviour is not so evident with equation (8) where a tighter fit has been achieved because of the smaller predrilled hole used in these joints. Also, it is seen from the graph of equation (42) that for the same value of reduced load the slip is greater than that associated with equation (8). At approximately 40% of the reduced load (ie 40% of the maximum load), the slip when using 3.2mm predrilled holes is approximately 0.6mm and when using 2.8mm predrilled holes is only 0.34mm. This means that for a 15% increase in the size of the predrilled hole there is an approximate increase of 75% in the slip at the serviceability state, which is a very significant difference.

To check if the change in predrill size had any effect on the other functions, the semi-empirical formulae for joint behaviour given in equations (41a) and (41b) were amended to incorporate the displacement function derived in equation (42) and compared with the results of sets of tests from the joint testing programme. Based on the displacement function in equation (42) the revised strength equations for steel gusset plate joints with 3.2mm predrilled holes becomes:

i) for nail row spacing between $0.7\times2\times5\times d$ and $0.7\times4\times7\times d$:

$$P\delta_x = AD(d)^{1.4468} f_u r(0.7428+0.0132(Sp/d))n(1-e^{-1.805\delta x})^{1.51}(0.1\delta x + 0.68)/f(mc) \quad \ldots.(43a)$$

ii) for nail row spacing greater than 0.7×4×7×d:

$$P\delta_x = AD(d)^{1.4468} f_u rn(1-e^{-1.805\delta x})^{1.51}(0.1\delta x + 0.68)/f(mc) \quad \ldots.(43b)$$

where the functions remain as defined in section 4.4.9 except for $P_{\delta x}$ which becomes:

$P_{\delta x}$ = load taken by the joint at displacement 'δx' with 3.2mm predrilled holes in the steel gussets - N.

These equations are used in other Chapters in the Thesis and to make them easier to use they have been simplified by the following functions:

$$S_{NS} = AD(d)^{1.4468} f_u(0.7428+0.0132(Sp/d))/f(mc) \quad \ldots.(43c)$$

$$S_N = AD(d)^{1.4468} f_u /f(mc) \quad \ldots.(43d)$$

Using the simplifications in equations (43c) and (43d), equations (43a) and (43b) are reduced to:

(i) for nail row spacing between $0.7\times2\times5\times d$ and $0.7\times4\times7\times d$:

$$P\delta_x = S_{NS}((1-e^{-2.341\delta x})^{0.785}(0.1\delta x + 0.68)rn \quad \ldots.(43e)$$

(ii) for nail row spacing exceeding $0.7\times4\times7\times d$:

$$P\delta_x = S_N(1-e^{-2.341\delta x})^{0.785}(0.1\delta x + 0.68)rn \quad \ldots.(43f)$$

Comparisons were made between five sets of tests which had been assembled using steel gussets with 3.2mm predrilled holes and equations (43a) and (43b) and the results are given in Table 4.16. The difference between the model result and the test result is also given, with a negative sign indicating an underestimation and a positive sign indicating an overestimation by the model

The joint test results and some of the model graphs based on the average properties of the respective test sets have also been plotted in Figure 4.27 and the model results are represented by the solid line.

Nailing pattern-number of nails	**Row spacing (mm)**	**Number of rows**	**Average timber density (kg/m^3)**	**Average moisture content (%)**	**Model load (N)**	**Test load (N)**	**Percentage error (%)**
M-4		1	582.27	13.33	6004.14	6131.92	-2.08
CS-8	16.67	2	508.7	13.90	17029.32	16985.98	+0.26
CR-12	16.67	4	530.36	14.40	13113.00	13597.74	-2.13
CR-12	16.67	4	511.41	14.07	12780.67	13397.87	-2.74
CW-20	16.67	5	524.46	13.46	22208.76	21984.89	+1.02

Table 4.16 Comparison of laterally loaded joints with steel gussets using 3.2mm predrilled holes for 2.65mm diameter nails of strength $804N/mm^2$ at a slip of 3.2mm.

From the results it will be seen that fit between the model and the average of the test results for each set is comparable to that obtained in section 4.4 when analysing the steel gusset joint formed using 2.8mm diameter predrilled holes. The behaviour of the test results continues to be variable however the fit at $P_{3.2}$ is good and the comparison over the full displacement curve is in line with the general behaviour of the tests.

The result indicates that the change effect arising from the alteration in the size of the predrilled hole is independent of the other functions in the joint model. On this basis, providing thick gusset plates are being used in the joint, the effect of different sizes of predrill can be taken into account in the model by inserting the associated displacement function in equation (41a) and (41b).

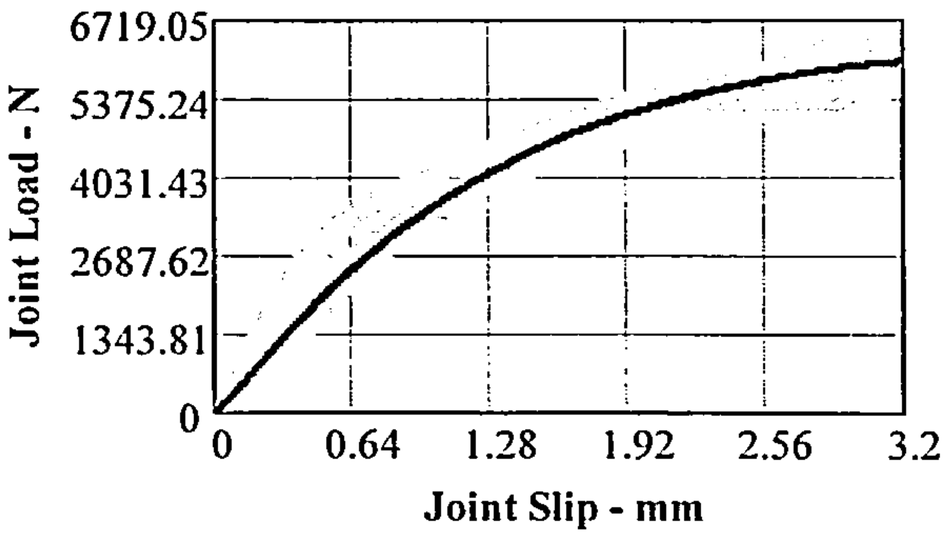

(a) Nailing Configuration 'MP'
(D = 582; mc = 13.33)

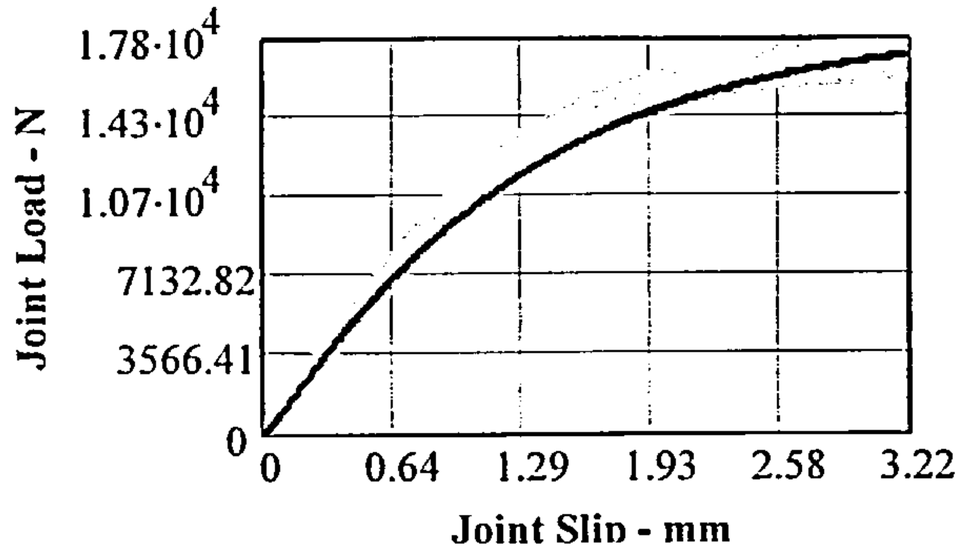

(b) Nailing Configuration 'CS'
(D = 509; mc = 13.90)

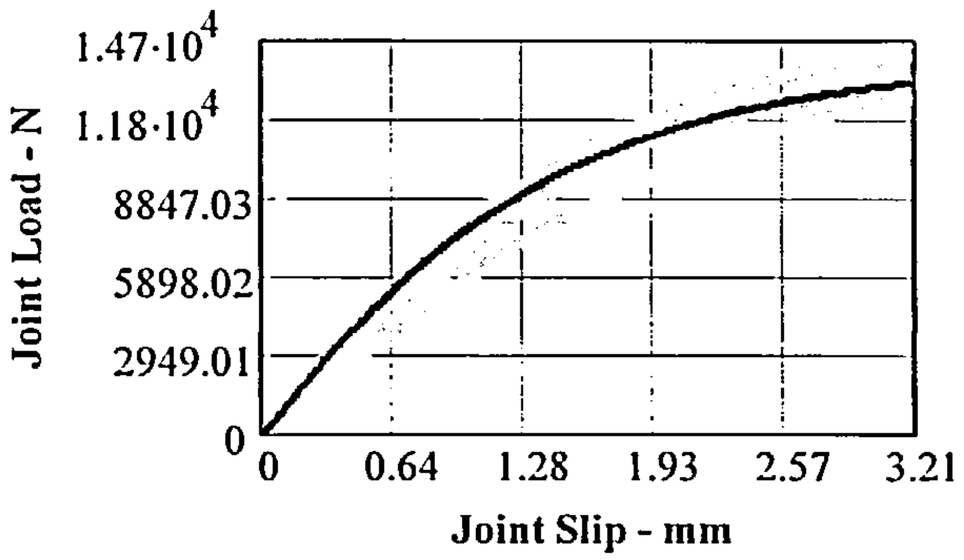

(c) Nailing Configuration 'CR'
(D = 530; mc = 14.40)

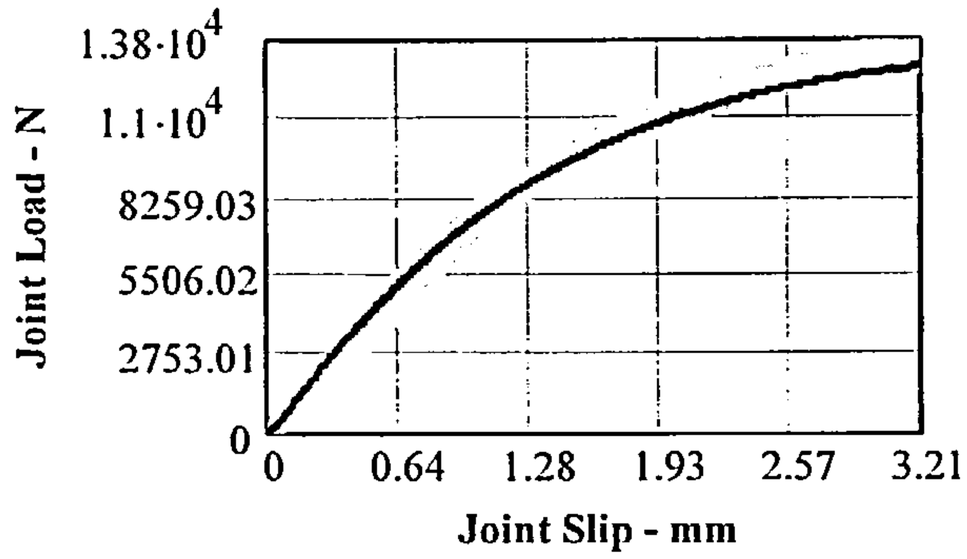

(d) Nailing Configuration 'CR'
(D = 511; mc = 14.07)

Figure 4.27 Load-Deformation behaviour of timber joints made with fully overlapping 2.65mm diameter nails and 6mm thick steel gusset plates with 3.2mm predrilled holes.

4.6 THE ANALYSIS OF LATERALLY LOADED STEEL GUSSET PLATE JOINTS FORMED USING PREDRILLED HOLES LESS THAN 1.1 TIMES THE NAIL DIAMETER AND WITHOUT A GAP

An objective of the programme was to determine lower bound solutions for the strength and stiffness of the joints and for this reason the gusset plates were assembled using 0.2mm spacers between the gusset plates and the timber. The spacers being removed after the joint had been assembled. The gap formed reduced the frictional interaction between the gusset and the timber in the joint and was in line with the approach adopted by other researchers [6, 17, 20, 53, 81, 104].

Eliminating the gap between the gusset plate and the timber changes the support condition for the nails and will also affect the joint displacement function. In addition the contact between the gusset plates and the timber introduces a friction force which will add to the joint strength. To investigate these effects sets of joints using nailing configuration RZJ, connected by 2.65mm 3.00mm and 3.35mm diameter Rynail nails were assembled without the use of spacers and then tested. The analysis of the test results was undertaken in two parts. The effect of the change in the support condition on the

displacement function was investigated first followed by the analysis of the effect of the additional friction force on the joint strength.

4.6.1 No Spacers in Joint - Effect on Displacement Function

As described in section 4.4.1, the results of the tests were converted to reduced load data and adopting the same type of exponential function as given in equation (7), using non linear regression analysis the displacement function for each nail size, and for the average for all nail sizes, was obtained. The functions are given in equations (44), (45), (46) and (47) and plotted against the associated reduced load data on Figures 4.28 and 4.29.

Nail Diameter	**Displacement Function**	
2.65mm	$f_{265hd}(\delta_x) = (1-e^{-2.307\delta x})^{0.601}(0.1\delta x + 0.68)$	....(44)
3.00mm	$f_{300hd}(\delta_x) = (1-e^{-1.988\delta x})^{0.896}(0.1\delta x + 0.68)$	....(45)
3.35mm	$f_{335hd}(\delta_x) = (1-e^{-1.486\delta x})^{0.669}(0.04597\delta x + 0.8548)$	....(46)
All diameters	$f_{hd}(\delta_x) = (1-e^{-2.341\delta x})^{0.785}(0.1\delta x + 0.68)$	....(47)

With the limited numbers of tests, the spread in the reduced load data for each nail size is much less than that obtained for the joints assembled with the use of spacers as reported in section 4.4.1. The coefficient of determination, R^2, for each fit, given below, is much improved.

Nail Diameter	**R^2 value**	**Nail Diameter**	**R^2 value**
2.65mm	0.977	3.35mm	0.948
3.00mm	0.995	All diameters	0.975

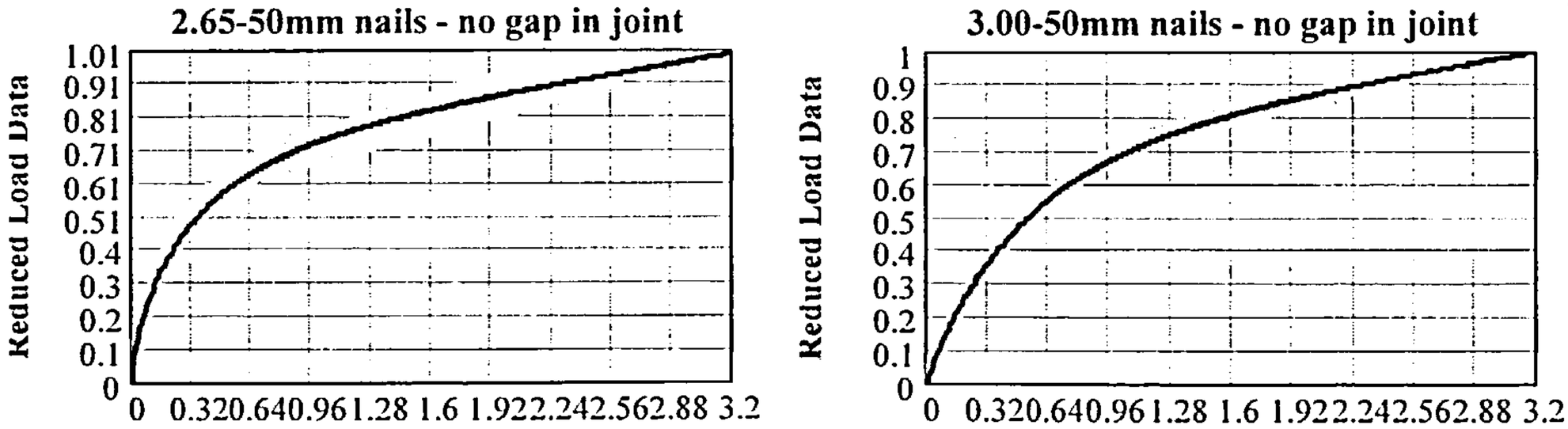

Figure 4.28 Regression graphs of the Displacement Functions for 2.65mm, 3.00mm, and 3.35mm diameter nails in joints with steel gusset plates in contact with the timber.

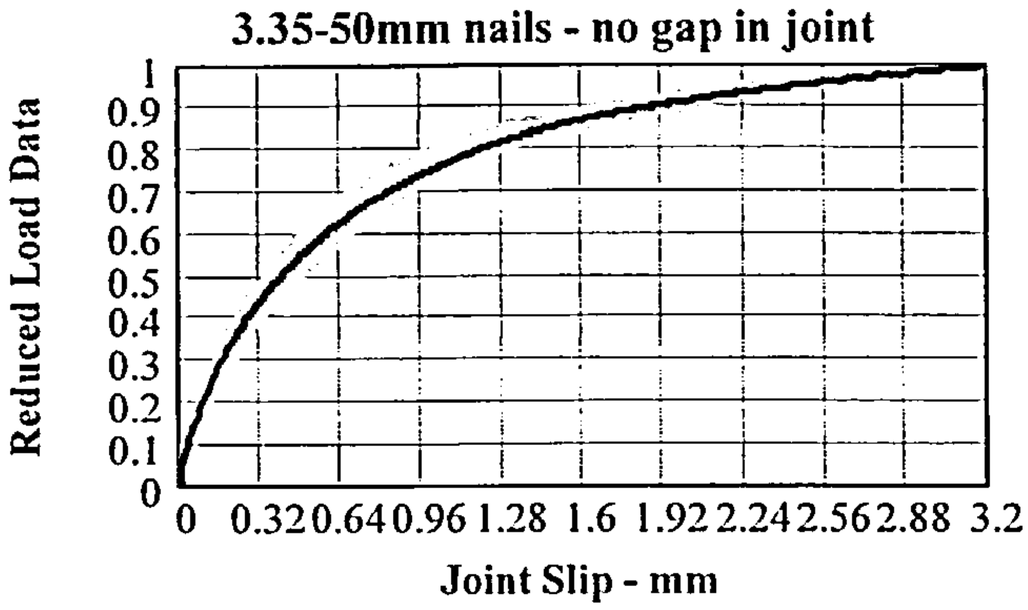

Figure 4.28 cont'd Regression graphs of the Displacement Functions for 2.65mm, 3.00mm, and 3.35mm diameter nails in joints with steel gusset plates in contact with the timber.

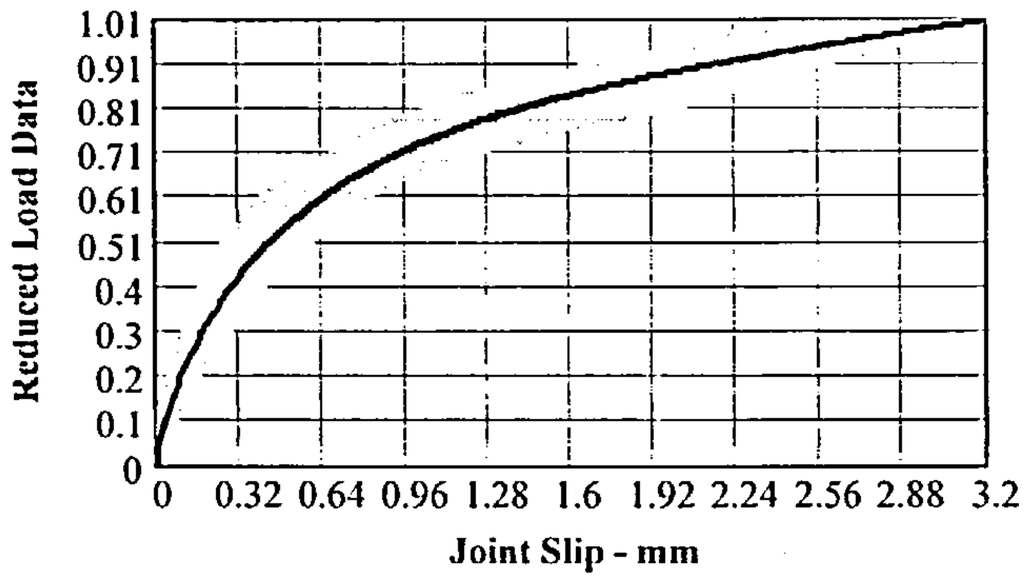

Figure 4.29 Regression graph of the Displacement Function for all nail sizes in joints with steel gusset plates in contact with the timber.

For comparison, the displacement functions in equations (44) to (47) are plotted together on Figure 4.30.

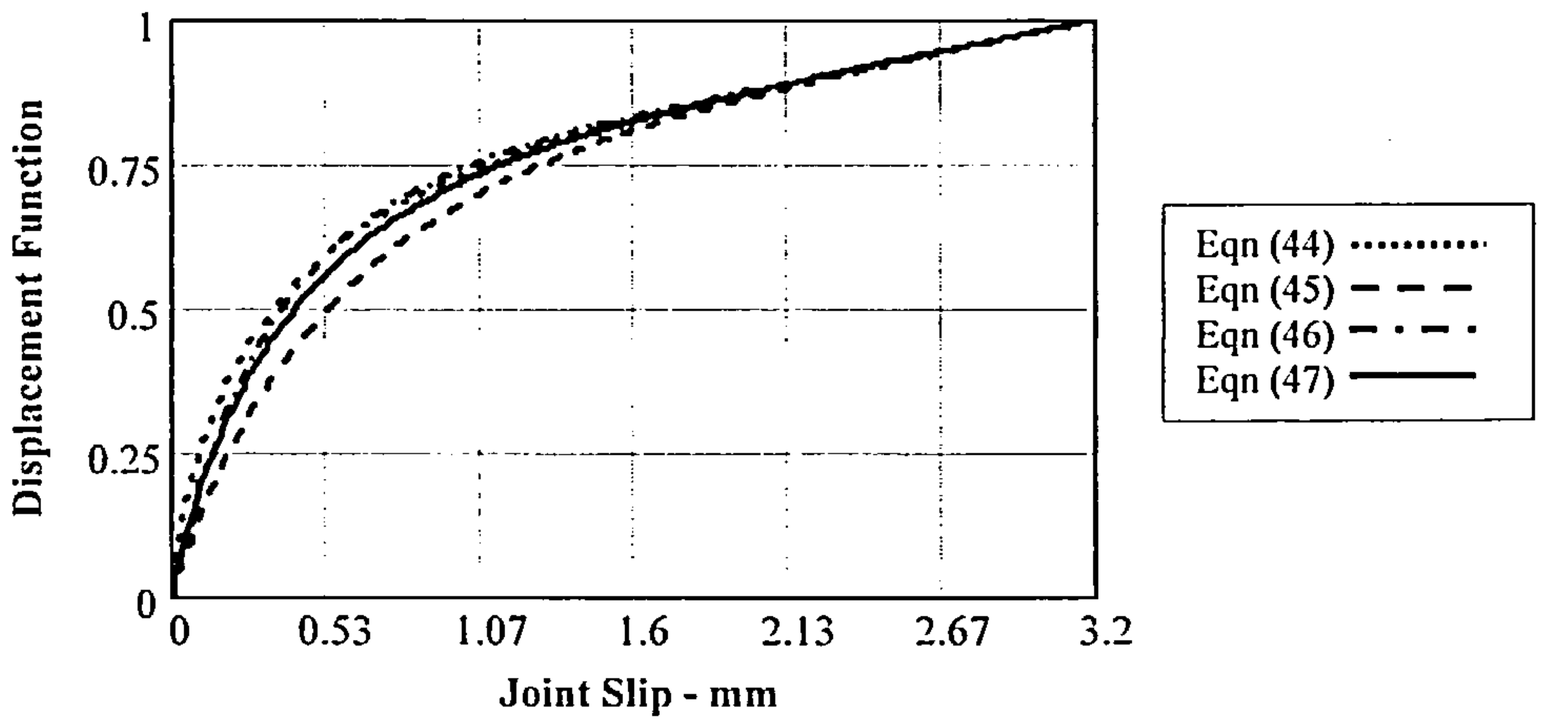

Figure 4.30 Displacement Functions given in equations (44),(45),(46) and (47).

As expected, relative to each other, the displacement function relationship remains the same as the relationship of the displacement functions derived for the steel gusset joints when using spacers as

shown in Figure 4.13. For the 2.65mm and 3.35mm diameter nails the functions remain reasonably comparable and again both exhibit much stiffer and stronger behaviour that the 3.00mm diameter displacement function. However, as shown in Figure 4.31, when the average displacement function, $f_{hd}(\delta x)$, (equation (47)), is compared with the average displacement function for joints assembled with a gap between the gusset plates and the timber, as given in equation (11), it is seen that equation (47) is a more stiff function.

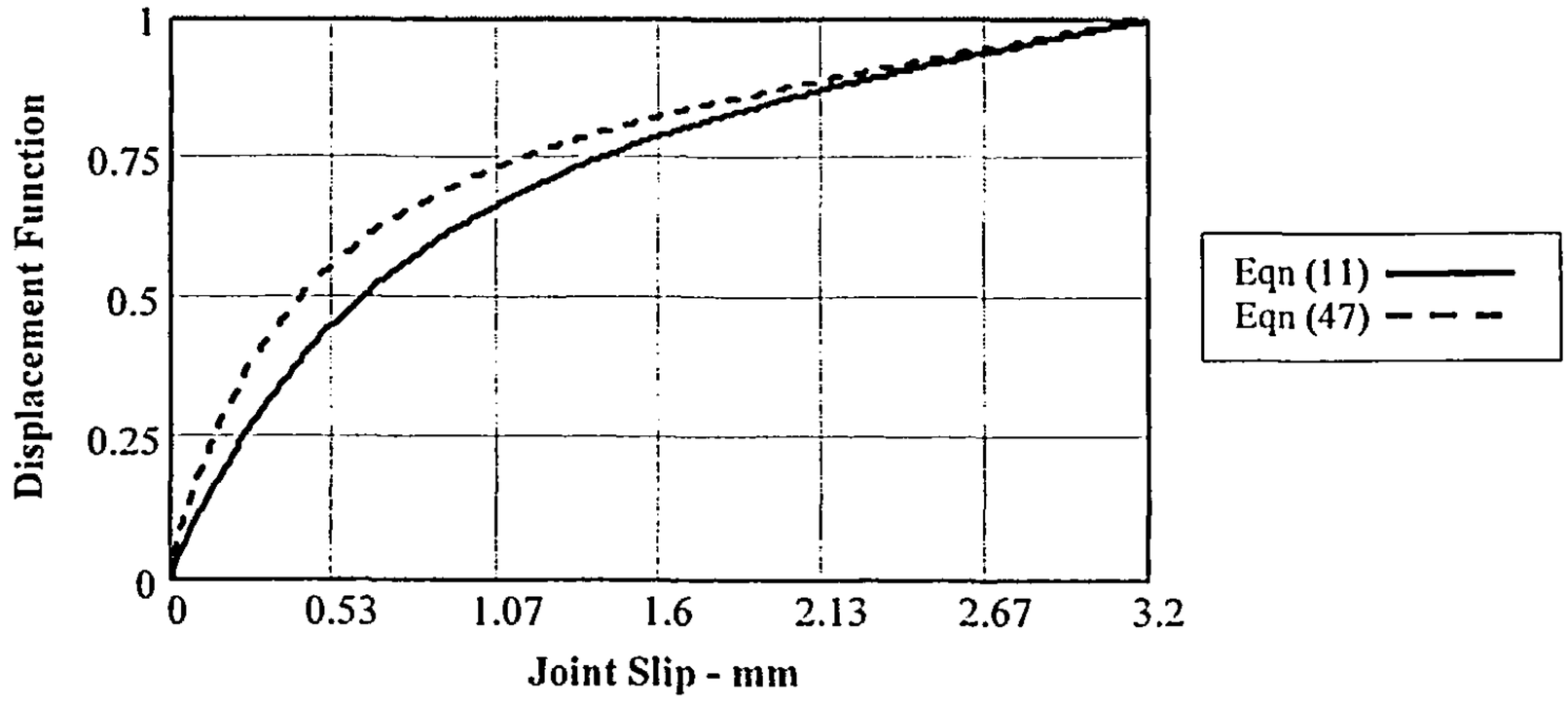

Figure 4.31. Comparison between the Displacement Function for steel gusset plate joints with a gap ($f(\delta_x)$) – equation (11) and without a gap ($f_{hd}(\delta x)$) – equation (47)

At 40% of the reduced load, which is equivalent to the serviceability limit state load condition, the joint slip for function $f_{hd}(\delta x)$ is approximately 0.28mm whilst for function $f(\delta_x)$ it is 0.44mm, resulting in an increase of 35% in stiffness. The slip of a structure formed using nailed joints with contact between the gusset plates and the timber will be considerably reduced over the same structure assembled using nailed joints with a gap between the gusset plates and the timber.

4.6.2 No Spacers in Joint - Frictional Force

Applying the displacement function in equation (47) to the semi-empirical model in equations (41a) and (41b), and including for a friction function, the semi-empirical model becomes:

i) for nail row spacing between 0.7×2×5×d and 0.7×4×7×d:

$$P_{hd}\delta_x = AD(d)^{1.446S} f_u r(0.7428+0.0132(Sp/d))n(1-e^{-2.341\delta x})^{0.785}(0.1\delta x + 0.68)f_f/f(mc) \quad \text{....(48a)}$$

ii) for nail row spacing greater than 0.7×4×7×d:

$$P_{hd}\delta_x = AD(d)^{1.446S} f_u rn(1-e^{-2.341\delta x})^{0.785}(0.1\delta x + 0.68)f_f/f(mc) \quad \text{....(48b)}$$

where the functions remain as described in section 4.4.9 and the friction function, f_f, has been added.

As the row spacing in Joint RZJ is 66.67mm c/c, equation (48b) will apply and inserting the average properties of the test sets of the joints, the $P_{3.2}$ value for each nail diameter will be obtained in terms of the friction function (f_f). Comparing the result with the average value obtained from the test set of joints for each nail diameter the following relationship can be set up:

$$P_{3.2Model} f_f = P_{3.2Test}$$

$$ie \quad f_f = P_{3.2Test} / P_{3.2Model} \qquad .....(49)$$

The result of the analysis for each nail diameter is given in Table 4.17.

Nail diameter mm	$P_{3.2}$ – Model N	$P_{3.2}$ – Tests N	Ratio $P_{3.2Test}/P_{3.2\ Model} = f_f$
2.66	$22493.20 f_f$	25755.11	1.14518
3.01	$25653.59 f_f$	29034.34	1.13178
3.36	$31533.16 f_f$	35537.47	1.1270
		Average f_f	**1.1346**

Table 4.17 Comparison between the $P_{3.2}$ value of the model and the tests

Although the trend of the friction function, f_f, is to slightly decrease as the nail diameter increases, the change associated with each nail size is only of the order of 1% and can be ignored. The average value of the friction function, f_f, is 1.1346, representing an increase of the order of 13% on the joint strength with no gap between the gusset plates and the timber. This is a significant factor and disagrees with the findings of Aune *et al* [17] where they report that the change in strength in joints where timber is in contact with steel gusset plates is minimal.

Adopting the average value of 1.1346 for each nail diameter and applying this factor to equations (48a) and (48b), the model becomes:

i) for nail row spacing between 0.7×2×5×d and 0.7×4×7×d:

$$P_{hd}\delta_x = A_1 D(d)^{1.446S} f_u r(0.7428+0.0132(Sp/d))n(1-e^{-2.341\delta x})^{0.785}(0.1\delta x + 0.68)/f(mc) \qquad ....(50a)$$

ii) for nail row spacing greater than 0.7×4×7×d:

$$P_{hd}\delta_x = A_1 D(d)^{1.446S} f_u rn(1-e^{-2.341\delta x})^{0.785}(0.1\delta x + 0.68)/f(mc) \qquad ....(50b)$$

where the functions are as described in section 4.4.9 except:

$P_{hd}\delta_x$ = load taken by the joint at displacement 'δx' for joints with steel gusset plates using predrilled holes less than 1.1 times the nail diameter and the joints are assembled with no gap between the gusset plates and the timber - N.

A_1 = constant = 1.826511×10^{-3}

These equations are used in other Chapters in the Thesis and to make them easier to use they have been simplified by the following functions:

$$S_{GS} = A_1 D(d)^{1.4468} f_u(0.7428+0.0132(Sp/d))/f(mc) \quad \text{....(50c)}$$

$$S_G = A_1 D(d)^{1.4468} f_u /f(mc) \quad \text{....(50d)}$$

Using the simplifications in equations (50c) and (50d), equations (50a) and (50b) are reduced to:

(i) for nail row spacing between $0.7\times2\times5\times d$ and $0.7\times4\times7\times d$:

$$P\delta_x = S_{GS}((1-e^{-2.341\delta x})^{0.785}(0.1\delta x + 0.68)rn \quad \text{....(50e)}$$

(ii) for nail row spacing exceeding $0.7\times4\times7\times d$:

$$P\delta_x = S_G(1-e^{-2.341\delta x})^{0.785}(0.1\delta x + 0.68)rn \quad \text{....(50f)}$$

Comparison between equation (50b) and the test results for the sets of joints used in the analysis (nailing configuration RZJ) are shown in Figure 4.32. The model result is shown as a solid line.

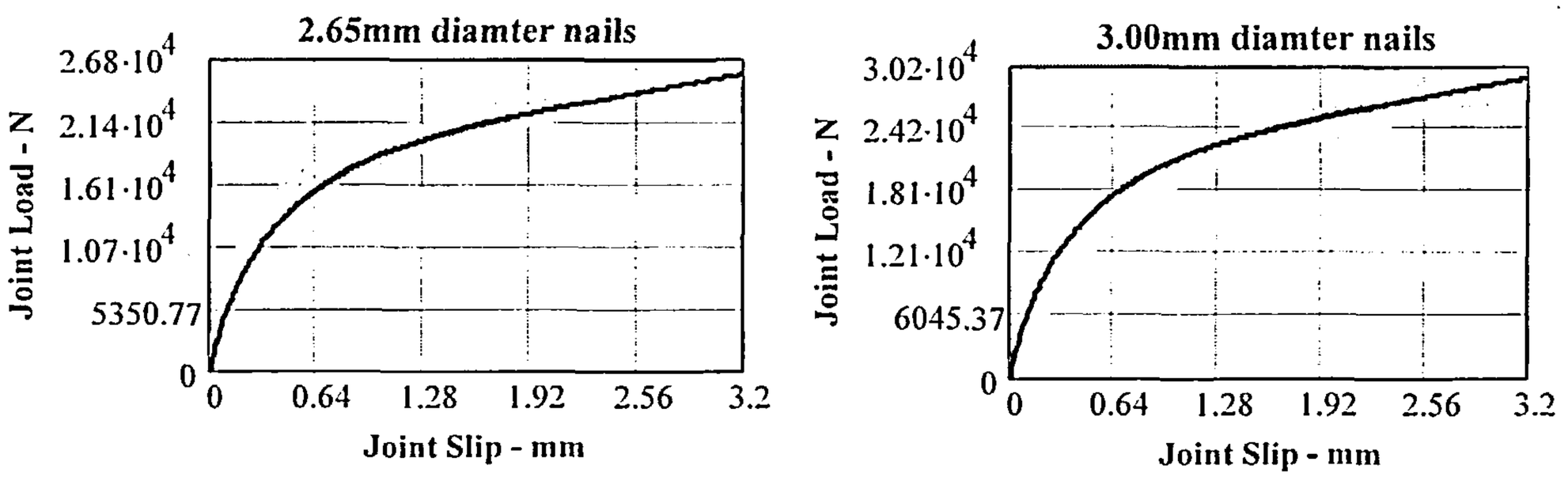

Figure 4.32 Comparison between equation (50b) and the test results for joints of nailing configuration RZJ using 2.65mm; 3.00mm and 3.35mm diameter nails.

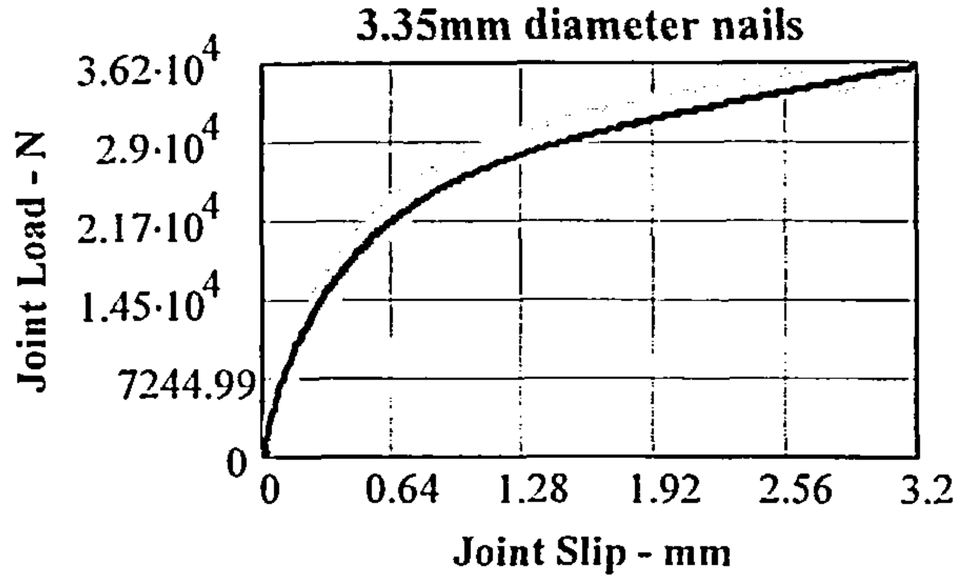

Figure 4.32 cont'd Comparison between equation (50b) and the test results for joints of nailing configuration RZJ using 2.65mm; 3.00mm and 3.35mm diameter nails.

The model achieves a good fit against the test data over the full length of the displacement curve.

4.7 THE ANALYSIS OF LATERALLY LOADED PLYWOOD GUSSET PLATE JOINTS FORMED WITH A GAP

4.7.1 General

Although plywood is a strong and stiff material, unlike thick steel gusset plates which provide a rigid support to the nail connector with minimal yielding under load, it behaves similarly to wood in that it yields under load [46] allowing the stress and deformation pattern across the gusset to change when the joint is loaded. A consequence of this is that the load-displacement relationship for joints with plywood gusset plates will differ from the relationship with steel gusset plates and the values derived for the other joint functions will not necessarily remain the same as those derived for the steel gusset plate joints. From section 4.3, the load-displacement relationship of joints with plywood gusset plates can be set out as a function of the joint displacement and the variables that affect the joint, and adopting the form given in equation (4), the relationship will be:

$$P_p = f_{p1}(\delta), f_{p2}(D), f_{p3}(mc), f_{p4}(d), f_{p5}(f_u), f_{p6}(k_g), f_{p7}(r), f_{p8}(S_p),), f_{p9}(l), f_{p10}(v) \quad \ldots.(51)$$

where the functions remain as previously described.

Before the commencement of testing the timber and plywood had been stored in the same environmental conditions for over a year and through the testing period the average moisture content of the timber was between 12.5% and 14%. As expected, the plywood recorded a lower range and was between 8% and 10%. Because of the relatively small variation it was considered that a moisture content function was not required and has not been developed. The analysis has been done on the premise that the load-displacement relationship can be taken to be valid for all joints using timber within a moisture content range of 12% to 14% and plywood within a range of 7.5% to 10%, nominally

equating to service class 1 conditions in EC5 [11].

Also, based on the work undertaken in section 4.2, the nail line function developed in section 4.4.8 will equally apply to joints with plywood gusset plates and has been used in this analysis.

Revisiting equation (51) taking account of the above, the load-displacement relationship to be developed for joints with plywood gusset plates will be:

$$P_p = f_{p1}(\delta), f_{p2}(D), f_{p4}(d), f_{p5}(f_u), f_{p6}(k_g), f_{p7}(r), f_{p8}(S_p), n \qquad \ldots.(52)$$

where:

P_p is the load taken by joints connected by fully overlapping nails using materials conditioned to service class 1 conditions - N

n, is the nail line function, $(f_{p9}(l))$, and equals the number of lines of nails of the same line configuration in the joint.

The joint functions are developed in sections 4.7.2 to 4.7.7.

4.7.2 The Joint Displacement Function $(f_{p1}(\delta_x))$

The procedure used to develop the displacement function $(f_{p1}(\delta_x))$, is the same as that used in section 4.4.1 for joints with steel gusset plates and to enable a comparison to be made between the functions, the slip limit for the analysis been taken as 3.2mm. It is to be noted however, unlike the steel gusset plate joints which were assessed to have reached their maximum withstand capability at a slip of 3.2mm, the majority of the plywood gusset plate joints exhibited an increasing capacity beyond this limit. Also, apart from 7 tests that failed at high loads by splitting of the timber, the remaining 557 tests exhibited ductile behaviour throughout the loading process.

The testing programme commenced using joints connected by 2.65mm diameter nails and as the loading was increased beyond the 3.2mm slip the withstand capacity of most of these joints increased in line with the increasing load. For several of the initial tests the joints were loaded to slips in excess of 7.5mm and still the joint capacity was increasing. Using joints connected by 3.00mm nails, there was also an increase in withstand capacity with increase in slip but there were signs of a falling off in the rate of increase and for joints connected by 3.35mm diameter nails, there was a marked fall off in the rate of increase just beyond the 3.2mm slip. What was clear was that as the nail diameter was increased the slip at which the joint started to show a sign of weakening reduced.

The results varied and examples of joint behaviour using 2.65mm, 3.00mm and 3.35mm diameter Castlenail nails with 19mm plywood gusset plates are shown in Figure 4.33.

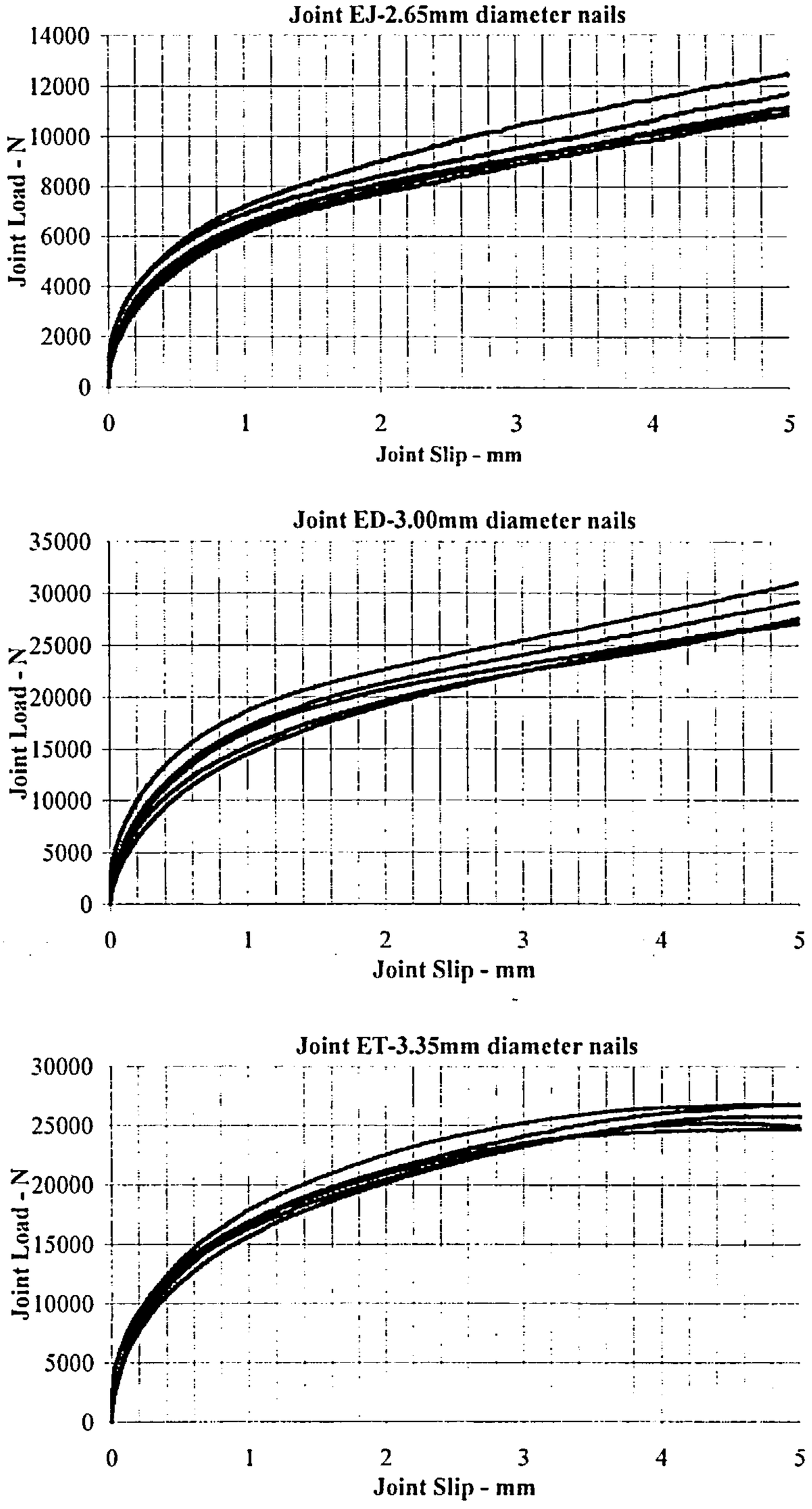

Figure 4.33 Typical load-displacement graphs for joints with plywood gusset plates

As stated, the displacement function will be determined for slips up to 3.2mm. To enable the model to be compared with joints designed in accordance with the requirements of EC5 [11], it will also be extended to the failure condition and that is addressed in Chapter 6.

Equation (52) can be rewritten in the form used in equation (5) and the displacement function, $f_{p1}(\delta_x)$, at the associated slip, δ_x, becomes:

$$f_{p1}(\delta_x) = P_x/P_{3.2} \qquad \ldots.(53)$$

where P_x is the load at any displacement δ_x and $P_{3.2}$ is the load on the joint at a slip of 3.2mm. $P_x/P_{3.2}$ is the reduced load and over the range of $\delta_x = 0$ to 3.2mm will define the displacement function of the joint. Examples of reduced load graphs for plywood gusset plate joints at that slip are shown in Figure 4.34.

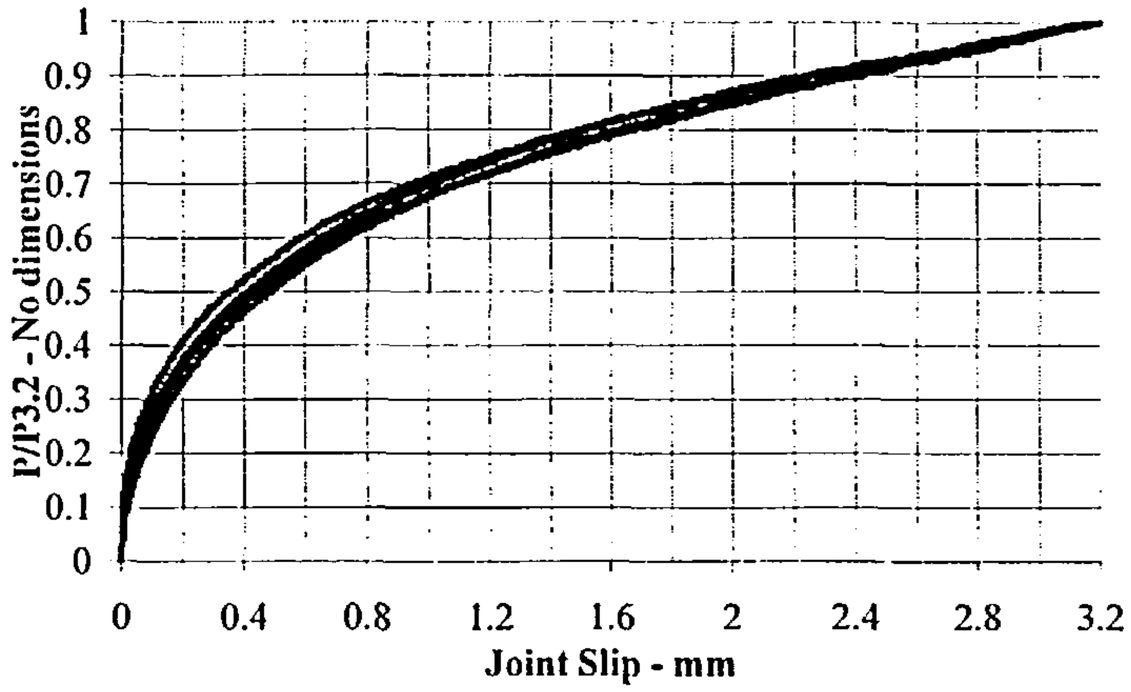

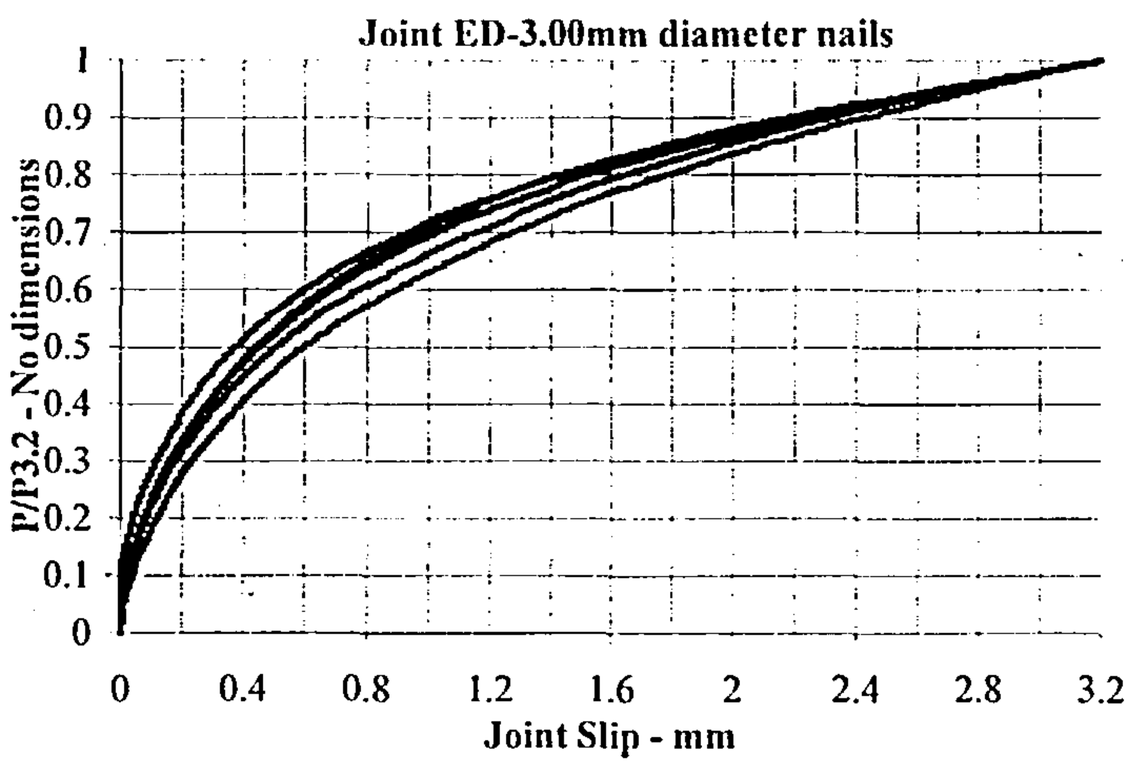

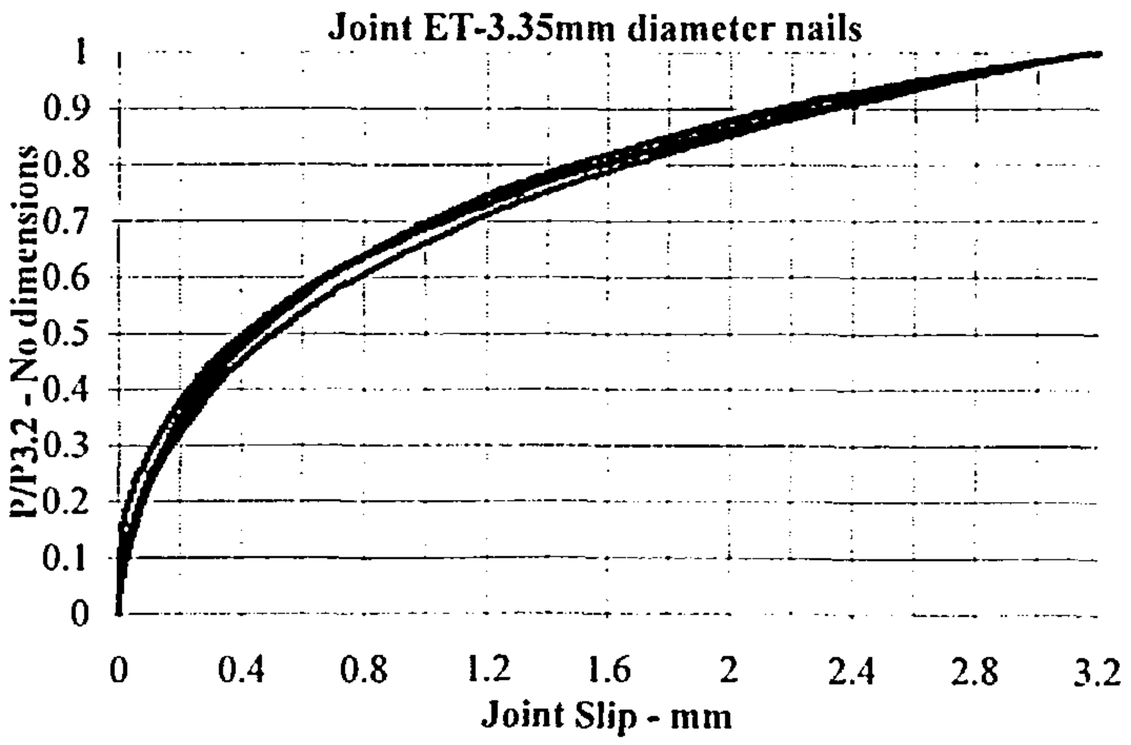

Figure 4.34 Reduced load ($P_x/P_{3.2}$) against joint slip for joint configurations using 2.65mm, 3.00mm, and 3.35mm diameter nails.

From a review of the reduced load curves it was clear that the four parameter non linear exponential equation defined in equation (7) and shown in graphical form in Figure 4.10 would also apply to joints with plywood gusset plates. The generalised function when used for plywood gusset plates can be written as:

$$f_{p1}(\delta_x) = (1 - e^{C\delta x/3.2})^D(A\,\delta_x/3.2 + B) \qquad \ldots.(54)$$

To determine the constants A, B, C and D the reduced load graphs of a selection of the 2.65mm, 3.00mm and 3.35mm diameter joint tests were combined to form a data base for each nail size against which least squares non linear regression analysis fits using Mathcad [51] were performed. As with the steel joint analysis, the data bases were also aggregated to enable a least squares non linear regression fit to be obtained for the combined nail sizes. The joint configurations selected for each nail size are given in Table 4.18 and at least five replicates were used for each test set:

Tests set nominal nail diameter	**Nail configurations used**
2.65	CO; ED; EG; EJ; EK; EQ
3.00	CO; ED; EJ; EK; EQ.
3.35	CO; ED; EG; EH; EJ, EK.

Table 4.18 Joint configurations used for test sets

The reduced data from the above tests was compiled up to a slip of 5.00mm as the displacement function was required to be extended to that limit to be able to do a later comparison of the model with EC5 [11]. For the derivation of the displacement function used in this section, only the data up to a slip of 3.2mm has been used. Again, the data was processed using Excel [50], limiting the maximum number of tests able to be used and, as with the steel gusset plate analysis, this had no significant effect on the accuracy of the displacement functions obtained.

The least squares non linear regression fit was carried out using the G*enfit* function within Mathcad [51] with values of 0.32 and 0.68 assigned to the constants A and B respectively as for the steel gusset plate analyses. The displacement functions obtained are given in equations (55), (56), (57) and (58) and are also plotted against the associated reduced load data plots on Figures 4.35 and 4.36. In the graphs, the displacement functions are shown as a solid line.

Nail Diameter	**Displacement Function**	
2.65mm	$f_{p265}(\delta_x) = (1\text{-}e^{-1.556\delta x})^{0.542}(0.1\delta x + 0.68)$	....(55)
3.00mm	$f_{p300}(\delta_x) = (1\text{-}e^{-1.854\delta x})^{0.587}(0.1\delta x + 0.68)$	....(56)
3.35mm	$f_{p325}(\delta_x) = (1\text{-}e^{-1.782\delta x})^{0.579}(0.1\delta x + 0.68)$	....(57)
All diameters	$f_{pall}(\delta_x) = (1\text{-}e^{-1.719\delta x})^{0.568}(0.1\delta x + 0.68)$	....(58)

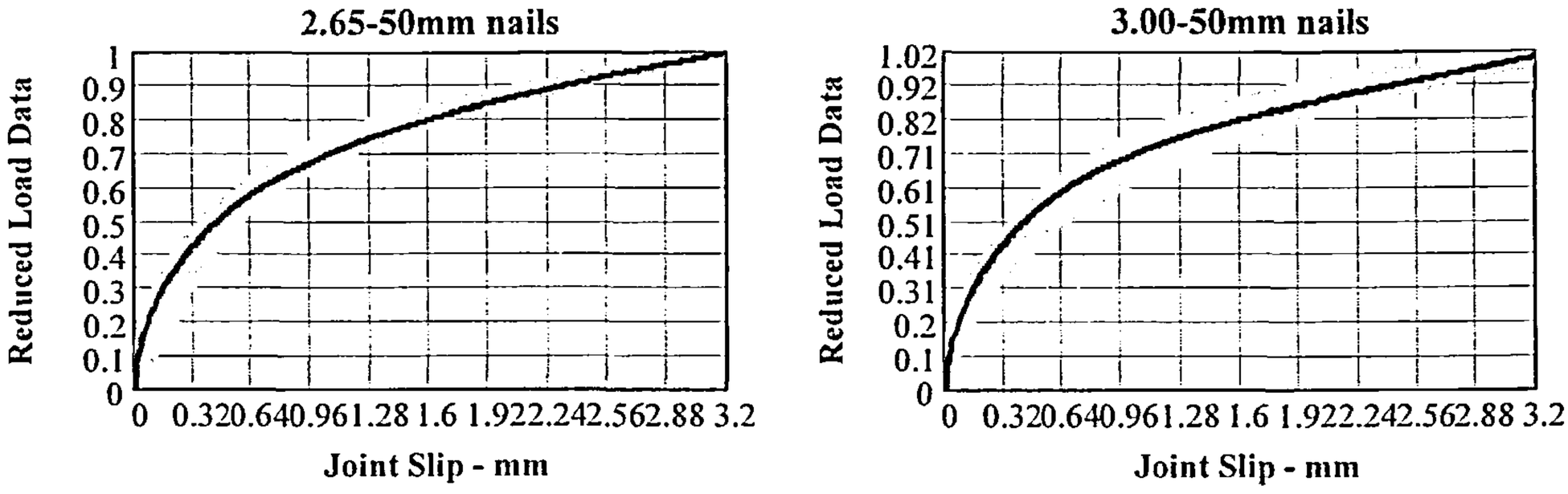

Figure 4.35 Regression graphs for 2.65mm and 3.00mm diameter nails

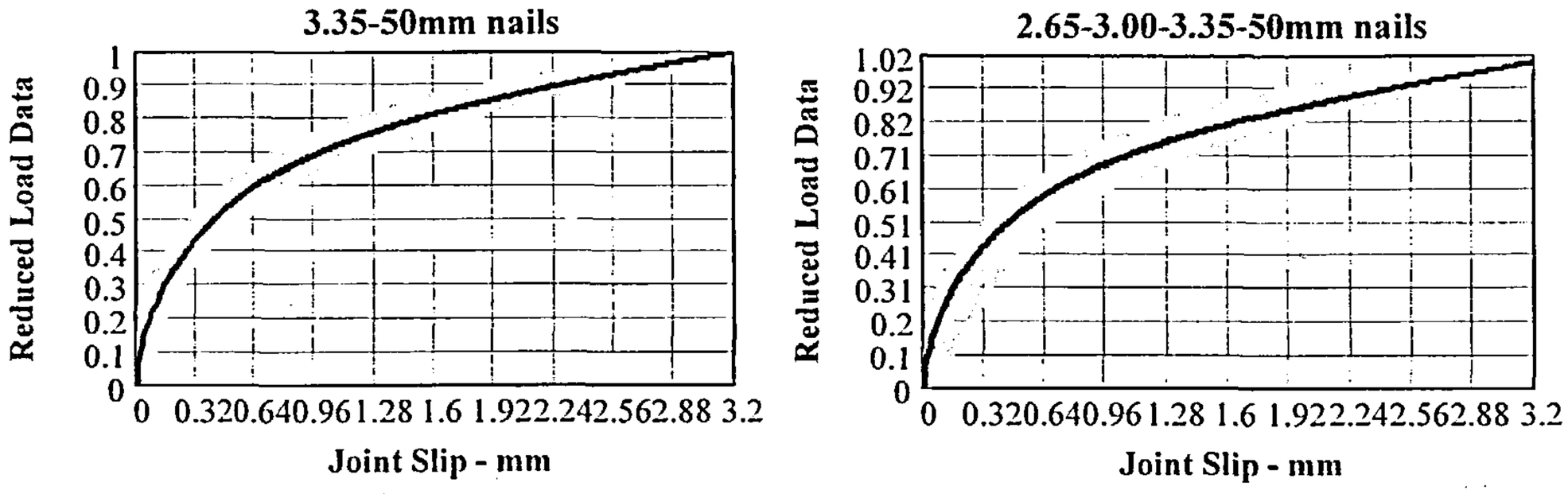

Figure 4.36 Regression graphs for 3.35mm diameter nails and for the all nail size fit.

To confirm that the use of pre-fixed values for A and B introduced no significant error to the equation a full regression fit was undertaken for each nail size and also for the combined data and the fits obtained confirmed there had been no loss in accuracy. The result of the full regression fit against the combined data is given in equation (59) and when compared with equation (58) in Figure 4.37 the plots are effectively coincident and cannot be discriminated.

$$g_1(\delta_x) = (1-e^{-1.473\delta x})^{0.545}(0.091\delta x + 0.711) \qquad \ldots.(59)$$

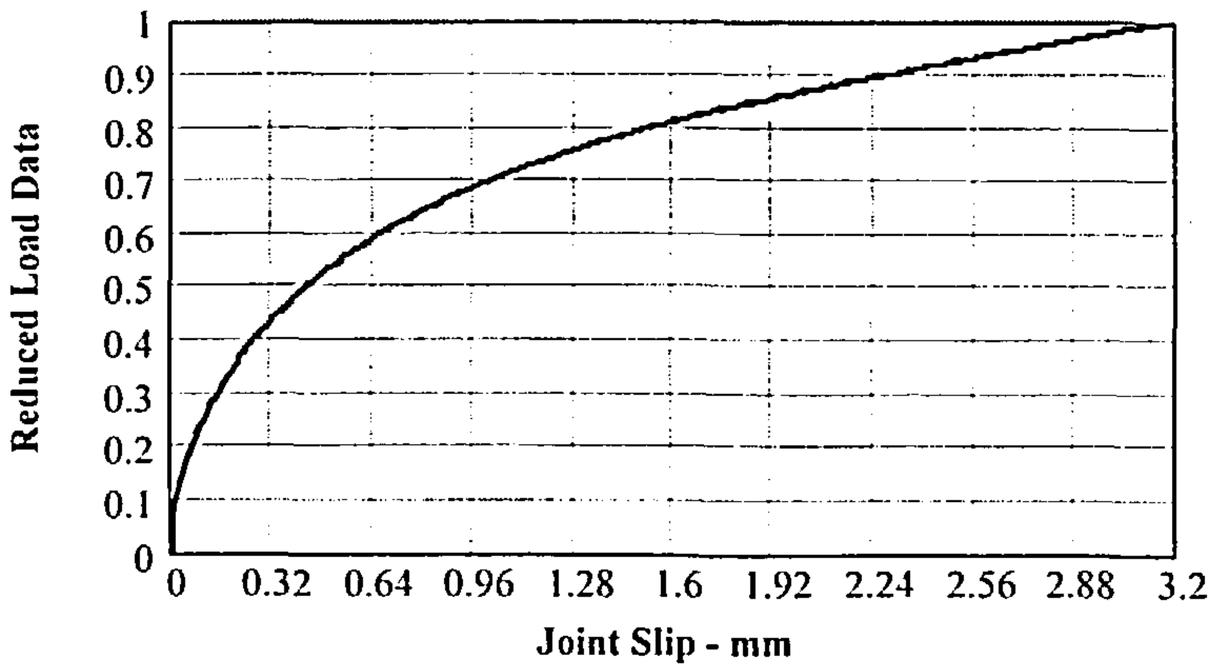

Figure 4.37 Regression graphs in equations (58) and (59) against the combined 2.65mm; 3.00mm and 3.35mm nail joint data.

It is to be noted that compared with the steel gusset plate joints in section 4.4.1, the spread of data is much more limited for each nail diameter and across the diameters and this is reflected in the value of the coefficient of determination, R^2, for each fit as shown below.

Nail Diameter	**R^2 value**	**Nail Diameter**	**R^2 value**
2.65mm	0.993	3.35mm	0.99
3.00mm	0.994	All diameters	0.992

The displacement functions in equations (55) to (58) inclusive are presented in graphical form in Figure 4.38.

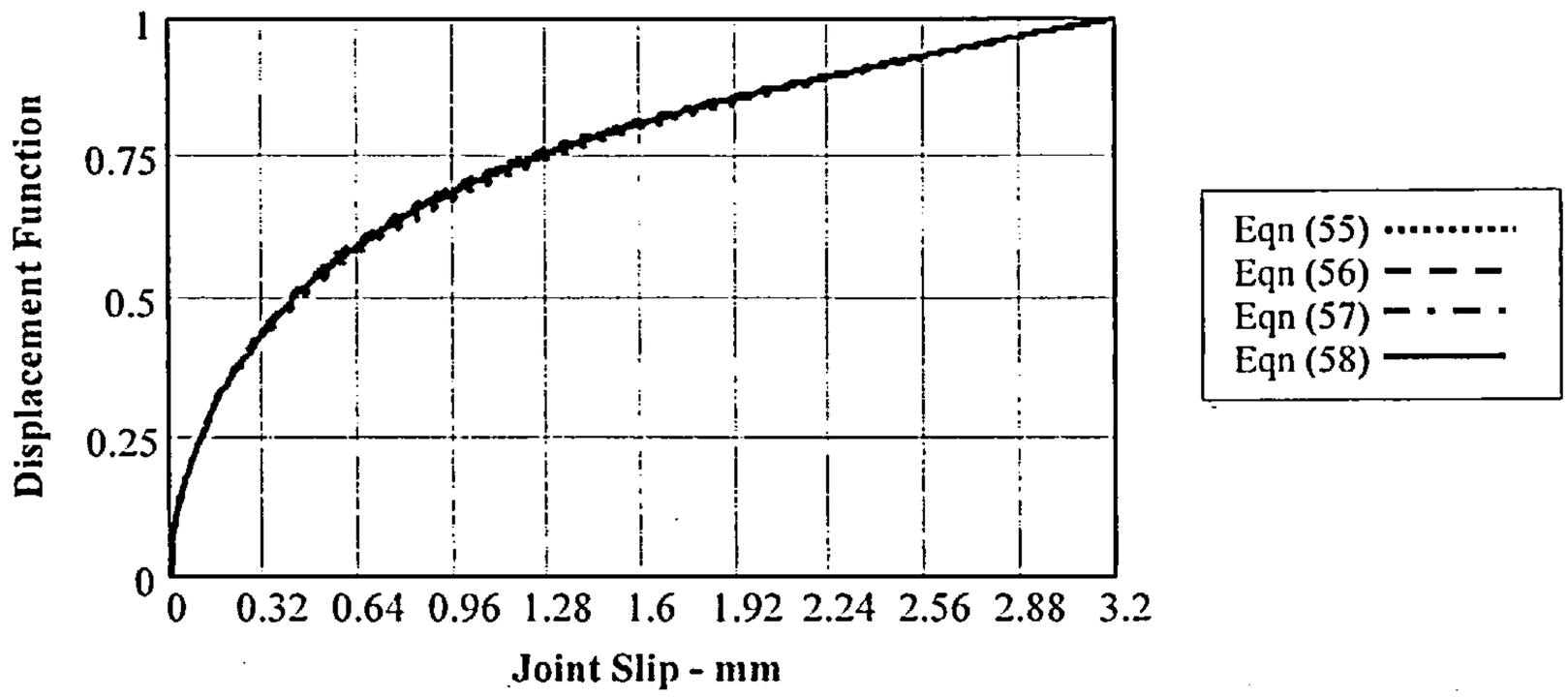

Figure 4.38 Displacement functions given in equations (55),(56),(57) and (58).

From Figure 4.38 it can be seen that the displacement function for each nail diameter is effectively the same. This is what was expected and reinforces the view expressed in section 4.4.1 that the displacement function for 3.00mm diameter nails with steel gusset plates was an unexpected occurrence and is more likely to relate to factors that were specific to the 3.00mm diameter Rynail nail than to factors common to all nail diameters.

The displacement function derived by Mack [6] for plywood gusset plates is given in equation (61) whilst Kermani *et al* [75] and McLain [7] use the same displacement function whether the gusset plates are made from plywood or from steel. For the reasons given in section 4.4.1, after reduction to unit values at the maximum slip and adjustment to a common base line slip of 2.54mm slip, the Kermani *et al* [75] and McLain [7] functions are as given in equations (14) and (15) respectively and together with the Mack displacement function are compared with equation (58), the average displacement function for the three nail sizes, in Figure 4.39. As the Kermani *et al* [75] displacement function is also a function of the number of nails in the joint, an average of 18 nails has been used for the comparison, equating to the average number of nails used for the joints in the reduced load data base. Also, in determining the coefficients for the McLain equation [7], a timber density of 600Kg/m^3 has been used.

$$fpMack(\delta x) = (1-e^{-2.953\delta x})^{0.6}(0.161\delta x+0.54) \quad \ldots.(61)$$

$$fKermani(\delta x) = (83(1-e^{-0.75\delta x}) - 0.73N\delta x e^{-0.75\delta x}) \quad \ldots.(14)$$

$$fMcLain(\delta x) = 0.545log(1+ 28.24\delta x) \quad \ldots.(15)$$

where x is the joint slip and N is the number of nails in the joint.

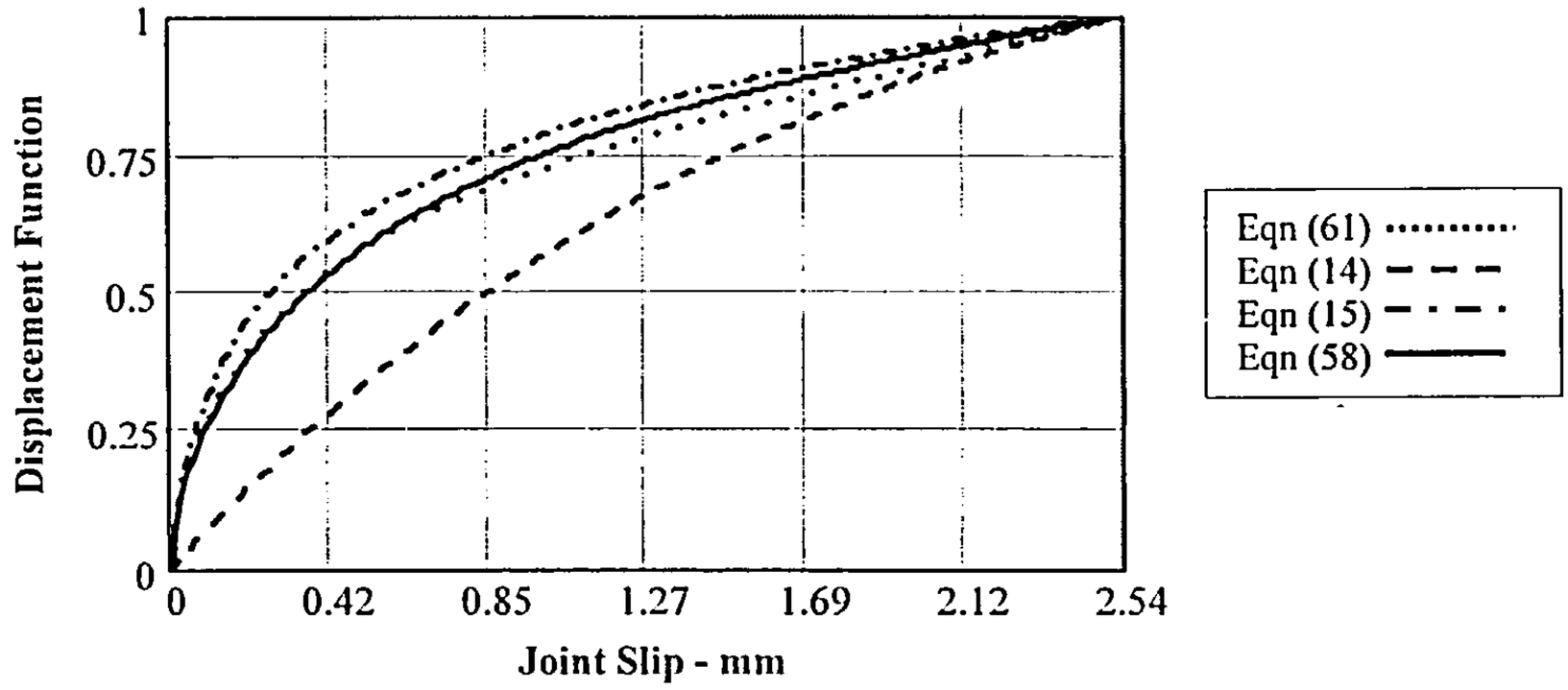

Figure 4.39 The average displacement function –eq'n (58); Mack's displacement unction –eq'n (61); Kermani *et al* displacement function – eq'n (14); McLain's displacement function – eq'n (15)

As was found with the steel gusset plate displacement function, the displacement function for plywood gusset plate joints is considerably stronger and stiffer than the Kermani *et al* equation over the full slip range. Also, as the number of nails in the joint increases the greater will be the difference. In regard to the comparison with the Mack function, there is an almost perfect fit along the graph with deviations of less than 4% in strength beyond 1mm slip. In the vicinity of the 0.25mm to 0.4mm slip, which can be considered to envelope the serviceability limit state of the joints, the functions coincide. The comparison with the McLain function is not quite as good but is still within 10% over the full range of slip.

To simplify equation (58), the exponential coefficients can be reduced in size and written as presented in equation (62) with minimal loss of accuracy and used as the displacement function, $fp_1(\delta_x)$.

$$fp_1(\delta_x) = (1-e^{-1.9\delta x})^{0.6}(0.1\delta x + 0.68) \quad \ldots.(62)$$

4.7.3 Density Function $(fp_2(D))$

From equations (52) and (62), at 3.2mm slip, $f_1(\delta_x) = 1$ and $P = P_{3.2}$ and the following relationship exists:

$$P_{p3.2} = (1), f_{p2}(D), f_{p4}(d), f_{p5}(f_u), f_{p6}(k_g), f_{p7}(r), f_{p8}(S_p), n \quad \ldots.(64)$$

To investigate the effect of the density function, $f_{p2}(D)$, on joint behaviour the influence of 'yielding' of the plywood gusset plate must be taken into account in addition to the yielding effect of the timber in the joint.

For each nail diameter, the results of tests on joints formed with the same nailing configurations were analysed using alternative relationships for the density function. These included the assumption that it could be a function of the ratio of the material densities; that it could be a power function of the product of the densities; finally reviewing the method proposed by Morris *et al* [83]. The best fit was obtained from the Morris *et al* approach and this method has in principle been followed.

The Morris *et al* approach takes into account material thickness and the basic density of the timber and plywood in the joint and was developed for joints using non-overlapping nails loaded in double shear. The approach has been modified to apply to joints with fully overlapping nails in single shear and using material density at the test programme moisture content, rather than the basic density. On this basis the relationship for the density function, $f_{p2}(D)$, becomes:

$$f_{p2}(D) = 2(b_1 D_{we} + b_2 D_{pe}) \qquad \ldots.(65)$$

where the function is based on the use of a pairs of fully overlapping nails in single shear as shown in Figure 4.40 and:

b_1 and b_2 = constants which modify the density of the timber and plywood and $(b_1+b_2 = 2)$

D_{we} = the weighted density of the timber $= t_w D_w/(t_w + t_p)$

D_{pe} = the weighted density of the plywood $= t_p D_p/(t_w + t_p)$

D_w = the density of the timber

D_p = the density of the plywood

t_w = the penetration of the nail into the central timber member

t_p = the thickness of each plywood gusset.

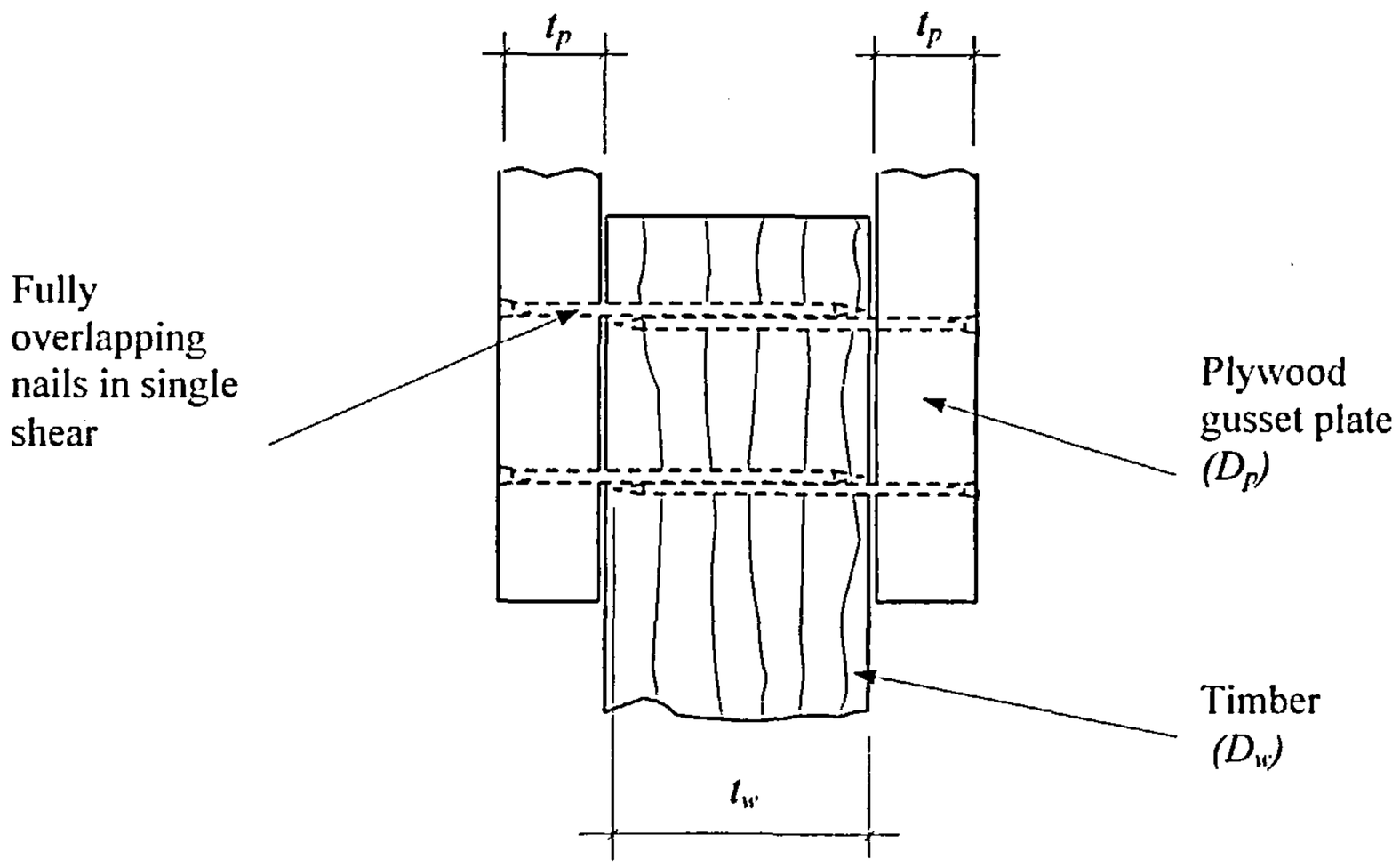

Figure 4.40 The Factors used in the Density Function for joints with plywood gusset plates

To determine the density function, the joint load at 3.2mm slip ($P_{3.2}$) was obtained for two sets of joints with differing density and thickness properties but having the same nailing configuration and the same nail diameter. This ensured that the effect of nail strength; nail diameter; number of nails; nail row and spacing functions would be the same between the sets and would not influence the comparison. On this basis for each nail diameter, for test sets 1 and 2, equation (64) can be written as:

$$P1_{p3.2} = (1), f_{p2}(D1),\ f_{p4}(d), f_{p5}(f_u), f_{p6}(k_g), f_{p7}(r), f_{p8}(S_p),\ n \qquad \text{.....(66a)}$$

$$P2_{p3.2} = (1), f_{p2}(D2),\ f_{p4}(d), f_{p5}(f_u), f_{p6}(k_g), f_{p7}(r), f_{p8}(S_p),\ n \qquad \text{.....(66b)}$$

Dividing equation (66a) by equation (66b) and using equation (64) for the density function, for each nail diameter the following relationship can be set up:

$$P1_{p3.2}/P2_{p3.2} \quad = (b_1 D1_{we} + b_2 D1_{pe})/\ (b_1 D2_{we} + b_2 D2_{pe}) \qquad \text{....(67)}$$

To ensure that ill conditioned equations were not used in the analysis, for each nail diameter one of the test sets was assembled using 19mm plywood gusset plates with the other used 12mm plates. Although not strictly necessary, it was also decided to use joints with nail row spacing greater than $4\times0.85\times7\times d$. A summary of the average properties of the test joint sets for each nail diameter together with the average $P_{p3.2}$ value is given in Table 4.19.

Nail diameter mm	Set number	Nailing conf'n	Timber density kg/m^3	Plywood density kg/m^3	Nail penetration mm	Plywood thickness mm	$P_{p3.2}$ N
2.65	1	EK	594.67	601.77	41.9	17.33	19516.57
2.65	2	EK	596.42	719.78	40.16	10.094	17275.57
3.00	1	ES	553.68	594	41.17	17.85	23832.4
3.00	2	ES	562.43	668.53	39.567	9.92	20196.87
3.35	1	ET	574.51	603.32	40.92	17.69	25303.3
3.35	2	ET	617.76	706.59	39.63	9.88	21577.88

Table 4.19 Average properties and $P_{P3.2}$ data of the joint test sets used to determine the density function for each nail diameter

Substituting into equation (67), the values of b_1 and b_2 were obtained for each nail diameter and are given in Table 4.20.

From a plot of the b constants against the ultimate nail strength f_u, it was observed that there was a linear relationship between the value of the constant and the associated nail strength and the plot of b_2 against f_u is shown on Figure 4.41.

Actual nail diameter mm	b_1	b_2	Ultimate nail strength f_u n/mm^2
2.66	0.289	1.711	827
3.01	0.259	1.741	792
3.33	0.171	1.829	697

Table 4.20 Value of b_1 and b_2 functions for each nail diameter

The fit is almost perfect and as $(b_1 + b_2) = 2$, the relationship between the constants and the ultimate nail strength can be written as:

$$b_1 = (0.000912f_u - 0.464) \text{ and } b_2 = (2.464 - 0.000912f_u) \quad \ldots.(68)$$

Substituting into equation (65), the Density Function, $f_{p2}(D)$, becomes:

$$f_{p2}(D) = 2((0.000912f_u - 0.464)D_{we} + (2.464 - 0.000912f_u)D_{pe}) \quad \ldots.(69)$$

where D_{we} and D_{pe} are the weighted density values of the timber and plywood respectively and are as defined under equation (65).

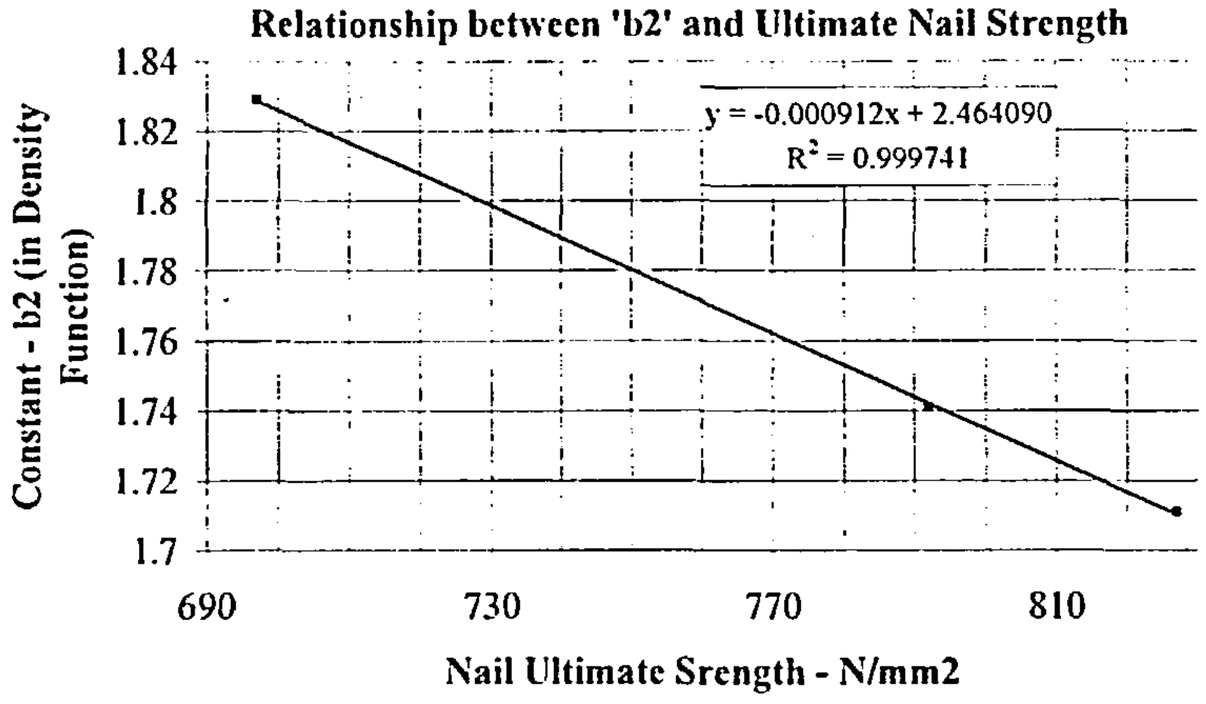

Figure 4.41 Relationship between constant b_2 and Ultimate Nail Strength f_u

4.7.4 Nail Diameter Function ($fp_4(d)$) and Nail Strength Function ($fp_5(f_u)$)

With single row joints and using two lines of fully overlapping nails, for each nail size the load displacement relationship per unit density at 3.2mm slip and at service class 1 conditions given in equation (52) can be written as:

$$Pp_{3.2}/f_{p2}(D) = f_{p4}(d), f_{p5}(f_u), f_{p6}(k_g), f_{p7}(r), f_{p8}(S_p), 2 \quad \ldots.(70)$$

where

$P_{3.2}$ is the load in the joint at a slip of 3.2mm.

$f_{p\,2}(D)$ is the density function

$f_{p7}(r)$ is the row function and will be taken as 1 for a single row of nails

$f_{p8}(S_p)$ is the row spacing function and will also be taken as unity for a single row of nails.

$f_{p9}(l)$ is the number of lines of overlapping nails in the joint = *2*

and the remaining functions $f_{p4}(d), f_{p5}(f_u), f_{p6}(k_g)$ being unknowns to be evaluated.

From the joint test results, values for $P_{p3.2}/f_{p2}(D)$ were obtained for joints with a single row of nails using nail configuration CO. Also values were obtained from the analysis of multi-row joints with row spacing equal to or greater than $4\times0.85\times7\times d$ by dividing the $P_{p3.2}/f_{p2}(D)$ result by the number of rows in the joint. The average result for each nail diameter was:

Nail Diameter	$P_{p3.2}/f_{p2}(D)$**/number of rows**	
2.65mm	4.591612	....(70a)
3.00mm	5.657876	....(70b)
3.35mm	6.406274	....(70c)

These values give the load taken at a unit density function for timber joints with plywood gusset plates at service class 1 conditions, at a slip of 3.2mm slip using pairs of overlapping nails in joint configuration CO. Applying the values to equation (70), the following relationships can be established:

$$4.591612/2 = f_{p4}(d_{2.65})\, f_{p5}(f_{u2.65})\, f_{p6}(k_g) \quad \text{....(71a)}$$

$$5.657876/2 = f_{p4}(d_{3.00})\, f_{p5}(f_{u3.00})\, f_{p6}(k_g) \quad \text{....(71b)}$$

$$6.406274/2 = f_{p4}(d_{3.35})\, f_{p5}(f_{u3.35})\, f_{p6}(k_g) \quad \text{....(71c)}$$

Equations (71a), (71b) and (71c) are functions of the nail diameter, nail strength and the generic function of the joint and by dividing by equation (71a) are reduced to functions of the nail diameter and nail strength only:

$$1 = f_{p4}(d_{2.65}/d_{2.65})\, f_{p5}(f_{u2.65}/f_{u2.65}) \quad \text{....(72a)}$$

$$1.28667 = f_{p4}(d_{3.00}/d_{2.65})\, f_{p5}(f_{u3.00}/f_{u2.65}) \quad \text{....(72b)}$$

$$1.65544 = f_{p4}(d_{3.35}/d_{2.65})\, f_{p5}(f_{u3.35}/f_{u2.65}) \quad \text{....(72c)}$$

In line with the argument in section 4.4.4 for joints with steel gusset plates, a linear function has been used for the nail strength function in the timber joint equation. On this basis the nail strength function becomes:

$$f_{p5}(f_u) = f_u/f_{u2.65} \quad \ldots(73)$$

where

f_u = the tensile strength of the nail size used in the joint

$f_{u2.65}$ = the tensile strength of the 2.65mm diameter nail

From tests on the Castlenail nails the tensile strength of the wire in the 2.65; 3.00 and 3.35mm diameter, 60m long nails was 827; 792 and 697 N/mm^2 respectively, as reported in Appendix B, and using equation (73) the nail strength functions for each nail size are given in Table 4.21:

Nail diameter – mm	Nail strength function $f_{p5}(f_u)$
2.65	827/827
3.00	792/827
3.35	697/827

Table 4.21 Nail Strength Functions for the nails used in the plywood gusset joints

Inserting the nails strength functions in equations (72a), (72b) and (72c) the nail diameter function is obtained. Using the actual nail diameter sizes of 2.66mm, 3.01mm and 3.33mm as given in Chapter 3, performing a least squares linear regression fit and adopting a power function, the nail diameter function $f_{p4}(d)$ is:

$$f_{p4}(d) = 0.1113\ (d)^{2.236} \quad \ldots.(74)$$

The coefficient of determination R^2 against the fit was 0.9967 and the regression plot against the data is shown in Figure 4.42.

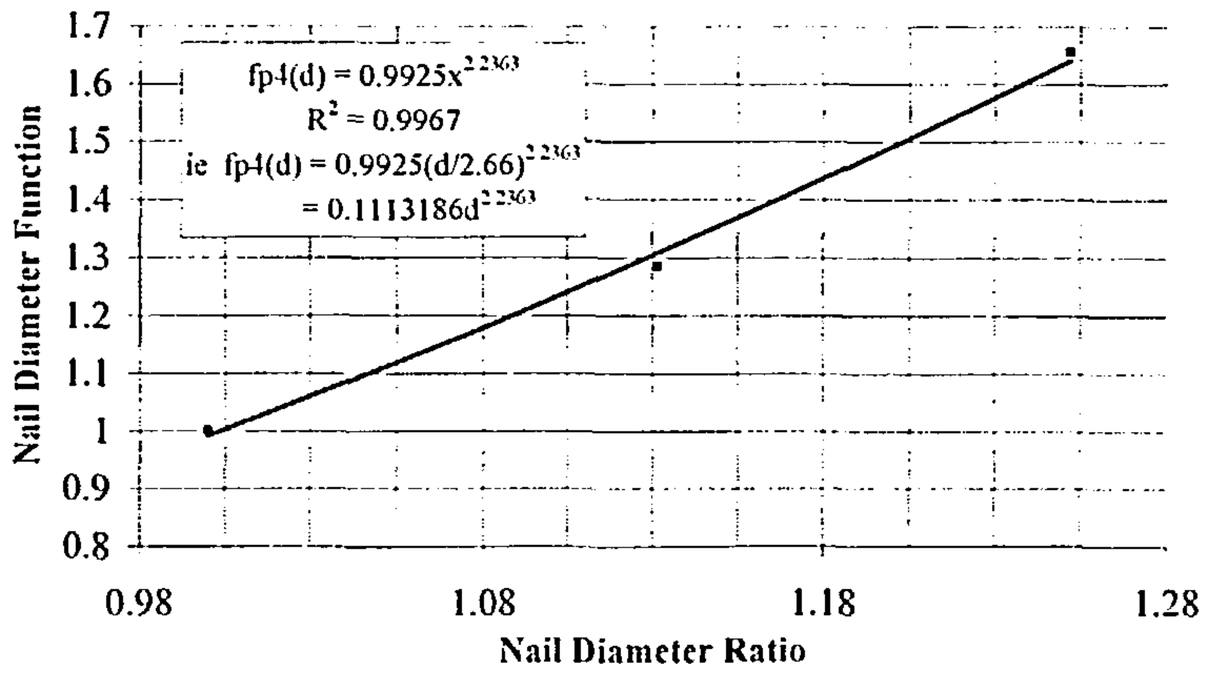

Figure 4.42 Nail diameter function regression fit

The function is different to the diameter function derived in section 4.4.4 for joints with steel gusset plates and in none of the published research has reference been made to the diameter function changing when using differing gusset plate materials. Although both types of joint are being loaded to 3.2mm slip, in the case of joints with plywood gussets the slip is the aggregate of the nail movement in the timber and the movement in the plywood. In the case of the steel gusset plate joints, there is negligible movement from the nail in the gusset plate and the slip is primarily due to the nail movement in the timber. This means that for the same joint slip the timber in joints with steel gusset plates is being subjected to greater stress resultants than in joints with plywood gusset plates and is likely to be a reason why the joint functions differ.

A comparison of the function in equation (74) with the nail diameter function for joints with steel gusset plates given in equation (24) as well as the $d^{1.75}$ function developed by Wilkinson [81] and the $d^{1.8}$ function used in EC5 [15] for small nail diameters in predrilled holes is shown on Figure 4.43.

As the nail diameter increases, equation (74) shows a much higher rate of increase than the other models and is 9.6% more than the Eurocode function with a nail diameter of 3.35mm. As the nail diameter gets smaller however, the diameter function gets closer to the others and will reduce below these models when the diameter is less than 2.65mm. The largest variation is between this function and the steel gusset plate diameter function. Only three nail sizes were used in the testing programme and the function can only be taken as valid for these nail sizes.

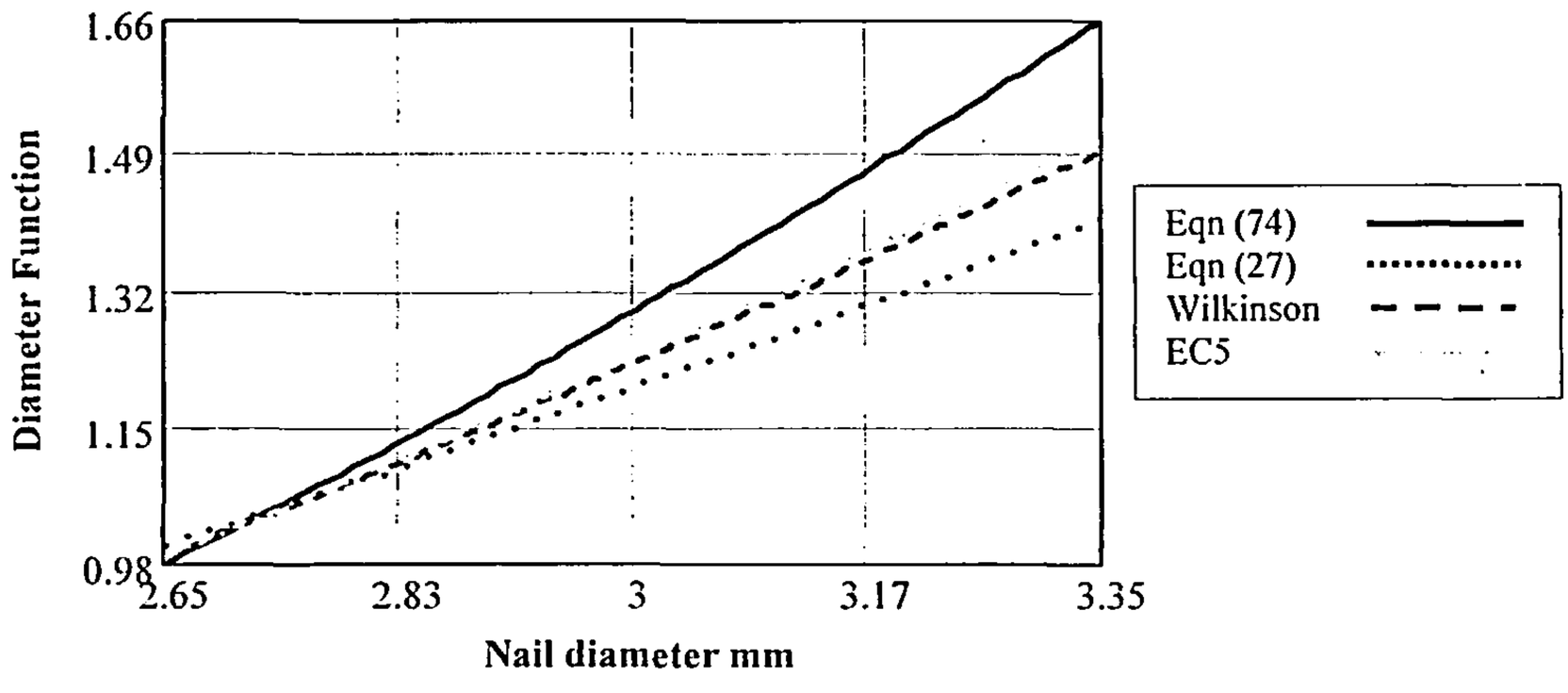

Figure 4.43 Comparison of equation (74) with the function for steel gusset plates in equation (27) and other diameter functions developed by Wilkinson and EC5.

4.7.5 Generic Function $(fp_6(k_g))$

The relationship between the generic function $f_{p6}(k_g)$ and the joint strength is given in equations (71a), (71b) and (71c) and inserting the nail strength functions given in Table 4.21 and the nail diameter function given in equation (74), the generic function associated with each nail diameter together with the average for each nail size is given in Table 4.22.

Nail diameter – mm	Generic function ($f_{p6}(k_g)$
2.66	2.31315
3.01	2.25745
3.33	2.31707
Average for all nail sizes	**2.296**

Table 4.22 The generic function ($f_{p6}(k_g)$) for plywood gusset late joints with a pair of fully overlapping nails

The function should be the same for all nail diameters and as the deviation from this figure is a maximum of +0.9% and a minimum of -1.7%, this is considered to be acceptable. The generic function ($f_{p6}(k_g)$) for plywood gusset plate joints with a pair of fully overlapping nails in single shear is taken as the average value for all nail sizes, 2.296.

Because the joints with plywood gusset plates are not stressed to the same degree as joints with steel gusset plates, the value of the respective generic functions should differ. This has also been found to be the case in this research.

It is further to be noted that Mack [6] did tests on timber joints with nails in single shear and converting his species factor coefficient from imperial to metric units, an equivalent generic function of 2.403 for a pair of overlapping nails is obtained. Also, from the research by Morris *et al* [83] into joints with plywood gusset plates using nails in double shear, an equivalent generic function of 2.519 can be derived. The value of the displacement function from this research appears to be in line with the values derived by other researchers for nailed joints using plywood gusset plates.

4.7.6 Nail Row Function ($f_{p7}(r)$)

The nail row function is investigated on the same basis as has been used in section 4.4.6 for joints with steel gussets.

An analysis was carried out on the results of those test joints with a row spacing approximately equal to or greater than 4 times the minimum values recommended in EC5 [15]. The row spacing criteria used for the selection of the joints to be analysed for each diameter has been chosen to try and align with the latest spacing criteria in EC5 [15] where Table 8.1 gives an upper limit of $14d$ and a lower limit of $5d$ as the extremes for nails which do not fully overlap. As stated, a factor of 2 is applied to these limits when using fully overlapping nails and also applying the 0.85 coefficient given in clause 8.3.1.4 of the code when using joints formed with plywood gusset plates, the row spacing criteria used for the joint selection will be as given in Table 4.23.

Nail diameter mm	Minimum spacing $0.85\times2\times5\times d$	Maximum spacing $0.85\times4\times7\times d$	Acceptable spacing for the nail row function analysis
2.65	22.53	63.07	≥ 63
3.00	25.5	71.40	≥ 72
3.35	28.49	79.73	≥ 80

Table 4.23 Criteria used for row spacing in the row function $(f_{p7}(r))$ analysis

With multi-row joints using two lines of fully overlapping nails, for each nail diameter the load displacement relationship per unit density function at 3.2mm slip and at service class 1 conditions given in equation (52) will apply. Using joints with row spacing equal to or greater than the criteria given in Table 4.23, the row spacing function $f_{p8}(S_p)$ will be unity. As all of the joints tested in the programme had 2 lines of nails, the nail line function $f_{p9}(l)$ will be 2 and, for each nail diameter, equation (52) can be rewritten as:

$$Pp_{3.2}/f_{p2}(D) = f_{p4}(d), f_{p5}(f_u), f_{p6}(k_g), f_{p7}(r) \times 1 \times 2 \qquad \ldots.(75)$$

For joints with a single row of nails (configuration CO), the row function will be taken as unity and applying equation (75) to each nail diameter and dividing by the equation for joint configuration CO, functions $f_{p4}(d), f_{p5}(f_u)$ and $f_{p6}(k_g)$ will be eliminated. By rearranging the equations the row function $f_{p7}(r)$ for each nail diameter will be given as:

$$f_{p7}(r)r = (P_{p3.2}/f_{p2}(D) \text{for multi-nail joint})/(P_{p3.2}/f_{p2}(D) \text{ for joint CO}) \qquad \ldots.(76)$$

where r is the number of rows in the joint.

Equation (76) was evaluated for all multi-nail joints for each nail diameter compliant with the row spacing criteria given in Table 4.23 and the results are given in Table 4.24.

A linear regression analysis was undertaken on the data for each nail diameter and for the combined data and the latter is shown in Figure 4.44.

The coefficient of determination R^2 exceeded 0.99 in all of the fits and the row function relationship for each nail diameter was:

2.65mm diameter nails	$f_{p7}(r) = 0.9921 \times r$	....(77a)
3.00mm diameter nails	$f_{p7}(r) = 1.0000 \times r$	....(77b)
3.35mm diameter nails	$f_{p7}(r) = 0.9859 \times r$	....(77c)
All nail diameters	$f_{p7}(r) = 0.9919 \times r$	....(77d)

2.65mm diameter conf'n	Number of rows in the joint	$f_{p7}(r)xr$	3.00mm diameter conf'n	Number of rows in the joint	$f_{p7}(r)xr$	3.35mm diameter conf'n	Number of rows in the joint	$f_{p7}(r)xr$
CO	1	1	CO	1	1	CO	1	1
EJ	3	3.021219	RZ	4	3.863196	RZA	4	3.761379
EJ	3	2.824727	ES	5	4.899719	RZA	4	3.883668
RY	4	3.761774	ES	5	5.104036	ET	5	4.928851
RY	4	3.82581	ES	5	5.106535	ET	5	4.915442
RY	4	4.055467				ET	5	5.150948
EK	5	4.981232				ET	5	4.914906
EK	5	5.017879						
EK	5	5.021314						
EQ	7	6.862555						
EQ	7	7.121509						

Table 4.24 Value of $f_{p7}(r) \times r$ for each nail diameter and joint configuration

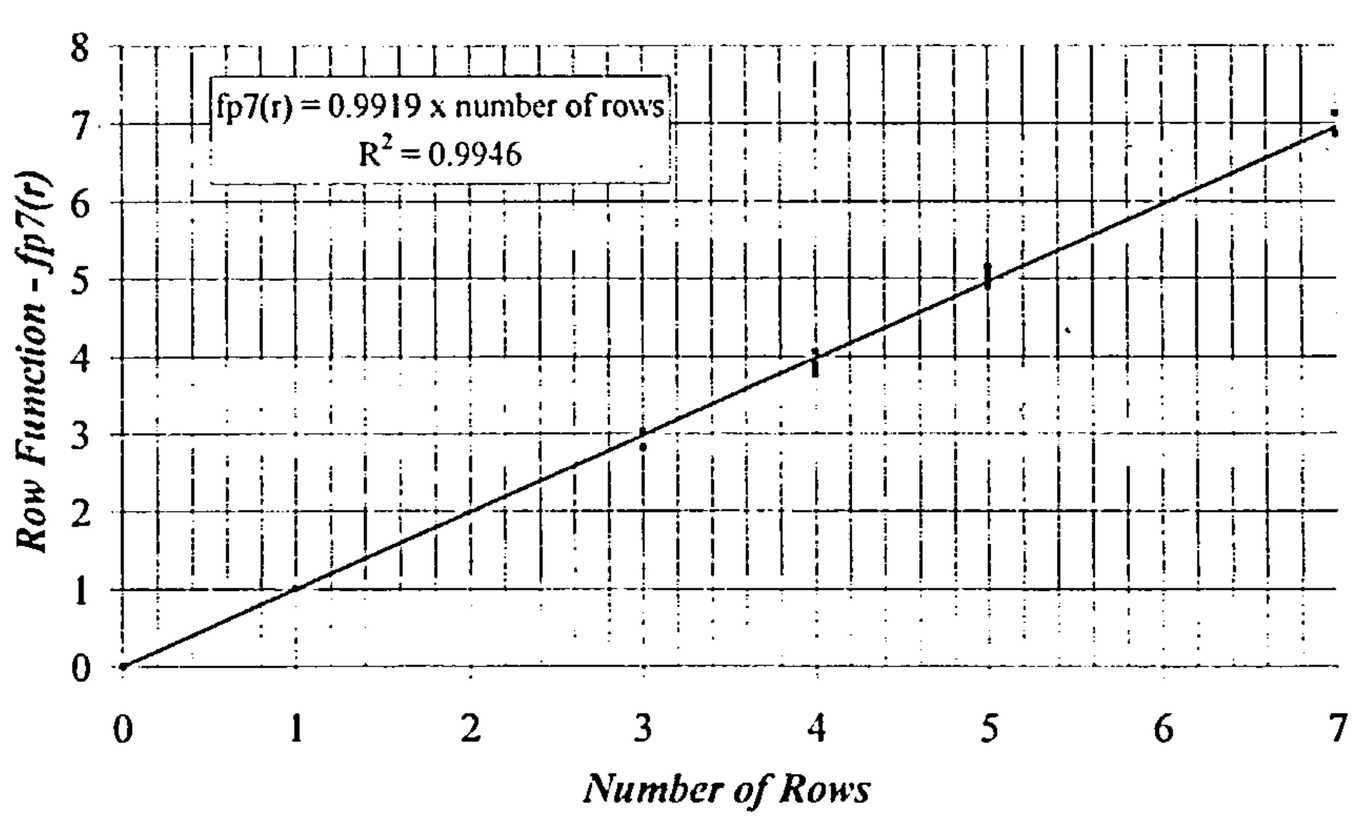

Figure 4.44 Linear regression fit of the row function data in Table 4.24 for 2.65mm, 3.00mm and 3.35mm diameter nails

The row function coefficient for the full data fit is 0.9919, which is effectively unity, and, as for joints with steel gusset plates, the row function for all nail diameters will be taken as:

$$f_7(r) = 1 \times r \qquad \ldots.(78)$$

where r is the number of rows in the joint.

The maximum number of rows used in the testing programme at this spacing was 7 and further testing is required to confirm that the finding will apply for joints with a greater number of rows.

4.7.7 Row Spacing Function ($f_{p8}(Sp)$)

4.7.7.1 Row Spacing Exceeding 4×0.85×7×d

In the analysis in section 4.7.6 the nail row function was obtained using joints with a row spacing exceeding $4\times0.85\times7\times d$ as summarised in Table 4.25.

2.66mm diameter-nailing conf'n	Row spacing in the Joint ($4\times0.85\times7\times d$=63.07) mm	3.01mm diameter-nailing conf'n	Row spacing in the joint ($4\times0.85\times7\times d$=71.4) mm	3.36mm diameter-nailing conf'n	Row spacing in the joint ($4\times.85\times7\times d$=79.73) mm
EJ	66.67	ES	75	ET	83.33
EK	66.67	RZ	75	RZA	83.33
EQ	66.67				
RY	66.67				

Table 4.25 The joint row spacing exceeding $4\times0.85\times7\times d$ used in the row function analysis

On this basis the row spacing function at and above $4\times0.85\times7\times d$ must also be unity:

$$f_{p8}(Sp) = 1 \qquad \ldots.(79)$$

4.7.7.2 Row Spacing Exceeding 4×0.85×5×d

The row spacing function between 4×0.85×5×d and 4×0.85×7×d was also investigated and the joint configurations used are given in Table 4.26.

A linear regression analysis was carried out on the data for each nail diameter and the coefficient of determination, R^2, exceeded 0.99 in all of the fits and the row spacing function for each nail diameter was:

2.66mm diameter nails	$f_{p8}(Sp) = 1.0012$	….(80a)
3.01mm diameter nails	$f_{p8}(Sp) = 0.9977$	….(80b)
3.33mm diameter nails	$f_{p8}(Sp) = 0.9837$	….(80c)
All nail diameters	$f_{p8}(Sp) = 0.994$	….(80d)

2.65mm diameter-nailing conf'n	Row spacing in the joint (4×0.85×5×*d*=45.22) mm	3.00mm diameter-nailing conf'n	Row spacing in the joint (4×0.85×5×*d*=51.7) mm	3.35mm diameter-nailing conf'n	Row spacing in the joint (4×.85×5×*d*=56.61) mm
EG	50	EJ	66.67	EJ	66.67
EJ	66.67	EK	66.67	EK	66.67
EK	66.67	EQ	66.67	EU	66.67
EQ	66.67	ES	75	ET	83.33
RY	66.67	RZ	75	RZA	83.33

Table 4.26 The joint row spacing used in the row function analysis for row spacing of 4×0.85×5×*d*.

The row spacing function for all nail diameters was 0.994, again effectively unity. Consequently, for all nail diameters with row a spacing of 4×0.85×5×*d* and above the row spacing function will be:

$$f_{p7}(Sp) = 1 \qquad \ldots.(81)$$

4.7.7.3 Row Spacing between 2×0.85×5*d* and 4×0.85×5×*d*

To obtain the relationship for the row spacing function for joints with row spacing between the minimum recommended spacing of 2×0.85×5×*d* up to the 4×0.85×5×*d* limit, using the approach adopted in 4.4.6, for joints with plywood gusset plates equation (35) can be rewritten as:

$$f_{p8}(Sp) = [(P_{p3.2}/f_{p2}(D) \text{for multi-nail joint})/r] \,/\, [(P_{p3.2}/f_{p2}(D) \text{ for joint CO}] \qquad \ldots.(82)$$

Equation (82) was evaluated for each nail diameter using a selection of the multi-nail joints with joint spacing within the range being investigated and the results are given in Table 4.27.

2.65mm diameter -nailing Conf'n	Row spacing	$fp_8(S_p)$	3.00mm diameter -nailing conf'n	Row spacing	$fp_8(Sp)$	3.35mm diameter -nailing conf'n	Row spacing	$fp_8(Sp)$
RT	23	0.90432	RU	26	0.924494	RV	28	0.901411
ED	33.33	0.93027	ED	33.33	0.98886	EC	33.33	0.97645
						ED	33.33	0.90551
						EG	50	0.98142

Table 4.27 Value of $f_{p8}(Sp)$ for each nail diameter and joint configuration for row spacing between 0.85×2×5×*d* and 0.85×4×5×*d*

For Sp/d equal to 0.85×4×5×*d* the function value was set at unity. The data in Table 4.27, including for Sp/d equal to unity at a spacing of 0.85×4×5×*d*, was plotted against *Sp/d* for each nail diameter and also for the combined 'all nail diameter' data case and the latter is shown in Figure 4.45.

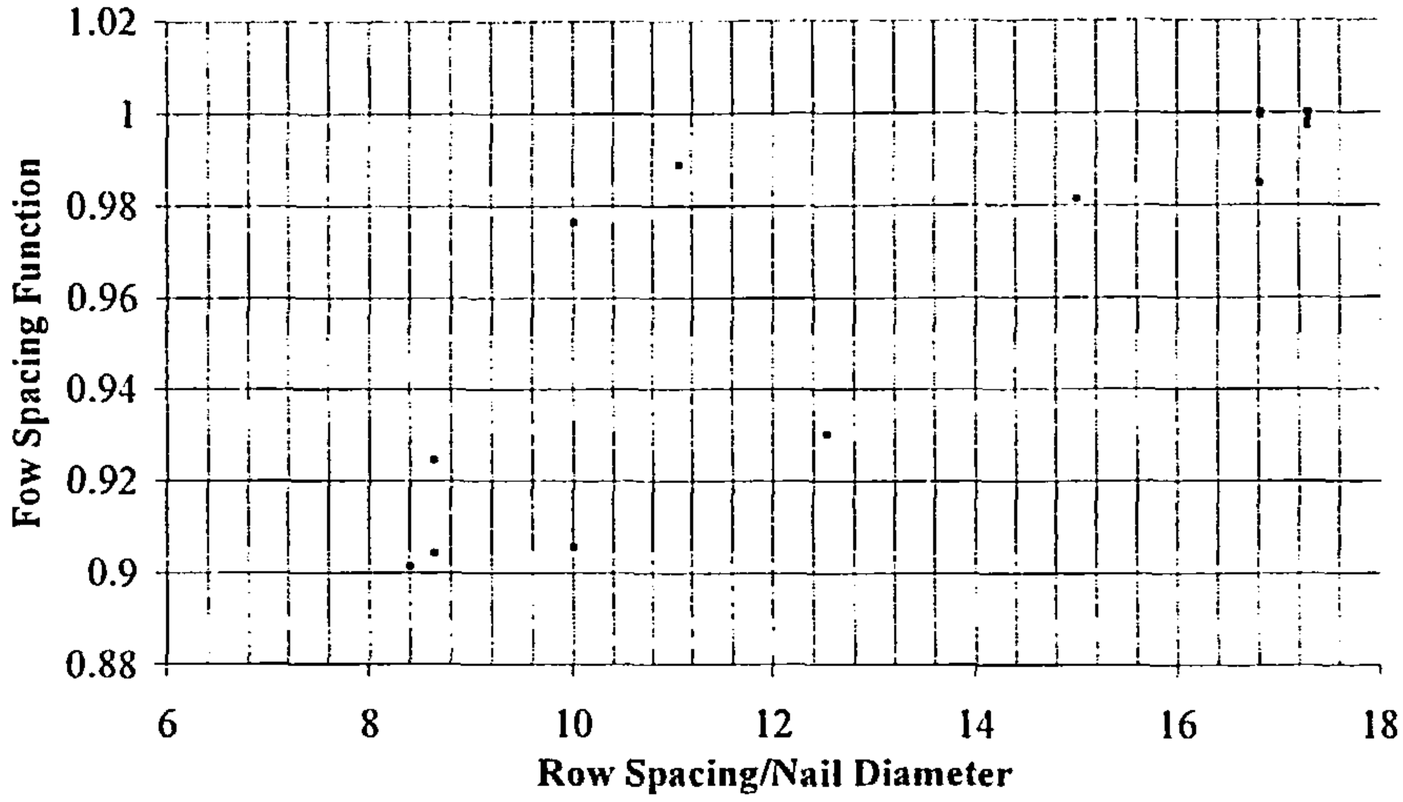

Figure 4.45 Plot of all nail diameter data against Row Spacing/Nail Diameter

As with the equivalent data in section 4.4.7, there is a high degree of variability. However there is also again a clear trend of a reducing row spacing function as the value of row spacing/nail diameter reduces. Noting that the maximum change in the value of the spacing function over the data range is less than 10%, it was felt that a linear relationship would be acceptable for the function. After a regression analysis fit using Axum [52] against the data for joints with row spacing between 2×0.85×5×*d* and 4×0.85×5×*d*, the row spacing function was:

$$f_{ps}(Sp) = 0.839 + 0.009489(Sp/d) \quad \ldots.(83)$$

4.7.7.4 Combined Expression for the Row Spacing Function

Combining the relationships in equations (79), (81) and (83), the row spacing function $f_{ps}(Sp)$ relationship for a joint with plywood gusset plates made with spacers and using fully overlapping nails in single shear is:

$$f_{p\,8}(Sp) = 1 \quad \text{when the row spacing exceeds } 0.85\times4\times5\times d$$
$$f_8(Sp) = 0.839 + 0.009489(Sp/d) \quad \text{when the row spacing is between } 0.85\times2\times5\times d \text{ and } 0.85\times4\times5\times d. \quad \ldots..(84)$$

Because the minimum and maximum row spacing criteria are different for joints with steel gusset plates and plywood gusset plates, the respective row spacing functions cannot be directly compared, however a plot of equation (84) is shown in Figure 4.46 together with the data shown on Figure 4.45.

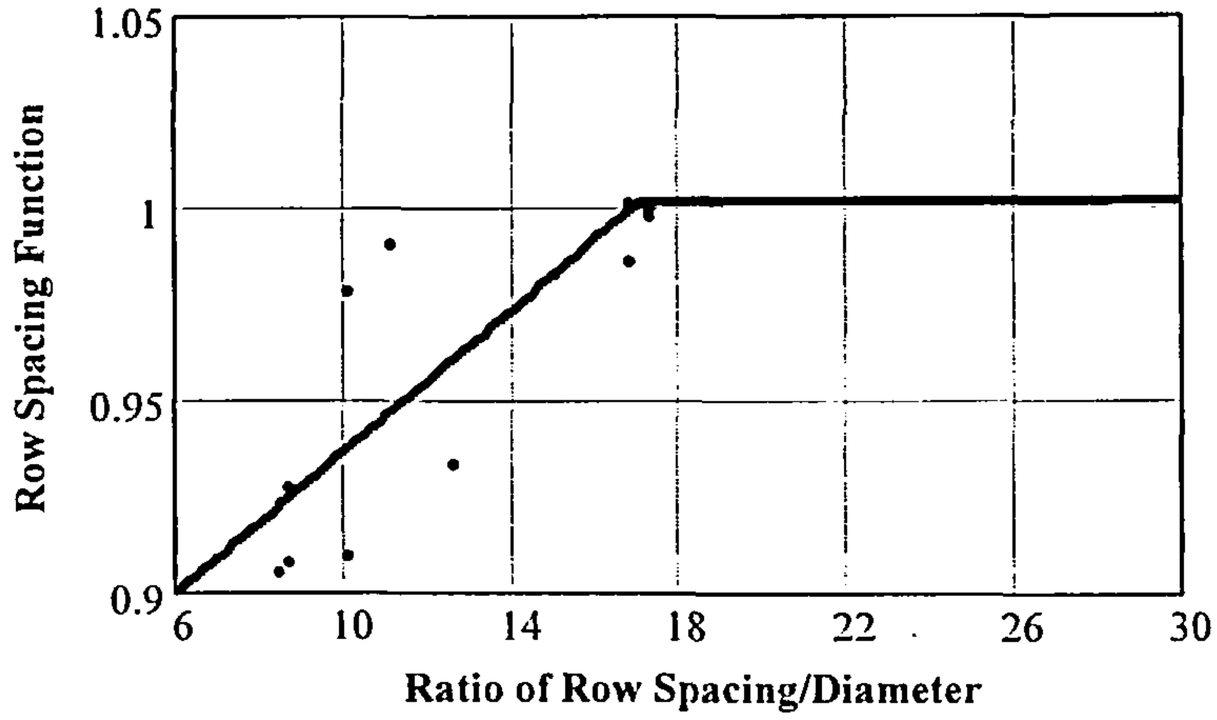

Figure 4.46 Nail Row Spacing Function for all nail diameters

The lowest ratio of row spacing/diameter can be taken as 8.5, giving a row spacing function of 0.92 and at a row spacing/diameter ratio of 17 or greater the function is unity. The greatest difference between the function and the data is associated with two joint configurations using 3.01mm and 3.33mm diameter nails where the function is approximately 5% greater than each test result, otherwise the maximum difference is around ± 2%.

4.7.8 Semi-Empirical Model for Laterally Loaded Plywood Gusset Plate Joints Formed with a Gap

In section 4.7.1 the load-displacement relationship for the joint in terms of the joint functions is given in equation (52) as follows:

$$P_p = f_{p1}(\delta), f_{p2}(D), f_{p4}(d), f_{p5}(f_u), f_{p6}(k_g), f_{p7}(r), f_{p8}(S_p), n \qquad \ldots(52)$$

Substituting the relationships developed in sections 4.7.2 to 4.7.7 for the individual functions, and including for the discontinuity in the row spacing function, the load-displacement equation is given in two forms:

$$P_p\delta_x=[(1-e^{-1.719x})^{0.568}(0.1\delta x+0.68)][D\ Function]\ [0.1113(d)^{2.236}][f_u/827][2.296]\ [r][(0.839+0.009489Sp/d)]n \qquad \ldots(85a)$$

$$P\delta_x=[(1-e^{-1.719x})^{0.568}(0.1\delta x+0.68)][D\ Function][0.1113(d)^{2.236}][f_u/827][2.296]\ [r]n \qquad \ldots(85b)$$

where equation (85a) is valid for nail row spacing between $2\times0.85\times5d$ and $4\times0.85\times5\times d$ and equation (85b) applies when the spacing exceeds $0.85\times4\times5\times d$. Rearranging and simplifying, the equations can be written:

i) for nail row spacing between $0.85\times2\times5\times d$ and $0.85\times4\times5\times d$:

$$P\delta_x = A_2(Density\ Function)(d)^{2.236} f_u r(0.839+0.009489(Sp/d))n(1-e^{-1.719\delta x})^{0.568}(0.1\delta x+0.68)...(86a)$$

ii) for nail row spacing exceeding 0.85×4×5×*d*:

$$P\delta_x = A_2\ (Density\ Function)(d)^{2.236} f_u rn(1-e^{-1.719\delta x})^{0.568}(0.1\delta x +0.68) \quad ....(86b)$$

where:

$P_{\delta x}$	= load taken by the joint at displacement 'δx' - N.
A_2	= constant = 3.090538×10^{-4}.
Density Function	= a function of the material density and nail penetration and is defined in equation (69). kg/m^3.
d	= nail diameter – mm.
f_u	= strength of the nail wire - N/mm^2.
r	= the number of rows of nails.
S_p/d	= ratio of nail row spacing (mm) divided by nail diameter (mm).
n	= the number of lines of nails.

Semi-empirical model equations (86a) and (86b) apply to joints with plywood gusset plates of different thickness assembled with a nominal gap between the plates and the timber; connected by fully overlapping nails in predrilled holes in accordance with the requirements of EC5 [15]; with nail lines of the same configuration and with uniform row spacing, subjected to short duration lateral loading.

These equations are used in other Chapters in the Thesis and to make them easier to use to they have been simplified by using the following functions:

$$P_{GS} = A_2(Density\ Function)(d)^{2.236} f_u\ (0.839+0.009489(Sp/d)) \quad ....(86c)$$

$$P_G\ = A_2(Density\ Function)(d)^{2.236} f_u \quad ....(86d)$$

Equations (86a) and (86b) reduce to

i) for nail row spacing between 0.85×2×5×*d* and 0.85×4×5×*d*:

$$P\delta_x = P_{GS}(1-e^{-1.719\delta x})^{0568}(0.1\delta x +0.68)rn \quad ....(86e)$$

(ii) for nail row spacing exceeding 0.85×4×5×*d*:

$$P\delta_x = P_G(1-e^{-1.719\delta x})^{0.568}(0.1\delta x +0.68)rn \quad ....(86f)$$

From the equations it is possible to determine the load-deformation characteristics of connections using a prescribed number of nails at a particular row spacing up to the joint failure slip limit of 3.2mm. Alternatively, for a prescribed displacement it is possible to determine and compare the load sustained by the joint for different nailing configurations.

4.7.9 Comparison of Semi-Empirical Model with Test Results

The model in equations (86a) and (86b) has been applied to the joint configurations used in the testing programme and the results are compared at the 3.2mm upper slip limit in Tables 4.28 to 4.31. The difference between the model result and the test result is also given, with a negative sign indicating underestimation and a positive sign indicating overestimation by the model. The majority of the testing was carried out using 19mm nominal thickness plywood however examples of the model applied to joints using 9mm and 12mm nominal thickness plywood are given on Table 4.31.

Nailing pattern-number of nails	Row spacing (mm)	Number of Rows	Average timber density (kg/m^3)	Average plywood density (kg/m^3)	Pen'n of nail into timber mm	Thickness of plywood mm	Model load (N)	Test load (N)	% error (%)
CO-4		1	552.12	419.96	42.32	16.93	2916.98	2782.73	+4.82
RT-16	23	4	556.14	607.84	41.62	17.64	14169.73	14041.4	+0.91
ED-20	33.33	5	549.93	471.55	42.13	17.12	15097.75	14651.07	+3.05
ED-20	33.33	5	552.71	475.24	42.13	17.12	15201.18	15045.09	+1.04
RZC-24	33.33	6	534.58	683.37	41.02	18.22	24411.01	23934.91	+1.99
RZC-24	33.33	6	494.78	548.66	41.16	18.09	20193.91	19435.60	+3.90
ER-28	33.33	7	548.16	456.61	42.01	17.20	20721.47	21287.55	-2.66
ER-28	33.33	7	535.31	471.7	42.24	17.07	20910.83	21284.00	-1.75
EG-20	50	5	581.85	394.61	42.29	16.97	14315.91	13114.3	+9.16
EJ-12	66.67	3	559.71	446.39	42.07	17.19	9218.96	9341.35	-1.31
EJ-12	66.67	3	567.36	466.80	42.25	17.08	9501.19	9001.19	+5.55
RY-16	66.67	4	563.69	521.1	41.22	18.03	14052.08	13296.59	+5.68
EK-20	66.67	5	594.67	601.77	41.80	17.33	19327.98	19516.57	-0.97
EK-20	66.67	5	541.97	458.8	42.36	17.12	15414.68	15394.17	+0.13
EQ-28	66.67	7	541.23	473.35	42.43	16.98	21944.20	21645.84	+1.38

Table 4.28 Comparison of laterally loaded joints using 19mm nominal thickness plywood and 2.66mm diameter nails of strength $827N/mm^2$ at a slip of 3.2mm.

Nailing pattern-number of nails	Row spacing (mm)	Number of rows	Average timber density (kg/m^3)	Average plywood density (kg/m^3)	Pen'n of nail into timber mm	Thickness of plywood mm	Model load (N)	Test load (N)	% error (%)
CO-4		1	527.8	573.49	41.58	17.40	4502.31	4576.22	-1.62
CO-4		1	553.44	601.01	41.20	17.78	4786.23	4788.01	+0.04
RU-16	26	4	576.56	615.56	41.36	17.64	17974.33	17772.67	-1.13
RU-16	26	4	530.31	664.15	41.55	17.45	18561.26	17081.07	+8.67
EV-16	33.33	4	553.98	597.59	41.27	17.71	17901.07	18654.30	-4.04
ED-20	33.33	5	536.33	572.00	41.64	17.32	21174.67	21798.54	-2.86
ED-20	33.33	5	678.99	594	41.70	17.33	23187.52	23999.57	-3.38
EJ-12	66.67	3	521.37	588.13	41.56	17.46	13751.62	13787.21	-0.26
EJ-12	66.67	3	673.62	589.84	41.60	17.35	14693.67	13688.37	+7.34
EK-20	66.67	5	530.88	582	41.55	17.40	22803.35	22764.77	+0.17
EK-20	66.67	5	671.68	600.10	41.59	17.41	24811.61	23883.44	+3.89
EQ-28	66.67	7	523.67	568.75	41.66	17.37	31206.80	31524.92	-1.01
RZ-16	75	4	560.65	514.87	40.93	18.07	17286.72	16397.11	+5.43
ES-20	75	5	553.68	594.00	41.17	17.85	23771.47	23832.40	-0.26
ES-20	75	5	669.8	598.00	41.65	17.37	24690.80	25056.50	-1.46

Table 4.29 Comparison of laterally loaded joints using 19mm nominal thickness plywood and 3.01mm diameter nails of strength $792N/mm^2$ at a slip of 3.2mm.

Nailing pattern-number of nails	Row spacing (mm)	Number of rows	Average timber density (kg/m^3)	Average plywood density (kg/m^3)	Pen'n of nail into timber mm	Thickness of plywood mm	Model load (N)	Test load (N)	% error (%)
CO-4		1	507.89	588.30	41.18	17.41	4819.83	4630.7	+4.08
CO-4		1	691.92	597.42	40.95	17.65	5213.20	5269.78	-1.07
RV-16	28	4	575.89	610.16	41.98	17.62	18604.00	18453.85	+0.81
RV-16	28	4	565.09	729.68	40.52	18.08	22294.35	20601.40	+8.22
ED-20	33.33	5	508.24	594.76	41.24	17.38	22712.42	21889.34	+3.76
ED-20	33.33	5	568.86	596.64	41.13	17.46	23291.75	23201.56	+0.39
EG-20	50	5	569.94	605.65	41.13	17.48	24807.47	25072.23	-1.06
EK-20	66.67	5	514.26	591.38	41.29	17.32	24150.46	22553.87	+7.08
EK-20	66.67	5	578.67	595.75	41.15	17.47	24953.75	25114.67	-0.64
EU-24	66.67	6	522.55	596.62	41.36	17.35	29271.04	29836.00	-1.89
EU-24	66.67	6	602.79	603.08	41.02	17.56	30595.73	30712.17	-0.38
RZA-16	83.33	4	536.03	510.79	40.58	18.02	17760.79	16909.9	+5.03
RZA-16	83.33	4	512.69	526.37	40.64	17.97	18023.31	17547.41	+2.71
RZA-16	83.33	4	477.86	518.16	40.68	17.92	17548.91	17251.38	+1.72
ET-20	83.33	5	513.47	595.47	41.22	17.34	24322.17	24275.58	+0.19
ET-20	83.33	5	574.51	603.32	40.92	17.69	25421.01	25303.30	+0.47

Table 4.30 Comparison of laterally loaded joints using 19mm nominal thickness plywood and 3.33mm diameter nails of strength $697N/mm^2$ at a slip of 3.2mm.

Nailing pattern-number of nails	Row spacing (mm)	Number of rows	Average Timber density (kg/m^3)	Average plywood density (kg/m^3)	Pen'n of nail into timber mm	Thickness of plywood mm	Model load (N)	Test load (N)	% error (%)
RY-16	66.67	2.66-4	477.54	719.58	41.32	9 - 8.69	11978.17	11527.12	+3.91
RY-16	66.67	2.66-4	460.00	708.52	41.285	9 - 8.72	11732.19	11958.15	-1.97
EK-20	66.67	2.66-5	596.42	719.78	40.16	12 - 10.09	17591.76	17775.57	-1.03
ES-20	75	3.01-5	562.43	668.53	39.57	12 - 9.92	20136.11	20196.87	-0.30
ET-20	83.33	3.33-5	617.76	706.59	39.63	12 - 9.88	21680.63	21577.88	+0.48

Table 4.31 Comparison of laterally loaded joints using 9mm and 12mm nominal thickness plywood at a slip of 3.2mm.

From the tables it can be seen that there is a reasonably good fit between the semi-empirical model and the average test results the average deviation of the model result is just over +1%. In the programme there has been a wide variation in the properties of the materials used and in the configuration of joints. The timber density has varied by just under 50%; the plywood density by 85%; three thicknesses of plywood have been used; row spacing has been varied to envelope the full range of row spacing effect and between one and seven rows of nails have been used in the joints. For all of these combinations there are only three cases where the deviation from the model exceeded +8% and in the majority of cases the results are within an acceptable deviation of approximately ±5%. It is also to be argued that a closer fit would be obtained had a moisture content function been developed and applied to the results.

The results of some of the joint tests and the model have also been plotted together for comparison and are presented in Figures 4.47 to 4.50. In the Figures the model result is represented by the solid line.

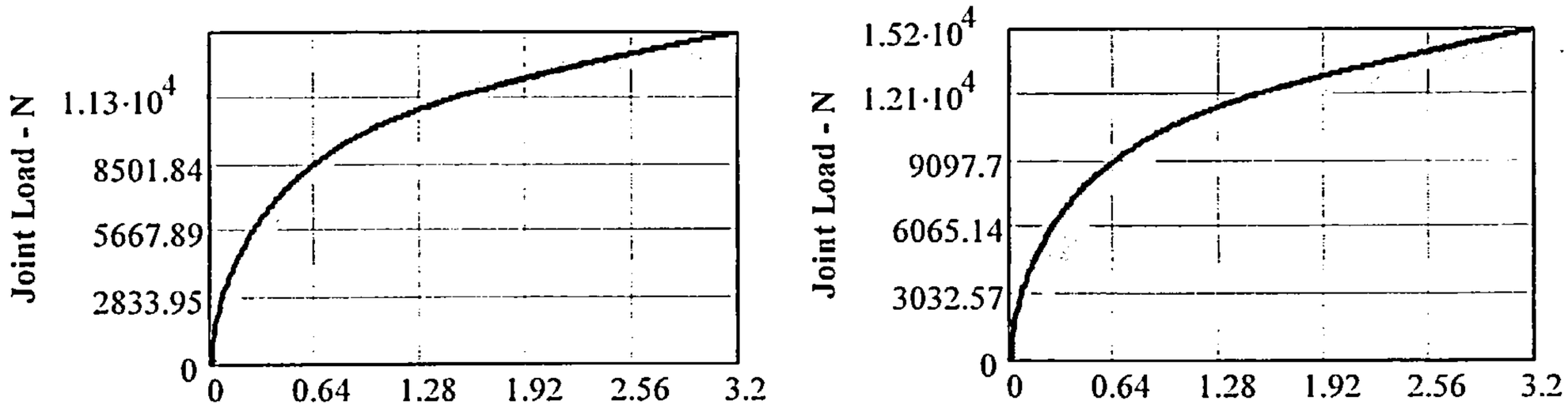

(a) Nailing Configuration 'RT' ($D_w = 556;\ D_P = 608$)

(b) Nailing Configuration 'ED' ($D_W = 550\ ;D_P = 472$)

Figure 4.47 Load-Deformation behaviour of timber joints made with fully overlapping 2.66mm diameter nails and 19mm thick plywood gusset plates.

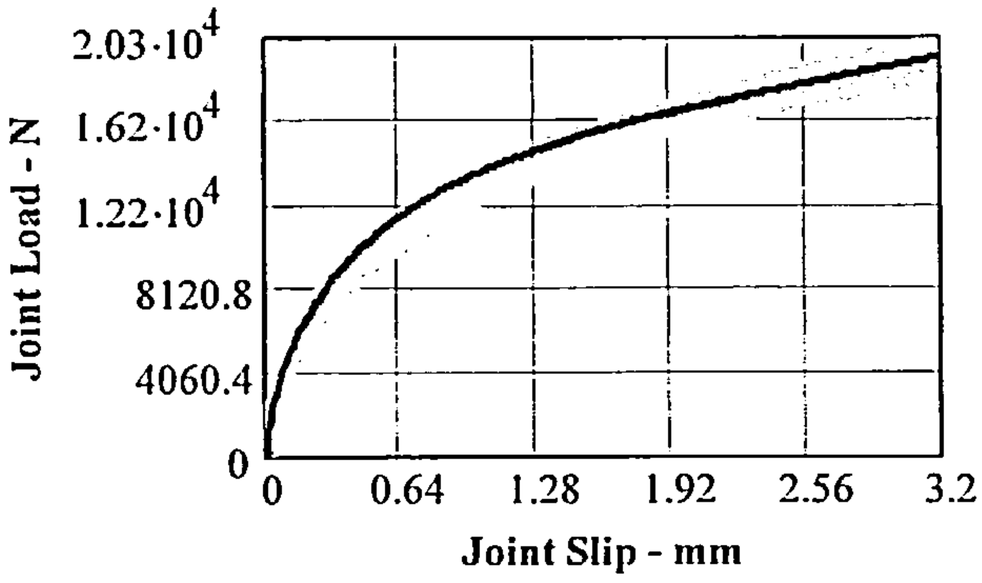

(c) Nailing Configuration 'EK'

(D_w = 595; D_P = 602)

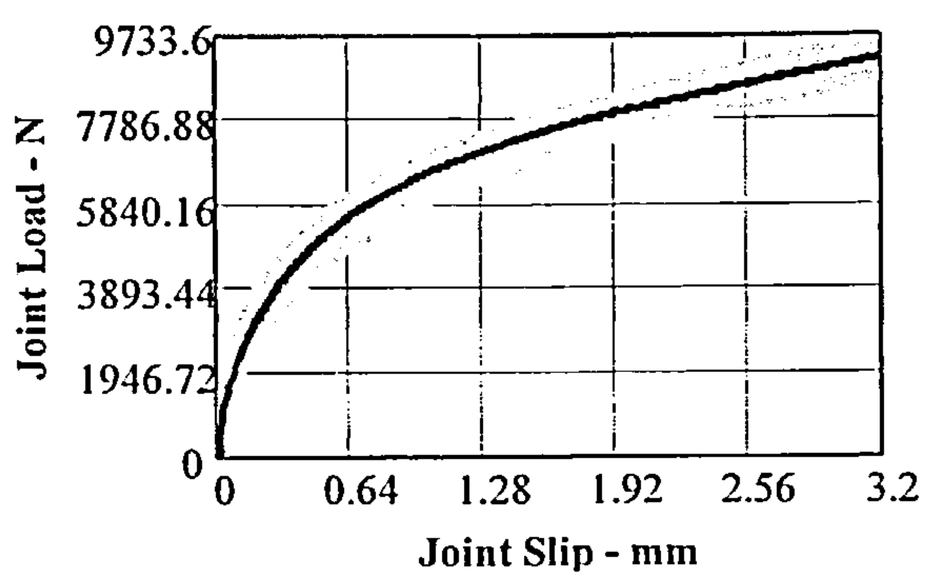

(d) Nailing Configuration 'EJ'

(D_W = 560 ; D_P = 446)

Figure 4.47 cont'd Load-Deformation behaviour of timber joints made with fully overlapping 2.66mm diameter nails and 19mm thick plywood gusset plates.

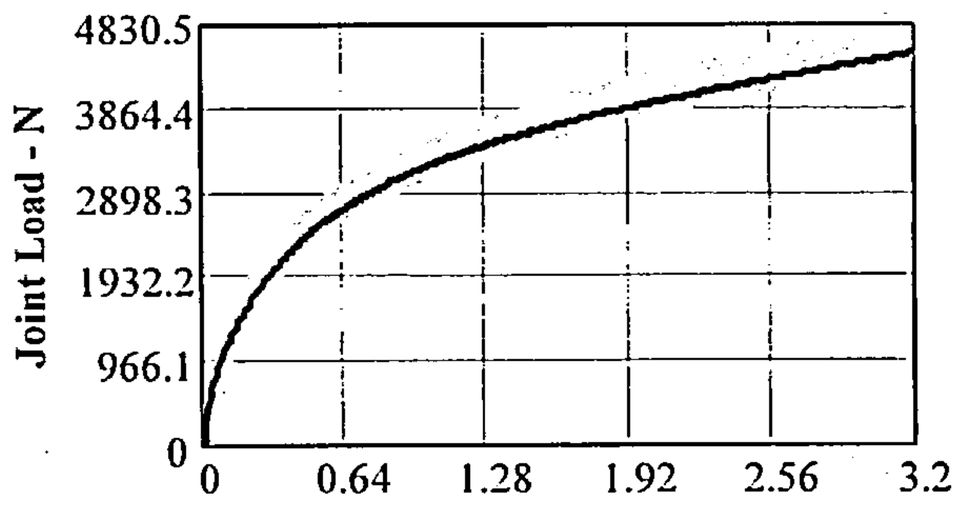

(e) Nailing Configuration 'CO'

(D_w = 528; D_P = 573)

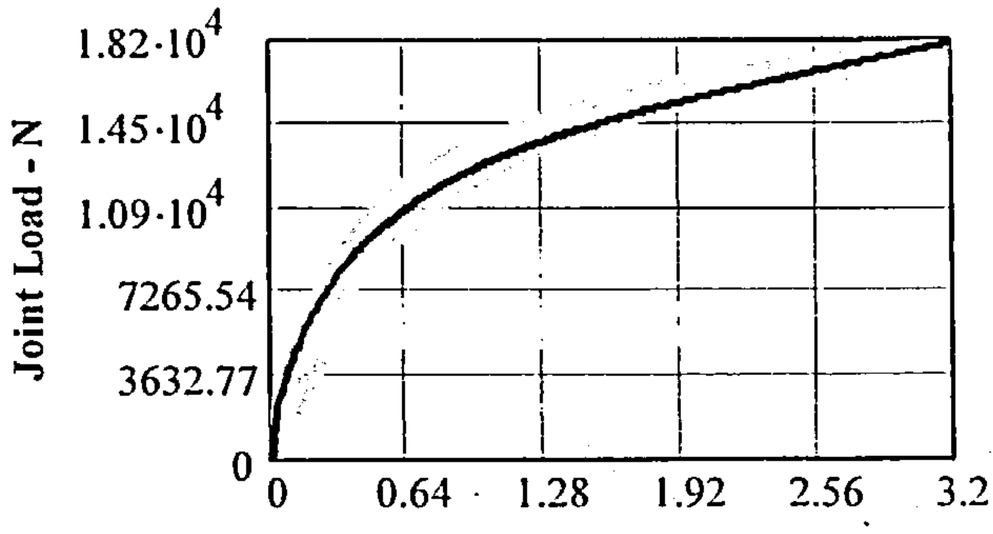

(f) Nailing Configuration 'RU'

(D_W = 577 ; D_P = 616)

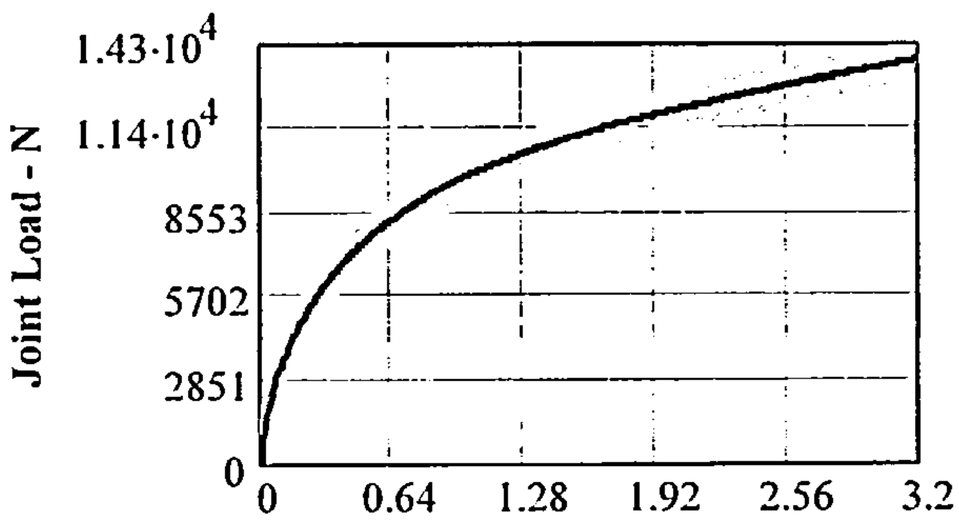

(g) Nailing Configuration 'EJ'

(D_w = 521; D_P = 588)

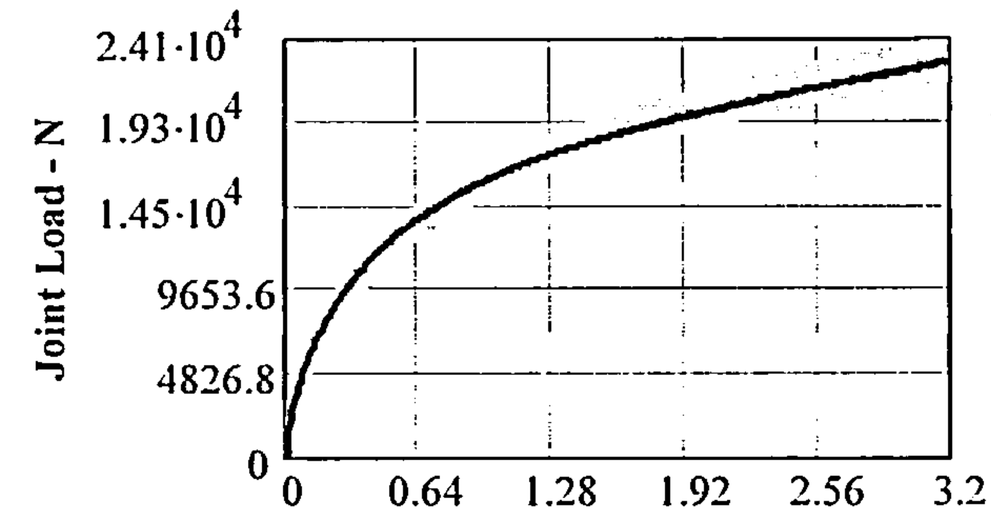

(h) Nailing Configuration 'EK'

(D_W = 531 ; D_P = 582)

Figure 4.48 Load-Deformation behaviour of timber joints made with fully overlapping 3.01mm diameter nails and 19mm thick plywood gusset plates.

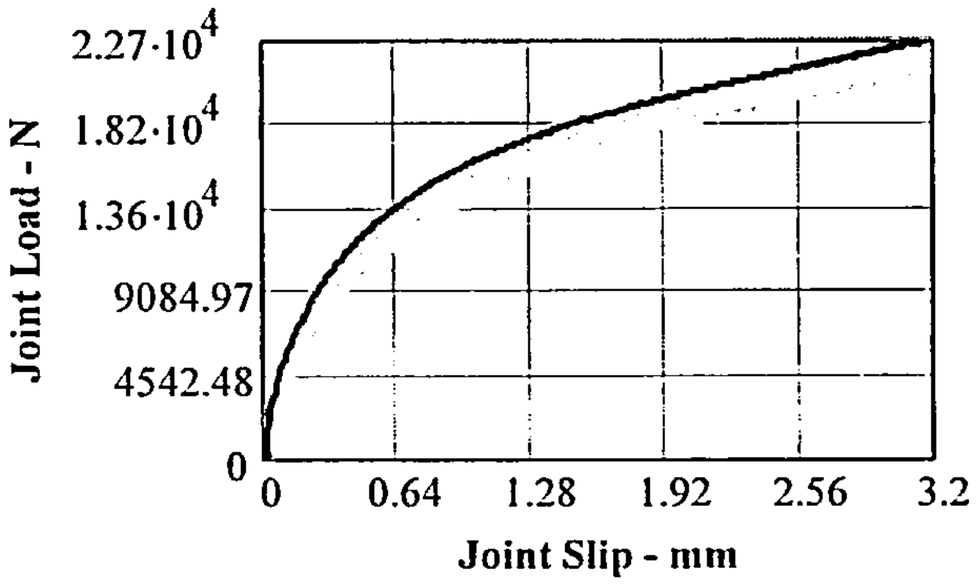

(i) Nailing Configuration 'ED'

(D_w = 508; D_P = 595)

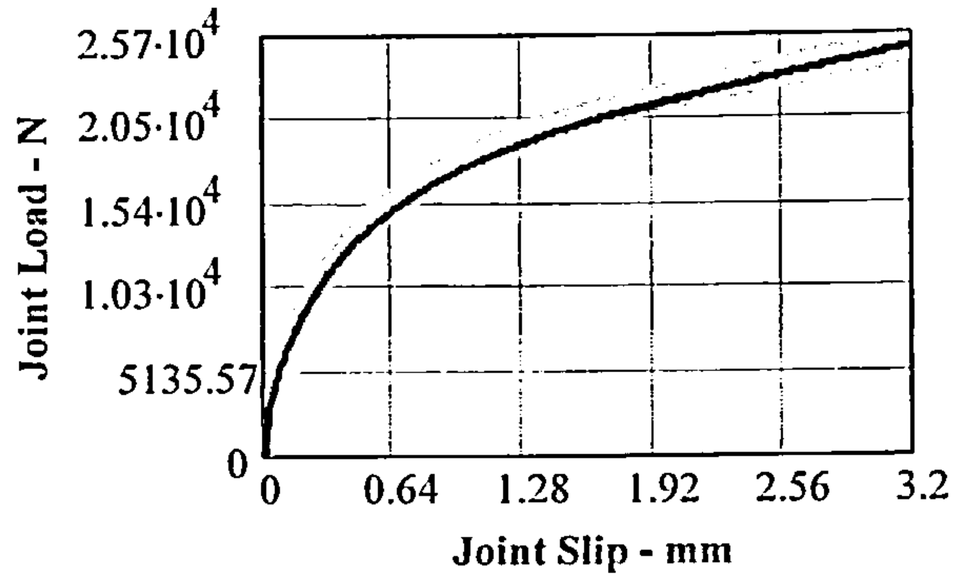

(j) Nailing Configuration 'EG'

(D_W = 570 ;D_P = 606)

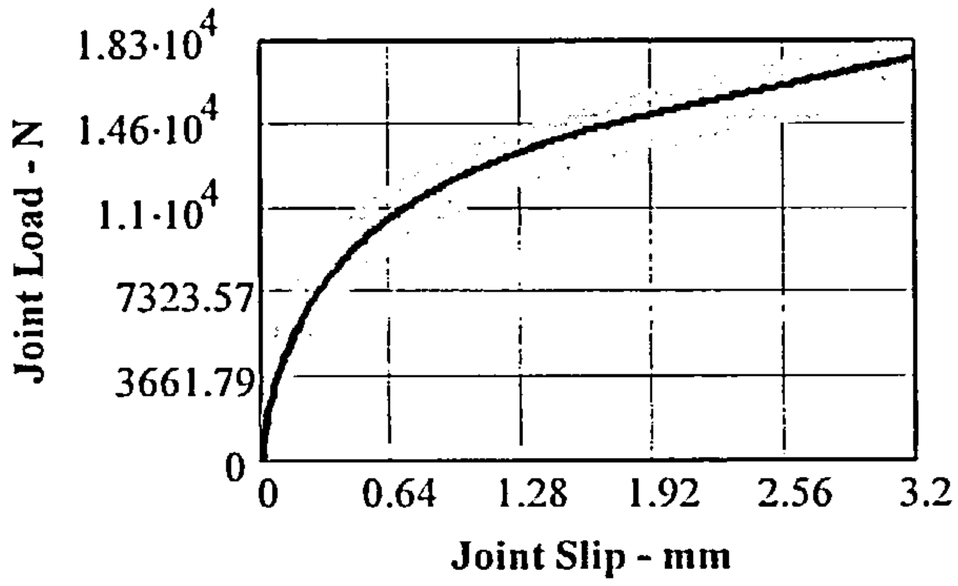

(k) Nailing Configuration 'RZA'

(D_w = 478; D_P = 518)

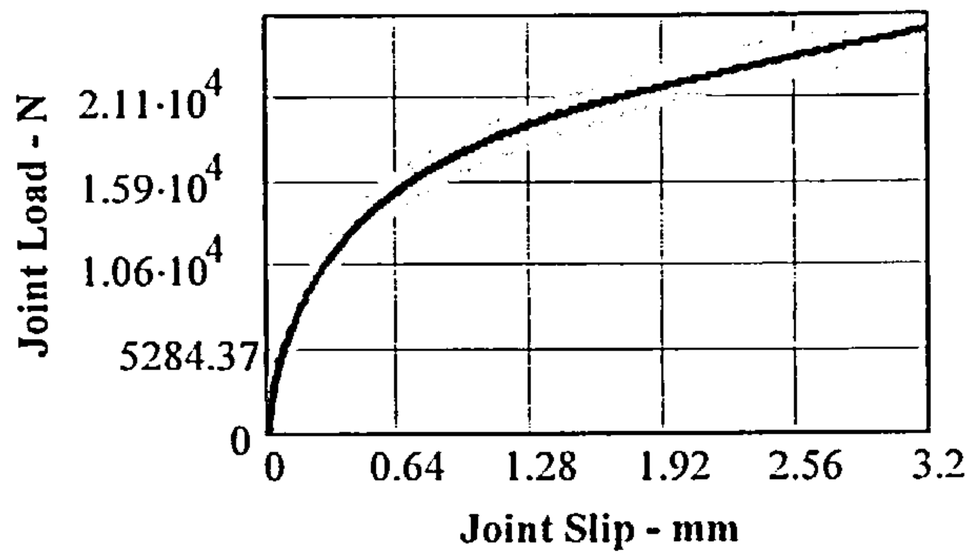

(l) Nailing Configuration 'ET'

(D_W = 575 ;D_P = 603)

Figure 4.49 Load-Deformation behaviour of timber joints made with fully overlapping 3.33mm diameter nails and 19mm thick plywood gusset plates.

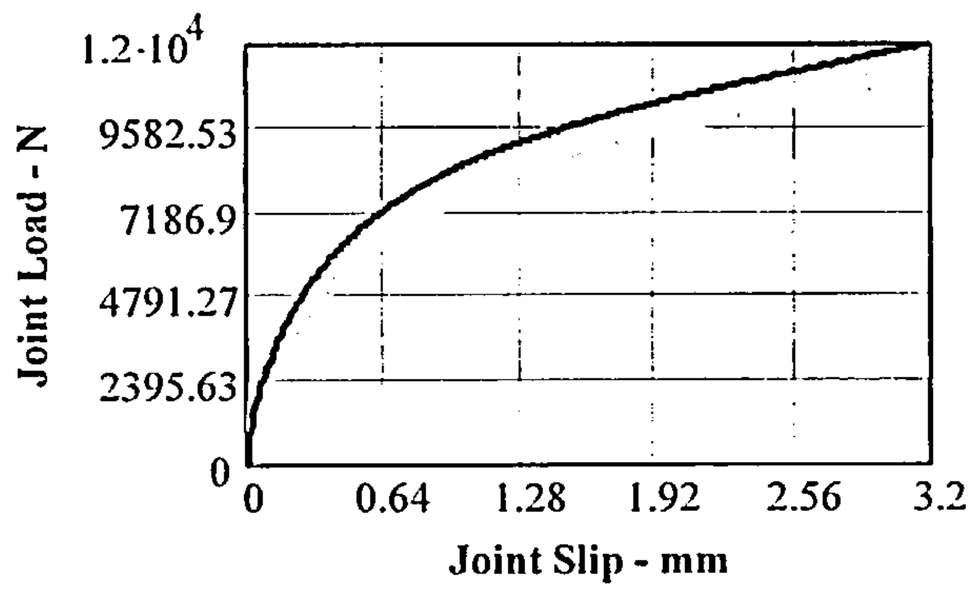

(m) Nailing Configuration 'RY'

(D_w = 478; D_P = 720)

2.66mm diameter nails and 9mm plywood

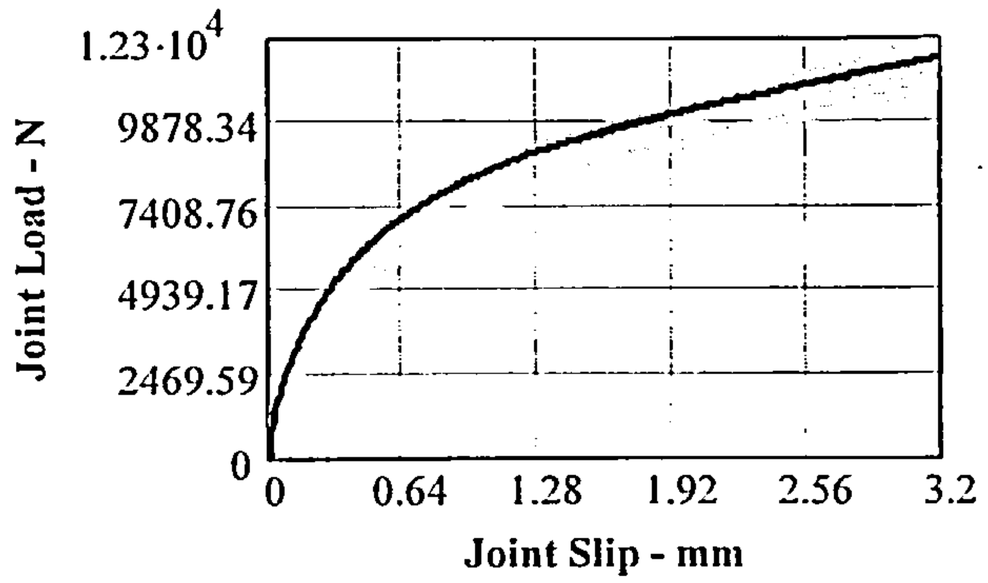

(n) Nailing Configuration 'RY'

(D_W = 460 ;D_P = 709)

2.66mm diameter nails and /9mm plywood

Figure 4.50 Load-Deformation behaviour of timber joints made with fully overlapping nails and 9mm and 12mm thick plywood gusset plates.

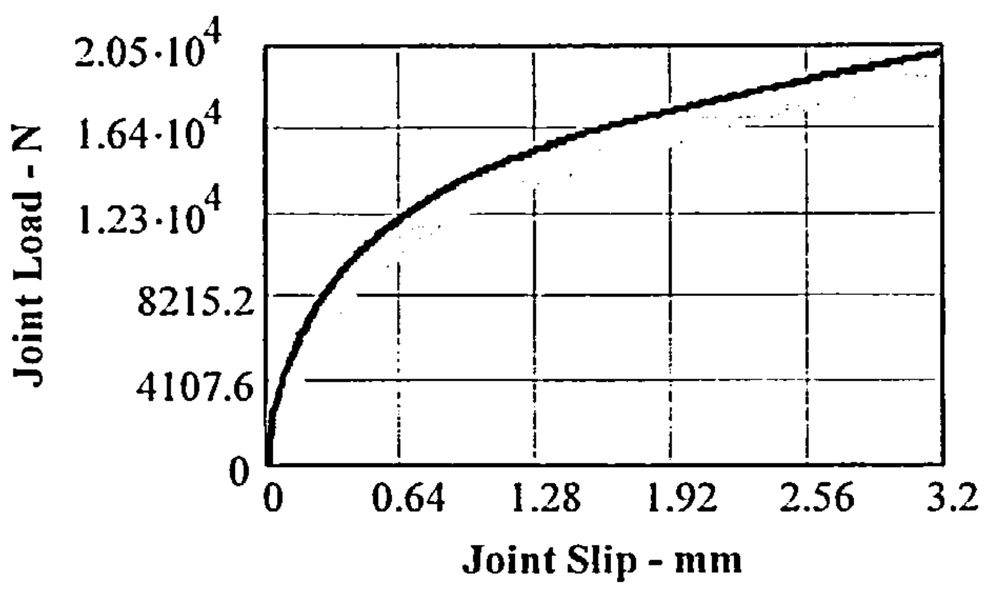

(o) Nailing Configuration 'ES'

(D_w = 562; D_P = 669)

3.01mm diameter nails and 12mm plywood

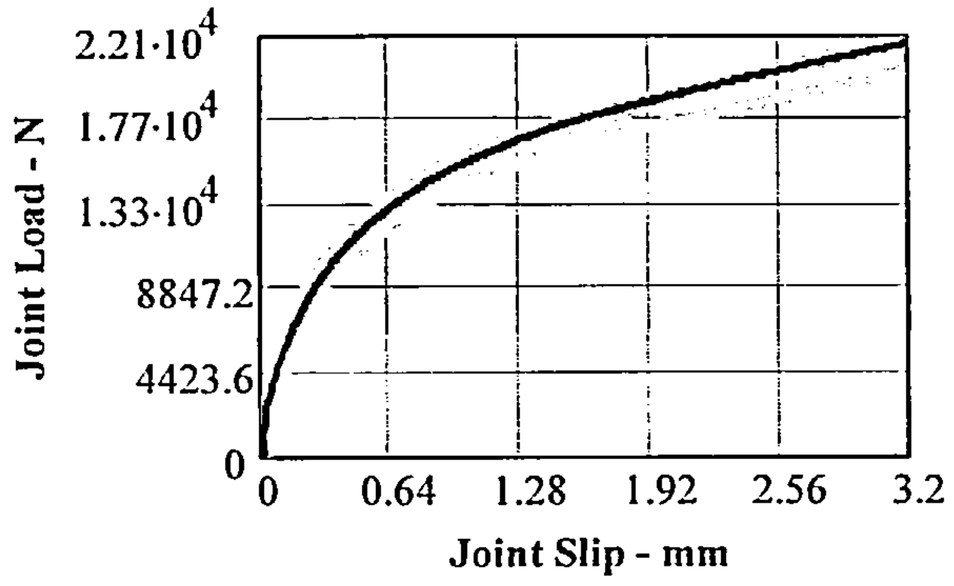

(p) Nailing Configuration 'ET'

(D_w = 618; D_P = 707)

3.33mm diameter nails and 12mm plywood

Figure 4.50 cont'd Load-Deformation behaviour of timber joints made with fully overlapping nails and 9mm and 12mm thick plywood gusset plates.

The results presented in Figures 4.47 to 4.50, which are typical of the test set results, show that there is a good fit between the model and the test sets over the full length of the displacement curve. The fit at a load of approximately 40% of the $P_{3.2}$ load, equivalent to the load at the 'serviceability limit state' of the joint, also compares very well with the test sets, giving a good comparison with the joint strength and stiffness at that condition.

4.8 THE ANALYSIS OF LATERALLY LOADED PLYWOOD GUSSET PLATE JOINTS FORMED WITHOUT A GAP

As for the joints with steel gusset plates, plywood gusset plate joints were also assembled without the use of spacers to investigate the effect on the model. Eliminating the gap between the gusset plate and the timber changes the support condition of the nails and will affect the joint displacement function. In addition, the contact between the gusset plates and the timber introduces a friction force that will add to the joint strength. To investigate these effects sets of joints of varying nailing configurations connected by 2.65mm 3.00mm and 3.35mm diameter Castlenail nails were assembled without a gap and tested.

The analysis of the test results was carried out in two parts. The effect of the change in the support condition on the displacement function was investigated first and followed by the analysis of the effect of the additional friction force on the joint strength.

4.8.1 No Spacers in Joint - Effect on Displacement Function

As described in section 4.7.2, the results of the tests were converted to reduced load data and adopting the same type of exponential function as given in equation (7), using non linear regression analysis the displacement function for each nail size, and for the average for all nail sizes, was obtained. The

functions are given in equations (87), (88), (89) and (90) and plotted against the associated reduced load data on Figures 4.51 and 4.52.

Nail Diameter	**Displacement Function**	
2.66mm	$f_{p266hd}(\delta_x) = (1-e^{-1.821\delta x})^{0.515}(0.1\delta x + 0.68)$	....(87)
3.01mm	$f_{p301hd}(\delta_x) = (1-e^{-2.133\delta x})^{0.511}(0.1\delta x + 0.68)$	....(88)
3.33mm	$f_{p333hd}(\delta_x) = (1-e^{3.051\delta x})^{0.584}(0.1\delta x + 0.68)$	....(89)
All diameters	$f_{phd}(\delta_x) = (1-e^{-2.227\delta x})^{0.529}(0.1\delta x + 0.68)$	....(90)

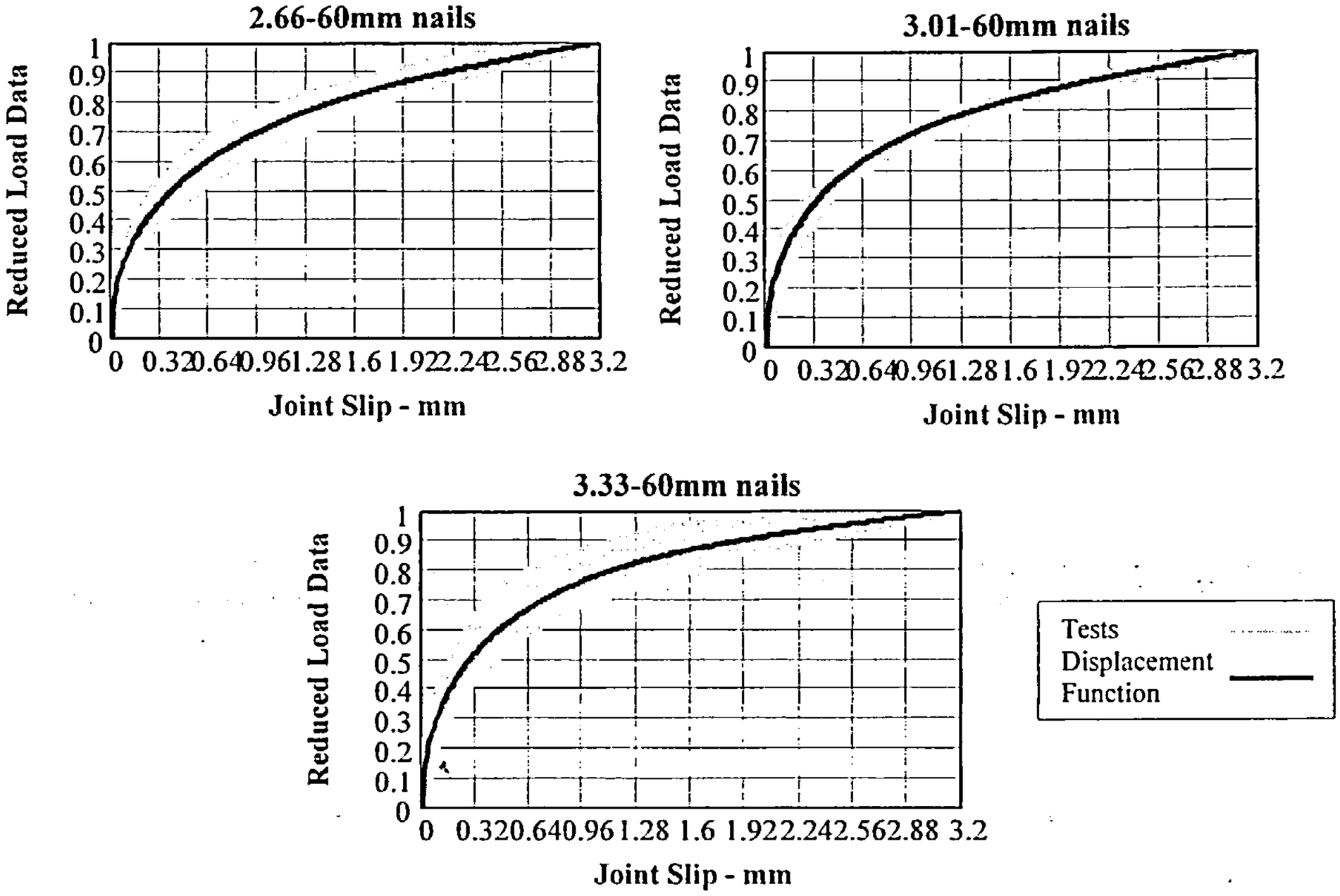

Figure 4.51 Regression graphs of the displacement functions for 2.66mm, 3.01mm, and 3.33mm diameter nails in joints with plywood gusset plates in contact with the timber.

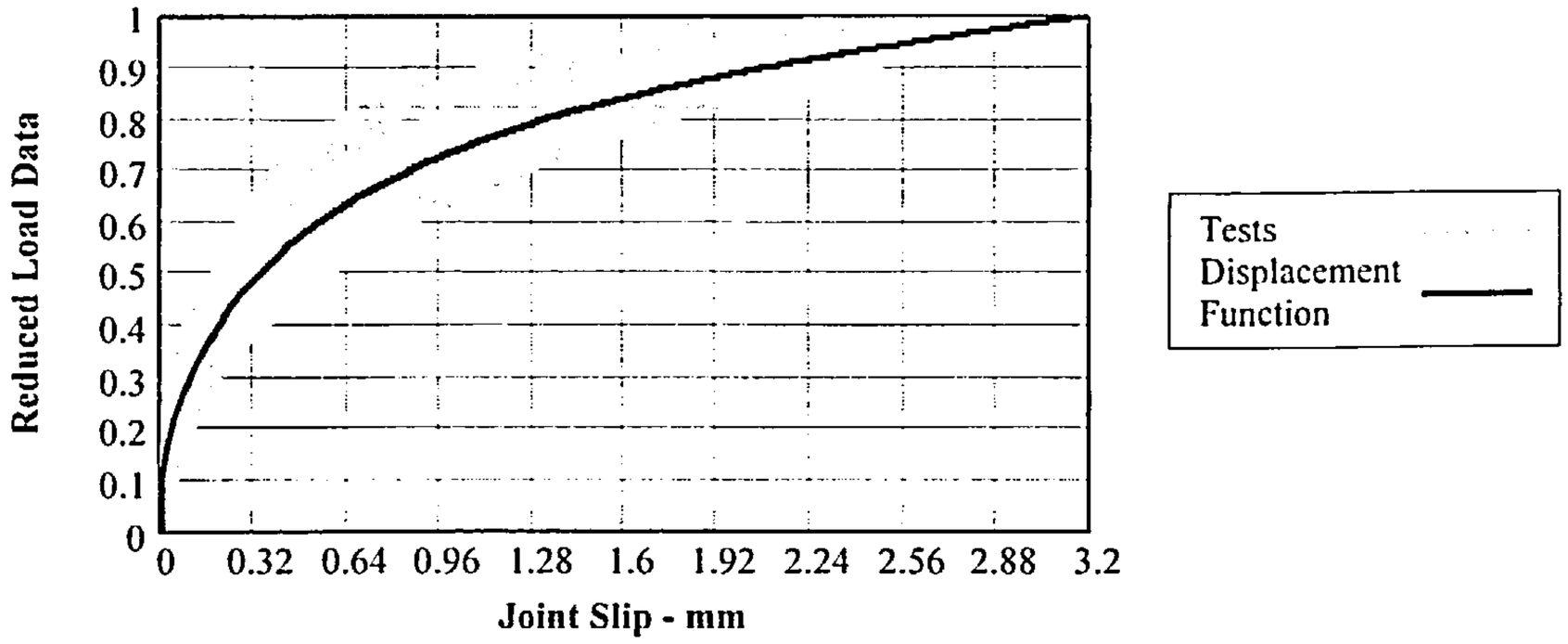

Figure 4.52 Regression graph of the displacement function for all nail sizes in joints with plywood gusset plates in contact with the timber.

With the limited number of tests the spread in the reduced load data for each nail size is much less than that obtained for the joints assembled with spacers reported in section 4.4.1, and the coefficient of determination, R^2, for each fit is much better. The figures are:

Nail Diameter	**R^2 value**	**Nail Diameter**	**R^2 value**
2.66mm	0.986	3.33mm	0.961
3.01mm	0.990	All diameters	0.974

The displacement functions in equations (87) to (90) are shown on Figure 4.53.

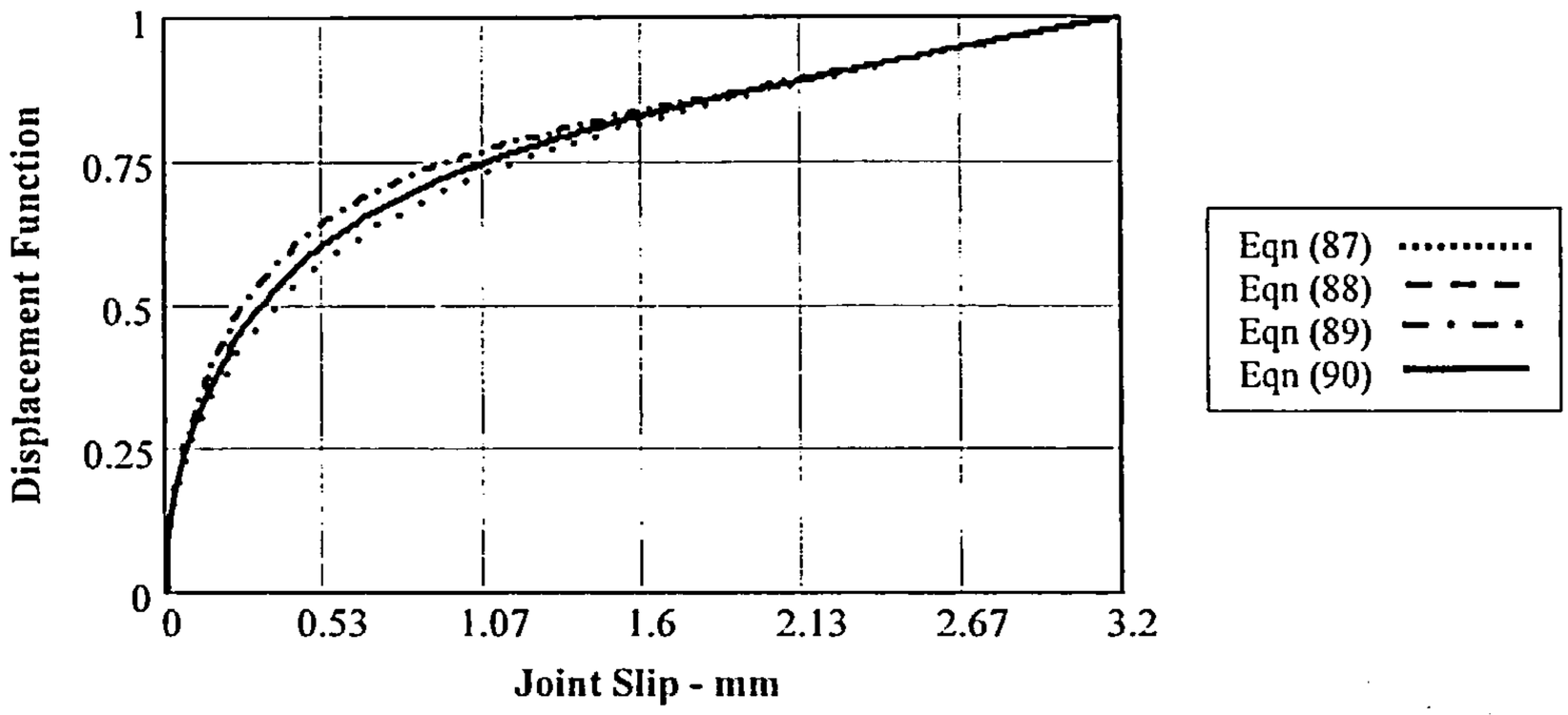

Figure 4.53 Displacement functions given in equations (87),(88),(89) and (90).

The fit is not as good as was obtained for the joints in section 4.7.2 however the variation in the function between nail diameters is still relatively small. It is to be noted that the average curve is almost in line with the curve for equation (88) and masks it on the graph. The average displacement function has also been compared with the average displacement function for plywood gusset joints assembled with a gap (equation (58)) and the graphs are shown on Figure 4.54.

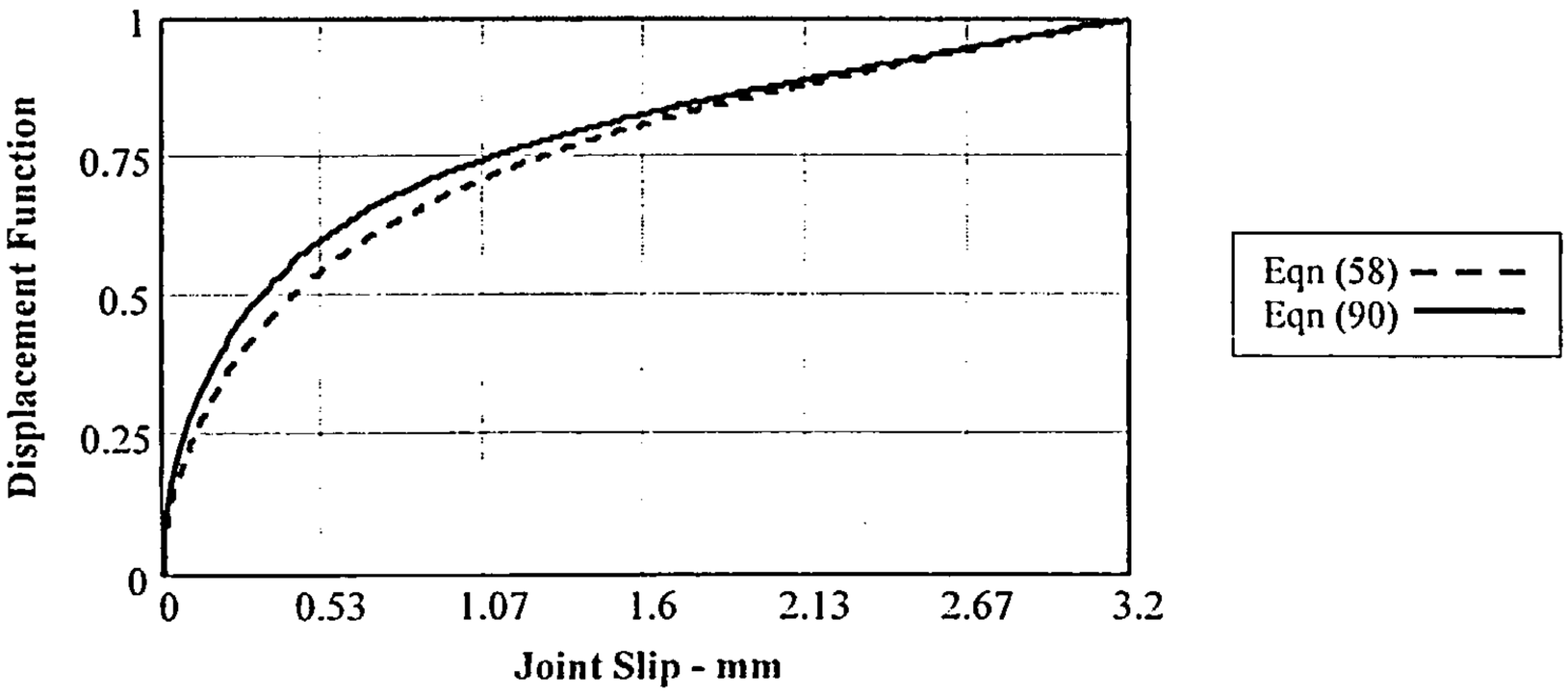

Figure 4.54 Comparison between the Displacement Function for plywood gusset plate joints with a gap (eq'n (58)) and without a gap (eq'n (90)) between the timber and the gusset plates.

At 40% of the reduced load, which is equivalent to the serviceability limit state load condition, the joint slip for equation (90) is approximately 0.19mm whilst for equation (58) is 0.27mm. This is an increase of approximately 42% in stiffness, which is less than the 57% increase obtained for the equivalent joints made with steel gusset plates, referred to in section 4.6.1. As for steel gusset plate joints, the slip of a structure formed using nailed joints with contact between the gusset plates and the timber will be considerably reduced over the same structure assembled using nailed joints with a gap between the gusset plates and the timber.

4.8.2 No Spacers in Joint - Frictional Force

Applying the displacement function in equation (90) to the semi-empirical model in equations (86a) and (86b), and including for a friction function, the semi-empirical model becomes:

i) for nail row spacing between $0.85\times2\times5\times d$ and $0.85\times4\times5\times d$:

$$P_{phd}\delta_x = A_2(Density\ Function)(d)^{2.236} f_u\, r(0.839+0.009489(Sp/d))n(1-e^{-2.227\delta x})^{0.529}(0.1\delta x\ +0.68)f_{pf} \quad ...(91a)$$

ii) for nail row spacing exceeding $0.85\times4\times5\times d$:

$$P_{phd}\delta_x = A_2(Density\ Function)(d)^{2.236} f_u\, rn(1-e^{2.227\delta x})^{0529}(0.1\delta x +0.68)f_{pf} \quad ....(91b)$$

where the functions are as described in section 4.7.8 except:

$P_{phd}\delta_x$ = load taken by the joint at displacement 'δx' for joints with plywood gusset plates and are assembled with no gap between the timber and the gusset plates - N.

f_{pf} = the friction function

By applying equations (91a) and (91b) to the joints and inserting the average properties of the test sets, the $P_{3.2phd}$ value for each nail diameter will be obtained in terms of the friction function (f_{pf}). Comparing the result with the average value obtained from the test set of joints for each nail diameter the following relationship can be set up:

$$P_{3.2phdModel} f_{pf} = P_{3.2Test}$$

ie $$f_{pf} = P_{3.2Test} / P_{3.2phdModel} \quad .....(91c)$$

The result of the analysis for each nail diameter is given in Table 4.32. There is no clear trend from the results and the maximum variation is of the order of 2.6% and can be ignored.

The average value of the friction function, f_{pf}, is 1.2373, representing an increase of the order of 24% in the joint strength when no spacers are used. In Mack's research [6] the friction function was 1.35 using timber gusset plates and in the work by Aune *et al* [17] the function was 1.47 to 1.56 using plywood

gusset plates. It is to be expected that this function will vary as it is dependent on the driving force behind the nail; the degree of embedment of the nail head into the gusset plate and the condition of the mating surfaces. What is to be noted, however, is that it represents a significant increase in strength over that to be obtained from equivalent joints assembled with a gap between the timber and the gusset plates. Also the function is around 9% higher than the equivalent function for joints with steel gusset plates, referred to in section 4.6.2.

Nail diameter mm	**$P_{3.2phd}$ – Model N**	**$P_{3.2}$ – Tests N**	**Ratio $P_{3.2Test}/P_{3.2phd\ Model}$ $=f_{pf}$**
2.66	$15003.31f_{pf}$	18570.24	1.23774
3.01	$16900.33f_{pf}$	20639.10	1.22123
3.36	$17213.42f_{pf}$	21567.48	1.25295
		Average f_{pf}	**1.2373**

Table 4.32 Comparison between the $P_{3.2}$ value of the model and the tests

Adopting the average value of 1.2373 for each nail diameter and applying this to equations (91a) and (91b), the model for a joint formed using plywood gusset plates and fully overlapping nails in single shear; with contact between the gusset plates and the timber becomes:

i) for nail row spacing between $0.85\times2\times5\times d$ and $0.85\times4\times5\times d$:

$$P_{phd}\delta_x = A_3(Density\ \ Function)(d)^{2.236}f_u\ r(0.839+0.009489(Sp/d))n(1-e^{-2.227\delta x})^{0.529}(0.1\delta x\ +0.68) \quad ...(92a)$$

ii) for nail row spacing exceeding $0.85\times4\times5\times d$:

$$P_{phd}\delta_x = A_3(Density\ Function)(d)^{2.236}f_u\, rn(1-e^{-2.227\delta x})^{0.529}(0.1\delta x +0.68) \quad ....(92b)$$

where the functions are as described in section 4.7.8 except:

$P_{phd}\delta_x$ = load taken by the joint at displacement 'δx' for joints with plywood gusset plates and assembled without spacers - N.

A_3 = constant $= 2.6003 \times 10^{-4}$.

These equations are used in other Chapters in the Thesis and to make them easier to use to they have been simplified by using the following functions:

$$P_{NS} = A_3(Density\ Function)(d)^{2.236}f_u\,(0.839+0.009489(Sp/d)) \quad ....(92c)$$

$$P_N = A_3(Density\ Function)(d)^{2.236}f_u \quad ....(92d)$$

Using the simplifications in equations (92c) and (92d), equations (92a) and (92b) are reduced to:

i) for nail row spacing between $0.7\times2\times5\times d$ and $0.7\times4\times7\times d$:

$$P\delta_x = P_{NS}((1-e^{-2.227\delta x})^{0.529}(0.1\delta x + 0.68))rn \qquad \ldots.(92e)$$

ii) for nail row spacing exceeding $0.7\times4\times7\times d$:

$$P\delta_x = P_{N}((1-e^{-2.227\delta x})^{0.529}(0.1\delta x + 0.68))rn \qquad \ldots.(92f)$$

A comparison between equations (92) and some of the test results for the sets of joints used in the analysis is shown in Figure 4.55. The equations are represented by the single line.

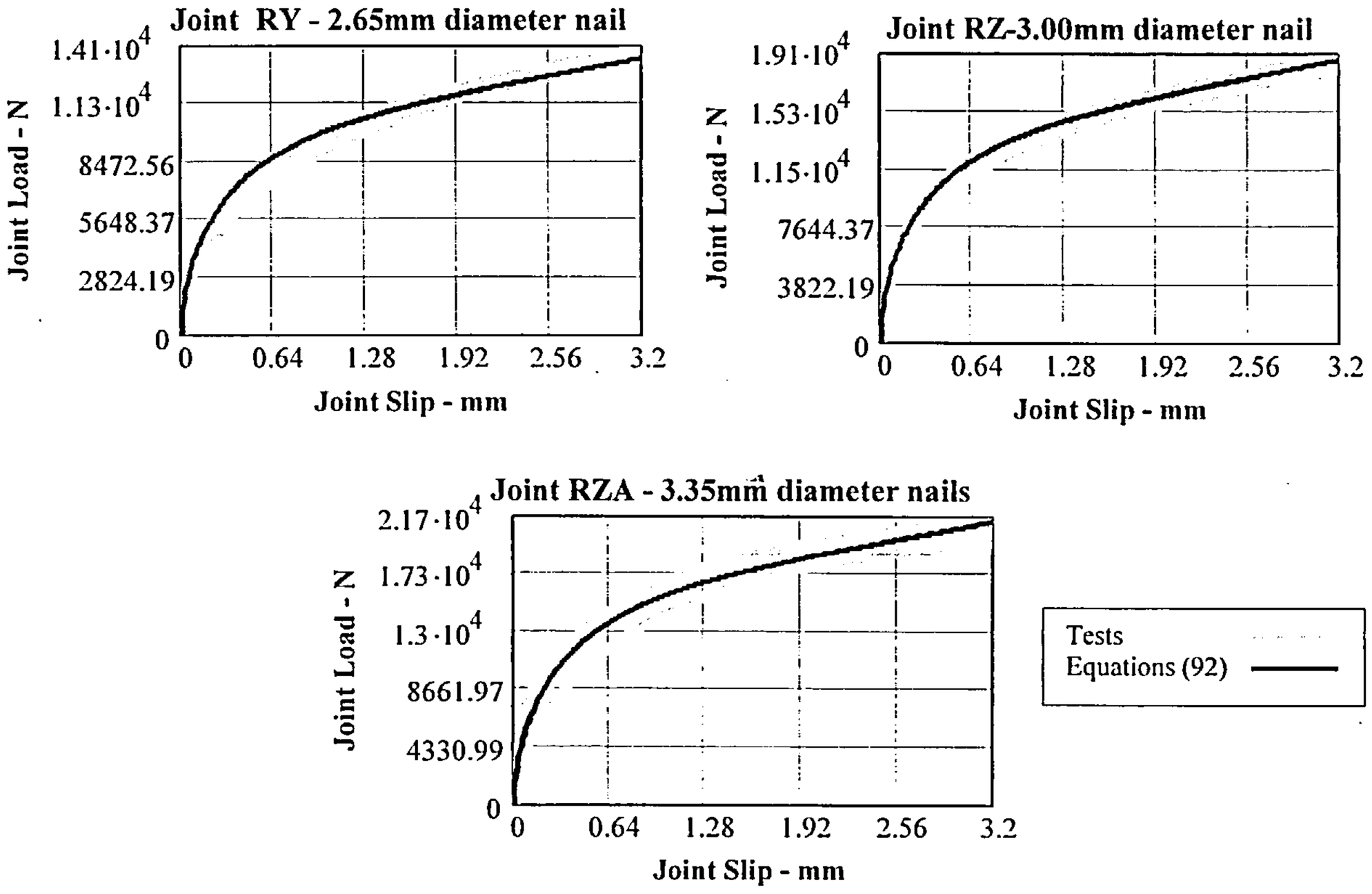

Figure 4.55 Comparison between equation (92) and the test results for joints of nailing configurations using 2.66mm; 3.01mm and 3.33mm diameter nails.

The model achieves a reasonably good fit against the test data over the full length of the displacement curves.

4.9 SUMMARY

In this Chapter it has been shown that it is possible to model the behaviour of joints assembled using fully overlapping nails and subjected to short duration lateral loading. This has been undertaken by

considering in isolation the effect of each of the functions which influence the joint. No evidence was found of any significant interaction between the functions. It has been shown, however, that for joints with steel and with plywood gusset plates the values of the respective functions will differ significantly. Consequently it is impractical for a single expression to be established that can readily be used to analyse joints with different types of gusset plates.

Semi-empirical models have been developed for joints with:

i) Steel gusset plates predrilled with holes less than 1.1 times the nail diameter and assembled with a gap between the gusset plates and the timber.
ii) Steel gusset plates predrilled with holes greater than 1.1 times the nail diameter and assembled with a gap between the gusset plates and the timber.
iii) Steel gusset plates predrilled with holes less than 1.1 times the nail diameter, assembled with no gap between the gusset plates and the timber.
iv) Plywood gusset plates assembled with a gap between the gusset plates and the timber.
v) Plywood gusset plates assembled without a gap between the gusset plates and the timber.

From a review of the results of the joint tests at 3.2mm slip, joints made with steel gusset plates were starting to show an increased frequency in the occurrence of brittle failure. This has been taken as the failure limit for the load-slip relationship for such joints. Joints with plywood gusset plates were able to sustain load beyond this limit and the failure limit for these joints is addressed in Chapter 6.

The models accurately predict the load-displacement behaviour of joints subjected to short duration lateral loading. They take into account the effect of the density and moisture content of the timber based materials; the effects of gusset plate thickness in plywood joints; the nail diameter and nail strength properties; the number of lines and rows of nails and the effect of nail row spacing. By inputting these properties in the models, joint strength and stiffness can be developed at any slip up to a limit of 3.2mm. The relationship can also be used in semi-rigid analyses of timber structures where joints with fully overlapping nails subjected to lateral loading are being used.

It has been shown for joints with steel gusset plates that the joint strength is a linear function of the timber density. For joints with plywood gusset plates the strength is also a linear function of the timber and the plywood density and the plywood thickness. A density function has been developed to incorporate these factors.

The effect of moisture content has been found to be an important factor in joint behaviour and a linear function has been developed which takes this into account for joints with steel gusset plates. A linear function was used because the variation in moisture content over the testing programme was limited to 4.5%. As the variation in the moisture content of the materials used for the plywood gusset plate joints

was small (between 1.5% and 2%) it was decided that a moisture content function was not required for these joints. The timber/plywood used in these tests was considered to effectively comply with the service class 1 condition given in EC5[11].

The behaviour of both steel and plywood gusset plate connections was found to be linearly related to the nail strength and a multiple of the number of lines of nails in the joint. For both types, up to 7 rows of nails were used and it was found that joint behaviour was also linearly related to the number of rows.

The nail diameter function was shown to be a power function of the nail diameter and differed substantially between the two types of joint. The functions, however, were unaffected by the use or otherwise of a gap between the timber and the gusset plates.

In all cases joint behaviour was affected by the spacing of the rows of nails. The closer the spacing the lower the load the joint could take. The minimum row spacing was found to be 2×0.7×5×nail diameter for joints with steel gusset plates, resulting in a reduction factor of 0.835. For joints with plywood gusset plates, the minimum row spacing was 2×0.85×5×nail diameter and the reduction factor was found to be 0.92. These reductions were independent of the number of rows of nails in the joint and are much smaller that the reductions recommended in Table 8.1 of EC5 [15]. The maximum spacing beyond which there was no reduction effect on joint strength was found to be 4×0.7×7×nail diameter for steel gusset plate joints and 4×0.85×5×nail diameter for joints with plywood gussets. Taking account of the relatively small effect of the row spacing function and the nature of the test results, linear functions have been used for the effect of intermediate row spacing. The functions were different for joints with steel and joints with plywood gusset plates and were not affected by the use or otherwise of a gap between the gusset plates and the timber.

Joints assembled with a gap between the gusset plates and the timber were stronger and stiffer than those assembled without a gap.

Although the joints all had the same type of exponential format for their displacement function, the exponential coefficients differed in all cases. The functions are however comparable with those developed by other researchers, and in particular the ones developed by Mack [6]. The function for the steel gusset plates extends to 3.2mm slip and represents the upper limit of the joint capacity. In the case of the plywood gusset plate joint the function can extend beyond 3.2mm slip and the upper limit for these joints is addressed in chapter 6.

5. SEMI-EMPIRICAL MODELLING OF MOMENT-ROTATION JOINTS CONNECTED BY FULLY OVERLAPPING NAILS

5.1 INTRODUCTION

Moment-rotation characteristics of nailed timber connections have been widely researched [12, 79, 91, 84, 92, 93, 95, 96, 97, 98, 99,179]. Various approaches have been used, mostly drawing on the well established methods for analysing equivalent types of connections in steelwork joints. Also there has been an increasing awareness of the need to address the splitting resistance of timber caused by the effects of nail loading perpendicular to the grain arising from this form of loading [91,118].

In this chapter alternative methods of analysis for joints connected by fully overlapping nails and subjected to a moment are examined. The methods incorporate, to varying degrees, the semi-empirical models for laterally loaded shear joints developed in Chapter 4 and the objective is to derive a method which best represents the actual joint behaviour. The study only considers the behaviour of joints subjected to in-plane moments. Because the joint nailing configurations in the testing programme did not use mixed nail sizes, the analyses have been developed on the assumption that only single nail size configurations will be used.

Linear and non-linear models are developed and their effectiveness compared with the results of moment tests. In the linear models the assumption has been made that the force in each nail is directly proportional to its distance from the centre of rotation of the joint. With the non-linear models, the nail force is taken to be a function of the displacement of the nail, each following the appropriate load-displacement relationships established in Chapter 4.

The first linear model assumes that the centre of rotation is at the centroid of the nailing configuration. It follows the conventional moment-rotation torsion formula relationship used in the design of bolted joints for steelwork connections and as also used by Morris [95, 96] and Goh [12] for the moment behaviour of nailed joints. In the second linear model the centre of rotation is assumed to be variable, arguably introducing an element of non-linearity to the method.

The first non-linear model assumes the centre of rotation is fixed and at the centroid of the nailing configuration, similar to the first linear analysis model, but incorporates the non-linear behaviour of the nails. The second non-linear model assumes a variable centre of rotation and in so doing is a more accurate representation of the joint behaviour. The third non-linear model includes for the effects of nail movement during the rotation of the joint, altering the nail positions and the force behaviour in the joint. This model achieves the most accurate theoretical representation of the joint behaviour. The fourth non-linear model is based on a truss analogy approach in which it is assumed that each nail is attached directly to the applied load and the nail force is a function of its distance from the applied load.

Each method is described in detail. Comparisons are also made between the models and the results of the moment tests referred to in Chapter 3 to determine the optimum approach.

Because of the transducer arrangement used for the tests, the effects of change in the joint geometry during rotation have to be taken into account. Also the implications of the fixed alignment of the transducers have to be addressed. A description of the methodology used to process the transducer readings to obtain nail displacements, incorporating the above has been given.

Where the plane of the grain of the timber is at an angle to the joint face, joints have been shown to be less strong than those in which the plane is parallel to the joint face. This behaviour has been investigated and a grain factor has been developed and incorporated into the preferred non-linear model.

The methods of analyses used have been based on the conventional premise that all of the rotation in a joint is caused by a combination of deformation of the nails and embedment of the timber and plywood. No deformation of the joint materials has been assumed to occur. To ensure the above condition is complied with, criteria have been given for the application of the recommended method of analysis.

Also, to demonstrate that joint material deformation is not a factor in the analysis of joints connected by the same gusset plates, double joints have been modelled and compared with the results of tests. This has been limited to joints with plywood gusset plates as any gusset deformation using joints with steel gusset plates will be much smaller.

5.2 MOMENT ROTATION CHARACTERISTICS OF NAILED JOINTS

When a nailed connection is subjected to a moment, the stress resultants in the joint are transferred between the timber and the gusset plates by the nails. The stiffness of the timber and of the gusset plates in the joint is generally large relative to the stiffness of the nailing configuration. Consequently their flexural, axial and shear deformations are small compared to the deformation arising from of the nails and can be neglected. This is the approach used by most researchers [79, 94, 101, 102] and follows the general recommendations given by Lui and Chen [100].

The rotational deformation of joints is customarily expressed as a function of the moment in the connection. Consider the simple case of a nailed joint subjected to a moment as shown in Figure 5.1(a). As the moment is increased the nails in the joint will deform allowing the timber to rotate relative to the gusset plates. The greater the moment the greater will be the rotation and the maximum rotation will depend on the stiffness of the connection. If the nail stiffness (k) was linear, the moment-rotation relationship would be a straight line as shown in Figure 5.1.(b). In Chapter 4, it has been shown that the stiffness of a nailed joint (k) reduces as the load increases and, on this basis, with increasing moment the moment-rotation relationship will fall away as shown in Figure 5.1.(c).

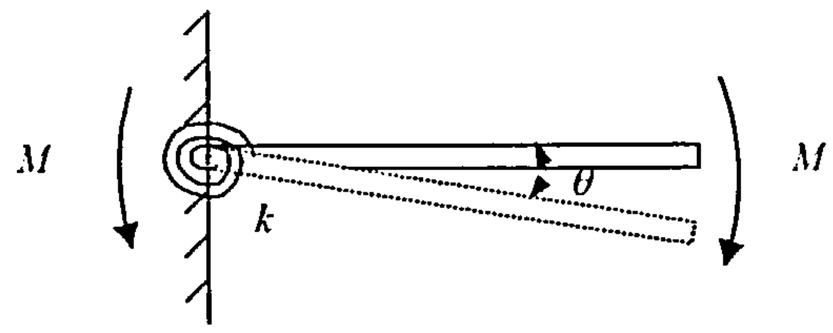

(a)

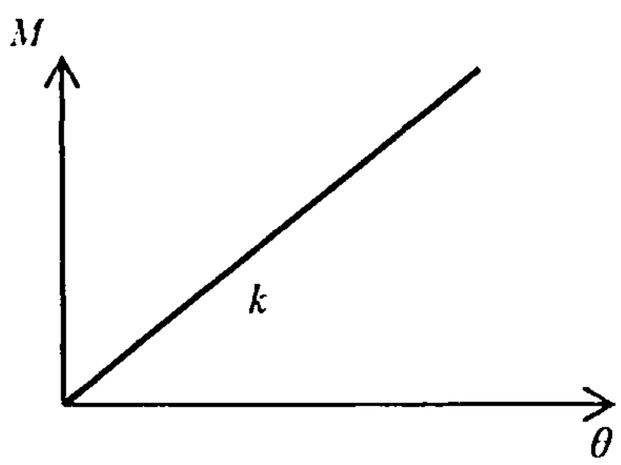

(b)

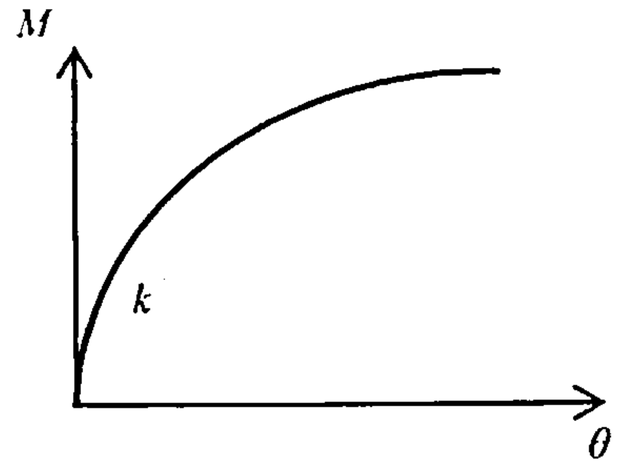

(c)

Figure 5.1 The moment (M) –rotation (θ) behaviour of a joint with stiffness k.

It may be acceptable to assume a linear approximation of the initial portion of the moment-displacement curve up to the serviceability limit state of the joint. To extend beyond that limit the behaviour of the joint would be unrealistic at intermediate and ultimate limit state conditions. For nailed joints the varying effect of the joint stiffness has to be taken into account and alternative approaches for this have been considered in sections 5.2.1 to 5.2.3.4.

In addition, when a joint is subjected to a moment, the timber and plywood are loaded at varying angles to their grain direction. For loading along the direction of the grain the nail load will be obtained from equations (41), (43), (50), (86) and (92). For loading perpendicular to the grain these equations have to be reviewed to take account of the effect of the direction of the loading and the relevance of the row spacing function.

From the analysis of embedment tests, Whale *et al* [104, 105] concluded there was negligible difference between the parallel and perpendicular veneer properties of plywood and similar results were also obtained for the effect of grain direction in timber. For nailed connections they recommend that the direction of loading relative to the grain of the timber and of the plywood had no effect on the strength and stiffness behaviour of the joint. This is also the approach taken in STEP 1 [79], Bouchar, *et al* [123] and EC5 [11]. To investigate this effect some plywood gusset plate joints with the face grain of the plywood at right angles to the direction of loading were tested in the programme. The results showed that the joints had the same stiffness behaviour and were approximately 4% stronger than equivalent joints tested with the face grain aligned along the direction of loading. This is a relatively small variation and for this research it has been accepted that joint strength can be taken to be the same irrespective of the grain direction.

Regarding the row spacing function, for the loading component along the direction of the grain, equations (41), (43), (50), (86) and (92) are directly applicable. For the loading component at right angles to grain, the direction of the grain prevents the timber from splitting or from reducing its withstand capability and the row spacing function can be taken to be unity. It is also to be appreciated that with the limited width of the timber in that direction only a few lines of nail can be fitted into the space and the effect of this change will in any case be relatively small.

Taking the above effects into account, the resultant force on any nail will be the combined effect of the forces along and at right angles to the grain and can be determined using the Hankinson formula [114].

Consider the forces on the timber due to any nail *i* to be as shown in Figure 5.2.

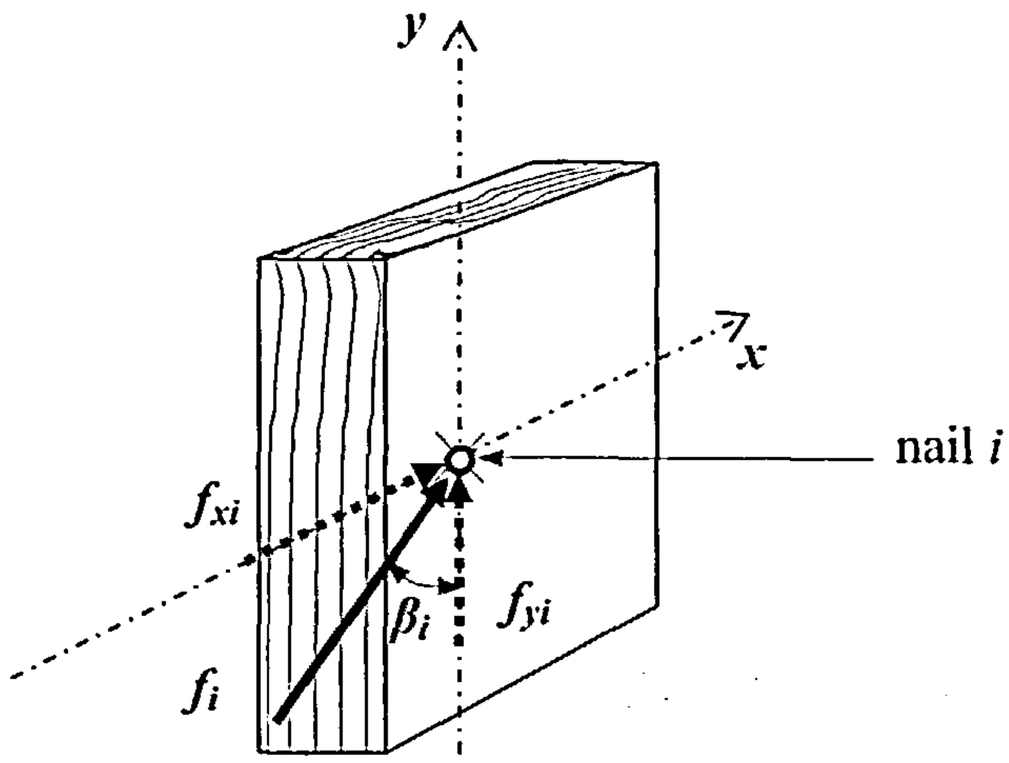

Figure 5.2 Force on nail *i* resolved into components along and at right angles to the grain direction.

The resultant force, f_i, on nail *i* acts at an angle β_i to the grain direction. Using the Hankinson formula the component force along the direction of the grain, f_{yi}, and perpendicular to it, f_{xi} can be related to f_i as follows:

$$f_i = \frac{f_{xi} f_{yi}}{f_{yi} \sin^2(\beta_i) + f_{xi} \cos^2(\beta_i)} \qquad \ldots.(93)$$

where:

f_{xi} is selected from equation (41f), (50f), (86f) or (92f) to suit the joint type being used.

f_{yi} is selected from equation (41e), (41f), (50e), (50f), (86e), (86f), (92e) or (92f) to suit the joint type and the row spacing being used.

In the above it has been assumed that the planes containing the timber grain are effectively parallel to the timber face as shown in Figure 5.3. The nail forces per growth ring act in the same plane as the grain of the timber.

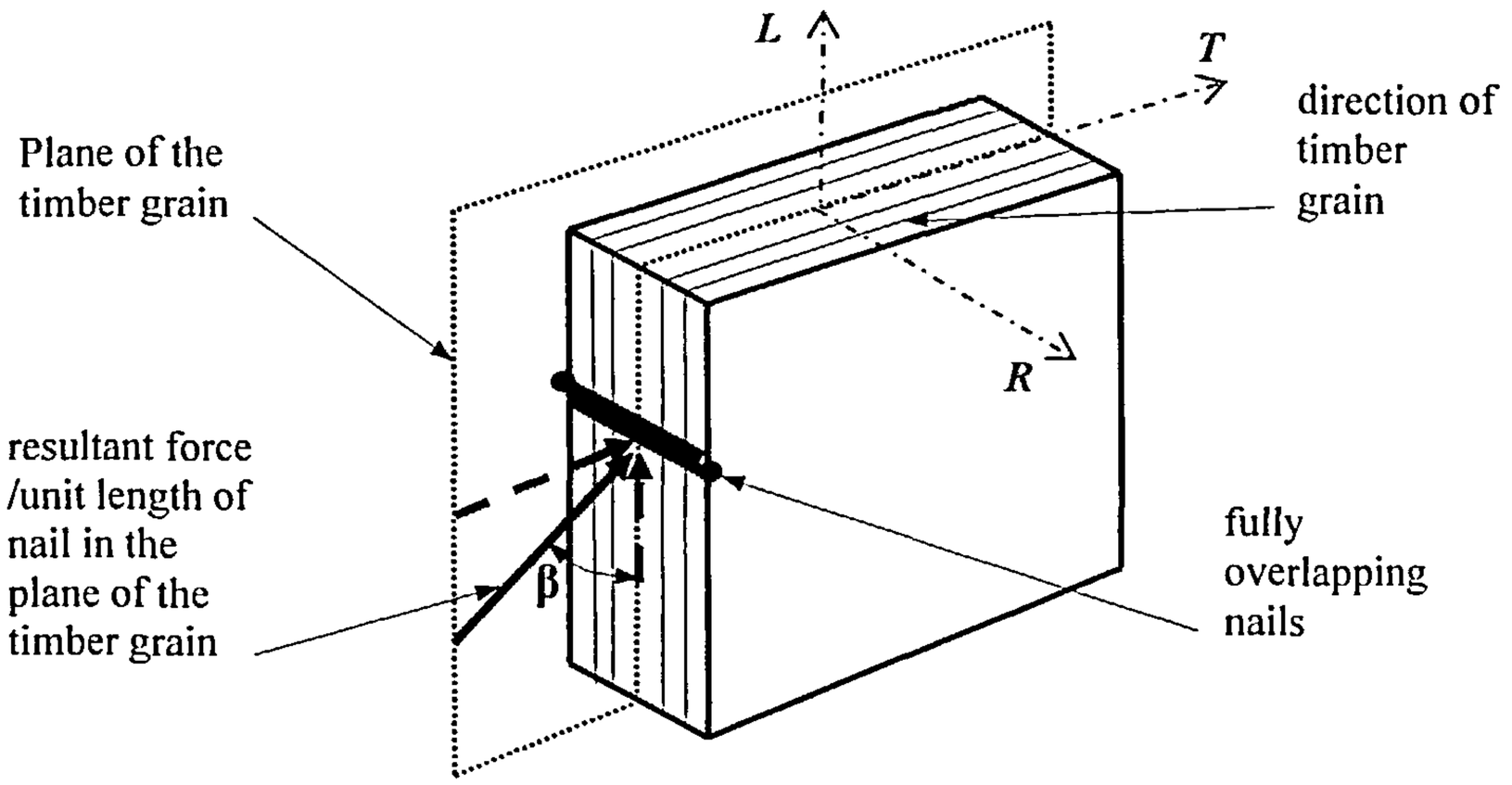

Figure 5.3 The timber grain is parallel to the face of the timber

The strength and stiffness properties of timber will differ depending on whether it is loaded relative to its radial (*R)*, tangential (*T)* or longitudinal (*L)* axis. The axes are shown on Figure 5.3 and are the conventional axes used when timber is idealised to behave in an orthotropic manner [1, 78, 117]. In Figure 5.3 the nail loading resolves into components acting in the direction of the tangential and longitudinal axes.

If the plane of the timber grain is at an angle *a* to its face, loading from the nail imposes a force component in the radial direction, F_R, in addition to components in the direction of the longitudinal axis, F_L, and tangential axis, F_T, as shown on Figure 5.4.

The force *F* imposed on the timber from the overlapping nails can be resolved into a vertical component, $Fcos(\beta)$, and a horizontal component, $Fsin(\beta)$. The vertical component will act along the direction of the *L* axis and the horizontal component can be resolved into further components along the direction of the *T* axis, ($F_H cos(a)$), and the *R* axis, ($F_H sin(a)$).

When timber is loaded along the *T* axis the earlywood and latewood elements of the growth ring [78] are compressed in parallel and the stronger latewood will dictate the strength of the timber. Loading in the *R* direction results in the earlywood and late wood being loaded in series and the softer earlywood will become the key factor in the timber strength and stiffness behaviour. From the results of tests using timber with the plane of the grain at an angle to the joint face it was observed that joint strength and stiffness were consistently lower than equivalent tests using timber with the plane of the grain parallel to the face. Because the size of the effect was significant, the matter has been investigated and reported in detail in section 5.4.2.

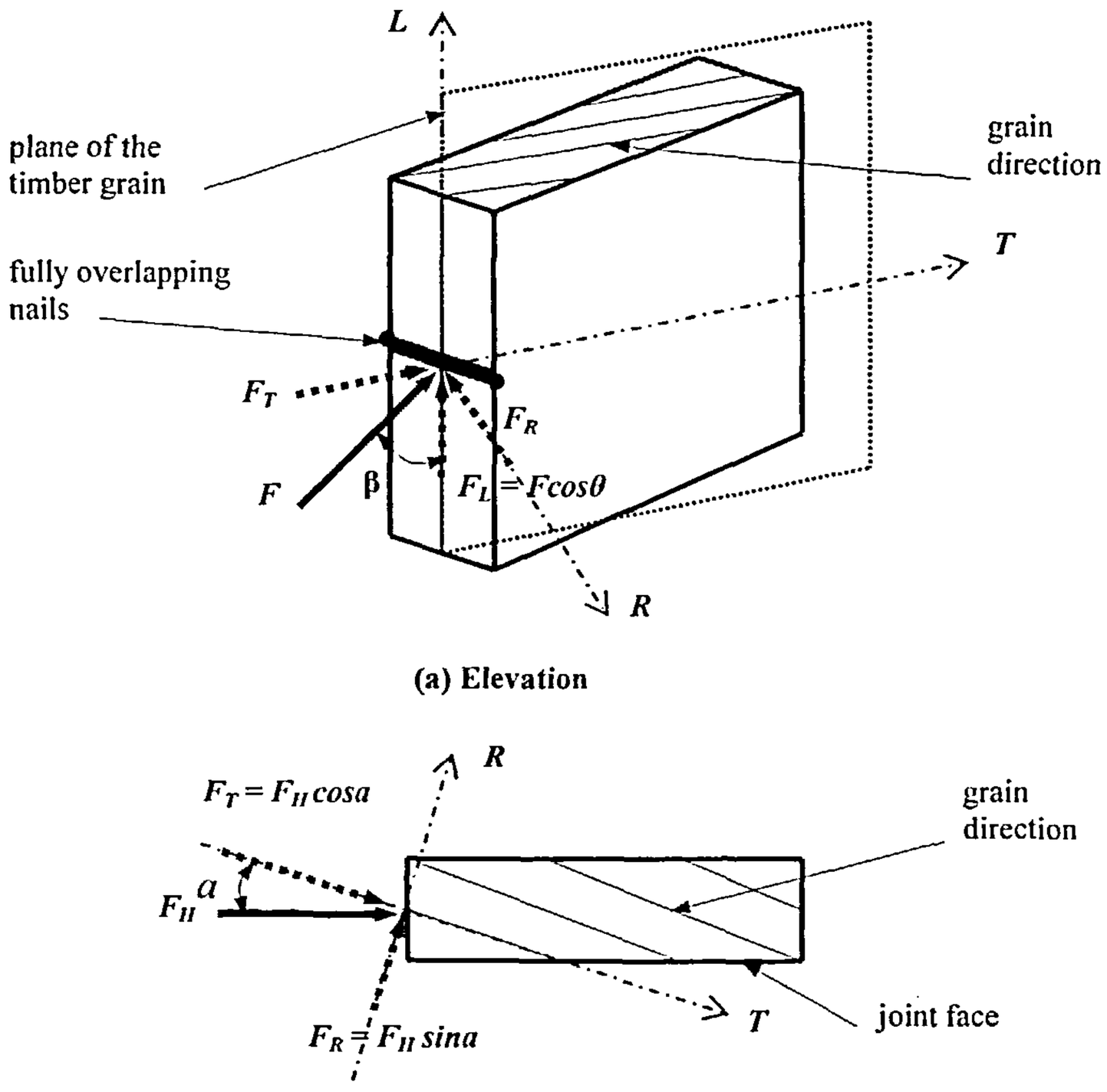

Figure 5.4 Timber grain at an angle *a* to the face of the timber

In the following analyses only the equations for joints using steel gusset plates or plywood gusset plates with a gap between the timber and the gusset plates have been used. Those applicable to the other types of joint assembly analysed in Chapter 4 can be developed by inserting the relevant model expressions in the moment equation. The models have been used for the calculation of the moment sustained by the moment connections tested and described in Chapter 3 and the solutions are presented and compared with the test results in section 5.4. In all of the methods the plane of the grain direction of the timber containing the *T* and *L* axes is taken to be parallel to the face of the joint.

5.2.1 Secant Stiffness-Fixed Centre of Rotation – (Secant Stiffness 1)

This is based on the conventional torsion theory used for the analysis of rigid steel joints connected by bolts or welds and has been applied to nailed timber joints by Morris [95, 96] and Goh [12].

It is assumed that each nail in the joint behaves in a perfectly elastic manner and as the joint is stressed the force in each nail will be directly proportional to its radius from the centre of rotation. The centre of rotation is taken to be the centroid of the nail group. Shear and axial force deformations are ignored and the position of the centroid is assumed to remain fixed under the action of the increasing moment. The

stiffness of all of the nails in the joint is taken to be the secant stiffness of the nail at the greatest distance from the centroid. With this assumption, the stiffness of the nails in the joints will generally be underestimated and a conservative solution will be obtained.

Consider a multi-nail joint subjected to a moment as shown in Figure 5.5(a).

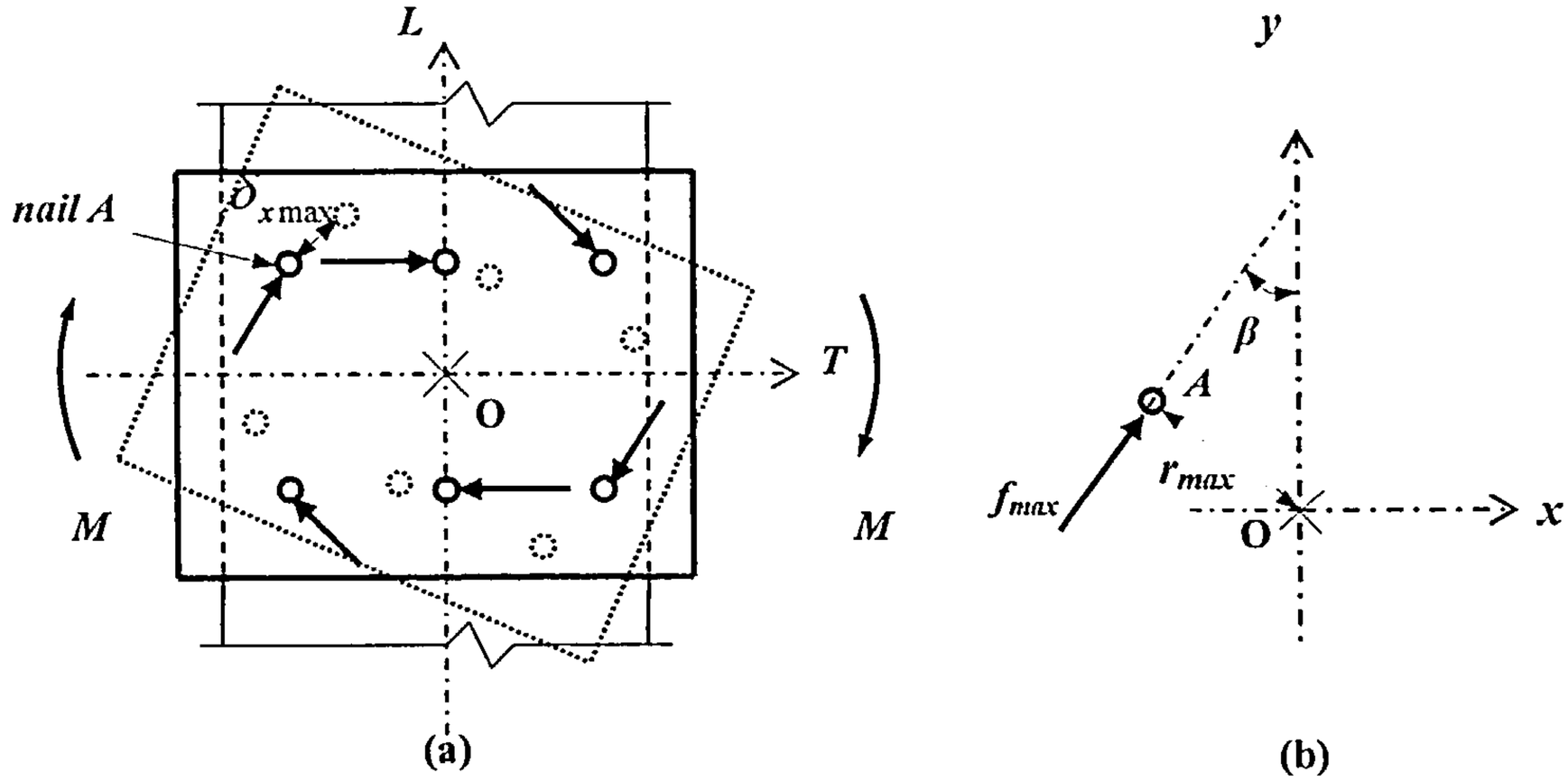

Figure 5.5 Multi-nailed joint subjected to a moment. (rotated position shown dotted)

The applied moment M causes the joint to rotate about the centre of rotation O. The force on each nail will be at right angles to the direction of the line between the nail and the centre of rotation and will be proportional to its distance from O. The force in nail A is at an angle β to the vertical as shown in Figure 5.5(b).

In Figure 5.6 the curved line represents the actual load-displacement behaviour of any nail in the joint. Each nail in the pair of overlapping nails furthest from the centre of rotation will be subjected to the greatest load f_{max} at a slip δ_{xmax}, where δ_{xmax} is the maximum slip caused by the joint rotation. Nails closer to the centroid will be subjected to smaller loads on the curve but will have a greater stiffness. In the secant stiffness method the stiffness of the extreme nail, taken to be the slope of the straight line between the origin and the load at δ_{xmax}, is applied to all of the nails in the joint.

Consider nail A, shown in Figure 5.5(a), to be one of the pair of overlapping nails at the greatest distance from the centre of rotation. In Figure 5.5(b) nail A is shown relative to a Cartesian co-ordinate system and based on the above assumption, the force f_i in a nail i at radius r_i and at angle β_i to the L axis will be:

$$f_i = \frac{r_i}{r_{\max}} f_{max} \qquad \ldots.(94)$$

The moment M_i taken by the nail at radius r_i will be the nail force times the lever arm from O:

$$M_i = f_i \; r_i \qquad \ldots.(95)$$

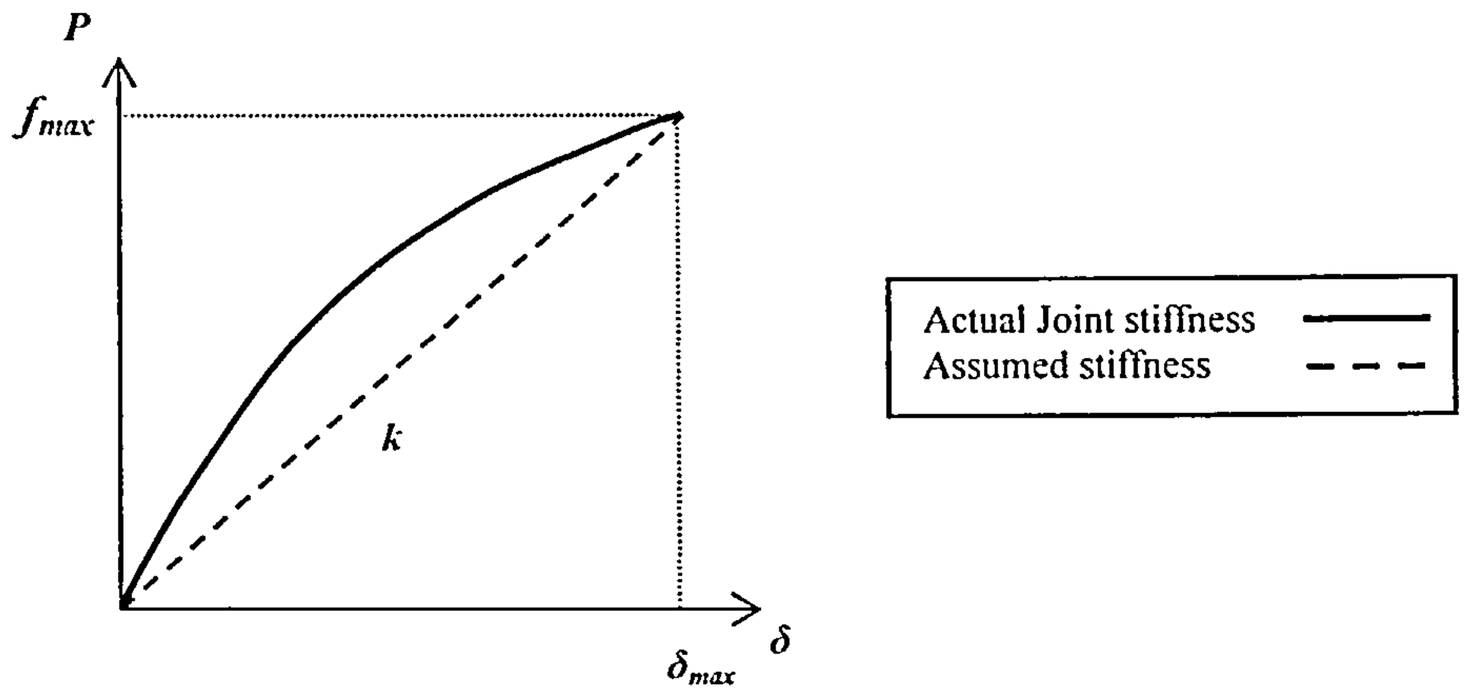

Figure 5.6 The stiffness of nail A in the multi-nail joint

Substituting for f_i, the moment in a joint with N nails will be:

$$M = \frac{f_{\max}}{r_{\max}} \sum_{i=1}^{i=N} r_i^2 \qquad \ldots.(96)$$

Applying equation (96) to joints with fully overlapping nails and taking the maximum nail load to be the appropriate value of $P_{\delta x}$ for joints with steel or plywood gusset plates given in equations (41), (43), (50), (86) and (92), the moment taken by the joint will be:

$$M_{\delta x} = \frac{P_{\delta x \max}}{r_{\max}} \sum_{i=1}^{i=\frac{N}{2}} \left(r_i^2\right) \qquad \ldots.(97)$$

The expression for $P_{\delta xmax}$ can be resolved into components along the direction of the T and L axes and the effects of loading relative to the grain direction applied in accordance with equation (93). For timber joints using fully overlapping nails with steel gusset plates or plywood gusset plates assembled with a gap between the gusset plates and the timber, moment equation (97) can be written as given in equations (98a) to (98d). The symbols used in these equations will be as given in equations (41) and (86).

(i) Joints with steel gusset plates and predrilled holes less than 1.1 times the nail diameter, assembled with a gap between the gusset plates and the timber:

(a) where the nail row spacing is between $0.7\times2\times5\times d$ and $0.7\times4\times7\times d$:

$$M_{\delta x} = (1/r_{max})\,(1-e^{-1.712\delta xmax})^{0.926}\,(0.1\delta xmax + 0.68)\sum_{i=1}^{i=\frac{N}{2}} (r_i^2)\,\frac{S_{GS}S_G}{S_{GS}\sin^2\beta_i + S_G\cos^2\beta_i} \quad \ldots.(98a)$$

(b) where the nail row spacing is greater than $0.7\times4\times7\times d$:

$$M_{\delta x} = (1/r_{max})\,S_G(1-e^{-1.712\delta xmax})^{0.926}(0.1\delta xmax + 0.68)\sum_{i=1}^{i=\frac{N}{2}}(r_i^2) \quad \ldots.(98b)$$

The symbols are as given against equations (41), and:

$M_{\delta x}$	=	moment taken by the joint - Nmm.
r_{max}	=	the distance of the furthest pair of nails from the nail group centroid – mm.
r_i	=	the distance of nail i from the nail group centroid. – mm.
δ_{xmax}	=	the slip of the nail at radius r_{max}.
$N/2$	=	the number of fully overlapping nails per side of the joint.
β_i	=	the angle between the force in the pair of nails at radius r_i from the centre of rotation and the direction of the L axis.

(ii) Joints with plywood gusset plates assembled with a gap between the gusset plates and the timber:

(a) where the nail row spacing is between $0.85\times2\times5\times d$ and $0.85\times4\times5\times d$:

$$M_{\delta x} = 1/r_{max}\,(1-e^{-1.719\delta xmax})^{0.568}(0.1\delta xmax + 0.68)\sum_{i=1}^{i=\frac{N}{2}} (r_i^2)\,\frac{P_{GS}P_G}{P_{GS}\sin^2\beta_i + P_G\cos^2\beta_i} \quad \ldots(98c)$$

(b) where the nail row spacing is greater than $0.85\times4\times5\times d$:

$$M_{\delta x} = P_G(1-e^{-1.719\delta xmax})^{0.568}(0.1\delta xmax + 0.68)/r_{max}\sum_{i=1}^{i=\frac{N}{2}}(r_i^2) \quad \ldots.(98c)$$

where the functions are as described in equation (86) and (i)(b).

5.2.2 Secant Stiffness–Variable Centre of Rotation – (Secant Stiffness 2)

In this method the centre of rotation is obtained using the principles of static equilibrium. It is the position where there is a balance between the forces generated by the moment and those due to the shear and axial forces on the joint.

Consider a multi-nail joint as shown in Figure 5.7(a). Setting the origin of a Cartesian co-ordinate system at the geometric centre of the nail group O, the centre of rotation of the joint C is assumed to be located at a radius r_c from O. The horizontal and vertical distances of C from O are x_c and y_c respectively. A shear force F is applied to the joint at a distance e from the geometric centre of the nailing configuration. Under the action of the force the joint will rotate about C and the displacement of the each pair of fully overlapping nails will be proportional to their radius from C.

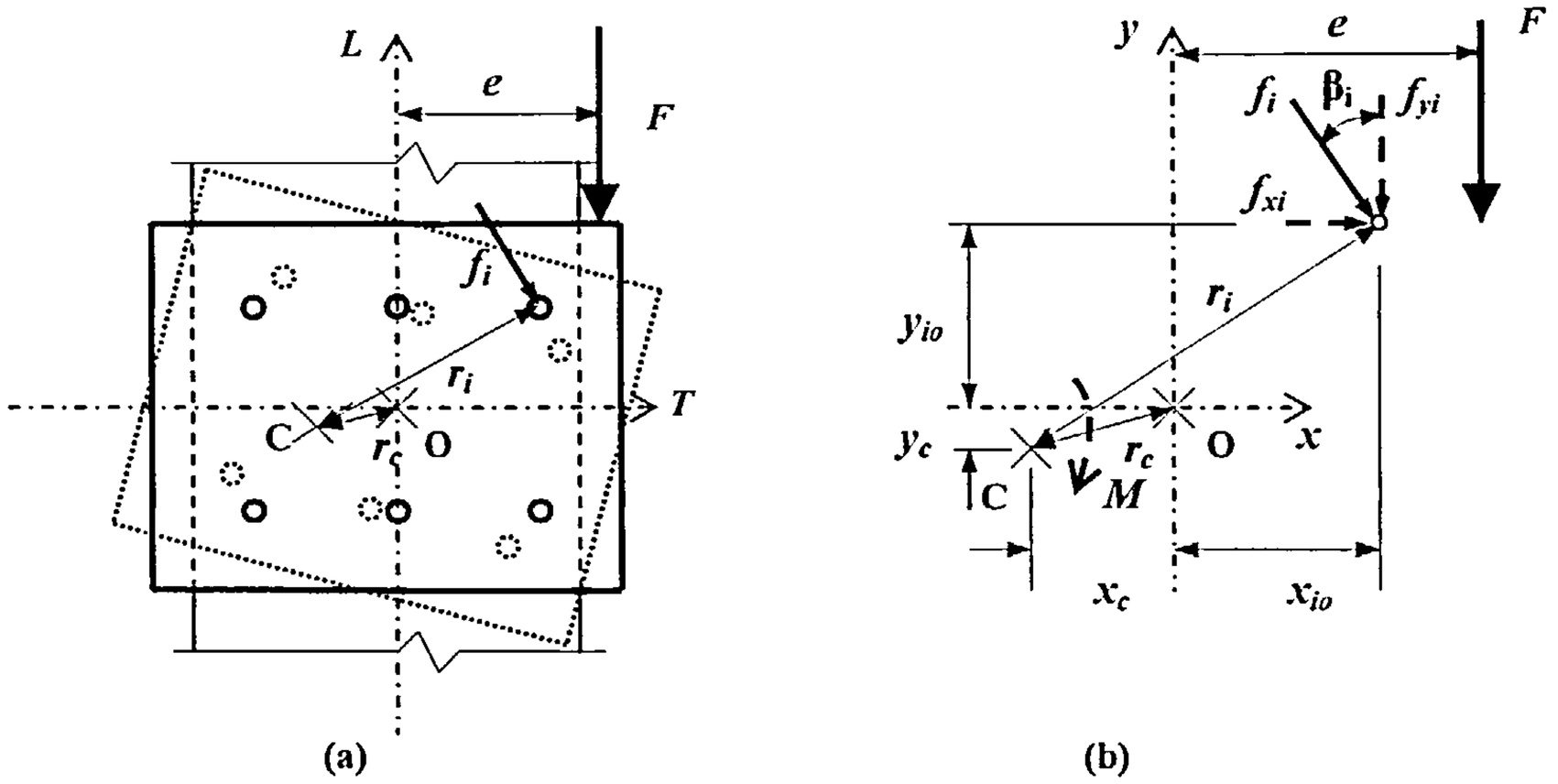

Figure 5.7 Ultimate strength approach. Dotted line shows rotated position.

The force f_i on nail i is at an angle β_i to the L axis as shown in Figure 5.7(b). Components of the force in nail i in the vertical and horizontal directions are f_{yi} and f_{xi} respectively.

For horizontal equilibrium, the sum of the horizontal forces must equal zero and as there is no external loading in that direction the value of y_c will also be zero as shown in Figure 5.8. This situation is common to all of the methods considered and will not be referred to in subsequent sections.

The radius, r_i, of nail i from C will be:

$$r_i = [(x_{io} - (x_c))^2 + y_{io}^2]^{0.5} \qquad \text{....(99)}$$

Assuming there are N nails in the joint, taking moments about C:

$$F\,(e + x_c) = \sum_{i=1}^{i=N} f_i(r_i) \qquad \text{....(100)}$$

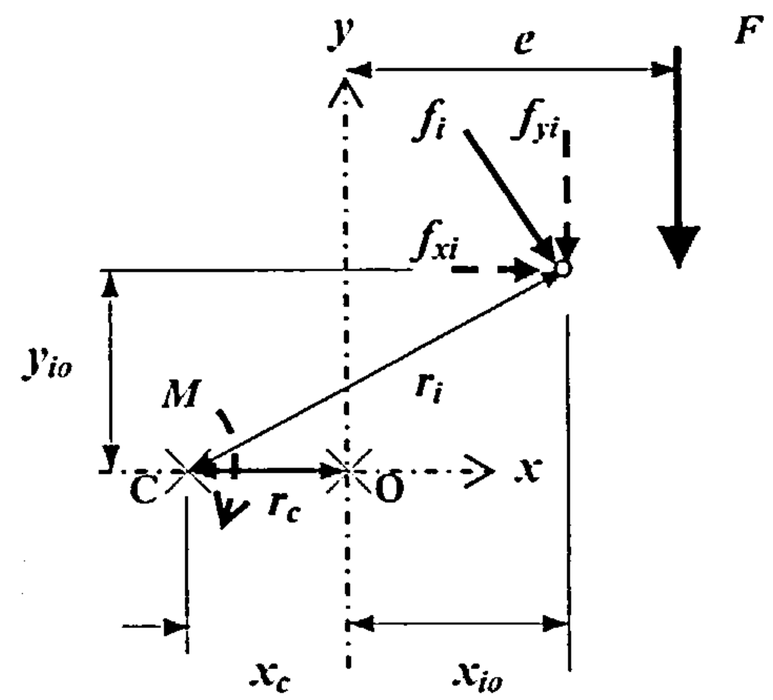

Figure 5.8 Ultimate strength approach showing $y_c = 0$.

Using equation (94) to express the nail force in terms of the maximum nail force, f_{max}, at radius r_{max} from C, applying equation (99) for r_i and rearranging, equation (100) becomes:

$$F = \frac{1}{(e + x_c)} \frac{f_{\max}}{r_{\max}} \sum_{i=1}^{i=N} r_i^{\,2} \qquad \ldots.(101)$$

The vertical force, f_{yi}, in nail i can be written in terms of the nail force as:

$$f_{yi} = f_i \frac{(x_{io} + x_c)}{r_i} \qquad \ldots.(102)$$

and again expressing f_i in terms of the maximum nail force, F can be written as:

$$F = \sum_{i=1}^{i=N} f_{yi} = \frac{f_{\max}}{r_{\max}} \sum_{i=1}^{i=N} (x_{io} + x_c) \qquad \ldots.(103)$$

Equating equation (101) and (103), the unknown x_c can be found. To solve the equations involves the use of an iteration process which can be readily done by setting up an algorithm in Mathcad [51] as shown in Appendix G.

Having determined x_c the force F is obtained from equation (103) and the moment in the joint can be obtained by multiplying equation (101) by the eccentricity $(e + x_c)$ giving:

$$M = \frac{f_{\max}}{r_{\max}} \sum_{i=1}^{i=N} r_i^{\,2} \qquad \ldots.(104)$$

Applying equation (104) to joints with fully overlapping nails and taking the maximum nail load to be the appropriate value of $P_{\delta x}$ for joints with steel or plywood gusset plates given in equations (41), (43), (50), (86) and (92), the moment taken by the joint will be:

$$M_{\delta x} = \frac{P_{\delta x \max}}{r_{\max}} \sum_{i=1}^{i=\frac{N}{2}} \left(r_i^2\right) \qquad \ldots.(105)$$

The expression for $P_{\delta xmax}$ can be resolved into components along the direction of the T and L axes and the effects of loading relative to the grain direction applied in accordance with equation (93). For timber joints using fully overlapping nails with steel gusset plates or plywood gusset plates assembled with and without gaps between the gusset plates and the timber, moment equation (105) can then be written as given in equations (106a) to (106d). The symbols used in these equations will be as given in equations (41) and (86).

(i) Joints with steel gusset plates and predrilled holes less than 1.1 times the nail diameter, assembled with a gap between the gusset plates and the timber:

(a) where the nail row spacing is between $0.7\times2\times5\times d$ and $0.7\times4\times7\times d$:

$$M_{\delta x} = (1-e^{-1.712\delta xmax})^{0.926}(0.1\delta xmax+0.68) \sum_{i=1}^{i=\frac{N}{2}} \frac{r_i^2}{r_{\max}} \left(\frac{S_{GS}S_G}{S_{GS}\sin^2\beta_i + S_G\cos^2\beta_i}\right) \qquad \ldots.(106a)$$

(b) where the nail row spacing is greater than $0.7\times4\times7\times d$:

$$M_{\delta x} = S_G\,(1-e^{-1.712\delta xmax})^{0.926}(0.1\delta xmax+0.68) \sum_{i=1}^{i=\frac{N}{2}} \frac{r_i^2}{r_{\max}} \qquad \ldots.(106b)$$

The symbols are as given against equations (41), in section 5.2.1 and:

r_{max} = the distance of the furthest pair of nails from C– mm.

r_i = the distance of nail i from C – mm.

(ii) Joints with plywood gusset plates assembled with a gap between the gusset plates and the timber:

(a) where the nail row spacing is between $0.85\times2\times5\times d$ and $0.85\times4\times5\times d$:

$$M_{\delta x} = (1-e^{-1.719\delta xmax})^{0.568}(0.1\delta xmax+0.68) \sum_{i=1}^{i=\frac{N}{2}} \frac{r_i^2}{r_{\max}} \left(\frac{P_{GS}P_G}{P_{GS}\sin^2\beta_i + P_G\cos^2\beta_i}\right) \qquad \ldots.(106c)$$

(b) where the nail row spacing is greater than $0.85\times4\times5\times d$:

$$M_{\delta x} = P_G(1-e^{-1.719\delta xmax})^{0.568}(0.1\delta xmax + 0.68)\sum_{i=1}^{i=\frac{N}{2}}\frac{r_i^2}{r_{\max}} \quad \text{....(106d)}$$

where the functions are as described in equation (86) and (i)(b).

5.2.3 Non-Linear Methods

In the previous methods the assumption was made that nail behaviour was linearly elastic and displacements of the joint were infinitesimally small such that changes in geometry of the nailing configuration relative to the timber could be ignored. In the following methods the non-linear behaviour of the nails is taken into account and in section 5.2.3.3 the effect of the movement of the nails on the geometry and the force configuration in the joint is also included for.

5.2.3.1 Fixed Centre of Rotation – (Non-Linear 1)

This method uses a similar procedure to that developed by Perkins *et al* [179] for the design of multi-nailed timber joints subjected to a moment.

Consider a multi-nailed joint as shown in Figure 5.9. The joint is subjected to a moment M caused by a shear force F at a lever arm e from the centre of rotation of the joint. The centre of rotation is taken to be the geometric centre of the nailing configuration, O. Nails in the joint will displace in proportion to their distance from O. At the maximum radius r_{max} from O the nail will have the greatest displacement, δ_{xmax}, and the maximum force, f_{max}. The force f_i on nail i is at an angle β_i to the vertical as shown in Figure 5.9(a).

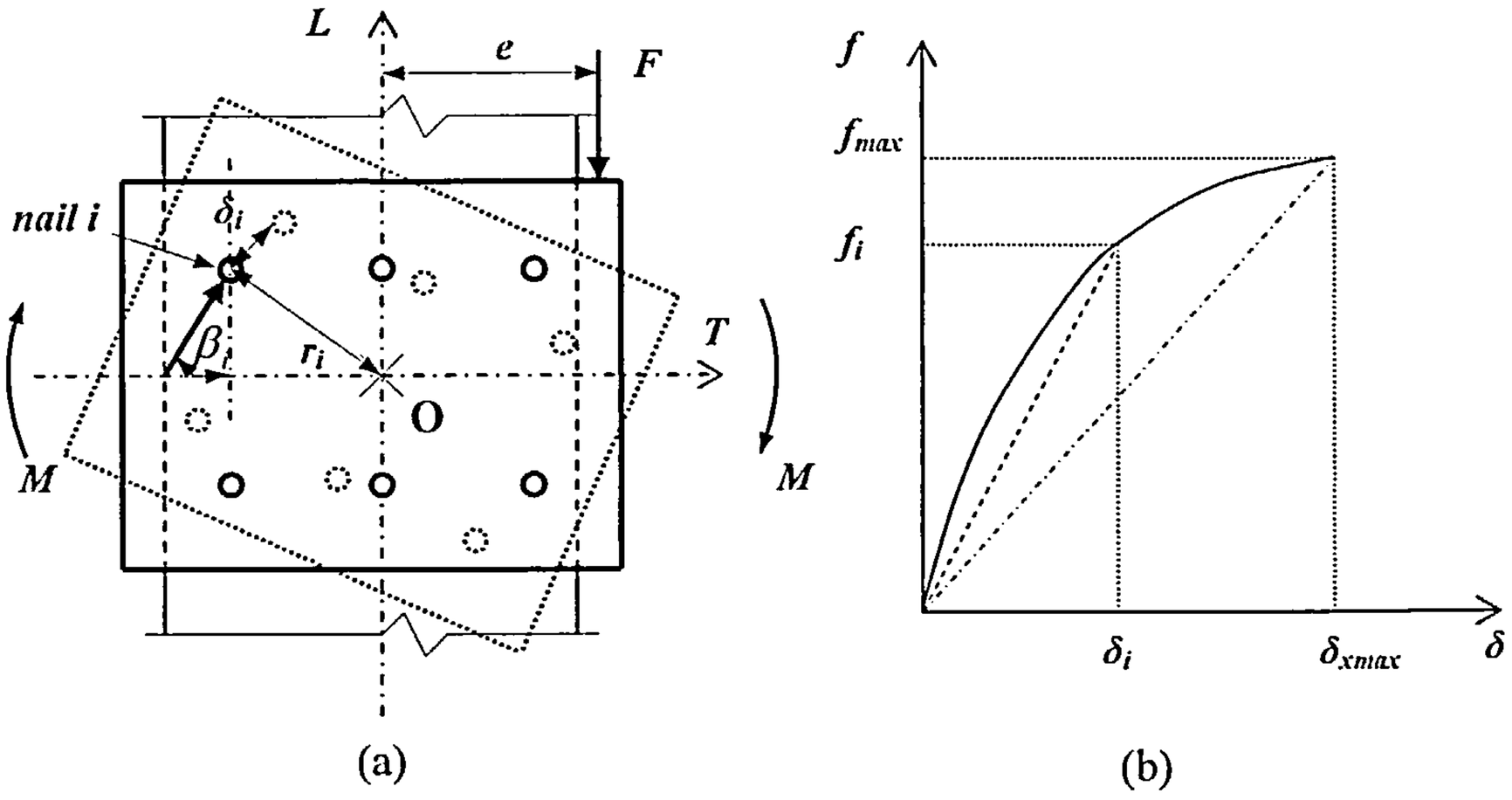

Figure 5.9 Non-Linear analysis. (dotted line shows rotated position)

The displacement relationship between the nail with the maximum force and nail *i* will be:

$$\delta_i = \frac{r_i}{r_{\max}} \delta_{xmax} \qquad \ldots.(107)$$

The force in nail *i* will be obtained from equation (94) using the displacement relationship for δ_i given in equation (107), as follows:

$$f_i = f_{(\delta xmax \frac{r_i}{r_{\max}})} \qquad \ldots.(108)$$

In Figure 5.9(b) the load-displacement relationship of a nail is shown with the load f_{max} at maximum slip δ_{xmax} and the load f_i at slip δ_i. What is to be noted is that for any displacement the full strength of the nail will be used in this approach. Summing the moments taken by all of the nails *N* in the joint about O:

$$M = \sum_{i=1}^{i=N} f_i r_i \qquad \ldots.(109)$$

Substituting for f_i as given in equation (108), the bending moment becomes:

$$M = \sum_{i=1}^{i=N} f(\delta x \max \frac{r_i}{r_{\max}})(r_i) \qquad \ldots.(110)$$

Applying equation (110) to joints with fully overlapping nails and taking the maximum nail load to be the appropriate value of $P_{\delta x}$ for joints with steel or plywood gusset plates given in equations (41), (43), (50), (86) and (92), the moment taken by the joint will be:

$$M_{\delta x} = \sum_{i=1}^{i=\frac{N}{2}} P(\delta x \max \frac{r_i}{r_{\max}})(r_i) \qquad \ldots.(111)$$

The expression for $P(\delta x \max \frac{r_i}{r_{\max}})$ can be resolved into components along the plane of the *T* and *L* axes and the effects of loading relative to the grain direction applied in accordance with equation (93). For timber joints using fully overlapping nails with steel gusset plates or plywood gusset plates assembled with a gap between the gusset plates and the timber, moment equation (111) can then be

written as given in equations (112a) to (112d). The symbols used in these equations will be as given in equations 41 and 86 and as given below.

(i) Joints with steel gusset plates and predrilled holes less than 1.1 times the nail diameter, assembled with a gap between the gusset plates and the timber:

(a) where the nail row spacing is between $0.7\times2\times5\times d$ and $0.7\times4\times7\times d$:

$$M_{\delta x}=\sum_{i=1}^{i=\frac{N}{2}} r_i \left(\frac{S_{GS}S_G}{S_{GS}\sin^2\beta_i + S_G\cos^2\beta_i}\right)\left(1-e^{-1.712\left(\delta\max\frac{r_i}{r_{\max}}\right)}\right)^{0.926}\left(0.1\left(\delta x max\frac{r_i}{r_{\max}}\right)+0.68\right) \quad \text{....(112a)}$$

(b) where the nail row spacing is greater than $0.7\times4\times7\times d$:

$$M_{\delta x}=\sum_{i=1}^{i=\frac{N}{2}} r_i \left(S_G\left(1-e^{-1.712\left(\delta\max\frac{r_i}{r_{\max}}\right)}\right)^{0.926}\left(0.1\left(\delta x max\frac{r_i}{r_{\max}}\right)+0.68\right)\right) \quad \text{....(112b)}$$

where the symbols are as given against equations (41) and in section 5.2.2.

(ii) Joints with plywood gusset plates assembled with a gap between the gusset plates and the timber:

(a) where the nail row spacing is between $0.85\times2\times5\times d$ and $0.85\times4\times5\times d$:

$$M_{\delta x}=\sum_{i=1}^{i=\frac{N}{2}} r_i \left(\frac{P_{GS}P_G}{P_{GS}\sin^2\beta_i + P_G\cos^2\beta_i}\right)\left(1-e^{-1.719\left(\delta\max\frac{r_i}{r_{\max}}\right)}\right)^{0.568}\left(0.1\left(\delta x max\frac{r_i}{r_{\max}}\right)+0.68\right) \quad \text{....(112c)}$$

(b) where the nail row spacing is greater than $0.85\times4\times5\times d$:

$$M_{\delta x}=\sum_{i=1}^{i=\frac{N}{2}} r_i P_G\left(1-e^{-1.719\left(\delta\max\frac{r_i}{r_{\max}}\right)}\right)^{0.568}\left(0.1\left(\delta x max\frac{r_i}{r_{\max}}\right)+0.68\right) \quad \text{....(112d)}$$

where the functions are as described in equation (86) and (i)(b).

5.2.3.2 Variable Centre of Rotation–(Non-Linear 2)

In this method the centre of rotation is determined using the approach given in section 5.2.2 and the forces in the nails are derived using the method in section 5.2.3.1.

Consider a multi-nailed joint subjected to a shear force F at a distance e from the geometric centre of the nailing configuration as shown in Figure 5.10(a). Setting the origin of a Cartesian co-ordinate system at the geometric centre O and using the argument followed in section 5.2.2, the centre of rotation of the joint, C, will be located at a horizontal distance r_c from O.

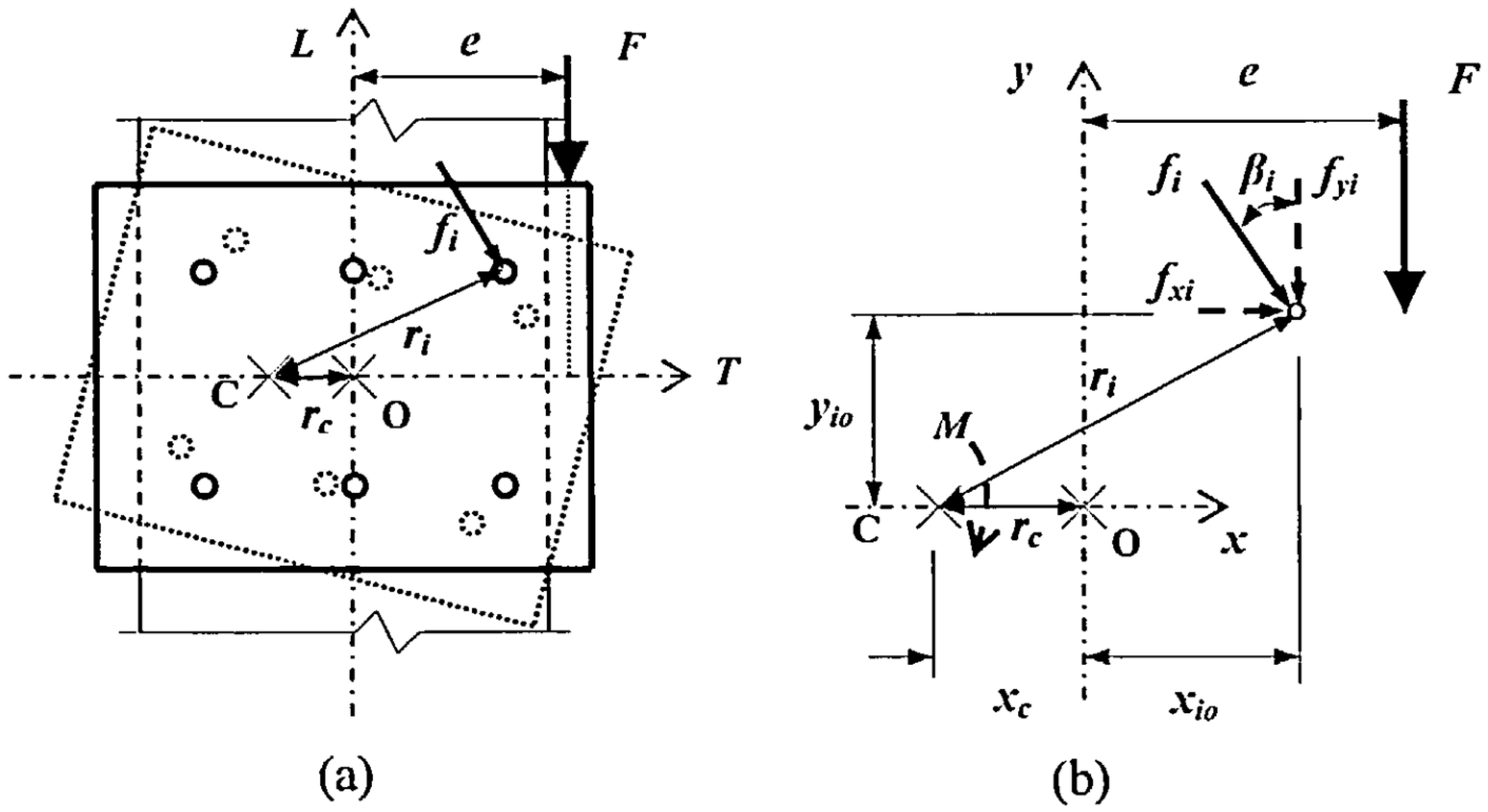

Figure 5.10 Variable centre approach. (dotted line shows rotated position)

Under the action of the shear force the joint will rotate about C. If the displacement of nail i at radius r_i from the centre of rotation is δ_i, it can be expressed in terms of the displacement of the nail with maximum displacement δ_{xmax} using equation (107) as follows:

$$\delta_i = \frac{r_i}{r_{\max}} \delta_{xmax}$$

where r_{max} is the radius of the maximum loaded nail from C.

The force f_i on nail i is at an angle β_i to the vertical as shown in Figure 5.10(b). Components of the force in nail i in the vertical and horizontal directions are f_{yi} and f_{xi} respectively.

The radius of nail i from C will be:

$$r_i = [(x_{io} - (x_c))^2 + y_{io}^2]^{0.5} \qquad \ldots.(113)$$

Assuming there are N nails in the joint, taking moments about C:

$$F\,(e-x_c) = \sum_{i=1}^{i=N} f_i(r_i) \qquad \ldots.(114)$$

From equation (107), the force in nail i is $f_i = f_{(\delta x max}\frac{r_i}{r_{\max}})$, and substituting into equation (114); including for r_i as given in equation (113) and dividing by $(e-x_c)$ gives:

$$F = \frac{1}{(e-x_c)} \sum_{i=1}^{i=N} f(\delta x \max \frac{r_i}{r_{\max}})\left(((x_{io}-x_c)^2 + y_{io}{}^2)^{0.5}\right) \qquad \ldots.(115)$$

The vertical force F can also be written as the sum of the vertical components of the nail forces in the joint:

$$F = \sum_{i=1}^{i=N} f_{yi} = \sum f(\delta x \max \frac{r_i}{r_{\max}}) \frac{(x_{io}-x_c)}{r_i} \qquad \ldots.(116)$$

Equating equations (115) and (116), the unknown x_c can be found by using the iteration method referred to in section 5.2.2 and described in Appendix G. Having determined x_c the bending moment in the joint can then be expressed in terms of the summation of the nail moments about the centre of rotation as follows:

$$M = \sum_{i=1}^{i=N} f(\delta x \max \frac{r_i}{r_{\max}}) r_i \qquad \ldots.(117)$$

Applying equation (117) to joints with fully overlapping nails and taking the maximum nail load to be the appropriate value of $P_{\delta x}$ for joints with steel or plywood gusset plates given in equations (41), (43), (50), (86) and (92), the moment taken by the joint will be:

$$M_{\delta x} = \sum_{i=1}^{i=\frac{N}{2}} P(\delta x \max \frac{r_i}{r_{\max}})(r_i) \qquad \ldots.(118)$$

The expression for $P(\delta x \max \frac{r_i}{r_{\max}})$ can be resolved into components in the plane of T and L axes and the effects of loading relative to the grain direction applied in accordance with equation (93). For timber joints using fully overlapping nails with steel gusset plates or plywood gusset plates assembled with a gap between the gusset plates and the timber, moment equation (118) can then be written as given in equations (119a) to (119d). The symbols used in these equations will be as given in equations (41) and, (86) and as given below.

(i) Joints with steel gusset plates and predrilled holes less than 1.1 times the nail diameter, assembled with a gap between the gusset plates and the timber:

(a) where the nail row spacing is between $0.7\times2\times5\times d$ and $0.7\times4\times7\times d$:

$$M_{\delta x} = \sum_{i=1}^{i=\frac{N}{2}} r_i \ (1-e^{-1.712(\delta x max \frac{r_i}{r_{\max}})^{0.926}} (0.1(\delta x max \frac{r_i}{r_{\max}}) + 0.68) \ \frac{S_{GS} S_G}{S_{GS} \sin^2 \beta_i + S_G \cos^2 \beta_i} \quad \text{...(119a)}$$

(b) where the nail row spacing is greater than $0.7\times4\times7\times d$:

$$M_{\delta x} = S_G \ (\sum_{i=1}^{i=\frac{N}{2}} r_i \ \ (1-e^{-1.712(\delta x max \frac{r_i}{r_{\max}})^{0.926}} (0.1(\delta x max \frac{r_i}{r_{\max}}) + 0.68)) \quad \text{....(119b)}$$

where the symbols are as given against equations (41) and in section 5.2.2.

(ii) Joints with plywood gusset plates assembled with a gap between the gusset plates and the timber:

(a) where the nail row spacing is between $0.85\times2\times5\times d$ and $0.85\times4\times5\times d$:

$$M_{\delta x} = \sum_{i=1}^{i=\frac{N}{2}} r_i \ (1-e^{-1.719\delta x max \frac{r_i}{r_{\max}})^{0.568}} (0.1(\delta x max \frac{r_i}{r_{\max}}) + 0.68) \ \frac{P_{GS} P_G}{P_{GS} \sin^2 \beta_i + P_G \cos^2 \beta_i} \quad \text{....(119c)}$$

(b) where the nail row spacing greater than $0.85\times4\times5\times d$:

$$M_{\delta x} = P_G \ (\sum_{i=1}^{i=\frac{N}{2}} r_i \ (1-e^{-1.719\delta x max \frac{r_i}{r_{\max}})^{0.568}} (0.1(\delta x max \frac{r_i}{r_{\max}}) + 0.68)) \quad \text{...(119d)}$$

where the functions are as described in equation (86) and (i)(b).

An example of the use of the model set up in Mathcad [51] is given in Appendix H.

5.2.3.3 Second-Order Solution–(Non-Linear 3)

In structural analysis, when the equilibrium relationships are written with respect to the undeformed original geometry of the structure, the analysis is referred to as a first-order analysis. This is the type of analysis that has been used in sections 5.2.1, to 5.2.3.2 inclusive. When the equilibrium relationships are written with respect to the deformed geometry of the structure the analysis is referred to as a second-order analysis [110, 112]. Second order analyses are always required for the stability analysis of structures to take account of the eccentricity effects of axial forces in what are commonly referred to as *P-Δ* effects or eigenvalue problems [111, 113, 115].

In the moment analyses of joints, the effect of the eccentricity of the force relative to the centre of rotation should always be taken into account and has been in the analyses given in this section. The second order effect being referred to in this method relates to the additional effects arising from the displacement of the nails relative to the joint geometry during the rotation process.

When nails are allowed to displace up to 3.2mm (the limit of the load-displacement relationships in Chapter 4) during rotation such a movement equates to a change of at least 4.5% in the nail position. The following analysis takes the effect of this movement into account. It also assumes that the centre of rotation of the joint will be variable using the approach given in section 5.2.3.2.

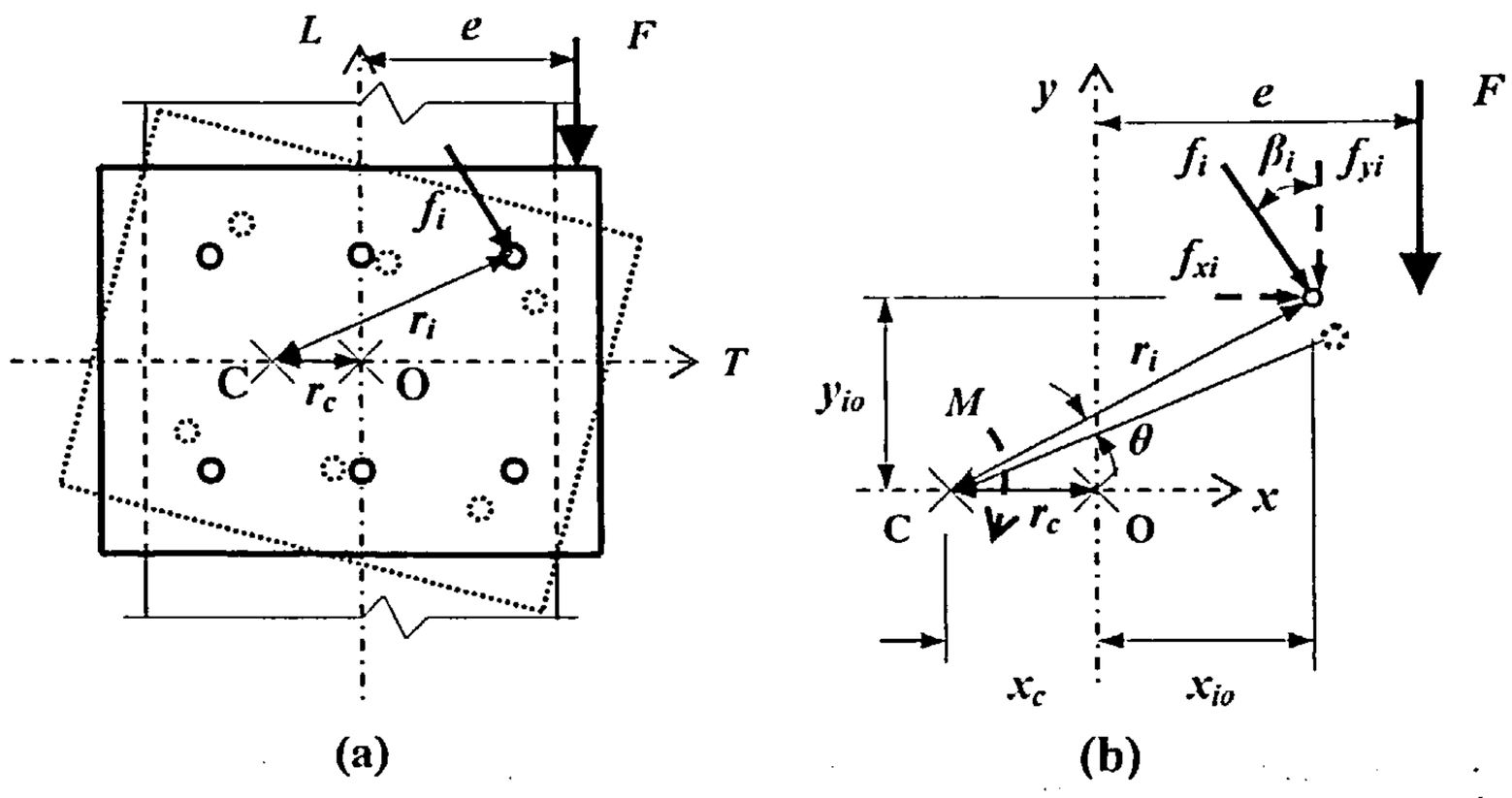

Figure 5.11 Moving nail position - Dotted line shows rotated position.

Consider the multi-nailed joint shown in Figure 5.11 where the behaviour and symbols remain as described in section 5.2.3.2. The joint is subjected to a shear force F at a distance e from the geometric centre of the nailing configuration O, and rotates by an amount θ about the centre of rotation C. The nails rotate to new positions (shown dotted on Figure 5.11(a)) and the displacement of nail i is shown in Figure 5.11(b) and enlarged on Figure 5.12. The force f_i on nail i is at an angle β_i to the vertical. Components of the force in nail i in the vertical and horizontal directions are f_{yi} and f_{xi} respectively.

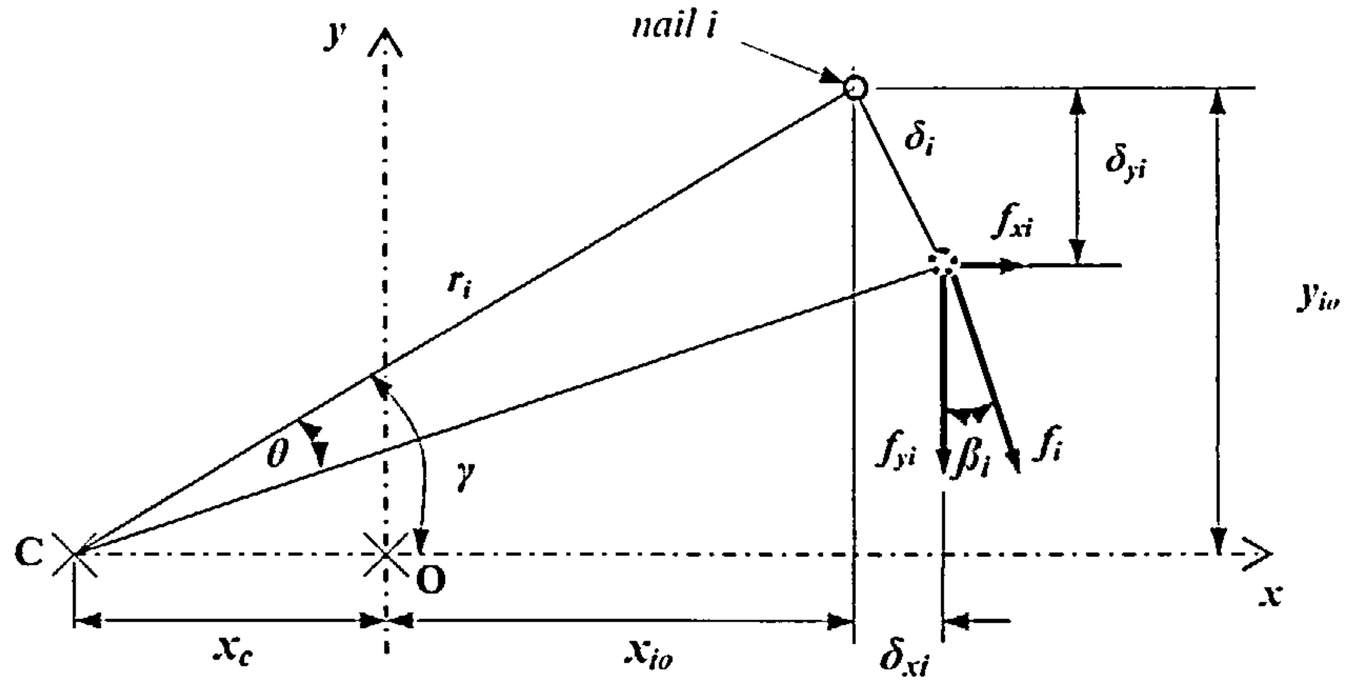

Figure 5.12 Displacement of nail i - (dotted circle shows displaced position)

The maximum nail displacement of the joint δ_{xmax}, is that associated with the nail at the greatest distance r_{max} from C. Expressing the rotation of the joint in terms of this displacement:

$$\theta = \frac{\delta_{x\max}}{r_{\max}} \qquad \ldots.(120)$$

The force in nail i can be expressed in terms of the maximum nail force f_{max} using equation (108). Assuming there are N nails in the joint, the vertical force F on the joint can be written as given in equation (115):

$$F = \frac{1}{(e - x_c)} \sum_{i=1}^{i=N} f(\delta x \max \frac{r_i}{r_{\max}})\left(((x_{io} - x_c)^2 + y_{io}{}^2)^{0.5}\right) \qquad \ldots.(115)$$

Resolving f_i into its horizontal and vertical components, these can be written in terms of the maximum nail force and the joint rotation:

$$f_{xi} = f(\delta x \max \frac{r_i}{r_{\max}}) \sin(\gamma - \theta) \qquad \ldots.(121)$$

$$f_{yi} = f(\delta x \max \frac{r_i}{r_{\max}}) \cos(\gamma - \theta) \qquad \ldots.(122)$$

where γ is the angle subtended by nail i about C before rotation.

The vertical force F can be written as the sum of the vertical components of the nail forces and using the expression for f_{yi} given in equation (122):

$$F = \sum_{i=1}^{i=N} f_{yi} = \sum_{i=1}^{i=N} f(\delta x \max \frac{r_i}{r_{\max}}) \cos(\gamma - \theta) \qquad \ldots.(123)$$

Equating equation (115) and (123) the unknown x_c can be found using the iteration approach referred to in section 5.2.2 and described in Appendix G. Having determined x_c the force F is obtained from (123) and the moment, M, in the joint can be written in terms of the force in the maximum loaded nail as given in equation (117):

$$M = \sum_{i=1}^{i=N} f(\delta x \max \frac{r_i}{r_{\max}}) r_i \qquad \ldots.(117)$$

where the functions are as described in section 5.2.2 and:

$f(\delta x \max \frac{r_i}{r_{\max}})$ = the value of the force in the nail i in terms of the force in maximum loaded nail - N.

γ = the angle of nail i subtended about C - degrees.

θ = the angle of joint rotation caused by displacement δ_{xmax} at the nail at radius r_{max} from C - degrees.

Applying equation (117) to joints with fully overlapping nails and taking the maximum nail load to be the appropriate value of $P_{\delta x}$ for joints with steel or plywood gusset plates given in equations (41), (43), (50), (86) and (92), the moment taken by the joint will be:

$$M_{\delta x} = \sum_{i=1}^{i=\frac{N}{2}} P(\delta x \max \frac{r_i}{r_{\max}})(r_i) \quad \ldots.(125)$$

The expression for $P(\delta x \max \frac{r_i}{r_{\max}})$ can be resolved into components in the plane of the T and L axes and the effects of loading relative to the grain direction applied in accordance with equation (93). For timber joints using fully overlapping nails with steel gusset plates or plywood gusset plates assembled with and without gaps between the gusset plates and the timber, moment equation (125) can then be written using the same equations as given in section 5.4.4.3.

5.2.3.4 Geometric Approach–(Non-Linear 4)

In this method nail forces are determined assuming a truss analogy and take into account the inelastic behaviour of the nails. The displacement of each nail is related linearly to the displacement of the highest loaded nail in the joint.

The method was developed by Nowak *et al* [107] for use with steel bolts and has been applied successfully to steel joints. In this approach the assumption is made that the applied load is directly transferred to the individual nails through the connection medium. Using a truss analogy, it is assumed that each nail is attached directly to the load by infinitely stiff truss members and the forces in the nails resist their share of the load through shear forces.

Consider the joint shown in Figure 5.13. The centroid of the nail group is taken as the point of origin for a Cartesian co-ordinate system x , y and the nails are located using the co-ordinate system as shown in Figure 5.14.

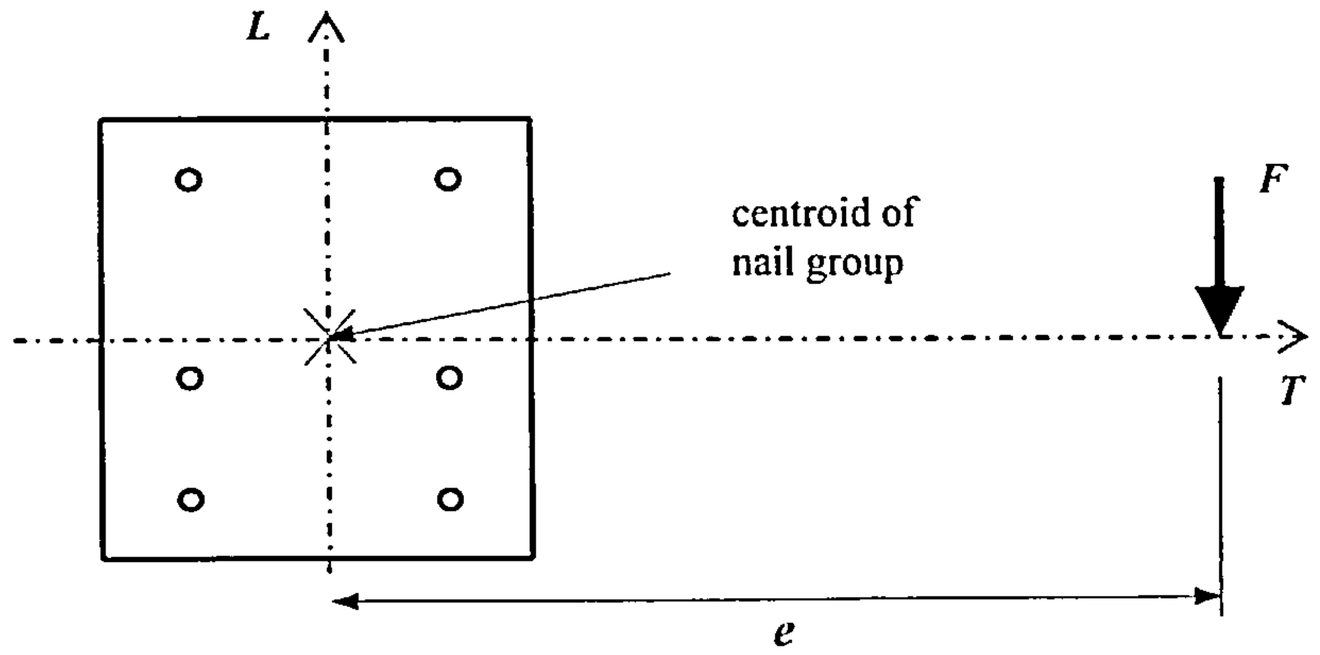

Figure 5.13 Joint subjected to a shear force F at eccentricity e.

The assumptions made in the geometric method are:

a) Point C is located at the intersection of the load and a line perpendicular to it through the centroid of the connection. The direction of the force f_i on any nail i acts through point C and has a vertical component f_{yi} and a horizontal component f_{xi} that resists the applied load.

b) The deformation of a nail is proportional to its distance from point C. The nail furthest from C has the greatest deformation δ_{xmax} and the others are proportional to the ratio of their distance to l_{max} such that for nail i, $\delta_i = \delta_{xmax}(\frac{l_i}{l_{\max}})$.

c) The force in each nail is a function of its deformation.

d) The equations of equilibrium of the forces and moments in the joint must be satisfied.

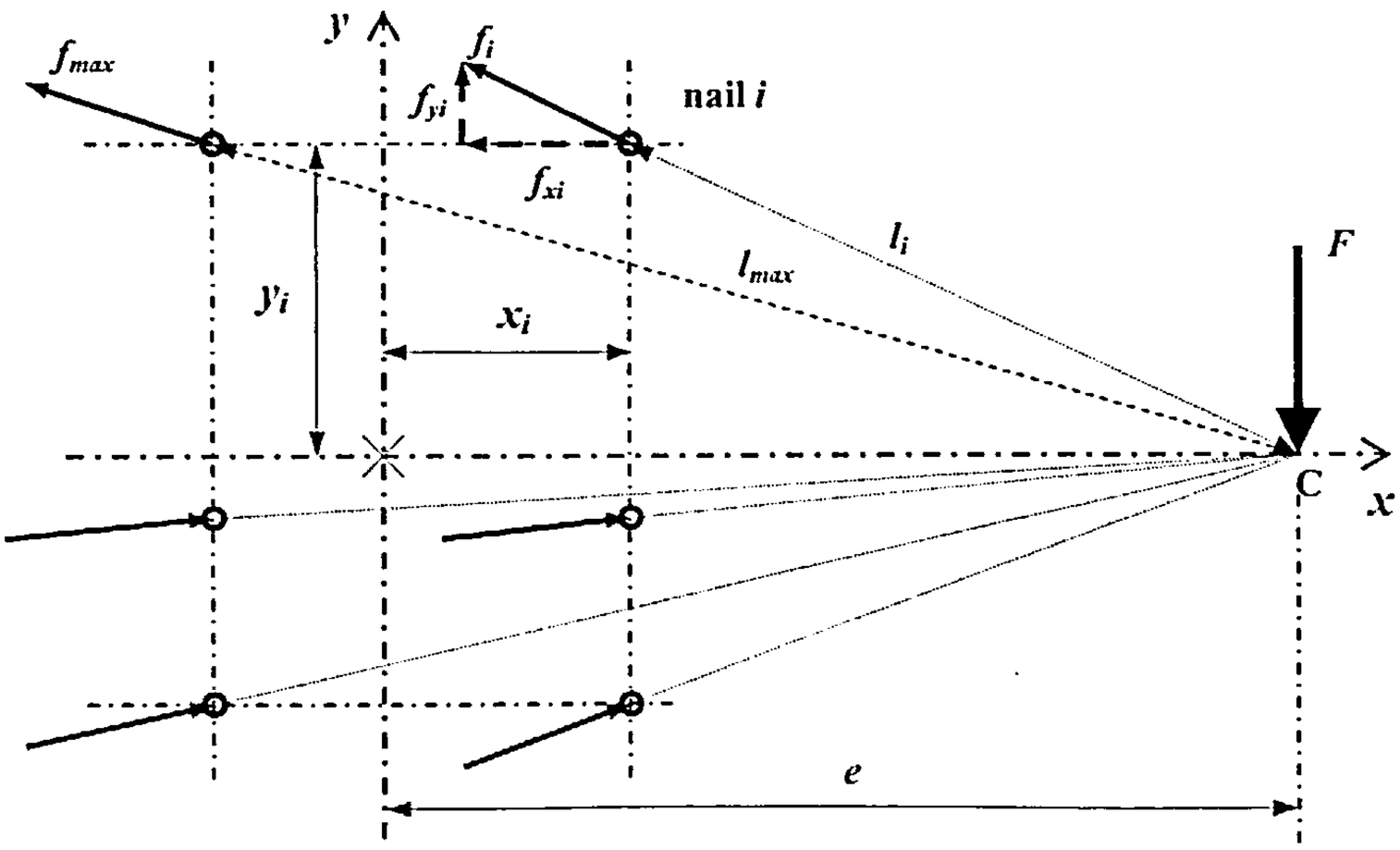

Figure 5.14 Basics of geometric method

Based on the above assumptions:

$$f_{yi} = f_i\left(\frac{|y_i|}{l_i}\right) \quad \text{....(126)}$$

and $$f_{xi} = -f_i\left(\frac{e-x_i}{l_i}\right) \quad \text{if } y_i>0 \quad \text{....(127)}$$

or, $$= f_i\left(\frac{e-x_i}{l_i}\right) \quad \text{if } y_i<0 \quad \text{....(128)}$$

where x_i and y_i are the co-ordinate distances of the nail. The negative sign in equation (127) is based on the Cartesian sign convention of the direction of the force due to assumption a).

The conditions of equilibrium dictate that the horizontal force components will sum to zero and the sum of the vertical components will equate to the vertical force on the joint, F. Due to assumption a), where all of the forces pass through point C the sum of the moments will also be zero. On this basis, with N nails in the joint the vertical force taken by the joint will be:

$$F = \sum_{i=1}^{i=N} f_{yi} = \sum_{i=1}^{i=N} f_i\left(\frac{|y_i|}{l_i}\right) \quad \text{....(129)}$$

The force in each nail, f_i, is determined using the relationship $\delta_i = \delta_{max}\left(\frac{l_i}{l_{\max}}\right)$ and the moment will be:

$$M = \sum_{i=1}^{i=N} f\left(\delta x \max \frac{l_i}{l_{\max}}\right)\left(\frac{|y_i|}{l_i}\right) e \quad \text{....(130)}$$

Applying equation (130) to joints with fully overlapping nails and taking the maximum nail load to be the appropriate value of $P_{\delta x}$ for joints with steel or plywood gusset plates given in equations (41), (43), (50), (86) and (92), the moment taken by the joint will be:

$$M_{\delta x} = \sum_{i=1}^{i=\frac{N}{2}} P\left(\delta x \max \frac{l_i}{l_{\max}}\right)\left(\frac{|y_i|}{l_i}\right) e \quad \text{....(131)}$$

The expression for $P\left(\delta x \max \frac{l_i}{l_{\max}}\right)$ can be resolved into components in the plane of the T and L axes and the effects of loading relative to the grain direction applied in accordance with equation (93). For timber joints using fully overlapping nails with steel gusset plates or plywood gusset plates assembled with and with a gap between the gusset plates and the timber, moment equation (131) can then be written as given in equations (132a) to (132d). The symbols used in these equations will be as given in equations 41, 43, 50, 86 and 92 and as given below.

(i) Joints with steel gusset plates and predrilled holes less than 1.1 times the nail diameter, assembled with a gap between the gusset plates and the timber:

(a) where the nail row spacing is between $0.7\times2\times5\times d$ and $0.7\times4\times7\times d$:

$$M_{\delta x} = \sum_{i=1}^{i=\frac{N}{2}} (1-e^{-1.712\delta x max}\frac{l_i}{l_{\max}})^{0.926}(0.1\delta_{x max}\frac{l_i}{l_{\max}} + 0.68)(\frac{|y_i|}{l_i})e\frac{S_{GS}S_G}{S_{GS}\sin^2\beta_i + S_G\cos^2\beta_i} \quad \ldots.(132a)$$

(b) where the nail row spacing is greater than $0.7\times4\times7\times d$:

$$M_{\delta x} = S_G \sum_{i=1}^{i=\frac{N}{2}} (1-e^{-1.712\delta x max}\frac{l_i}{l_{\max}})^{0.926}(0.1\delta_{x max}\frac{l_i}{l_{\max}} + 0.68)(\frac{|y_i|}{l_i})e \quad \ldots.(132b)$$

where the functions are as described in equation (41) and section 5.2.2 and:

l_{max} = the distance of the furthest pair of fully overlapping nails from C– mm.

l_i = the distance of nail i from C – mm.

δ_{xmax} = the slip of the nail at distance $l_{max.}$-mm.

$|y_i|$ = is the absolute value of the y co-ordinate of nail I – mm.

(ii) Joints with plywood gusset plates assembled with a gap between the gusset plates and the timber:

(a) where the nail row spacing is between $0.85\times2\times5\times d$ and $0.85\times4\times5\times d$:

$$M\delta x = \sum_{i=1}^{i=\frac{N}{2}} (1-e^{-1.719\delta x max}\frac{l_i}{l_{\max}})^{0.568}(0.1\delta x max\frac{l_i}{l_{\max}} + 0.68)(\frac{|y_i|}{l_i})e\frac{P_{GS}P_G}{P_{GS}\sin^2\beta_i + P_G\cos^2\beta_i} \quad \ldots(132c)$$

(b) where the nail row spacing is greater than $0.85\times4\times5\times d$:

$$M_{\delta x} = P_G \sum_{i=1}^{i=\frac{N}{2}} (1-e^{-1.719\delta x max}\frac{l_i}{l_{\max}})^{0.568}(0.1\delta x max\frac{l_i}{l_{\max}} + 0.68)(\frac{|y_i|}{l_i})e \quad \ldots.(132d)$$

where the functions are as described in equation (86) and (i)(b).

It is to be noted that when the eccentricity is within the nailing zone or is very far from it, the use of the truss analogy approach is unrealistic and the theory has to be modified.

5.3 PROCESSING OF MOMENT TEST DATA

In the test set-up the displacement transducers were securely fixed to the gusset plates and to minimise any movement due to gusset plate deformation the plates were made larger and stiffer than was required to meet the minimum joint strength criteria. This ensured the transducers were held in a rigid manner and effectively all of the movement being recorded was due to rotation of the nails; embedment of the timber and plywood and possible deformation of the timber.

As a joint is loaded the timber member rotates relative to the gusset plates and the transducers record the movement of the timber face, not the movement of the nails in the joint. Also, because the transducers are fixed to the gusset plates, only movement in the line of the transducers is recorded. The transducer readings have to be processed to obtain the movement of the nail furthest from the centre of rotation in the joint. And the nail movement being referred to is the movement at right angles to the direction of the line between the extreme nail and the centre of rotation.

The processing procedure used in the programme is given for the case where transducers are fitted to record vertical movements, having been set up to read on the top horizontal face of the joint timber as shown in Figure 5.15. The Figure shows a generalised layout of the transducers relative to the timber and the nailing configuration in a joint.

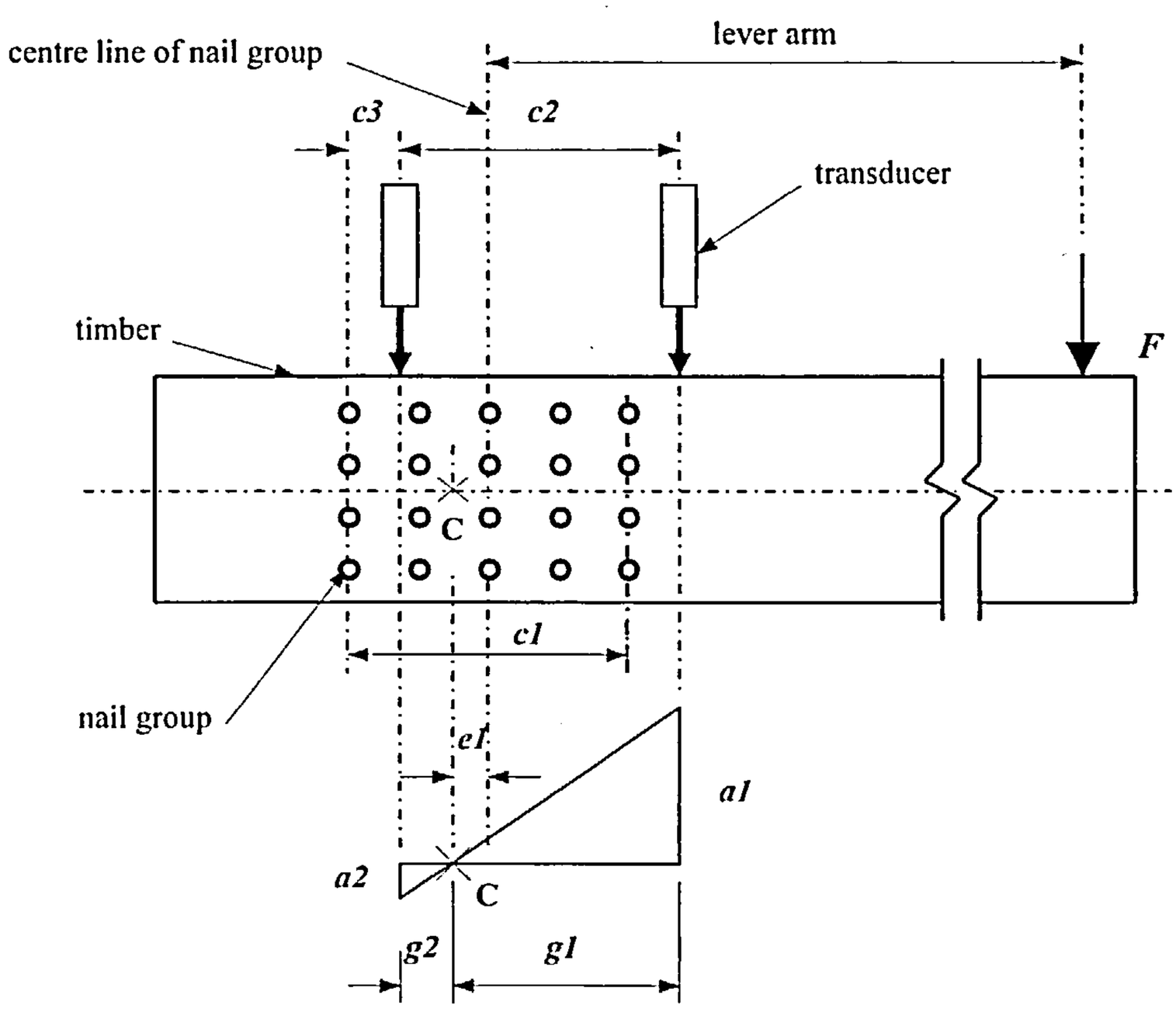

Figure 5.15 Transducer arrangement relative to nail group

where;

a1 = the reading on the transducer closest to the applied load *F* (for this set-up this transducer will record the maximum movement).

a2 = the reading on the transducer furthest from the applied load *F* (for this set-up this transducer will record the minimum movement).

c1 = horizontal distance between the extreme nail positions.

c2 = horizontal distance between the centre lines of the transducers.

c3 = horizontal distance between the transducer furthest from *F* and the adjacent end line of nails.

The centre of rotation of the joint *C*, will be at the position where the line joining the transducer readings crosses the horizontal as shown on Figure 5.15. It is to be noted that the position of *C* will change as the moment is increased and the one to be used in the analysis is the position when the extreme nail in the joint has been moved by the maximum slip $\delta_{xmax.}$

From the geometry of the transducer set-up the distance between the centre of rotation and the position of the lower reading transducer will be :

$$g2 = \frac{c2}{(1+\frac{a1}{a2})} \qquad \ldots.(133)$$

As the timber in the joint rotates the relationship between the transducer with the maximum reading; the position of the nail at the maximum distance from *C* and the geometry of the set-up will be as shown in Figure 5.16.

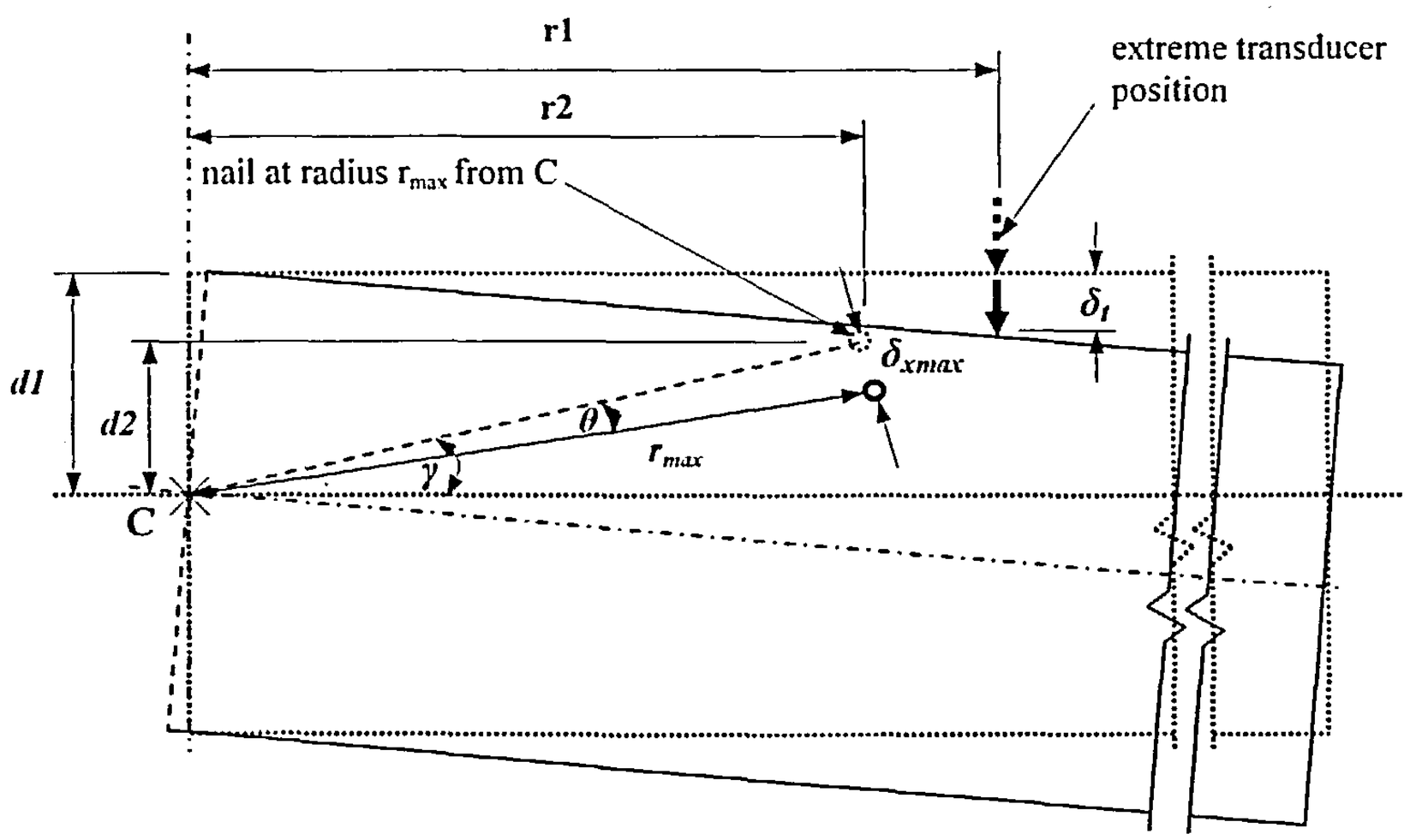

Figure 5.16 The movement of the extreme nail and the transducer with the maximum reading. (original position is shown dotted)

The joint will be rotated until the nail with the greatest radius r_{max} from C has moved by the maximum slip. During the rotation, the transducer remains in its vertical aspect and records the **vertical** movement of the timber δ_t, not the movement of the nail. To obtain the movement at the nail a multiplication factor, *mf*, has to be applied to the transducer reading such that:

$$mf\,\delta_t = \delta_{xmax} \qquad \ldots.(134)$$

Using the geometry of the joint at the position when the extreme nail has been displaced by $\delta_{\delta max}$, it can be shown that *mf* is:

$$mf = \frac{[(r2-(r2^2+d2^2)^{0.5}\cos(\theta+\gamma))^2+((r2^2+d2^2)^{0.5}\sin(\theta+\gamma)-d2)^2]^{0.5}}{[(r1+d1\sin(\theta))\tan(\theta)-(d1-d1(\cos(\theta))]} \qquad \ldots.(135)$$

where the symbols represent:

r1 = horizontal distance from the centre of rotation to the transducer closest to the applied load – mm.

r2 = horizontal distance from the centre of rotation to the nail at the greatest distance from the centre of rotation – mm.

d1 = the vertical distance between the horizontal axis through *C* and the top face of the timber in the joint – mm.

d2 = the vertical distance between the horizontal axis through *C* and the position of maximum loaded nail – mm.

θ = the angle of rotation of the joint about *C*.

γ = the angle subtended at *C* by the horizontal axis and the maximum loaded nail.

At the start of the processing procedure the position of the centre of rotation is unknown and an approximate value has to be assumed. Using equation (133) and adjusting the angle of the joint rotation until equation (134) equals 3.2mm, an iteration process is set up. After two to three iterations at most the correct position of the centre of rotation will be found. The multiplying factor *mf* is then applied to the readings from the transducer closest to the force allowing the load in the nail to be obtained at δ_{xmax}. Although the procedure has been explained using transducers fitted to read vertically, the same process will apply to joints where the transducers are fitted to read horizontally.

5.4 COMPARISON OF SEMI-EMPIRICAL MODEL AND TEST RESULTS

The model solutions are compared against the test results of joints that used plywood and steel gusset plates assembled with a gap between the gusset plates and the timber. The steel gusset plates were predrilled using drills less than 1.1 times the nail diameter. The analyses assume the highest loaded nail in the joint has been displaced by 3.2mm. Also, to obtain a more realistic assessment of the validity of the models the comparison has been undertaken using the results of single tests rather than the average

of test sets. Comparison with joints made with 19mm plywood gusset plates is given in Table 5.1 and joints with 12mm/9mm plywood gusset plates is given in Table 5.2. Joints made with steel gusset plates are compared in Table 5.3. Validation of the models was primarily against joints with plywood gusset plates, using a variety of nailing configurations. The model results were also compared against joints made with steel gusset plates to confirm the application of the theory. Only one nailing configuration was used.

The Tables give the moment in the joint when the most highly loaded nail has been displaced by 3.2mm. Nail slip has been used as the monitoring function rather than angular rotation as the latter will vary between joint configurations whereas the former does not. A summary of the joint rotations of some of the nailing configurations used in the programme is given in Table 5.4. Two values are given. One is based on rotation about the centroid of the nailing configuration and the other on the use of a variable centre of rotation obtained from an analysis of the transducer readings. As stated earlier, the rotation varies with the joint configuration and it is to be noted that the variation can be quite significant depending on the nailing configuration being used. Test and model results for joints in which the plane of the grain in the timber is parallel to the timber face are given in Tables 5.1 to 5.3. Joints in which the plane of the grain in the timber is at an angle to the timber face are compared in Table 5.8. The majority of the testing used timber where the grain was essentially parallel to the face and these results are discussed in section 5.4.1. The results using timber with its grain at varying angles to the face are discussed in section 5.4.2.

Only those test results in which no flexural movement of the timber was recorded across the length of the joint have been included in the Tables. This is because the model theory used has been developed on the premise that all joint movement is solely due to nail flexure and bearing failure of the timber and/or the plywood gussets plates

A summary of the percentage difference between the test and model results is given in Tables 5.4 to 5.7, and also in Table 5.8. Negative signs indicate an underestimation and positive signs indicate an overestimation by the model being referred to.

5.4.1 Results Using Timber with the Plane of the Grain Parallel to the Face of the Joint

The Secant Stiffness models are essentially elastic models assuming the load-displacement behaviour of the nails is linear. These models should and do underestimate the moment capacity of the joint. The Non-Linear models take the load-displacement behaviour of the nails into account and in the case of the Non-Linear 3 model, second order effects arising from the modelling of the nail movement in the joint are also included. A model was also developed to include for the effect of shear force on the centre of rotation but as it showed that the effect on joint capacity was less than 0.1%, it has not been incorporated into the analyses. In general the model solutions fluctuate above and below the test results.

The least amount of fluctuation is obtained from the Secant Stiffness models as these give the more conservative results. These models predicted capacities which were within 4% to 7% of each other and both gave a mixture of results when compared with the tests. For joints with two lines of nails the results are reasonably close to the test values. However, as the number of lines is increased these models become less accurate and, in the case of Secant Stiffness model 2, with 5 lines of nails it is 18.2% below the test result. In general it can be concluded that these models will underestimate the moment capacity of the joint and the amount of underestimation will increase as the number of lines of nails in the joint increases

With the exception of the Non-Linear 4 model, the non-linear models give the most consistent comparison and the best overall approximation to the test results. The Non-Linear 4 model gives a poor fit because it ignores the effect of nails lying on the x-axis and the majority of the nailing configurations used in the tests had this feature. The extreme case is joint RO where all of the nails are on the *x*-axis and the model cannot be used as it will predict a zero moment capacity. It is not a method that can be recommended for general use. Of the three remaining Non Linear models, where a fixed centre of rotation has been used the model will predict a greater capacity than one using a variable centre approach. This is seen from an inspection of the results in Tables 5.1 to 5.3. Model Non-Linear 1 has a fixed centre of rotation and the results exceed Non-Linear models 2 and 3. However, if a joint is subjected to a pure moment, the centre of rotation will not vary and model Non-Linear 1 will give the best theoretical solution. For joints that are subjected to moment by a shear force, Non-Linear 3 is theoretically the most accurate of the non-linear models. In addition to including for the effect of the movement of the centre of rotation as loading increases, it also includes for the effect of the movement of the nails on the geometry of the joint. However, it is to be noted that with this method the results only vary by less than 1% from those obtained using Non-Linear 2. On this basis it is considered that the additional modelling and computational effort involved in the use of model Non-Linear 3 cannot be justified.

The model recommended for use is Non-Linear 2. With this method the majority of the results were within $\pm$ 5% of the test values with a few cases where there was an exceedance beyond this limit. The greatest overestimate was 8.36% for the plywood gusset joints and 4.34% for the steel gusset joints and the maximum underestimates were 6.97% and 6.85% respectively. Overall the comparison was very good.

The load-deformation behaviour of a sample of the tests compared with the results calculated using model Non-Linear2 have been plotted together for comparison and are presented in Figures 5.17 to 5.19. In the figures the model result is shown as a dotted line.

Test Ref.	Nailing conf'n	Nail Ø mm	No of nails in joint	Timber density kg/m^3	Plywood density kg/m^3	Plywood thickness mm	Lever arm mm	Experiment moment kNm	Secant stiffness 1 kNm	Secant stiffness 2 kNm	Non-linear 1 kNm	Non-linear 2 kNm	Non-linear 3 kNm	Non-linear 4 kNm
P1	RA	3.01	32	647.03	620.36	17.69	517	1.77663	1.548	1.478	1.833	1.792	1.804	1.285
P2	RA	3.33	32	550.00	624.23	17.60	513	1.77148	1.564	1.493	1.852	1.810	1.823	1.300
P3	RS	2.66	32	607.73	644.59	17.53	489	1.73317	1.596	1.480	1.861	1.828	1.836	1.030
P4	RS	3.01	32	591.83	651.62	17.85	489	2.23337	1.976	1.833	2.306	2.265	2.275	1.279
P5	RS	3.33	32	598.15	681.79	17.65	489	2.40208	2.158	2.002	2.518	2.474	2.485	1.399
P6	RB	3.01	40	567.44	653.68	17.53	433.5	2.45243	2.120	2.006	2.532	2.499	2.512	1.583
P7	RK	3.01	56	594.42	606.92	17.64	510	2.5373	2.334	2.161	2.740	2.710	2.727	1.850
P8	RK	3.33	56	608.63	614.25	17.61	510	2.70547	2.481	2.303	2.921	2.889	2.908	1.970
P9	RM	3.01	24	557.02	611.51	17.67	460	2.55114	2.595	2.433	2.667	2.536	2.541	0.6356
P10	RN	3.01	12	568.64	611.51	17.67	426.7	1.27891	1.305	1.255	1.309	1.227	1.227	1.415
P11	RO	3.01	4	583.74	627.21	17.77	460	0.46042	0.4993	0.49885	0.4991	0.46503	0.46479	Not relevant
P12	RP	3.01	28	583.74	627.21	17.61	426.7	3.1855	3.130	2.952	3.254	3.121	3.128	0.8808
P13	RQ	3.01	16	580.91	636.40	17.69	460	1.69335	1.805	1.709	1.821	1.713	1.715	0.2931
P14	RR	3.01	20	574.16	639.17	17.66	426.7	2.16253	2.255	2.134	2.294	2.173	2.176	0.4414

Table 5.1 Summary of the results of the moment taken by joints constructed with19mm plywood gusset plates when the highest loaded nail moves by 3,2mm.

Test ref	Nailing conf'n	Nail Ø mm	No of nails in joint	Timber density kg/m^3	Plywood density kg/m^3	Plywood thickness mm	Lever arm mm	Experiment moment kNm	Secant stiffness 1 kNm	Secant stiffness 2 kNm	Non-linear 1 kNm	Non-linear 2 kNm	Non-linear 3 kNm	Non-linear 4 kNm
P15	RA	3.01	32	551.45	563.17	11.15	513	1.213	1.131	1.079	1.325	1.309	1.318	0.9386
P16	RA	2.66	32	567.96	635.19	11.52	513	1.10187	1.032	0.98472	1.208	1.194	1.202	0.8551
P17	RB	3.01	40	558.19	705.53	11.47	495	2.18295	1.841	1.751	2.198	2.170	2.181	0.954
P18	RS	3.33	32	537.25	497.94	11.18	489	1.50946	1.301	1.207	1.518	1.491	1.498	0.8431
P19	RS	2.66	32	539.41	534.92	11.13	489	1.3068	1.130	1.048	1.318	1.294	1.300	0.7296
P20	RS	2.66	32	549.69	536.17	7.36	489	1.08578	0.9591	0.88945	1.119	1.099	1.104	0.6194
P21	RA	3.33	32	546.38	675.50	9.75	513	1.42832	1.219	1.164	1.429	1.412	1.421	1.014
P22	RS	3.01	32	534.24	551.45	7.33	489	1.33451	1.143	1.060	1.334	1.310	1.316	0.7397
P23	RS	3.33	32	510.99	546.70	7.55	489	1.34586	1.092	1.013	1.275	1.252	1.258	0.7081

Table 5.2 Summary of the results of the moment taken by joints constructed with12mm and 9mm plywood gusset plates when the highest loaded nail moves by 3.2mm.

Test ref	Nailing conf'n	Nail Ø mm	No of nails in joint	Timber density kg/m^3	Moisture content of timber %	Lever arm mm	Experiment moment kNm	Secant stiffness 1 kNm	Secant stiffness 2 kNm	Non-linear 1 kNm	Non-linear 2 kNm	Non-linear 3 kNm	Nin-linear 4 kNm
S1	RA	2.66	32	480.93	11.06	525	1.90425	1.566	1.497	1.816	1.791	1.805	1.309
S2	RA	2.66	32	485.42	11.00	525	1.92313	1.583	1.513	1.836	1.810	1.825	1.323
S3	RA	2.66	32	504.31	11.01	525	2.01819	1.644	1.572	1.907	1.880	1.895	1.375
S4	RA	2.66	32	506.89	11.01	525	2.01582	1.653	1.580	1.917	1.890	1.905	1.382
S5	RA	3.01	32	568.24	11.06	525	2.37022	2.094	2.001	2.428	2.394	2.413	1.754
S6	RA	3.01	32	577.64	11.07	525	2.3734	2.128	2.034	2.467	2.433	2.452	1.782
S7	RA	3.01	32	565.29	11.12	525	2.282	2.080	1.988	2.412	2.378	2.397	1.742
S8	RA	3.01	32	569.26	11.08	525	2.29722	2.096	2.004	2.431	2.397	2.416	1.756
S9	RA	3.36	32	504.65	11.01	525	2.61062	2.332	2.229	2.705	2.667	2.688	1.957
S10	RA	3.36	32	493.24	11.01	525	2.62596	2.280	2.179	2.644	2.607	2.627	1.913
S11	RA	3.36	32	486.56	11.00	525	2.66418	2.249	2.150	2.608	2.572	2.592	1.888

Table 5.3 Summary of the results of the moment taken by joints constructed with 6mm thick steel gusset plates when the highest loaded nail moves by 3.2mm

Joint configuration	a -Joint rotation about centroid of nail group – radians	b - Joint rotation about centre of rotation based on transducer readings – radians	% Difference between rotations (a-b)/a
RA	0.04526	0.04315	4.66
RB	0.0384	0.03678	4.22
RC	0.03292	0.02966	9.93
RF	0.02862	0.02437	14.84
RG	0.03157	0.02352	25.50
RH	0.04657	0.03935	15.50
RI	0.03036	0.02508	17.39
RK	0.04526	0.04348	3.93
RM	0.02954	0.01927	34.77
RN	0.03157	0.01973	37.50
RO	0.032	0.01632	49.01
RP	0.02862	0.02036	28.87
RQ	0.03105	0.01945	37.35
RR	0.03036	0.02016	33.61
RS	0.0355	0.03153	11.18

Table 5.4 Joint Rotation in radians when the highest loaded nail in the joint is displaced by 3.2mm.

Test ref	Nailing pattern	Nail Ø	Secant stiffness1	Secant stiffness2	Non-linear1	Non-linear2	Non-linear3	Non-linear4
P1	RA	3.01	-12.87	-16.81	+3.17	+0.87	+1.54	-27.67
P2	RA	3.33	-11.71	-15.72	+4.55	+2.17	+2.91	-26.62
P3	RS	2.66	-7.91	-14.61	+7.38	+5.47	+5.93	-40.57
P4	RS	3.01	-11.52	-17.93	+3.25	+1.42	+1.86	-42.73
P5	RS	3.33	-10.16	-16.66	+4.83	+2.99	+3.45	-41.76
P6	RB	3.01	-13.56	-18.20	+3.24	+1.90	+2.43	-35.45
P7	RK	3.01	-8.01	-14.83	+7.99	+6.81	+7.48	-27.09
P8	RK	3.33	-8.30	-14.88	+7.97	+6.78	+7.49	-27.18
P9	RM	3.01	+1.72	-4.63	+4.54	-0.59	-0.4	-75.09
P10	RN	3.01	+1.33	-2.56	+1.64	-4.73	-4.73	+9.87
P11	RO	3.01	+8.44	+8.35	+8.40	+1.00	+0.95	Not relevant
P12	RP	3.01	-1.74	-7.33	+2.15	-2.02	-1.81	-72.35
P13	RQ	3.01	+6.59	+0.92	+7.54	+1.16	+1.28	-82.69
P14	RR	3.01	+4.28	-1.32	+6.08	+0.48	+0.62	-79.59

Table 5.5 Percentage difference between test and model results - 19mm plywood gusset joints

Test ref	Nailing pattern	Nail Ø	Secant stiffness1	Secant stiffness2	Non-linear1	Non-Linear2	Non-linear3	Non-linear4
P15	RA	3.01	-6.76	-11.05	+9.23	+7.91	+8.66	-22.62
P16	RA	2.66	-6.34	-10.63	+9.63	+8.36	+9.09	-22.40
P17	RB	3.01	-15.66	-19.79	+0.69	-0.59	-0.09	-56.30
P18	RS	3.33	-13.81	-20.04	+0.57	-1.22	-0.76	-44.15
P19	RS	2.66	-13.53	-19.80	+0.86	-0.98	-0.52	-44.17
P20	RS	2.66	-11.67	-18.08	+3.06	+1.22	-1.68	-42.95
P21	RA	3.33	-14.65	-18.51	+0.05	-1.14	-0.51	-29.01
P22	RS	3.01	-14.35	-20.57	-0.04	-1.84	-1.39	-44.57
P23	RS	3.33	-18.86	-24.73	-5.27	-6.97	-6.53	-47.39

Table 5.6 Percentage difference between test and model results - 12mm and 9mm plywood gusset joints

Test ref	Nailing pattern	Nail Ø	Secant stiffness1	Secant stiffness2	Non-linear1	Non-linear2	Non-linear3	Non-linear4
S1	RA	2.66	-17.76	-21.39	-4.63	-5.95	-5.21	-31.26
S2	RA	2.66	-17.69	-21.33	-4.53	-5.88	-5.10	-31.21
S3	RA	2.66	-18.54	-22.11	-5.51	-6.85	-6.10	-31.87
S4	RA	2.66	18.00	-21.62	-5.90	-6.24	-5.50	-31.44
S5	RA	3.01	-11.65	-15.58	+2.44	+1.00	+1.80	-26.00
S6	RA	3.01	-10.34	-14.30	+3.94	+2.51	+3.31	-24.92
S7	RA	3.01	-8.85	-12.88	+5.70	+4.21	+5.04	-23.66
S8	RA	3.01	-8.76	-12.76	+5.82	+4.34	+5.17	-23.56
S9	RA	3.36	-10.67	-14.62	+3.62	+2.16	+2.96	-25.04
S10	RA	3.36	-13.17	-17.02	+0.69	-0.72	+0.04	-27.15
S11	RA	3.36	-15.58	-19.30	-2.11	-3.46	-2.71	-29.13

Table 5.7 Percentage difference between test and model results – 6mm steel gusset joint

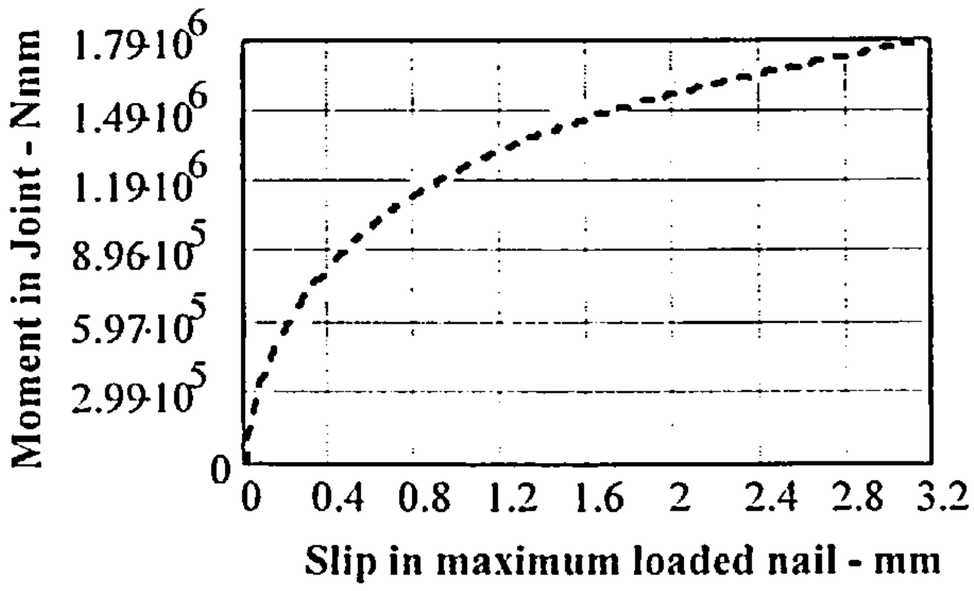

Nailing configuration RA-Joint P1

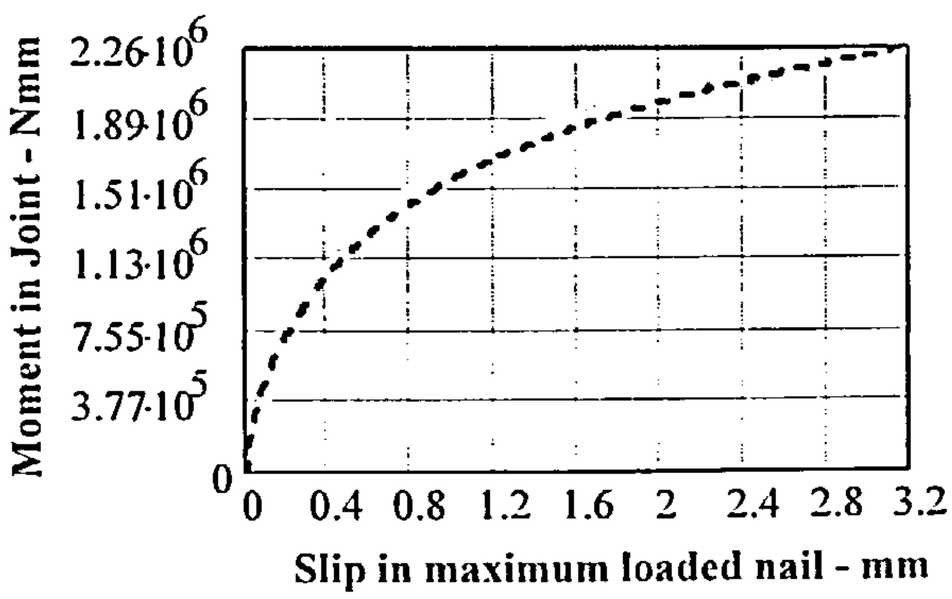

Nailing configuration RS-Joint P4

Figure 5.17 Comparison of model NL2 and test results of joints made with 19mm thick plywood gusset plates when maximum loaded nail is displaced by up to 3.2mm.

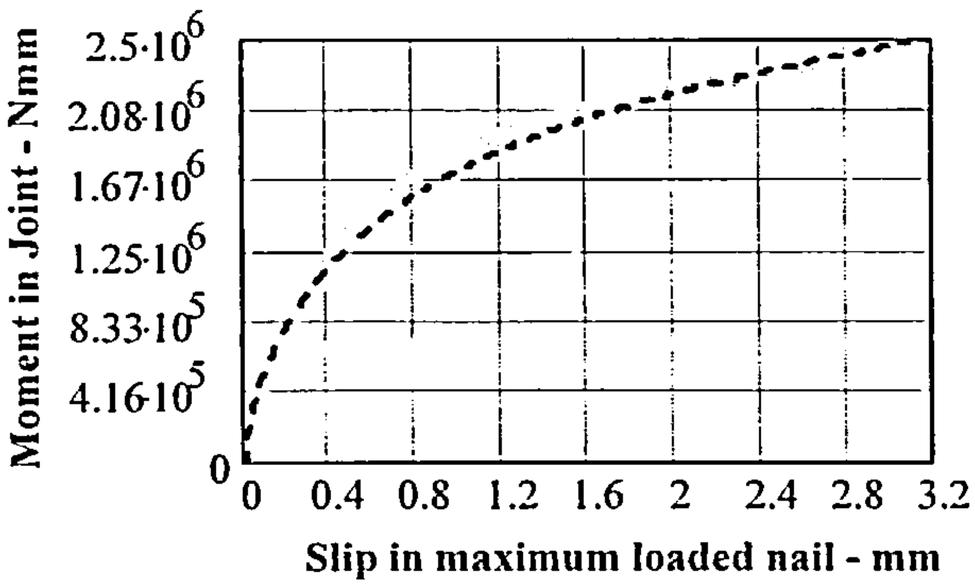

Nailing configuration RB- Joint P6

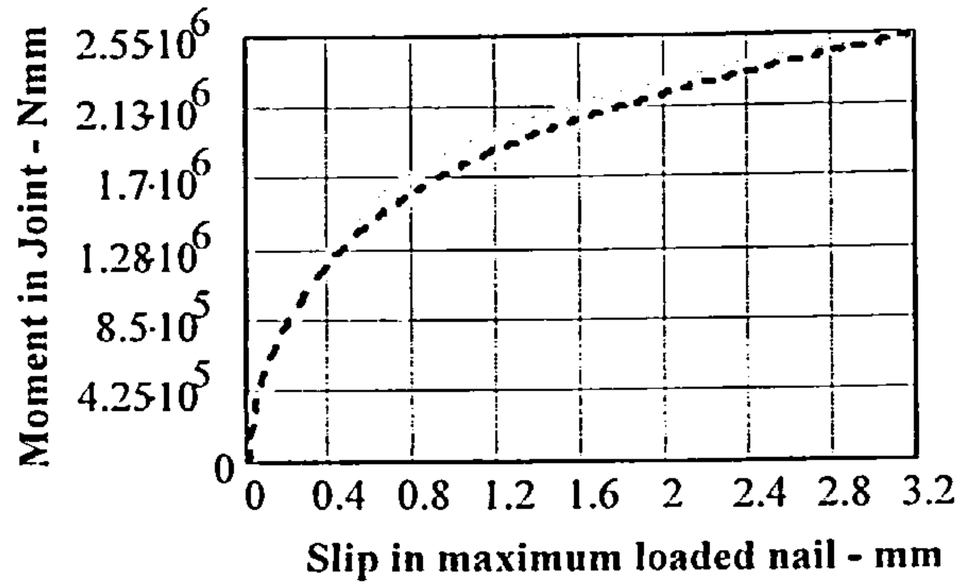

Nailing configuration RM-Joint P9

Figure 5.17 cont'd Comparison of model NL2 and test results of joints made with 19mm thick plywood gusset plates when maximum loaded nail is displaced by up to 3.2mm.

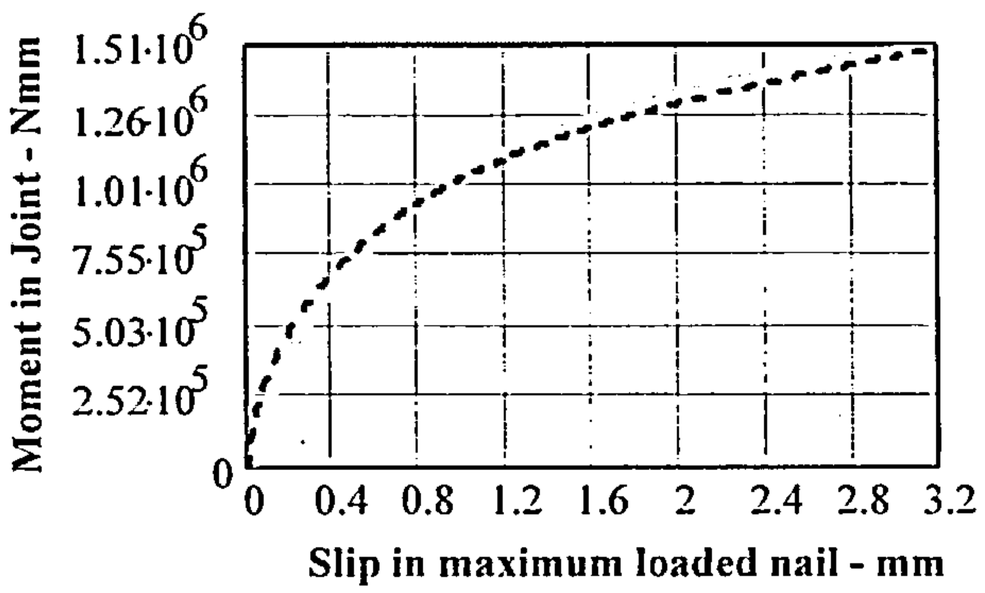

Nailing configuration RS-Joint P18

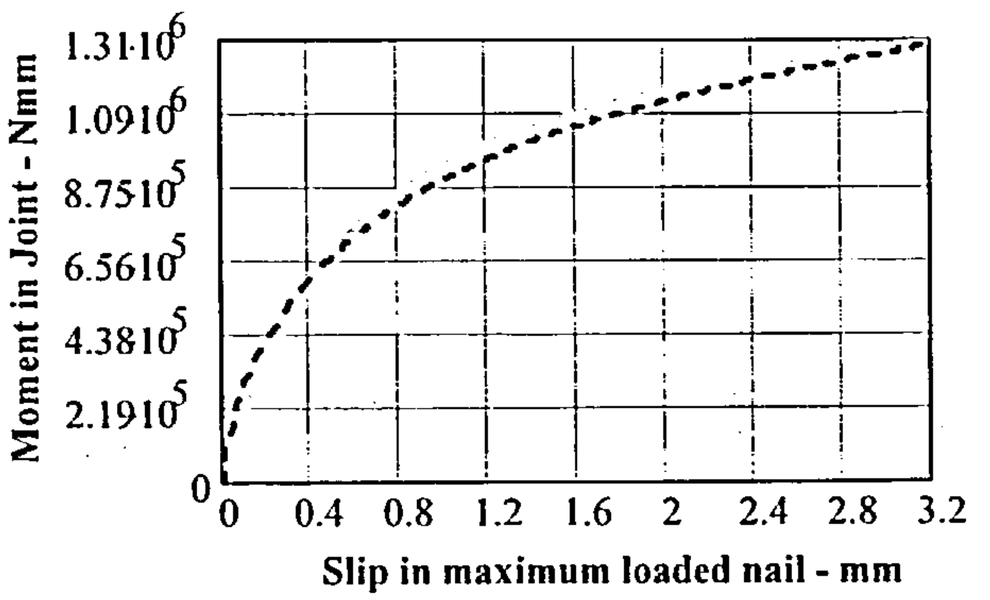

Nailing configuration RS-Joint P19

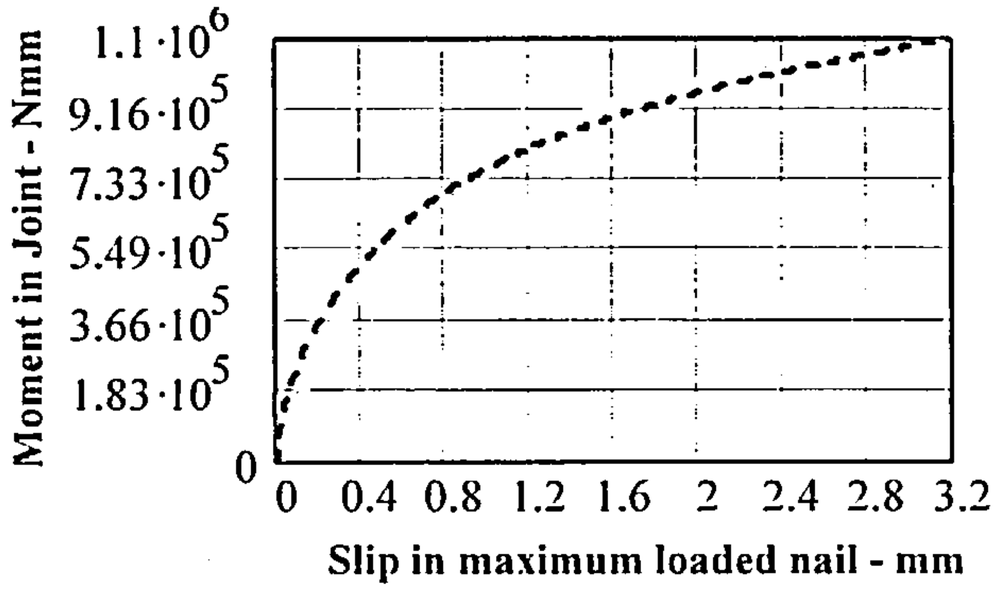

Nailing configuration RS-Joint P20

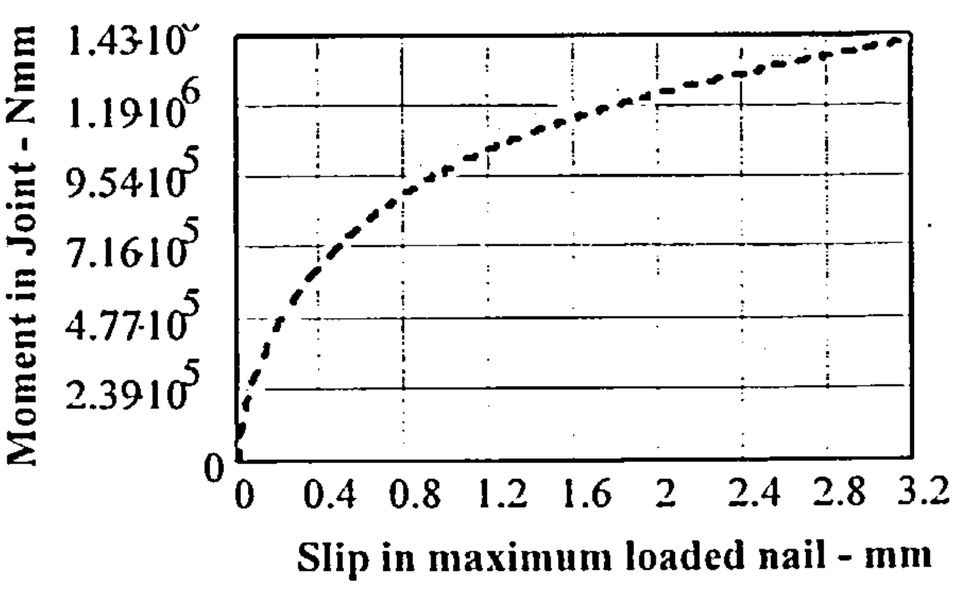

Nailing configuration RA-Joint P21

Figure 5.18 Comparison of model NL2 and test results of joints made with 9mm and 12mm thick plywood gusset plates when maximum loaded nail is displaced by up to 3.2mm.

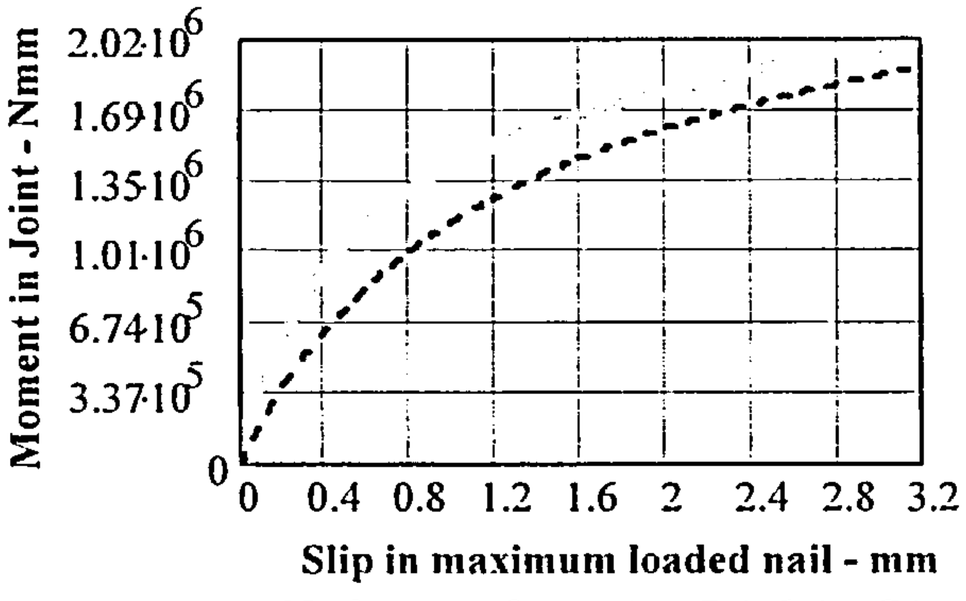

Nailing configuration RA-Joint S4

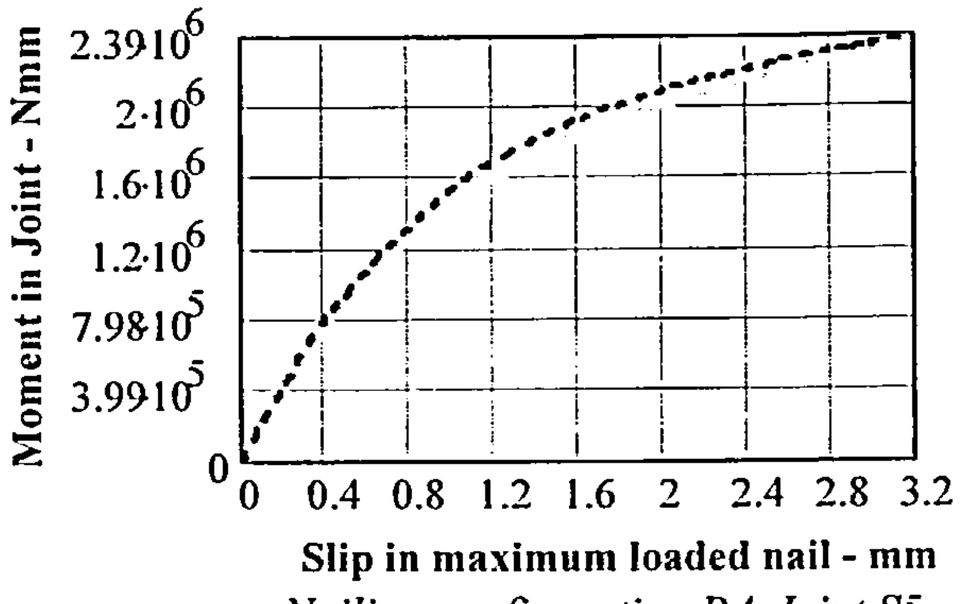

Nailing configuration RA-Joint S5

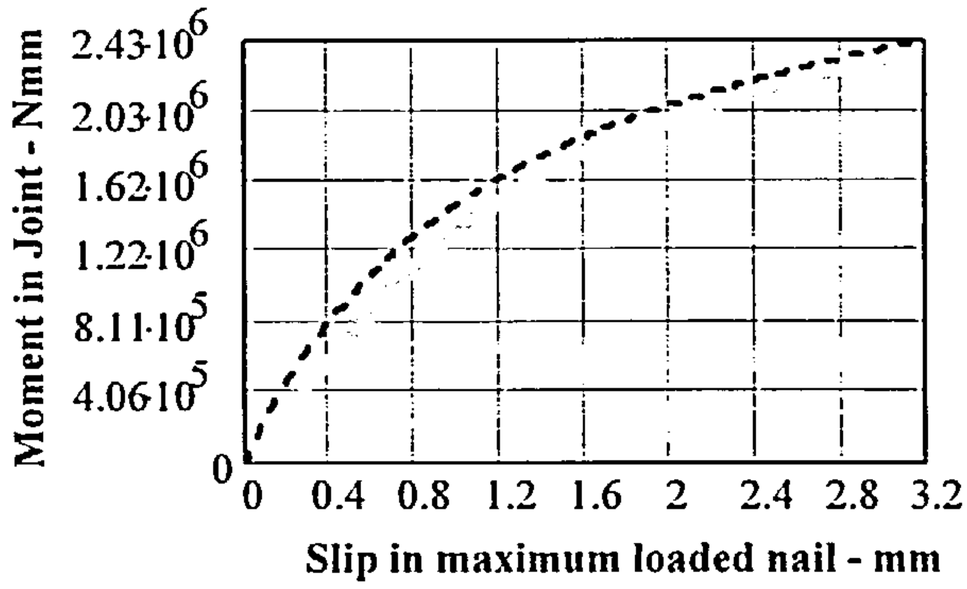

Nailing configuration RA-Joint S6

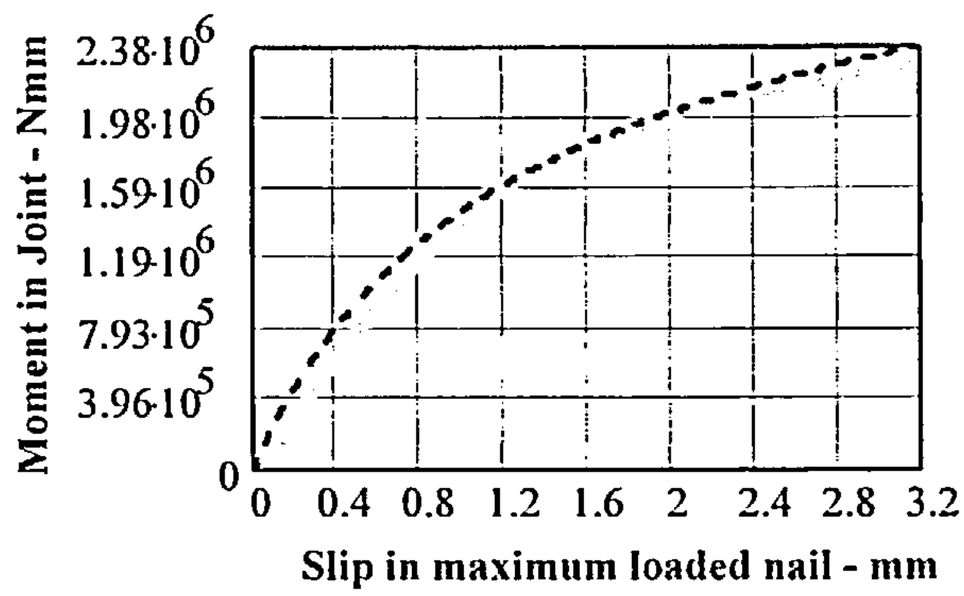

Nailing configuration RA-Joint S7

Figure 5.19 Comparison of model NL2 and test results of joints made with 6mm thick steel gusset plates (with predrilled holes less than 1.1 times the nail diameter), when maximum loaded nail is displaced by up to 3.2mm.

From the graphs it is seen that there is a good comparison between the tests and the models over the full range of nail displacement. The fit with the joints using steel gusset plates is not as good as that with the joints using plywood gusset plates. That is considered to be due to the effects of joint friction in the samples or variations in the material properties of the samples rather than to matters relating to the model.

The results demonstrate that the moment behaviour of timber joints can be modelled using the load-displacement relationships developed in Chapter 4 for laterally loaded joints. To obtain the most accurate result for all nailing configurations, a non linear analysis incorporating a variable centre of rotation approach, as given in model Non-Linear 2, should be used. The applied shear force on the joints was less than 10% of the direct shear strength and the effect of shear deformations were found to be negligible and can be ignored in the analysis.

5.4.2 Results Using Timber with the Plane of the Grain at an Angle to the Face of the Joint

When timber was used with the plane of its grain set at an angle to the face of the joint, as shown in

Figure 5.4, the moment taken by the joint was less than that predicted by the models developed in section 5.3.

This was considered to be due to the effect of the weaker strength of the timber when loaded in the direction of the *R* orthotropic axis. The following approach has been developed to take this into account.

Tests were carried out on joints made with 19mm plywood gusset plates having varying nailing configurations and using timber with the plane of its grain at varying angles to the face of the joint. Initially, sets of joints were tested using nailing configuration RA and with timber having the direction of the plane of its grain set at right angles to the timber face. In this case the nail loading is applied to only the *R* and *L* orthotropic axes. Using the Non-Linear 2 model the moment in the joint was calculated at a slip of 3.2mm in the highest loaded nail and the average of the ratio of test moment to model moment for these tests was found to be 0.88. Based on the test results for joints made with nailing configuration RA and timber with the direction of the plane of its grain parallel to the timber face, it was found that the ratio of test moment to model moment was 0.97. In this case the nail loading was applied to only the *T* and *L* orthotropic axes.

Using the model as a datum reference, the relative relationship of these results gives a radial/transverse factor of 0.91. From this result the factor to be applied to the force on a joint where the plane of the timber grain is at an angle *a* to the face of the timber, as shown in Figure 5.20, can be established.

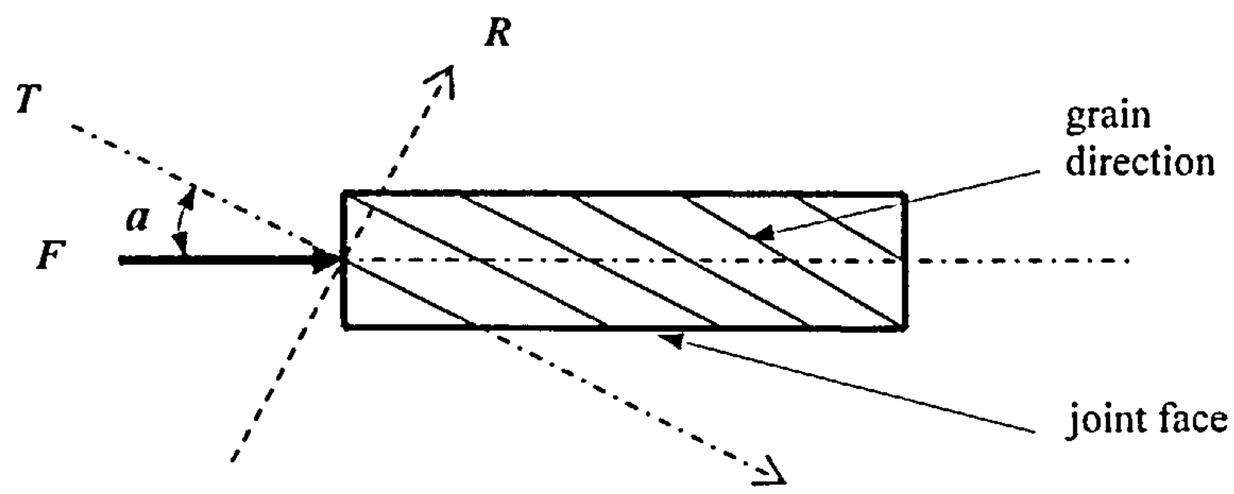

Figure 5.20 Force on joint relative to the T and R axes.

Applying Hankinson's equation [114], the grain direction factor to be applied to the force component parallel to the face of the joint will be

$$f_{TR} = \frac{0.91}{\sin^2(\alpha) + 0.91\cos^2(\alpha)} \qquad \ldots.(136)$$

where

f_{TR} = the grain direction factor applied to the nail force F on the timber face.

a = the angle between the plane of the grain and the face of the timber.

Combining the effect of the grain direction factor and the function in equation (93), the resultant force on nail i in the joint will be:

$$f_i = \frac{f_{xi} f_{yi} f_{TR}}{f_{yi} \sin^2(\beta_i) + f_{xi} \cos^2(\beta_i)} \qquad \ldots.(137)$$

where:

f_{xi} = selected from equation (41f), (50f), (86f) or (92f) to suit the joint type being used.

f_{yi} = selected from equation (41e), (41e), (50e), (50f), (86e), (86f), 92(e) or (92f) to suit the joint type and the row spacing being used.

β_i = the angle between the force in the nail and the direction of the longitudinal orthogonal axis.

A comparison between a sample of the tests and solutions calculated using Non-Linear 2 model, incorporating equation (137), is given in Table 5.8. A negative sign in the right hand column indicates an underestimation and a positive sign indicates an overestimation by the model.

The results using the Non-Linear 2 model incorporating the grain direction factor f_{TR} compare very favourably with the tests. From the examples given there are two instances, NV18 and NV24 where the model predicts results which are around +10%. However the paired results, NV17 and NV23, which used the same materials, are +6.88% and +2.69% respectively, suggesting that the high results are more likely to have been influenced by factors associated with the joint materials or the assembly process rather than the application of the model.

The load-deformation behaviour of a sample of tests compared with the model results have also been plotted together for comparison over the full slip range and are given in Figure 5.21. In the figures the model result is represented by a dashed line.

It can be seen from the graphs that there is a good comparison between the tests and the models over the full range of nail displacement. The results demonstrate that the moment behaviour of joints with the plane of the grain of the timber at an angle to the face of the joint can be modelled using the Non-Linear 2 model by into account the grain direction factor as given in equation (137). An example of the use of Non-Linear 2 model set up in Mathcad [51] incorporating the grain direction factor is given in Appendix I.

Test ref	Nailing conf'n	Nail Ø mm	No of nails in the joint	Angle of the plane of the grain - a^0	Timber density kg/m^3	Plywood density kg/m^3	Lever arm mm	Experiment moment A kNm	Non-linear 2 B kNm	-(A-B)/A %
NV2	RA	2.66	32	90	554.77	645.98	509	1.2656	1.301	+2.80
NV3	RA	3.33	32	90	534.16	668.52	504	1.71169	1.741	+1.71
NV5	RB	3.01	40	75	519.97	574.65	497	1.98893	2.033	+2.22
NV6	RB	3.01	40	75	526.39	579.54	497	2.0677	2.052	-0.76
NV7	RB	3.01	40	45	614.72	653.27	490	2.43583	2.434	-0.08
NV10	RB	3.33	40	45	553.16	617.07	490	2.38642	2.396	+0.40
NV14	RC	2.66	48	45	547.2	608.13	601.6	2.34226	2.420	+3.32
NV17	RF	2.66	28	45	602.79	635.10	550	1.84888	1.976	+6.88
NV18	RF	2.66	28	45	612.94	639.95	550	1.80802	1.994	+10.65
NV19	RG	2.66	8	45	612.94	639.95	549	0.68071	0.7155	+5.11
NV21	RH	2.66	8	45	612.94	639.95	545	0.47943	0.4893	+1.99
NV22	RH	2.66	8	45	599.82	638.38	545	0.48441	0.487	+0.53
NV23	RI	2.66	8	45	608.41	636.16	544	0.75882	0.7792	+2.69
NV24	RI	2.66	8	45	612.94	636.58	544	0.71583	0.7816	+9.19

Table 5.8 The moment taken by joints constructed with 19mm plywood gusset plates using timber with the plane of the grain direction angled to the joint face. Joints were assembled with a gap between the timber and gussets plates.

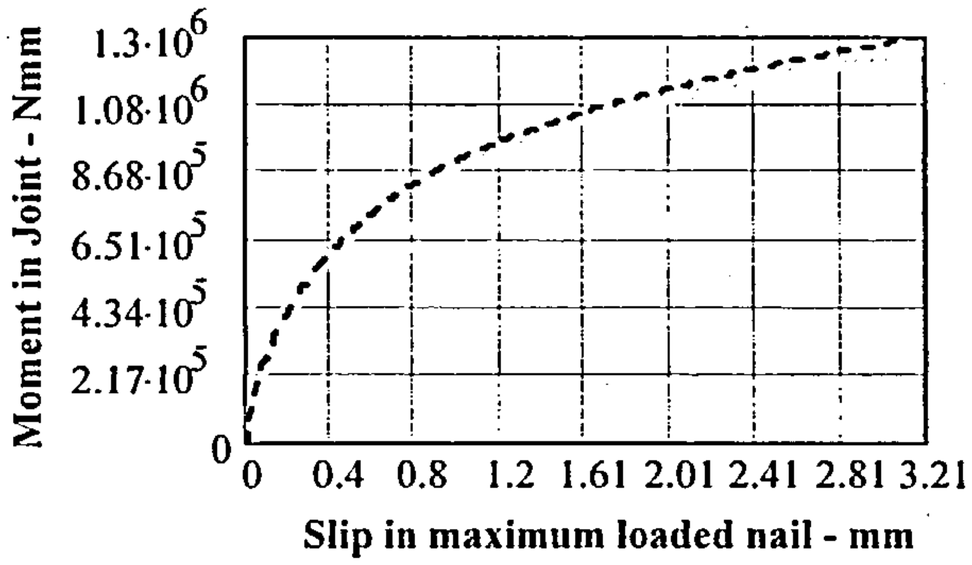

Nailing configuration RA-Joint NV2

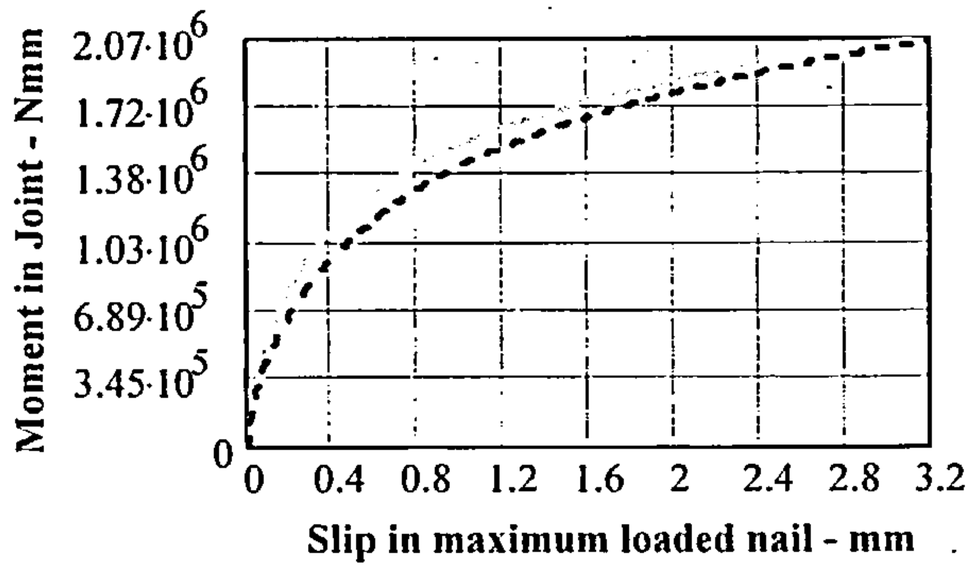

Nailing configuration RB-Joint NV6

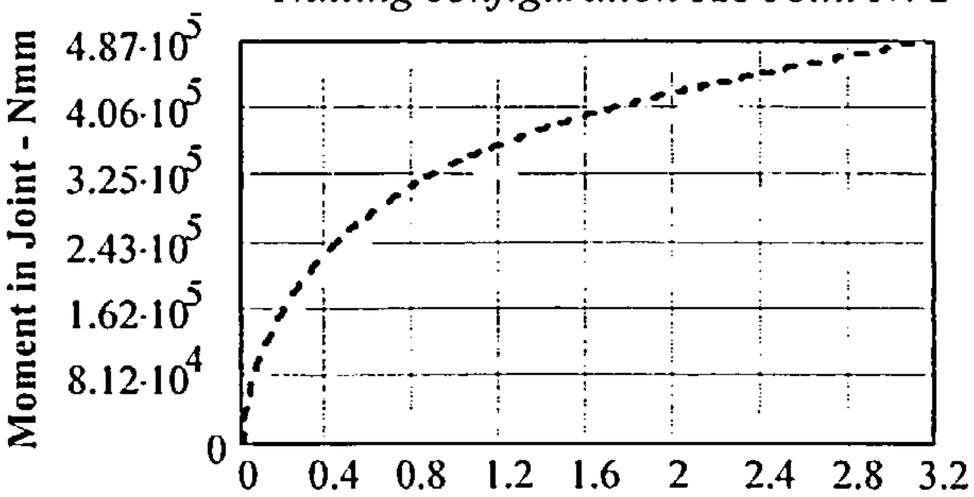

Nailing configuration RH-Joint NV22

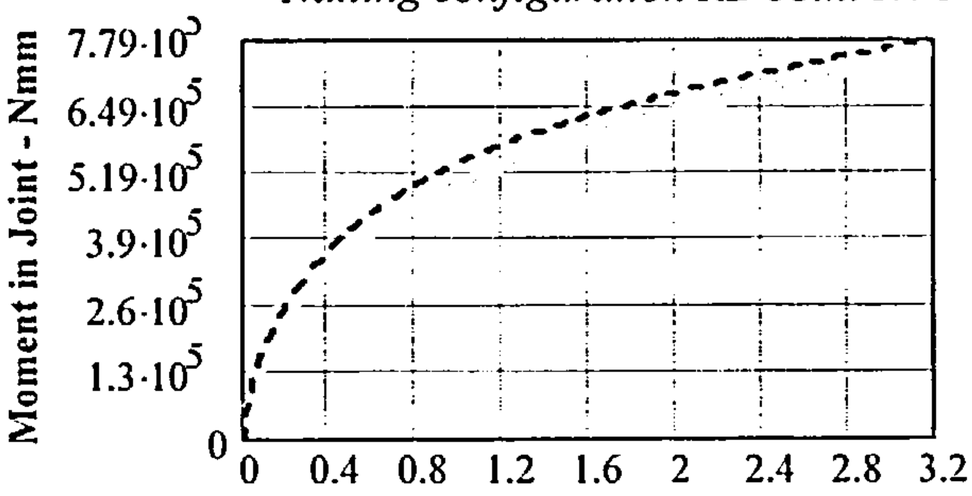

Nailing configuration RI-Joint NV23

Figure 5.21 Comparison of model NL2 and test results of joints made with 19mm plywood gusset plates, using timber with the plane of the grain angled to the joint face when the maximum loaded nail is displaced by up to 3.2mm.

5.5 LIMITATION OF THE VALIDITY OF THE MODELS

In the analyses in section 5.3 a key premise was that joint rotation was caused primarily by a combination of deformation of the nails and embedment of the nails into the timber and plywood. Flexural displacements caused by bending and shear force displacements of the timber and gusset plates were assumed to be negligible.

This was confirmed to be the case for the nailing configurations referred to in section 5.4 by using four transducers to check the linearity of the timber along the length of the joint during the test procedure. For each joint configuration one of the tests was carried out using a four transducers set-up, spaced along the joint length. This enabled the exterior face of the timber to be checked for curvature effects over the duration of the test. In all cases the joint configurations referred to in section 5.4 remained straight.

Tests were also undertaken using nailing configurations with more nails than have been reported in section 5.4 and in these instances flexure of the timber was recorded. A combination of nail numbers and nail spacing resulted in joints which exhibited flexure in addition to nail deformation and this occurred using joints RC, RD, RE and RL. In these instances Non-Linear 2 model will not give a reasonable prediction of the moment capacity of the joint.

Because of the number of variables influencing the joint behaviour it is not possible to set simple criteria that will define a limit beyond which the model will not apply. The limit of applicability has been determined using a combination of joint moment capacity; design bending strength and the design splitting capacity of the timber in the joint.

a) Joint moment capacity – Limiting nailing configuration

Using Non-Linear 2 model to determine the moment capacity of the joint nailing configurations used in the programme, the one that gives the highest value without showing signs of flexure in the timber is taken to be the upper bound limit of applicability of the model. For the joints assembled with plywood gusset plates, the limiting nailing configuration was found to be RK. For joints with steel gusset plates only nailing configuration RA was used and this showed no sign of flexure. However, as stronger joints were not used further work will be required to establish an upper limit for this type of joint.

b) Moment capacity based on the design bending strength of the timber and gusset plates

The design moment strength of the gusset plates and the timber will be determined in accordance with the requirements of EC5 [15] and the joint strength will be the element with the lowest moment

strength. To maximise the benefit of the joint the bending strength of the timber and the gusset plates should ideally exceed the strength of the nailing configuration.

c) Splitting resistance of the timber

When the force in a connection acts at an angle to the grain there is the possibility of splitting in the timber caused by the tension component perpendicular to the grain. The investigation into the splitting behaviour of timber lends itself to the use of the theory of fracture mechanics and the application of linear elastic fracture mechanics to timber commenced in the early 1990's [119]. At that time the research was principally associated with the evaluation of fracture properties of timber test specimens [118]. Since then a number researchers have investigated the splitting behaviour of joints [119, 120, 121, 122] using linear elastic fracture mechanics and recommendations for the design of joints subjected to splitting forces are now included in EC5 [15].

Consider a nailed joint subjected to a moment caused by a shear force *F*. From the application of Non-Linear 2 model, it will be found that the centre of rotation will be at a location offset from the centroid of the nailing configuration as shown in Figure 5.22.

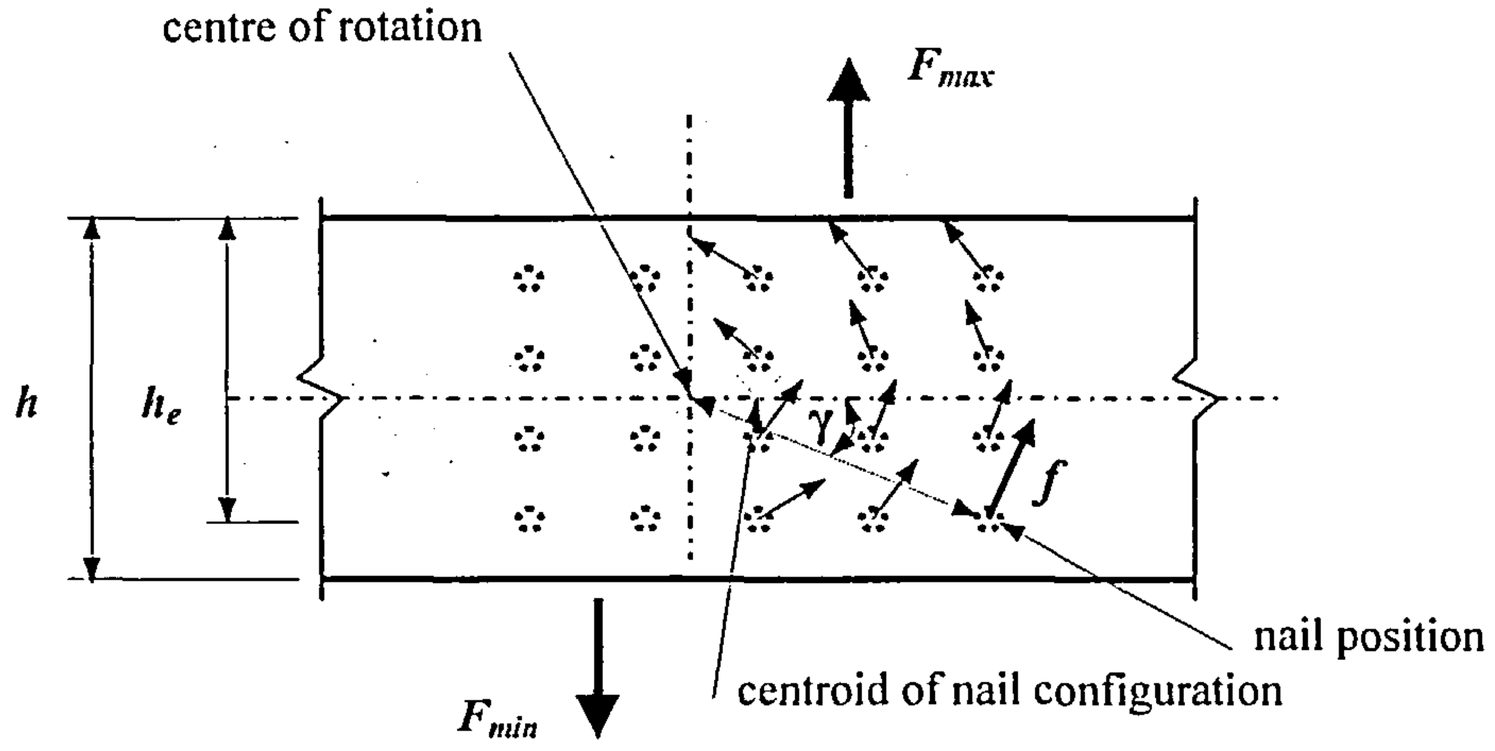

Figure 5.22 The forces in the nails giving the greatest shear force perpendicular to the grain of the timber.

The resultant force *f* in each nail will be at right angles to the line jointing the nail and the centre of rotation and summing the vertical components of the nail forces gives the splitting force in the joint. In the example shown the nails located to the right of the centre of rotation will have a resultant vertical force $F_{max.}$ acting upwards and to the left the resultant, F_{min}, will act downwards. The maximum force, F_{max} will be obtained by the summation of the vertical components of the nail forces acting in the same direction and will include the nail at the greatest distance from the centre of rotation. In Figure 5.22, that will be the nails to the right of the centre of rotation.

For equilibrium, $F + F_{max} + F_{min} = 0$ ....(138)

and $F_{max} = \sum (f \cos(\gamma))$ ....(139)

where γ is the angle of the line between the nail and the centre of rotation and the horizontal axis.

From EC5 [15], the design splitting capacity of the timber is:

$$F_{90.Rd} = \frac{k_{\text{mod}}}{\gamma_{\text{mod}}} (14bw) \sqrt{\frac{h_e}{\left(1 - \frac{h_e}{h}\right)}} \quad \text{....(140)}$$

For the splitting capacity of the timber to exceed F_{max}:

$$F_{max} \leq \frac{k_{\text{mod}}}{\gamma_{\text{mod}}} (14bw) \sqrt{\frac{h_e}{\left(1 - \frac{h_e}{h}\right)}} \quad \text{....(141)}$$

which reduces to $$F_{max} \leq (14b) \sqrt{\frac{h_e}{\left(1 - \frac{h_e}{h}\right)}} \quad \text{....(142)}$$

where:

F_{max} = the maximum force in the joint perpendicular to grain – N.

b = the member thickness – mm.

w = a width factor = 1

h = the timber member height – mm.

h_e = the loaded edge distance from the centre of the most distant nail – mm.

Based on the above, the limitation of applicability of the Non-Linear 2 model will be:

i) For plywood gusset plate joints, Non-Linear 2 model will apply where:

a) the moment capacity of the joint does not exceed the capacity obtained from the model when fitted to nailing configuration RK.

b) the moment capacity will be the least of the joint capacity, the design moment strength of the timber or of the plywood gusset plates designed in accordance with EC5 [15].

c) the maximum force in the joint perpendicular to the grain complies with the requirement of equation (142).

ii) For steel gusset plate joints the same approach can be applied as for the plywood joints but using pattern RA as the limiting nailing configuration. This will provide a lower bound safe solution. Further testing using different nailing configurations is required to establish the upper bound limit.

5.6 THE BEHAVIOUR OF DOUBLE JOINTS

To demonstrate that joint gusset deformation is not a factor in the analysis of joints connected by the same gusset plates, double joints have been modelled and compared with the results of tests. The comparison has been limited to the use of joints with plywood gusset plates as these will be less stiff than joints made with steel gusset plates.

The configuration of the joints and the test and monitoring set-up used are as described in Chapter 3. Nailing configurations RA and RB were used. Joints with nailing configuration RA were assembled without a gap between the gusset plates and the timber and those using nailing configuration RB were assembled with a gap.

The joints were loaded until the maximum loaded nails had slipped by 3.2mm. Because of the geometry of the set-up this occurred at different loadings for the joint in the vertical 'leg' member and the joint in the horizontal 'arm' member. The arm joint reaching the maximum slip criteria at a higher load than that required to achieve the same slip in the leg joint. Also, under test the combined effect of the rotation of the gusset plates relative to the leg joint and the rotation of the horizontal member relative to the gusset plates resulted in significant changes in geometry. Horizontal reaction forces were also introduced at the loading point on the test machine due to the joint movement. All of these effects have been taken into account in the analysis process.

Under load the double joint deforms as indicated in Figure 5.23, where:

P = the load applied to the joint by the test machine.
H = the horizontal load from the test machine due to rotation of the joint.
h = the distance between the centres of rotation of the joints.
l = the lever arm - the distance between the applied load and the centre of the nailing configurations.
ε = the angle of rotation of the gusset plates relative to the vertical leg.
η = the angle of rotation of the arm joint relative to the original position of the centre line of the horizontal arm

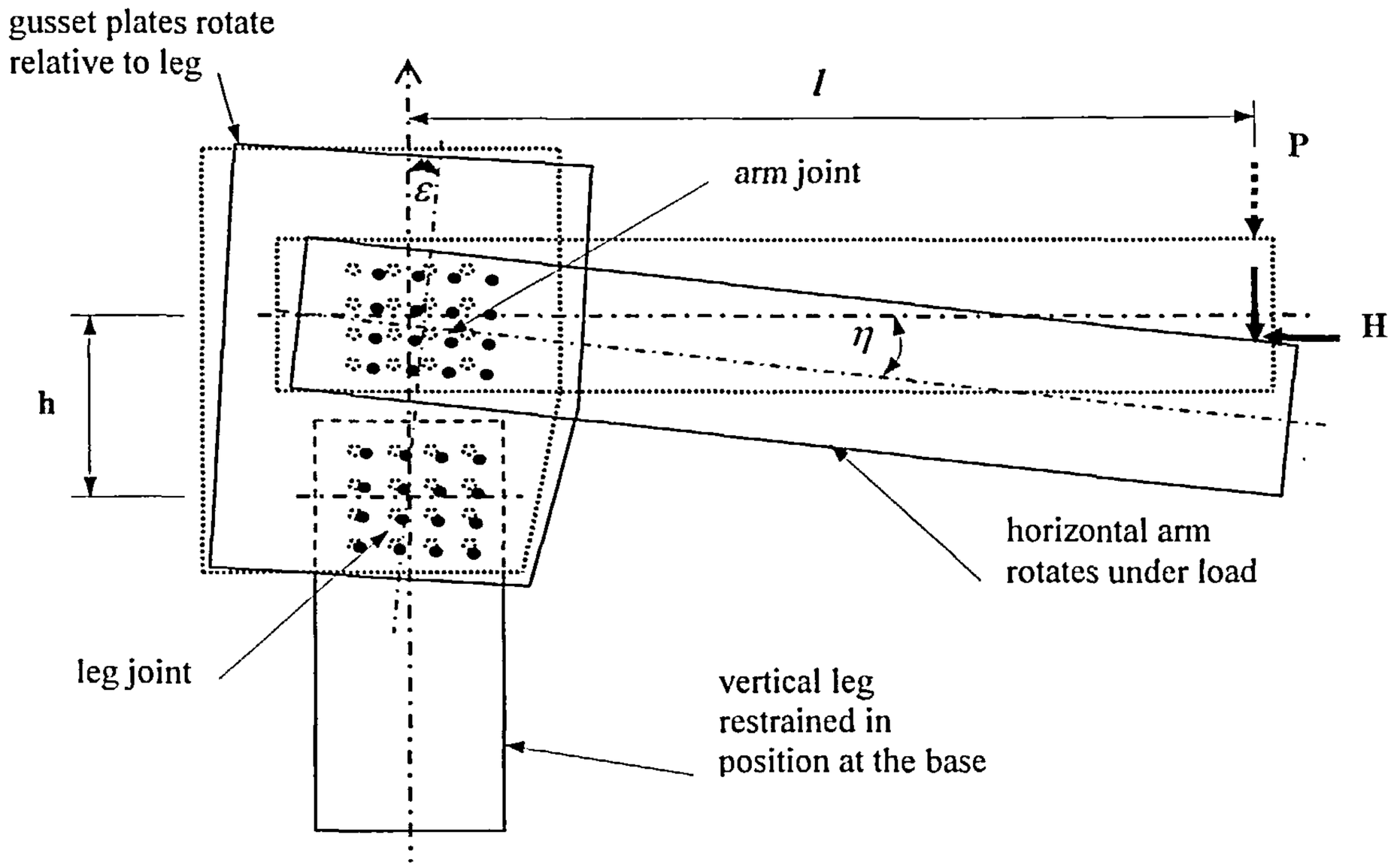

Figure 5.23 Behaviour of the double joint under load. (the unloaded connection is shown dotted)

The loading causes the gusset plates to rotate by an angle ε relative to the vertical leg. The horizontal arm rotates by η, a combination of the rotation of the gusset plates and the arm relative to the gusset plates. There are three main effects arising from these rotations:

i) The length of the lever arm on the arm joint is reduced.
ii) The joint is displaced towards the loading arm. As the test machine is rigid it imposes a horizontal force H on the joint in addition to the vertical force P.
iii) The horizontal force reduces the bending moment on the joint in the leg. Because of the small lever arm at the arm joint the effect of the horizontal force on that joint can be ignored.

The reduction in the lever arm is $h\sin(\varepsilon)$; the horizontal force on the joint is $P\sin(\eta)$; and the lever arm between the horizontal force and the centre of the nailing group in the leg is $(l-h\sin(\varepsilon))\sin(\eta)$.

Incorporating these adjustments into the processing procedure, the results from the tests are compared in Table 5.9 with the solution using the Non-Linear 2 model. Two pairs of transducers were used per joint in each test, a pair being connected to each gusset plate. This checked the rotation of the timber relative to each gusset plate and enabled an average load to be obtained at each joint should the gusset plates rotate by differing amounts. From the processed results the gusset plates rotated by the same amount and the averaging procedure was not required. The figures in Table 5.9 are based on the most highly loaded nail in each joint being displaced by 3.2mm. The actual diameter of the 2.65mm diameter nails used in these tests was 2.63mm and this size has been used in the analyses. The difference

between the model result and the test result is also given, with a negative sign indicating an underestimation and a positive sign indicating an overestimation by the model.

Test ref	Joint	Nailing Pattern	Nail Ø mm	Timber density kg/m^3	Plywood density kg/m^3	Plywood thickness mm	Test moment kNm	Non-linear 2 moment kNm	% difference
C1	ARM	RA	2.63	550.17	543.89	17.99	1.41969	1.549	+9.11
C2	LEG	RA	2.63	568.15	543.89	17.99	1.47687	1.564	-+5.90
C3	ARM	RB	2.63	528.71	514.47	17.89	1.56447	1.645	+5.15
C4	LEG	RB	2.63	515.63	514.47	17.89	1.62617	1.634	+0.48
C5	ARM	RB	3.01	523.98	509.99	17.88	2.04311	2.059	+0.78
C6	LEG	RB	3.01	521.78	509.99	17.88	2.06204	2.057	-0.24

Table 5.9 Comparison between the double joint test result and model Non-Linear 2 when the maximum loaded nail in each joint is displaced by 3.2mm.

In the majority of the tests the model solution exceeds the test result and apart from one joint the test and model results compare well with each other. The greatest exceedance is 9.11% and is associated with test reference C1 in joint RA. Joint RA was assembled without a gap between the gusset plate and the timber and noting that the paired joint C2, which used the same materials, was only 5.90% under the model value, it is probable that variations in the material surfaces and the assembly process have resulted in a lower friction function for that joint.

The load-deformation behaviour of a selection of the tests compared with the results using model Non-Linear2 have also been plotted together for comparison and are presented in Figure 5.24. In the graphs the model result is represented by a dashed line.

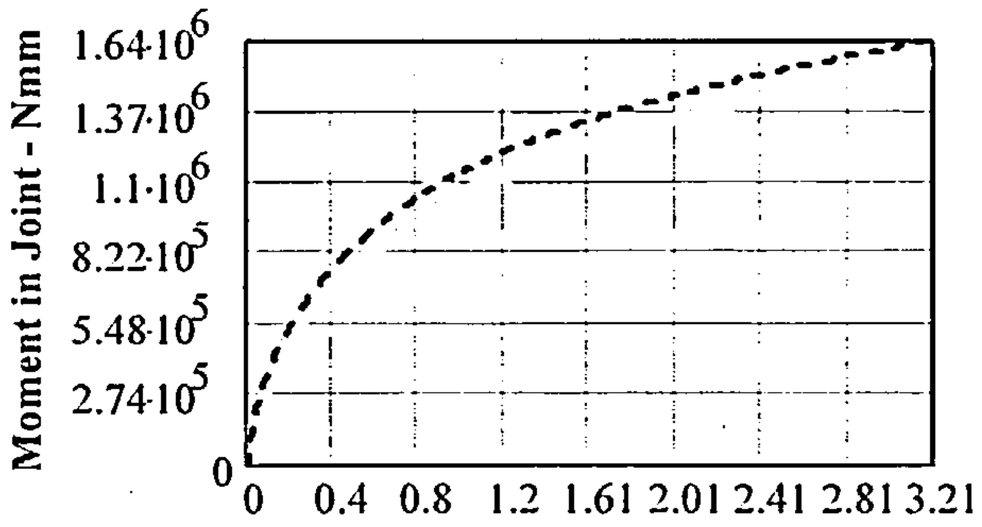

Nailing configuration RB-Joint C3

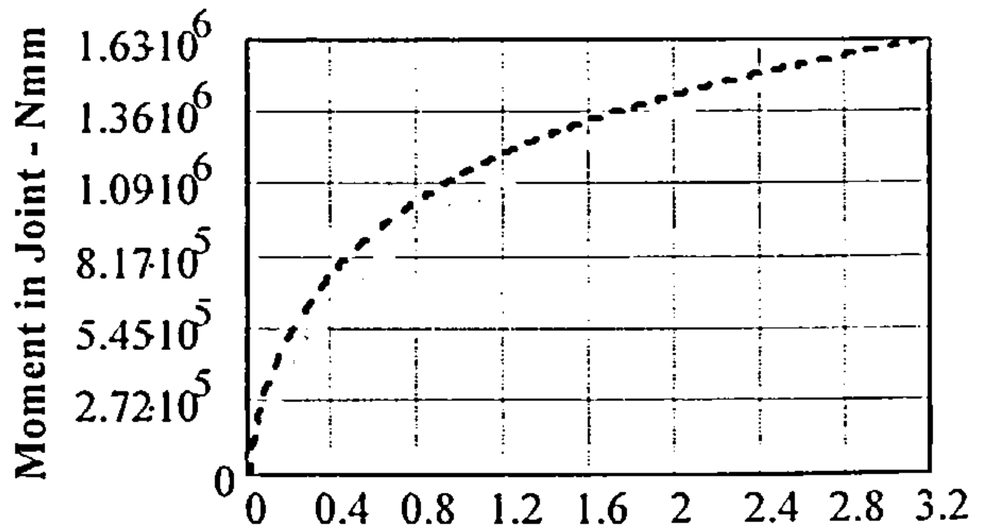

Nailing configuration RB-Joint C4

Figure 5.24 Comparison of model NL2 and test results of double nailed joints made with plywood gusset plates (with predrilled holes less than 1.1 times the nail diameter), when the maximum loaded nail is displaced by up to 3.2mm.

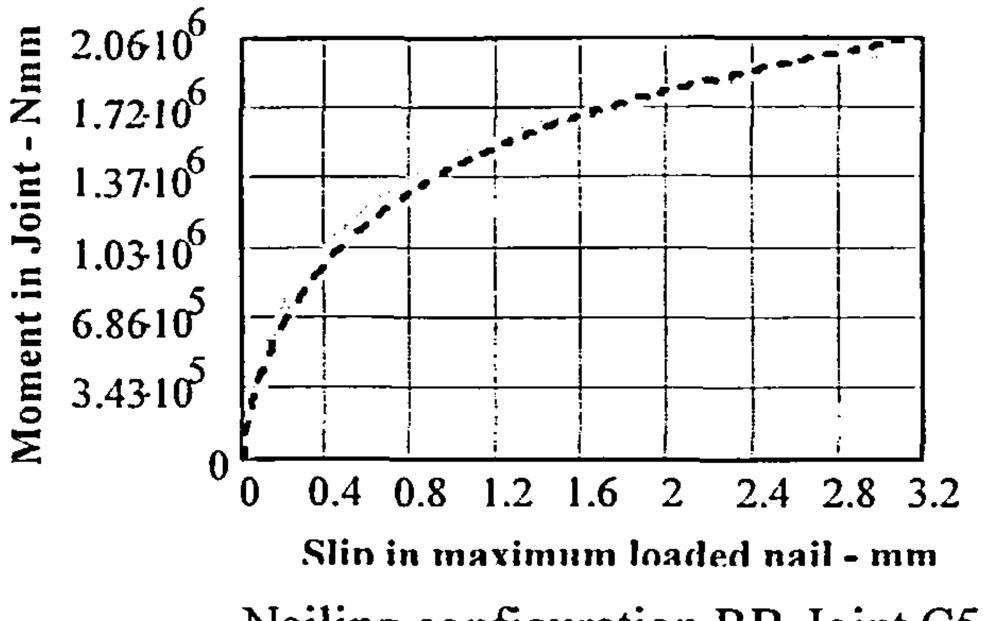

Nailing configuration RB-Joint C5

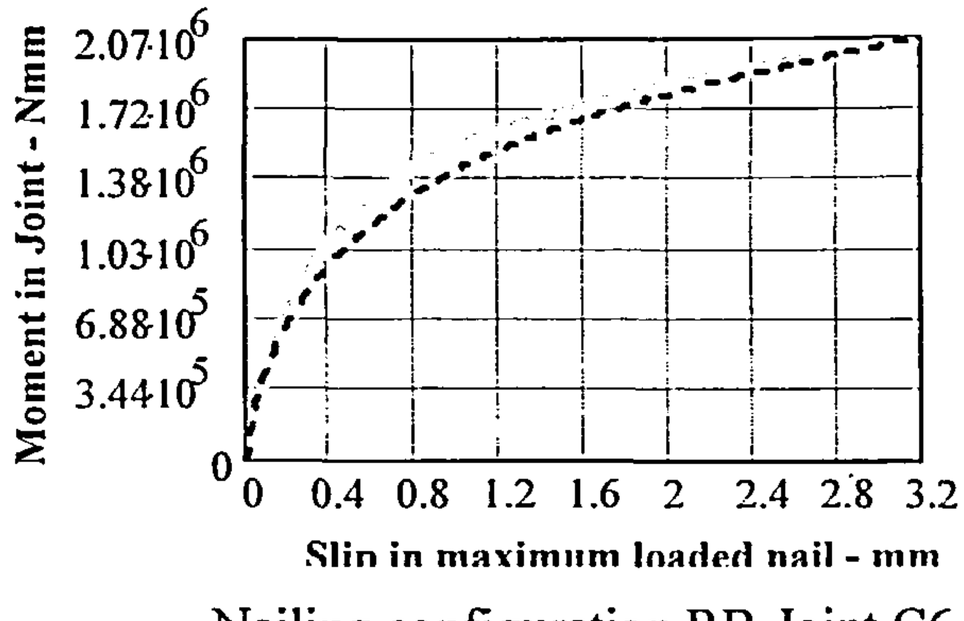

Nailing configuration RB-Joint C6

Figure 5.24 cont'd Comparison of model NL2 and test results of double nailed joints made with plywood gusset plates (with predrilled holes less than 1.1 times the nail diameter), when maximum loaded nail is displaced by up to 3.2mm.

The overall comparison is good and the conclusion from these tests is that the model will satisfactorily predict the behaviour of multiple joints connected to the same gusset plates.

5.7 SUMMARY

In this chapter a description is given of alternative methods of analyses that have been developed to investigate the moment-displacement behaviour of joints using fully overlapping nailed connections. Linear and non-linear models have been used and their effectiveness in simulating the moment-displacement behaviour of the nailed connections has been examined. Because the behaviour of these joints is a function of the load-displacement behaviour of the nails, the displacement of the maximum loaded nail in the joint has been used in the analyses as the monitoring criteria rather than joint rotation. Based on the load slip limits set in Chapter 3 for laterally loaded joints, an upper slip limit of 3.2mm has been used as the limiting movement.

In the test set-up used in the programme, the transducers record the adjacent movement of the timber face, not the movement of the nails in the joint. Further, because the transducers are fixed to the gusset plates only movements in the line of the transducers were recorded. As the nails were loaded at right angles to the line joining the nail head to the centre of rotation, the transducer readings had to be processed to obtain the movement of the extreme nail. A description is given of the method used taking account of the above factors.

Six methods of analysis have been presented. All use the load-displacement models developed in Chapter 3 and have been incorporated into linear or non-linear methods. Two of the methods – Secant Stiffness 1 and 2 - assume the nails have linear load-displacement behaviour and use either a fixed or a

variable centre of rotation. These models give approximations which generally underestimate the moment capacity of the joint.

The four remaining methods use non-linear approaches. They model the actual nail load-displacement behaviour and, as for the linear models, use fixed or variable centres of rotation. One of the models – Non-Linear 3 - includes for second order joint movements but as it contributes less than 1% to the degree of accuracy obtained when using the Non-Linear 2 method, the additional complexity and computational effort associated with the method is not considered to be justified. Non- Linear 1 assumes a fixed centre of rotation and is appropriate for use with joints subjected to a pure moment. Non-Linear 4 is the least accurate as it ignores the effect of nails lying on the x-axis. For joints subjected to moment by shear forces, Non-Linear 2, which incorporates a variable centre of rotation approach, has been shown to give the best simulation of the moment displacement behaviour.

The methods are based on joints in which failure takes place by deformation of the nails and embedment of the timber and plywood rather than by failure of the timber. Limiting criteria has been established for use with the Non-Linear 2 method for joints with plywood gusset plates. Only approximate criteria have been given for joints with steel gusset plates. The objective of the programme was primarily to demonstrate that the method of analysis would also apply to joints with steel gusset plates and only joint configuration RA was used.

Plywood gusset and steel gusset plate joints have been used in the model assessment exercise and all joints have been assembled with a gap between the timber and the gusset plates.

Joints made with plywood gusset plates, also assembled with a gap between the timber and the gusset plates, but using timber with the plane of the grain at an angle to the face of the timber have also been investigated. A grain factor which takes account of the behaviour of the timber when loaded in this manner has been developed and applied to the spacing function used in the Non-Linear 2 model. The model results give a good comparison with the test results.

The Non-Linear 2 method has also been applied to connections using double joints. It is shown that the model works well in such instances making it suitable for use in the analysis of the behaviour of structures assembled with nailed joints. In these tests only plywood gusset plate joints were used and assembled with and without a gap between the timber and the gusset plates.

6. COMPARISON BETWEEN THE MODELS FOR JOINTS WITH LATERALLY LOADED NAILS AND EUROCODE 5

6.1 INTRODUCTION

In this Chapter the models developed in Chapter 4 for joints assembled with steel gusset plates and plywood gusset plates, using fully overlapping nails and subjected to lateral loading, are compared with the behaviour of joints designed in accordance with EC5 [11]. As EC5 is currently being revised and several draft revisions have been issued for comment, the comparison has been carried out against the first draft issue, EC5 [11], and the latest draft, EC5 [15].

The background to the strength and stiffness equations used in EC5 [11] has been given, drawing on the work by Ehlbeck *et al* [68] and STEP 1 [79]. This has been carried out to ensure the appropriate factors embodied in the relevant equations in the Eurocode are able to be read across to the model, allowing a proper comparison to be undertaken. The Eurocode is a limit state probabilistic code and to equate to the strength and stiffness equations, the models, which have been developed on a mean property basis, have been converted to a characteristic value basis. This has been achieved using a Log-Normal distribution and the confidence limits proposed for test results given in EC5 [13].

A comparison has been given between the results of properties derived from sample testing with those determined using the EC5 rules. In particular the results of embedment tests on nails in timber and plywood samples and nail pull out tests.

For each joint type, a parametric exercise has been undertaken to compare the effects of variations in the joint parameters on the model and the Eurocode results. The variation in parametric value has been limited to the extreme values used in the testing programme to ensure the model behaviour is bounded by the results of the testing programme. Joint strength and stiffness have been compared at the ultimate limit state (ULS) and the serviceability limit state (SLS). Also the EC5 strength and stiffness results at the ULS and the SLS are combined into one graph for each joint type to compare with the respective model behaviour.

6.2 JOINT STRENGTH AND STIFFNESS CRITERIA IN EC5

6.2.1 EC5 Safety Format

The basis for EC5, "Design of Timber Structures", was the CIB Structural Timber Design Code, 1983 [124]. The Timber Design Code was developed and changed into the Eurocode through the CIB W18 forum with discussions and changes documented in the proceedings of the working commission meetings. Development of the document took a significant period of time. A first draft was published by the Commission of the European Communities in 1987 (Report EUR 9887) for comment [128] and

the first formal publication of a draft edition in the United Kingdom was in late 1994 as DD ENV 1995-1-1:1994 [11]. Publication of the definitive EN EC5 has still to be achieved and is expected in 2003.

To date three revisions of the 1995 draft have been issued [13, 14, 15] and to ensure a realistic comparison will be achieved, the models have been compared with the current issue [11] as well as with the Final Draft Version, 2002-02-28 [15]. This covers for the possibility of retention of the existing code or replacement with the latest revision.

EC5 is a limit state code in which the design is related to clearly defined states beyond which the structure will no longer satisfy the design performance requirements. Limit states are classified into ULS and SLS. ULS are those associated with collapse and other forms of structural failure which may endanger safety and become a risk to life. SLS correspond to states beyond which specified service criteria are no longer met, leading to damage to finishes, discomfort to people, or adversely affecting functional effectiveness or appearance.

Structural reliability is ensured by the use of a partial coefficient system, following the same principle used in the permissible stress approach. Partial load factors, γ_G or γ_Q increase the value of the applied loads and partial factors for materials, γ_M, reduce the value of the strength property.

For strength and stiffness calculations, characteristic values of load, (G_k for permanent actions and Q_k for variable actions); of strength properties of materials, X_k, or of a load carrying capacity, R_k, are generally used. In the case of joints, fifth percentile values are used for the characteristic values and are derived from a statistical analysis or from the results of laboratory tests in accordance with BSEN 26891 1991 [27] and other related standards. The characteristic strength is the value below which the strength will lie in no more than 5% of cases and the characteristic load is the load which will not be exceeded in more than 5% of cases.

The design value of a load is obtained by multiplying the characteristic load by the appropriate partial load factor, γ_G and/or γ_Q. Design value of a strength property or a resistance is obtained by dividing the characteristic resistance property by the partial factor for the material property, γ_M, and multiplying by a moisture content and load duration factor, k_{mod}.

The material factor has been estimated on the basis of a calibration exercise taking permissible state design codes as the benchmark. Generally the safety factors in the codes were about 2.5 and by adopting a value of γ_M = 1.3 comparable safety factors were obtained [128]. K_{mod} is a modification factor that varies in value and takes into account the combined effect of moisture content and of the duration of load.

In regard to moisture content, there are three service classes corresponding approximately to the following moisture contents in the structure: service class 1 = less than 12%; service class 2 = less than

20%; and service class 3 = an unlimited value. For the duration of load effect, there are five load-duration classes given in EC5. Using a constant load, the classes correspond to: permanent = more than 10 years; long-term = 6 months to a year; medium-term = 1 week to 6 months; less than one week; instantaneous. The case of short term test results is not referred to in the code and from discussions with TRADA, this is a special category for which the value of k_{mod} is taken to be unity.

Ignoring the effect of combination factors, which take into account the reduced possibility of more than one action having its full characteristic value, the design action effect can be written:

$$S_d = \Sigma(\gamma_G G_k + \gamma_Q Q_{kj}) \quad \ldots.(143)$$

and the design value of the load carrying capacity of a joint can be written:

$$R_d = k_{mod}\frac{R_k}{\gamma_M} \quad \ldots.(144)$$

The key safety principle to be followed in the code is that $S_d \leq R_d$ giving:

$$\Sigma(\gamma_G G_k + \gamma_Q Q_{kj}) \leq k_{mod}\frac{R_k}{\gamma_M} \quad \ldots.(145)$$

6.2.2 Joint Strength Criteria

6.2.2.1 Ultimate Limit State Strength

When a joint formed with dowel type connectors is loaded to failure it can fail in either a ductile or a brittle mode. The ductile mode is one in which the bedding material and dowel connector fail by yielding, in accordance with Johansen's plastic theory [43]. In this form of failure the joint sustains load whilst deformation continues to take place and there is no sudden loss of joint strength or stiffness. Brittle mode failure is one in which failure occurs by material splitting; connectors shearing; shear plug failure or tension failure arises. This type of failure will result in a sudden loss in strength and stiffness and is to be avoided if possible. To cover for this situation, in EC5 the detailing requirements of the code are written to try and ensure that only ductile failures will be able to occur [47].

Plastic theory forms the foundation for the strength calculations of lateral load-carrying dowel-type connectors. Dowel-type connectors envelope connections using nails, bolts, screws, staples and dowels and in this Chapter only joints using nail connectors will be considered.

The failure model used in the theory is based on the assumption of elastic-ideally plastic material

behaviour of the nail in bending and of the timber/gusset material in bearing. The effect of the reduction in plastic moment capacity in the nail due to the nail axial force is ignored, as is the influence of the nail shear force on the plastic moment. The bearing stress, referred to as the embedment stress for timber and for plywood, is assumed to be uniform.

The basic parameters used in the analysis are the characteristic nail yield moment, $M_{y,Rk}$, and the characteristic timber (or plywood) embedment strength, $f_{h,k}$, from which the yield equations are developed.

Considering only ductile modes of failure, the assumption of an elastic–ideally plastic behaviour result in the possibility of three basic failure modes:

Mode 1 - where the connector remains rigid and the bedding material fails by yielding.
Mode 2 - where there is bedding material yield failure in conjunction with partial yielding of the dowel.
Mode 3 - where the bedding material again fails by yielding and there is full plastic failure of the dowel.

As mentioned in Chapter 3, these types of failure are commonly referred to as the European yield model [47] and if applied to joints using overlapping nails in a three member joint, the most likely mode failures, including possible variations to the basic mode, are shown in Figure 3.13.

Prior to publication, the early drafts of EC5 excluded the effect of friction in the joint and tension in the nails [68]. There are two types of friction effect which can arise in a joint. One is due to the occurrence of friction when a joint is assembled with the gusset plates in direct contact with the timber. The other arises when the nail pulls the gusset plate onto the timber as the joint is deformed under load. The former can be eliminated by having a gap between the timber and the gusset plates but the latter will always arise. Larsen's research [45] demonstrated that for joints with a gap between the timber and the gusset plates and using non-overlapping nails, the combined effect of the withdrawal resistance of the nail and the additional friction force caused by the nail pulling action, gave a load carrying capacity about 20% higher than the theoretical capacity based on Johansen's theory. This magnitude of increase was confirmed by Aune *et al* [17] using joints assembled with non-overlapping nails. Aune *et al* also found that when using joints with members driven in tight contact, the capacity increased by about 50%, concluding that the direct friction effect on its own could be up to 30%. It is also to be noted from the analysis of the test results in Chapter 4 the direct friction effect for joints using plywood gusset plates was 24%, which is comparable with the Aune *et al* finding.

Taking 20% as an upper bound level of increase in load due to nail tension effects, it is possible to review the EC5 assumptions that nail tension and shear effects on the nail strength can be ignored.

Consider a single shear joint using a plywood gusset plate in its failure state (ULS) as shown in Figure 6.1.

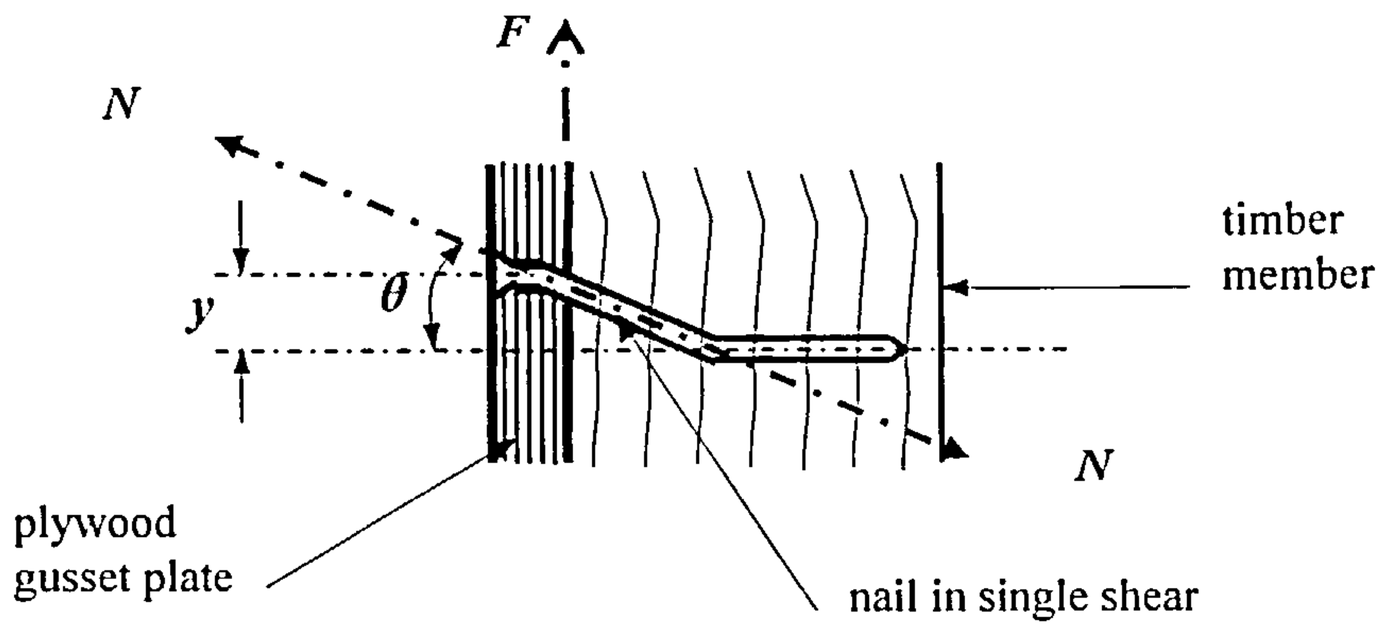

Figure 6.1 Joint with nail in single shear at the ULS condition.

The material strengths are taken to be such that a Mode 3 type failure will occur and at this state the nail is assumed to have rotated by an angle θ and displaced by a distance y, as shown on Figure 6.1. The coefficient of friction between the gusset plate and timber is taken to be μ. Nail yield will occur in the gusset plate as well as in the timber and the nail will also be subjected to a tension force N due to the withdrawal effect during loading. Force N can be resolved into a vertical force component, $N\sin\theta$, and a horizontal force component, $N\cos\theta$, the latter resulting in an additional vertical friction force, $\mu N\cos\theta$. The force in the joint, F, will equate to the sum all of the vertical forces in the joint, giving:

$$F = N(\sin\theta + \mu\cos\theta) + \text{Johansen's Yield Load } (F_Y) \qquad \ldots.(146)$$

From the application of Johansen's yield theory it is readily shown that the yield load of the joint will be:

$$F_Y = \sqrt{\frac{4\beta}{(1+\beta)} M_{y,Rk} f_{h,p,k} d} \qquad \ldots.(147)$$

where

$M_{y,Rk}$ = the characteristic value of the yield moment in the nail -Nmm.

$f_{h,p,k}$ = the characteristic value of the embedment strength of the plywood–N/mm^2.

d = the nail diameter – mm.

β = ratio of the characteristic embedment strength of the timber to the plywood.

From EC5 [15], with round nails $M_{y,Rk} = \frac{f_u}{600} 180 d^{2.6}$; $f_{h,w,k} = 0.082(1\text{-}0.01d)\,\rho_k$ for timber; $f_{h,p,k} = 0.11\,\rho_k\, d^{0.3}$ for plywood. Assuming d = 2.66mm; f_u = 800 N/mm^2 for the nail strength and taking the characteristic density ρ_k of the timber and plywood as 550Kg/m^3, substituting into equation (147):

$$F_Y = 850.3 \text{ N} \quad \ldots.(148)$$

Taking the tension force in the nail as 20% of *Fy* and assuming a coefficient of friction of 0.33, also found from Larsen's tests [45], from equation (146) the nail force *N* can be expressed as:

$$N = \left(\frac{0.2Fy}{(\sin\theta + \mu\cos\theta)} \right) \quad \ldots.(149)$$

From Johansen's theory, the angle of tilt of the nail at yield can be shown to be:

$$tan\theta = \frac{yf_{h,p,k}d}{F_y}\left(\frac{\beta}{(1+\beta)} \right) \quad \ldots.(150)$$

Taking the level of slip around which nail yield will occur to be 3.2mm, and substituting into equation (150) gives $tan\theta = 0.223$. Substituting for θ in equation (149):

$$N = \frac{0.2 \times 850.3}{\sin\theta + 0.33\cos\theta} = 313.3 \text{ N} \quad \ldots.(151)$$

This is just over 7% of the failure stress of the nail and if a sensitivity analysis is done on the effect of increasing the value of *y* it will be found that the value of *N* decreases. Using the conventional design approach that in a yield analysis the direct stress area is located in the central zone, *N* equal to 313.3N equates to strip of nail less than 0.1mm thick. This will have a negligible effect on the plastic modulus of the nail.

For steel sections, where the shear stress is less than 0.6 times the shear capacity, the effect of shear stress on the plastic modulus can be ignored [59, 125]. Adopting this criterion for nails, as the shear stress is much lower than 0.6 times the shear capacity of the nail the shear stress effect can also be safely disregarded.

The case for ignoring the effect of axial and shear force reductions to the yield moment in the nail is clearly demonstrated in this exercise.

In the 1994 issue of EC5 [11] it was accepted that the friction effect due to direct contact between the timber and the gusset plates should be ignored but that an allowance should be included in the appropriate failure mode equations for the tension effects from the nails. To cover for this, in the draft issue the relevant equations for joint strength derived from yield theory were multiplied by a factor of 10%. In the subsequent draft revisions this has been modified and a function has been included to cover the nail withdrawal resistance. Also the coefficients used in the basic yield equations have been altered.

From a review of the ULS equations, within the extreme values used for the variable parameters in the testing programme, for joints using fully overlapping nails Modes 1B, 2A and 3B type failures are potential options for the failure of plywood gusset plate joints and Mode 3A type failure for steel gusset plate joints. The relevant equations in EC5 [11] and [15] for these failure modes will be used for comparison with the appropriate model. These equations are given in the code in terms of the characteristic strength of a joint formed by a single nail acting in single shear as follows:

(i) EC5 [11]

for single shear joints with plywood gusset plates:

Mode 1A $$F_{v,Rk} = f_{h,p,k} t_p d \quad \text{....(152a)}$$

Mode 2A $$F_{v,Rk} = 1.1 \frac{f_{h,p,k} t_p d}{(2+\beta)} \left(\sqrt{2\beta(1+\beta) + \frac{4\beta(2+\beta) M_{y,Rk}}{f_{h,p,k} d t_p^2}} - \beta \right) \quad \text{....(152b)}$$

Mode 3B $$F_{v,Rk} = 1.1 \sqrt{\frac{2\beta}{(1+\beta)}} \sqrt{\left(2 M_{y,Rk} f_{h,p,k} d\right)} \quad \text{....(152c)}$$

for single shear joints with steel gusset plates:

Mode 3A $$F_{v,Rk} = 1.5 \sqrt{\left(2 M_{y,Rk} f_{h,p,k} d\right)} \quad \text{....(152d)}$$

(ii) EC5 [15]

for single shear joints with plywood gusset plates:

Mode 1A $$F_{v,Rk} = f_{h,p,k} t_p d \quad \text{....(153a)}$$

Mode 2A $$F_{v,Rk} = 1.05 \frac{f_{h,p,k} t_p d}{(2+\beta)} \left(\sqrt{2\beta(1+\beta) + \frac{4\beta(2+\beta) M_{y,Rk}}{f_{h,p,k} d t_p^2}} - \beta \right) + \frac{F_{ax,Rk}}{4} \quad \text{....(153b)}$$

Mode 3B $$F_{v,Rk} = 1.15 \sqrt{\frac{2\beta}{(1+\beta)}} \sqrt{\left(2 M_{y,Rk} f_{h,p,k} d\right)} + \frac{F_{ax,Rk}}{4} \quad \text{....(153c)}$$

for single shear joints with steel gusset plates:

Mode 3A $$F_{v,Rk} = 2.3 \sqrt{\left(M_{y,Rk} f_{h,w,k} d\right)} + \frac{F_{ax,Rk}}{4} \quad \text{....(153d)}$$

and $F_{ax,Rk}$ is the lesser of $(f_{ax,k}\, d t_w)$ or $(f_{ax,k}\, d t_p + f_{head,k}\, d_h^2)$ ....(154)

where, for smooth nails:

$F_{ax,Rk}$ = the characteristic withdrawal capacity of the nail for nailing perpendicular to the grain.

$f_{ax,k}$ = the characteristic point side withdrawal strength = $20 \times 10^{-6} \times \rho_k^2$.

$f_{head,k}$ = the characteristic head side pull-through strength. = $70\times10^{-6}\times\rho_k^2$ for $d_h \geq 2d$.

t_w = the point side penetration length (penetration of the nail into the timber).

t_p = the thickness of the head side member (plywood thickness).

d = the nail diameter-mm.

d_h = the nail head diameter-mm.

ρ_k = the characteristic density of the timber – kg.m^3.

$M_{y,Rk}$ = the characteristic value of nail yield moment – Nmm.

$f_{h,p,k}$ = the characteristic value of the embedment strength of plywood – N/mm^2.

$f_{h,w,k}$ = the characteristic value of the embedment strength of timber – N/mm^2.

β = the ratio of the embedment strength of the timber to the plywood.

To obtain the ULS capacity, the characteristic strength equations given above are converted to design strength in accordance with the requirements of equation (144):

$$F_{v.Rd} = k_{mod}\frac{F_{v,Rk}}{\gamma_M} \qquad \ldots.(155)$$

When comparing the Eurocode equations with the results from tests on joints, the value of k_{mod} is taken to be unity and from both versions of the code, γ_m is 1.3, giving:

$$F_{v.Rd} = \frac{F_{v,Rk}}{1.3} \qquad \ldots.(156)$$

The full value of the load in the joint will be obtained by multiplying equation (156) by the number of lines of nails in the joint and the effective number of nails in a row. The latter is taken as the number of rows of nails in EC5 [11] and as a function of the nail row spacing in EC5 [15] and is discussed in section 6.4.

In determining the strength of joints the two most significant factors in the equations are the nail yield moment and the embedment strength of the timber and plywood. A brief background comment on these factors is given in the following paragraphs together with some observations on their testing procedure requirements.

(i) Nail Yield Moment

When a nail is subjected to a moment and it is bent beyond the yield limit, it will eventually develop a plastic moment and, based on conventional plastic theory, the theoretical value of the plastic moment will be:

$$M_y = f_y Z_P \qquad \text{....(157)}$$

where Z_P is the plastic modulus of the nail. For a circle this will be $d^3/6$.

Because of the strain hardening effect in nail wire, the plastic moment (or yield moment as referred to in the Eurocode) will be higher than the theoretical solution based on equation (157). From research by Smith *et al* [126] into the strength of nails manufactured in the UK, when taking account of strain hardening it was concluded that nail yield strength could be expressed as $fy = (950\text{-}50d_{nom})$ $\pm$150 N/mm^2. Also in the pre-publication draft of EC5 it was proposed that the nail wire strength should be the average of the nail tensile strength and the yield strength [68]. In EC5 [11] the minimum tensile strength of the nail has been taken to be 600N/mm^2 and in EC5 [15] the actual nail strength of the nail wire has been used. The latter is also the strength that has been used for the nails in the modelling work used for joint strength in Chapter 4. After extensive testing in Germany the nail strength equation was adjusted to relate the yield moment to the tensile strength of the nail wire and its diameter [68] and the equation for the characteristic value of smooth round wire nails given in the EC5 [15] is:

$$M_{y,Rk} = \frac{f_u}{600} 180 d^{2.6} \qquad \text{....(158)}$$

where f_u is the minimum tensile strength of the nail and in EC5 [11] f_u is set equal to 600N/mm^2. It is to be noted that from the tests undertaken for the strength of the nails used in the programme, the mean strengths varied from 697 N/mm^2 to 829 N/mm^2.

The nail yield moment can also be determined using BS EN 409 [38] however, because of the nature of the loading frame required, the accuracy of the results using that method are to be questioned.

(ii) Embedment Strength

The embedment strength, f_h, is the average compressive stress at maximum load in a piece of timber or wood-based product under the action of a stiff straight dowel with its axis perpendicular to the surface of the timber and when loaded perpendicular to the axis.

For a piece of timber t mm thick, loaded with a nail d mm in diameter, under a maximum load F_{max} the embedment strength can be written:

$$f_h = \frac{F_{\max}}{dt} \qquad \text{....(159)}$$

Because of the complex cellular structure of timber and wood based products, the embedment strength is not a material property. It is a theoretical property. For joints using smooth round nails, it is dependent on the nail diameter; whether or not the material has been predrilled; the tolerance and size of the predrill used, and the material density.

As mentioned in Chapter 2, the embedment equations given in EC5 have been based on the research by Whale *et al* [41, 127]. In the research predrilling was used for all hardwood and no predrilling was used for softwood. The upper limit for softwood density used in the tests was only 500Kg/m^3. Different equations were derived for embedment in softwood and in hardwood and it was concluded that the difference was due to the effect of the predrilling [127]. This was subsequently adjusted in EC5. The same equations were adopted for softwood and hardwood with the difference solely relating to the whether or not predrilling was being used. For plywood, only one equation was used. The EC5 [11] and EC5 [15] equations for characteristic embedment strength relevant to timber with predrilled holes and to plywood are the same and are:

(i) Timber using nails up to 6mm in diameter with predrilled holes:

$$f_{h.k} = 0.082(1-0.01d)\,\rho_k \qquad \ldots.(160)$$

(ii) Plywood using nails with a head diameter of at least 2*d*:

$$f_{h.k} = 0.11\,\rho_k\, d^{-0.3} \qquad \ldots.(161)$$

In the research by Whale *et al* is was found that when using timber and plywood no grain orientation effects existed and the above equations will apply irrespective of the grain direction.

To check on the validity of the Eurocode rules for embedment, tests were carried out on the embedment strength of the timber and plywood being used in the programme in accordance with the requirements of BS EN 383 [37]. The standard does not give details of the type of rig to be used and from a review of the testing rigs developed by Aune *et al* [17] and also Rodd *et al* [40] the rig shown in Appendix A was designed and fabricated. The procedure used for the tests and photographs of the test set-up are also given in Appendix A.

BS EN 383 sets an upper limit of four times the nail diameter as the maximum thickness of material to be used in an embedment test. This requirement is imposed to ensure that all of the test energy will be used to compress the timber/plywood with only a small risk of some being used to bend the nail. The samples were predrilled in line with the predrilling criteria used for the test joints and care had to be taken to ensure the predrilled hole was exactly perpendicular to the timber face. Unless this was achieved, it was found that invariably the timber would split as the nail was secured onto the rig.

For timber based products the code states that the test piece shall be the thickness of the panel. Using 17mm plywood with 2.65mm nails results in an aspect ratio of 6.4, which well exceeds the limit of 4 given in the code, leading to premature failure by bending in the nail rather than embedment failure of the plywood. Preliminary tests were carried out using full thickness plywood and the nails did indeed fail by bending and the test results were unsatisfactory. The tests were redone using plywood reduced in thickness to approximate four times the nail diameter and the results of these tests are given in Table 6.2.

Samples of timber, three times the nail thickness, were initially used but it was found that at this thickness the samples were consistently failing by splitting. The thickness had to be increased and the final ratio of sample thickness to nail diameter used was as given in Table 6.1.

Nominal nail diameter	t/d ratio – timber and plywood
2.65	4.4
3.00	3.9
3.35	3.5

Table 6.1 Ratio of material thickness to nail diameter used in embedment tests

The use of a 4.4 ratio for the timber samples was found to be necessary to prevent timber splitting. However, if using material with a high density, with this ratio the 2.65mm nails suffered permanent deformation. This also occurred in the plywood tests where the density was 740Kg/m^3. It did not occur when the density was 550 Kg/m^3 and only these test results have been used.

The overall load-slip behaviour of timber samples was similar to that found by Whale *et al*. There was a uniform slope to the load-displacement graph up to a maximum load, which was generally sustained as the slip continued. The load started to fall away around 70% to 80% of the failure load, which normally occurred within a slip of 1mm to 2mm from the start of the test. The tests results using plywood were different. With plywood there was no definitive failure load. As the load increased, there was a gradual reduction in the load being taken but there was no clearly defined failure limit. However it was found that in these tests the load-slip curve had a close fit with the displacement function derived in Chapter 4 for laterally loaded joints with plywood gusset plates. To obtain the embedment figure, a slip limit had to be selected. BS EN 383 sets an upper limit of 5mm however, as the testing programme has limited nail slip to a maximum value of 3.2mm, this value has been used to derive the embedment strength.

Typical examples of embedment test results using timber and plywood samples are given in Figure 6.2.

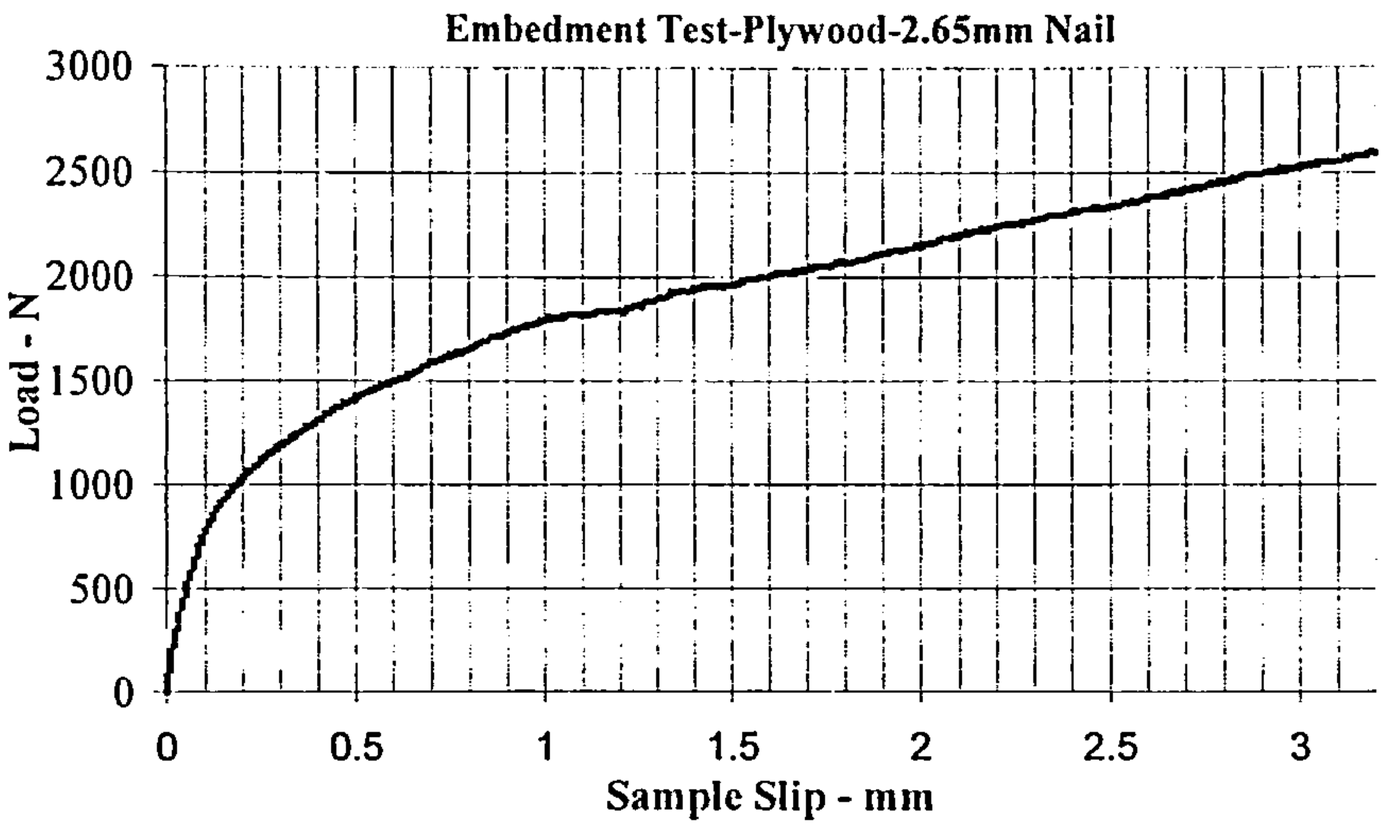

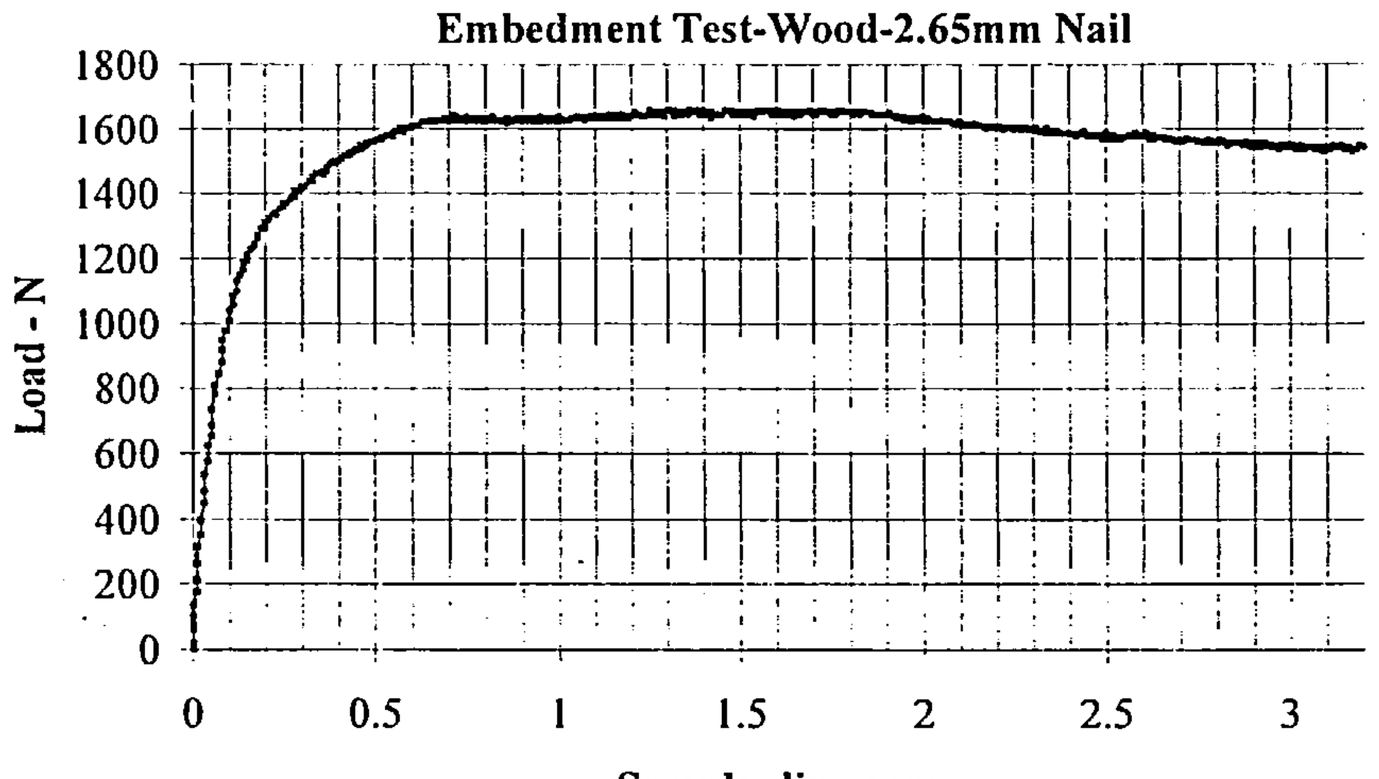

Figure 6.2 Embedment test results

To compare the results, the embedment strength has been divided by the density of the timber or plywood test sample. The results are given in Table 6.2 for the three nail sizes used in the programme together with the associated standard deviation and coefficient of variation values.

To convert the strengths to characteristic values, a factor of 0.853 has been applied to the average density used in the tests. This is the statistical factor required to convert an average value to a 5-percentile value assuming a log-normal distribution and a coefficient of variation of 10%. The average moisture content of the timber and plywood samples was 11.72% and 9.13% respectively and as nail strength is not a factor in the embedment test, the tests were only carried out using Rynail nails.

There is no clear pattern of behaviour from either the timber or the plywood test results. The unit density embedment figures show no relationship with the nail size or between the two materials. As stated earlier, the success of the test was found to be very sensitive to the accuracy of the alignment

of the nail through the sample and it could be that this has had an effect on sample behaviour and embedment strength. If this is the case, because of the importance of embedment strength in determining ultimate strength behaviour, more thought needs to be given to the significance of the test rig set-up used and the procedure to be followed in BS EN 383 [37].

Nail size/ material	Number of tests	Average embedment strength	Standard deviation	Coef. of variation
2.65mm ø in timber	5	0.1052 $N/mm^2/kg/m^3$	0.0048 $N/mm^2/kg/m^3$	0.046
3.00mm ø in timber	5	0.1261 $N/mm^2/kg/m^3$	0.0072 $N/mm^2/kg/m^3$	0.057
3.35mm ø in timber	5	0.1027 $N/mm^2/kg/m^3$	0.0027 $N/mm^2/kg/m^3$	0.026
2.65mm ø in plywood	5	0.1600 $N/mm^2/kg/m^3$	0.0105 $N/mm^2/kg/m^3$	0.049
3.00mm ø in plywood	5	0.1480 $N/mm^2/kg/m^3$	0.0073 $N/mm^2/kg/m^3$	0.055
3.35mm ø in plywood	5	0.1243 $N/mm^2/kg/m^3$	0.0050 $N/mm^2/kg/m^3$	0.040

Table 6.2 Embedment test results

A comparison of the unit density embedment strength from the tests and the equivalent values obtained from equations (160) and (161) divided by the characteristic density of the timber and the plywood respectively, is given in Table 6.3.

The test results consistently exceed the Eurocode values. For timber, the average exceedance is 19.35% and with plywood it is 54.45%. Also, in the case of the plywood results, the values were determined at a slip of 3.2mm and the BS EN 383 requirement is that the upper limit of slip should be 5mm. If this were used the difference with the EC5 result would be of the order of 65%.

Although the level of difference in the case of the timber results can be tolerated, the difference in the plywood results is extreme. Because of the importance of this function in the strength equations, it is to be recommended that the test equipment requirement and test procedure are reviewed and further consideration is given to the slenderness ratio criteria to be used for the plywood tests.

Nominal nail diameter mm	Material	Test embedment /characteristic density $N/mm^2/(kg/m^3)$ A	EC5 embedment /characteristic density $N/mm^2/(kg/m^3)$ B	Difference (A-B)/A %
2.65	Timber	0.08974	0.0798	+12.43
3.00	Timber	0.10757	0.0796	+35.2
3.35	Timber	0.08756	0.0793	+10.41
2.65	Plywood	0.13652	0.0802	+66.44
3.00	Plywood	0.12626	0.0793	+59.11
3.35	Plywood	0.10605	0.0766	+37.81

Table 6.3 Comparison between test and EC5 embedment results.

6.2.2.2 Serviceability Limit State Strength

Joint strength at the SLS is obtained by multiplying the design strength equation (156) by the ratio of the loading at the SLS to the loading at the ULS. At the SLS the partial load factors are taken to be unity and the function will become:

$$F_{d.ser} = F_{v.Rd}\left(\frac{G_K + Q_K}{(\gamma_G G_K + \gamma_Q Q_K)}\right) \quad \ldots.(162)$$

6.2.3 Joint stiffness criteria

6.2.3.1 General

Timber has a relatively low stiffness-to-strength ratio resulting in comparatively flexible structural systems. The focus of code development in most countries has been on the ULS and as a result serviceability requirements, where they exist, may be insufficient to ensure acceptable building performance [129]. Although the significance of the potentially catastrophic consequences associated with a violation of joint strength criteria is readily understood, failure by non compliance with stiffness criteria is likely to be the more common reason for problems arising during the design life of a structure.

The stiffness of a joint is the ratio of the load in the joint divided by the joint slip and from this relationship the joint slip can be obtained at any particular load. In EC5 the stiffness property is referred to as the slip modulus. With steel and concrete, a stiffness property is only given for the SLS [58, 59], but for timber, different values are given for the SLS and the ULS.

When timber design codes were based on a permissible stress design approach, stiffness criteria was given at the working load condition and in most codes the slip limit for joints was set at 0.15 inches, nominally 0.4mm [72, 86, 87, 88]. In EC5, different values of stiffness are given for the SLS and the ULS and no limit is set for the joint slip at these states. It is left to the designer to decide on the value of slip that will be acceptable for the structure being designed.

EC5 refers to joint stiffness as the slip modulus and an instantaneous slip modulus is given for the SLS, K_{ser}, and for the ULS, K_u. The derivation of each modulus is given in the following sections, starting with the SLS slip modulus, which is the more important.

6.2.3.2 Serviceability Limit State Stiffness

In EC5 the instantaneous slip modulus for SLS design, K_{ser}, is taken to be the secant modulus of the load-displacement curve at a load level of approximately 40% of the load carrying capacity of the joint [68]. The use of a 40% factor was adopted as it was in line with the safety factor of 2.5 that was being used in most permissible stress design codes and which had been used as a benchmark for the calibration of the materials factor [128]. Also, the approximation to a straight line relationship up to this limit was considered to be acceptable relative to the actual joint behaviour.

The original solution derived in EC5 for the modulus was based on the use of design properties and on property values which had been recommended prior to its publication in 1994. Because of the importance of the modulus and of its relationship to the model behaviour, the derivation of the property is given. The modulus was developed assuming that the most common type of failure in joints would be Mode type 3. Using the design strength based on the Johansen theory, the load carrying capacity of a Mode3 type joint can be written as:

$$F_{v,Rk} = \sqrt{\frac{2\beta}{(1+\beta)}}\sqrt{2M_{y,Rk} f_{h,w,k} d} \qquad \ldots.(163)$$

where:

$M_{y,Rk}$ = the nail yield moment. At that time the value was $180d^{2.6}$

$f_{h,w,k}$ = the characteristic embedment strength of the timber. Using predrilled holes, the value is $0.082(1\text{-}0.01d)\,\rho_k$ - (equation (160))

β = the ratio of the timber to gusset plate embedment strength, and taken to be unity.

For smooth round wire nails, substituting for the above into equation (163), the load carrying capacity (ULS) of the joint can be expressed in terms of the nail diameter and the characteristic density of the joint materials, ρ_k as:

$$F_{v,Rk} = \sqrt{(360d^{2.6})(0.082(1-0.01d))\rho_k} \qquad \text{....(164)}$$

From the results of many tests on joints with predrilled holes available from various test laboratories, the slip at the serviceability limit state at approximately 40% of the load carrying capacity of the connector was found to be as given in equation (1). The instantaneous slip modulus is obtained by multiplying equation (164) by 0.4 to reduce the load to the SLS condition and dividing by equation (1):

$$K_{ser} = \frac{0.4F_{y,Rk}}{\delta_{inst}} = \frac{0.5433}{100}\sqrt{(100-d)d\rho_k^{1.5}} \qquad \text{....(165)}$$

for nails between from 2 to 8mm diameter, equation (165) can be simplified to:

$$K_{ser} = \frac{\rho_k{}^{1.5}d}{19.19} \qquad \text{say } \frac{\rho_k{}^{1.5}d}{20} \qquad \text{....(166)}$$

Equation (166) was used as the instantaneous slip modulus at the SLS in the 1994 draft issue of EC5 [11] and is the force in N/mm per shear plane per fastener. In the latest issue of EC5 [15] the modulus has been adjusted and is now based on the mean rather than the characteristic value of density. Assuming a log-normal distribution for the density property, the characteristic value can be shown to be k_l times the mean value [13], where:

$$k_l = e^{(-(2.645+\frac{1}{\sqrt{n}})v+0.15)} \qquad \text{....(167)}$$

where n is the number of tests done and v is the coefficient of variation.

Using the minimum number of tests, n = 5, and assuming the minimum value of the coefficient of variation (v = 0.1) is achieved, from equation (167) the coefficient k_l will be 0.853. Incorporating this factor into equation (166), the value of the modulus in terms of the mean density ρ_m becomes:

$$K_{ser} = \frac{\rho_m{}^{1.5}d}{25.3} \qquad \text{say } \frac{\rho_m{}^{1.5}d}{25} \qquad \text{....(168)}$$

If the density of the timber based materials in the joint differs, as will normally be the case, the value of mean density ρ_m to be used in the equation will be:

$$\rho_m = \sqrt{\rho_{m1}\rho_{m2}} \qquad \text{....(169)}$$

where ρ_{m1} and ρ_{m2} are the characteristic densities of the respective materials. The same value of modulus was also to be used for steel to timber joints, which was clearly an error, and has since been corrected in EC5 [15]. Also, in EC5 [15] the instantaneous slip modulus for nails in timber to timber and timber based panel to timber connections has been further adjusted to take into account the effect of alterations that have been made to the basic joint strength equation (163) and is now:

$$K_{ser} = \frac{2}{3} \times \frac{\rho_m^{1.5} d}{35} \qquad \ldots.(170)$$

In EC5 [15], for steel to timber connections, the modulus may be multiplied by 2.

The instantaneous slip modulus for the SLS was initially developed from the Johansen strength equation without the addition of any factor to include for the nail tension effect referred to in section 6.2.2.1. In the 1994 issue of the code a tension factor of 1.1 was included and in the latest draft, for joints made from timber with timber (or plywood) gusset plates, the strength is given by equation (153c). This has increased the basic Johansen strength by at factor of 1.15 and it also incorporates an additional factor to cover for the nail withdrawal resistance. As a conservative estimate the combined factor will be in excess of (1.1×1.15) and including for this the instantaneous slip associated with the slip modulus in the latest draft of the code can be estimated.

To check on the EC5 value for nail withdrawal resistance, some nail withdrawal tests were carried out on timber and also on plywood. For timber, point side withdrawal tests were undertaken and for plywood, head side tests were carried out. In the latter the nail was positioned such that the head was clear of the plywood surface to enable an element of point side penetration to also be measured before the nail head made contact with the plywood. To eliminate the effect of variation in density, the same sample of timber and plywood was used for all of the tests. Five tests were carried out for each nail size for the timber tests and five, using only 3.00mm diameter nails, for the plywood tests. A typical test result for timber and for plywood using Castlenail nails is shown in Figure 6.3.

The timber sample was 44mm thick and the plywood was 18mm thick. In the timber point side penetration tests, there was a reasonably linear increase in withdrawal resistance up to a maximum at a slip, which for all tests, gave an average of approximately 0.23mm. In the case of the plywood penetration tests, there was also a linear increase up to a maximum point side resistance at about 0.07mm slip after which it followed a fluctuating path varying between a maximum and minimum value until the nail head started to make contact with the plywood. At this point the level of fluctuation started to reduce until it was eliminated when there was complete contact with the nail head. As the nail was drawn further into the plywood the resistance increased at a uniform rate. Although the test was stopped after a slip of 2.5mm the nail head side resistance was increasing and showing no sign of tailing off and levelling out.

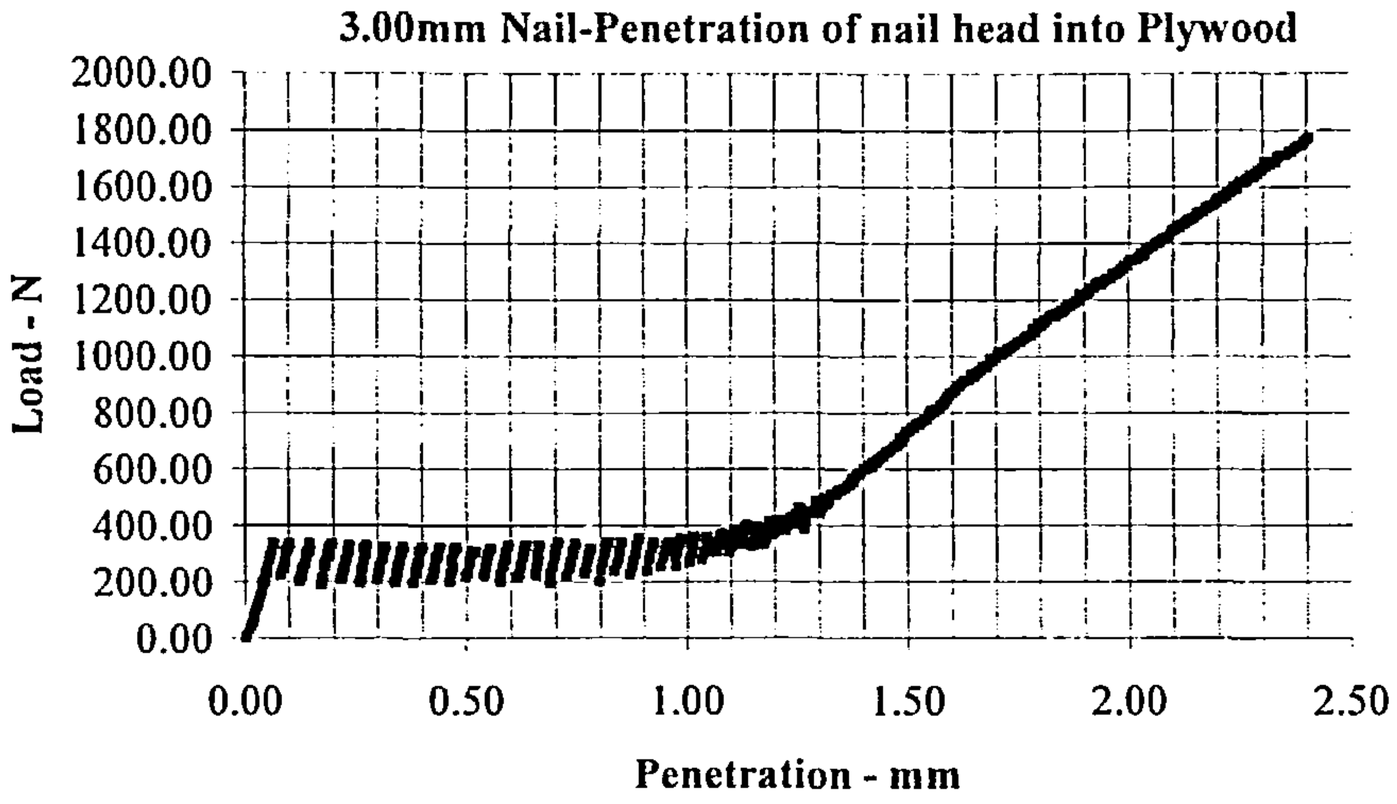

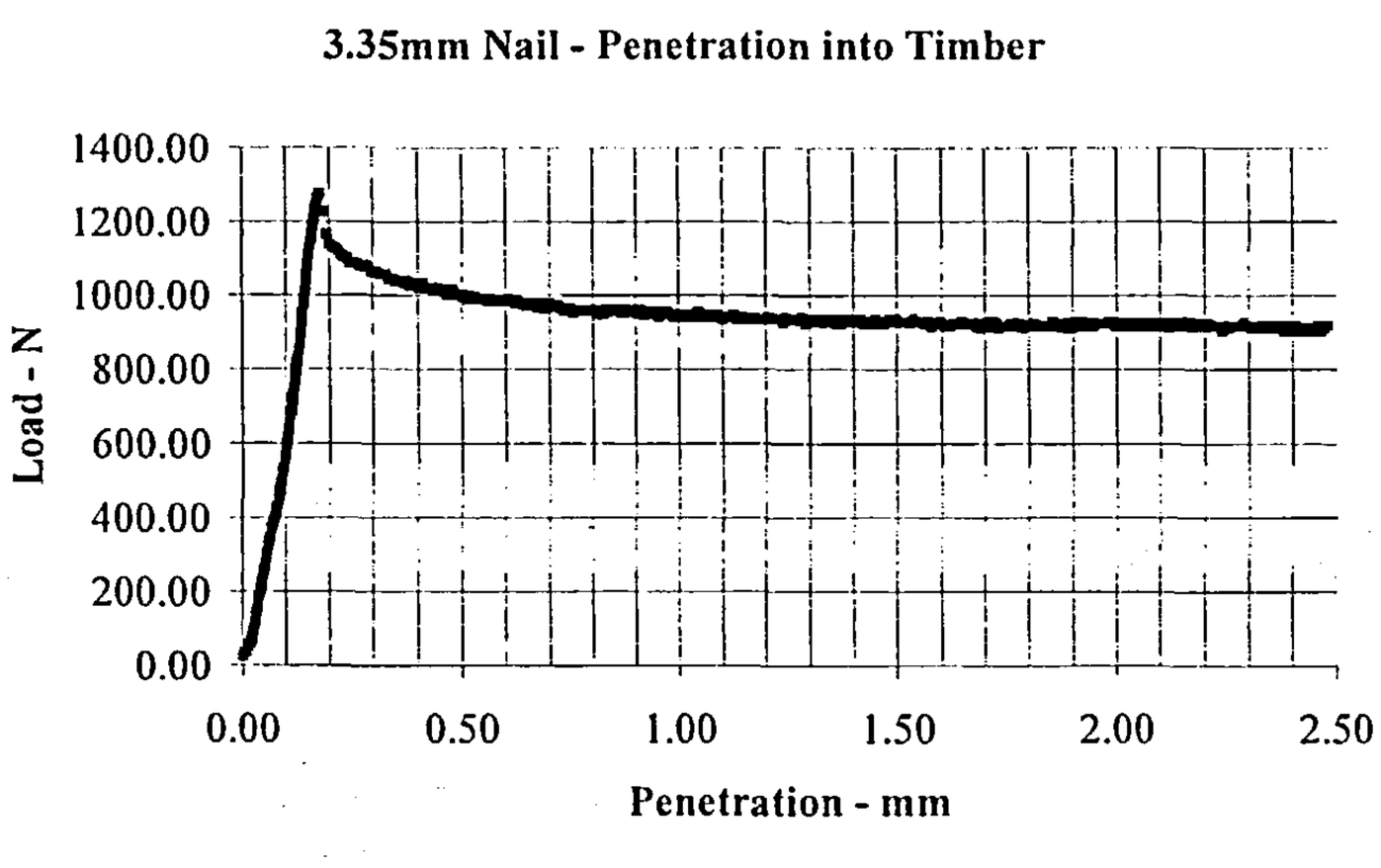

Figure 6.3 Withdrawal test results of a nail into timber and into plywood

The characteristic value of the nail point side withdrawal strength compared with the equivalent value in EC5 [15] is given in Table 6.4. The head side pull through strength is not given in the Table as the test result well exceeded the Eurocode value and the limiting criteria in the test programme will be point side withdrawal.

In general the test strengths varied with the nail size, but on a random basis. The plywood result was about 21% below the Eurocode value and the timber results all exceeded the Eurocode values by varying percentages. The variation was considered to be likely to be due to sample related factors and matters associated with nail size and it is considered that the Eurocode equations will predict an acceptable result for this property.

From EC5 [11] , using the load factor of 40%; including for the tension factor of 1.1; based on the use of mean rather than characteristic density, the relationship between the nail slip and the instantaneous slip modulus at the SLS can be reduced to:

$$\frac{0.4\times1.1}{40}\approx\frac{1}{25} \qquad \ldots.(171)$$

Similarly, using EC5 [15], the equivalent relationship will be:

$$\frac{0.4\times1.1\times1.15}{x}\approx\frac{1}{35}\times\frac{2}{3} \qquad \ldots.(172)$$

Adopting the same relative relationship for each version of the code, equating equations (171) and (172), the value of x will be 96.6. On this basis, in EC5 [15] the instantaneous slip at the SLS is approximately:

$$\delta_{inst} = 96.6d^{0.8}/\rho_m \qquad \ldots.(173)$$

The result has been to increase the slip at the SLS by approximately 140% over the value used in EC5 [11]. The final slip however is also a function of the SLS load and the combined effect is addressed in the comparison studies given section 6.4.

Material	Nominal nail diameter mm	Material density kg/m^3	Characteristic point-side withdrawal from tests	EC5 point-side withdrawal Strength	Percentage Difference
Timber	3.35	566.00	1179	942	+26.16
Timber	3.00	566.00	1583	857	+84.75
Timber	2.65	566.00	830	749	+10.85
Plywood	3.00	511.00	274	347	-21.11

Table 6.4 Comparison between nail point side withdrawal strength from tests and from EC5 [15]

6.2.3.3 Ultimate Limit State Stiffness

In EC5 [11], the instantaneous slip modulus for the ULS – denoted K_u – is taken to be the secant modulus of the load slip curve at a load level of approximately 60% to 70% of the maximum load. The load level is that associated with the ULS design load of the joint and is obtained from the $\frac{k_{\text{mod}}}{\gamma_m}$ factor applied to the characteristic load. At this load, the stiffness of the joint has been taken to be approximately two thirds of the stiffness at the SLS and the instantaneous slip modulus in EC5 [11] and EC5 [15] is approximated to:

$$K_u = \frac{2}{3} K_{ser} \qquad \ldots.(174)$$

In limit state philosophy the ULS is that state corresponding to structure collapse or any other state which may endanger the safety of people or result in considerable financial loss and for timber structures it is difficult to see where the ultimate limit deflection of a structure will become the ULS failure condition.

6.3 CONVERSION OF MODEL TO CHARACTERISTIC STRENGTH

6.3.1 General

6.3.1.1 Models to be used in the Comparison Exercise

In Chapter 4, models have been developed for timber joints with 6mm thick steel gusset plates and for timber joints with plywood gusset plates of varying thickness. In the case of the steel gusset plate joints, alternative models have been developed to account for the effect of varying the size of the predrill used in the gusset plate. Also, different methods of assembly have been used in both types of joint to investigate the friction effect in joints with and without a space between the gusset plates and the timber.

In EC5, steel gusset plate joints are classified into two categories. Joints in which the thickness of the gusset plate is less than 0.5 times the nail diameter are called thin plate joints. Those with a thickness greater than 0.5 times the nail diameter are called thick plate joints and in EC5 [15] a further requirement that the predrilled holes in the gussets must be less than 1.1 times the nail diameter is also included. The comparison between the model and EC5 for joints with steel gusset plates will be based on the use of thick plate joints.

As confirmed by Ehlbeck *et al* [68], the ultimate strength equations used for joints in EC5 [11] do not include for joint friction effects. The only factor included for in the published code is a nail tension effect where a factor of 1.1 has generally been incorporated into the relevant strength equations. Also, from the testing work done for the code during the code development and calibration period, the joints were fabricated with small gaps between the joint members. This provided a lower-bound estimate of strength and stiffness, eliminating the frictional interactions between the members [53, 127]. Further, despite the requirement in EC5 that nails be driven to a depth that the surface of the nail heads are flush with the timber surface, in these tests the nail heads were not fully driven home into the side members.

Taking the above into account, for the comparison with EC5 the model equations to be used for joints with steel or plywood gusset plates will be those applicable to joints assembled with a gap between the timber and the gusset plate.

6.3.1.2 Probability Distribution Function to be used

The testing programme has been carried out with materials that have had a relatively limited variation in strength and as such it is not possible to determine from the programme the probabilistic distribution function which should be used to represent the joint behaviour.

From a review of the distribution function options available, the Log-Normal probability distribution function, which is logarithmically related to the Normal function, has been selected. It has been extensively applied to model material strength phenomena [130] and, together with the 2-parameter Weibull distribution function, it is the function commonly used for timber related properties [131]. It is however to be noted that where there is a relatively small coefficient of variation, say 0.1 or less, it does not matter very much what function is used as there are only small differences between the distributions [132].

The strength values will be based on the 5 percentile value estimated as the lower endpoint in the one-sided 84.1% confidence interval and the coefficient of variation taken to be 0.1 or the value derived from the test results, if greater. From the results of the tests the coefficient of variation was less than 0.1 and based on a sample size of 5 for each test set, from equation (167), the coefficient used to convert the mean value to the 5 percentile value is 0.853.

The model equations have been developed from the analysis of mean value properties and the 0.853 coefficient has been incorporated into the equations to equate to the EC5 strength equations.

6.3.2 Model Applied to Joints with Steel Gusset Plates

In Chapter 4, the model equations for joints with thick steel gusset plates predrilled with holes less than 1.1 times the nail diameter and with a gap between the gusset plates and the timber and using fully overlapping nails, developed from the use of mean properties, are given in equations (41a) and (41b). These give the failure load at a slip of 3.2mm based on mean properties and by incorporating the statistical factor of 0.853 are converted to characteristic models as follows:

(i) for nail row spacing between $0.7\times2\times5\times d$ and $0.7\times4\times7\times d$:

$$P\delta_{x(char)} = 0.853AD(d)^{1.4468} f_u r(0.7428+0.0132(Sp/d))n(1-e^{-1.712\delta x})^{0.926}(0.1\delta x + 0.68)/f(mc) \quad \ldots.(175a)$$

(ii) for nail row spacing exceeding $0.7\times4\times7\times d$:

$$P\delta_{x(char)} = 0.853AD(d)^{1.4468} f_u rn(1-e^{-1.712\delta x})^{0.926}(0.1\delta x + 0.68)/f(mc) \quad \ldots.(175b)$$

Comparison between these equations and the equivalent Eurocode strength equations is given in section

6.4.

6.3.3 Model applied to joints with plywood gusset plates

In chapter 4 the model developed for joints with plywood gusset plates is applicable to joints with slips up to 3.2mm to provide a common basis of comparison with the behaviour of joints made with steel gusset plates. However, as these joints will continue to take an increasing load beyond the 3.2mm slip, the failure condition model to be used for comparison with the EC5 ultimate limit state equations is developed below.

From a review of the joint behaviour, it was observed that beyond approximately 3.5mm slip the load taken by joints with 3.35mm diameter nails started to fall off and show signs of failure. With 3.00mm diameter nails the signs of failure did not appear until higher slips and with 2.65mm diameter nails, there was no sign of load reduction even up to slips of 7.00 mm or more.

A review of the displacement functions was undertaken for each nail size up to a joint slip of 5.00mm. The review followed the approach used in Chapter 4, fitting against the generalised four parameter-non linear exponential equation (54):

$$f_{p1}(\delta_x) = (1 - e^{C\delta r/3.2})^D(A\,\delta_x/3.2 + B) \qquad \ldots(54)$$

To determine the constants A, B, C and D the reduced load graphs of a selection of the 2.65mm, 3.00mm and 3.35mm diameter joint tests were combined to form a data base for each nail size against which least squares non linear regression analysis fits using Mathcad [51] were performed. The data bases were also aggregated to enable a least squares non linear regression fit to be obtained for the combined nail diameters. The joint configurations selected for each nail diameter are given in Table 6.5 and at least five replicates were used for each test set:

Tests set nominal nail diameter	Nail configurations used
2.65	CO; ED; EG; EJ; EK; EQ
3.00	CO; ED; EJ; EK; EQ
3.35	CO; ED; EG; EH; EJ, EK

Table 6.5 Joint configurations used for test sets

The above data was that used in Chapter 4 for the analysis of plywood joints up to 3.2mm slip and had been converted to reduced data at that slip. In this exercise the data is still applicable and has been extended up to a 5.00mm slip. The data was processed using Excel [50] as discussed in Chapter 4.

The least squares non linear regression fit was again carried out using the G*enfit* function within Mathcad [51] and on this occasion the regression coefficients for the four constants were used. The displacement functions obtained are given in equations (176) to (179) and are also plotted against the associated reduced load data plots on Figure 6.4. The displacement function is shown as a solid line.

Nail Diameter	**Displacement Function**	
2.65mm	$f_{p265e}(\delta_x) = (1\text{-}e^{-1.513\delta x})^{0.533}(0.101\delta x + 0.681)$	....(176)
3.00mm	$f_{p300e}(\delta_x) = (1\text{-}e^{-1.64x})^{0.565}(0.095x + 0.702)$	....(177)
3.35mm	$f_{p32e5}(\delta_x) = (1\text{-}e^{-1.085\delta x})^{0.523}(0.066\delta x + 0.802)$	....(178)
All diameters	$f_{palle}(\delta_x) = (1\text{-}e^{-1.406\delta x})^{0.54}(0.088\delta x + 0.725)$	....(179)

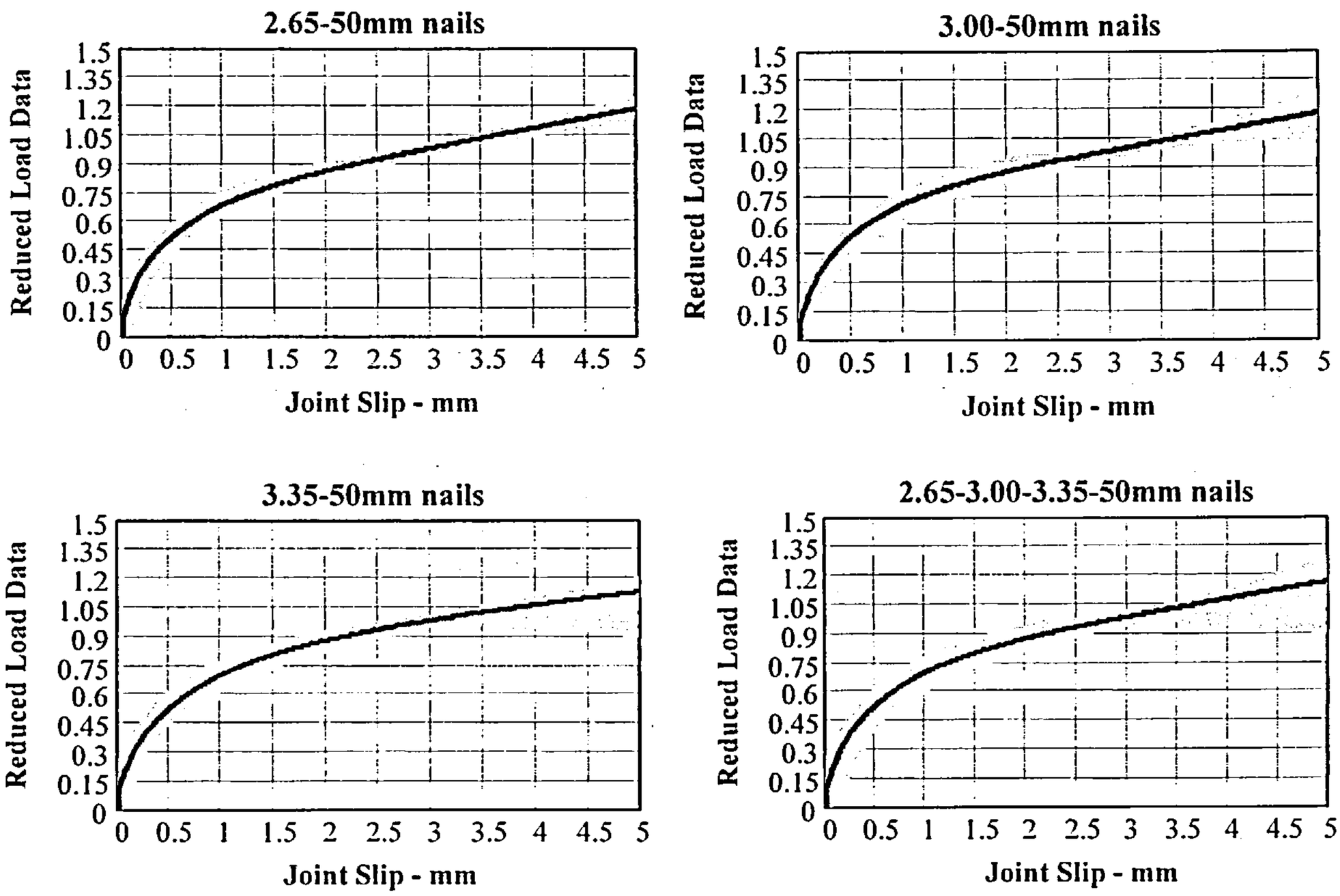

Figure 6.4 Regression graphs for 2.65mm; 3.00mm; 3.35mm diameter nails and for the all nail size fit.

To show that the function fits well with the displacement function for plywood joints up to 3.2mm slip, given in equation (62), the functions were plotted against one another and the result is shown on Figure 6.5.

From the graph alignment it can be seen that the functions are effectively the same. There is a marginal deviation at the upper end of the slip range but it is not significant for analysis purposes. The coefficient of determination for the combined fit data is 0.993 and the displacement functions in equations (176) to (179) inclusive are shown together in graphical form on Figure 6.6.

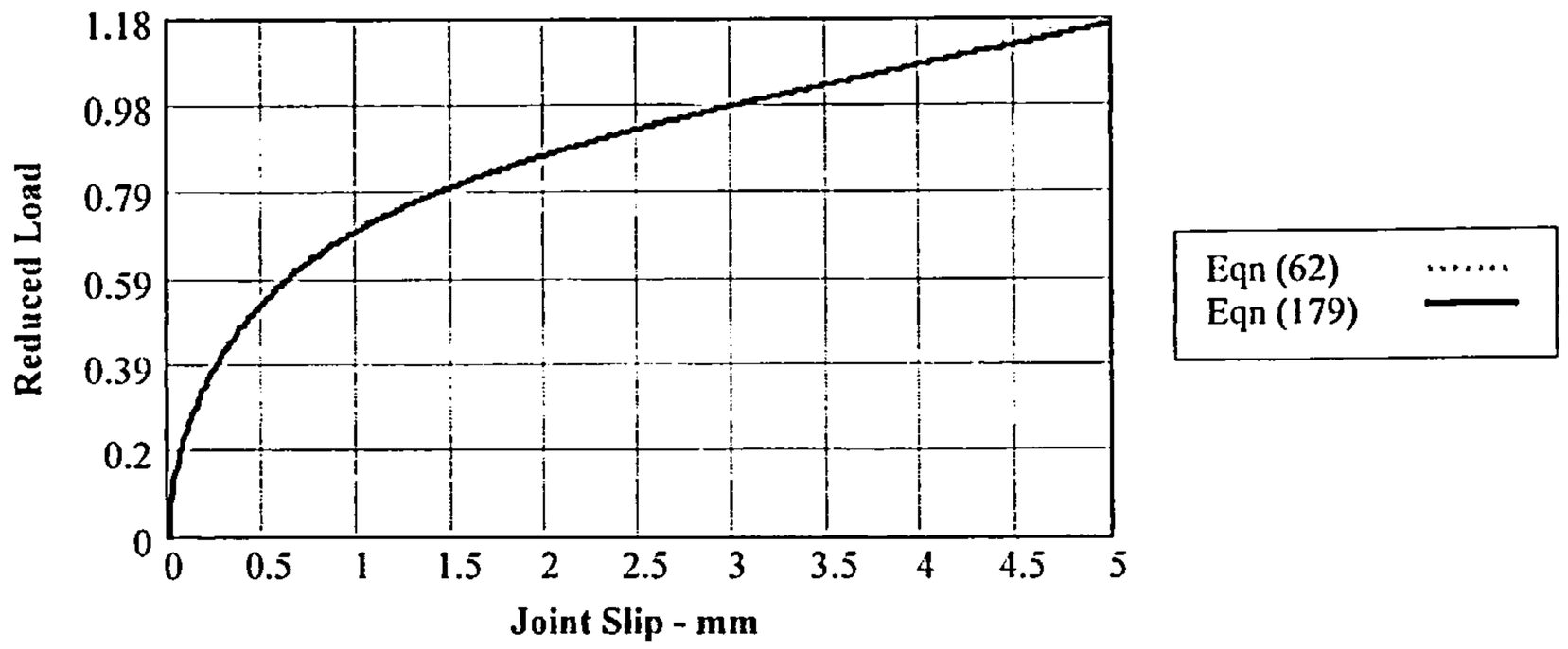

Figure 6.5 Regression graphs in equations (62) and (179) against the combined 2.65mm; 3.00mm and 3.35mm nail joint data up to 5.00m slip.

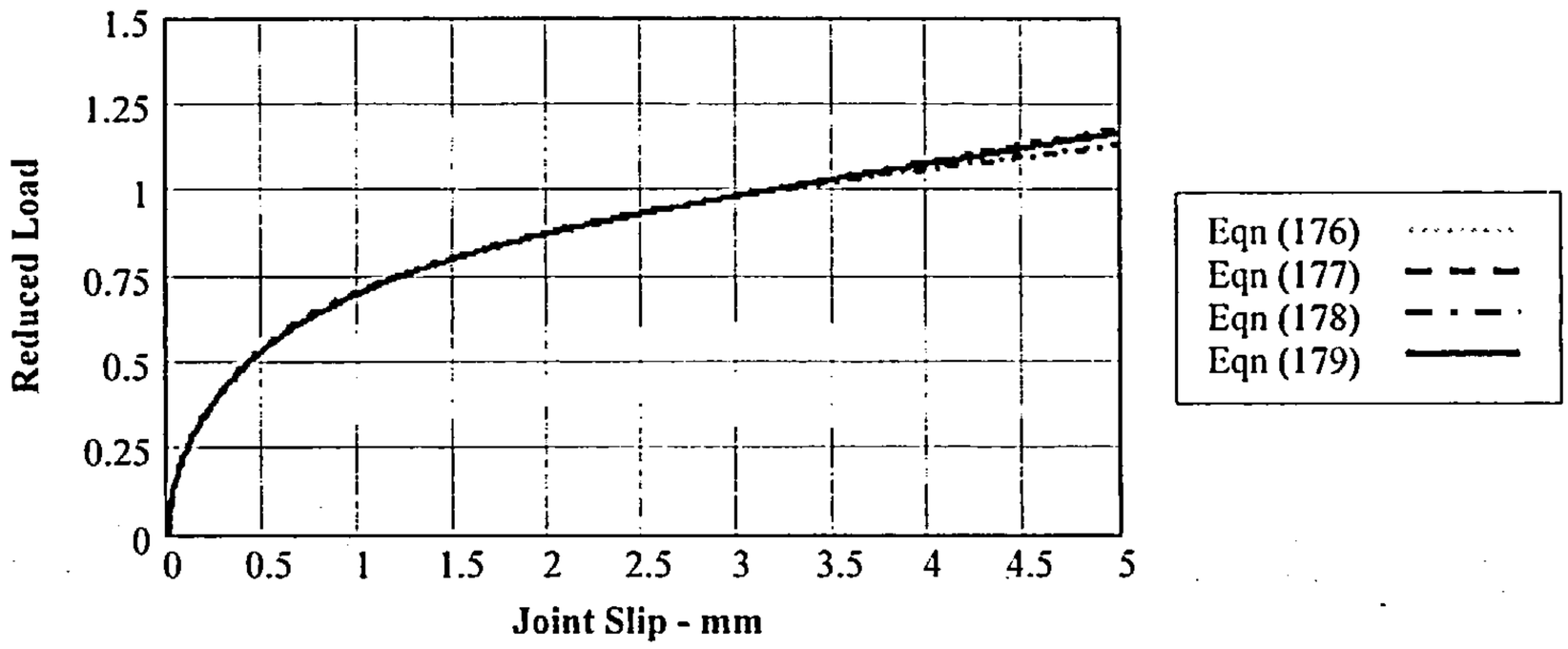

Figure 6.6 Displacement Functions given in equations (176),(177),(178) and (179)

From Figure 6.6 it is seen that the displacement function for each nail diameter is almost the same up to 3.5m slip. Beyond that the 3.35mm diameter nail displacement function starts to fall off and the combined displacement function overestimates the strength by just over 3%. From a comparison between the test results and the joint model incorporating equation (179) as the displacement function, the optimum limit of slip for the function has been assessed to be 4.5mm. This is taken to be the failure limit for all joints with plywood gusset plates and at this slip the value of the displacement function equates to 1.12.

Using the displacement function in equation (179) and incorporating the relevant functions from equation (85), the load-displacement model becomes:

(i) for nail row spacing between $0.85\times2\times5\times d$ and $0.85\times4\times5\times d$:

$$P\delta_{xe} = Ae(\text{Density Function})(d)^{2.236} f_u r(0.839+0.009489(Sp/d))n(1-e^{-1.406\delta x})^{0.54}(0.121\delta x+1) \quad \ldots.(180a)$$

(ii) for nail row spacing exceeding $0.85\times4\times5\times d$:

$$P\delta_{xe} = Ae(\text{Density Function})(d)^{2.236} f_u rn(1-e^{-1.406\delta x})^{0.54}(0.121\delta x+1) \quad \ldots.(180b)$$

where the functions remain as defined for equation (85) and constant $Ae = 2.24064\times10^{-4}$. Note this also includes for the effect of adjusting the value of constant B to equate to unity to simplify the function.

Semi-empirical model equations (180a) and (180b) apply to joints with plywood gusset plates of variable thickness assembled with a nominal gap between the plates and the timber; connected by fully overlapping nails in predrilled holes in accordance with the requirements of EC5 [15]; with nail lines of the same configuration and with uniform row spacing, subjected to short term lateral loading.

A comparison of some of the test results with the model is given in Tables 6.6 to 6.8. The difference between the model and the test result is also given, with a negative sign indicating underestimation and a positive sign indicating overestimation by the model. The majority of the testing was carried out using 19mm nominal thickness plywood and some examples of the model applied to joints using 9mm nominal thickness plywood are also given. From the tables it can be seen that there is a good fit between the semi-empirical model and the average test results at 4.5mm slip. A more accurate fit would have been obtained by deriving the displacement function at the 4.5mm slip rather than extending the graph based on a fit at 3.2mm slip. However the difference would not have been significant and the rework involved would not have been justified.

The results of some of the joint tests and the model have been plotted together for comparison and are presented in Figure 6.7. In the figure the model result is represented by the solid line. The results, which are typical of the test set results, show that there is a good fit with the model over the full length of the displacement curve. The tailing away of the test loads in joints using 3.35mm diameter nails is shown in the graphs for joints Pe43 and Pe48. The fit at a load of approximately 34% (ie 0.853 times 40%) of the $P_{4.5}$ load, equivalent to the load at the SLS of the joint, compares very well with the test sets, giving a good basis for comparison with the EC5 joint strength and stiffness at that condition

Equations (180a) and (180b) model the failure load of the joint based on average properties. Incorporating the statistical coefficient of 0.853 given in section 6.3.1.2 to convert the model to the 5 percentile failure load, the equations become:

(i) for nail row spacing between $0.85\times2\times5\times d$ and $0.85\times4\times5\times d$:

$$P\delta_{xe(char)}=0.853(Ae)(DensityFunction)(d)^{2.236}f_u r(0.839+0.009489(Sp/d))n(1-e^{-1.406\delta x})^{0.54}(0.121\delta x+1) \quad \ldots.(181a)$$

(ii) for nail row spacing exceeding $0.85\times4\times5\times d$:

$$P\delta_{xe(char)} = 0.853(Ae)(Density\ Function)(d)^{2.236}f_u rn(1-e^{-1.406\delta x})^{0.54}(0.121\delta x +1) \quad \ldots.(181b)$$

Comparison between equations (181a) and (181b) and the Eurocode strength equations is given in section 6.4.

Test ref	Nailing conf'n-number of nails	Row spacing (mm)	Number of rows	Average timber density (kg/m^3)	Average plywood density (kg/m^3)	Average penetration of nail into timber (mm)	Average thickness of plywood (mm)	Model load (N)	Test load (N)	% error (%)
Pe1	RT-16	23	4	556.14	607.84	41.62	17.64	15873.22	15252.61	+4.07
Pe2	ED-20	33.33	5	549.93	471.55	42.13	17.12	16912.80	17048.1	-0.79
Pe3	ED-20	33.33	5	552.71	475.24	42.13	17.12	17028.66	17581.84	-3.15
Pe4	RZC-24	33.33	6	534.58	683.37	41.02	18.22	27345.7	27200.91	+0.53
Pe5	RZC-24	33.33	6	551.12	555.72	41.20	18.05	23471.64	23392.33	+0.34
Pe6	ER-28	33.33	7	548.16	456.61	42.01	17.20	23212.61	23687.24	-2.00
Pe7	ER-28	33.33	7	535.31	471.7	42.24	17.07	23424.73	24265.75	-3.47
Pe8	ER-28	33.33	7	499.7	504.75	41.28	17.97	24789.89	25693.11	-3.52
Pe9	RY-16	75	4	460.00	708.52	41.29	8.72	13142.63	14023.30	-6.28
Pe10	EJ-12	66.67	3	559.71	446.39	42.07	17.19	10327.26	10627.21	-2.82
Pe11	EJ-12	66.67	3	567.36	466.80	42.25	17.08	10643.42	11066.34	-3.82
Pe12	RY-16	66.67	4	563.69	521.1	41.22	18.03	15741.42	14520.83	+8.41
Pe13	EK-20	66.67	5	543.45	458.93	42.18	17.07	17295.50	17600.92	-1.74
Pe15	EK-20	66.67	5	596.42	719.78	40.16	10.094	19706.64	21298.36	-7.47
Pe16	EQ-28	66.67	7	541.23	473.35	42.43	16.98	24582.33	24610.84	-0.12

Table 6.6 Comparison of laterally loaded joints using 19mm and 9mm nominal thickness plywood, 2.66mm diameter nails of strength $827N/mm^2$, at a slip of 4.5mm.

Test ref	Nailing pattern-number of nails	Row spacing (mm)	Number of rows	Average timber density (kg/m^3)	Average plywood density (kg/m^3)	Average penetration of nail into timber (mm)	Average thickness of plywood (mm)	Model load (N)	Test load (N)	% error (%)
Pe19	CO-4	-	1	527.8	573.49	41.58	17.40	5043.58	5200.92	-3.03
Pe20	CO-4	-	1	553.44	601.01	41.20	17.78	5361.62	5550.81	-3.41
Pe21	RU-16	26	4	576.56	615.56	41.36	17.64	20135.20	19562.43	+2.93
Pe22	RU-16	26	4	575.02	629.87	41.25	17.75	20566.54	20719.66	-0.74
Pe23	ED-20	33.33	5	536.33	572.00	41.64	17.32	23720.29	23865.14	-0.61
Pe24	ED-20	33.33	5	678.99	594	41.70	17.33	25975.12	27209.98	-4.54
Pe25	EJ-12	66.67	3	521.37	588.13	41.56	17.46	15404.84	15367.21	+0.24
Pe26	EJ-12	66.67	3	673.62	589.84	41.60	17.35	16460.14	15564.37	+5.76
Pe27	EK-20	66.67	5	530.88	582	41.55	17.40	25544.77	25506.77	+0.15
Pe28	EK-20	66.67	5	671.68	600.10	41.59	17.41	27794.46	27416.84	+1.38
Pe29	EQ-28	66.67	7	523.67	568.75	41.66	17.37	34958.48	34913.5	+0.13
Pe30	EQ-28	66.67	7	659.26	593.60	41.72	17.24	38196.79	36715.2	+4.04
Pe31	ES-20	75	5	562.43	668.53	39.57	9.92	22556.87	23876.07	-5.53
Pe32	ES-20	75	5	495.75	586.00	41.60	17.35	25216.01	24365.38	+3.49

Table 6.7 Comparison of laterally loaded joints using 19mm and 9mm nominal thickness plywood; 3.01mm diameter nails of strength $792N/mm^2$, at a slip of 4.5mm.

Test Ref	Nailing pattern-number of nails	Row spacing (mm)	Number of rows	Average timber density (kg/m^3)	Average plywood density (kg/m^3)	Average penetration of nail into timber (mm)	Average thickness of plywood (mm)	Model load (N)	Test load (N)	% error (%)
Pe33	CO-4	-	1	692.56	585.66	40.85	17.74	5770.64	5811.05	-0.70
Pe34	CO-4	-	1	691.92	597.42	40.95	17.65	5839.93	5847.4	-0.13
Pe35	RV-16	28	4	575.89	610.16	41.98	17.62	20840.57	19940.09	+4.52
Pe36	ED-20	33.33	5	508.24	594.76	41.24	17.38	25442.90	24151.94	+5.35
Pe37	ED-20	33.33	5	568.86	596.64	41.13	17.46	26091.88	24333.56	+7.23
Pe38	ED-20	33.33	5	595.11	599.65	41.14	17.53	26467.25	25967.84	+1.92
Pe39	EG-20	50	5	569.94	605.65	41.13	17.48	27789.82	27789.89	-0.00
Pe40	EJ-12	66.67	3	500.95	598.64	41.3	17.29	16313.28	15340.9	+6.34
Pe41	EJ-12	66.67	3	574.49	593.03	41.27	17.37	16607.64	16713.74	-0.63
Pe42	EK-20	66.67	5	578.67	595.75	41.15	17.47	27953.69	28207.67	-0.90
Pe43	EU-24	66.67	6	522.55	596.62	41.36	17.35	32790.00	32219.25	+1.77
Pe44	EU-24	66.67	6	602.79	603.08	41.02	17.56	34273.94	33767.69	+1.50
Pe45	RZA-16	83.33	4	477.86	518.16	40.68	17.92	19658.64	18614.91	+5.61
Pe46	ET-20	83.33	5	617.76	706.59	39.63	9.88	24287.07	24896.63	-2.45
Pe47	ET-20	83.33	5	574.51	603.32	40.92	17.69	28477.13	27569.90	+3.29
Pe48	ET-20	83.33	5	513.47	595.47	41.22	17.34	27246.18	25717.38	+5.94

Table 6.8 Comparison of laterally loaded joints using 19mm and 9mm nominal thickness plywood; 3.33mm diameter nails of strength $697N/mm^2$, at a slip of 4.5mm.

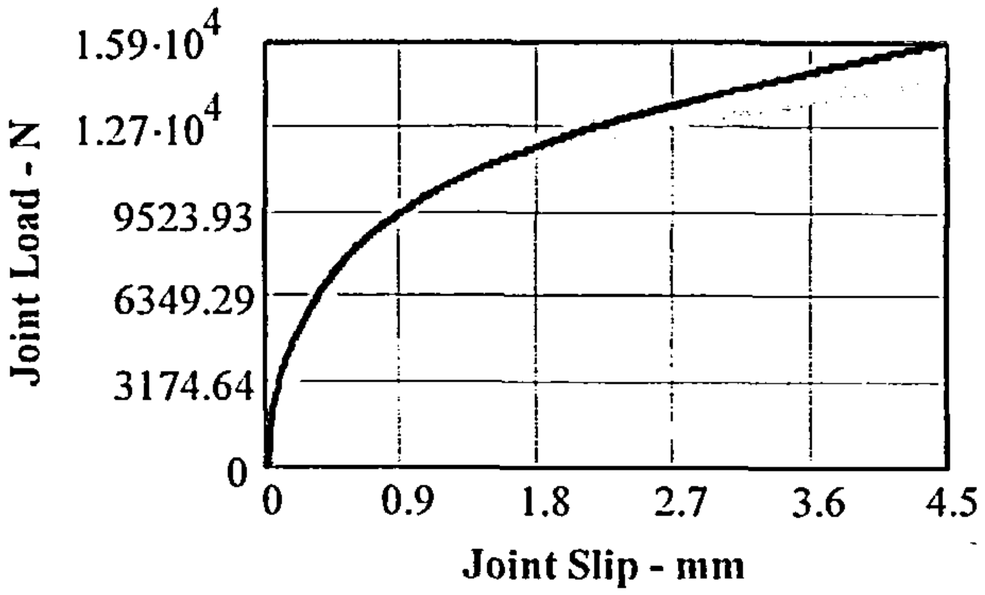

Nailing configuration RT-Joint Pe1

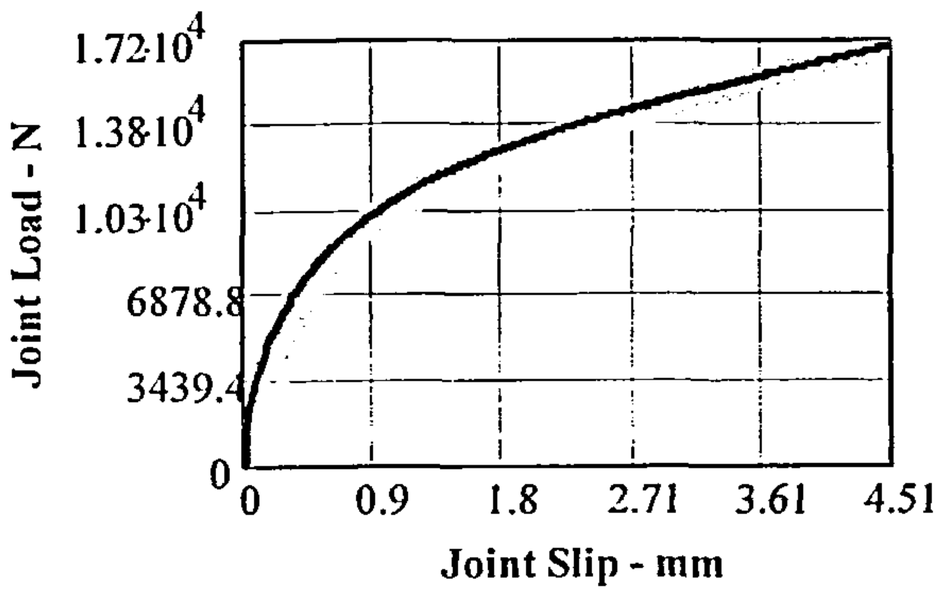

Nailing configuration ED-Joint Pe2

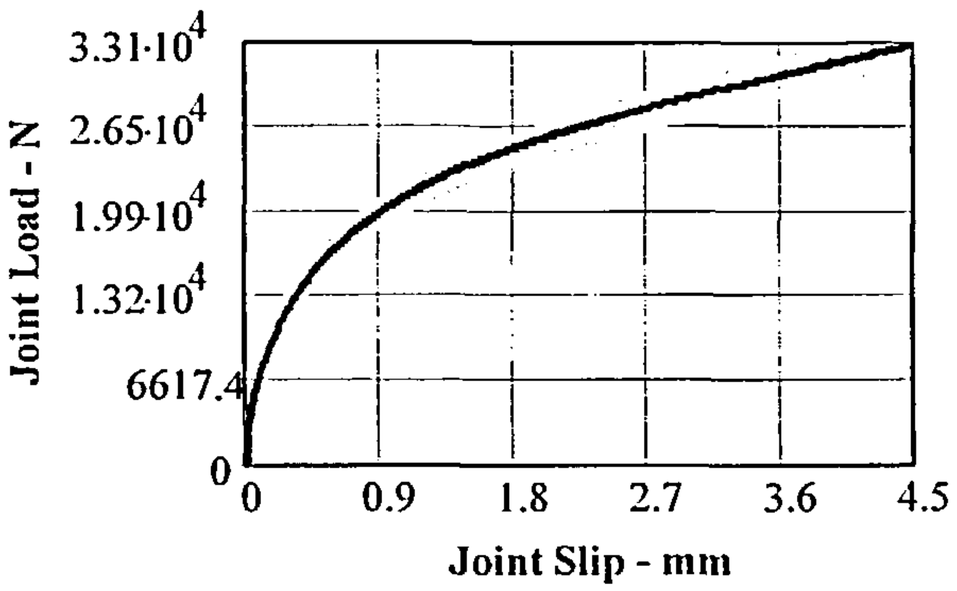

Nailing configuration EU-Joint Pe43

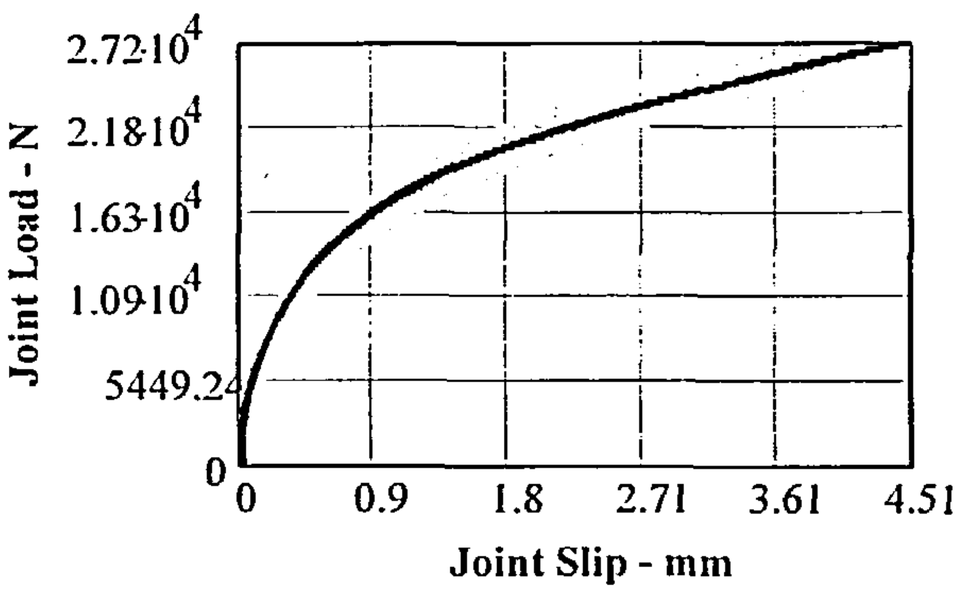

Nailing configuration ET-Joint Pe48

Figure 6.7 Comparison of model and test results of timber joints made with fully overlapping nails and 19mm and 9mm thick plywood gusset plates up to 4.5mm slip.

6.4 COMPARISON OF MODELS WITH EC5 RULES

6.4.1 Strength at the Ultimate Limit State

6.4.1.1 General

To ensure the validity of the model is retained, the comparison with EC5 has been constrained to a parametric study which limits the parameter values to lie within the extreme values used for the material in the test programme.

The timber moisture content will be equated to 12%, with the plywood having an equivalent value. Only joints with predrilled holes and gusset plates with a gap between the gusset plate and the timber will be considered. Also, only joints with a nail penetration of 41mm, the average of the test regime, will be used.

The parametric study will be constrained within the following parameter values:

Parameter	Value
Mean timber density	450Kg/m^3 to 700Kg/m^3.
Mean plywood density	400Kg/m^2 to 700Kg/m^3
Plywood thickness	7.5mm to 17.5mm.
Nail diameters	as used in the testing programme
Nail yield strength	as derived from the nail tests
Number of rows of nails in joint	1 to 7
Nail row spacing	(i) Minimum 7d for steel gusset plate joints 8.5d for plywood gusset plate joints (ii) Maximum 19.6d for steel gusset plate joints. 17d for plywood gusset plate joints

6.4.1.2 Joints with Steel Gusset Plates

(i) Timber Density Effect

From a review of EC5 [11], EC5 [15] and the model equation at the ULS, the Eurocode equations for joint strength are directly proportional to the square root of timber density whereas in the model equation, strength is directly proportional to the timber density. EC5 [15] also includes a nail withdrawal term that is a function of the square of the density but as this only represents a small fraction of the joint strength, it still means that as the density increases the model capacity will increase at a higher rate than the Eurocode values.

Consider a joint made with a pair of fully overlapping nails. Applying equations (152d), (153d) and (175b) all modified by equation (156) the characteristic strength equations are converted to the ULS strength equations, as follows:

EC5 [11]
$$F_{v,d} = 1.5\sqrt{\left(2M_{y,Rk} f_{h,w,k} d\right)}\frac{n}{1.3} \quad \text{....(182a)}$$

EC5 [15]
$$F_{v,d} = (2.3\sqrt{\left(M_{y,Rk} f_{h,w,k} d\right)} + \frac{F_{ax,Rk}}{4})\frac{n}{1.3} \quad \text{....(182b)}$$

Model
$$P\delta_{xd} = 0.853AD(d)^{1.4468} f_u rn(1-e^{-1.712\delta x})^{0.926}(0.1\delta x + 0.68)/f(mc)\frac{1}{1.3} \quad \text{....(182c)}$$

Applying equations (182) to a joint with nail diameter d = 2.66mm; number of nails n = 2; nail strength = 804N/mm^2 and mean density D ranging from 450kg/m^3 to 700Kg/m^3, and A is 1.6098284×10^{-3}, the joint strength relationships will be as shown in Figure 6.8.

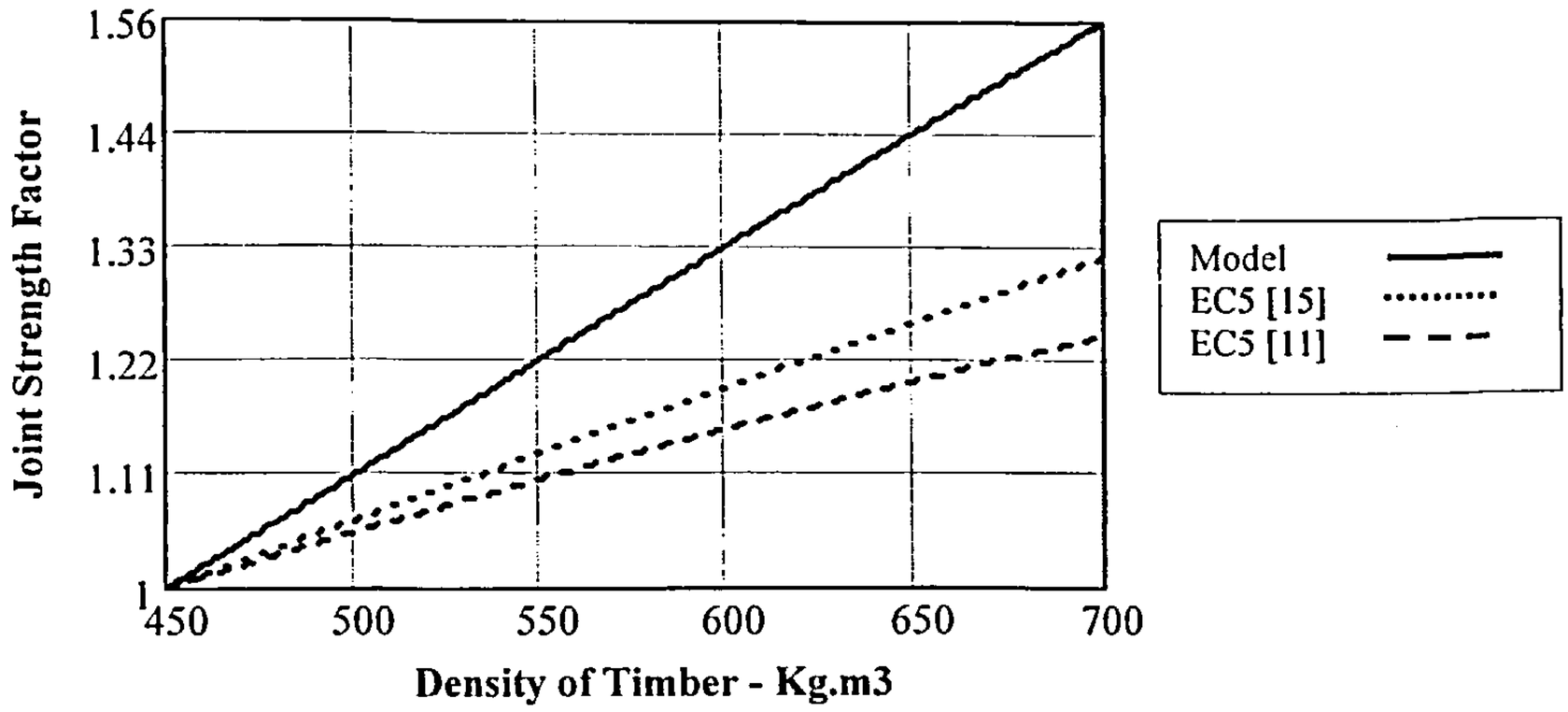

Figure 6.8 The effect of variation in the timber density between the model, EC5 [11] and EC5 [15].

To enable the influence of change in density to be more clearly shown for each equation, in the Figure each strength equation has been divided by its strength at a density of 450Kg/m^3. It is seen that the greatest increase is obtained from the model where there will be a 56% increase in strength over the range of density selected. EC5 [15] and EC5[11] increase by 32% and 25% respectively, the difference between these results being due to the withdrawal strength function in EC5[15].

(ii) Nail Diameter Effect

Applying equations (182) to a joint with timber density D = 450Kg/m^3; number of nails n = 2; nail strength = 804N/mm^2 and nail diameter d ranging from 2.66mm to 3.36mm, the Joint strength relationships will be as shown in Figure 6.9.

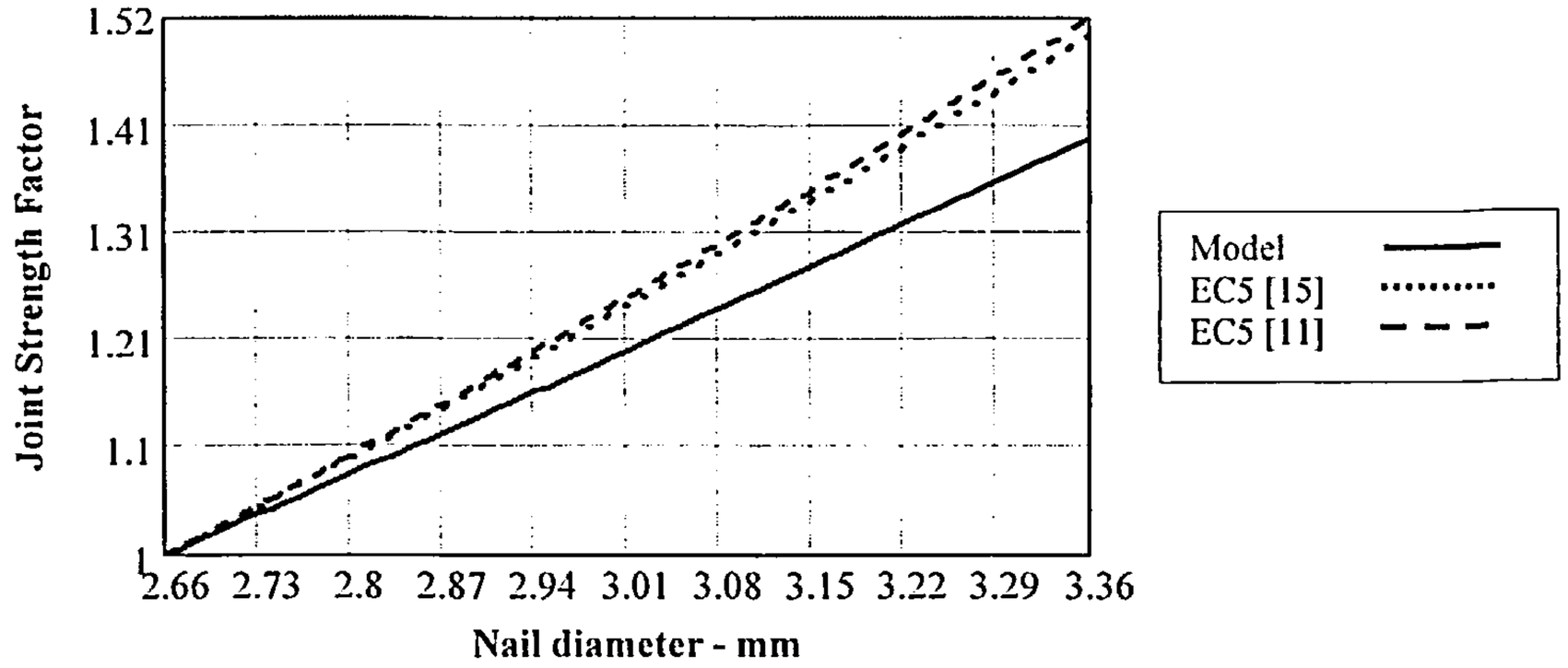

Figure 6.9 The effect of variation in nail diameter between the model, EC5 [11] and EC5[15].

In the model equation, joint strength is a function of $d^{1.4468}$ and in the Eurocode equations it is a function of $d^{1.8}$ and the increase in strength using the Eurocode equations over the model is clearly shown in the graph. To enable the influence of change in nail diameter to be more clearly shown each strength equation has been divided by the joint strength using a 2.66mm diameter nail.

The greatest increase is obtained from EC5 [11] where there will be a 52% increase in strength over the nail diameter range selected. EC5 [15] is slightly less at 50% and the model gives the smallest increase of 40%.

(iii) Nail Strength Effect

Applying equations (182) to a joint with timber density $D = 450\text{Kg/m}^3$; number of nails $n = 2$; nail diameter $d = 2.66\text{mm}$ and nail strength ranging from 769N/mm^2 to 804N/mm^2, the joint strength relationships will be as shown in Figure 6.10.

In the model equation, joint strength is a function of nail strength and in the Eurocode equations it is a function of the square root of the strength and the increase in strength from the model equation over the Eurocode equations is clearly shown in the graph. To enable the influence of change in nail diameter to be more clearly shown each strength equation has been divided by the joint strength using a nail strength of $769\ \text{N/mm}^2$.

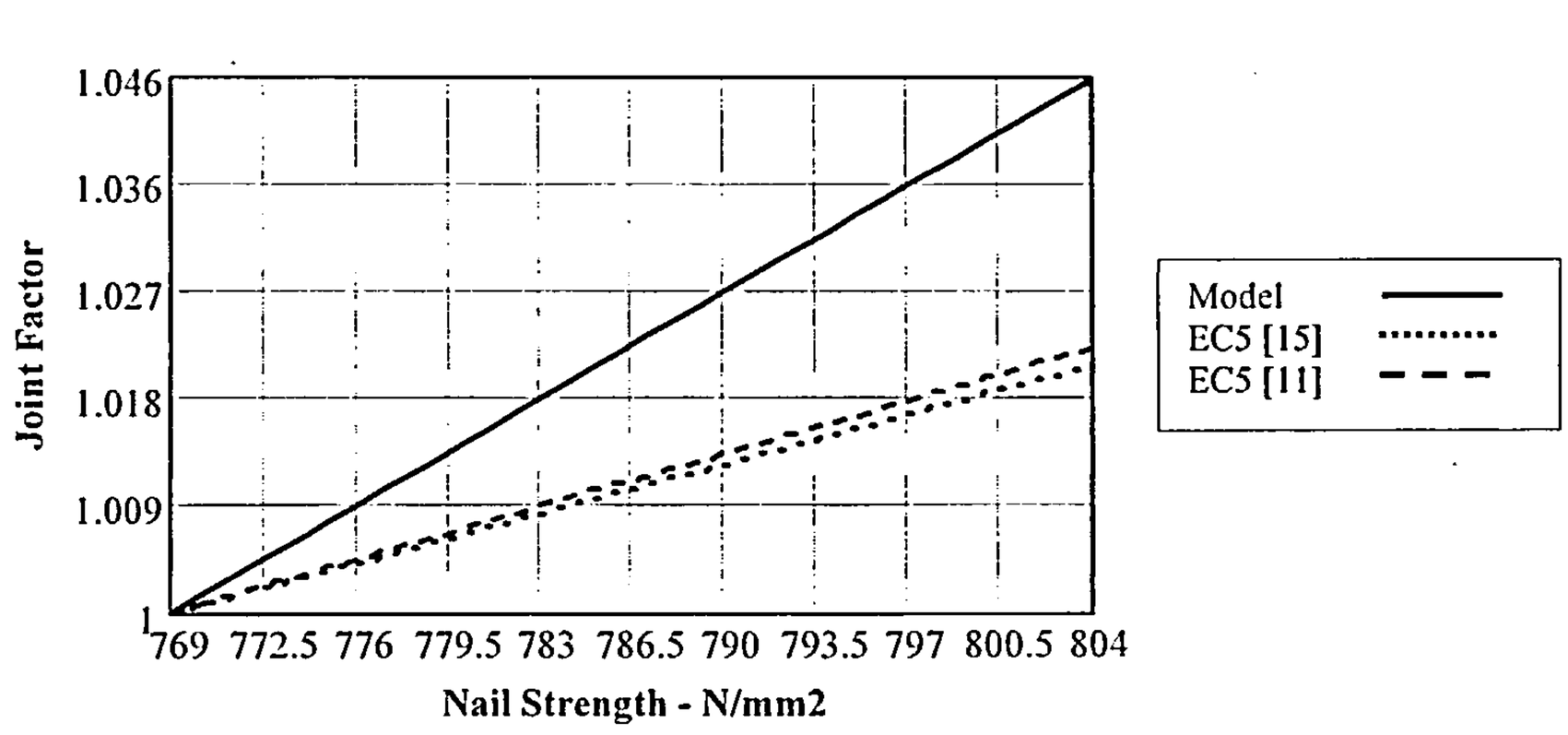

Figure 6.10 The effect of variation in nail strength between the model,EC5 [11] and EC5[15].

The model increase over the range is 4.6% compared to 2.3% and 2.1% respectively for EC5 [15] and EC5 [11]. The strength increases are small because of the limited range used for the nail strength.

(iv) Number of Rows of Nails and Row Spacing Effect

To equate the model with EC5 [15] the effect of the number of rows of nails in the joint and of the row spacing function are combined to form one function.

In the model, joint strength is a multiple of the number of rows of nails, *r*, in the joint and the row spacing function. The row spacing function is given in equation (38), where the function is unity at a spacing greater than *19.6d* and *(0.7428 + 0.0132Sp/d)* for spacing between *7d* and *19.6d.*

In EC5 [15], joint strength is a function of r^{kef}, where k_{ef} is given in Table 8.1 of the code. For joints with predrilled holes the values of k_{ef} are given in Table 6.9.

Row spacing	k_{ef}
≥ 14d	1.0
= 10d	0.85
= 7d	0.7
= 5d	0.5

Table 6.9 Value of k_{ef} taken from Table 8.1 in EC5 [15].

In EC5 [11], the joint strength is a linear function of the number of rows of nails and is not affected by the nail row spacing used.

The joint strengths are compared using the combined nail row-spacing functions referred to above. The comparison is undertaken using up to 7 rows of nails and at a spacing of *7d, 10d, 14d* and *19.6d* to envelope the model criteria and also align with the criteria given in EC5 [15]. A comparison cannot be made with the EC5 [15] limit of *5d* as the minimum row spacing for joints with fully overlapping nails is *7d.*

Nail Row Spacing – *7d, 10d, 14d and 19.6d*

Using the combined row-spacing functions at a spacing of *7d, 10d, 14d* and *19.6d*, the effect of the functions on the joint strength will be as shown in Figure 6.11.

In EC5 [15] the row-spacing reduction factor is a function of the number of rows of nails in the joint. This is not the case for the model or EC5[11]. For a joint with 7 rows of nails at a row spacing of *7d*, the reduction in joint strength will be 44.2% for EC5 [15] and only 16.5% for the model. At a spacing of *10d* the reductions are 25.3% and 12.5% respectively and at a spacing of *14d* the Eurocode row-spacing function is unity and the graph aligns with EC5 [11]. At this spacing however, the row-spacing function in the model will still reduce the joint strength by 7.2%. At a spacing of *19.6d* in all cases there will be no reduction factor.

As explained in Chapter 3, the spacing used for joints with fully overlapping nails is of the order of two times that required for equivalent joints made with fully overlapping nails. Because the comparison has been made using the same row spacing, a close fit between the model and EC5 [15] is not to be

expected. It is to be noted, however, that had a reduced spacing been used for the EC5 [15] joints, an even greater difference than reported above would be exhibited. In the model the spacing at which the row-spacing factor becomes unity is *19.6d.* With EC5 [15], for joints with nails which do not fully overlap, the equivalent spacing is *14d.* If one applies a factor of *2* to this spacing to equate to a joint with fully overlapping nails, and in addition applies the spacing factor of *0.7* allowed by the code for joints with steel gusset plates, the equivalent spacing for such joints will also be *19.6d.* This fully aligns with the model spacing for a combined row-spacing factor of unity.

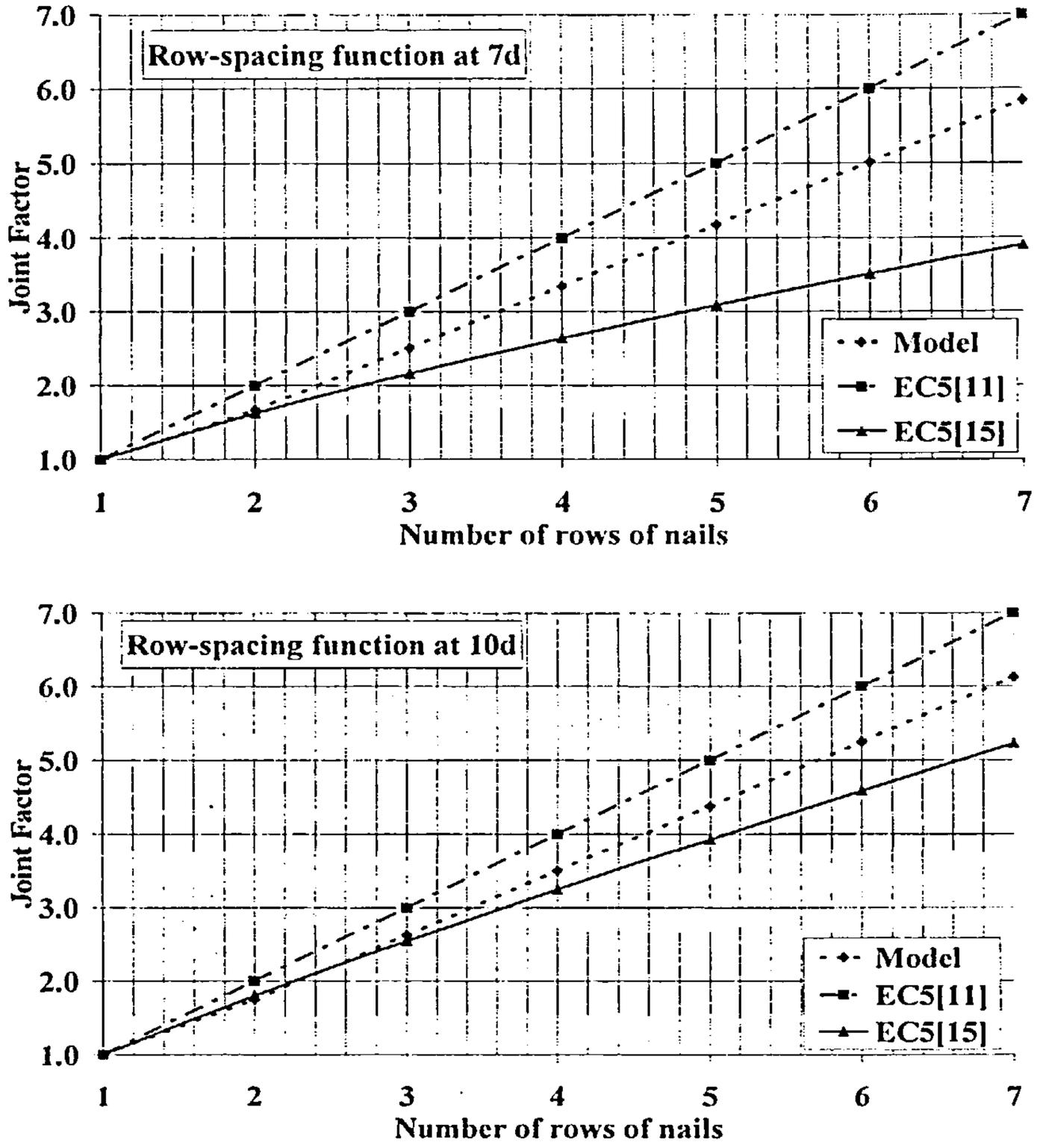

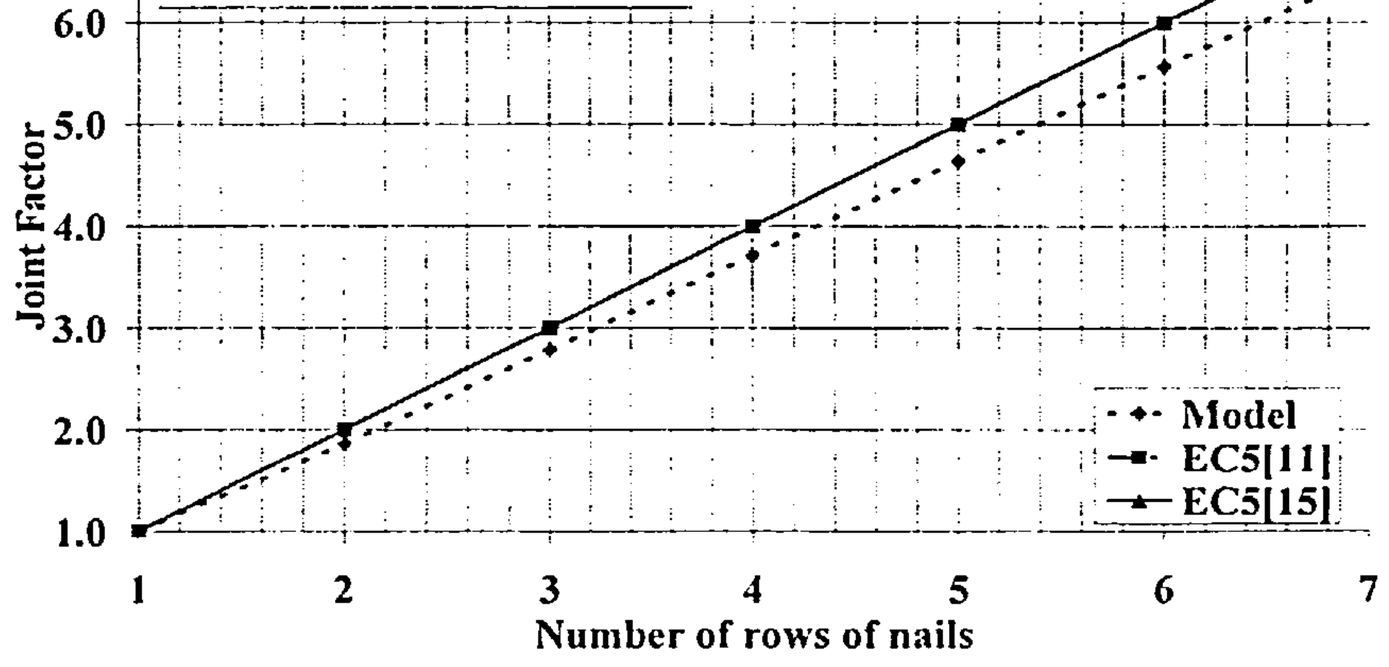

Figure 6.11 The effect of nail row spacing of *7d,10d,14d* and *19.6d* between the model, EC5 [11] and EC5[15].

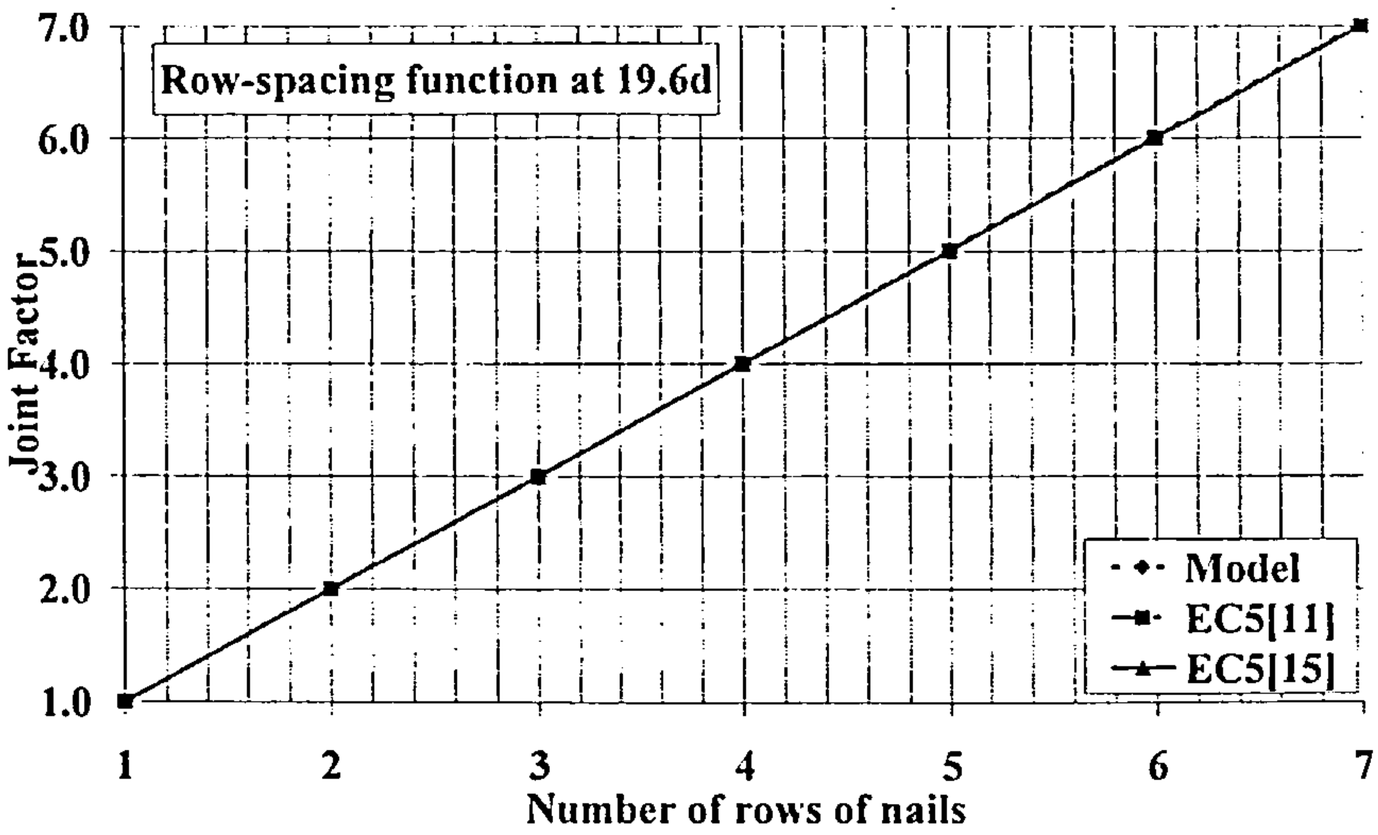

Figure 6.11 cont'd The effect of nail row spacing of *7d,10d,14d* and *19.6d* between the model, EC5 [11] and EC5[15].

(v) Combined effect

For joints where the row spacing is equal to or greater than *19.6d* the model predicts joint strength to be consistently below that obtained from EC5 [15] and above that using the EC5 [11] rules.

Examples of the ULS strength of such joints at the extremes of the parameter properties used in the programme are shown in Figure 6.12. Two joints are considered, one made with a pair of 2.66mm diameter nails using timber with a density of 450kg/m^3 and the other with a pair of 3.36mm diameter nails using timber with a density of 700kg/m^3. Both joints use nails with a strength of 804N/mm^2 and timber at a moisture content of 12%.

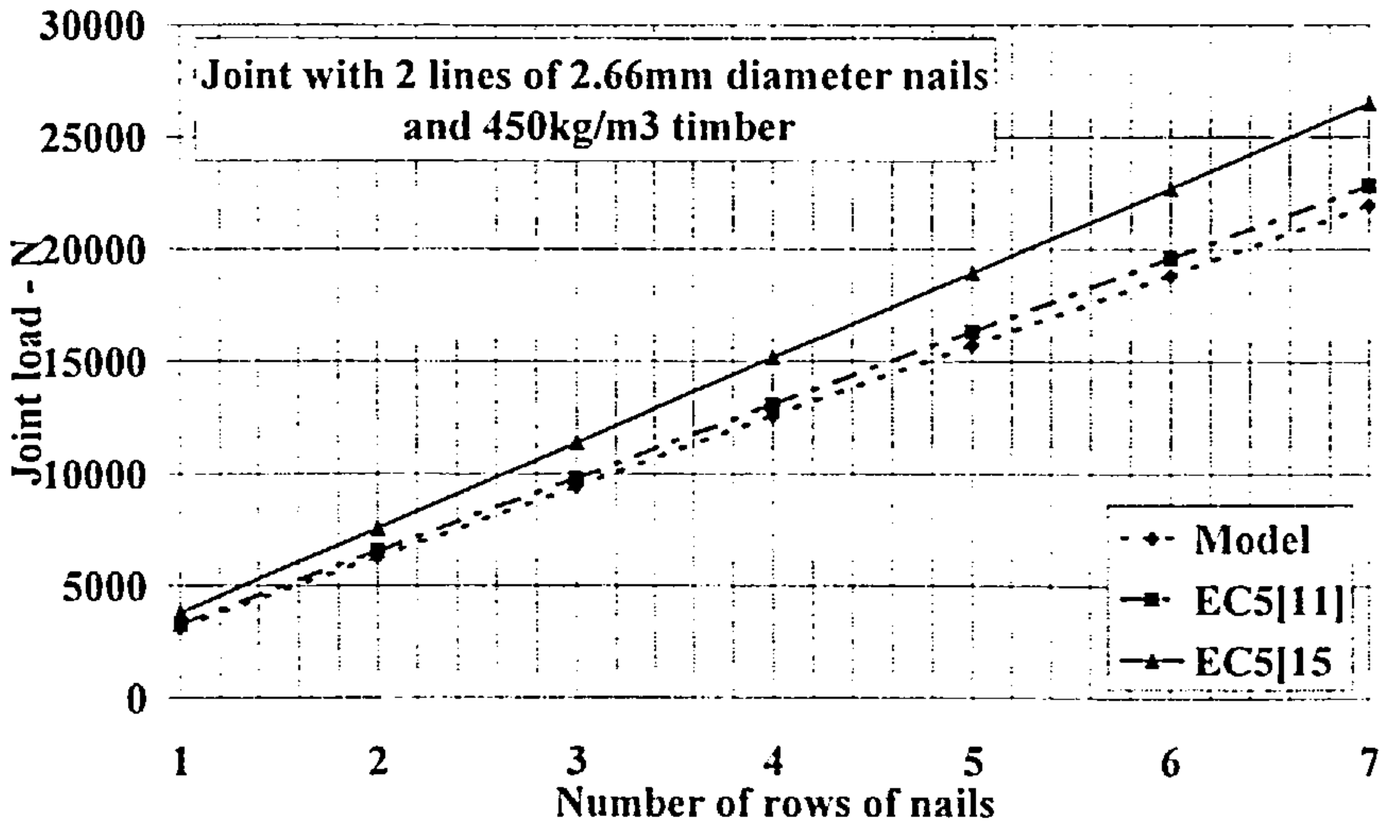

Figure 6.12 Comparison of joint strength using the model, EC5 [11] and EC5 [15] at the ultimate limit state

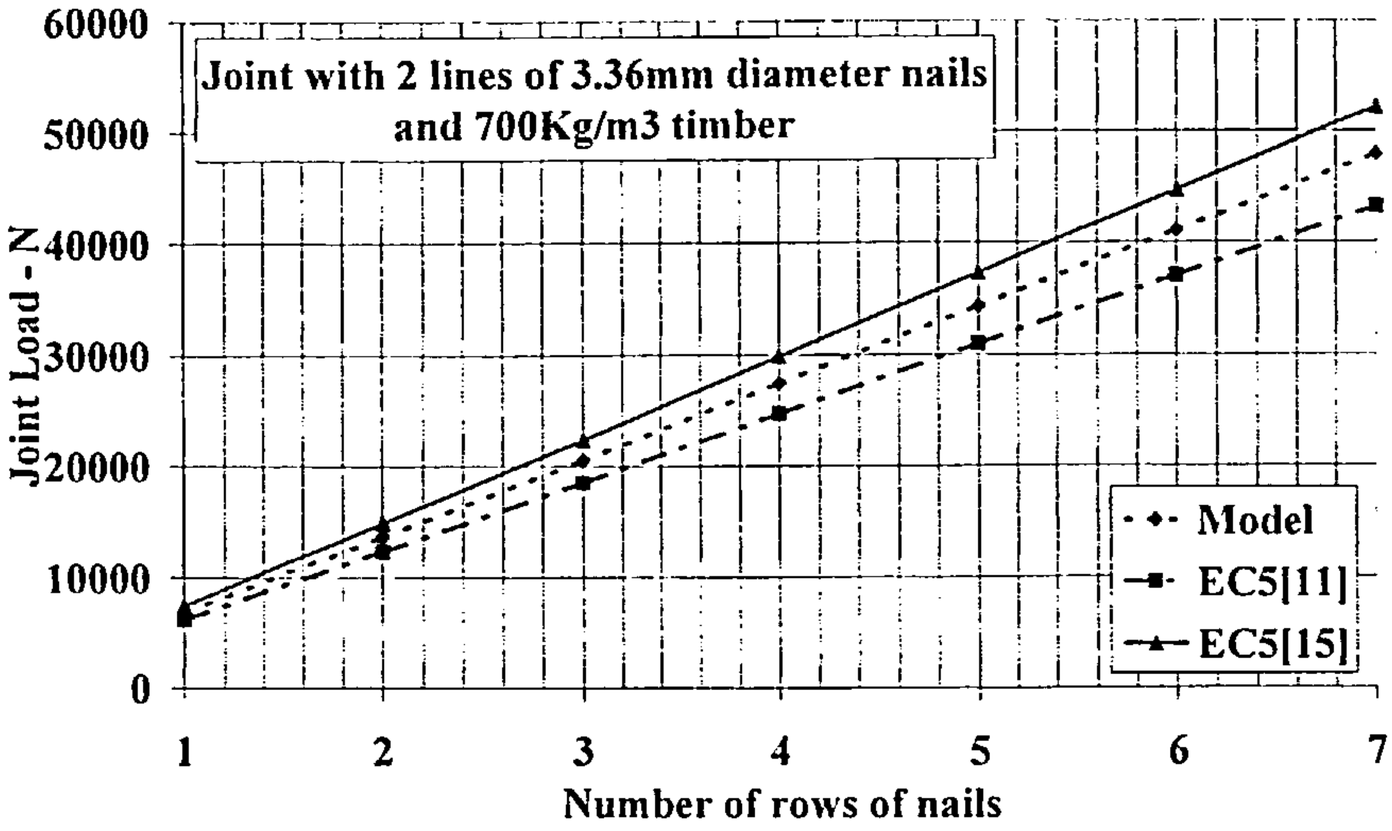

Figure 6.12 cont'd Comparison of joint strength using the model, EC5 [11] and EC5 [15] at the ultimate limit state.

EC5 [11] is consistently smaller in value than EC5 [15], being 16.6% less using 450kg/m^3 timber and 2.66mm diameter nails and 18.6% less using 700kg/m^3 timber with 3.36mm diameter nails. From the results of the parametric study, the increase in strength is due to the effect of the timber density. Using 450kg/m^3 timber and 2.66mm diameter nails the model is 4% less than the EC5 [11] result and as the nail diameter and density increases the model result increases relative to the code values. With 700kg/m^3 timber and 3.36mm diameter nails the model result is 9.8% above EC5 [11] and 8.8% below the EC5 [15] result. A summary of the difference between the model and the EC5 [11] and EC5 [15] results is given in Table6.10.

Nail diameter mm	**Percentage difference in joint strength between model and EC5 [11]**		**Percentage difference in joint strength between model and EC5 [15]**	
	Timber density = 450kg/m^3	Timber density = 700kg/m^3	Timber density = 450kg/m^3	Timber density = 700kg/m^3
2.66	-4.0	16.6	-20.6	-2.6
3.01	-8.4	13.1	-25.0	-5.8
3.36	-12.5	9.8	-29.1	-8.8

Table 6.10 The percentage difference between the model and EC5 [11] and EC5 [15] in joints where the spacing exceeds 19.6*d*.

When the nail row spacing is reduced below *19.6d,* with the exception of joints designed to EC5 [11], the row-spacing function will apply, and as shown in item (iv),(a) above, this will reduce the joint strength in multi-row joints. Because of the requirement to adopt a greater row spacing in joints with fully overlapping nailed joints over that required for equivalent joints assembled using nails which do

not fully overlap, the model and EC5 [15] row-spacing functions cannot be directly compared. What can be noted, however, is that using the EC5 [15] rules the value of the reduction increases as the number of rows increase. If using the minimum row spacing of *7d* on a 7 row joint, the strength of EC5 [15] joints will be reduced by 44.2% and the model results by only 16.5%. If the EC5 [15] spacing is reduced to *5d* to better equate to joints with fully overlapping nails the comparison will be as shown in Figure 6.13. The strength reduction will be even greater and for the joint type referred to above will equate to 62.2%.

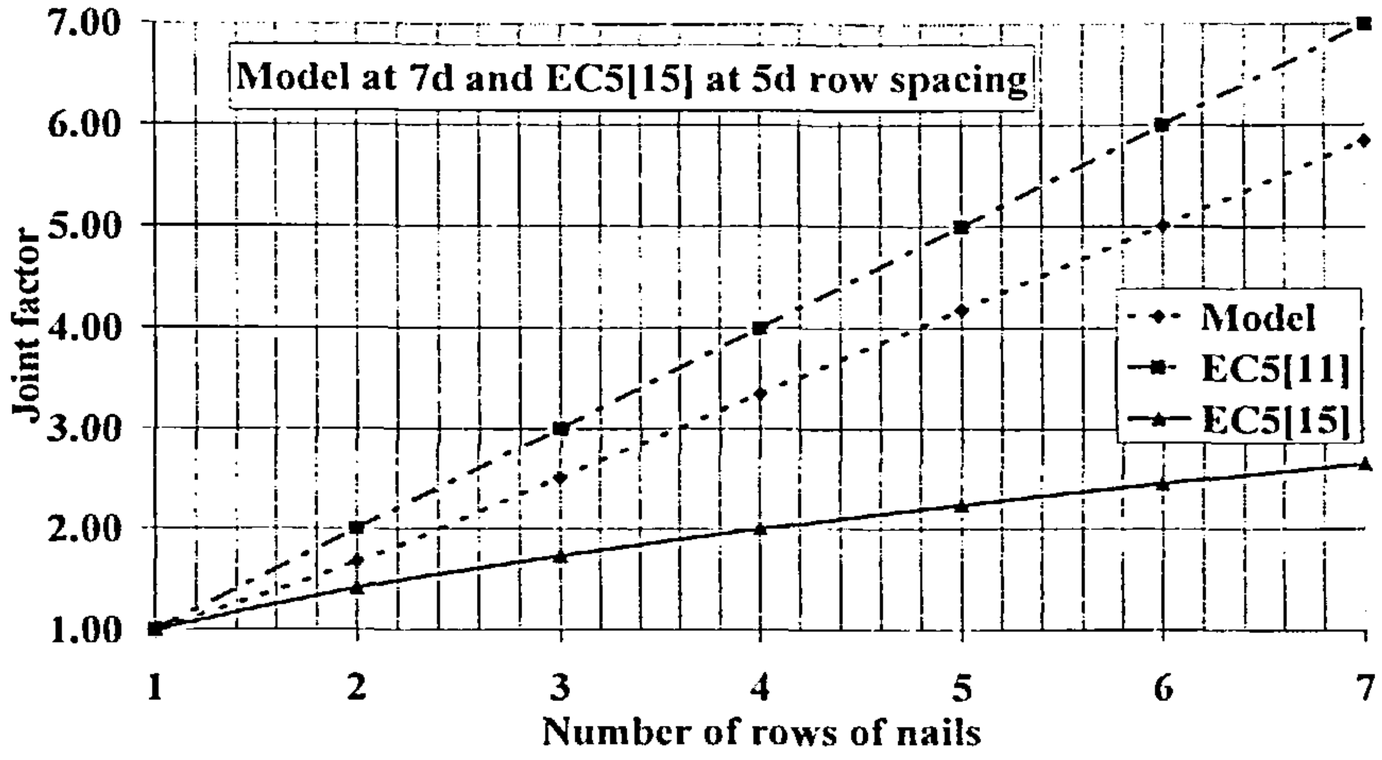

Figure 6.13 The effect of nail row spacing at *7d* in the model compared with EC5 [11] and a nail row spacing of *5d* in EC5 [15].

From Figure 6.13 it is seen that the row spacing factor in EC5 [15] will greatly overestimate the reduction to be applied to the strength of multi-row joints. Because the row spacing requirement with fully overlapping nails is of the order of two times that required for joints made with nails which do not fully overlap, the row-spacing factor cannot be directly equated to the model row-spacing factor at the same spacing

6.4.1.3 Joints with Plywood Gusset Plates

(i) Timber Density Effect

From a review of EC5 [11], EC5 [15] and the model equation at the ULS, the Eurocode equations for joint strength are complex functions of the timber and plywood densities whereas in the model equation, strength is directly proportional to the density of these materials. EC5 [15] also includes a nail withdrawal term that is a function of the square of the density.

Consider a joint made with a pair of fully overlapping nails. Applying equations (152a) to (152c), (153a) to (153c) and (181b) modified by equation (156) the characteristic strength equations are converted to the ULS strength equations, as follows:

(i) EC5 [11]:

Mode 1A

$$F_{v,d} = f_{h,p,k} t_p d \frac{n}{1.3} \quad \text{....(183a)}$$

Mode 2A

$$F_{v,d} = 1.1 \frac{f_{h,p,k} t_p d}{(2+\beta)} \left(\sqrt{2\beta(1+\beta) + \frac{4\beta(2+\beta) M_{y,Rk}}{f_{h,p,k} d t_p^2}} - \beta \right) \frac{n}{1.3} \quad \text{....(183b)}$$

Mode 3B

$$F_{v,d} = 1.1 \sqrt{\frac{2\beta}{(1+\beta)}} \sqrt{\left(2 M_{y,Rk} f_{h,p,k} d\right)} \frac{n}{1.3} \quad \text{....(183c)}$$

(ii) EC5 [15]:

Mode 1A

$$F_{v,d} = f_{h,p,k} t_p d \frac{n}{1.3} \quad \text{....(183d)}$$

Mode 2A

$$F_{v,d} = (1.05 \frac{f_{h,p,k} t_p d}{(2+\beta)} \left(\sqrt{2\beta(1+\beta) + \frac{4\beta(2+\beta) M_{y,Rk}}{f_{h,p,k} d t_p^2}} - \beta \right) + \frac{F_{ax,Rk}}{4}) \frac{n}{1.3}$$

....(183e)

Mode 3B

$$F_{v,d} = (1.15 \sqrt{\frac{2\beta}{(1+\beta)}} \sqrt{\left(2 M_{y,Rk} f_{h,p,k} d\right)} + \frac{F_{ax,Rk}}{4}) \frac{n}{1.3} \quad \text{....(183f)}$$

(iii) Model:

$$P\delta_{xd} = 0.853(Ae)(Density\ Function)(d)^{2.236} f_u rn(1-e^{-1.406\delta x})^{0.54}(0.121\delta x + 1) \frac{n}{1.3}$$

....(183g)

Applying equations (183) to a joint with nail diameter d = 2.66mm; number of nails n = 2; nail strength = 827N/mm^2; plywood mean density 700Kg/m^3, plywood thickness 17.5mm, nail penetration into the timber tw = 41.00mm and timber mean density ranging from 450kg/m^3 to 700Kg/m^3, the joint strength relationships will be as shown in Figure 6.14.

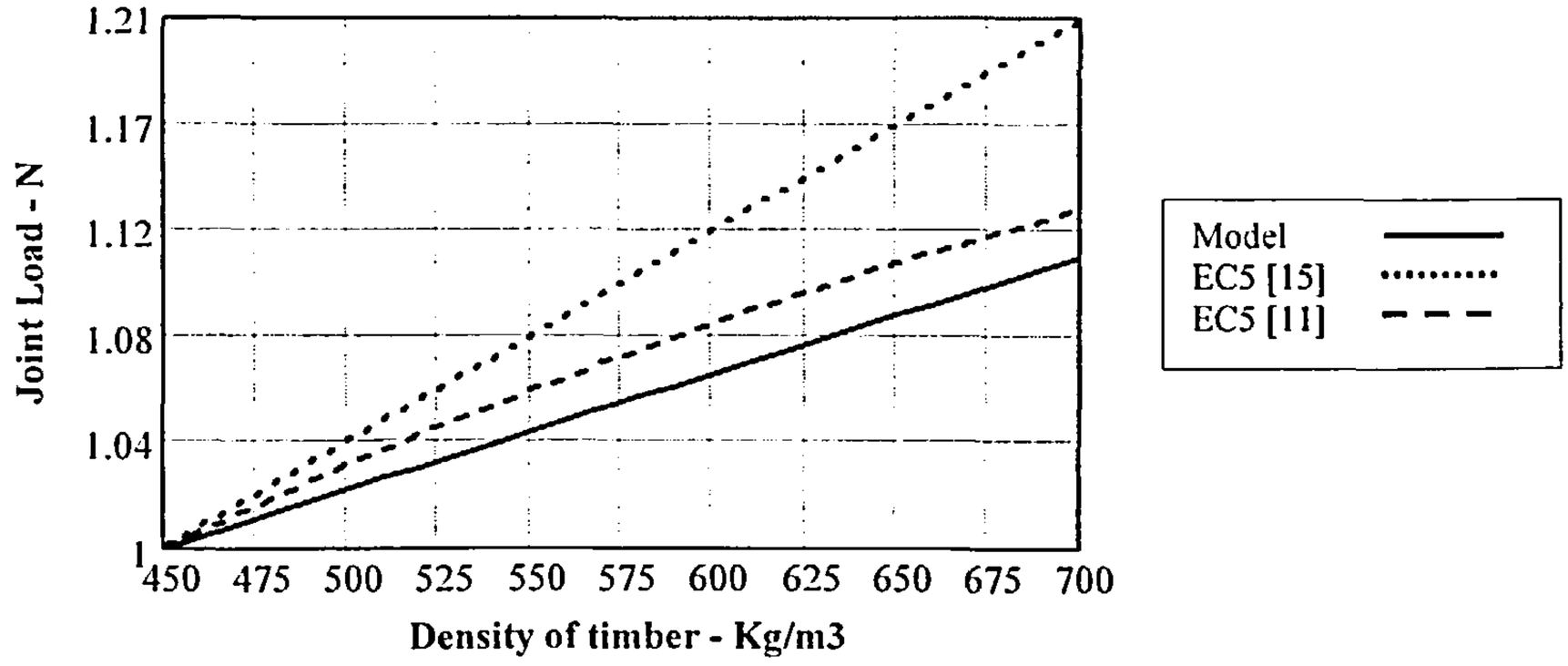

Figure 6.14 The effect of variation in the timber density between the model, EC5 [11] and EC5 [15].

As for the steel gusset plate joints, to enable the influence of change in density to be more clearly shown each strength equation has been divided by the joint strength using a timber density of 450Kg/m^3.

It is seen that for plywood gusset plate joints the greatest increase is obtained from EC5 [15] where there will be a 21% increase in strength over the range of density selected. EC5 [11] will increase by 13% and the model increases by 11%. The increase in strength shown by EC5 [15] over EC5 [11] is caused by the addition of the nail withdrawal term which is a function of the square of the timber density. It is also to be noted that under EC5 [15] rules the joint will fail in Mode 2A whereas under EC5 [11] rules it will fail in Mode 3B. In both instances there is only a small percentage difference in strength between the modes.

(ii) Plywood Density Effect

Applying equations (183) to a joint with nail diameter d = 2.66mm; number of nails n = 2; nail strength = 827N/mm2, timber density D = 450Kg/m^3, plywood gusset thickness tp = 17.5mm, nail penetration into the timber tw = 41.00mm and plywood density ranging from 400Kg/m^3 to 700Kg/m^3, the joint strength relationships will be as shown in Figure 6.15.

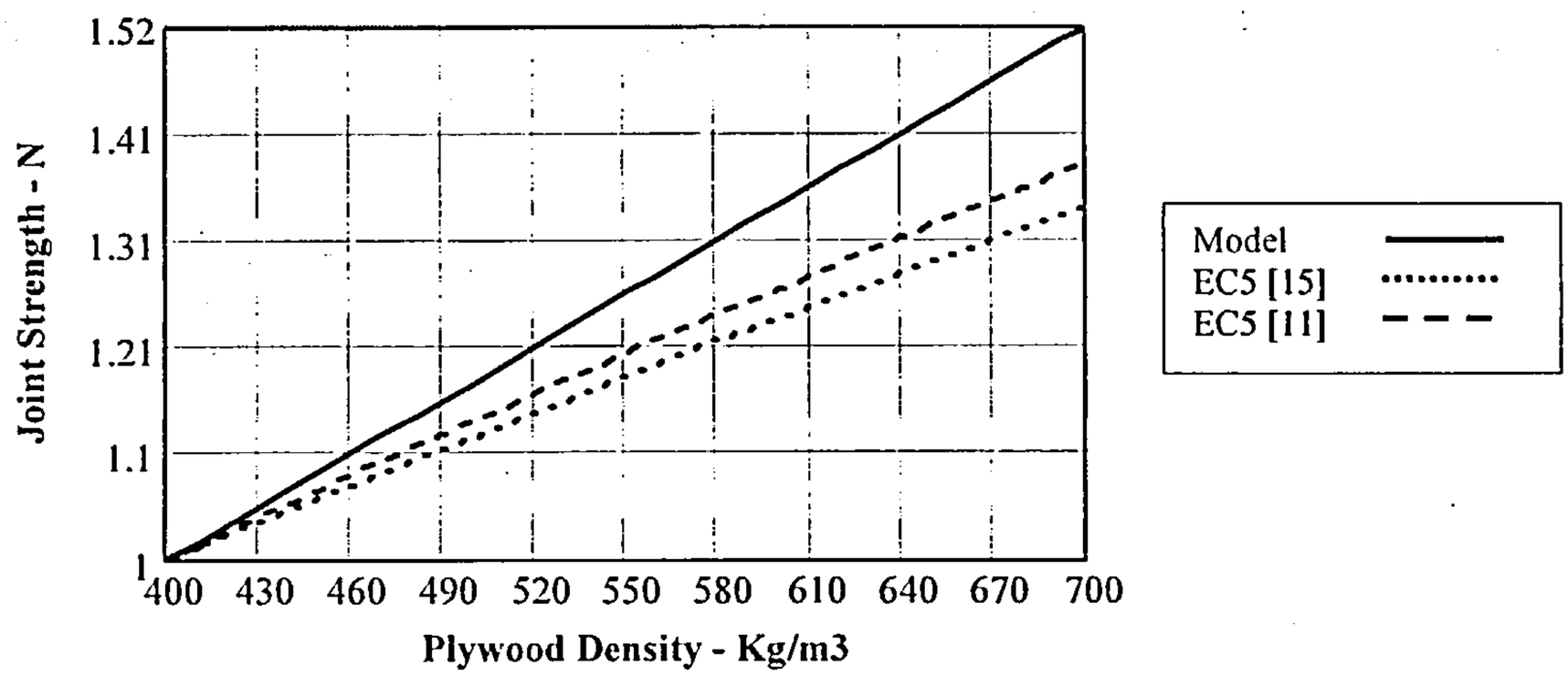

Figure 6.15 The effect of variation in the plywood density between the model, EC5 [11] and EC5 [15].

To enable the influence of change in plywood density to be more clearly shown each strength equation has been divided by the joint strength using a plywood density of 400Kg/m^3. The greatest increase is obtained from the model where there is a 52% increase in strength over the range of density selected. EC5 [11] will increase by 39% and EC5 [15] by 34%. The mode of failure remains as Mode 2A for the EC5 [15] joints and under EC5 [11] rules the failure mode changes from Mode 2A at low densities to Mode 3 as the density increases.

(iii) Plywood Thickness Effect

Applying equations (183) to a joint with nail diameter d = 2.66mm, ; number of nails n = 2; nail strength = 827N/mm2, timber density 450Kg/m^3, plywood density 700Kg/m^3, nail penetration into the timber tw = 41.00mm, and plywood thickness ranging from 7.5mm to 17.5mm, the joint strength relationships will be as shown in Figure 6.16.

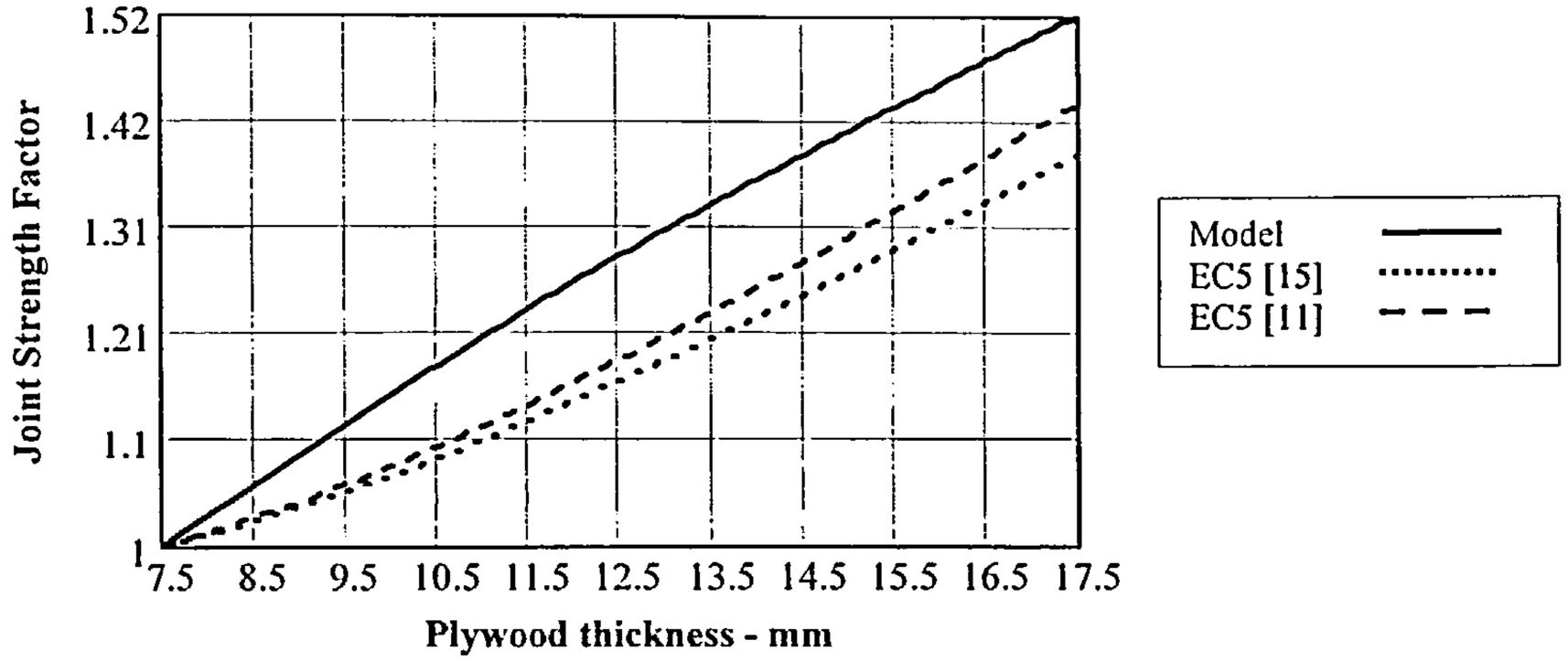

Figure 6.16 The effect of variation in the plywood thickness between the model, EC5 [11] and EC5 15].

To enable the influence of change in plywood thickness to be more clearly shown each strength equation has been divided by the joint strength using a plywood thickness of 7.5mm. The model strength increases by 52% over the thickness range whilst joints designed to the EC5 [11] rules increase by 44% and to EC5 [15] rules by 39%. For both sets of Eurocode rules, the modes of failure are Mode 2A at 7.5mm thickness but as the thickness increases, the joints designed to EC5 [11] rules change to failure Mode 3B.

(iv) Nail Diameter Effect

Applying equations (183) to a joint with timber density D = 450Kg/m^3, plywood density 700Kg/m^3, number of nails n = 2; nail strength = 827N/mm2, nail penetration into the timber tw = 41.00mm, plywood thickness tp = 17.5mm and nail diameters ranging from 2.66mm to 3.33mm, the joint strength relationships will be as shown in Figure 6.17.

To enable the influence of change in nail diameter to be more clearly shown each strength equation has been divided by the joint strength using a nail diameter of 2.66mm.

The model strength increases by 65% over the nail diameter range whilst joints designed to the EC5 [11] rules increase by 48% and to EC5 [15] rules by 29%. For both sets of Eurocode rules over the full range of nail diameters the modes of failure are Mode 2A.

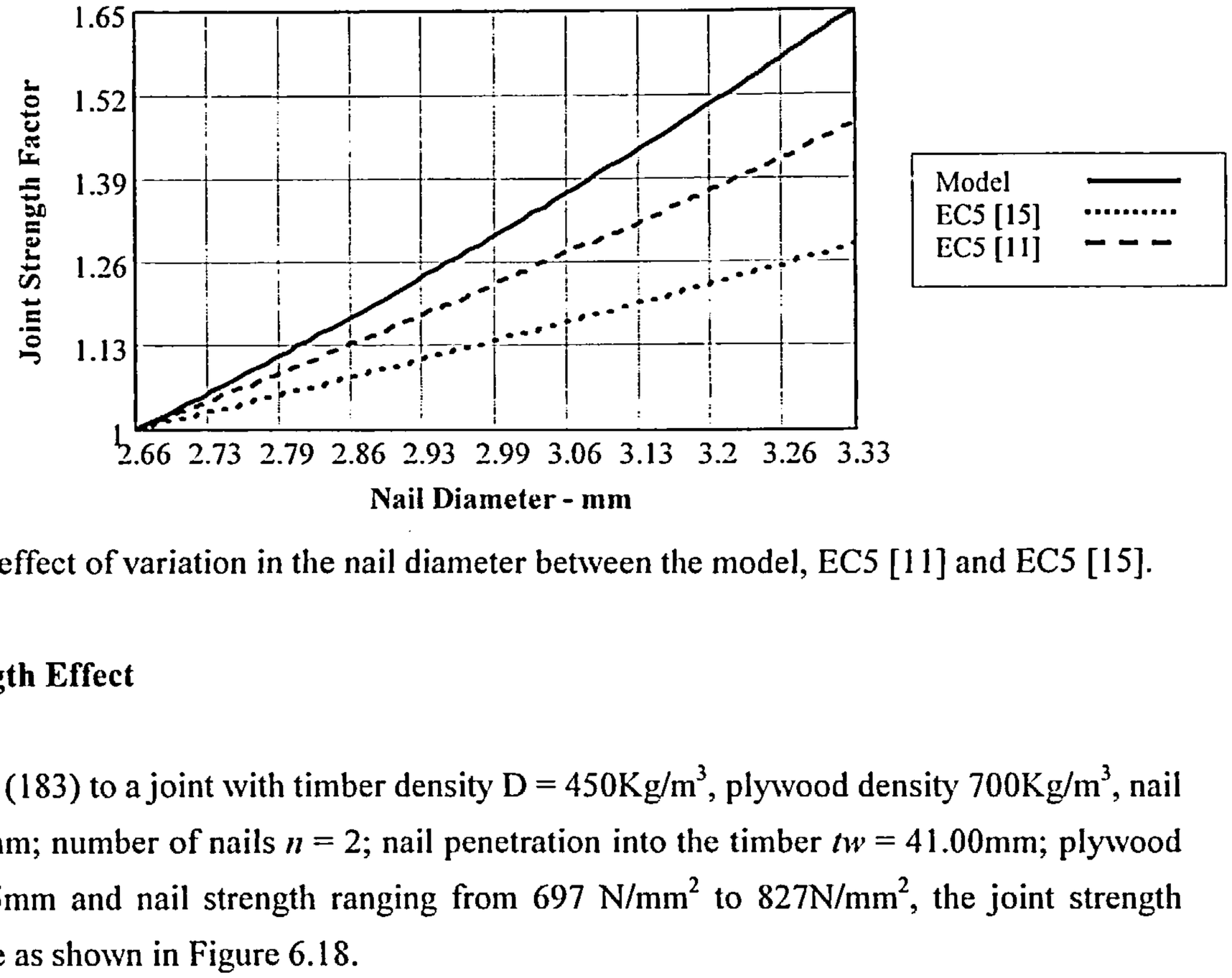

Figure 6.17 The effect of variation in the nail diameter between the model, EC5 [11] and EC5 [15].

(v) Nail Strength Effect

Applying equations (183) to a joint with timber density D = 450Kg/m^3, plywood density 700Kg/m^3, nail diameter d = 2.66mm; number of nails n = 2; nail penetration into the timber tw = 41.00mm; plywood thickness tp = 17.5mm and nail strength ranging from 697 N/mm^2 to 827N/mm^2, the joint strength relationships will be as shown in Figure 6.18.

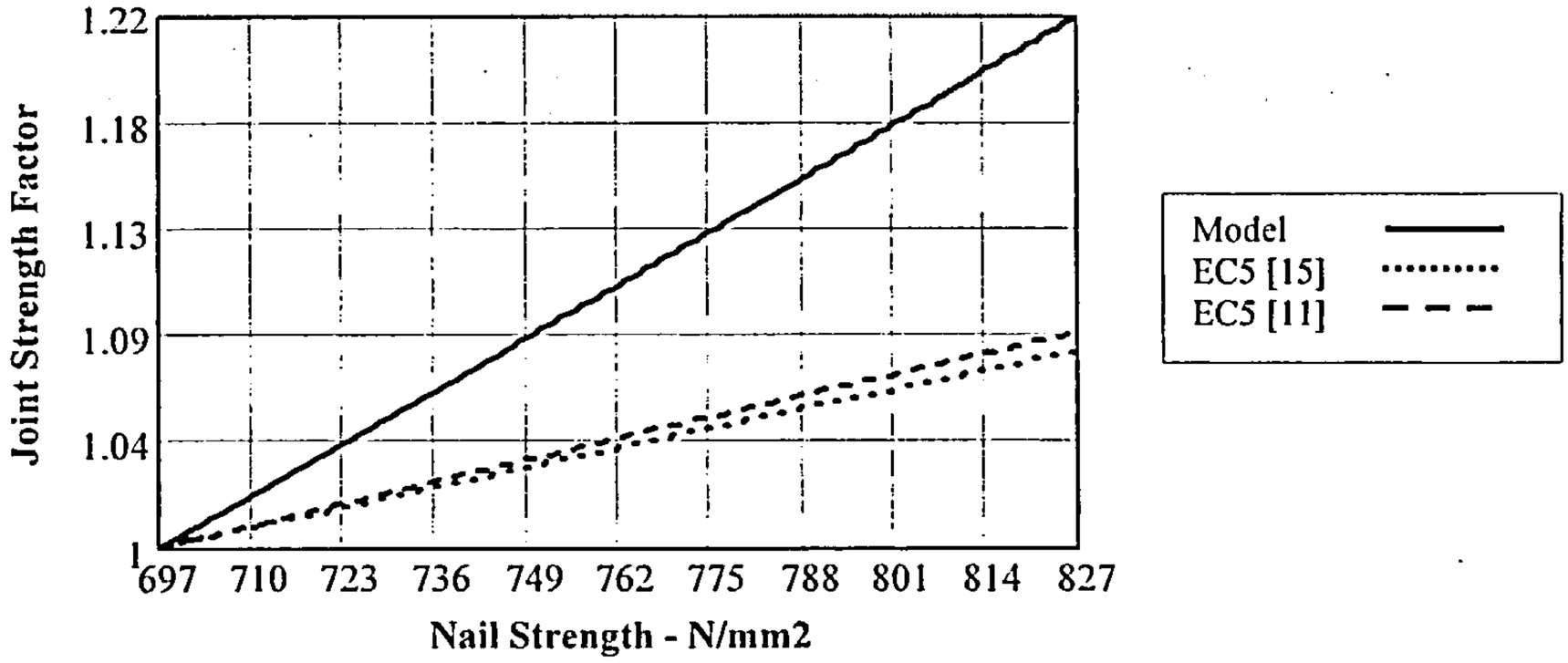

Figure 6.18 The effect of variation in the nail strength between the model, EC5 [11] and EC5 [15].

To enable the influence of change in nail strength to be more clearly shown each strength equation has been divided by the joint strength using a nail strength of 697N/mm^2. The model strength increases by 22% over the nail diameter range whilst joints designed to the EC5 [11] rules increase by 9% and to EC5 [15] rules by 8%. For both sets of Eurocode rules, at 697N/mm^2 the failure modes were Mode 3B and as the nail strength increased, under EC5 [11] rules the failure mode changes to Mode 2A.

(vi) Number of Rows of Nails and Row Spacing Effect

To equate the model with EC5 [15], as for the steel gusset plate joints, the effect of the number of rows of nails in the joint and of the row spacing function are combined to form one function.

In the model, joint strength is a multiple of the number of rows of nails, *r*, in the joint times the row spacing function. The row spacing function is given in equation (84), where the function is unity at spacing greater than *17d* and *(0.839 + 0.009489Sp/d)* for spacing between *8.5d* and *17d.*

In EC5 [15], joint strength is a function of r^{kef}, as explained in section 6.4.1.2(iv), and in EC5 [11], the joint strength is a linear function of the number of rows of nails and is not affected by the nail row spacing used.

The joint strengths are compared using the combined nail row-spacing functions referred to above. The comparison has been carried out at a spacing of *8.5d, 10d, 14d* and *17d* to envelope the model criteria and also align with the criteria given in EC5 [15]. At the spacing limit of *8.5d,* from Table 8.1 in EC5 [15], k_{ef} will be 0.775.

Nail row spacing – *8.5d, 10d, 14d and 17d*

Using the combined row-spacing functions at a spacing of *8.5d, 10d, 14d* and *17d*, the effect of the functions on the joint strength will be as shown in Figure 6.19.

As for joints with steel gusset plates, in EC5 [15] the row-spacing reduction factor for plywood gusset plate joints is also a function of the number of rows of nails in the joint. For a joint with 7 rows of nails at a row spacing of *8.5d*, the reduction in joint strength will be 35.5% for EC5 [15] and only 8% for the model function, At a spacing of *10d* the reductions are 25.3% and 6.6% respectively and at a spacing of *14d* the Eurocode row-spacing function is unity and the graph aligns with EC5 [11]. At this spacing however, the row-spacing function in the model will still reduce the joint strength by 2.8%.

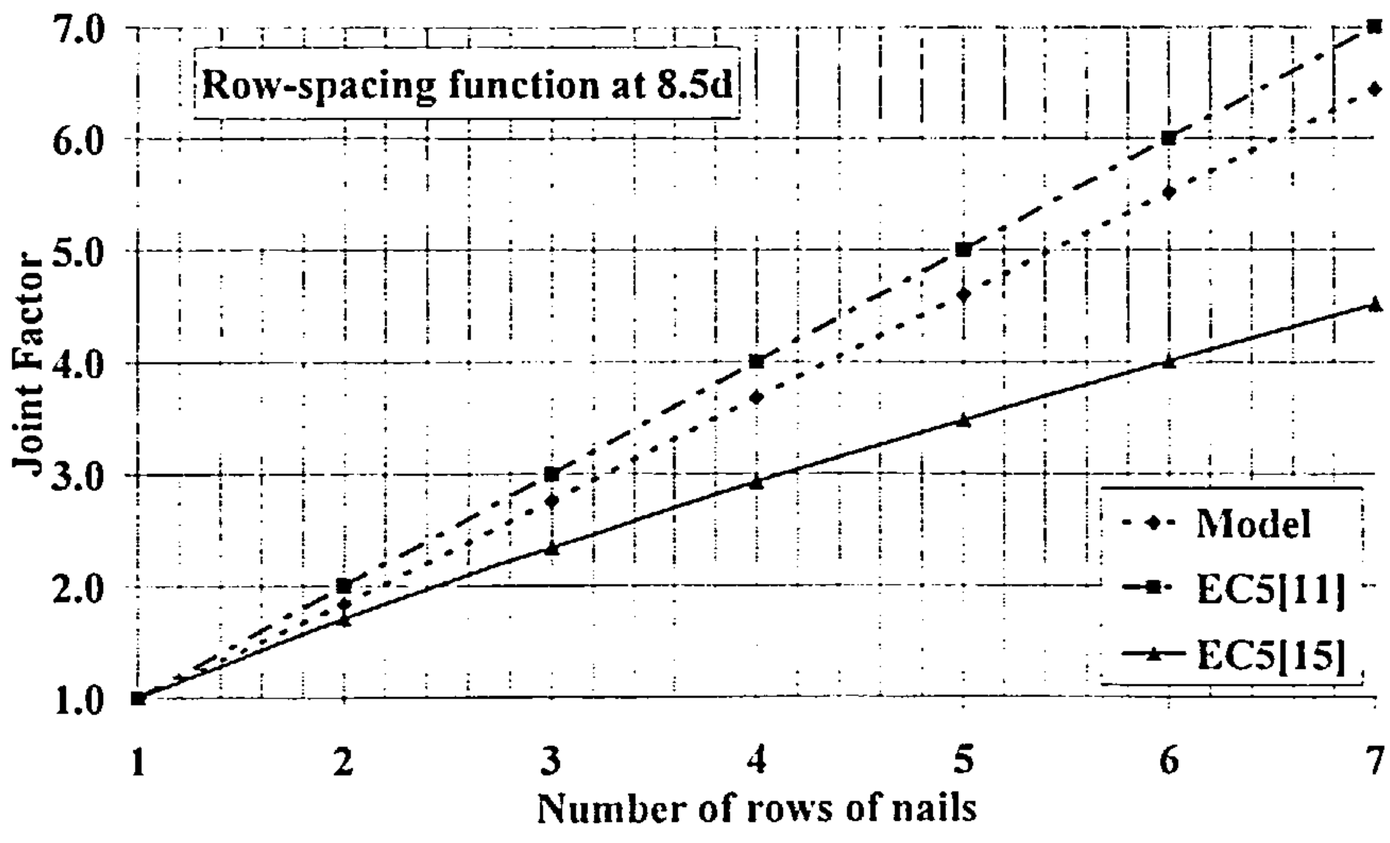

Figure 6.19 The effect of nail row spacing of *8.5d,10d,14d* and *17d* between the model, EC5 [11] and EC5[15].

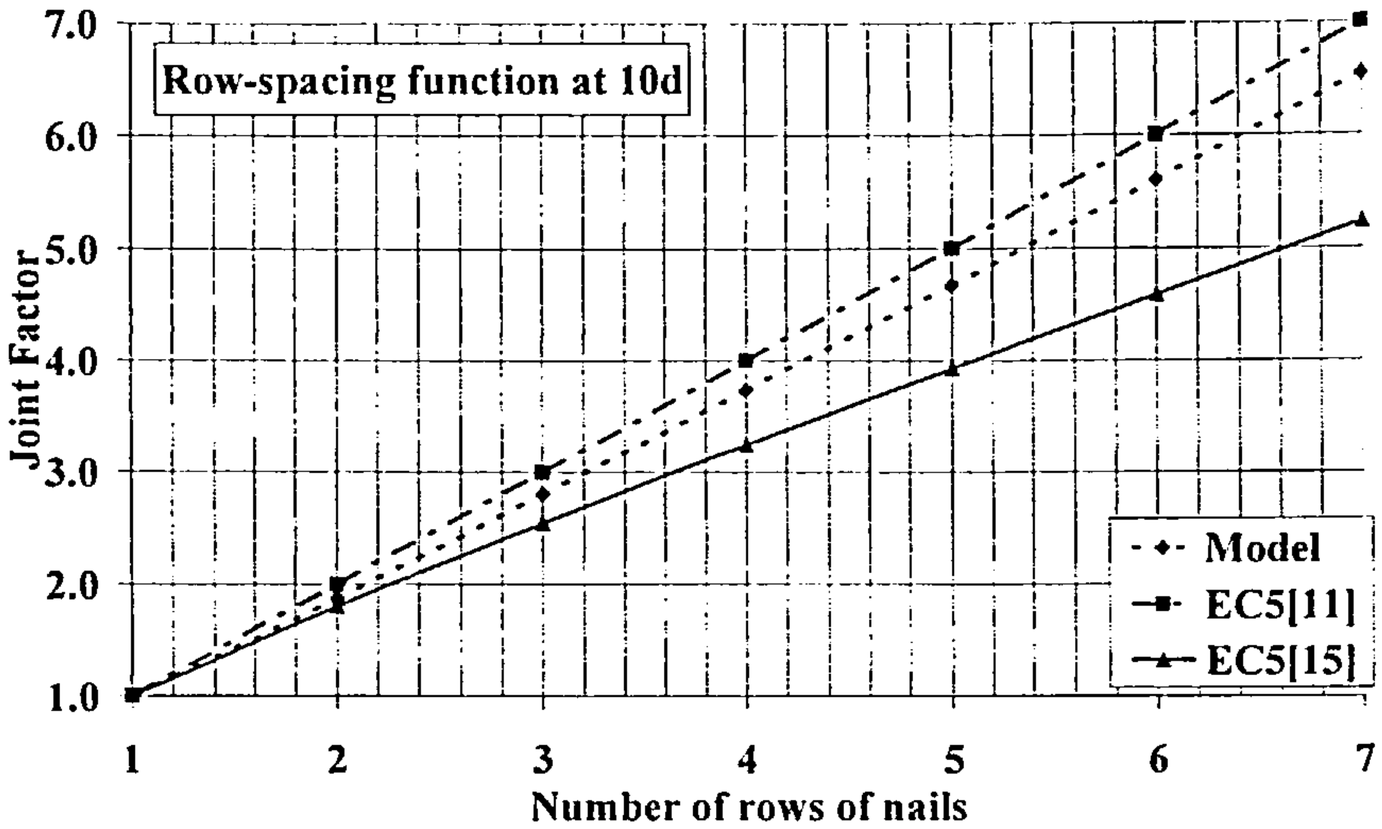

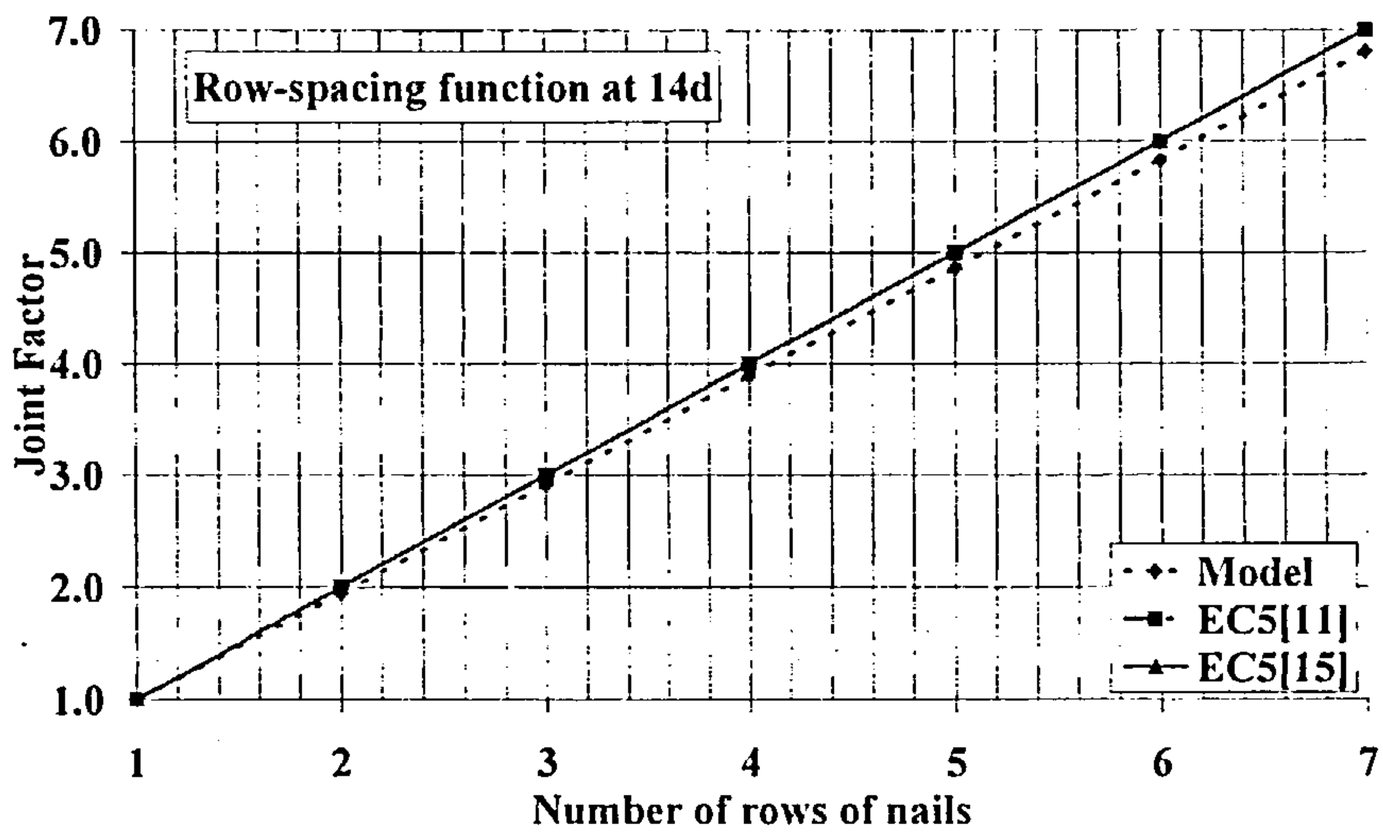

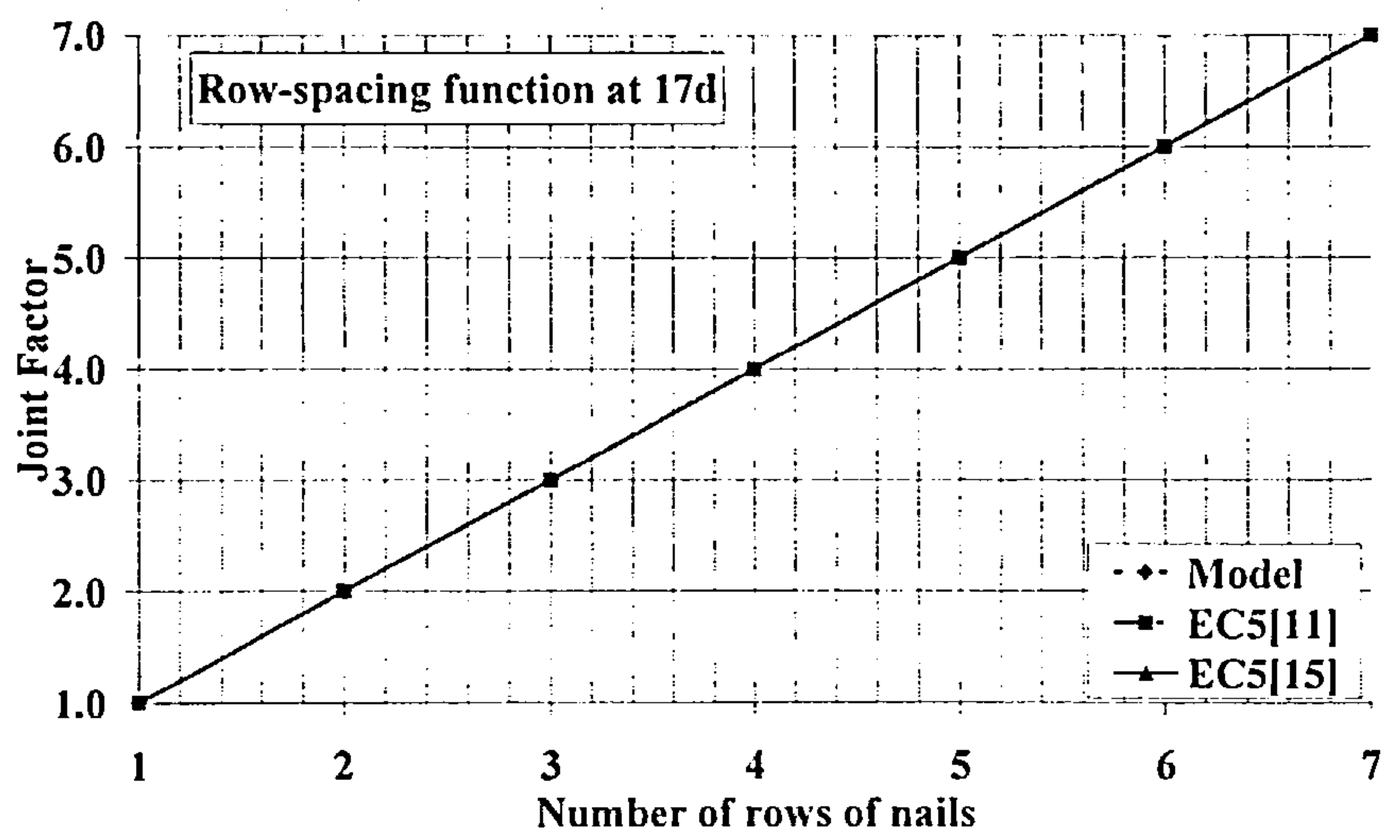

Figure 6.19 cont'd. The effect of nail row spacing of *8.5d,10d,14d* and *17d* between the model, EC5 [11] and EC5[15].

As explained in Chapter 3, the spacing used for joints with fully overlapping nails, is of the order of two times that required for equivalent joints made with non-overlapping nails. Because the comparison has

been made using the same row spacing, a close fit between the model and EC5 [15] is not to be expected. However, as found in section 6.4.1.2 for joints with steel gusset plates, if a reduced spacing had been used for the EC5 [15] joints, an even greater difference than reported above would be exhibited.

(vii) Combined Effect

For joints in which the row spacing is equal to or greater than *17d* there is no consistent relationship between the model, EC5 [11] and EC5 [15] joint behaviour. Examples of the ULS strength of such joints at the extremes of the parameter properties used in the programme are shown in Figure 6.20. Eight joints are considered, enveloping the extremes of timber and plywood density and nail size used in the programme. The joints are made from a pair of nails with a timber-side penetration of 41mm, nail strength of 827N/mm^2 and a material moisture content of 12%.

For joints using 3.33mm diameter nails, the model strength always exceeds the Eurocode results and as the nail size reduces the model value reduces below the EC5 [15] value and fluctuates about the EC5 [11] result. The reduction in strength as the nail size reduces is to be expected as the model has been based on setting the joint capacity at a fixed slip (4.5mm) for all nail sizes, but being aware that for joints with 2.65mm or 3.00mm diameter nails the joint can continue to take higher loads beyond that limit. Using the 3.33mm nail results as the comparator with EC5 rules, the exceedance varies depending on the density of the timber and the plywood. When compared with EC5 [11], the maximum exceedance (36.7%) occurs when the density of the timber and plywood are at the maximum values and the minimum exceedance occurs when they are at minimum density values. In the comparison with EC5 [15], the maximum exceedance (29.8%) occurs when the density of the timber is at its minimum value and the plywood is at its maximum value and the minimum exceedance (11.2%) occurs when they are at minimum density values.

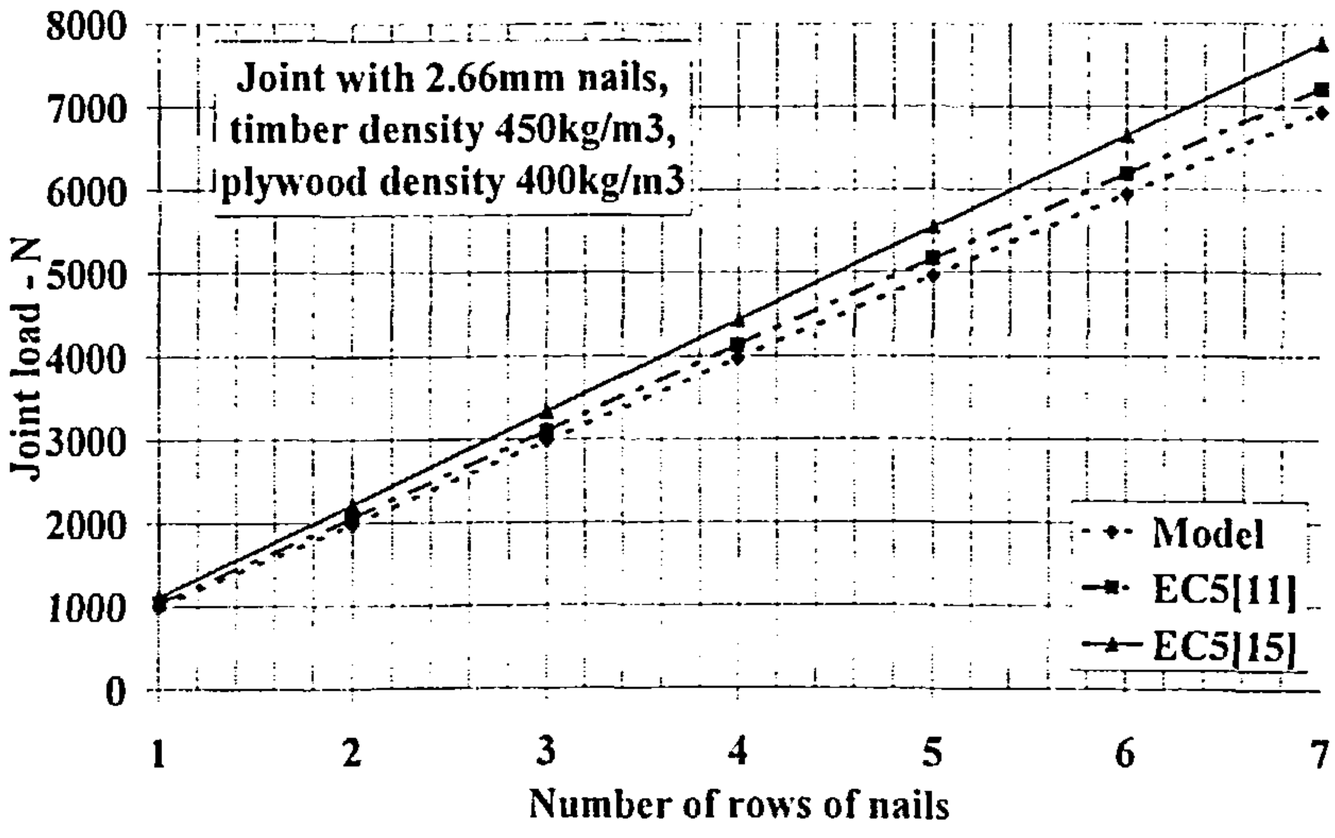

Figure 6.20 Comparison of joint strength using the model, EC5 [11] and EC5 [15] at the ULS

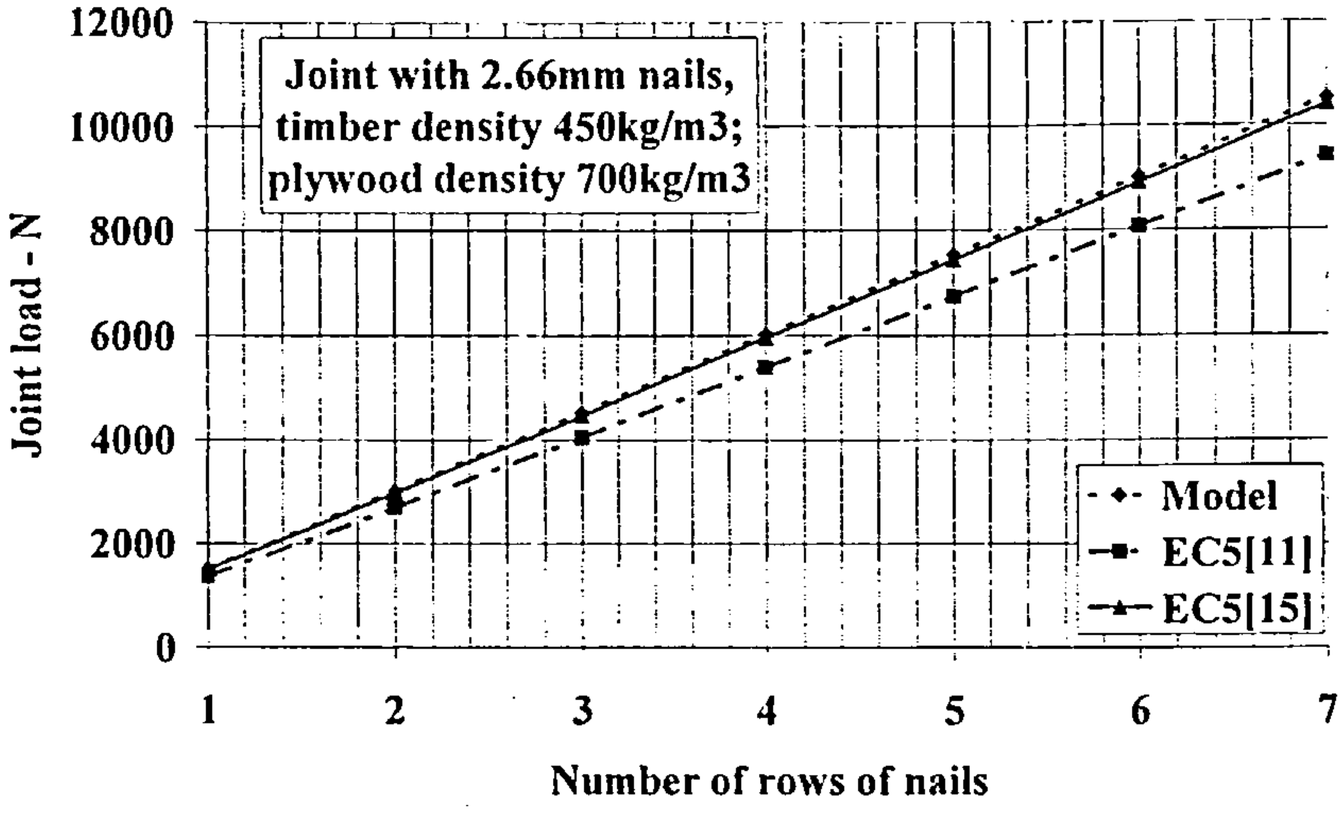

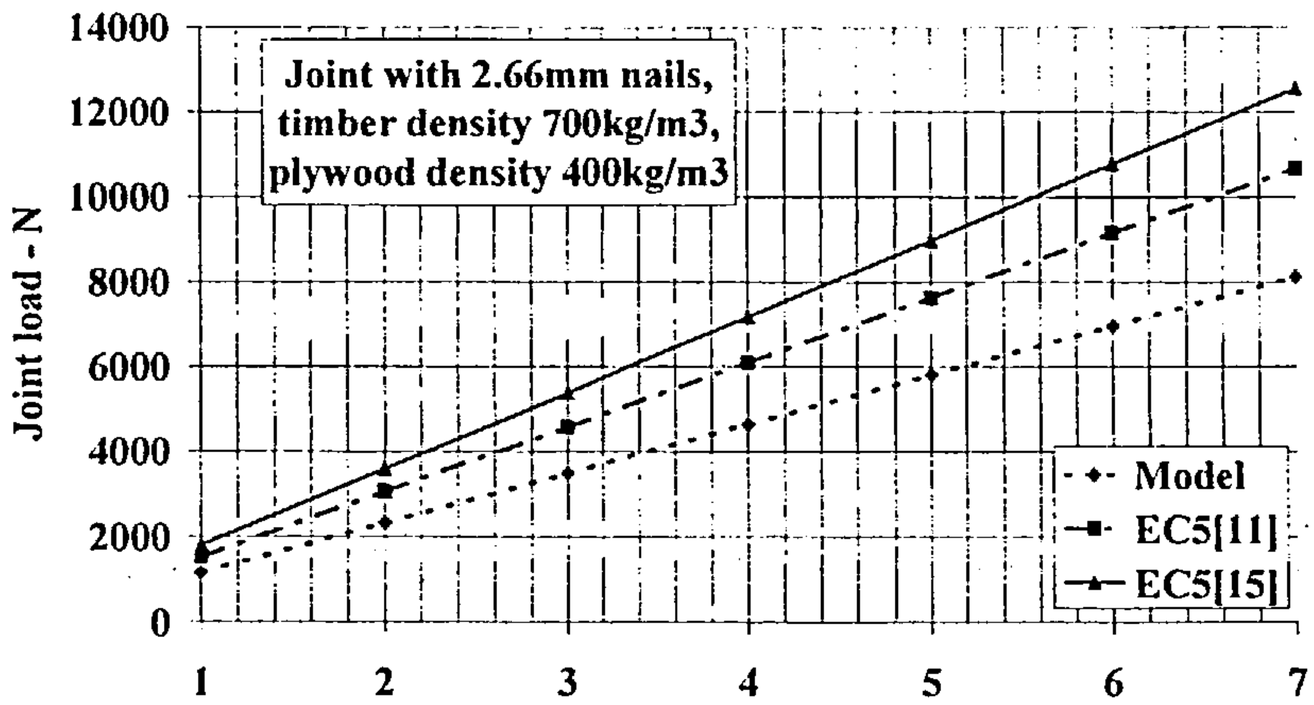

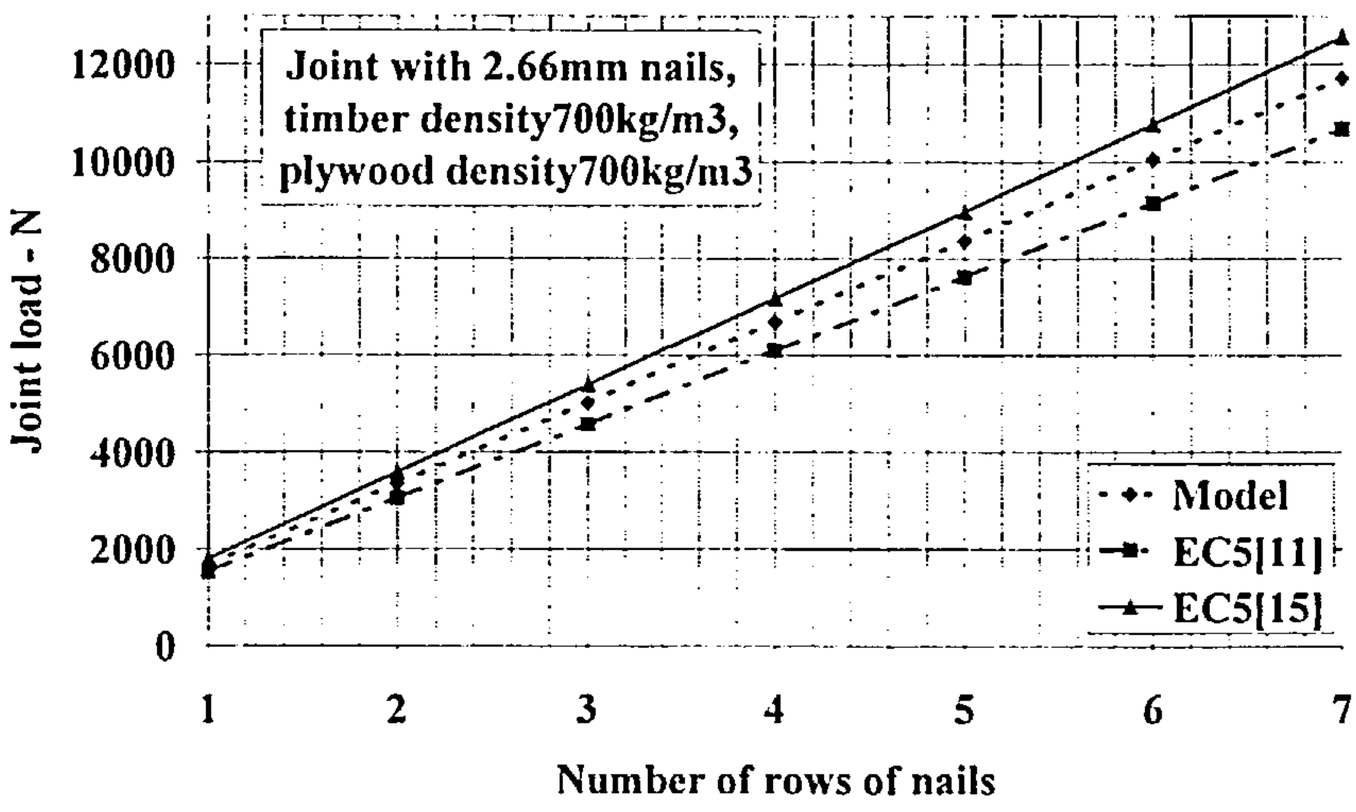

Figure 6.20 cont'd Comparison of joint strength using the model, EC5 [11] and EC5 [15] at the ULS

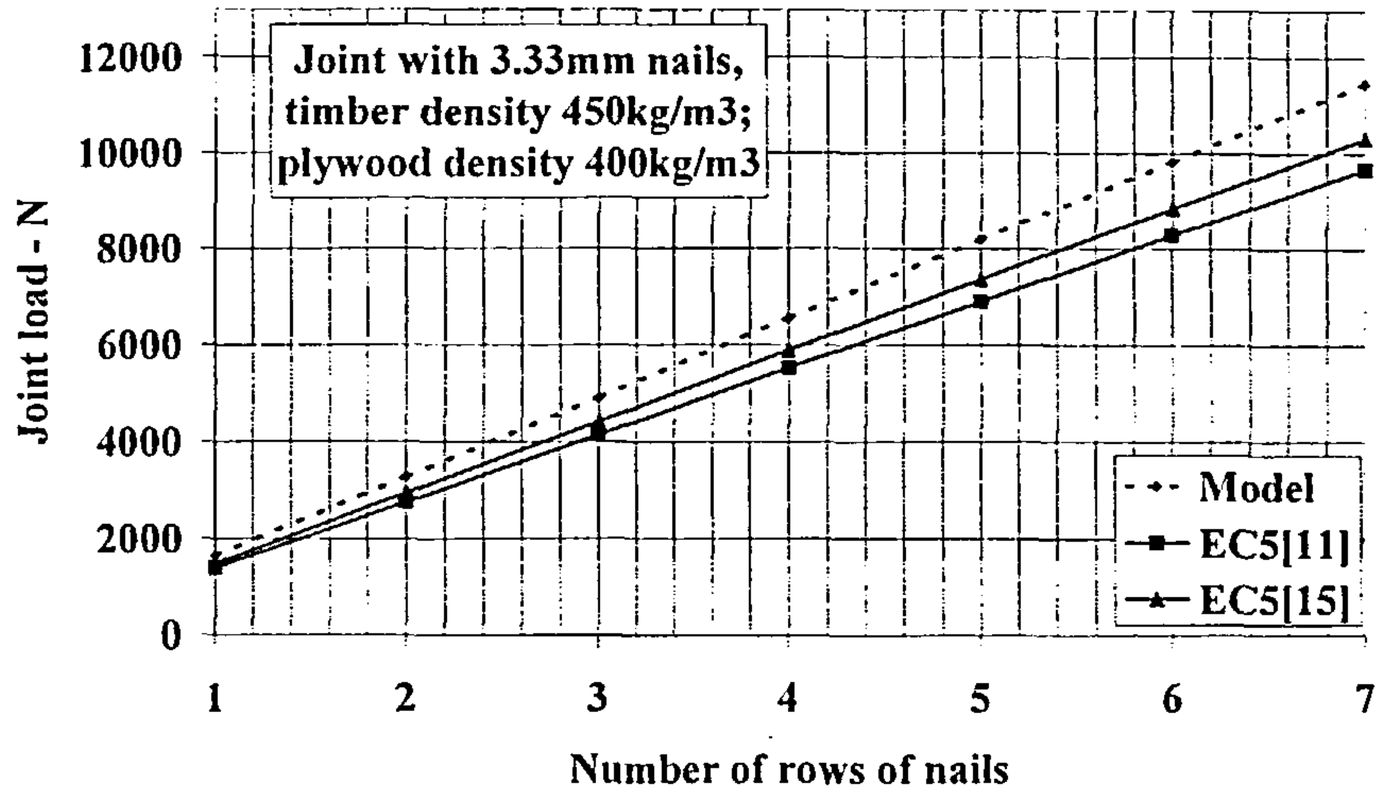

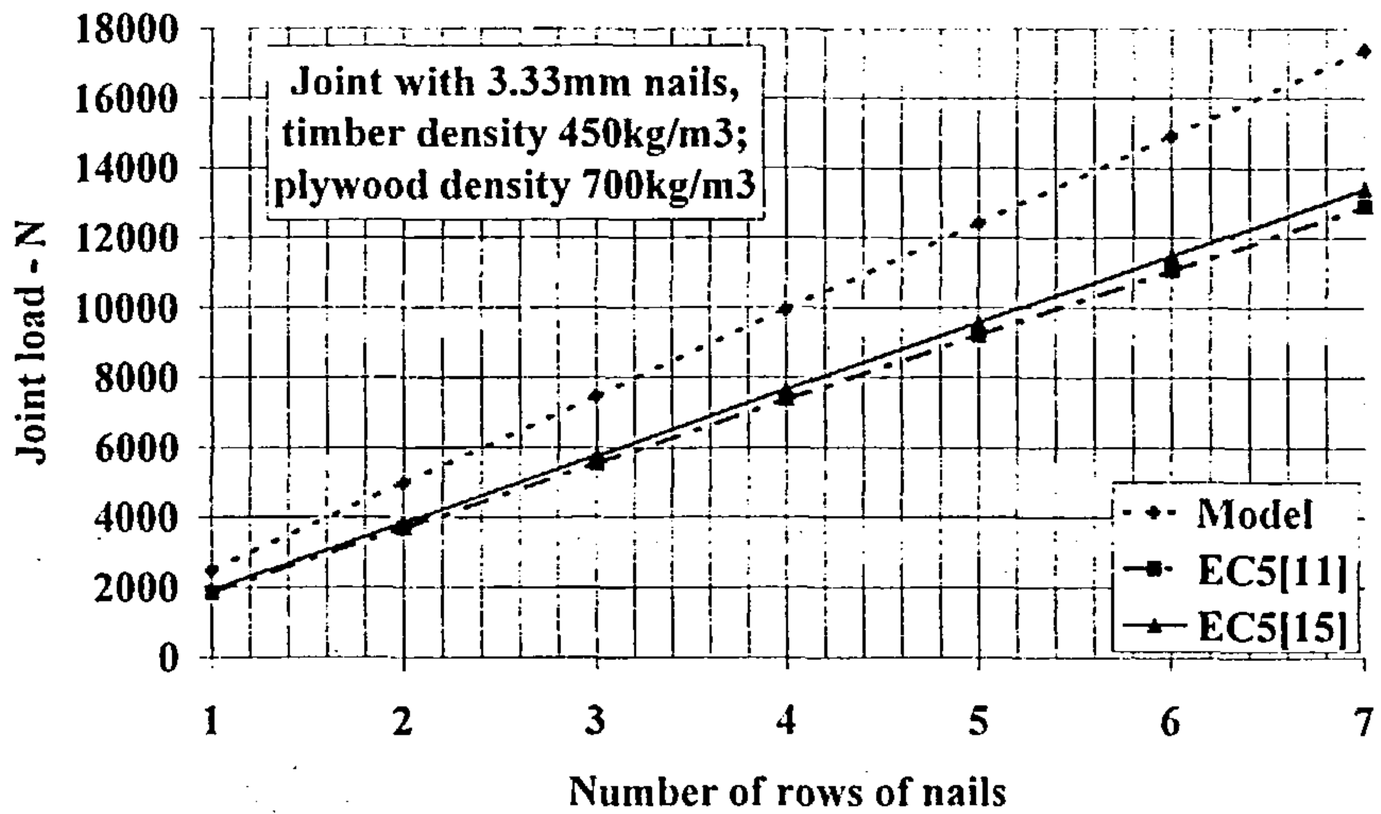

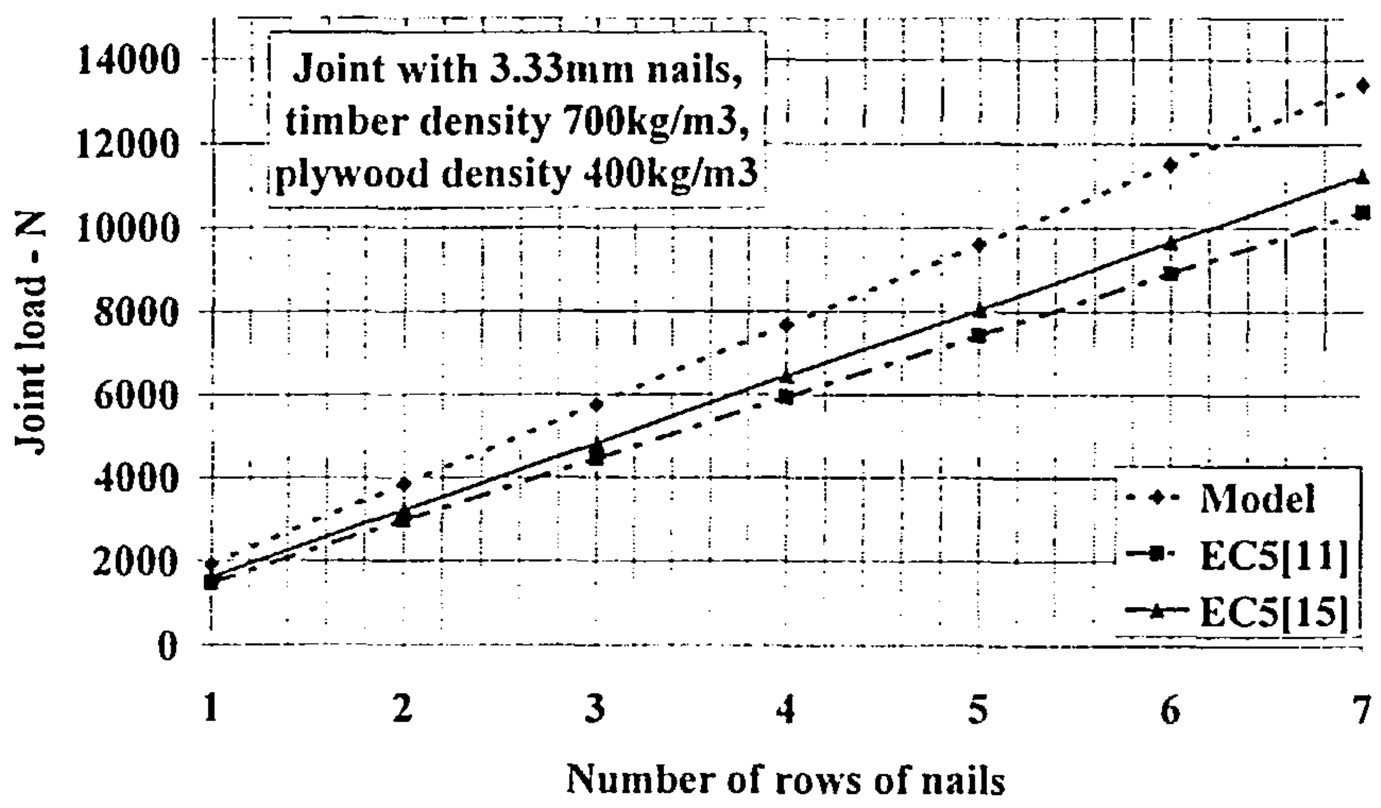

Figure 6.20 cont'd. Comparison of joint strength using the model, EC5 [11] and EC5 [15] at the ULS

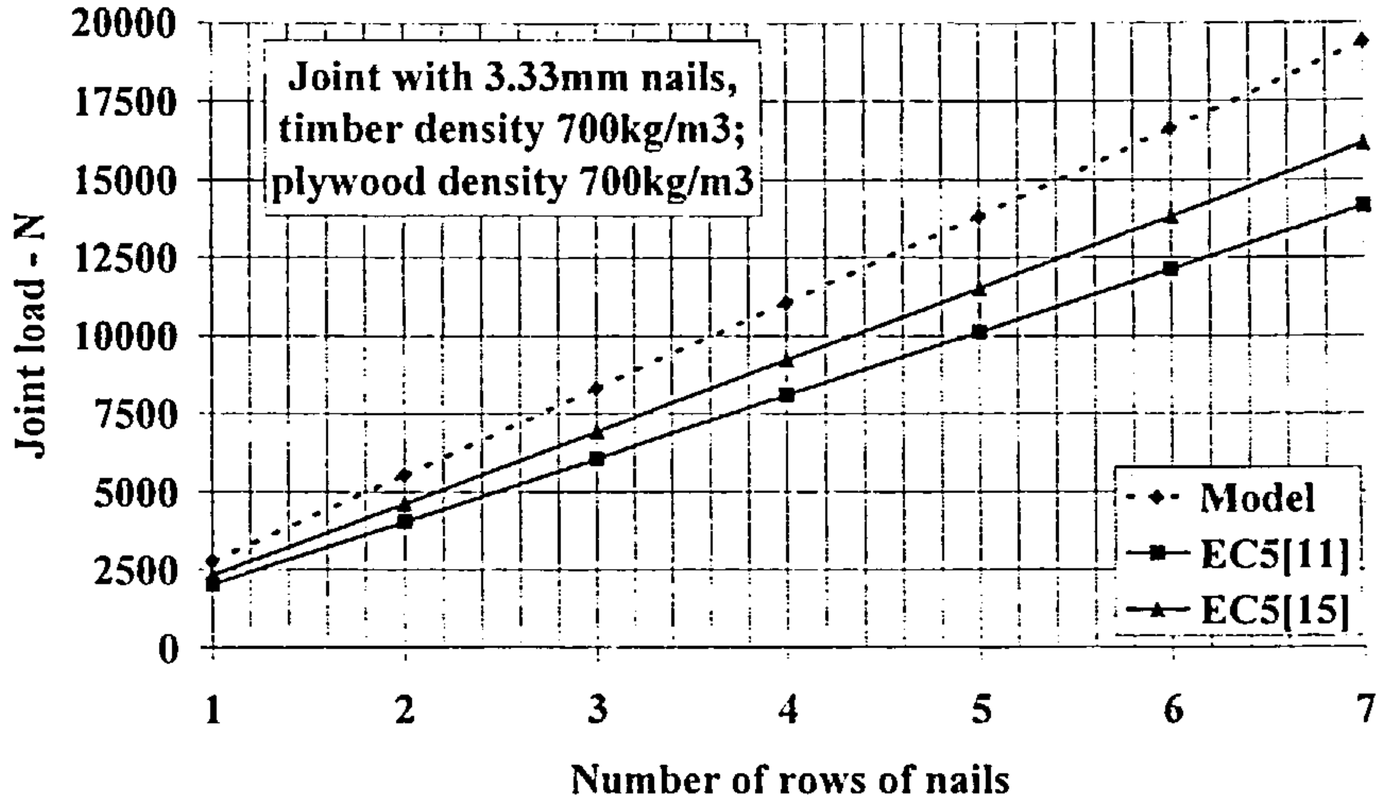

Figure 6.20 cont'd. Comparison of joint strength using the model, EC5 [11] and EC5 [15] at the ULS

The modes of failure predicted by the Eurocode rules are given in Table 6.11 and the failure mode reference used is that given in section 6.2.2.1.

Nail diameter mm	Timber density kg/m^3	Plywood density kg/m^3	EC5 [11] failure mode	EC5 [15] failure mode
2.66	450	400	2A	2A
2.66	450	700	3B	2A
2.66	700	400	2A	2A
2.66	700	700	3B	2A
3.33	450	400	2A	2A
3.33	450	700	2A	2A
3.33	700	400	2A	2A
3.33	700	700	2A	2A

Table 6.11 The joint failure modes based on EC5 [11] and EC5 [15] rules.

It is to be noted in Table 6.11 that the strength equation revisions from EC5 [11] to EC5 [15] result in changes in the mode of joint failure. A comprehensive record of the precise mode of failure of the joints in the test programme was not kept however a sample of the test results is compared with the failure modes obtained from the EC5 equations in Table 6.12.

Where a Type 2A/3B failure is referenced in the Table, these are instances where the nail had fully yielded in the timber and exhibited some elasto-plastic failure in the plywood gussets. From the Table it is seen that the failure modes observed from the tests did not always comply with those projected by EC5. In particular, Mode 3B type failures are not projected by either version of the code but in about 50% of the cases Mode 3B or 2A/3B were noted to have occurred.

Joint conf'n	Timber density kg/m^3	Plywood density kg/m^3	Plywood thickness mm	Nail diameter mm	Nail strength N/mm^2	EC5[11] failure mode	EC5[15] failure mode	Test failure mode
EQ	550	450	17.5	2.66	827	2A	2A	3B
ES	516	582	17.5	3.01	792	2A	2A	3B
CO	542	670	11.6	3.01	792	2A	2A	2A/3B
EU	609	606	17.5	3.33	697	2A	2A	2A/3B
ET	601	597	17.5	3.33	697	2A	2A	2A
EJ	582	588	17.5	3.33	697	2A	2A	2A
EG	557	601	17.5	3.33	697	2A	2A	2A
CO	544	574	17.5	3.33	697	2A	2A	2A/3B
ET	694	715	10.11	3.33	697	2A	2A	2A
ET	637	710	10.13	3.33	697	2A	2A	2A

Table 6.12 Comparison between test failure modes and EC5 [11] and EC5 [15] modes.

The difference between the model and Eurocode results will vary depending on the material parameters used and the parametric study in sections (i) to (iv) shows how variations in each parameter affect the model behaviour and how it also relates to equivalent joints analysed using the Eurocode rules. When the nail row spacing is reduced below *17d,* with the exception of joints designed to EC5 [11], the combined row-spacing function will apply. This function reduces the joint strength in multi-row joints. Because of the requirement to adopt a greater row spacing in joints with fully overlapping nailed joints over that required for equivalent joints assembled using nails which do not fully overlap, the model and EC5 [15] row-spacing functions cannot be directly compared. What can be noted, however, is that using EC5 [15] rules the value of the reduction increases as the number of rows increase and if using the minimum row spacing of *8.5d* on a 7 row joint, the strength of EC5 [15] joints will be reduced by 35.5% and the model results by only 8%. If the EC5 [15] spacing is reduced to *5d* to better equate to joints with fully overlapping nails the comparison will be as shown in Figure 6.21. The strength reduction will be even greater and for the joint type referred to above will equate to 62.2%. It should also be noted that when *14d* spacing is used, EC5 [15] rules will underestimate the strength reduction by 2.8%.

As was found for joints with steel gusset plates, for plywood gusset plate joints designed to EC5 [15] rules the row spacing factor greatly reduces the joint strength over that obtained from the equivalent model function. Because the row spacing requirement with fully overlapping nails is of the order of two times that required for joints made with nails which do not fully overlap, the row-spacing factor cannot be directly equated to the model row-spacing factor at the same spacing.

For joints with fully overlapping nails, using the unity row–spacing factor in EC5 [11], the joint strength will be overestimated. Relative to the model reduction, the maximum overestimate will be 8%,

occurring in joints with 7 rows of nails and using the minimum row spacing of *8.5d.* The overestimate reduces to nil as the row spacing is increased to *17d*

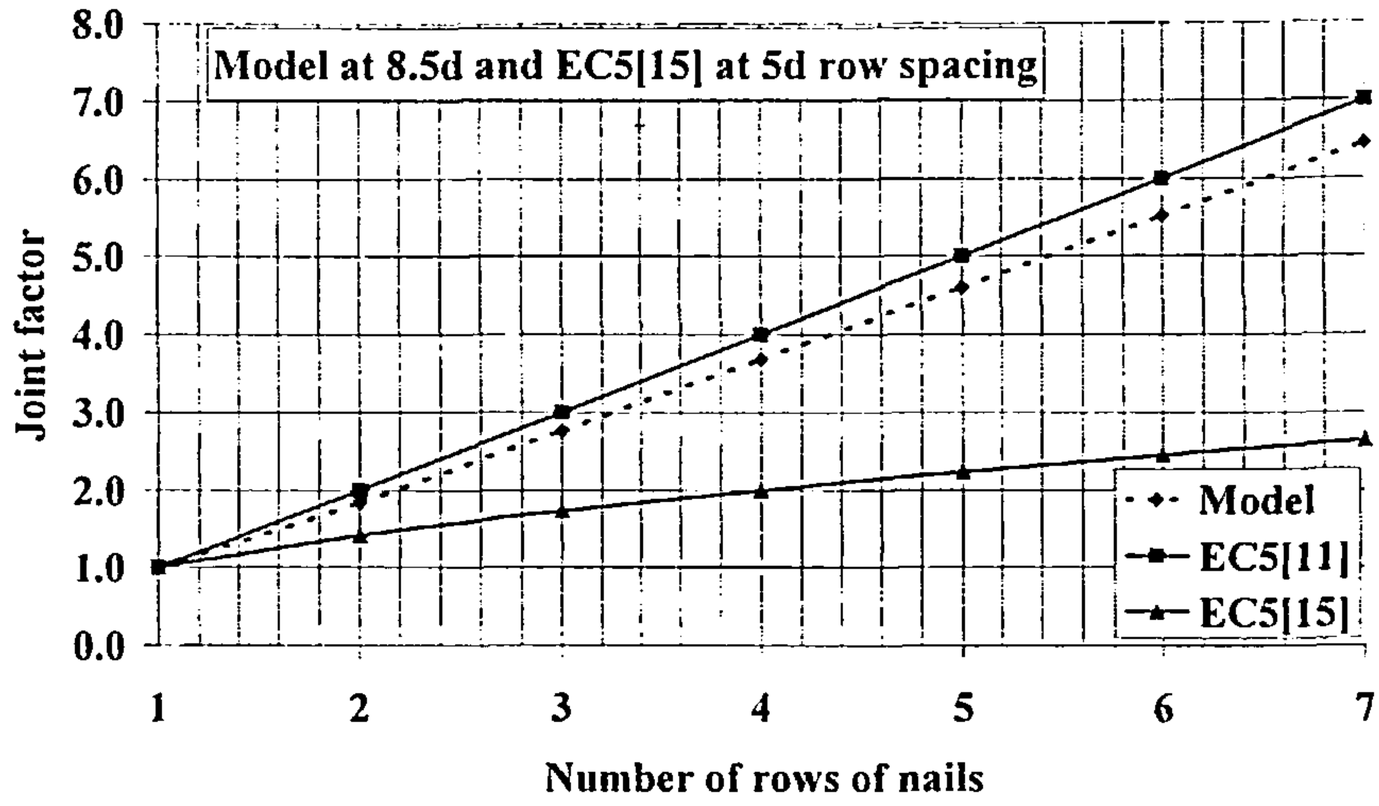

Figure 6.21 The effect of nail row spacing at *8.5d* in the model compared with EC5 [11] and a nail row spacing of *5d* in EC5 [15].

6.4.2 Strength at the Serviceability Limit State

The design load strength at the SLS, $F_{d.ser}$, is obtained by applying a load factor to the ULS design strength, as given in equation (162). Applying the same factor to the model design strength to obtain the equivalent SLS load in the model, the comparison with EC5 will remain as described in section 6.4.1.

6.4.3 Stiffness at the Serviceability Limit State

6.4.3.1 Joints with Steel Gusset Plates

The SLS stiffness of the model is obtained by dividing the joint strength at the SLS by the joint displacement at that load. As explained in section 6.2.3.2, to obtain the SLS instantaneous slip modulus, a load factor of 2.5 has been used in EC5. The same factor will be applied to the model strength equation to obtain the equivalent SLS load for the model. Considering any joint with a row spacing equal to or exceeding *19.6d,* using equation (175b) and applying a load factor of 2.5, the SLS load for the model will be:

$$P\delta_{xd.ser} = [0.853AD(d)^{1.4468} f_u rn(1-e^{-1.712\delta x})^{0.926}(0.1\delta x + 0.68)/f(mc)]\frac{1}{2.5} \qquad \ldots.(184)$$

From the displacement function, at the SLS load the slip in the joint will be 0.437mm and the model stiffness, $K_{sermodel}$, per pair of fully overlapping nails in joints with steel gusset plates at the SLS becomes:

$$K_{sermodel} = [0.853AD(d)^{1.4468} f_u (1-e^{-1.712\delta x})^{0.926}(0.1\delta x + 0.68)/f(mc)] \frac{1}{2.5 \times 0.437} \quad \ldots.(185)$$

The stiffness equation is valid for joints with a pair of fully overlapping nails and also for multi-row joints where the nail row spacing is equal to or greater than *19.6d*.

The development of the stiffness of joints with a single nail designed to EC5 [11] and EC5 [15] has been discussed in section 6.2.3.2. For joints with steel gusset plates, EC5 [15] allows the application of a factor of 2 to obtain the stiffness and applying a further factor of 2 to obtain the stiffness of predrilled joints with 2 nails, the EC5 slip modulus at the SLS are:

(i) *EC5 [11]*
$$K_{serEC11} = 2 \times \frac{\rho_k^{1.5} d}{20} \equiv 2 \times \frac{\rho_m^{1.5} d}{25} \quad \ldots.(186)$$

(ii) *EC5 [15]*
$$K_{serEC15} = 2 \times 2 \times \frac{2}{3} \times \frac{\rho_m^{1.5} d}{35} \quad \ldots.(187)$$

where ρ_m is the mean density of the timber in the joint and d is the nail diameter.

These stiffness equations apply to joints with a pair of nails in single shear and in multi-row joints where the nail row spacing is equal to or greater than the upper limit of *14d* given in the code. In the model equation, (185), the slip at the SLS is fixed at 0.437mm for all nail sizes. The EC5 stiffness equations are based on a slip which is variable, being a function of $d^{0.8}$ and the inverse of the material density, as given in equations (1) and (173) for EC5 [11] and EC5 [15] respectively. The nail slip at the SLS for each nail size is given in Table 6.13 and a graphical comparison of the associated stiffness at the extreme density values of 450Kg/m^3 and 700Kg/m^3 against the model behaviour is given in Figure 6.22.

Nail diameter Mm	**Slip at the SLS using the model. mm**		**Slip at the SLS using EC5 [11]. mm**		**Slip at the SLS using EC5 [15]. mm**	
	Timber Density *450kg/m^3*	Timber Density *700kg/m^3*	Timber Density *450kg/m^3*	Timber Density *700kg/m^3*	Timber Density *450kg/m^3*	Timber Density *700kg/m^3*
2.66	0.437	0.437	0.418	0.269	0.509	0.347
3.01	0.437	0.437	0.460	0.296	0.557	0.378
3.36	0.437	0.437	0.502	0.323	0.605	0.409

Table 6.13 Joint slip from the model; EC5 [11] and EC5 [15] at the serviceability limit state in a joint formed with a pair of nails

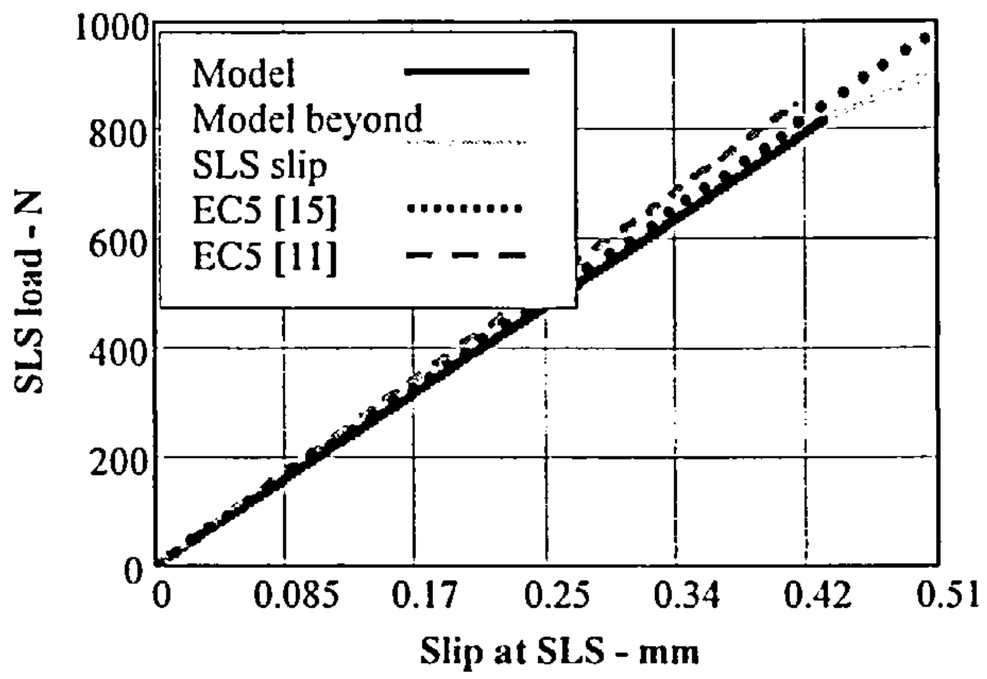

2-2.65mm nails; timber density-450kg/m^3

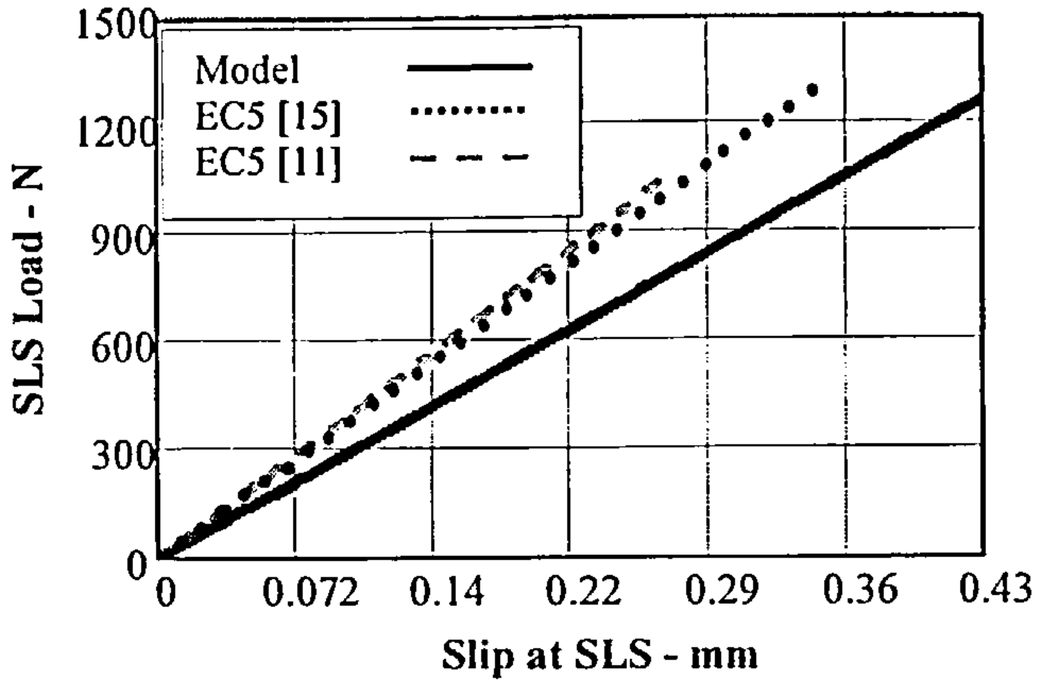

2-2.65mm nails; timber density-700kg/m^3

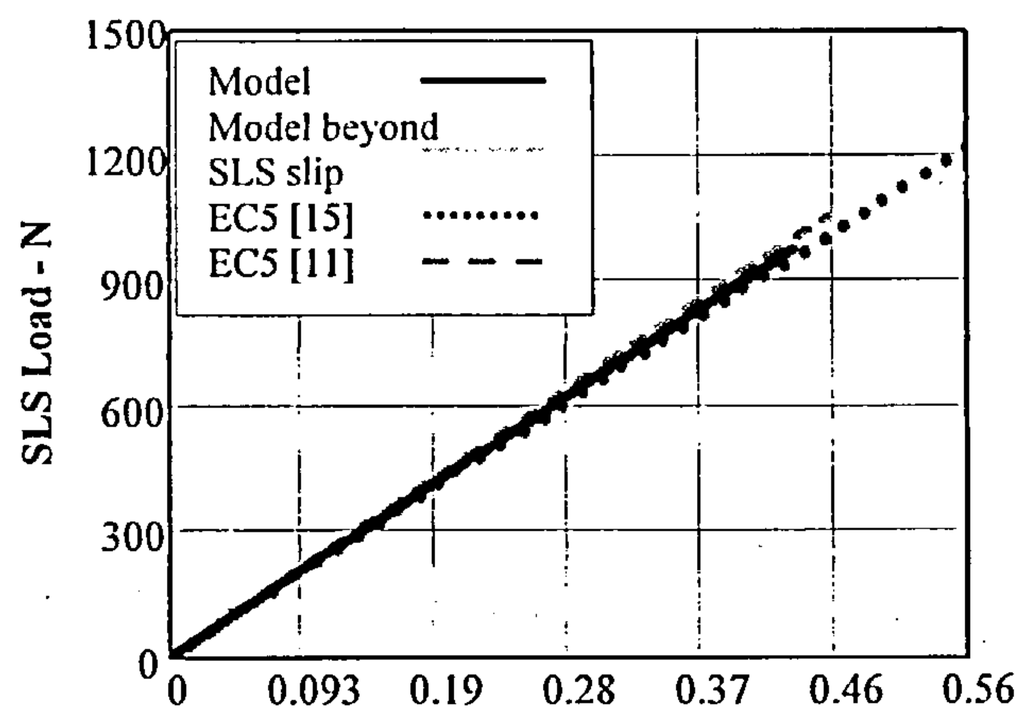

2-3.0mm nails; timber density-450kg/m^3

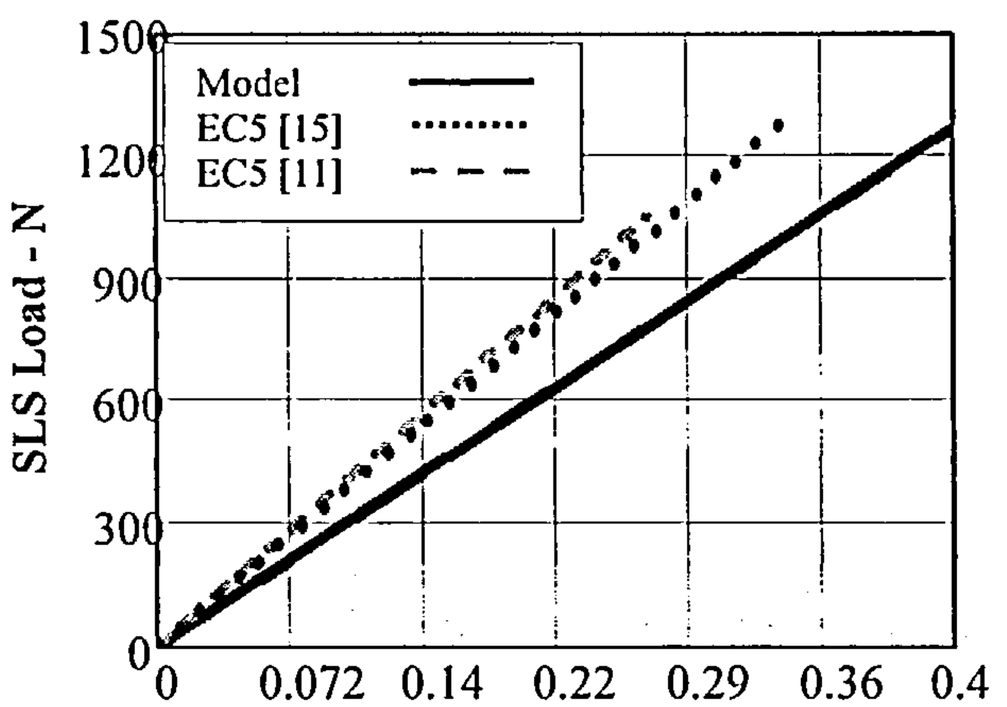

2-3.00mm nails; timber density-700kg/m^3

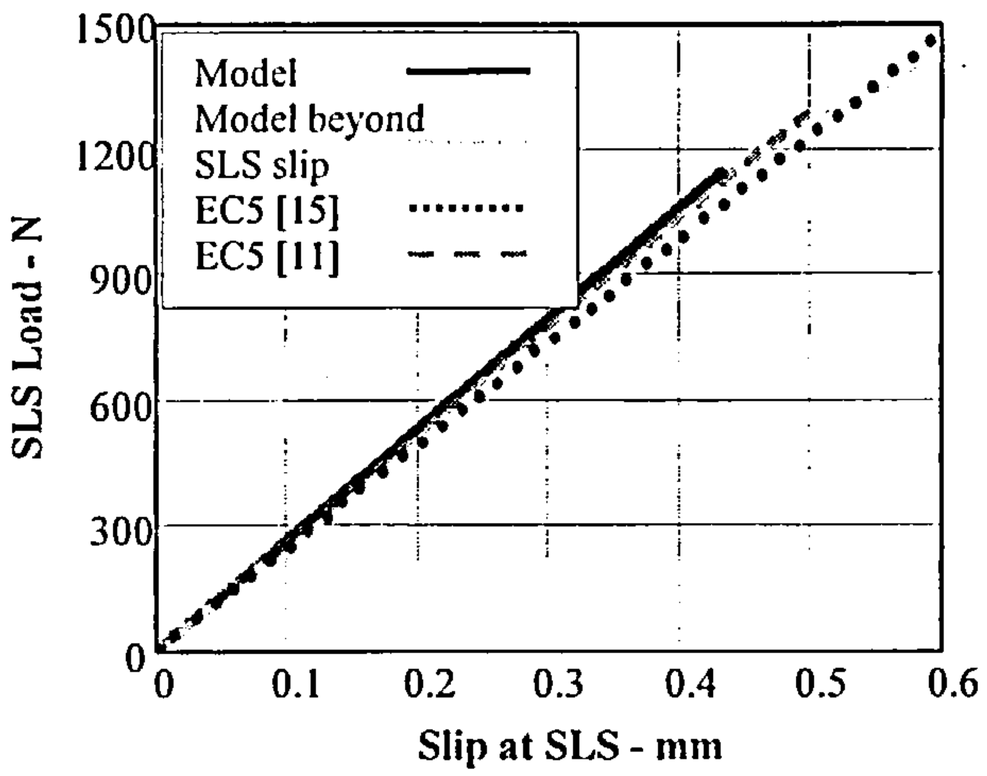

2-3.35mm nails; timber density-450kg/m^3

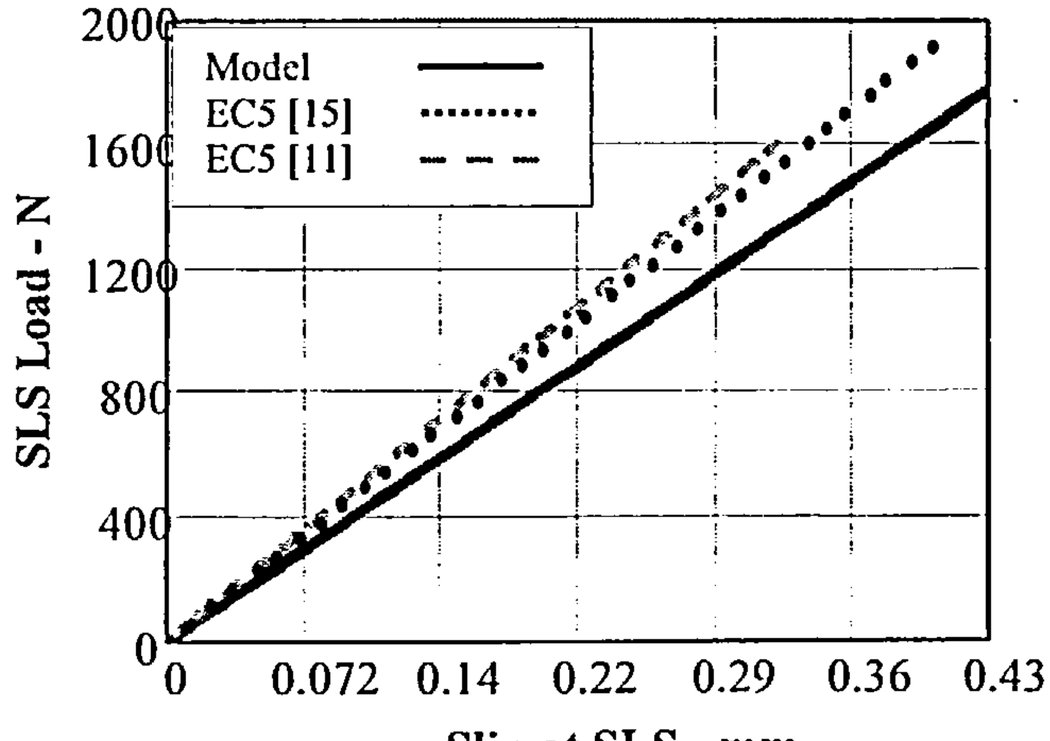

2-3.35mm nails; timber density-700kg/m^3

Figure 6.22 Comparison of the stiffness of the model, EC5[11] and EC5 [15] for a pair of 2.66mm, 3.01mm and 3.36mm diameter nails at the SLS.

In each case the EC5 [11] and EC5 [15] stiffness is within 5% of each other in value, with EC5 [15] consistently being the lesser. The stiffness of the model equates closely with EC5 [11] and EC5 [15] for all nails sizes at a density of 450kg/m^3 and as the density increases, the EC5 [11] and EC5 [15] slip modulus exceed the model value. The percentage difference between the model and the Eurocode values for each nail size is given in Table 6.14. A negative sign in the table denotes that the model is less stiff than the relevant Eurocode value.

Nail diameter mm	**% difference between model stiffness and EC5 [11] slip modulus.**		**% difference between model stiffness and EC5 [15] slip modulus**	
	Timber Density *450kg/m^3*	Timber Density *700kg/m^3*	Timber Density *450kg/m^3*	Timber Density *700kg/m^3*
2.66	-8.2	-35.0	-3.1	-28.6
3.01	-2.4	-27.7	+2.5	-21.6
3.36	+2.5	-21.6	+7.1	-15.8

Table 6.14 Percentage difference between model stiffness and EC5 slip modulus at the SLS for a joint with a pair of nails.

With timber at a density of 700kg/m^3, EC5 [11] exceeds the model stiffness by values ranging from 21.6% to 35% depending on the nail diameter and EC5 [15] exceeds it by 15.8% to 28.6%, again depending on the nail diameter. Although the exceedance reduces as the nail diameter increases, the Eurocode values are such that if applied to joints using fully overlapping nails with timber at an average density above 500kg/m^3, the rules would significantly underestimate the slip in the joint and result in an unsafe design.

The graphs in Figure 6.22 apply to joints with nail row spacing equal to or exceeding *19.6d*. For joints with multi-rows of nails at row spacing less than *19.6d* the row spacing reduction factors will modify the joint strengths and the difference relative to the model will reduce.

6.4.3.2 Joints with Plywood Gusset Plates

The SLS stiffness of the model is obtained by dividing the joint strength at the SLS by the joint displacement at that load.

As explained in section 6.2.3.2, to obtain the SLS instantaneous slip modulus, a load factor of 2.5 has been used in EC5. The same factor has been applied to the ULS model strength equation to obtain the

equivalent SLS load for the model. Considering any joint with a row spacing equal to or exceeding *17d,* using equation (183g) and applying a load factor of 2.5, the SLS load for the model will be:

$$P\delta_{xdpser} = [0.853(Ae)(Density\ Function)(d)^{2.236} f_u rn(1-e^{-1.406\delta x})^{0.54}(0.121\delta x + 1)]\ \frac{1}{2.5} \qquad \ldots.(188)$$

From the displacement function, at the SLS load the slip in the joint will be 0.34mm and the model stiffness, $K_{psermodel}$, per pair of fully overlapping nails in joints with plywood gusset plates at the SLS becomes:

$$K_{psermodel} = [0.853(Ae)(Density\ Function)(d)^{2.236} f_u rn(1-e^{-1.406\delta x})^{0.54}(0.121\delta x + 1)]\ \frac{1}{2.5} \times \frac{1}{0.34} \qquad \ldots.(189)$$

The stiffness equation is valid for joints with a pair of fully overlapping nails and for joints with multi-rows of nails where the nail row spacing is equal or greater than *17d.*

The development of the stiffness of joints with a single nail designed to EC5 [11] and EC5 [15] has been discussed in section 6.2.3.2. For joints with plywood gusset plates, applying a factor of 2 to obtain the stiffness of predrilled joints with 2 nails the EC5 stiffness equations at the SLS are:

(i) *EC5 [11]* $$K_{serEC11} = 2 \times \frac{\rho_k^{1.5} d}{20} \equiv 2 \times \frac{\rho_m^{1.5} d}{25} \qquad \ldots.(190)$$

(the same as for joints with steel gusset plates)

(ii) *EC5 [15]* $$K_{serEC15} = 2 \times \frac{2}{3} \times \frac{\rho_m^{1.5} d}{35} \qquad \ldots.(191)$$

where d is the nail diameter and ρ_m is the mean density of the timber and plywood, such that:

$$\rho_m = \sqrt{\rho_{mtimber} \times \rho_{mplywood}} \qquad \ldots.(192)$$

These stiffness equations apply to joints with a pair of nails in single shear and in joints with multi-rows of nails where the nail row spacing is equal to or greater than the upper limit of *14d* given in the code,

Because of the extent of variables involved, the comparison of the model and EC5 stiffness equations has been limited to 2.66mm and 3.33mm diameter nails; using timber with a mean density ranging from 450Kg/m^3 to 700 Kg/m^3; plywood 17.5mm thick and a nail length with a timber side penetration of

41mm. The nail yield strength has been taken as 827N/mm^2. These parameters envelope the extremes used in the testing programme.

In the model equation, (189), the slip at the SLS is fixed at 0.34mm for all nail sizes. As with joints using steel gusset plates, the EC5 stiffness equations for plywood gusset plate joints are based on a variable slip. A summary of the SLS slip for the model, EC5 [11] and EC5 [15] is given in Table 6.15.

Nail diameter-plywood density		**Slip at the SLS using model. mm**		**Slip at the SLS using EC5 [11]. mm**		**Slip at the SLS using EC5 [15]. mm**	
mm	kg/m^3	Timber Density *450kg/m^3*	Timber Density *700kg/m^3*	Timber Density *450kg/m^3*	Timber Density *700kg/m^3*	Timber Density *450kg/m^3*	Timber Density *700kg/m^3*
2.66	400	0.34	0.34	0.288	0.222	0.651	0.501
	700	0.34	0.34	0.247	0.201	0.574	0.497
3.33	400	0.34	0.34	0.308	0.238	0.691	0.542
	700	0.34	0.34	0.271	0.213	0.590	0.510

Table 6.15 Joint slip from the model; EC5 [11] and EC5 [15] at the serviceability limit state in a joint formed with a pair of nails using 2.66mm and 3.33mm nails.

The comparison between the model, EC5 [11] and EC5 [15] stiffness at the SLS is given in Figure 6.23.

There is a considerable difference between EC5 [11] and EC5 [15] stiffness, caused by the changes in the respective strength and stiffness equations in EC5 [15]. With 2.66mm diameter nails the model stiffness lies between the Eurocode values and with 3.33mm diameter nails the model stiffness approximates the EC5 [11] slip modulus. In all cases EC5 [15] rules underestimate the joint stiffness and would result in a safe, albeit uneconomic design. If EC5 [11] rules were applied, the stiffness would be overestimated, resulting in an unsafe design for joints using nails with a diameter less than 3.33mm.

The graphs in Figure 6.23 apply to joints with nail row spacing equal to or exceeding *17d*. For joints with multi-rows of nails at row spacing less than *17d* the row spacing reduction factors will modify the joint strengths of both the model and EC5 [15]. This will lead to a reduction in the model stiffness relative to EC5 [11] and the EC5 [15] curve will reduce even further relative to the model and to EC5 [11]. Because of the poor comparison between the model and the EC5 [15] reduction factors, graphs incorporating these factors have not been given.

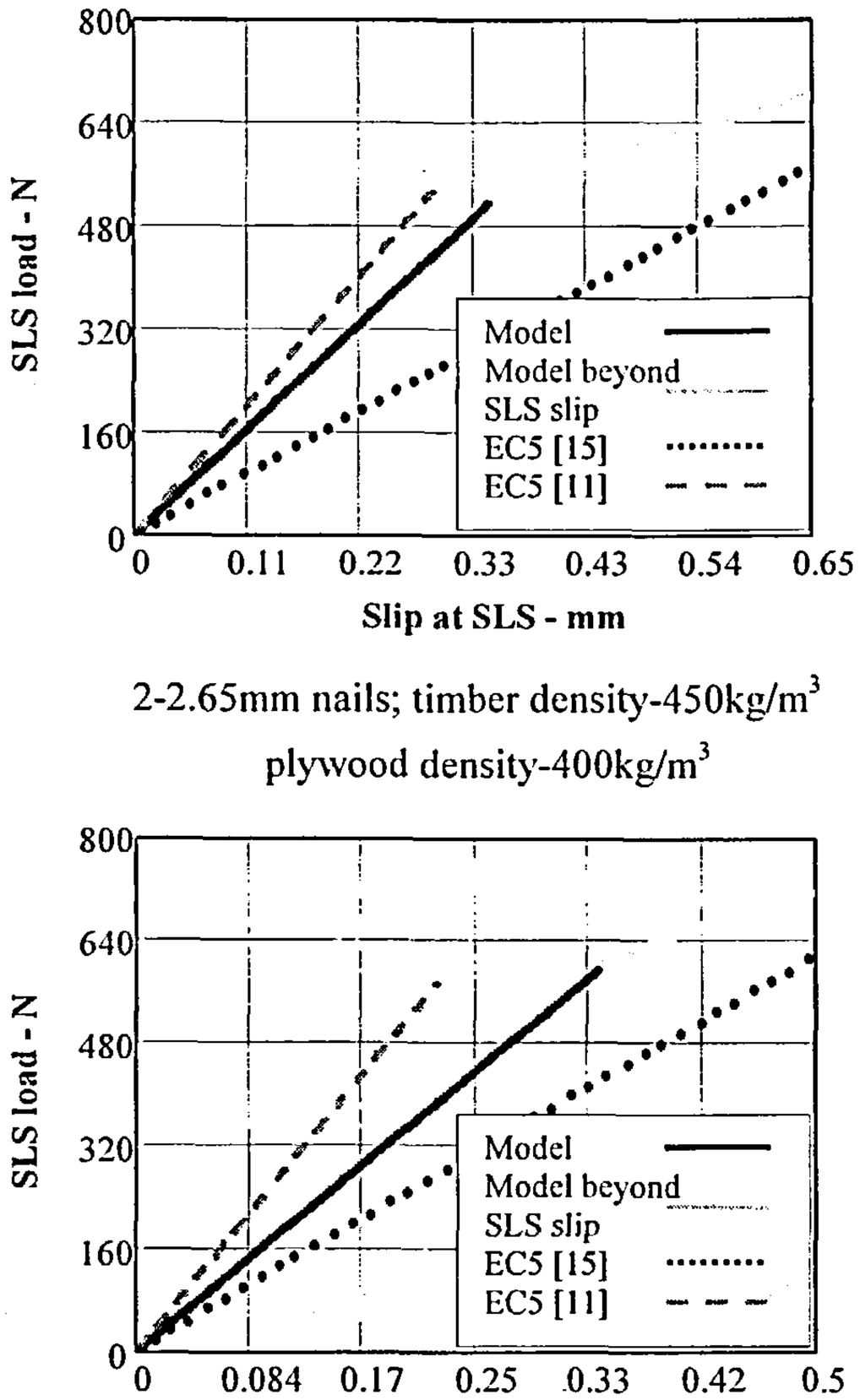

2-2.65mm nails; timber density-450kg/m^3
plywood density-400kg/m^3

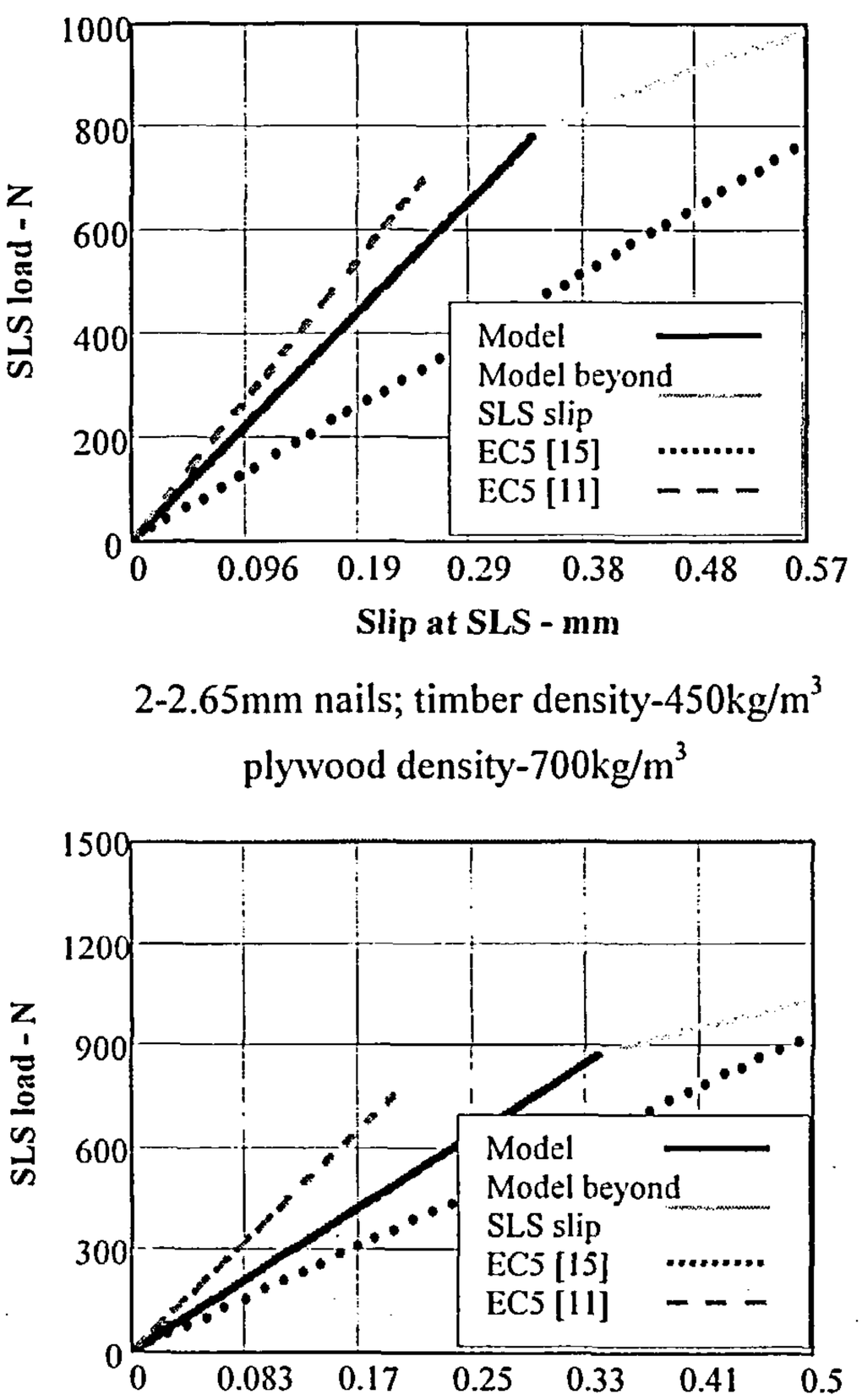

2-2.65mm nails; timber density-450kg/m^3
plywood density-700kg/m^3

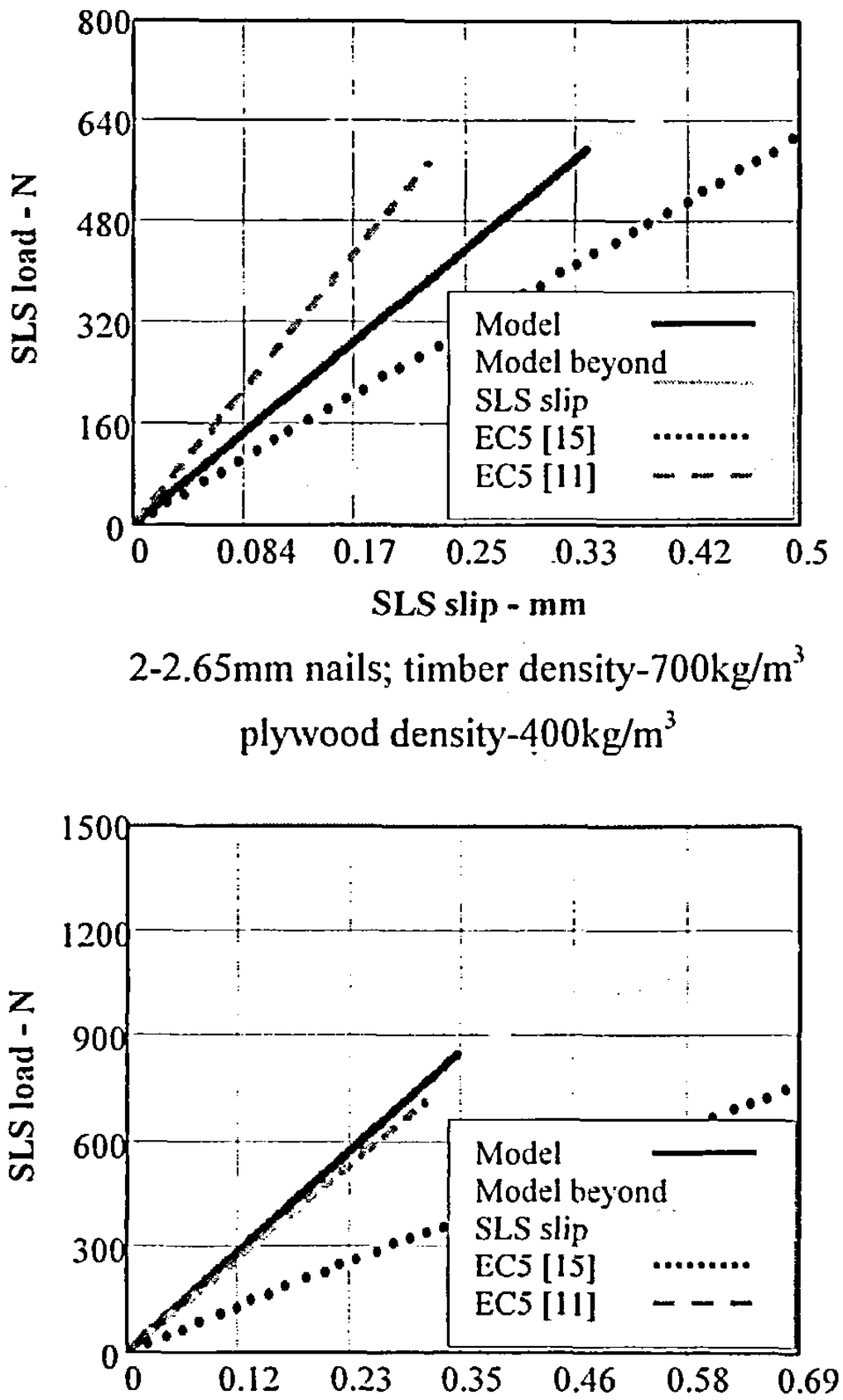

2-2.65mm nails; timber density-700kg/m^3
plywood density-400kg/m^3

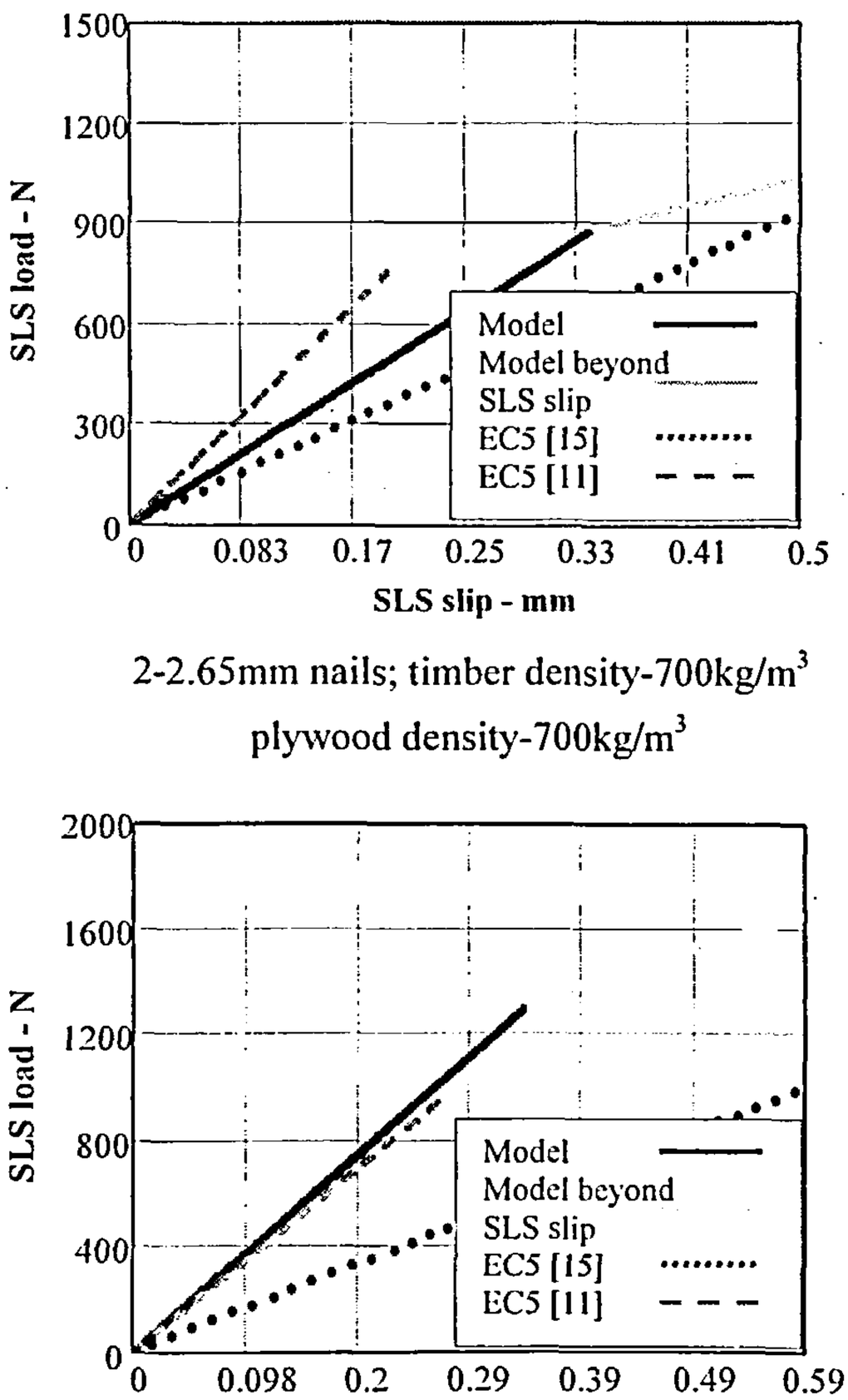

2-2.65mm nails; timber density-700kg/m^3
plywood density-700kg/m^3

2-3.35mm nails; timber density-450kg/m^3
plywood density-400kg/m^3

2-3.35mm nails; timber density-450kg/m^3
plywood density-700kg/m^3

Figure 6.23 Comparison of the stiffness of the model, EC5[11] and EC5 [15] for a pair of 2.66 and 3.33mm diameter nails at the SLS.

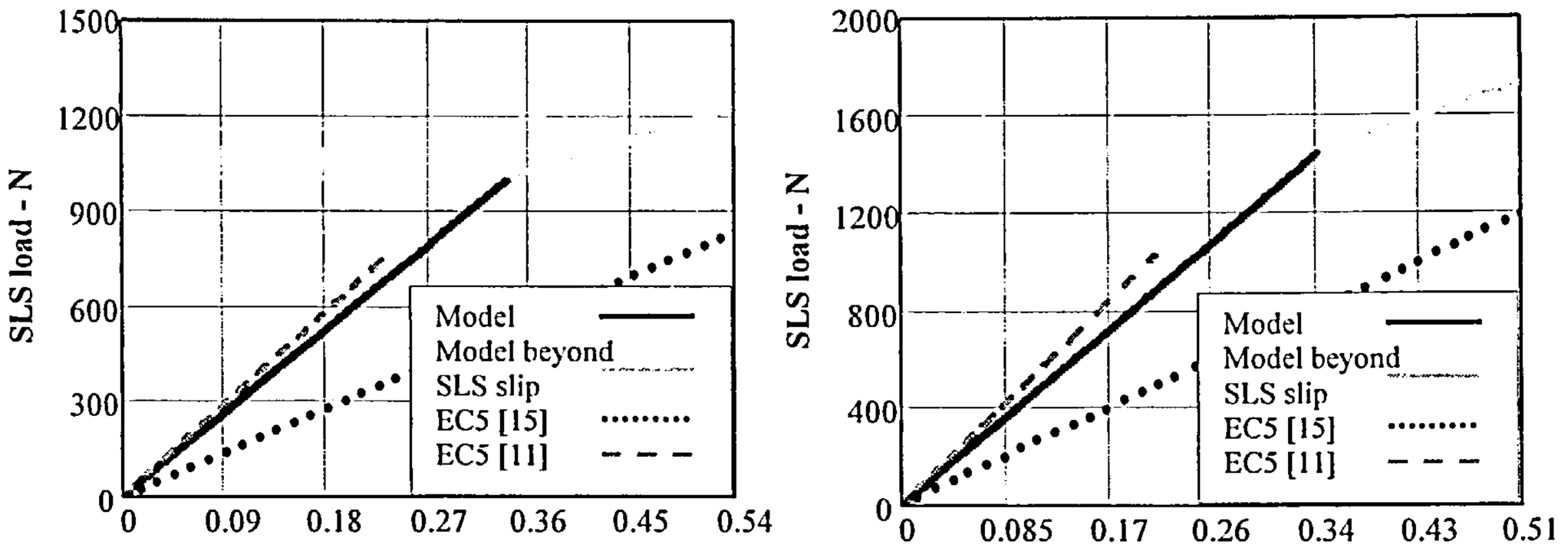

Figure 6.23 cont'd. Comparison of the stiffness of the model, EC5[11] and EC5 [15] for a pair of 2.66 and 3.33mm diameter nails at the SLS.

6.4.4 Stiffness at the Ultimate Limit State

6.4.4.1 Joints with Steel Gusset Plates

The ULS stiffness of the model is obtained by dividing the joint strength at the ULS by the joint displacement at that load.

For any joint with a row spacing equal to or exceeding *19.6d* the characteristic load carrying capacity of the model will be as given in equation (175b).

To obtain an exact value for the slip at the ULS the joint load should be taken as the load obtained by dividing equation (175b) by the material factor, γ_M. However, to compare directly with the method used in EC5 for the derivation of the slip modulus, a factor of 0.667 will be applied to the characteristic load and at this load the slip in the model will be 1.07mm. The model stiffness, $K_{ulsmodel}$, per pair of fully overlapping nails in joints with steel gusset plates at the ULS then becomes:

$$K_{ulsmodel} = [0.853AD(d)^{1.4468} f_u (1-e^{-1.712\delta x})^{0.926}(0.1\delta x + 0.68)/f(mc)] \frac{2}{3\times 1.07} \quad \ldots.(193)$$

The stiffness equation is valid for joints with a pair of fully overlapping nails and where the nail row spacing is equal or greater than *19.6d.*

In EC5 [11] and EC5 [15] the ULS slip modulus is 0.667 times the SLS slip modulus and for joints with

steel gusset plates, the values are:

(i) *EC5 [11]* $$K_{ulsEC11} = \frac{2}{3} \times 2 \times \frac{\rho_m{}^{1.5} d}{25} \quad \text{....(194)}$$

(ii) *EC5 [15]* $$K_{ulsrEC15} = \frac{2}{3} \times 2 \times 2 \times \frac{2}{3} \frac{\rho_m{}^{1.5} d}{35} \quad \text{....(195)}$$

where ρ_m is the mean density of the timber in the joint and d is the nail diameter.

These stiffness equations apply to joints with a pair of nails in single shear and for multi-row joints where the nail row spacing is equal to or greater than the upper limit of *14d* given in the code,

In the model equation, (193), the slip at the ULS is fixed at 1.07mm for all nail sizes. The EC5 stiffness equations are based on a slip which is variable, being a function of $d^{0.8}$ and the inverse of the material density, as given in equations (1) and (173) for EC5 [11] and EC5 [15] respectively. The nail slip at the ULS for each nail size is given in Table 6.16 and a graphical comparison of the associated stiffness at the extreme density values of 450Kg/m^3 and 700Kg/m^3 against the model behaviour is given in Figure 6.24.

Nail diameter Mm	**Slip at the ULS using model. mm**		**Slip at the ULS using EC5 [11]. mm**		**Slip at the ULS using EC5 [15]. mm**	
	Timber Density *450kg/m^3*	Timber Density *700kg/m^3*	Timber Density *450kg/m^3*	Timber Density *700kg/m^3*	Timber Density *450kg/m^3*	Timber Density *700kg/m^3*
2.66	1.07	1.07	1.045	0.672	1.272	0.868
3.01	1.07	1.07	1.151	0.74	1.394	0.946
3.36	1.07	1.07	1.255	0.807	1.512	1.022

Table 6.16 Joint slip from the model; EC5 [11] and EC5 [15] at the ULS in a joint formed with a pair of nails

As with the comparison at the SLS condition, the EC5 [11] and EC5 [15] slip modulus are within 5% of each other, EC5 [15] being the lesser. The stiffness of the model equates closely with EC5 [11] and EC5 [15] for all nails sizes at a density of 450kg/m^3, and as the density increases EC5 [11] and EC5 [15] slip modulus increases over the model value. The percentage difference between the model and the Eurocode values for each nail size is given in Table 6.17. A negative sign in the table denotes that the model is less stiff than the relevant Eurocode value.

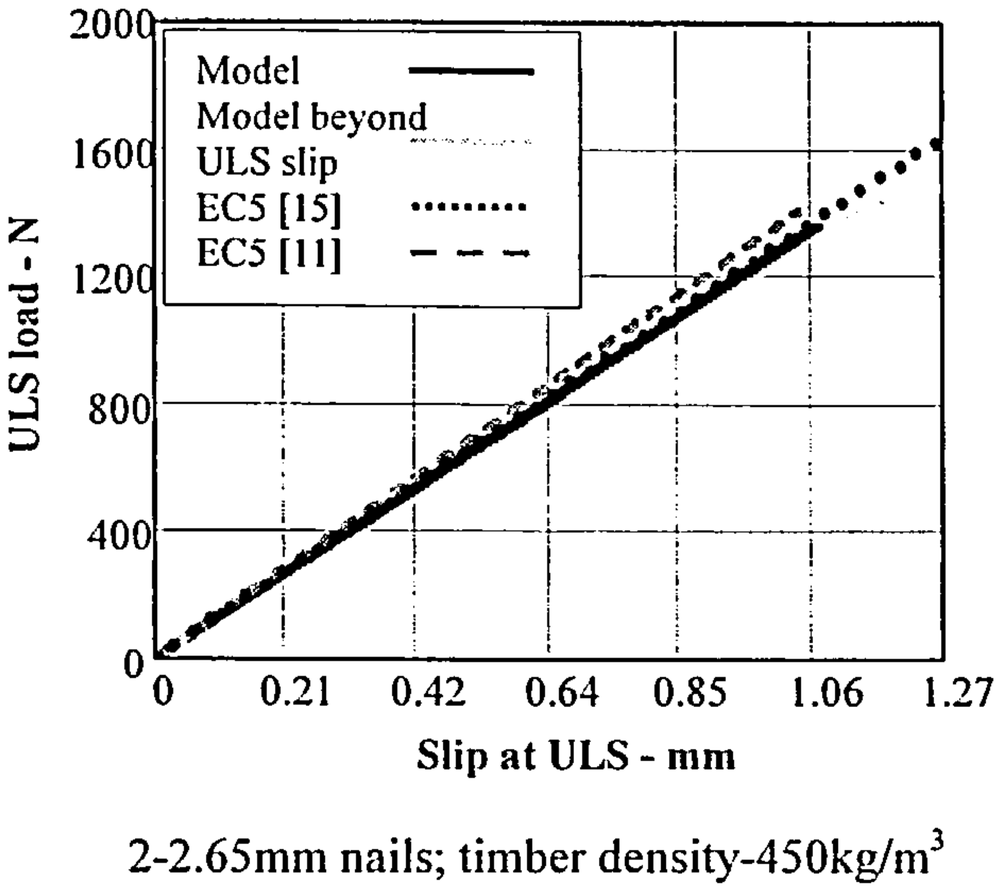

2-2.65mm nails; timber density-450kg/m^3

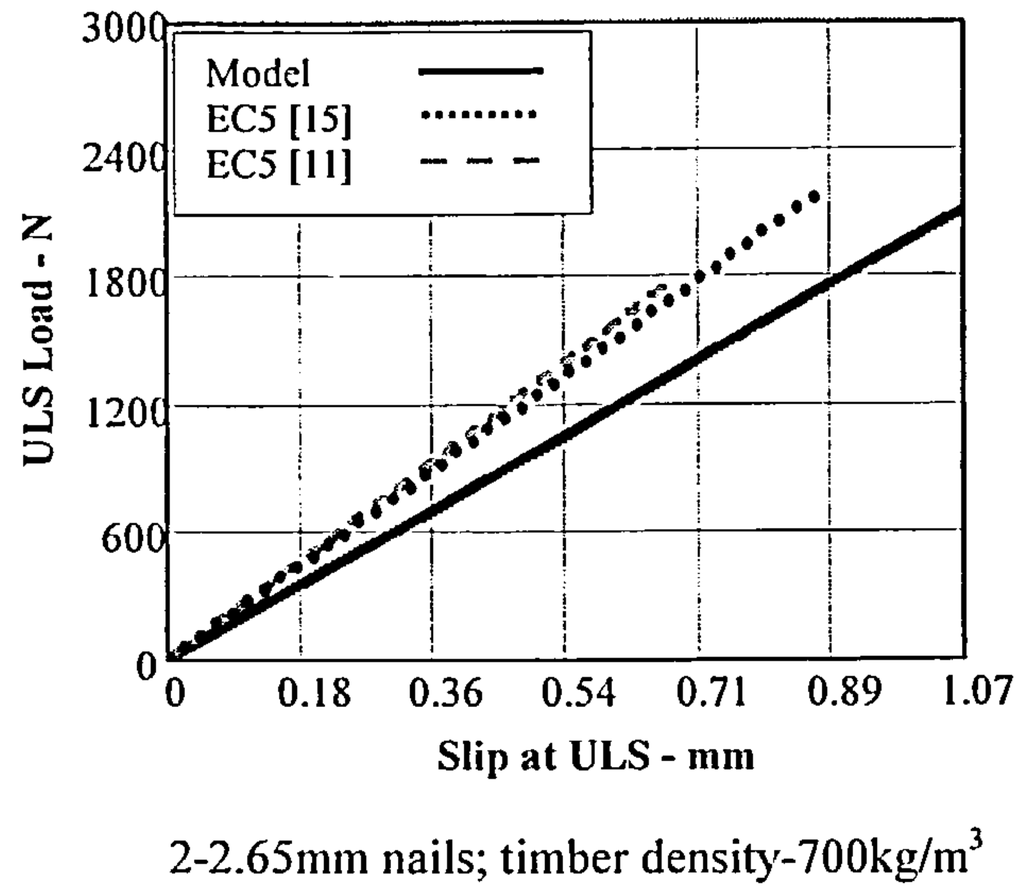

2-2.65mm nails; timber density-700kg/m^3

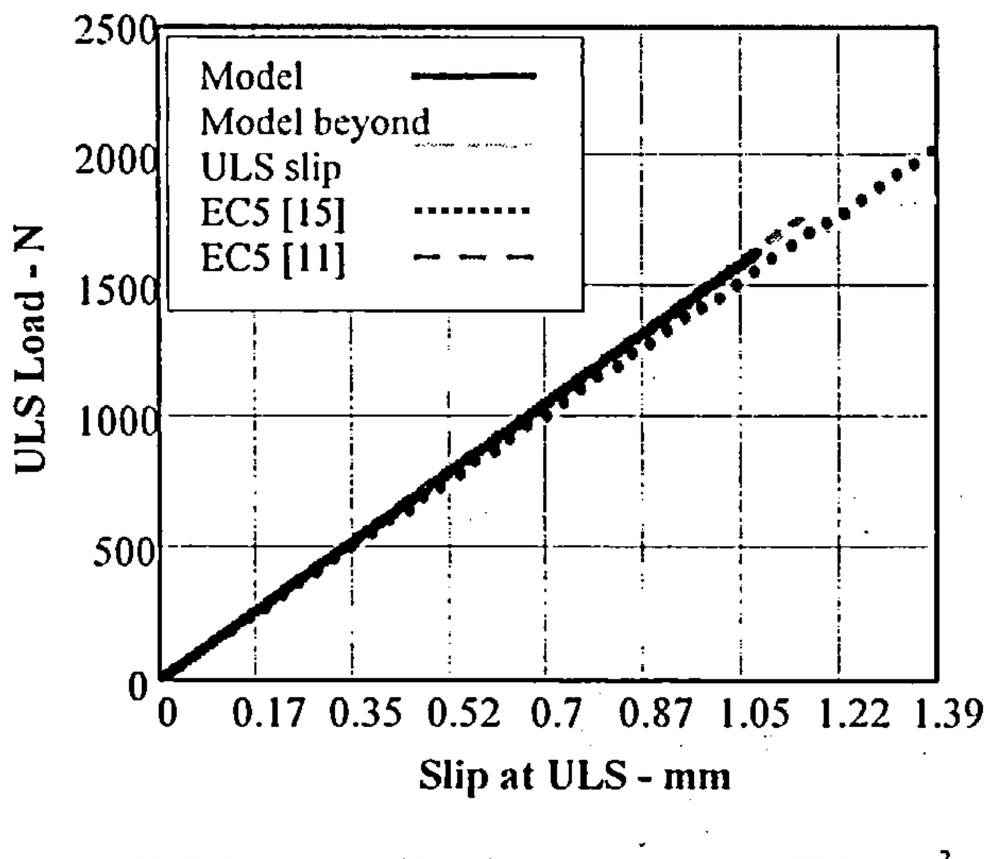

2-3.00mm nails; timber density-450kg/m^3

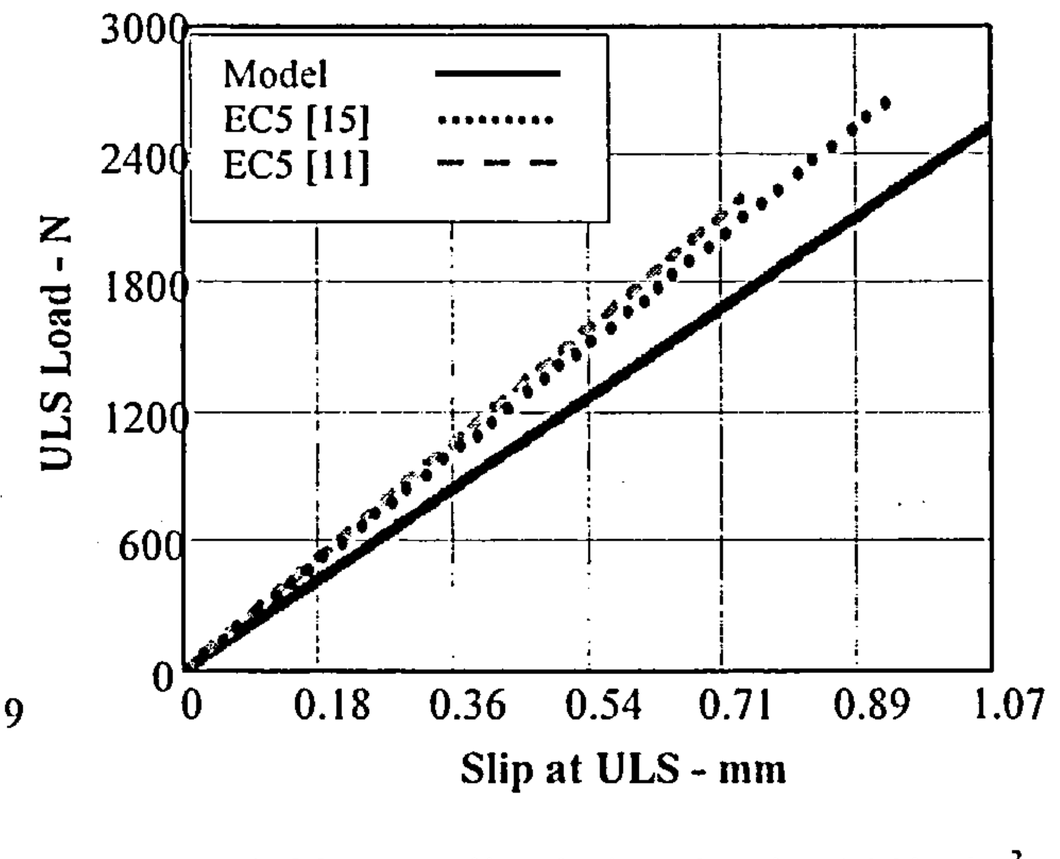

2-3.00mm nails; timber density-700kg/m^3

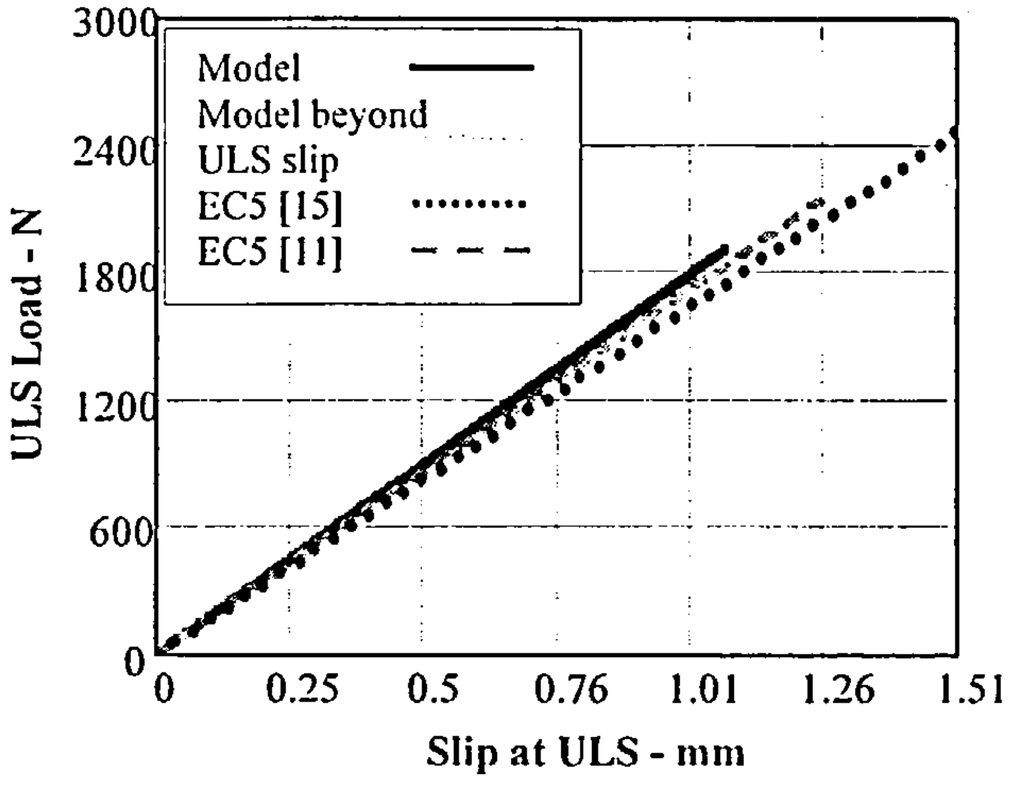

2-3.35mm nails; timber density-450kg/m^3

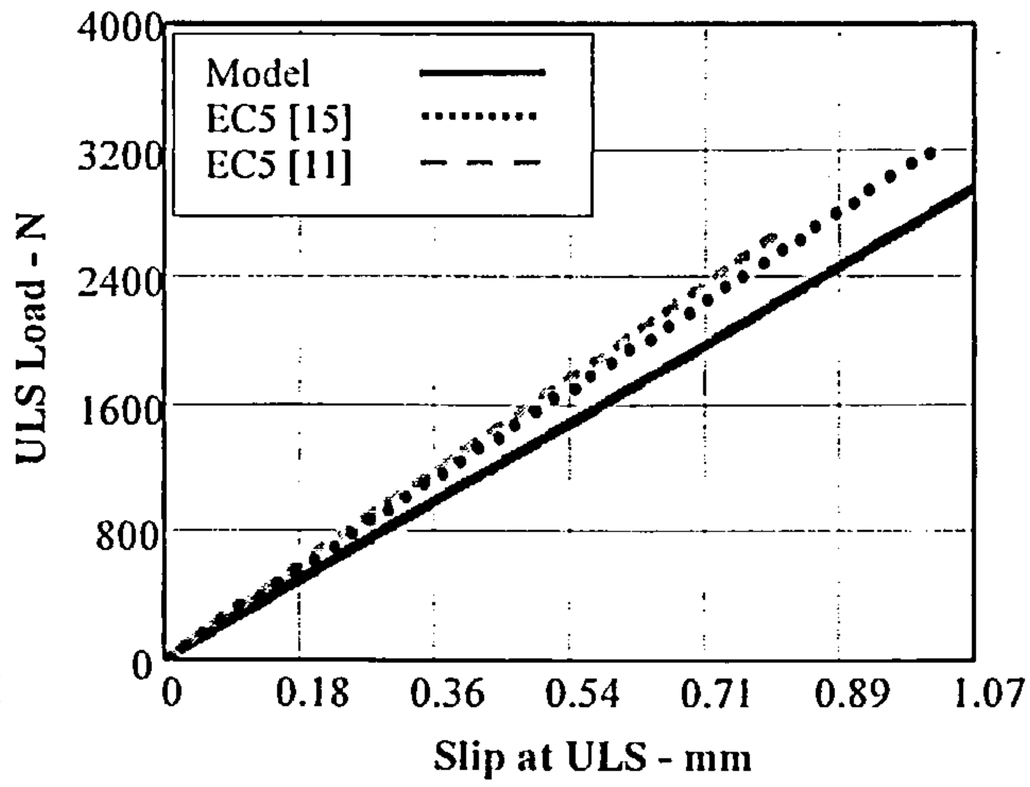

2-3.35mm nails; timber density-700kg/m^3

Figure 6.24 Comparison of the stiffness of the model, EC5 [11] and EC5 [15] for a pair of 2.66mm; 3.01mm and 3.36mm diameter nails at the ULS.

Nail diameter mm	% difference between model stiffness and EC5 [11] slip modulus.		% difference between model stiffness and EC5 [15] slip modulus	
	Timber Density *450kg/m^3*	Timber Density *700kg/m^3*	Timber Density *450kg/m^3*	Timber Density *700kg/m^3*
2.66	-6.5	-32.2	-1.4	-26.5
3.01	-0.8	-25.7	+4.0	-19.7
3.36	+4.1	-19.6	+8.6	-13.9

Table 6.17 Percentage difference between model stiffness and EC5 slip modulii at the SLS for a joint with a pair of nails.

With timber at a density of 700kg.m^3, EC5 [11] exceeds the model stiffness by values ranging from 19.6% to 32.2 depending on the nail diameter and EC5 [15] exceeds it by 13.9% to 26.5%, again depending on the nail diameter.

Although the exceedance reduces as the nail diameter increases, the Eurocode values are such that if applied to joints using fully overlapping nails with timber at an average density above approximately 500kg/m^3, the rules would significantly underestimate the slip in the joint and result in an unsafe design.

The graphs in Figure 6.24 apply to joints with nail row spacing equal to or exceeding *19.6d.* For joints with multi-rows of nails at row spacing less than *19.6d* the row spacing reduction factors will modify the joint strengths and the difference relative to the model will reduce.

6.4.4.2 Joints with plywood gusset plates

The ULS stiffness of the model is obtained by dividing the joint strength at the ULS by the joint displacement at that load.

For any joint with a row spacing equal to or exceeding *17d,* the characteristic strength of the model is given by equation (183g).

From the displacement function, at the ULS load the slip in the joint will be 1.214mm and the model stiffness, $K_{ulspmodel}$, per pair of fully overlapping nails in joints with plywood gusset plates at that load becomes:

$$K_{ulspmodel} = 0.853(Ae)(Density\ Function)(d)^{2.236} f_u rn(1-e^{-1.406\delta x})^{0.54}(0.121\delta x+1) \times \frac{2}{3} \times \frac{1}{1.214} \quad .(196)$$

The stiffness equation is valid for joints with a pair of fully overlapping nails and where the nail row spacing is equal or greater than *17d.*

In EC5 [11] and EC5 [15] the ULS modulus for joints with plywood gusset plates is 0.667 times the SLS modulus, giving:

(i) *EC5 [11]* $$K_{ulsEC11} = \frac{2}{3} \times 2 \times \frac{\rho_m{}^{1.5} d}{25}$$

....(197)

(ii) *EC5 [15]* $$K_{ulsEC15} = \frac{2}{3} \times 2 \times \frac{2}{3} \frac{\rho_m{}^{1.5} d}{35} \quad ....(198)$$

where ρ_m is the mean density of the combined timber and plywood as given in equation (192).

These stiffness equations apply to joints with a pair of nails in single shear and for multi-row joints where the nail row spacing is equal to or greater than the upper limit of *14d* given in the code,

Because of the extent of variables with these joints, as for the SLS analysis, the comparison of the model and EC5 stiffness equations is limited to 2.66mm and 3.33mm diameter nails, using timber with a mean density ranging from 450Kg/m^3 to 700 Kg/m^3; plywood 17.5mm thick and nail length with a timber side penetration of 41mm. The nail yield strength has been taken as 827N/mm^2. These parameters envelope the extremes used in the testing programme.

In the model equation, (196), the slip at the ULS is fixed at 1.214mm for all nail sizes. As with joints using steel gusset plates, the EC5 stiffness equations for plywood gusset plate joints are based on a variable slip. A summary of the ULS slip for the model, EC5 [11] and EC5 [15] is given in Table 6.18 and a graphical comparison is given in Figure 6.25.

As with the comparison at the SLS, there is a considerable difference between the EC5 [11] and EC5 [15] stiffness, caused by the changes in the respective strength and stiffness equations in EC5 [15]. With 2.66mm diameter nails the model stiffness approaches the EC5 [15] slip modulus. As the nail diameter increases the model stiffness increases relative to the Eurocode slip modulus and with 3.33mm diameter nails it lies almost midway between EC5 [11] and EC5 [15].

The graphs in Figure 6.25 apply to joints with nail row spacing equal to or exceeding *17d.* For joints with multi-rows of nails at row spacing less than *17d* the row spacing reduction factors will modify the

joint strengths of the model and Eurocode5 [15]. This will lead to a reduction in the model stiffness relative to EC5 [11] and the EC5 [15] curve will reduce even further relative to the model and to EC5 [11]. Because of the poor comparison between the model and EC5 [15] reduction factors, graphs incorporating these factors have not been given.

Nail diameter-plywood density mm		**Slip at the ULS using model. mm**		**Slip at the ULS using EC5 [11]. mm**		**Slip at the ULS state using EC5 [15]. mm**	
mm	kg/m^3	Timber Density *450kg/m^3*	Timber Density *700kg/m^3*	Timber Density *450kg/m^3*	Timber Density *700kg/m^3*	Timber Density *450kg/m^3*	Timber Density *700kg/m^3*
2.66	400	1.214	1.214	0.721	0.556	1.626	1.252
	700	1.214	1.214	0.619	0.503	1.435	1.243
3.33	400	1.214	1.214	0.771	0.595	1.727	1.354
	700	1.214	1.214	0.677	0.533	1.476	1.276

Table 6.18 Joint slip from the model; EC5 [11] and EC5 [15] at the ultimate limit state in a joint formed with two a pair of nails using 2.66mm and 3.33mm nails.

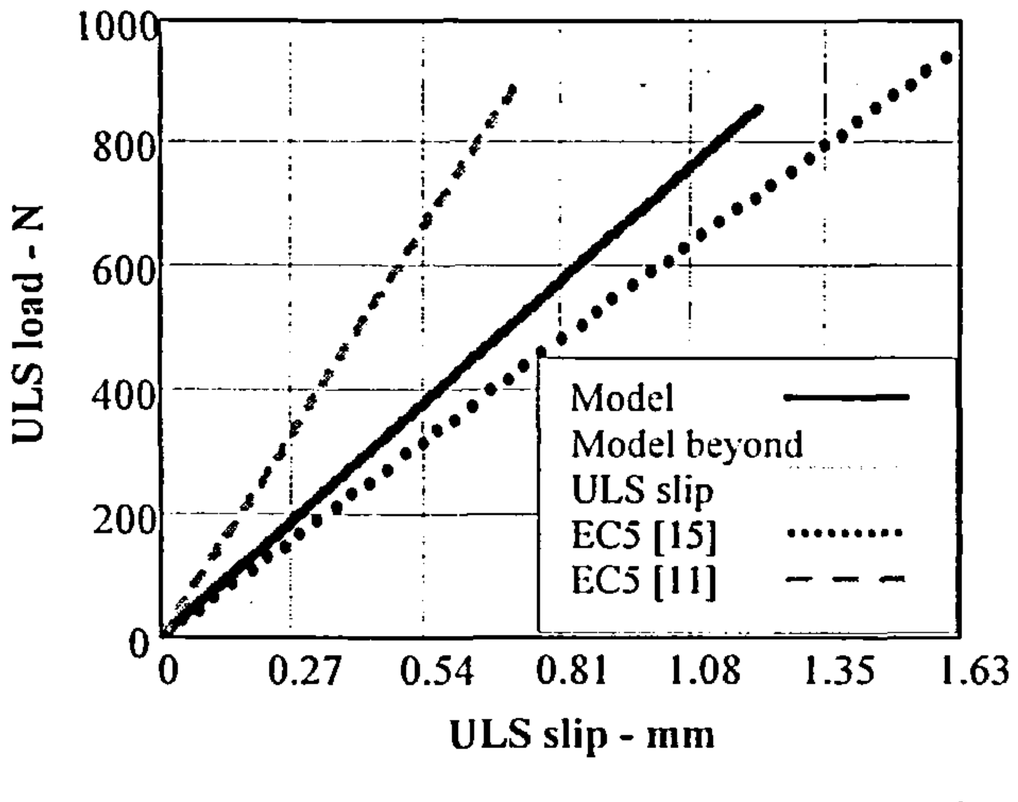

2-2.65mm nails; timber density-450kg/m^3
plywood density-400kg/m^3

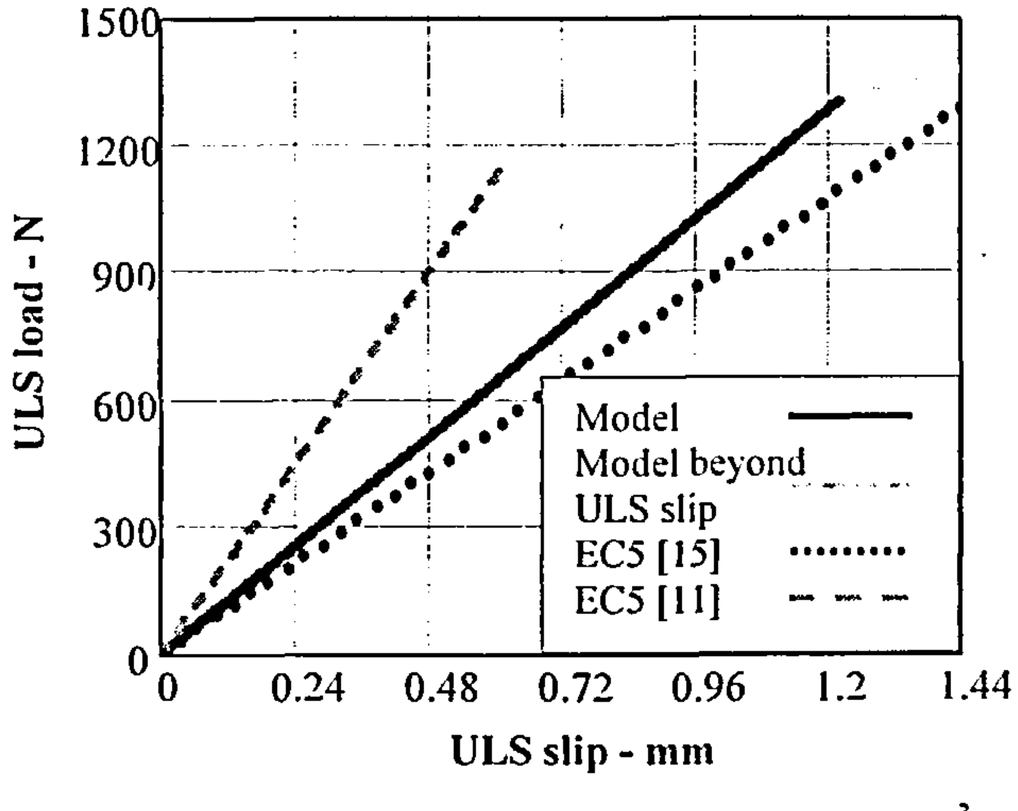

2-2.65mm nails; timber density-450kg/m^3
plywood density-700kg/m^3

Figure 6.25 Comparison of the stiffness of the model, EC5[11] and EC5 [15] for a pair of 2.66mm and 3.33mm diameter nails at the ULS.

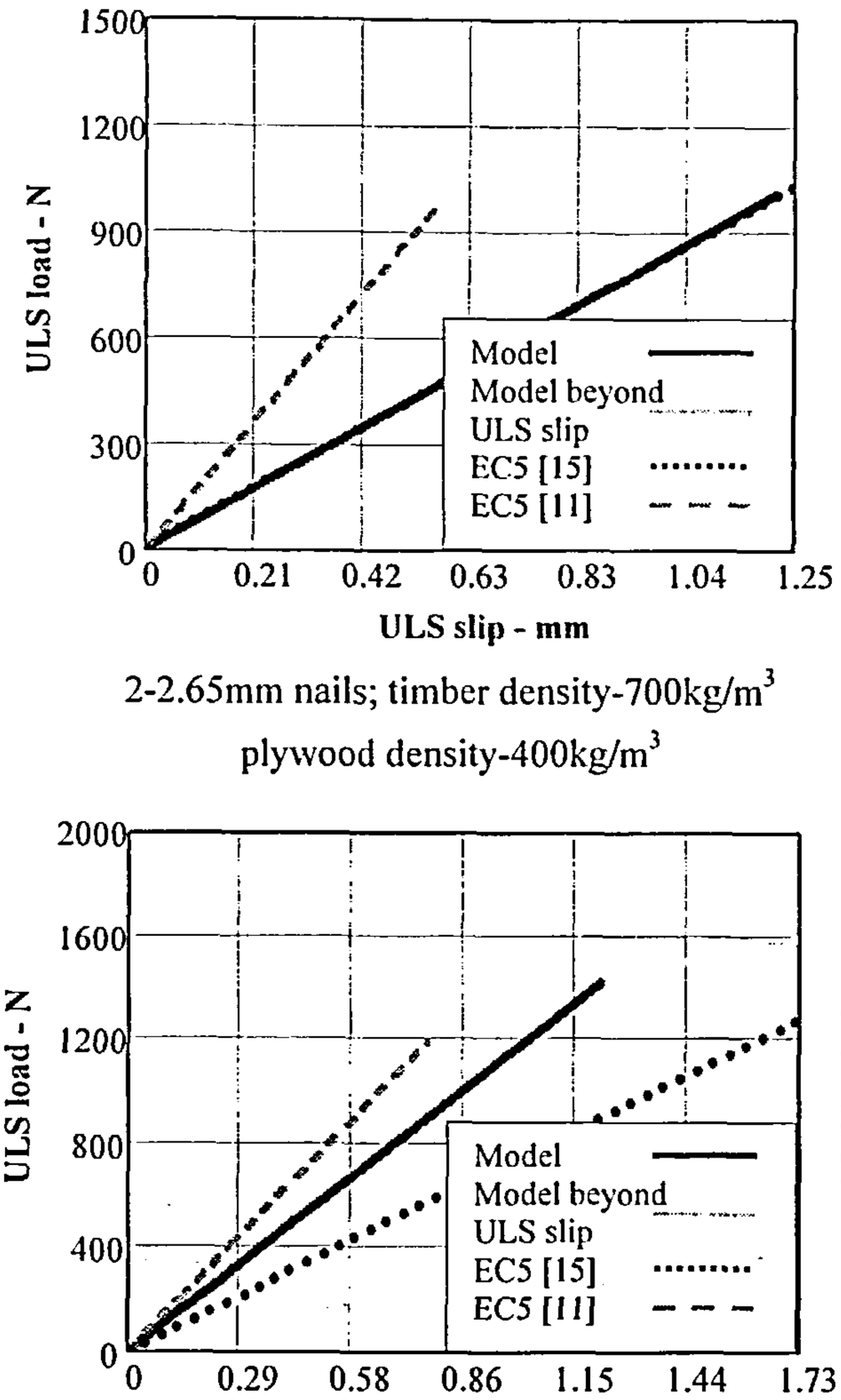

2-2.65mm nails; timber density-700kg/m^3
plywood density-400kg/m^3

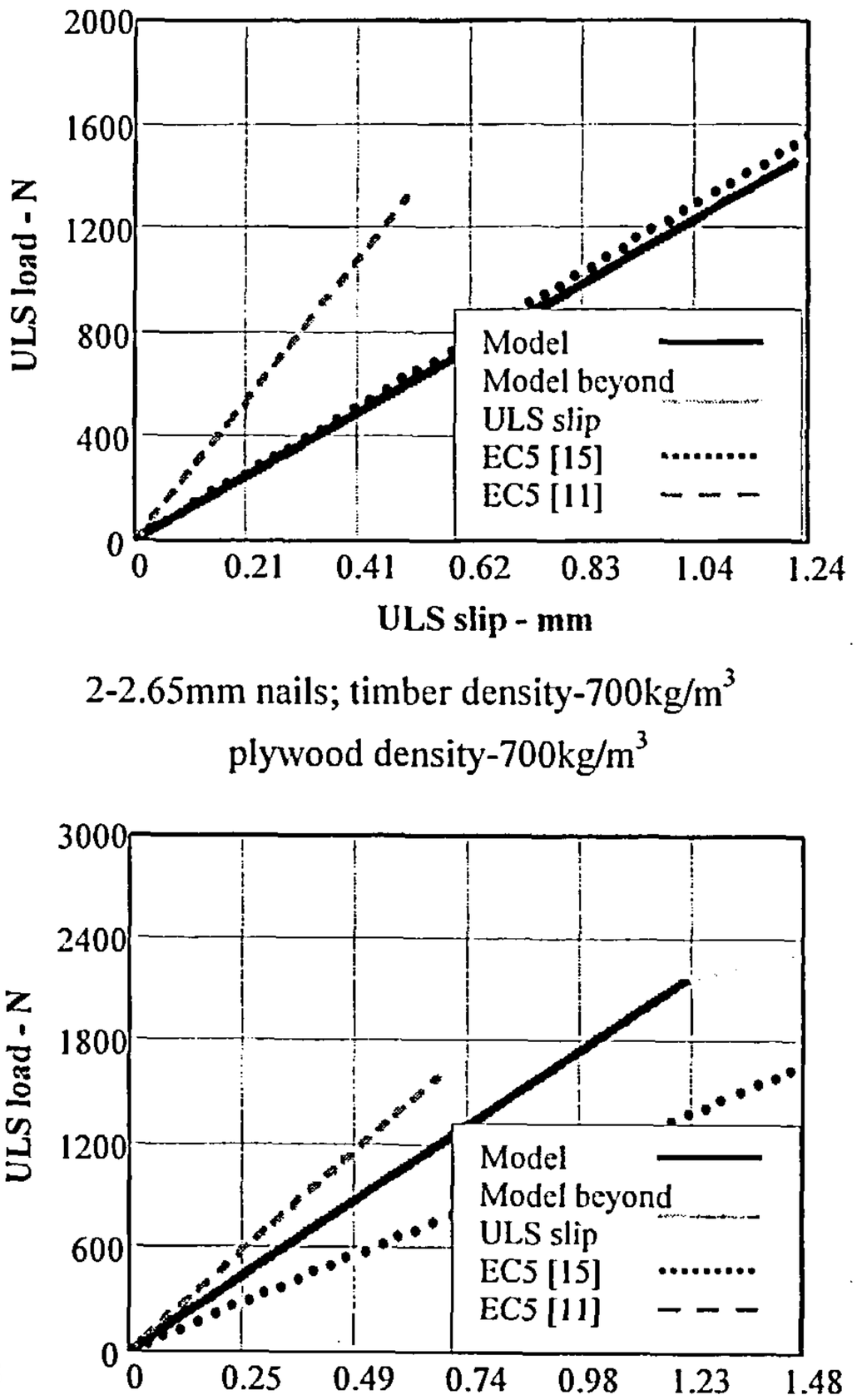

2-2.65mm nails; timber density-700kg/m^3
plywood density-700kg/m^3

2-3.35mm nails; timber density-450kg/m^3
plywood density-400kg/m^3

2-3.35mm nails; timber density-450kg/m^3
plywood density-700kg/m^3

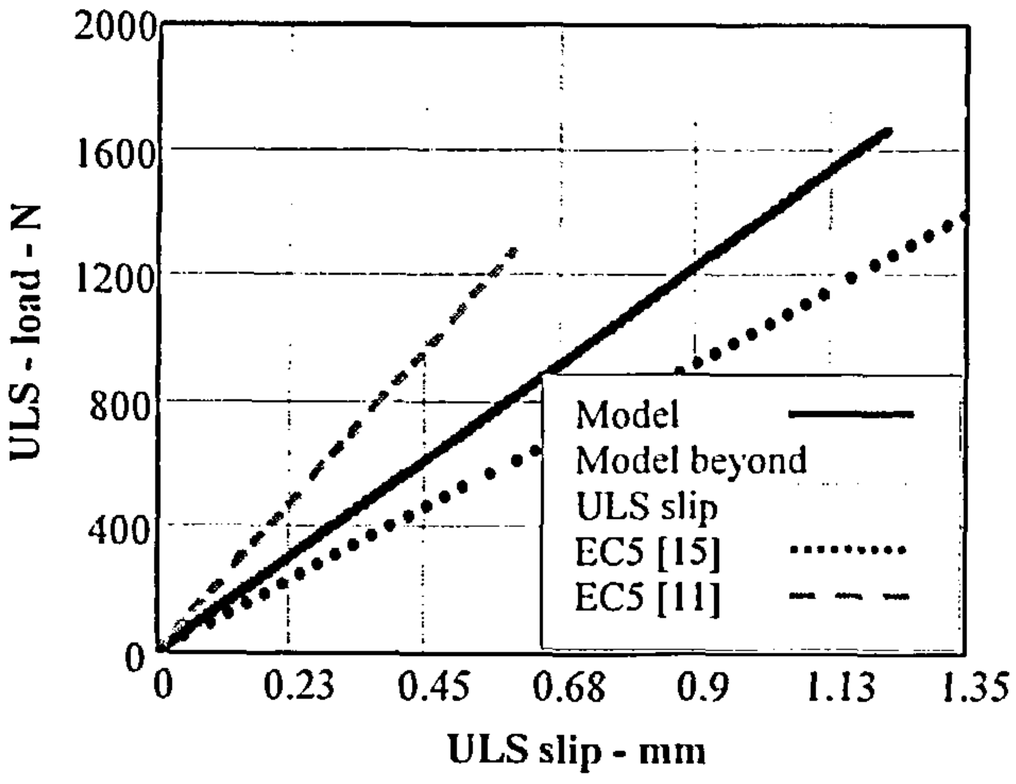

2-3.35mm nails; timber density-700kg/m^3
plywood density-400kg/m^3

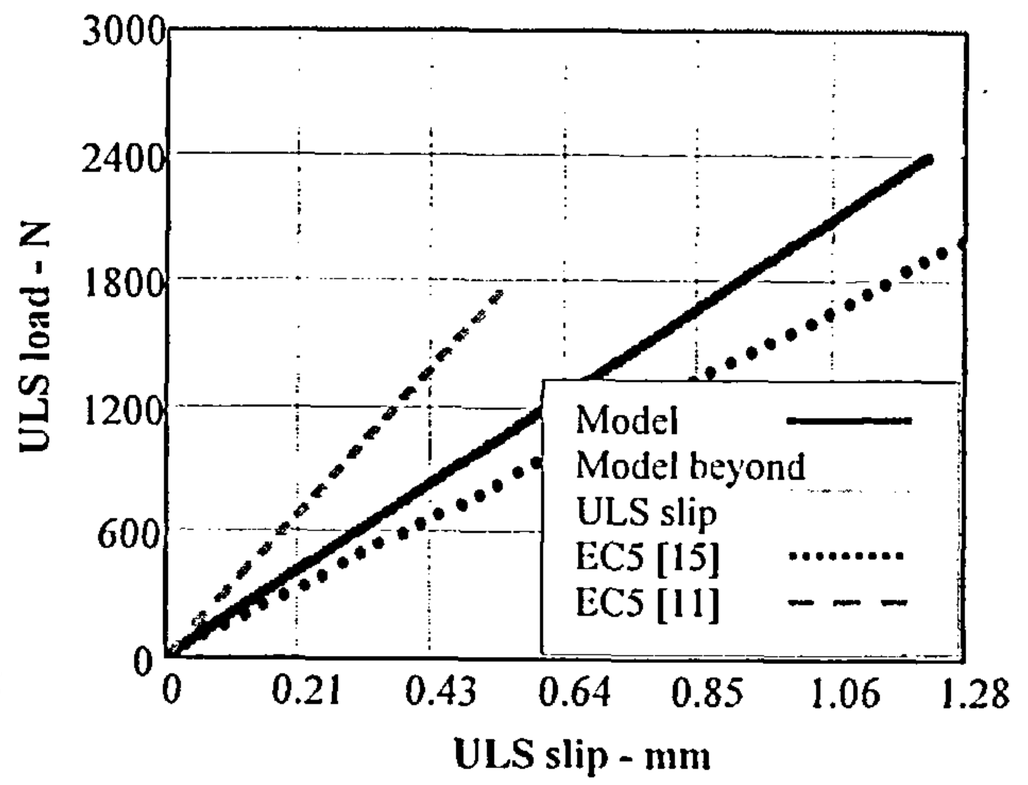

2-3.35mm nails; timber density-700kg/m^3
plywood density-700kg/m^3

Figure 6.25 cont'd Comparison of the stiffness of the model, EC5[11] and EC5 [15] for a pair of 2.66mm and 3.33mm diameter nails at the ULS.

6.4.5 Overall Strength-Stiffness Comparison

To obtain an overall comparison of the model against the EC5 rules, the Eurocode strength and stiffness criteria have been combined for each joint type and compared using the extreme material properties. For EC5 [11] and EC5 [15], the strength profile is taken to be bounded by the respective slip modulus up to the SLS load and by the line joining that load and the ULS load. To form an upper boundary to the joint behaviour, at the ULS load of the model, EC5 [11] and EC5 [15], the graphs are extended to the greatest ULS slip limit. In this zone, the model will follow its displacement function profile and the Eurocode graphs have been assumed to be able to sustain their ULS load. The latter is not strictly in line with the Eurocode rules as no criteria is given for ductility behaviour, but it gives a more realistic representation of the joint behaviour.

The Eurocode rules for strength reduction due to row spacing factors cannot be applied to joints with fully overlapping nails. EC5 ignores the matter altogether and the factors used in EC5 [15] greatly overestimate the reduction effect. For this reason comparative examples have not been given for such joints.

6.4.5.1 Steel gusset plate joints

The strength and stiffness data for steel gusset plate joints using a pair of 2.66mm nails with timber at a mean density of 450Kg/m^3 and a pair of 3.36mm diameter nails with timber at a maximum average density of 700Kg/m^3 has been plotted in Figure 6.26. In both instances the nail yield strength has been taken as 804N/mm^2.

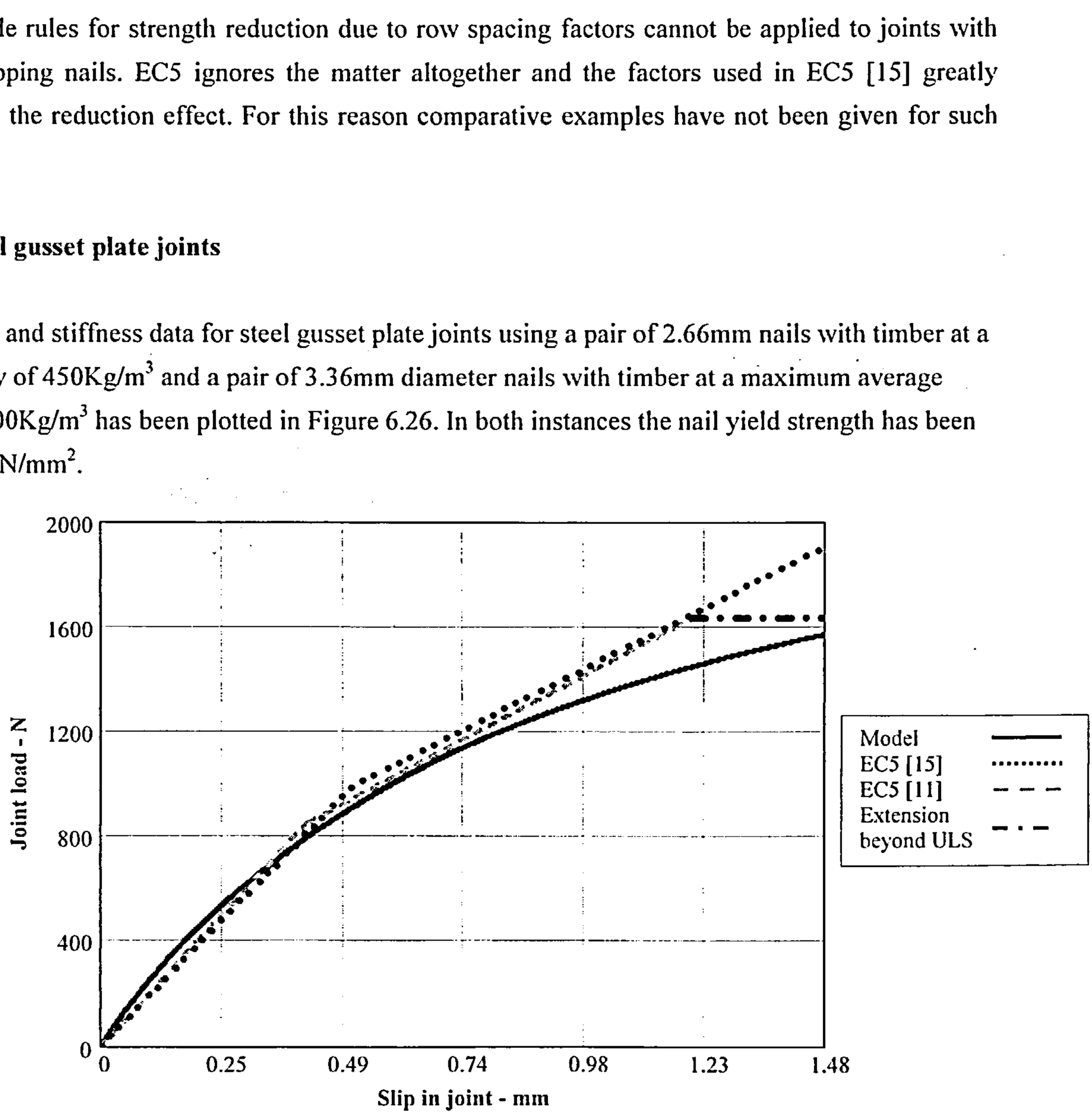

Figure 6.26 Comparison of the model, EC5[11] and EC5 [15] against a joint with a pair of nails.

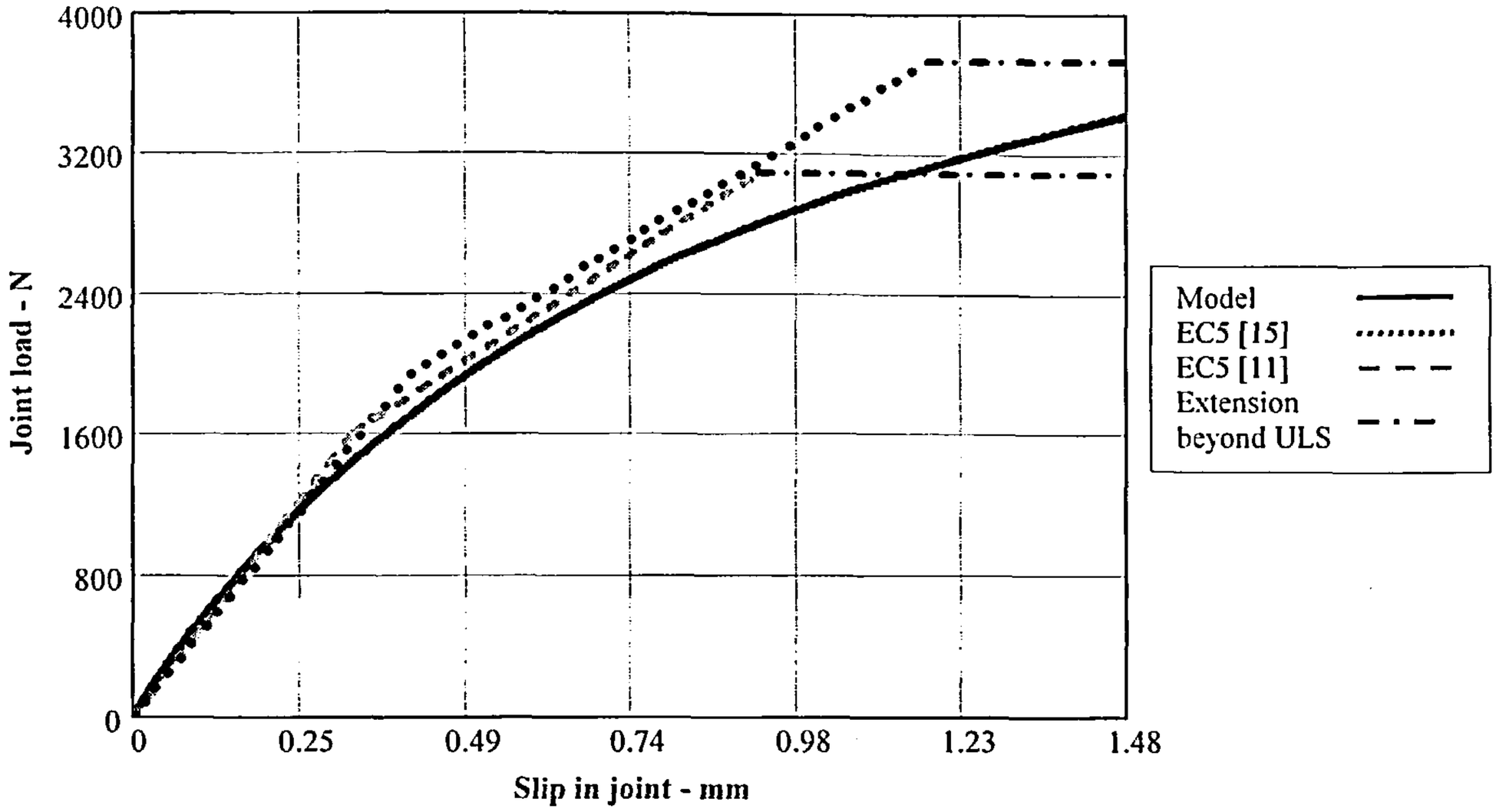

2-3.35mm nails; timber density – 700kg/m^3

Figure 6.26 cont'd Comparison of the model, EC5[11] and EC5 [15] against a joint with a pair of nails.

Although the graphs shown are for a joint with only a pair of overlapping nails, the relative relationship will apply to all joints with multi-rows of nails in which the row spacing is equal to or greater than *19.6d*.

As will be observed, the model conforms in principle with the Eurocode strength and stiffness profile, however, its strength and stiffness values vary relative to the EC5 values as the material properties change. At extremes values either the strength or stiffness or both will be exceeded by EC5 [11] and EC5 [15] by more than 5%. The Eurocode rules cannot be used for joints using fully overlapping nails.

6.4.5.2 Plywood Gusset Plate Joints

Because of the extent of variables with these joints, the comparison of the model and EC5 for plywood gusset plate joints is more complex. To envelope the extremes of behaviour, the comparison is limited to 2.66mm and 3.33mm diameter nails, using timber with a mean density ranging from 450Kg/m^3 to 700 Kg/m^3; 17.5mm thick plywood with a mean density ranging from 400kg/m^3 to 700kg/m^3 and nails having a timber side penetration of 41mm. The nail yield strength has been taken as 827N/mm^2. These parameters envelope the extremes used in the testing programme and the results for each nail size are given in Figure 6.27. The relative relationship of the model and the EC5 results shown in the Figure will apply to all joints with multi-rows of nails in which the row spacing is equal to or greater than *17d*.

The EC5 [11] and EC5 [15] ULS loads are closer to each other than is the case for joints assembled using steel gusset plates. However, as the material properties vary the differences with the model results are considerable. With 2.66mm diameter nails, the ultimate strength of the model compares reasonably with EC5 [11] as does the stiffness at the SLS. With 3.33mm diameter nails, however, EC5 [11] considerably underestimates the joint strength at the ULS and the fit using EC5 [15] is extremely variable. The variation in stiffness behaviour is also significant, albeit in the case of EC5 [15], generally on the conservative side. As for joints assembled with steel gusset plates, the graphs show that for joints with plywood gusset plates using fully overlapping nails, the behaviour cannot be satisfactorily modelled using either version of EC5.

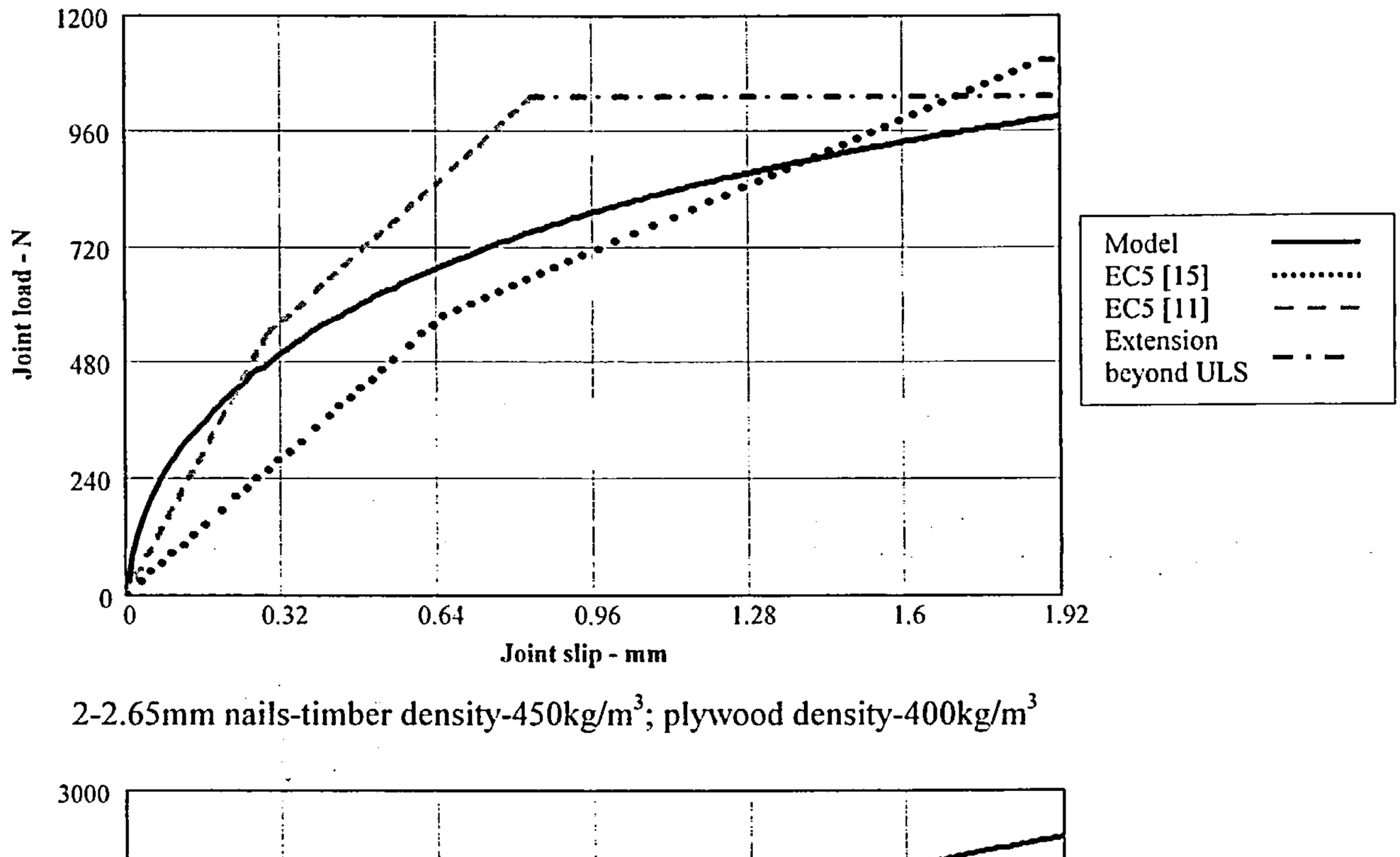

Figure 6.27 Comparison of the behaviour of the model , EC5[11] and EC5 [15] using a joint with a pair of 2.66mm and 3.33mm nails

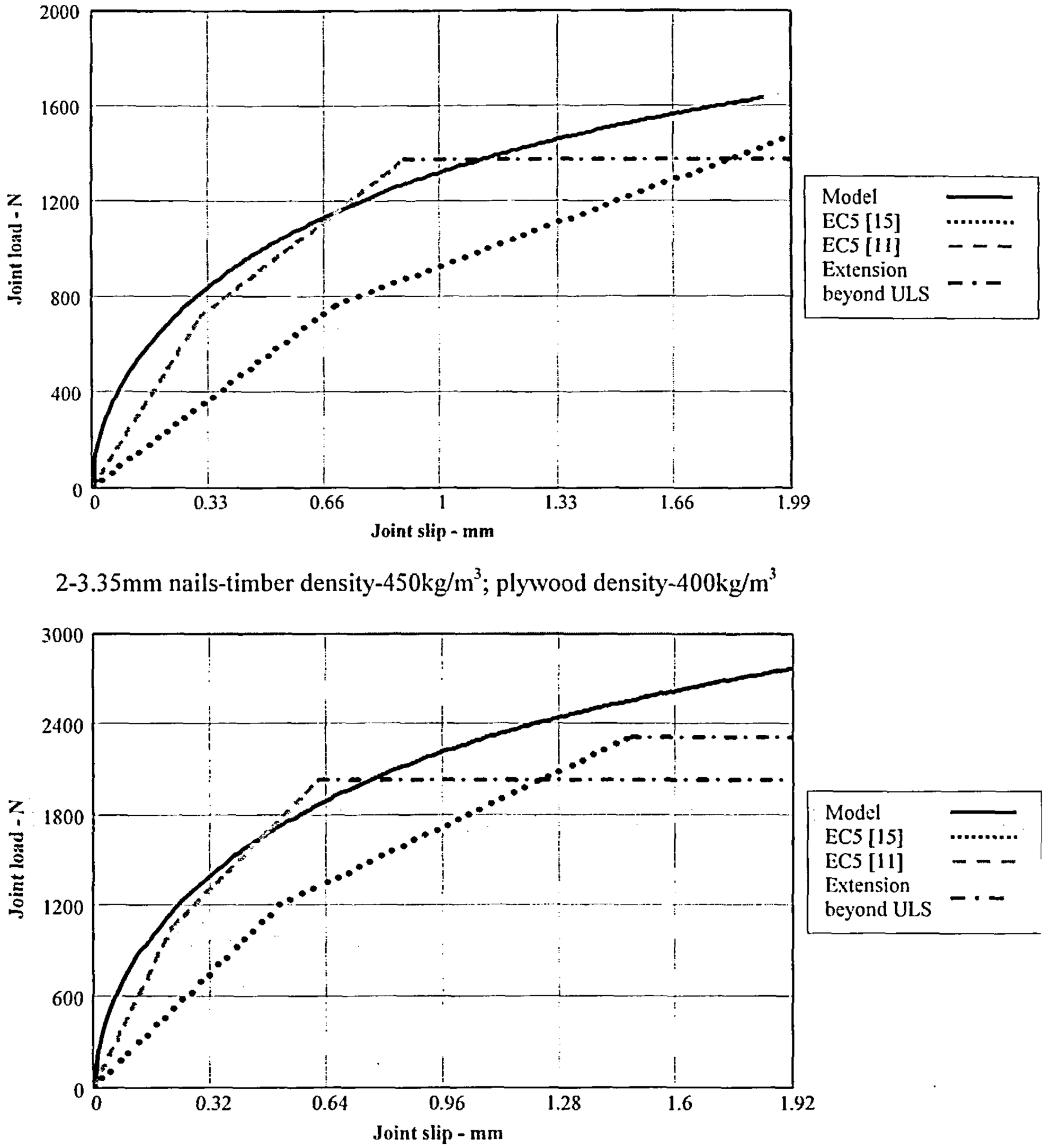

Figure 6.27 cont'd Comparison of the behaviour of the model , EC5[11] and EC5 [15] using a joint with a pair of 2.66mm and 3.33mm nails.

6.5 SUMMARY

In this Chapter the models developed in Chapter 4 for joints with steel gusset plates and plywood gusset plates using fully overlapping nails subjected to lateral loading are compared with the EC5 [11] and EC5 [15]. Because the revision process of the code is still ongoing and subject to change, the comparison has been carried out against the original issue of the code and the latest draft. To equate to

the EC5 strength equations, the models used for the comparison are those for joints assembled with a gap between the timber and the gusset plates.

To ensure the models are compared with the Eurocode on the same basis, the strength and stiffness equations in EC5 [11] and EC5 [15] have been reviewed, drawing on the work by Ehlbeck *et al* [68] and STEP 1 [79]. This identified the load factors to be used for the strength and stiffness comparisons. For the ULS load comparison the characteristic value of the model has been divided by 1.3, the material factor for connections; for the SLS stiffness comparison the load has been obtained by dividing the characteristic value of the model by a partial load factor of 2.5; for the ULS stiffness comparison the load has been taken as two thirds of the characteristic value of the model. These factors were used in the development of EC5 [11] and have been read over into EC5 [15].

The model for steel gusset plate joints has an upper slip limit of 3.2mm, which was the joint failure slip limit determined from the testing programme. For the joints with plywood gusset plates, the model has been reviewed to define the joint failure limit. An upper slip limit of 4.5mm has been determined and the model has been revised to incorporate the new displacement function. A good comparison is shown to exist between the model and the test results up to this limit.

The 5 percentile characteristic value of each model has been developed using a Log-Normal probability distribution function, adopting the confidence limits proposed for test results given in EC5 [13]. Based on the use of a 5 test sample regime for the joint strength and taking a coefficient of variation of 0.1, which exceeded the test value result, a factor of 0.853 has been applied to each model to obtain the characteristic strength.

As expected, the failure modes for the steel gusset plate joints were as predicted using the EC5 strength equations. However, from a review of some of the joints assembled with plywood gussets, the EC5 failure mode based on calculation did not always agree with what was observed from the test. The difference related to Mode 2 and 3 type failures where the test showed a Mode 3 failure had arisen and EC5 rules predicted a Mode 2. However, it is to be noted that there is not a large difference in value between the results of the EC5 equations for Mode 2 and Mode 3 type failures.

The Eurocode strength equations ignore the effect of tension and shear in the connector and calculations have been carried out to validate this approach. Embedment tests have also been carried out to compare the test values with the results from the Eurocode embedment equations. Poor results were obtained. It was concluded that for this important test, the test regime needed to be reviewed by the code committee and better advice given on the maximum sample thickness to be used for plywood samples. Nail pull out tests were also done and the results, although not in complete agreement with the code, were considered to be acceptable.

A parametric exercise has been undertaken for each joint type to compare the effects of variations in the joint parameters on the model and the Eurocode results. The variation in parametric value has been limited to the extreme values used in the testing programme to ensure the model behaviour is bounded by the results of the testing programme. Joint strength and stiffness have been compared at the ULS and the SLS. The results of the exercise show that as material properties are varied, the strength and stiffness values of the model and the Eurocodes vary considerably relative to each other. The variations are well outside what could be considered to be acceptable for design purposes.

The significant findings from the exercise are:

(i) The spacing and distance rules for nails in EC5 cannot be directly applied to joints using fully overlapping nails. A factor of 2 should be applied to the Eurocode rules to obtain a joint which can be assembled without splitting and will behave in a predominantly ductile manner. This will also give a basis for comparison with joints which use nails that do not fully overlap.

(ii) EC5 [11] does not include for any reduction in joint strength when using nail spacing less than 2 times the minimum nail spacing given in the code. This rule is unsafe and will be superseded by the proposals in EC5 [15].

(iii) In EC5 [15], for joints having a nail row spacing equal to or greater than *14d* the joint strength is a multiple of the number of rows of nails in the joint. Similarly, with the models for steel or plywood joints using fully overlapping nails with a nail row spacing $\geqslant$ *19.6d* and *17d* respectively, the joint strength is a multiple of the number of rows of nails in the joint.

(iv) In EC5 [15] for joints with a nail row spacing less than *14d* the joint strength will be reduced. In the models for steel or plywood joints using fully overlapping nails, the joint strength is reduced in joints having a nail row spacing less than *19.6d* and *17d* respectively.

(v) In EC5 [15] for joints with a row spacing less than *14d*, the joint strength will be reduced by a factor which is a power function of the number of rows of nails in the joint. With the models for steel or plywood joints using fully overlapping nails, for all row spacings the joint strength is a linear function of the number of rows of nails in the joint.

(vi) In EC5 [15] the strength reduction factor is a power function of the number of rows of nails in the joint. For each ratio of nail row spacing to nail diameter, the strength reduction factor will increase as the number of rows of nails in the joint increases. With the models for steel or plywood joints using fully overlapping nails, the respective strength reduction factors are linear functions of the nail row spacing divided by the nail diameter. For each ratio of nail row spacing to nail diameter, the strength reduction factor will be a constant and will not be influenced by the number of rows of nails in the joint.

(vii) Because the material relationships in the model and Eurocode strength equations differ significantly, the EC5 rules cannot be safely applied to predict the strength or stiffness behaviour of joints formed with fully overlapping nails.

7. APPLICATION TO DESIGN AND ANALYSIS

7.1 INTRODUCTION

In Chapter 6 it was concluded that the rules in EC5 [11] or EC5 [15] are not directly applicable to joints made with fully overlapping nails and if the Eurocode strength and stiffness equations are used, the results will not accurately represent the behaviour of such joints.

In this section a design method for joints with fully overlapping nails subjected to lateral load or to moment, using the models developed in Chapters 4, 5 and 6 is given. It is structured to be read in conjunction with the rules in EC5 [15] with guidance given on the methodology to be used where changes are required. Only joints with a gap between the gusset plate and the timber are considered, in line with the approach used in EC5.

Characteristic values of the models for joints subjected to direct shear and to moment conditions are given together with design rules for strength and stiffness behaviour at the SLS and ULS states.

The semi-rigid behaviour of the moment models has been investigated and methods for determining the rigidity factor and the end moment reduction factor of the joints have been developed. A procedure for obtaining the secant rotational stiffness coefficient of each joint type is also given. In addition methods of analysis for sway and no-sway frames using these joints have been suggested.

7.2 GENERAL

The design philosophy uses a limit state approach related to clearly defined states beyond which the joint is deemed to no longer satisfy the design performance requirements. It fits within the framework for the basis of structural design set out in EN 1990 [133].

The ULS and SLS states used in EC5 apply, with the states being established using the same development criteria used for the code and discussed in Chapter 6. Characteristic value models are used, adopting fifth percentiles based on a log-normal distribution and assuming a coefficient of variation of not less than 0.10. Average values of functions are used in the models. To simplify the strength and stiffness equations, minor adjustments have been made to some of the coefficients derived for the original equations.

The classification of actions and the partial coefficient system as defined in EN 1991 [134] will apply and the partial factor for connections, γ_m, has been taken as 1.3, in line with EC5. As the joint testing regime used to derive the model only used timber with a moisture content within the range 11% to 15.5%, the methodology has been limited to the design of joints that come within the requirements of

service class 1 in EC5 (i.e. the moisture content will not exceed 12%). The moisture content factor for steel gusset plate joints has been removed.

To ensure lower bound results are obtained, as for the joint strength and stiffness equations developed in EC5, the design rules are based on the assumption there will be a gap between the timber and the gusset plates. Only those models associated with such joints have been used.

The key safety principle followed in the proposed design methodology is the same as is applicable to EC5. It complies with the framework given in equation (145) in which factored stress resultants caused by design action effects must be less than or equal to the equivalent design resistance of the joint.

7.2.1 Limitations to the Application of the Joint Models

The joint models are semi-empirical equations developed from a combination of the results of tests and analyses. To ensure they will adequately represent joint behaviour, only joints with material properties that have been enveloped within the testing programme can be used and the relevant limitations are given in Table 7.1. It is highly probable that for the majority of factors the models will be valid beyond these limits, however, for the above reason, this constraint has been imposed.

Where reference is made to 'lines' of nails in the models, this refers to the run of nails along any line which lies in the direction of the applied load. Where reference is made to 'rows' of nails, this means the run of nails along any line at right angles to the direction of the applied load. These definitions have been shown diagrammatically in Figure 4.1, Chapter 4.

Ref	Parameter	Limitations
i	Nail diameter	2.65mm to 3.35mm inclusive
ii	Nail type	Smooth round wire nails
iii	Nail strength	the minimum tensile strength of the nail wire is to be within the range 600 N/mm^2 to 830N/mm^2.
iv	Nail shear	The overlapping nails will be in single shear
v	Timber density	within the range 450Kg/m^3 to 700Kg/m^3.
vi	Plywood density	within the range 400Kg/m^3 to 700Kg/m^3
vii	Timber thickness	Minimum thickness of 40mm. Maximum thickness unlimited.
viii	Plywood thickness	5 ply to 7 ply; in the range 9mm to 19mm nominal thickness.

Table 7.1 Limitations to the application of the joint models

Ref	Parameter-cont'd	Limitations cont'd
ix	Steel gusset plate Thickness	6mm or greater.
x	Predrilling of timber and plywood	must be used and be compliant with the requirements of Eurocode 5 [15]
xi	Pre-boring of steel gusset plates	the tolerance on the hole diameter must be less than 0.1 times the nail diameter.
xii	Gap between timber and gusset plates	a nominal gap is to be present
xiii	Nail row spacing	the nail row spacing must be the same for all rows in a joint. It cannot be varied within a joint.
xiv	Max'm number of rows	the maximum number of rows will be 7.
xv	Nail lines	all nail lines must have the same number of nails and cannot be staggered relative to each other.
xvi	Material moisture content	The timber and plywood will comply with the requirements of service class1 in Eurocode5 [15].

Table 7.1 cont'd. Limitations to the application of the joint models

7.3 CRITERIA RELEVANT TO THE JOINT MODEL

The rules for the assembly of a joint will be as given in EC5 [15] unless otherwise stated in the following paragraphs.

i) Fully overlapping nails.

The nails will be driven adjacent to each other and will extend into the central timber member of the joint for at least 90% of the member thickness, as shown in Figure 7.1. The nails will not project into the adjacent gusset plate.

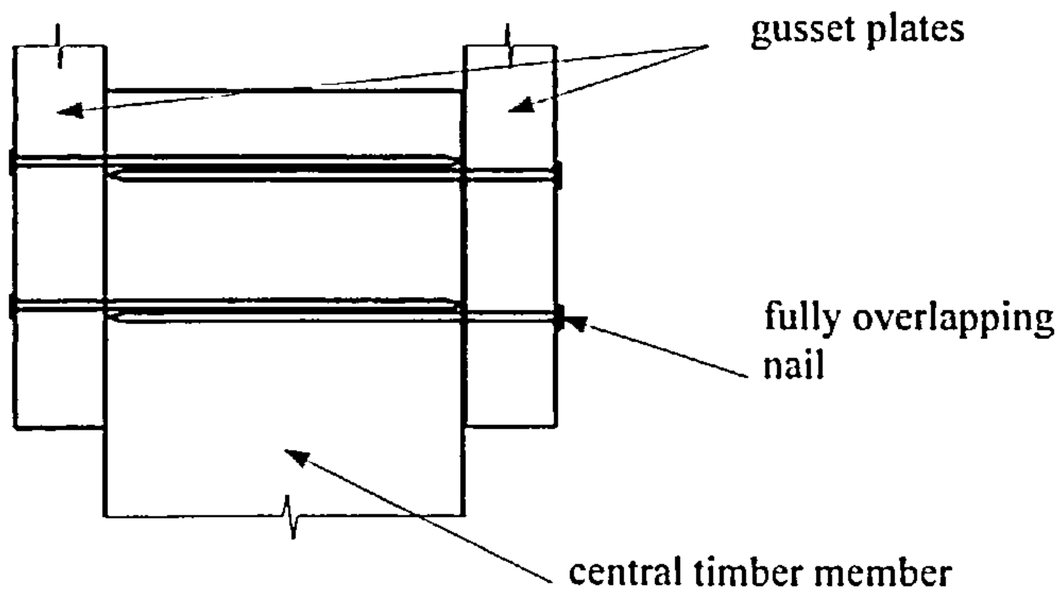

Figure 7.1 Fully overlapping nail configuration

ii) Minimum Nail Spacing and Distances in timber

The minimum spacing and distances applicable to timber in joints with fully overlapping nails are given in Table 7.2, with the symbols illustrated in Figure 7.2. Unless otherwise stated in the Table, the criteria will apply to joints with steel gusset plates and joints with plywood gusset plates.

Spacing or distance (see Figure 7.3)	**Angle**	**Minimum Distance (d – is the nail diameter)**
		Predrilled holes must be used
Spacing a_1 (//'l to the grain)	$0^\circ \le \beta \le 360^\circ$	Steel gusset joints - $7d$ Plywood gusset joints - $8.5d$
Spacing a_2 ($\perp$'r to the grain)	$0^\circ \le \beta \le 360^\circ$	$(3+\lvert\sin\beta\rvert)\,d$
Distance $a_{3,t}$ (loaded end)	$-90^\circ \le \beta \le 90^\circ$	Timber - $(14+10\lvert\cos\beta\rvert)d$;Ply - $(3+4\lvert\cos\beta\rvert)d$
Distance $a_{3,c}$ (unloaded end)	$90^\circ \le \beta \le 270^\circ$	Timber - $14d$; Ply – $3d$
Distance $a_{4,t}$ (loaded edge)	$0^\circ \le \beta \le 180^\circ$	Timber - $(6+4\lvert\sin\beta\rvert)\,d$; Ply – $(3+4\lvert\sin\beta\rvert)d$
Distance $a_{4,c}$ (unloaded edge)	$180^\circ \le \beta \le 360^\circ$	$3d$

Table 7.2 Minimum nail spacing and distances

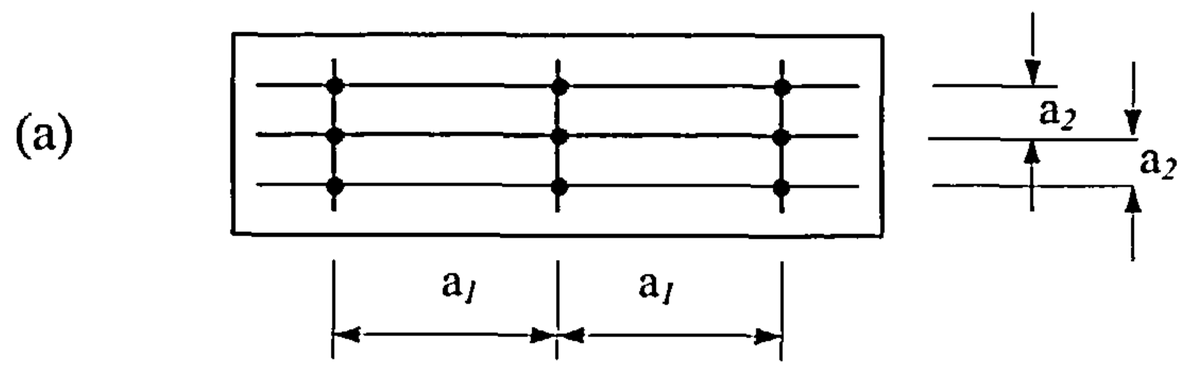

Figure 7.2 Spacing and distances – definitions (a) Spacing parallel and perpendicular to the grain, (b) Edge and end distances (β is the angle between the force and the grain direction)

7.4 DESIGN OF JOINTS USING FULLY OVERLAPPING NAILS

7.4.1 Models to be used for the Design of Laterally Loaded Joints with Steel or Plywood Gusset Plates

7.4.1.1 Characteristic load

The generalised characteristic strength behaviour for joints using steel gusset plates is given by equations (199) and (200) in Table 7.3. For these joints the joint displacement at the characteristic load will be 3.2mm and at that slip the characteristic load will be obtained from equations (201) and (202).

For joints with plywood gusset plates, the generalised characteristic strength behaviour is given by equations (203) and (204) in Table 7.4. For these joints the displacement at the characteristic load will be 4.5mm and at that slip the characteristic load will be obtained from equations (206) and (207), with the density function being obtained using equation (205).

The terms used in the equations are:

$P_S\delta x_{char}$ = the characteristic load of the steel gusset plate joint - at a slip of 3.2mm- N.

$P_P\delta x_{char}$ = the characteristic load of the plywood gusset plate joint - at a displacement of 4.5mm – N.

DF = is the density function and is defined in equation (205) - kg/m^3.

d = nail diameter – mm.

f_u = tensile strength of the nail wire - N/mm^2.

r = the number of rows of nails.

S_p/d = ratio of nail row spacing (mm) divided by the nail diameter (mm).

n = the number of lines of nails.

t_w = the length of penetration of the nail into the central timber - mm.

t_p = the thickness of each plywood gusset plate – mm.

D_W = density of the timber – kg/mm^3.

D_P = density of the plywood - kg/mm^3.

7.4.1.2 The ULS load

The design value of the joint load at the ULS will be as given in equation (208) for steel gusset plate joints and (209) for joints with plywood gusset plates. The functions remain as described in section 7.4.1.1, and in addition:

$P_S\delta x_d$ = the ULS load of the steel gusset plate joint – N

$P_P\delta x_d$ = the ULS load of the plywood gusset plate joint – N

k_{mod} = the strength modification factor given in Table 3.1 of EC5[15] for the appropriate load-duration class applicable to joints made with timber and plywood at service class 1 conditions.

7.4.1.3 The SLS load

The design value of the joint load at the SLS will be as given in equation (210) for steel gusset plate joints and (211) for plywood gusset plate joints. The functions remain as described in section 7.4.1.2 and in addition:

$P_S \delta x_{ser}$ = the SLS load of the joint – N

$P_P \delta x_{ser}$ = the SLS load of the joint – N

$\left(\frac{G_K + Q_K}{(\gamma_G G_K + \gamma_Q Q_K)} \right)$ = the ratio of the SLS load to the ULS load on the joint.

7.4.1.4 Joint slip under lateral loading

To evaluate the slip at any load on the joint, the load is inserted into the left hand side of the generalised characteristic strength equation and solved for δx. The solution can be obtained manually, by numerical analysis or more readily by using Mathcad [51] or an equivalent software package.

Where all of the joints are efficiently designed, for a reasonable approximation at the SLS and ULS states, the respective stiffness $K_S\ ser_{sls}$ and $K_S\ ser_{uls}$ can be taken as given in equations (212) and (213) for joints with steel gusset plates, given in Table 7.3. The SLS and ULS loads are as defined in sections 7.4.1.2 and 7.4.1.3 respectively; δx_{ser} is the slip at the serviceability load and is obtained from equation (199) or (200); and at the ULS the joint slip is 1.488mm.

For joints with plywood gusset plates, at the SLS and ULS states the respective stiffness $K_P\ ser_{sls}$ and $K_P\ ser_{uls}$ are as given in equations (214) and (215) in Table 7.4. The SLS and ULS loads are as defined in sections 7.4.1.2 and 7.4.1.3 respectively; δx_{ser} is the slip at the serviceability load and is obtained from equation (203) or (204); and at the ULS the joint slip is 1.924mm.

7.4.2 Models used for the Design of Moment Connections

7.4.2.1 General

In Chapter 5, the model recommended for the analysis of moment connections is that associated with the Non-Linear 2 method of analysis. It takes account the variation in the non-linear behaviour of the

Strength and stiffness equations for joints with steel gusset plates

i) Generalised characteristic strength equation:

(a) for nail row spacing between $7d$ and $19.6d$:

$$P_S \delta x_{char} = \frac{1.373}{1000} D_W d^{1.45} f_u r(0.743 + 0.013(\frac{S_p}{d}))n(1 - e^{-1.71\delta x})^{0.93}(0.1\delta x + 0.68) \quad \ldots.(199)$$

(b) for nail row spacing exceeding $19.6d$:

$$P_S \delta x_{char} = \frac{1.373}{1000} D_W d^{1.45} f_u rn(1 - e^{-1.71\delta x})^{0.93}(0.1\delta x + 0.68) \quad \ldots.(200)$$

ii) Characteristic strength:

(a) for nail row spacing between $7d$ and $19.6d$:

$$P_S \delta x_{char} = \frac{1.373}{1000} D_W d^{1.45} f_u r(0.743 + 0.013(\frac{S_p}{d}))n \quad \ldots.(201)$$

(b) for nail row spacing exceeding $19.6d$:

$$P_S \delta x_{char} = \frac{1.373}{1000} D_W d^{1.45} f_u rn \quad \ldots.(202)$$

iii) ULS load:

$$P_S \delta x_d = P_S \delta x_{char} \frac{k_{\text{mod}}}{1.3} \quad \ldots.(208)$$

iv) SLS load:

$$P_S \delta x_{ser} = P_S \delta x_d \left(\frac{G_K + Q_K}{(\gamma_G G_K + \gamma_Q Q_K)} \right) \quad \ldots.(209)$$

v) The SLS stiffness of the joint:

$$K_S ser_{sls} = \frac{P_S \delta x_{ser}}{\delta_{Sser}} \quad \ldots.(212)$$

vi) The ULS stiffness of the joint:

$$K_S ser_{uls} = \frac{P_S \delta x_d}{1.488} \quad \ldots.(213)$$

Table 7.3 Strength and stiffness equations for joints with steel gusset plates.

Strength and stiffness equations for joints with plywood gusset plates

i) Generalised characteristic strength equation:

(i) for nail row spacing between 8.5d and 17d:

$$P_P\delta x_{char} = \frac{1.911}{10000}(DF)d^{2.236}f_u r(0.839+0.0095(\frac{S_p}{d}))n(1-e^{-1.41\delta x})^{0.54}(0.121\delta x+1) \quad \ldots.(203)$$

(ii) for nail row spacing exceeding 17d:

$$P_P\delta x_{char} = \frac{1.911}{10000}(DF)d^{2236}f_u rn(1-e^{-1.41\delta x})^{0.54}(0.121\delta x+1) \quad \ldots.(204)$$

ii) Characteristic strength:

(i) for nail row spacing between 8.5d and 17d:

$$P_P\delta x_{char} = \frac{2.949}{10000}(DF)d^{2.236}f_u r(0.839+0.0095(\frac{S_p}{d}))n \quad \ldots.(206)$$

(ii) for nail row spacing exceeding 17d:

$$P_P\delta x_{char} = \frac{2.949}{10000}(DF)d^{2.236}f_u rn \quad \ldots.(207)$$

$$\text{and } DF = 2((0.000912f_u - 0.464)\frac{t_w}{(t_w+t_p)}D_W + (2.464-0.000912f_u)\frac{t_p}{(t_w+t_p)}D_P \quad \ldots.(205)$$

iii) ULS load:

$$P_P\delta x_d = P_P\delta x_{char}\frac{k_{\text{mod}}}{1.3} \quad \ldots.(209)$$

iv) SLS load:

$$P_P\delta x_{ser} = P_P\delta x_d\left(\frac{G_K+Q_K}{(\gamma_G G_K+\gamma_Q Q_K)}\right) \quad \ldots.(211)$$

v) The SLS stiffness of the joint:

$$K_P ser_{sls} = \frac{P_P\delta x_{ser}}{\delta_{Sser}} \quad \ldots.(214)$$

vi) The ULS stiffness of the joint:

$$K_P ser_{uls} = \frac{P_P\delta x_d}{1.924} \quad \ldots.(215)$$

Table 7.4 Strength and stiffness equations for joints with plywood gusset plates.

nails in the joint as well as the effect of movement of the centre of rotation of the joint during the loading process.

When dealing with the moment behaviour of joints in statically determinate beam or frame configurations, the solution is relatively straight forward, as has been shown in Chapter 5 using cantilever beams. With joints in indeterminate situations, the moment in the joint is a function of its rotational rigidity and before this can be determined the centre of rotation must first be identified. Because there is not a linear relationship between the moment and the shear force in such structures, the solution necessitates a numerical analysis or equivalent approach, considerably adding to the effort required to solve the problem. Such a requirement has also been identified by Hirai [134] in his analysis of moment connections in statically indeterminate structures using timber joints.

From a review of the results of the methods of analysis proposed in Chapter 5, Non-Linear 1 method, which is based on the use of a fixed centre of rotation at the centroid of the nail group, is readily solvable irrespective of the state of determinacy of the structure. It also gives answers that are generally within 1% to 2% of the Non-Linear 2 result and as the stiffness of the joint increases, the difference between the results reduces. In addition, for joints subjected to pure moment the centre of rotation will, in any event, be the centroid of the nail group. And, with indeterminate structures, when using joints designed for moment transfer the joint will tend to be stiffer with the moment becoming the more dominant action and approximating to the pure moment condition. For the above reasons, rather than adopt the Non-Linear 2 method with a numerical analysis approach, Non-Linear 1 has been used.

To use the models, the radius of the extreme nail, r_{max}, from the nail group centroid is first determined and by applying a displacement of $\delta x \max$ to this nail the joint rotation will be $\frac{\delta x \max}{r_{\max}}$. Because the testing programme for steel gusset plate joints was restricted to joints with nailing configuration RA, this has been used as the upper bound limit for the moment equation for these joints. For joints with plywood gusset plates, the upper bound nailing configuration is RK.

The following analysis is only applicable to joints with a gap between the gusset plates and the timber and where the limitations given in Table 7.1 have been fully complied. The model also includes for joints where the plane of the timber grain is at an angle to the face of the timber, as shown in Figure 5.20, and discussed in Chapter5.

7.4.2.2 Evaluation of the Characteristic Moment of Steel Gusset Plate Joints.

The characteristic moment strength equation for the model is given in equations (216) and (217) to suit the nail row spacing being used. The model will give the characteristic moment of the joint at a rotation of $\frac{3.2}{r_{\max}}$ radians by substituting for $\delta x \max = 3.2$mm.

The validity of the result will be dependent on achieving full compliance with other relevant design criteria and the requirements to be met are given in item (c) below.

(a) where the nail row spacing is between $7d$ and $19.5d$:

$$M_S\delta x_{char} = (\sum_{i=1}^{i=\frac{N}{2}} r_i \ (1\text{-}e^{-1.71\delta xmax\frac{r_i}{r_{\max}}})^{0.93}(0.1(\delta xmax\frac{r_i}{r_{\max}}) +0.68)\frac{P_1P_2f_{TR}}{P_1\sin^2\beta+P_2\cos^2\beta} \quad ...(216)$$

(b) where the nail row spacing greater than $19.5d$:

$$M_S\delta x_{char} = P_2f_{TR}(\sum_{i=1}^{i=\frac{N}{2}} r_i \ (1\text{-}e^{-1.71\delta xmax\frac{r_i}{r_{\max}}})^{0.93}(0.1(\delta xmax\frac{r_i}{r_{\max}}) +0.68)) \quad ...(217)$$

and

$$P_1 = \frac{1.373}{1000}D_W d^{1.45} f_u(0.743 + 0.013(\frac{S_p}{d})) \quad ....(218)$$

$$P_2 = \frac{1.373}{1000}D_W d^{1.45} f_u \quad ....(219)$$

$$f_{TR} = \frac{0.91}{\sin^2(\alpha) + 0.91\cos^2(\alpha)} \quad ....(136)$$

where:

$M_S\delta x_{char}$ = the characteristic moment taken by the joint – Nmm.

r_{max} = the distance of the furthest pair of fully overlapping nails from the centroid of the nail group– mm.

r_i = the distance of nail i from the centroid of the nail group – mm.

$\delta xmax$ = the slip of the nail at radius $r_{max.}$-mm.

N = the total number of nails in the joint. $\frac{N}{2}$ is the number of fully overlapping pairs of nails in the joint.

β = the angle between the force in the pair of fully overlapping nails at r_{max} and the direction of the L axis, as shown in Figure 5.3.

f_{TR} = the grain direction factor.

a = the angle of between the plane of the grain and the face of the timber as shown in Figure 5.20.

and the other terms remain are as described in section 7.4.1.1.

(c) The joint moment from the above equations will be valid providing the following criteria are also complied with:

(i) There must be no significant bending of the timber over the length of the joint. For joints using 150mm deep timber, this will be satisfied providing the moment from the model equations is ≤ that obtained using nailing configuration RA.

(ii) The moment capacity of the timber member in the joint must exceed the joint moment.

(iii) To prevent splitting of the timber, the maximum force in the joint perpendicular to the grain, F_{max}, defined below, must satisfy:

$$F_{max} \leq \frac{k_{\text{mod}}}{\gamma_{\text{mod}}}(14bw)\sqrt{\frac{h_e}{\left(1-\frac{h_e}{h}\right)}} \qquad \ldots.(141)$$

where:

F_{max} = the maximum force in the joint perpendicular to the grain at the ULS moment. It is obtained by the summation of the vertical components of the nail forces acting in the same direction and will include the nail at the greatest distance from the centre of rotation, as shown in Figure 5.22 and defined in equation (139) – N.

b = the member thickness – mm.

w = a width factor = 1.

h = the timber member height – mm.

h_e = the loaded edge distance from the centre of the most distant nail – mm.

7.4.2.3 The ULS Moment of Joints with Steel Gusset Plates.

Subject to compliance with the conditions in section 7.4.2.2 (c), the design value of the joint moment at the ULS will be:

$$M_S\delta x_d = M_S\delta x_{char}\frac{k_{\text{mod}}}{1.3}. \qquad \ldots.(220)$$

where the functions remain as described in sections 7.4.1.2 and 7.4.2.2 and in addition $M_S\delta x_d$ = the ULS moment of the joint – N.

7.4.2.4 The SLS Moment of Joints with Steel Gusset Plates.

Subject to compliance with the conditions in section 7.4.2.2 (c), the value of the joint moment at the SLS will be:

$$M_S\delta x_{ser} = M_S\delta x_d\left(\frac{G_K+Q_K}{(\gamma_G G_K+\gamma_Q Q_K)}\right) \qquad \ldots.(221)$$

where the functions remain as described in section 7.4.1.3, and 7.4.2.3 and in addition $M_S \delta x_{ser}$ = the SLS moment of the joint – N

7.4.2.5 Evaluation of the Characteristic Moment of Plywood Gusset Plate Joints.

The characteristic moment strength equation for the model is given in equations (222) and (223) to suit the nail row spacing being used. The model will give the characteristic moment of the joint at a rotation of $\frac{4.5}{r_{\max}}$ radians by substituting for $\delta x \max$ = 4.5mm in the equations.

The validity of the result will be dependent on achieving full compliance with other design criteria and the requirements to be met are given in item (c) below.

(a) where the nail row spacing is between 8.5*d* and 17*d*:

$$M_P \delta x_{char} = \sum_{i=1}^{i=\frac{N}{2}} r_i \ (1\text{-}e^{-1.41 \delta x max \frac{r_i}{r_{\max}}})^{0.54} (0.121(\delta x max \frac{r_i}{r_{\max}}) + 1) \ \frac{P_3 P_4 f_{TR}}{P_3 \sin^2 \beta + P_4 \cos^2 \beta} \quad ...(222)$$

(b) where the nail row spacing greater than 17*d*:

$$M_P \delta x_{char} = P_4 f_{TR} (\sum_{i=1}^{i=\frac{N}{2}} r_i \ (1\text{-}e^{-1.41 \delta x max \frac{r_i}{r_{\max}}})^{0.54} (0.121(\delta x max \frac{r_i}{r_{\max}}) + 1)) \quad ...(223)$$

and

$$P_3 = \frac{1.911}{10000} (DF) d^{2.236} f_u (0.839 + 0.0095(\frac{S_p}{d})) \quad ....(224)$$

$$P_4 = \frac{1.911}{10000} (DF) d^{2.236} f_u \quad ....(225)$$

where $M_P \delta x_{char}$ is the characteristic moment taken by the joint in Nmm and other terms remain as described in sections 7.4.1.1 and 7.4.2.2.

(c) The joint moment from the above equations will be valid providing the following criteria are also complied with:

(i) There must be no significant bending of the timber over the length of the joint. For joints using 150mm deep timber, this requirement will be satisfied providing the moment from the model equations is $\leq$ the moment obtained from nailing configuration RK.

(ii) The requirements of items (ii) and (iii) in section 7.4.1.2 (c) are fully complied with.

7.4.2.6 The ULS Moment of Joints with Plywood Gusset Plates.

Subject to compliance with the conditions in section 7.4.2.5 (c), the design value of the joint moment at the ULS will be:

$$M_p \delta x_d = M_p \delta x_{char} \frac{k_{\text{mod}}}{1.3} \qquad \ldots.(226)$$

where the functions remain as described in section 7.4.1.2, and 7.4.2.5 and in addition $M_p \delta x_d$ = the ULS moment of the joint – N.

7.4.2.7 The SLS Moment of Joints with Plywood Gusset Plates.

Subject to compliance with the conditions in section 7.4.2.5 (c), the value of the joint moment at the SLS will be:

$$M_p \delta x_{ser} = M_p \delta x_d \left(\frac{G_K + Q_K}{(\gamma_G G_K + \gamma_Q Q_K)} \right) \qquad \ldots.(227)$$

where the functions remain as described in section 7.4.1.3, and 7.4.2.6 and in addition $M_p \delta x_{ser}$ = the SLS moment of the joint – N.

7.5 ANALYSIS OF STRUCTURES WITH JOINTS FORMED USING FULLY OVERLAPPING NAILS WHEN SUBJECTED TO MOMENT

7.5.1 Joint Behaviour

When the joint in a structure formed using gusset plates is subjected to rotation, providing there is no relative movement between the joint members and the gusset plates, the members and plates will rotate by the same amount. In this condition the joint is referred to as rigid, providing maximum rotational stiffness to the structure. At the other extreme, where, when subjected to rotation the gusset plates rotate but the joint members remain unflexed, the joint is referred to as pinned. Between these conditions the joint is referred to as semi-rigid. With timber structures, the traditional approach in analysis has been to assume joints are either rigid or pinned.

From the investigations into joint behaviour in Chapter 5 it has been shown by loading cantilever members secured by fully overlapping nailed joints that a rigid joint condition will not be obtained. The tests have demonstrated that when subjected to a moment the cantilever member will rotate relative to

the gusset plates in a semi-rigid manner, allowing the deflection of the member to increase and the joint stiffness and moment transfer capability to reduce. Despite the prevailing tendency by designers to classify joints as either fully fixed or pinned, semi-rigidity is the most common type of behaviour in timber joints formed with gusset pates using dowel type connectors and should be taken into account in the design process. The above tests have also shown that the effect of shear forces on the joint behaviour is small compared to the moment effect and, in line with the assumptions made by other researchers when analysing the moment behaviour if joints, shear (and axial) deformation effects can be ignored [79, 94, 100, 101, 102].

Joint behaviour varies with the type of connection being used and several experimental studies have been carried out by researchers to establish moment-rotation relationships for different connection types. Several models have been developed and these have been outlined in Chapter 2. The model type most relevant to this research is the exponential power model. Exponential models have been developed by other researchers [2, 150, 151, 152] and the model derived in Chapter 5 for joints with steel gusset plate or plywood gusset plate connections using fully overlapping nails is of this type. It lends itself to an analytical solution where the moment in the joint, M, can be related to the relative rotation θ_r between the joint gusset plates and the joint member in the following manner:

$$M = k\theta_r \qquad \ldots.(228)$$

where k is the rotational stiffness of the connection in the form of an exponential relationship. The physical representation of a joint with a rigid, pinned or semi-rigid connection is shown in Figure 7.3.

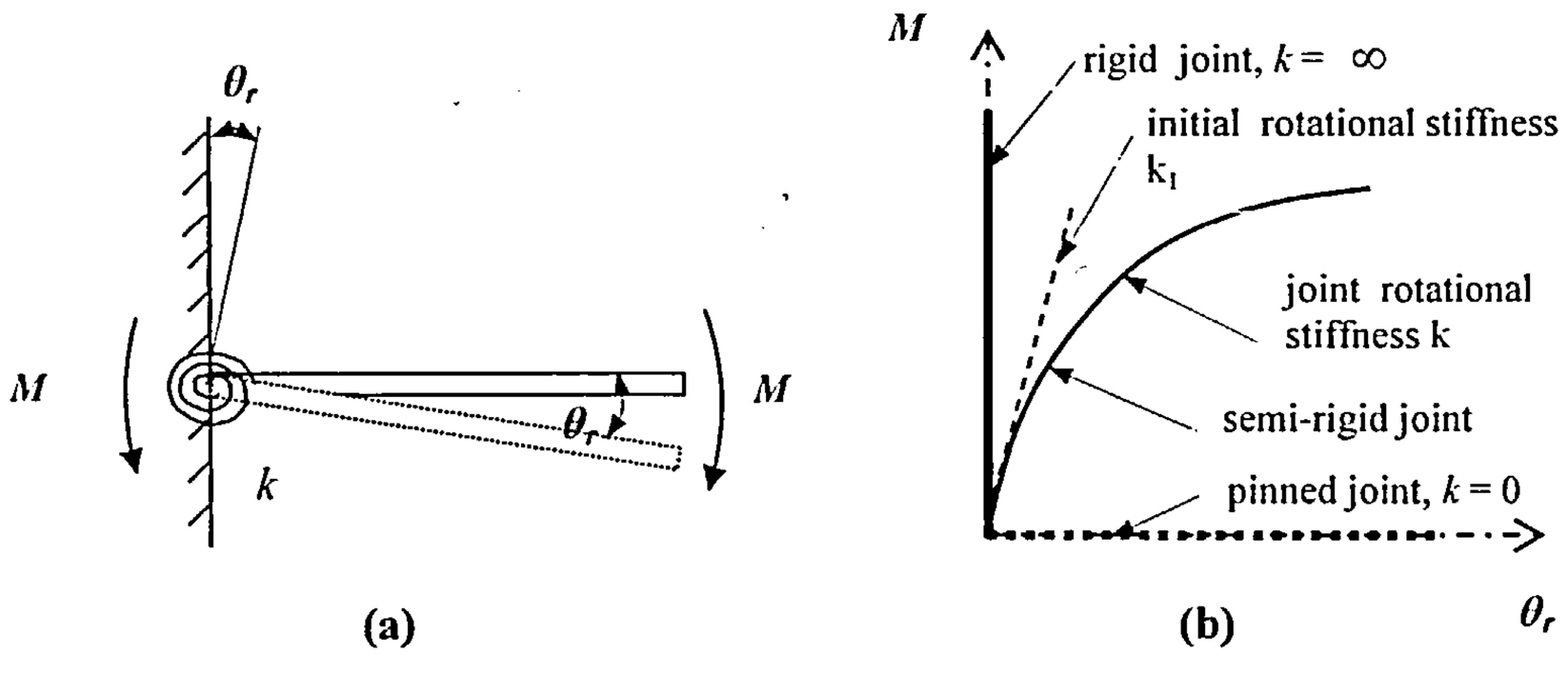

Figure 7.3 Different types of connection rotational stiffness in a timber joint.

With a rigid connection, irrespective of the value of the moment, the relative rotation θ_r will be zero and the M - θ_r relationship will be a vertical line through the origin as shown in Figure 7.3(b). The rotational stiffness for this condition is infinity. With a pinned joint connection, no moment can develop and the M - θ_r relationship will be a horizontal line also through the origin. The rotational stiffness for this condition is zero. All conditions between these extremes constitute semi-rigid behaviour.

A possible method for taking into account the effect of semi-rigid connections on member behaviour is to represent the connection by a rotational spring and this has been widely used in the analysis of steel structures [102, 137, 112, 143, 145]. In timber analysis, this approach was proposed by Porteous [141] and developed by Brynildsen and Booth [142] for the study of semi-rigid joints in W-braced trusses and has been further developed by other researchers [94, 134, 144] in nailed timber joint and frame analyses.

The simplest form is the use of a linear rotational spring which is modelled to represent the initial stiffness k_1 of the connection, shown in Figure 7.3(b). By incorporating an iteration procedure in the analysis the spring properties can be varied over the joint rotation cycle to fit the rotational stiffness k of the joint.

Consider any prismatic member ab of length L and flexural rigidity EI within a frame fitted with linear rotational spring elements of stiffness k_a and k_b of negligible length at each end, as shown in Figure 7.4. As axial load effects will be ignored, the member can be considered to be axially rigid. Ends *1* and *2* are the joint connections to the frame and elements *1,a* and *b,2* are the rotational spring elements. Under the action of an end moment M at a joint, it will rotate and there will also be a relative rotation θ_r between the joint and the member, represented by the rotation of the spring. The joint rotations are designated θ_1 and θ_2 at ends *1* and *2* respectively. The moment required to be applied to the end of a prismatic member to cause a unit rotation when the other end is fixed in position is referred to as the member stiffness. For a member of length L and flexural rigidity EI, from basic principles the member stiffness can be shown to equal $\frac{4EI}{L}$ [135]. To align with the member stiffness definition, the spring rotational stiffness will be written in a similar format as follows:

$$k_1 = \frac{EI}{L}\beta_a; \qquad k_2 = \frac{EI}{L}\beta_b \qquad \ldots.(229)$$

where $M_1 = k_1\theta_{r1}$ and $M_2 = k_2\theta_{r2}$ and β_a and β_b will be referred to as the secant rotational stiffness coefficients of the joints.

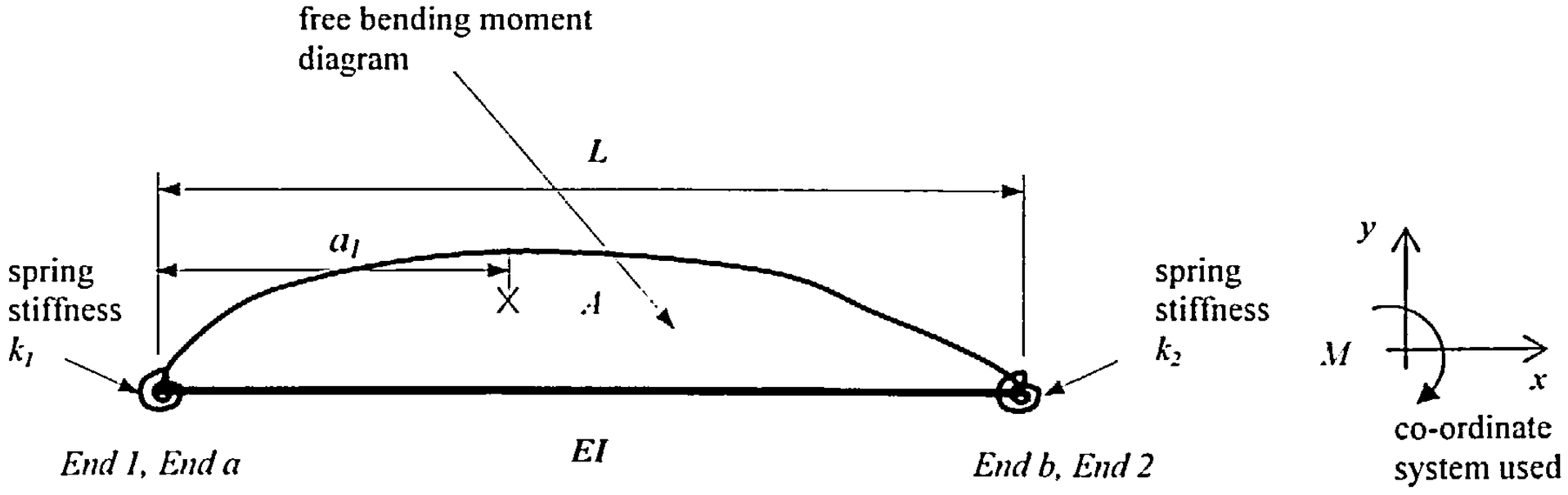

Figure 7.4 Member with rotational springs at each end

Consider the beam to be loaded in a generalised manner and the area of the free bending moment diagram to be A with its centre of area at a distance a_1 from end a. Using unit load theory, a combination of flexibility coefficients and the stiffness method of analysis, and assuming ends 1 and 2 to be unyielding supports, it will be shown that:

$$M_1 = (\frac{1}{1+\frac{3EI}{k_1 L}})(\frac{3EI\vartheta_1}{L} + \frac{M_2}{2} - \frac{3A(L-a_1)}{L^2}) \quad \ldots.(230)$$

$$M_2 = (\frac{1}{1+\frac{3EI}{k_2 L}})(\frac{3EI\vartheta_2}{L} + \frac{M_1}{2} + \frac{3Aa_1}{L^2}) \quad \ldots.(231)$$

The functions $(\frac{1}{1+\frac{3EI}{k_1 L}})$ and $(\frac{1}{1+\frac{3EI}{k_2 L}})$ modify the prismatic member relationship to take account of the effects of the end springs and are referred to by Monforton *et al* [137] as the fixity factors of the member and by Kermani [94] as the rigidity factors. They are dimensionless parameters, and are functions of the respective spring stiffness and the stiffness properties of the beam. Expressing the rigidity factors in terms of the symbol γ, they can be written:

$$\gamma_1 = (\frac{1}{1+\frac{3EI}{k_1 L}}) \quad \ldots.(232)$$

$$\gamma_2 = (\frac{1}{1+\frac{3EI}{k_2 L}}) \quad \ldots.(233)$$

After solving (230) and (231) for M_1 and M_2 the equations can be written in terms of the rigidity factors:

$$M_1 = (\frac{6\gamma_1}{(4-\gamma_1\gamma_2)})\frac{EI}{L}(2\vartheta_1 + \gamma_2\vartheta_2 - \frac{A}{EIL}(2(L-a_1) - \gamma_2 a_1)) \quad \ldots.(234)$$

$$M_2 = (\frac{6\gamma_2}{(4-\gamma_1\gamma_2)})\frac{EI}{L}(2\vartheta_2 + \gamma_1\vartheta_1 + \frac{A}{EIL}(2a_1 - \gamma_1(L-a_1)) \quad \ldots.(235)$$

The above are referred to as the modified slope equations. They are simplifications of the more generalised format which includes for deflection effects at the ends of the beam, developed by Monforton *et al* [137] using the conjugate beam approach and by Livesley [136], McGuire *et al* [138] and Dhillon *et al* [112] using a combined flexibility and stiffness approach. Those elements in the

equations containing the free bending moment are the modified end fixing moments on the beam and can be written as:

$$M_{F1} = \frac{6A}{L^2}\frac{\gamma_1}{(4-\gamma_1\gamma_2)}(2(L-a_1)-\gamma_2 a_1) \qquad \ldots.(236)$$

$$M_{F2} = \frac{6A}{L^2}\frac{\gamma_2}{(4-\gamma_1\gamma_2)}(2a_1-\gamma_1(L-a_1) \qquad \ldots.(237)$$

where M_{F1} and M_{F2} are the modified end fixing moments at ends 1 and 2 of the beam.

The above are general relationships applicable to prismatic members with rotational springs at each end resting on unyielding supports. If the joint is rigid k will be infinity and the rigidity factor γ will be unity. If the joint is a frictionless pin, k will be zero and the rigidity factor will also be zero.

7.5.2 Rigidity Factors for Joints Formed using Fully Overlapping Nails

The expressions in section 7.5.1 have been developed on the assumption that the initial rotational spring stiffness of the joint is constant for the full range of loading. In this section the effect of the reduction in joint stiffness associated with joints using fully overlapping nails is taken into account.

Consider the generalised joint configuration shown in Figure 7.5(a) where the joint is subjected to a moment M and rotates about the centroid of the nail group O.

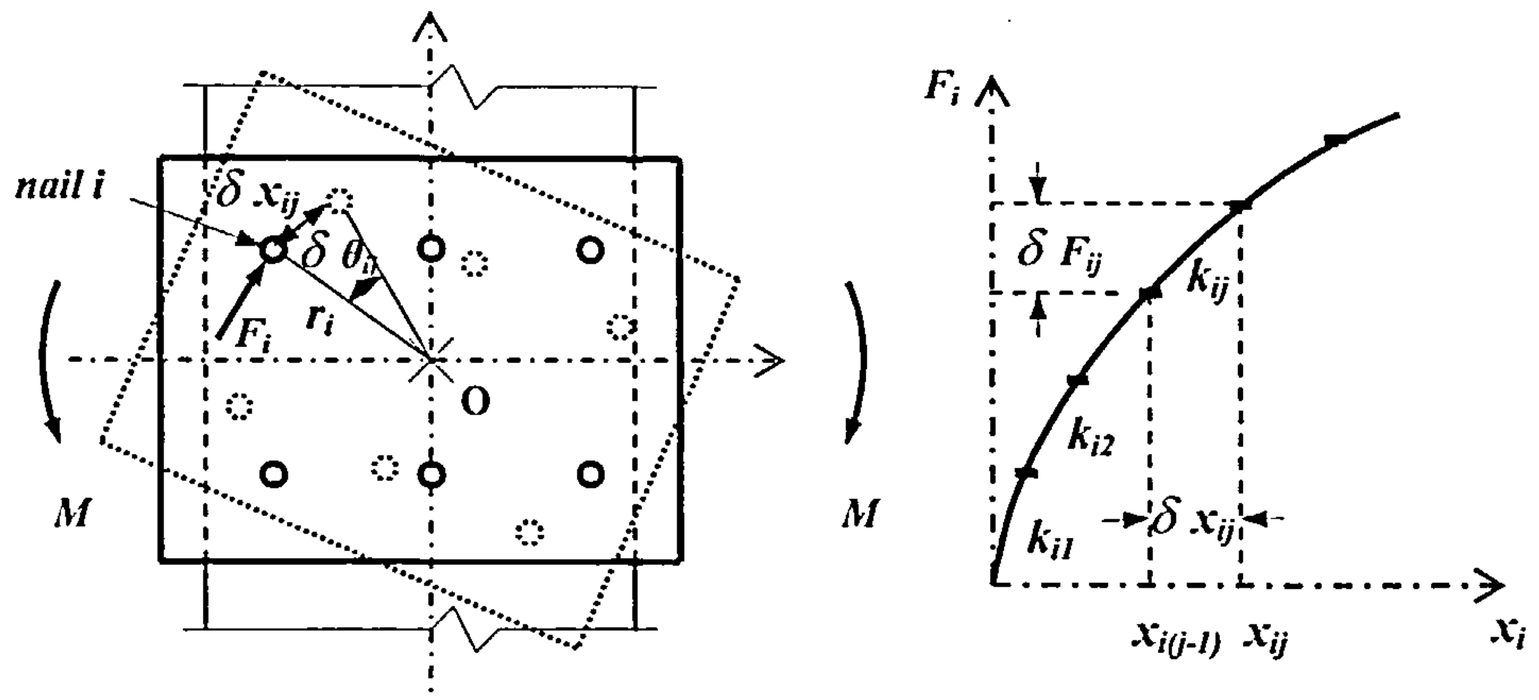

(a) **(b)**

Figure 7.5 Joint rotation about nail group centroid

Under the moment the nails will displace and the relationship between the force F_i in any nail i at radius r_i from O and the slip x_i of the nail in the joint will be as shown in Figure 7.5(b). Under the general

increment of slip, $x_{i(j-1)}$ to x_{ij}, let nail i move distance δx_{ij} and the joint rotate by amount $\delta\theta_{ij}$ and the relationship between the nail force and the nail slip will be:

$$\delta F_{ij} = k_{ij}\, \delta x_{ij} \qquad \ldots.(238)$$

The relationship between nail slip and joint rotation is $\delta x_{ij} = r_i \delta\theta_{ij}$ and substituting for δx_{ij} in equation (238) gives:

$$\delta F_{ij} = k_{ij}\, r_i\, \delta\theta_{ij} \qquad \ldots.(239)$$

To obtain the increment of moment δM_{ij} taken by the joint due to the force δF_{ij} in nail i during increment $x_{i(j-1)}$ to x_{ij}, the force is multiplied by its lever arm r_i, giving:

$$\delta M_{ij} = k_{ij}\, r_i^2\, \delta\theta_{ij} \qquad \ldots.(240)$$

The total moment M in the joint causing it to rotate through θ will be the summation of the incremental moments taken by each nail over the full displacement range:

$$M = \sum_{1}^{i}\sum_{1}^{j} k_{ij} r_i^2 \vartheta \qquad \ldots.(241)$$

where

M = the moment taken by the joint when rotation is about the centroid of the nailing configuration

k_{ij}= the **tangential** stiffness of nail i at displacement j

r_j= the radius of nail i from the centroid

θ = the angular rotation of the joint about the centroid.

The tangential stiffness of the models for joints using steel gusset plates and plywood gusset plates with fully overlapping nails will be obtained by differentiating the exponential load-slip relations in equations (216), (217) and (222), (223) respectively giving:

(i) for steel gusset plate joints:

(a)where the nail row spacing is between $7d$ and $19.5d$:

$$k_{ij} = \frac{P_1 P_2 f_{TR}}{P_1 \sin^2\beta + P_2 \cos^2\beta}\left(1 - e^{-1.71\delta_{ij}}\right)^{0.93}\left(\frac{1.5903\,(0.1\delta_{ij} + 0.68)e^{-1.71\delta x_{ij}}}{(1 - e^{-1.71\delta_{ij}})} + 0.1\right) \qquad \ldots.(242)$$

(b) where the nail row spacing greater than 19.5*d*:

$$k_{ij} = P_2 f_{TR} \left(1 - e^{-1.71\delta_{ij}}\right)^{0.93} \left(\frac{1.5903\,(0.1\delta_{ij} + 0.68)e^{-1.71\delta x_{ij}}}{(1 - e^{-1.71\delta_{ij}})} + 0.1\right) \quad \ldots(243)$$

(ii) for plywood gusset plate joints:

(a) where the nail row spacing is between 8.5*d* and 17*d*:

$$k_{ij} = \frac{P_3 P_4 f_{TR}}{P_3 \sin^2\beta + P_4 \cos^2\beta} \left(1 - e^{-1.41\delta_{ij}}\right)^{0.54} \left(\frac{0.7614\ (0.121\,\delta_{ij} + 1)e^{-1.41\delta_{ij}}}{(1 - e^{-1.41\delta_{ij}})} + 0.121\right) \quad \ldots.(244)$$

(b) where the nail row spacing greater than 17*d*:

$$k_{ij} = P_4 f_{TR} \left(1 - e^{-1.41\delta_{ij}}\right)^{0.54} \left(\frac{0.7614\ (0.121\,\delta_{ij} + 1)e^{-1.41\delta_{ij}}}{(1 - e^{-1.41\delta_{ij}})} + 0.121\right) \quad \ldots(245)$$

In the above equations, $\delta_{ij} = \frac{r_i}{r_{max}} \delta x_{ij}$; r_{max} is the radius of the nail at the greatest distance from the centroid of the nailing configuration and the remaining items are as described in sections 7.4.2.2 and 7.4.2.5.

Substituting for the relevant rotational stiffness in equation (232) and using array calculations set up in Mathcad [51], the value of the rigidity factors associated with the model equations for steel and plywood joints with fully overlapping nails can be determined. In the analyses, to allow for a better focus on the more relevant aspects of the behaviour of the joints, the same nailing configuration has been used at each end of the beam. An example using the calculation procedure derived for joints with plywood gusset plates is given in Appendix J. Using the extreme values of the material properties the rigidity factors for joints with plywood gusset plates and steel gusset plates using fully overlapping nails are shown graphically in Figures 7.6 and 7.7 respectively.

In the analyses, nailing configuration RA has been used. The modulus of elasticity has been kept the same, using a mean value of 9000N/mm^2 as given in Table 1 of BS EN 338: 1995 [115] for timber of strength class C18 (used in the testing programme). The beam properties have all been based on the average geometric properties of the beam used for the cantilever moment tests.

For both types of joint, at the commencement of rotation it is noted that the rigidity factor is always less than unity and as rotation increases the factor falls away, becoming almost asymptotic at values less than 0.2 at the maximum nail slip for each joint type. From consideration of the rigidity factor equation,

this is to be expected as the tangent stiffness k_{ij} of the load-slip curve gets smaller with increasing joint slip thereby reducing the value of the factor.

As the nail diameter increases the rigidity factor also increases but the change between nail sizes is relatively small. The initial value of the rigidity factor is higher using plywood gusset plate joints but the factor falls off more slowly as the joint rotation increases when using steel gusset plate joints. This is shown in Figure 7.8 where a steel gusset plate joint is compared with one using plywood gusset plates and a maximum slip of 3.2mm is used for both joints. Beyond a slip of 1mm, the rigidity factor of the steel gusset plate joint is almost 50% more than the plywood joint factor.

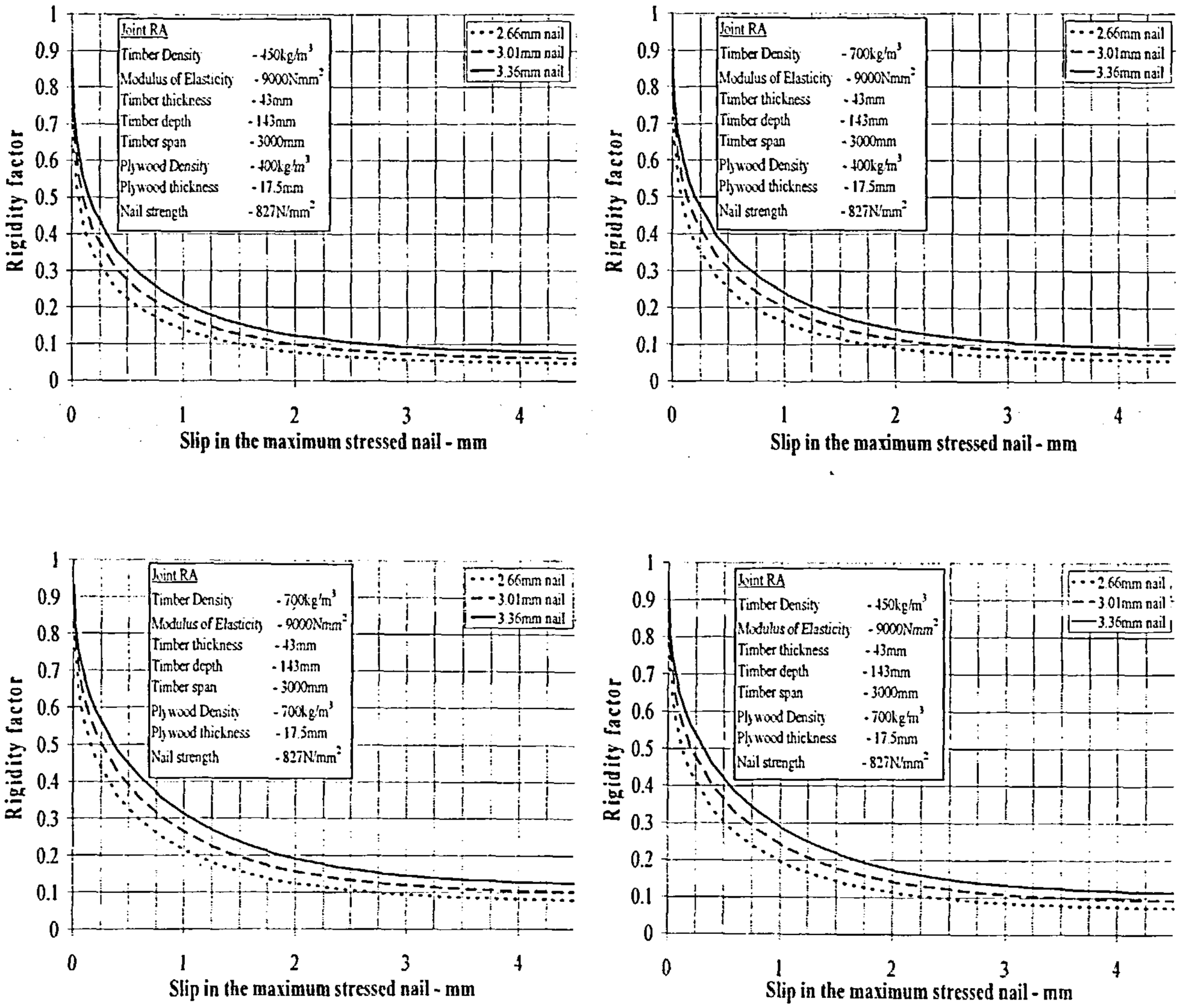

Figure 7.6 Rigidity factors for joints with plywood gusset plates

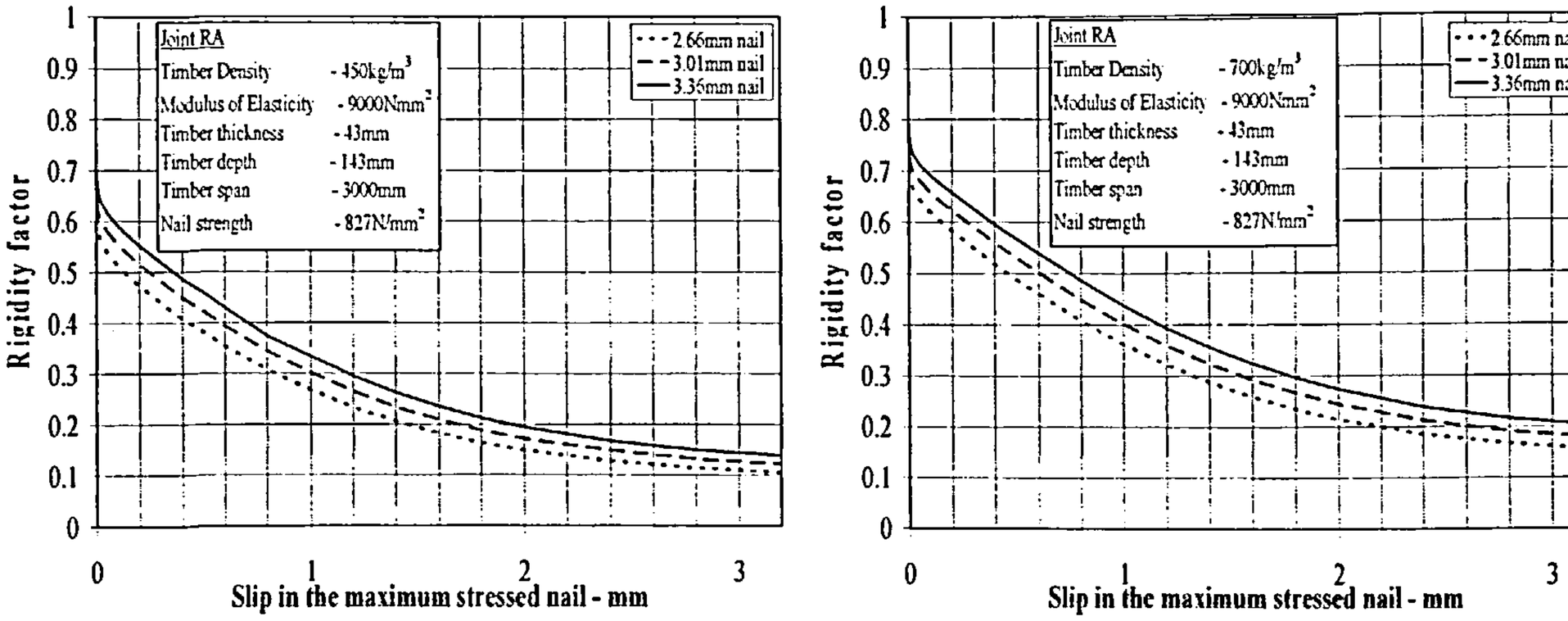

Figure 7.7 Rigidity factors for joints with steel gusset plates

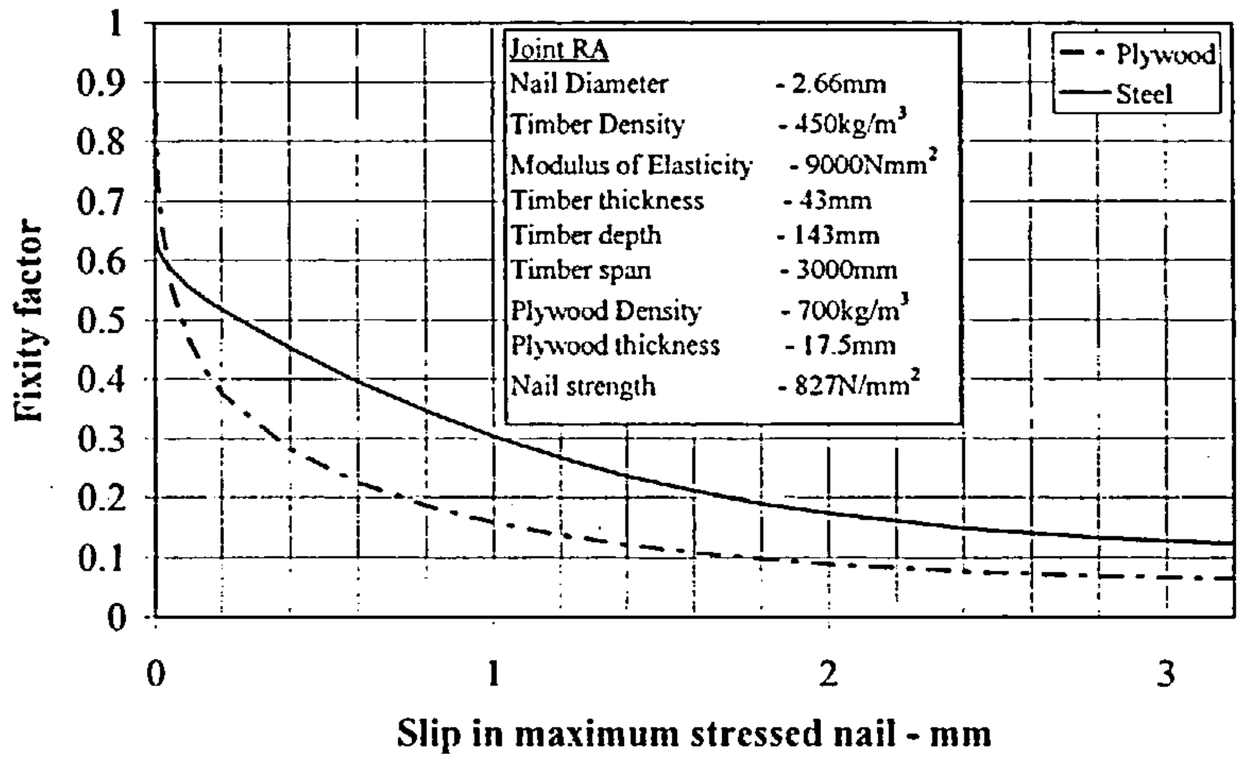

Figure 7.8 Comparison of the rigidity factor of a plywood gusset joint and steel gusset joint

From equations (236) and (237), the end moment resistance provided to a beam fitted with semi-rigid joints is a function of the joint rigidity factor and from the above graphs, whether using steel or plywood gusset plate joints, the value will reduce as the ends of the beam rotate. The withstand capacity will be dependent on the rotation of the ends of the beam, which is a function of the beam loading, and is investigated in the following section.

7.5.3 Withstand Capacity of Joints in Beams

In section 7.5.1, the end fixing moments in a beam with semi-rigid connections are given by equations (236) and (237). Considering a beam fitted with the same joint at each end and subjected to a point load at mid-span, these equations reduce to:

$$M_{F1} = M_{F2} = \frac{PL}{8}\left(\frac{3\gamma_1}{(2+\gamma_1)}\right) \qquad \ldots.(246)$$

Substituting for the value of the rigidity factor given in equation (232), and using the rotational stiffness derived from equation (241), the above equation becomes:

$$M_{F1} = M_{F2} = \frac{PL}{8}\left(\frac{1}{\left(1+\frac{2EI}{\sum_{1}^{i}\sum_{1}^{j} k_{ij} r_i^2 L}\right)}\right) \qquad \ldots.(247)$$

Function $\left(\frac{1}{\left(1+\frac{2EI}{\sum_{1}^{i}\sum_{1}^{j} k_{ij} r_i^2 L}\right)}\right)$ is termed the end fixing moment factor, and using an array calculation approach in Mathcad, it can be determined for the joints.

Under each increment of load on the beam, p_{ij}, the increment of moment taken by the joint will be m_{ij} and by rearranging equation (247), the relationship between the functions can be written as:

$$p_{ij} = \frac{8}{L} m_{ij}\left(1+\frac{2EI}{k_{ij} r_i^2 L}\right) \qquad \ldots.(248)$$

In a fully fixed condition the load taken by the joint will be $P = \frac{8M}{L}$, where M is the moment taken by the joint at maximum slip. By increasing the value of j until the sum of equation (248) over all of the nails equals P, the value of the joint slip at the equilibrium condition will be obtained:

$$P = \sum_{1}^{i}\sum_{1}^{j} p_{ij} \qquad \ldots.(249)$$

Substituting for the value of j obtained from (249) into equation (247), the end fixing moment, M_{FI}, at the equilibrium position will be obtained.

For this moment, the secant rotational stiffness of the joint, k_{sec}, will be obtained by dividing by the joint rotation at increment j:

$$k_{\text{sec}} = \frac{M_{F1}}{\left(\frac{j}{r_{\max}}\right)} \qquad \ldots.(250)$$

where r_{max} is the radius of the nail in the joint with the maximum slip.

Equating (250) and equation (229) and rearranging, the secant rotational stiffness coefficient of the joint

can be obtained as follows:

$$\beta = \frac{k_{sec} L}{EI} \qquad \ldots.(251)$$

An example of the use of the above method for a beam fitted with the same steel gusset plate joint at each end is given in Appendix K. It shows the derivation of the end fixing moment factor and the secant rotational stiffness coefficient for beam joints at the equilibrium position when subjected to the point load at mid span associated with the maximum moment able to be taken by the joint. Because the joint rotational stiffness curve has no points of contraflexure up to the slip limit, incremental analysis can be used without the need to have to include for a Newton-Raphson algorithm. After investigating the degree of fit obtained by reducing the size of slip increment, an incremental value of $\frac{1}{500}$mm was chosen to give optimum results and has been used in all of the analyses.

The end moment reduction factors for a beam with end joints using steel gusset plates and another with end joints using plywood gusset plates, both using nailing configuration RA and rotated through the maximum joint displacement, are shown in Figure 7.9. The beams have a span of 6000mm; timber density 450Kg/m^3; plywood density 400Kg/m^3; nail strength 827N/mm^2 and the plywood thickness is 17.5mm. In these examples, as soon as the joint rotates the reduction factor is 0.822 for the steel gusset plate joint and 0.935 for the plywood gusset plate joint and as the rotation increases the factors are 0.506 and 0.364 respectively when the maximum nail slip in both joint types is 3.2mm. The reduction factor for the plywood joint is 0.312 at a maximum nail slip of 4.5mm. Also it is seen that the rate of reduction in the factors associated with the plywood gusset plate joints is much greater than with the steel gusset plate joint.

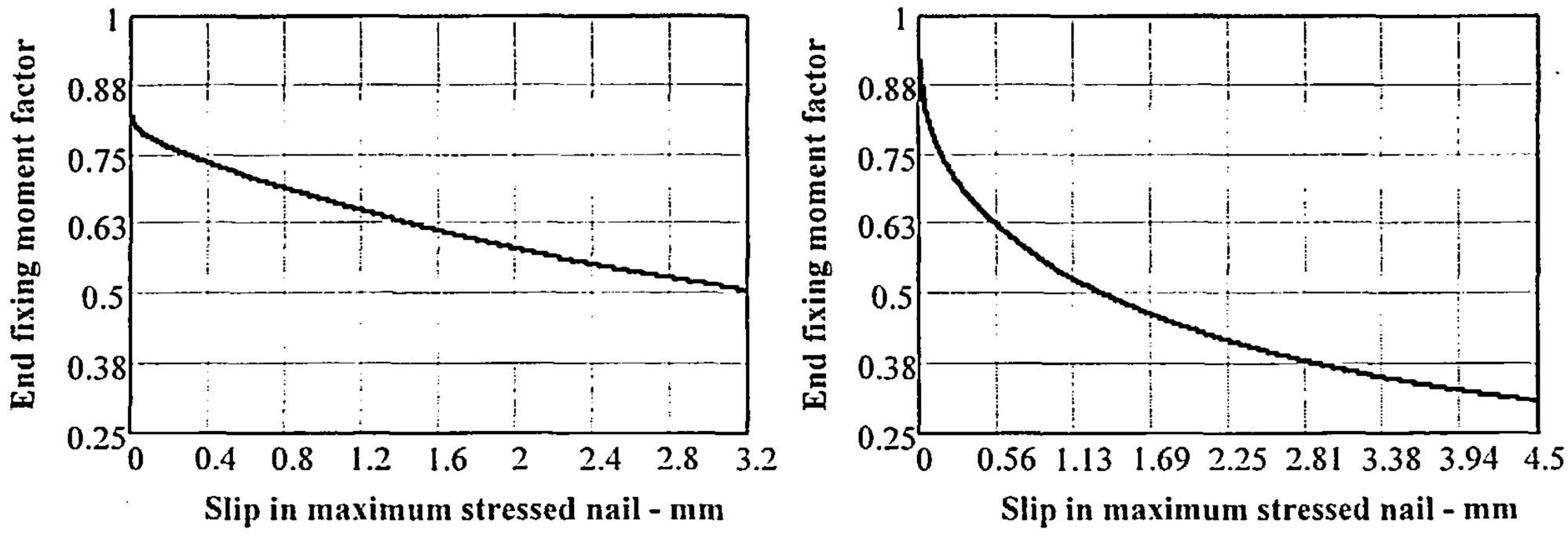

Figure 7.9 End fixing moment factor plotted against joint slip

This behaviour is typical over the joint material property range and confirms that when this type of joint

is being used in timber structures its semi-rigidity must be taken into account in the analysis process.

The graphs give the end fixing moment factors over the full range of joint rotation. To obtain the value of the factor at the equilibrium position of the beam, an analysis of steel and plywood gusset plate joints using nailing configuration RA at each end has been carried out using equations (247) to (249). The beams have spans ranging from 2m to 6m and are subjected to a point load at mid-span. The results of the analyses are shown in Figure 7.10. For both types of joint the end fixing moment factors are relatively large. However it is interesting to note that despite this the joint rotations at equilibrium are relatively small. For the beams with a 6000mm span fitted with steel gusset joints, the rotation will be $1.6\text{x}10^{-2}$ radians and when fitted with plywood gusset joints it will be $1.2\text{x}10^{-2}$ radians, both using 2.66mm diameter nails. These values increase to $1.9\text{x}10^{-2}$ and $1.7\text{x}10^{-2}$ respectively for joints with 3.36mm diameter nails.

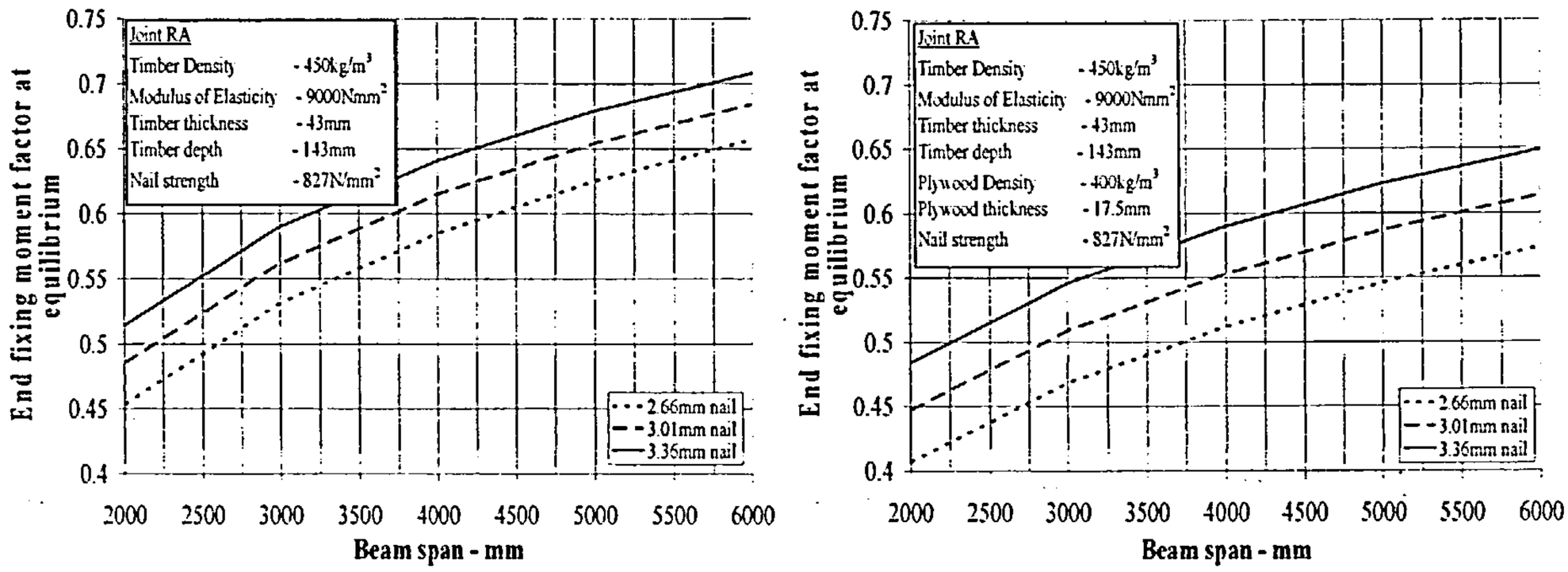

Steel gusset plate joints Plywood gusset plate joints

Figure 7.10 The end fixing moment factor for beams fitted with steel or plywood gusset plate joints and subjected to a point load at mid-span

The associated secant rotational stiffness coefficients for the above beam configurations are shown in Figure 7.11.

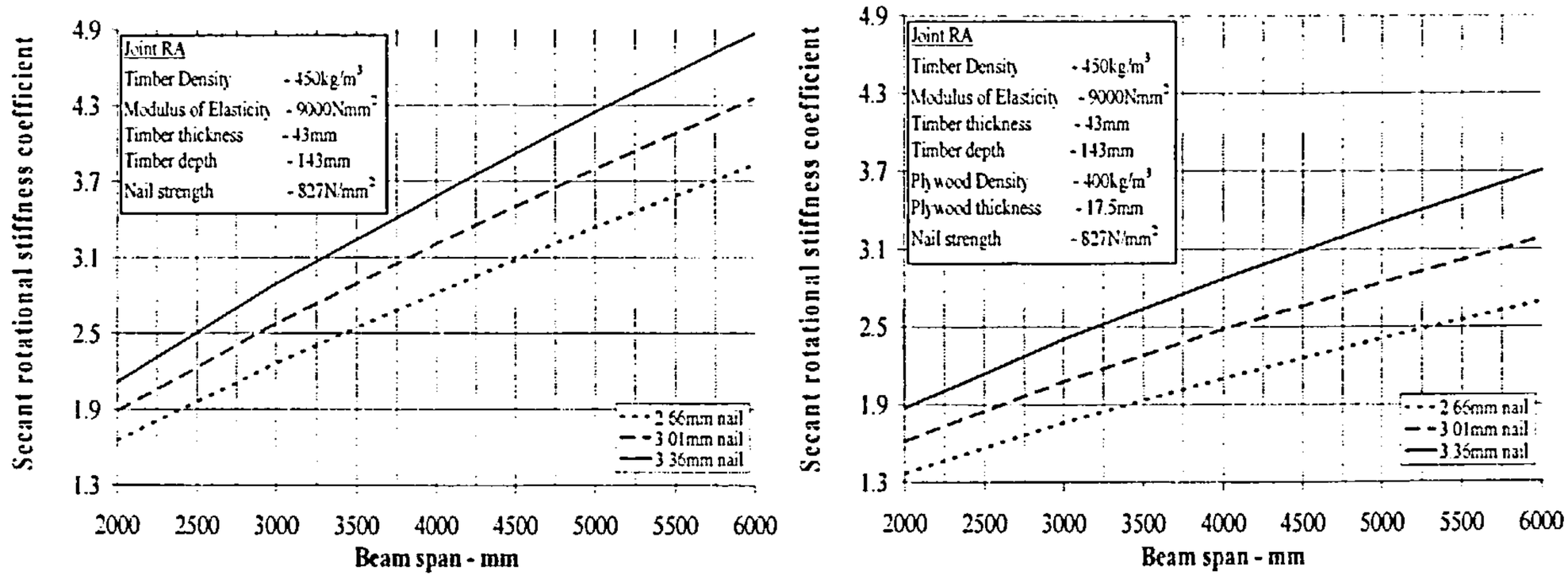

Steel gusset joints Plywood gusset joints

Figure 7.11 Secant rotational stiffness coefficients for the joints used in Figure 7.10.

The limits given for the secant rotational stiffness coefficient in Eurocode 3 [140] for semi-rigid joints are that for members in braced frames the coefficient must be between 0.5 and 8. Below 0.5 the joint will be classed as pinned and above 8 it can be considered to be rigid. From Figure 7.11 it will be seen that the value of the secant rotational stiffness coefficient varies and both types of joint clearly come within the criteria for semi-rigid joints, both being closer to the lower end of the limit. The secant rotational stiffness coefficient is also dependent on the joint nailing configuration being used. Various configurations used in the testing programme have been analysed using plywood gusset plate joints with 2.66mm diameter nails and the results of four different configurations are given in Figure 7.12.

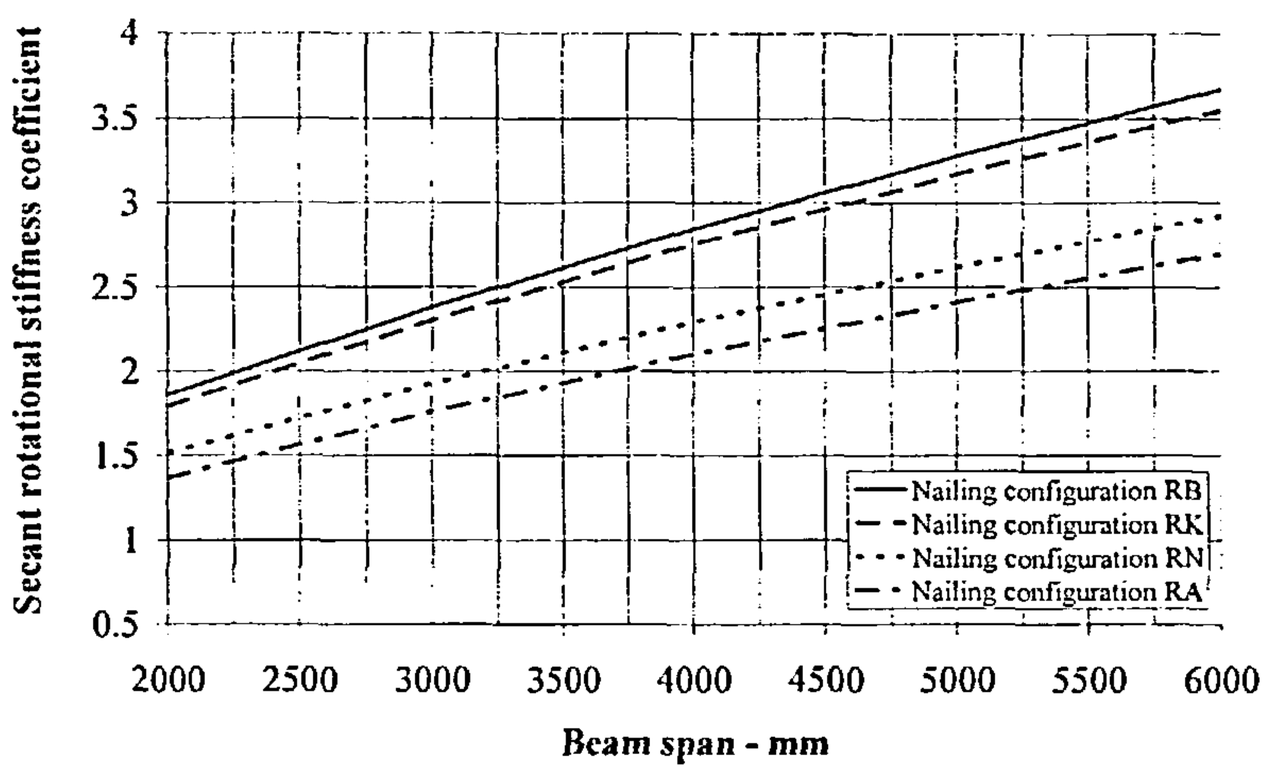

Figure 7.12 Secant rotational stiffness coefficients for various nailing configurations

Although the value of the coefficient varies for the selected joints, the behaviour is typical of what was obtained over the range of joints tested in the programme. The range of coefficients always comes within the semi-rigid category of joint behaviour, confirming the need to analyse structures fitted with such joints on a semi-rigid basis.

7.5.4 Method of Analysis

In the model for moment behaviour, the upper limit of slip has been set at 3.2mm and 4.5mm in the highest stressed nail(s) in the joints using steel gusset plates and plywood gusset plates respectively. An important requirement, however, is that a joint will be able to take load without sudden failure should rotation continue beyond the ULS design limit. With models used for structural steel connections, a common approach is to set a limiting moment plateau at the ultimate moment capacity of the joint. This allows the joint to continue to rotate as a plastic hinge whilst sustaining the ultimate moment [102, 140, 153,]. In the development of the models in Chapter 4 and 5, with the exception of a few cases, the joints tested were able to continue to slip beyond the above limits without failure. The displacement functions showed signs of levelling off, or, more commonly, a tendency to continue to increase the load carrying capacity of the joint. Adopting a plateau condition at the ULS load, or at the characteristic load, will be an acceptable assumption for structures incorporating these types of joint.

It has been shown by Ahmed *et al* [154] that for no-sway steel frames designed with semi-rigid connections under all possible variations of frame geometry and loading to simulate extreme conditions, at the design failure condition the maximum connection rotation was only 1% of its failure limit rotation, coming well inside the SLS design condition. His conclusion was that there was no need to focus at the failure end of a joint as with semi-rigid joints this condition will never be achieved. This has been investigated for the steel gusset and plywood gusset plate joints and for the joints reported in Figure 7.10, at the equilibrium design condition the maximum joint rotation was 35.5% of the rotation at 3.2mm slip limit for joints with steel gusset plates and for joints with plywood gusset plates the maximum rotation was 18.8% of the rotation at 4.5mm slip. These rotations will result in slips exceeding the SLS limit, and the conclusion reached by Ahmed *et al* for steel joints cannot be read across to timber joints using fully overlapping nails.

To determine the load and slip behaviour of structures with prismatic members fitted with joints using steel or plywood gusset plates and fully overlapping nails at the SLS, the analysis can be simplified by assuming the joint to have a linear behaviour based on the joint stiffness at the SLS load. Up to this limit the shape of the load-slip curve reasonably approximates straight line behaviour. On this basis the analysis can be undertaken using a linear elastic analysis programme with adjustment for joint stiffness in line with the method presented by Monforton *et al* [137]. For analyses at the ULS however, although the joint rotation will not reach the value at the ULS slip limit, it will nevertheless significantly exceed the SLS value and a non linear analysis in line with the methods presented by Dhillon *et al* [112] or Kermani [94] *et al*, taking into account the stiffness behaviour of the gusset plates should be used.

7.6 SUMMARY

In this Chapter a design and analysis procedure has been defined for timber joints using steel or plywood gusset plates with fully overlapping nails. Equations for the characteristic, ULS and SLS strengths of the respective joint types are defined for direct shear and moment conditions, together with associated stiffness criteria.

The design rules comply with the requirements of EC5 [15] and where deviations are necessary, they have been detailed. To ensure the procedure has been enveloped by the results of the testing programme in Chapter 3, the application of the rules has been restricted to the extreme values of the variables used in the programme. Limitations on the application of the rules and the criteria that can be used have been given.

The semi-rigid moment-rotation behaviour of the joints has been investigated and to eliminate the need for a complex numerical analysis approach, the Non-Linear 1 moment model developed in Chapter 5 has been used. The reduction in accuracy associated with this model rather than the more accurate Non-Linear 2 model is approximately 1% and this more than compensated for by the saving in complexity of the analysis method otherwise required. Equations have been developed for the rigidity factor; the end

fixing moment reduction factor and the secant rotation stiffness coefficient of the joints. These are factors which describe the semi-rigid behaviour of the joints; give the strength reduction from the fully fixed end moment situation and enable the joint to be categorised.

From the semi-rigid analyses it has been shown that the behaviour of timber joints using steel or plywood gusset plates comes within the semi-rigid limits set by Eurocode 3. It has also been shown that there is a significant reduction in fixing moment when using these joints and the analysis of indeterminate structures will require the effect of the change in joint stiffness as joint rotation takes place to be included for. For structures at the SLS, the modified elastic method of analysis as proposed by Monforton *et al* [137] will be acceptable. For structures analysed at states beyond the SLS and up to the ULS, a non-linear method of analysis, as proposed Dhillon *et al* III [139] or Kermani [94] *et al*, taking into account the stiffness behaviour of the gusset plates should be used.

8 CONCLUSIONS AND RECOMMENDATIONS FOR FUTURE WORK

8.1 CONCLUSIONS

The investigation reported in this thesis has addressed the behaviour of steel and plywood gusset plate joints connected by fully overlapping nails when subjected to short duration lateral or moment loading. The research has been undertaken in a considered, controlled and structured manner and has included for the effect of material properties as well as those other variables that influence the strength and stiffness behaviour of such joints.

The core objectives of the research as listed in section 1.2 have been achieved and the findings from the investigations are briefly summarised as follows:

1) General

The lateral spacing between adjacent rows of nails along the direction of the grain of the timber in joints using fully overlapping nails is twice the lateral spacing required when using staggered or partially overlapping nails. At right angles to the grain direction the code spacing rules are not affected.

2) Lateral Loading of Nailed Joints.

a) It has been shown from an analysis of joint behaviour using steel gusset plates and using plywood gusset plates that joint strength is a linear function of the density of the timber used in the joint.

b) Joint strength has also been found to be a linear function of the number of rows of nails in the joint. Tests were carried out with up to seven rows of nails and in all instances the joint behaviour was shown to be a linear multiple of the single row behaviour.

c) The spacing of the rows of the nails in the joint influences joint strength. Joint strength has been shown to be a linear function of the row spacing divided by the nail diameter, with different functions applying for joints with steel gusset plates and with plywood gusset plates.

d) The effect of changes in moisture content can be incorporated into the joint strength equation by the inclusion of a linear function relationship. The relationship, developed from tests using steel gusset plate joints, gives a strength decrease of 2.66% per 1% increase in moisture content, comparable with 3% recommended in EN 384:1995 [80] and less than 5% recommended in STEP 1 [79].

e) It was found that the nail diameter function was a power function but the power factor was different

for joints with steel gusset plates and joints with plywood gusset plates. The influence of gusset plate material on the nail diameter factor has not been identified as a factor by other researchers.

f) It was found that a generalised four parameter non-linear exponential function best fitted the test results, in line with the findings of other researchers. The functions are different for joints with steel gusset plates and joints with plywood gusset plates. The plywood gusset plate function has a steeper initial stiffness than the steel gusset plate function but the rate of decrease in stiffness with slip in the steel gusset plate function is much slower. The lower initial stiffness behaviour in the steel gusset plate joint was due to the take up of slack between the nail and the bearing face of the predrilled hole in the gusset plate and will be a feature of such joints.

g) The nail strength function has been found to be a linear factor of the tensile strength of the nail for both types of joint.

h) As expected, joints with a gap between the gusset plate and the timber are less strong that those without a gap. In the strength models for joints with and without a gap, it was found that the individual property functions remain unaltered except for the displacement functions and for the addition of a friction factor in the model for joints assembled without a gap.

i) The strength of both types of joint is a linear multiple of the number of lines of nails in the joint.

j) With the empirical method of analysis, most researchers have developed their joint strength equations on the basis that joint failure occurs at a pre-fixed slip. This was not found to be the case. Joint displacement is a combination of the displacement of the nail in the gusset plate and in the timber and as the stiffness of the gusset plate changes so will the joint displacement at the failure condition. From the research the failure limit for joints with steel gusset plate joints has been found to be 3.2mm whereas the failure limit for joints using the less stiff plywood gusset plates has been shown to be at least 4.5mm.

k) Because of the different slip behaviour between joints using gusset plates of different stiffness, and the different values of the variable functions associated with such joints, it is not practical to develop a single relationship for the strength of joints that use variable types of gusset plate. In this research separate expressions have been developed for each type of joint.

l) Using the approach developed by Mack [6], load-displacement relationships that have been shown to compare well with the results from tests have been developed for nailed joints with steel gusset plates with and without a gap between the gusset plate and the timber. Also for steel gusset plate joints using varying sizes of predrilling. Accurate load-displacement relationships have also been developed for nailed joints with plywood gusset plates with and without a gap between the timber and the plywood.

3) Moment Behaviour of Nailed Joints

a) It has been found from the measurement of joint rotation behaviour that the position of the centre of rotation of a multi-nailed joints is not fixed when a joint is subjected to the action of an increasing moment caused by a shear force. The movement was, however, not found to be excessive and ignoring the effect will result in a loss of accuracy of less than 2%.

b) If linear methods of analysis based on the classical torsion formula are used, the model will significantly underestimate the joint strength, giving a safe but uneconomic solution The moment-rotation behaviour of a nailed joint can be accurately modelled from the lateral load-slip relationship by assuming a non-linear displacement approach based on the method used by Perkins *et al* [179]. The most accurate model is obtained by also including for the second order effect of the nail movements in the joint however this only increases the accuracy by less than 1%. The preferred model, Non-Linear 2, ignores this effect but incorporates the effect of movement of the centre of rotation.

c) Moment-displacement models for joints with steel gusset plates and with plywood gusset plates have been developed on the above basis and give good comparisons with test results. The models are limited to situations where there is no bending in the timber over the length of the joint and where the nail splitting force in the timber is within the limit set by EC5 [15].

d) Joint behaviour is affected by the direction of the plane of the timber grain across the thickness of the timber. The effect increases as the angle of the plane of the T and L axes increases relative to the direction of the nail force. A grain factor has been developed and incorporated into the moment-displacement equations to include for this effect. The equations gave a good comparison with the results from tests.

e) The effect of variation in nail line spacing at right angles to the grain has not been found to be a factor in the moment models. The effect of row spacing along the grain direction is a factor.

f) From tests using double joints sharing the same gusset plates, it has been shown that the moment-displacement model will accurately predicts the joint behaviour of multiple joints.

4) Comparison with EC5.

a) In EC5 the nail spacing criteria has been developed for joints using staggered nails or for nails with a limited overlap and it cannot be applied directly to joints using fully overlapping nails. To have a basis for comparison the spacing rules given in the code for loading along the direction of the grain must be increased by a factor of 2.

b) Even when increased by a factor of 2, the spacing and distance rules given in EC5 still result in instances of failure by splitting rather than in the expected ductile mode in joints subjected to lateral load. Particularly when using joints with steel gusset plates. The code rules require to be reviewed.

c) Taking account of the spacing change, the failure modes for steel gusset plate joints were in general found to be as predicted by the code. For the plywood gusset plate joints there were variations between the test results and the code predictions for mode 2 and 3 failures but they were not considered to be significant.

d) When using the procedure given in BS EN383:1993 for embedment tests the results were very poor compared with those derived from the embedment equations given in EC5. It was found to be unrealistic to obtain a valid result using the full thickness of the plywood in the test and the samples should be reduced to align with the slenderness ratio used for timber samples. The slenderness ratio applied to timber samples also needs to be reviewed to include for the effect of density. As the density increases the slenderness ratio should be reduced. The tests procedure also requires to be reviewed to give better guidance on the preparation requirements to reduce the risk of premature splitting during the assembly stage of the test sample.

e) EC5 [11] does not include for any reduction in joint strength when using nail spacing less than 2 times the minimum nail spacing given in the code. This rule is unsafe and will be superseded by the proposals in EC5 [15].

f) The joint strength functions in the model differ from the equivalent relationships in the EC5 [11] and EC5 [15] strength equations and the aggregate effect leads to variable results between the model and the EC5 equations.

g) In EC5 [15], for joints having a nail row spacing equal to or greater than *14d* the joint strength is a multiple of the number of rows of nails in the joint. Similarly, with the models for steel or plywood joints using fully overlapping nails with a nail row spacing $\geqslant$ *19.6d* and *17d* respectively, the joint strength is a multiple of the number of rows of nails in the joint.

h) In EC5 [15], for joints with a nail row spacing less than *14d* the joint strength will be reduced. In the models for steel or plywood joints using fully overlapping nails, the joint strength is reduced in joints having a nail row spacing less than *19.6d* and *17d* respectively.

i) In EC5 [15], for joints with a nail row spacing less than *14d*, the joint strength will be reduced by a factor which is a power function of the number of rows of nails in the joint. With the models for steel or plywood joints using fully overlapping nails, for all nail row spacings the joint strength is a linear function of the number of rows of nails in the joint.

j) In EC5 [15] the strength reduction factor is a power function of the number of rows of nails in the joint. For each ratio of nail row spacing to nail diameter, the strength reduction factor will increase as the number of rows of nails in the joint increases. With the models for steel or plywood joints using fully overlapping nails, the respective strength reduction factors are linear functions of the nail row spacing divided by the nail diameter. For each ratio of nail row spacing to nail diameter, the strength reduction factor will be a constant and will not be influenced by the number of rows of nails in the joint.

k) When compared to the findings from the testing programme, the proposed changes to EC5 for the effect of nail row spacing less than 2 times the minimum spacing will greatly overestimate the reduction in strength of the joint.

l) For joints with a nail row spacing greater than 2 times the minimum value, the strength and stiffness behaviour using fully overlapping nails does not compare well with the behaviour obtained by the application of the EC5 [11] or EC [5] strength and stiffness equations. Because the material relationships in the model and Eurocode strength equations differ significantly, the EC5 rules cannot be safely applied to predict the strength or stiffness behaviour of joints formed with fully overlapping nails.

5) Semi-Rigid Behaviour

a) It is acceptable to use a method of analysis that is based on a fixed centre of rotation to analyse the semi-rigid behaviour of the joint.

b) Joints using steel gusset plates and plywood gusset plates with fully overlapping nails will come within the limits set in Eurocode 3 for semi-rigid behaviour.

c) The semi-rigid behaviour of this type of joint is significant and must be included for in the analysis procedure in structures fitted with such joints to be able to accurately predict strength and stiffness.

d) With structures designed for a serviceability limit state condition, it has been shown to be acceptable to use a modified elastic method of analysis as prepared by Monforton *et al* [137] or equivalent.

e) For structures loaded beyond the SLS condition, a non-linear method of analysis as proposed by Dhillon *et al* [139] or Kermani [94] should be used.

8.2 RECOMMENDATIONS FOR FUTURE WORK

Although the investigation has met the requirements of the core objectives of the research programme

outlined in section 1.2 and made a contribution to the solution of the mentioned problems, the effects of several factors have still to be investigated to obtain an optimum solution for the design and analysis of joints using fully overlapping nails.

The objective of this section is to briefly outline the areas of research that are considered to be relevant and should be addressed.

1. To further enhance the capability of the load-displacement relationships by developing the models to including for the effect of varying the amount of nail penetration in the timber; extending the range of nail diameter up to 6mm; refining the effect of nail strength and including for joints with timber-timber connections.

2. To fully investigate the ductility of this type of joint in direct shear and when subjected to a moment. The investigation should be extended to include for reverse loading and then followed by cyclic loading.

3. To further investigate the behaviour of joints when subjected to moment and extend the moment-rotation model to be able to determine joint capacity where there is bending in the timber over the length of the joint.

4. To carry out full scale testing on timber structures assembled with joints using fully overlapping nails and compare the behaviour with the results from the models. This should include sway-type structures to investigate the extent of joint rotations obtained and to review the method of analysis required.

5. To develop a finite element model and compare with the results using the empirical method.

REFERENCES:

1. Dinwoodie, J. M., 2000, "Timber: Its nature and behaviour", Second Edition, pp. 1-3.
2. Latham, M., 1998, "Rethinking Construction", Department of the Environment, Transport and the Regions.
3. Statutory Instrument, 1998, "The Landfill Tax Regulations", Statutory Instrument 1527, H.M.S.O.
4. Lovelace, N, 2002, "Seeing Wood for the Trees", New Civil Engineer, July 2002, pp 20-21.
5. Milner, M.W., Edwards, S., Turnbull, D.B. and Enjily, V., 1998, "Verification of the robustness of a six-storey timber-frame building 2", The Structural Engineer, Volume 76/No 16, pp.307-312.
6. Mack, J.J., 1966, "The Strength and Stiffness of Nailed Joints under Short-duration loading", Division of Forest Products Technological Paper No. 40, Commonwealth Scientific and Industrial Research Organisation, Australia, pp. 3-28.
7. McLain, T.E., 1976, "Curvilinear Load- Slip Relations in Laterally-Loaded Nail Joints", Forest Products Research Society, Madison, Wisconsin. Proc. No P-76-16; pp 33-51.
8. Foschi, R. O., July 1974 "Load Slip Characteristics of Nails" Wood Science Journal, Vol. 7, No. 1.
9. Morris, E.N., Feb 1970 "An Analysis of the Load-Slip Curve for a Nailed Joint and the effect of Moisture Content", Journal of Institute of Wood Science, Vol. 5, No 1, Issue 25, pp.3-9.
10. BSI 5268, 1996, "Structural use of timber Part 2. Code of practice for permissible stress design, materials and workmanship"
11. BSI, DD ENV 1994-1-1 : EC5 "Design of timber structures – Part 1-1 General Rules and rules for buildings (together with United Kingdom National Application Document".
12. Goh, H. C-C., April 1997, "Semi-Rigid and Rheological Behaviour of Mechanical Joints in Timber Structures", PhD Thesis, Department of Civil and Transportation Engineering, Napier University.
13. BSI, EC5 "Design of timber structures – Part 1-1 General Rules , General Rules and rules for buildings" Second Draft CEN/TC 250/SC5 N316 prEN 1995-1-1
14. BSI, EC5 "Design of timber structures – Part 1-1 General Rules , General Rules and rules for buildings" CEN/TC 250/SC5 N158 prEN 1995-1-1 Final Draft (Stage 34).
15. BSI, EC5 "Design of timber structures – Part 1-1 General Rules , General Rules and rules for buildings" Final Draft Version 2002-02-28.
16. Ehlbeck, J. Sept 1979, "Nailed Joints in Wood Structures", Virginia Polytechnic Institute and State University Wood Research and Wood Construction Laboratory, pp. 1-145.
17. Aune, P., and Patton-Mallory, M., 1986, "Lateral Load Bearing Capacity of Nailed Joints Based on the Yield Theory – Experimental Verification", United States Department of Agriculture, Forest Service, Forest Products Laboratory, Research Paper FPL 470.

18. Brock, C. R. 1957 "The Strength of Nailed Joints" Bulletin No 41, Forest Products Research Department of Scientific and Industrial Research, London, England.
19. Wilkinson, T. L. 1972 "Analysis of Nailed Joints with dissimilar members" J. Struct. Div., ASCE, 98(9), pp. 2005-2013.
20. Bullen, F. and Stringer, G. "Mechanistic Design of Nailed Timber Joints with Australian Timbers" Pacific Timber Engineering Conference, 1994, Gold Coast, Australia, pp. 49-57.
21. BS, EN314 – 2, 1993, "Plywood – Bonding Quality – Part 2; Requirements".
22. BS, EN315, 1993, "Plywood – Tolerances for Dimensions".
23. BS, 1202, 1974, "Part 1 Specification for Nails".
24. BS EN, 10 025 1993, "Hot Rolled Products of Non-Alloy Structural Steels".
25. Hunt, R. D. H. and Bryant, A. H., Jan 1990 "Laterally Loaded Nail Joints in Wood", Journal of Structural Engineering, ASCE, Vol. 116, No. 1, pp. 111-124.
26. BS EN, 1380, 1999 "Timber structures – Tests Methods – Load bearing nailed joints".
27. BS EN, 26891: 1991 "Timber structures – Joints made with mechanical fasteners – General principles for the determination of strength and deformation characteristics".
28. BS EN, 322: 1993 "Wood-based panels – Determination of moisture content".
29. ISO 3131:1975, Wood – Determination of density for physical and mechanical tests".
30. BS EN, 323:1993 "Wood – based panels – Determination of density".
31. BSI, 373, 1957, "Testing Small Clear Specimens of Timber".
32. BSI, 4512, 1969, "Methods of Test for Clear Plywood".
33. BSI, 5820, 1979, "Methods of Test for Determination of Certain Physical and Mechanical Properties if Timber in Structural Sizes".
34. BSI, 18, 1987, "Tensile Testing of Metals".
35. BSI, 6948, 1989, "Methods for Mechanically Fastened Joints in Timber and Wood based Material".
36. BS EN, 28970, 1991, "Timber structures – Testing of joints made with mechanical fasteners – Requirements for wood density".
37. BS EN, 383, 1993, "Timber structures – Test methods – Determination of embedding strength and foundation values for dowel fasteners".
38. BS EN, 409, 1993, "Timber structures – Test methods – Determination of yield moment of dowel type fasteners – Nails".
39. BS EN, 408, 1995, "Timber structures – Structural timber and glued laminated timber – Determination of some physical and mechanical properties".
40. Rodd, P.D., Anderson, C., Whale, L.R.J. and Smith, I., 1987, "Characteristic Properties of Nailed and Bolted Joints under Short-Term Lateral Load – Part 2 – Embedment Test Apparatus for Wood and Wood-Based Sheet Material", Journal of the Institute of Wood Science Vol. 11 Part 2 – pp. 208-212.
41. Whale, L.R.J., Smith, J. and Hilson, B.O., 1988, "Characteristic Properties of Nailed and Bolted Joints under Short Term Lateral Loading – Part 4 – The Influence of Testing Mode

and Fastener Diameter upon Embedment Testing Data", Journal of the Institute of Wood Science, Vol.11 Part 5 pp. 156-161.

42. Draper, R. and Smith, H., 1998, "Applied Regression Analysis" Third Edition, Wiley Interscience.
43. Johansen, K.W., 1949, "Theory of Timber Connections", International Association of Bridge and Structural Engineering, Publication N9, Berne, pp. 249-262.
44. Aune, P. 1966, "The load carrying capacity of nailed joints. Calculations and experiments", The Norwegian Institute of Technology, Trondheim, Norway.
45. Larsen, H.J. 1977, "K.W. Johansen's Nail Tests", Institute of Building and Structural Engineering, Alborg University Centre, Denmark, pp. 1-22.
46. Hilson, B.O., Whale, L.R.J. and Smith, I., 1990, "Characteristic properties of nailed and bolted joint under short-term lateral load. Part 5 – Appraisal of current design data in BS5268:Part 2:1984 Structural Use of Timber." Journal of the Institute of Wood Science. Vol. 11(6), pp. 208-212.
47. Jorrison, A,. 1996, "Multiple Fastener Timber Connections with Dowel Type Fasteners", International Wood Engineering Conference, 1996, Publication 4, pp189-196.
48. Deam, L., King, A.B. and Button, C.R., 1996, "Timber Fastener Capacities-A Limit State Approach", International Wood Engineering Conference, 1996, Publication 4, pp. 205-211.
49. System 5000, Vishay Measurements Group, USA.
50. Microsoft Excel 2002.
51. Mathsoft Mathcad 2001i., Mathsoft Inc. USA.
52. Mathsoft Axum 6, Mathsoft Inc, USA.
53. Hilson, B., and Whale, L.R.J., 1990, "Developments in the design of timber joints", The Structural Engineer, Volume 68, No.8, pp.148-150.
54. Smith, I., Whale, L.R.J., Anderson, C., Hilson, B. and Rodd, P.D., 1988 "Design Properties of Laterally Loaded Nailed or Bolted Joints", Canadian Journal of Civil Engineering, 15, pp. 633-643.
55. NZS 3603:1993 "Timber Structures Standard" Standards New Zealand.
56. ASCE. 1996 "Standard for load and resistance factor design for engineering wood construction." ASCE 2(3) 16-95.
57. Moehler, K., and Maier, G. 1969, "Der Reibbeiwert bei Fichtenholz im Hinblick auf die Wirksamket reibschluessiger Holzverbindungen." Holz als Roh-u Werkstoff 27(8):303-307.
58. BSI, 8110, 1997, "Strutural Use of Concrete. Code of practice for design and construction".
59. BSI, 5980, 2000, "Structural use of steelwork in building. Part 1:Code of practice for design. – Rolled and Welded Sections".
60. BSI, 8002, 1994, "Code of practice for earth retaining structures".
61. Kermani, A., 1999, "Structural Timber Design", Blackwell Science Limited.
62. Bertero, R.D. and Bertero, V.V., 1999, "Redundancy in Earthquake-Resistant Design", Journal of Structural Engineering Vol. 125(1), pp. 81-88.

63. C.S.A., 1994, "Engineering design in wood (limit states design)." CSA Standard No 086.1-94, Canadian Standards Association, Toronto.
64. Standards Australia. 1997, "AS 1720.1-1997. Timber Structures, Part 1: Design methods." Standards Australia, Sidney, Australia.
65. Chui, Y.H. and Smith, I., 1993, "Capacity design of wood structures", Canadian Society for Civil Engineers Annual Conference, June 8-11, 1993, pp. 365-374.
66. Smith, I., Craft, S.T. and Quenneville, P., 2001 "Design capacities of joints with laterally loaded nail", Canadian Journal of Civil Engineering, Vol. 28, pp. 282-290.
67. Bullen, F. and Stringer, G., 1994, "Mechanistic design of nailed timber joints with Australian timbers", Pacific Timber Engineering conference, 1994, pp. 49-57.
68. Ehlbeck, J. and Larsen, H.J., 1993, "EC5 – Design of timber structures: Joints." Proceedings of International Workshop on Wood Connectors, No. 7361, Forest Products Society, Madison, Wisconsin, pp. 9-23.
69. Ivanov, I.M. 1949, "The new measure of the strength of wood and methods of its determination. Bulletin of the Forest Institute of Academy of Sciences of USSR, Vol.4. pp. 34-45.
70. SaRibiero, R.A. and SaRibiero, M.G., 1991, "Load-slip behaviour of nailed joints: an improved model." Proceedings of the International Timber Engineering Conference, London, Vol. 3, pp. 3-10.
71. Mack, J.J., 1977, "The Load Displacement Curve for Nailed Joints", Journal of the Institute of Wood Science", Vol.7(6), pp. 34-36.
72. BSI, 1984, "BS 5268 Part 2: Structural Use of Timber – Part 2 – Code of Practice for Permissible stress design, materials and workmanship".
73. Smith, I. and Whale, L.R.J., 1987, "Characteristic Properties of Nailed and Bolted Joints under Short-Term Lateral Load – Part1-Research Philosophy and Tests Programme", Journal of the Institute of Wood Science, 11: (2), pp. 53-59.
74. Smith, I., 1982, "Interpretation and adjustment of results from short-term lateral load tests on whitewood joint specimens with nails or bolts." Research Report, Timber Research and Development Association. No 5/82.
75. Kermani, A. and Goh, C-C. G., 1998, "Load-Slip Characteristics of Multi-Nailed Joints," Procedings of the Institution of Civil Engineers, Structures and Buildings, Vol134, Issue 1February 1999, pp. 31-43.
76. Chapra, S.C. and Canale, R.P., 1998, "Numerical Methods for Engineers with programming and software applications, Third Edition." W.C.B. McGraw-Hill.
77. Morris, E.N. 1973, "The application of the slip modulus in the design of nailed joints." Journal of the Institute of Wood Science, Vol. 6(2), pp17-21.
78. Bodig, J. and Jayne, B.A., 1993, "Mechanics of Wood and Wood Composites", Krieger Publishing Company, Malabar, Florida,, 1993 edition.
79. Structural Timber Education Programme (STEP) 1, 1995, "Timber Engineering STEP 1" Centrum Hout, Postbus 1350, 1300 BJ Almere, pp. A4/16.

80. E.N. 384: 1995, "Structural Timber – Determination of characteristic values of mechanical properties and density."
81. Wilkinson, T.L. 1971, "Theoretical Lateral Resistance of Nailed Joints." American Society of Civil Engineers, Journal of the Structural Division 97, pp. 2005-2013.
82. Keunzi, E.W. 1955, "Theoretical Design of a Nailed or Bolted Joint Under Lateral Load." U.S.D.A Forest Products Laboratory Report No D 1951. Madison, Wisconsin.
83. Morris, E.N. and Gajjar, S., 1981 "Load-Displacement relationship for nailed joints with solid timber and plywood members", Journal of the Institute of Wood Science, Vol. 9, Issue 2, pp. 62-64.
84. Boult, B.F., 1988, "Multi-Nailed Moment Resisting Joints", Timber Engineering Research Report, Auckland University.
85. Lantos, G, 1967, "Load Distribution in Multiple Mechanical Fasteners in joints subjected to direct load." Timber Research and Development Association, Research Report No E-RR-28.
86. American Forest & Paper Association, 1987, "National Design Specification (NDS) for Wood Construction." A.F&P.A., Washington, D.C.
87. Canadian Standards Association, 1984, "Engineered Design in Wood (working stress version), CAN3-086.1-M84". C.S.A., Rexdale, Ontario.
88. Standards Association of Australia, 1974, "Determination of working loads for metal fasteners in timber." AS 1649-1974.
89. Moss, P, 1994, "Row Modification Factors for Multiple-Bolted Timber Joints", Pacific Timber Engineering Conference 1994, Gold Coast Australia, 00360-369.
90. Wilkinson, T.L., 1986, "Load Distribution among bolts parallel to load", Journal of Structural Engineering, ASCE, Vol. 112, no 7, pp. 835-852.
91. Structural Timber Education Programme (STEP) 2, 1995, "Timber Engineering STEP 1" Centrum Hout, Postbus 1350, 1300 BJ Almere. pp. D8/1-7.
92. Kermani,A. and Lee, B.S., 1991, "Performance of Nailed Joints in Rigid Timber Portals", Journal of Forest Engineering, Vol.3, No1, pp. 13-28.
93. Kermani, A., 1992, "Timber Portal Frames with Moment Resisting Nailed Joints", Journal of the Institute of Wood Science, Vol.12, Issue 72, pp. 325-334.
94. Kermani, A., 1995, "A Study of Semi-Rigid and Non-Linear Behaviour of Nailed Joints in Timber Portal Frames", Journal of Forest Engineering, pp.17-33.
95. Morris, E.N., 1966, "The Rotational Rigidity of Nailed Joints in Double Shear and Subject to Short Term Loading", TRADA Research Report: E/RR/25.
96. Morris, E.N., 1968, "The Rotational Rigidity of Nailed Joints with Plywood Gussets Subject to Short Term Loading", TRADA Research Report: E/RR/32.
97. Larsen, H.J., 1998, "Influence of Semi-Rigidity of Joints in the Structure", COST C1 Conference, Liege, 17-19 September 1998, pp. 265-273.
98. Rodd, P.D. and Pope, D.J., 1999, "The Stiffness of Moment Transmitting Joints in Reinforced Glulam", PTEC 14-18 March 1999, Volume 3, pp. 280-285.

99. Engstrom, D., 1999, "Design and Buildability of Connections for Timber-Framed Structures", PTEC 14-18 March 1999, pp. 259-266.
100. Lui, E.M. and Chen, W.F., 1987, "Steel Frame Analysis with Flexible Joints", Journal of Constructional Steel Research, Vol. 8, pp. 161-202.
101. Kishi, N. and Chen, W.F. 1999, "Moment-Rotation Relations of Semi-Rigid Connections with Angle", Journal of Structural Engineering, American Society of Civil Engineers, pp. 1813-1834.
102. Anderson, D. and Kavianpour, K., 1991, "Analysis of steel frames with semi-rigid connections", Structural Engineering Review, Chapman and Hall, Vol3, pp. 79-87.
103. Nozynski, W., June 1980, "Investigation of the effect of number of nails in a joint on its loading capacity", C.I.B-W18, Helsinki.
104. Whale, L.R.J., Smith, I. and Larsen, H.J., 1987 "Design of nailed and bolted joints. Proposals for the revision of existing formulae in draft EC5 and the CIB Code", WC W18A-Timber Structures, Meeting No 20, September 1987, Dublin.
105. Whale, L.R.J. and Smith, I., 1986, "Mechanical Joints in Structural Timber – Information for Probabilistic Design", T.R.A.D.A., Research Report 17/86.
106. Smith, I. and Whale, L.R.J., June1985, "The influence of the orientation of mechanical joints on their mechanical properties", C.I.B. Meeting – W18, Haifa, Israel.
107. Nowak, P.S. and Hartmann, T.W., Feb. 1993, "Eccentric Connection Design: Geometric Approach", Journal of Structural Engineering, A.S.C.E., Vol. 119, No.2, pp. 606-618.
108. McLain, T.E., Soltis, L.A., Pollock Jr, D.E. and Wilkinson, D.G., Oct. 1993, "LRFD for Engineered Wood Structures – Connection Behaviour Equations", Journal of Structural Engineering, ASCE, Vol. 119, No 10, pp. 3024-3038.
109. Guarracino, F. and Walker, A. 1999, "Energy Methods in Structural Mechanics", published by Thomas Telford, pp. 354.
110. Chen, W.F. and Lui, E.M. 1991, "Stability Design of Steel Frames", C.R.C Press, pp.145.
111. Makode, P.F., Corotis, R.B. and Ramirez, M.R., 1999, "Geometric Nonlinear Analysis of Frame Structures by Pseudodistortions", Journal of Structural Engineering, A.S.C.E., November 1999, pp.1318-1327.
112. Dhillon, B.S. and O'Malley, J.W., May 1999, "Interactive Design of Semirigid Steel Frames", Journal of Structural Engineering, A.S.C.E., Vol. 125, pp.556-564.
113. Kim, S-E. and Chen, W-F., 1996, "Practical Advanced Analysis for Semi-rigid Frame Design", Engineering Journal, Fourth Quarter, 1996, pp. 129-141.
114. Hankinson, R.L., 1921, "Investigation of the crushing of spruce at varying angles of grain", Air Service Information Circular 3(259), Material Section Paper No. 130.
115. BS EN 338:1995 "Structural Timber. Strength Classes".
116. Rathbone, A.J., 2002, "Second-order effects-who needs them", The Structural Engineer, 5 November 2002, Vol., 80, No 21.
117. Goh, H.C.C and Kermani, A., 1994, "Finite Element Analysis of Timber Joints made with Welded Steel Gussets and Dowels", proceedings of the Second International Conference on

Computational structural Technology, Civil-Comp Press, Advances in Structural Engineering Computing, Athens, Greece, pp. 85-95.

118. Valentin, G., Bostrom, L., Gustafsson, P.J., Ranta-Maunus, A. and Gowda, S., 1991, "Application of fracture mechanics to timber structures", RILEM state-of-art Report. Technical Research Centre of Finland, Espoo Finland, Research Notes 1262. ISBN 951.38.3891.1.
119. Daudeville, L., Davenne, L. and Yasumura, M., 1996 "Experimental and Numerical Analysis of Failure in Bolted Joint", Proceedings of the International Wood Engineering Conference 1996, New Orleans, Louisiana, U.S.A., pp. 1-1523-1-171.
120. Yasumara, M., 2002 "Design Criteria for Bolted Timber Joints Subjected to Force Perpendicular to the Grain", The 7th World Conference on Timber Engineering, WTCE 2002, August 12-15, 2002., Volume 3, pp. 137-144.
121. Leijten, A.J.M., 2002, "Perpendicular to grain failure of beams caused by concentrated load of joints", The 7th World Conference on Timber Engineering, WTCE 2002, August 12-15, 2002, Volume 3, pp145-152.
122. Larsen, H.J. and Gustaffson, P.J., 2001, "Dowel joints loaded perpendicular to grain." Proceeding s of CIB/W18, paper 34-7-3, August 2001.
123. Bouchair, A., Boucquet, J.F., Racher, P. and Peuchot, B., 1996 "Behaviour of moment resisting connections", Proceedings of the International Wood Engineering Conference, New Orleans, Louisiana, U.S.A, 1996. pp. 2-153 to 2-160.
124. CIB Working Commission W 18., 1983, "Structural Timber Design Code." Publication 66.
125. Davies, J.M. and Brown, B.A., 1996, "Plastic Design to BS 5950", The Steel Construction Institute, Blackwell Science, pp. 16.
126. Smith, I. and Whale,L.R.J., 1985, "Mechanical properties of nails and their influence on mechanical properties of nailed timber joints subjected to lateral load. Part 1. Background and tests on nails of UK origin." TRADA Research Report 4/85 1985, High Wycombe, Bucks., pp. 1-34.
127. Whale, L.R.J., Smith, I. and Larsen, H.J., 1987 "Design of nailed and bolted joints. Proposals for the revision of existing formulae in draft EC5 and the CIB code." International Council for Building Research Studies and Documentation, Working Commission W18A – Timber Structures, 1987, pp. 1-35.
128. Larsen, H.J., 1991, "Safety Format of EC5" Reliability Based Design of Engineered Wood Structures, Jozsef Bodig, Proceedings of the NATO Advanced Research Workshop on Reliability-Based Design of Engineered Wood Structures, Florence, Italy, pp.125-128.
129. Ellingwood, B., Kovacs, Z. and Zahn, J., 1991 "Fundamentals of Reliability Assessment", Reliability Based Design of Engineered Wood Structures, Jozsef Bodig, Proceedings of the NATO Advanced Research Workshop on Reliability-Based Design of Engineered Wood Structures, Florence, Italy, pp.147-157.
130. Bury, K., 199, "Statistical Distributions in Engineering", Cambridge University Press, pp. 115.

131. Rammer, D., R., Winistorfer, S.G., and Bender, D.A., 2001, "Withdrawal strength of threaded nails", Journal of Structural Engineering, ASCE, April 2001, pp. 442-449.
132. Bryant, A.H. and Hunt, R.D., 1999, "Estimates of joint strength from experimental tests", Pacific Timber Engineering Conference, Rotorua, New Zealand, 1999, pp. 225-229.
133. EN 1990 Eurocode – Basis of design .....
134. Hirai, T., 1987, "Deformation of Semi-Rigid Wooden Frames", Reasearch Bulletins of College Experiment Forests, Vol. 44, pp. 297-326.
135. Coates, R.C., Coutrie, M.G., and Kong, F.K., 1992, "Structural Analysis", Third Edition, Chapman and Hall, pp. 217.
136. Livesley, R.K., 1964, "Matrix Methods in Structural Analysis", Pergammon Press, The Macmillan Company, New York, pp. 93-111.
137. Monforton, G.R. and Wu, T.S., 1963, "Matrix Analysis of Semi-Rigidly Connected Frames", Journal of the Structural Division, Proceedings of the American Society of Civil Engineers, Vol. 89, No ST6, pp. 13-42.
138. McGuire, W., Gallagher, R.H. and Ziemian, R.D., 2000, "Matrix Stuctural Analysis", Second Edition, John Wiley and Sons, Inc., pp. 393-397.
139. Love, A.E.H., 1892, "A treatise on the mathematical theory of elasticity", Cambridge Press, 1892.
140. DD ENV 1993-1-1:1992 "Eurocode3 –Design of Steel Structures-Part 1.1: General rules and rules for buildings."
141. Porteous, A, 1965, "Analysis of timber roof trusses, taking into consideration flexibility of joints", M.Sc. Thesis, Imperial College, London University.
142. Brynildsen, O.A, and Booth, L.G., 1967, "Structural analysis of timber trusses with semi-rigid joints", Paper presented at IUFRO, section 41,Munich, September 1967, pp. 1-14.
143. Lightfoot, E. and LeMessurier, A.P., 1974, "Elastic analysis of frameworks with elastic connections", Journal of the Structural Division, A.S.C.E, 100, st6: pp. 1297-1309.
144. Komatsu, K., 1989 "Behaviour of nailed timber joints with steel side plates", Proceedings Pacific Timber Engineering Conference, Auckland New Zealand, Vol2, pp. 89-94.
145. Lui, E.M. and Chen, W.F., 1987, "Steel frame analysis with flexible joints", Journal of Constructional Steel Research, Vol. 8, pp. 161-202.
146. Lui, E.M. and Chen, W.F., 1986, "Strength of H-columns with small end restraints", Journal of the Institution of Structural Engineers, 61B, 1; pp.17-26.
147. Simitses, G.J. and Swisshelm, J.D., 1984, "Flexibly jointed unbraced portal frames", Journal of Constructional Steel Research, Vol.4; pp. 27-44.
148. Frye, M.J. and Morris, G.A., 1976, "Analysis of flexibly connected steel frames," Canadian Journal of Civil Engineers, Vol. 2, No.3; pp. 280-291.
149. Ang, K.M. and Morris, G.A., 1984, "Analysis of three-dimensional frames with flexible beam-column connections," Canadian Journal of Civil Engineers, Vol11; pp. 245-254.
150. Lui, E.M. and Chen, W.F., 1986, "Analysis and behaviour of flexibly-jointed frames", Engineering Structures, Vol. 8; pp. 107-118.

151. Kishi, N. and Chen, W.F., 1986, "Data base of steel beam-to-column connections," Structural Engineering Report No. CE-STR-86-26, School of Civil Engineering, Purdue University, West Lafacyette, USA., pp. 1-653.
152. Yee, Y.L., and Melchers, R.E., 1986, "Moment-rotation curves for bolted connections", Journal of Structural Engineering, A.S.C.E, Vol. 112, 3; pp. 615-635.
153. Disque, R.O., 1975, "Directional moment connections – a proposed design method for unbraced steel frames," Engineering Journal, A.I.S.C., Vol. 12, 1; pp. 14-18.
154. Ahmed, I. and Kirby, P.A., 1996, "Maximum connection rotations in non-sway semi-rigid frames," Journal of Constructional Steel Research, Vol. 40, No 1, pp. 1-15.
155. Maier-Leibnitz, H., 1936, "Test results, their interpretation and application", Preliminary Publication, International Association for Bridge and Structural Engineering, 2nd Congress, Berlin.
156. Ewing, J.A., 1899, "The strength of materials" Cambridge Press, 1899.
157. Baker, J.F. and Roderick, J.W., 1938, "An experimental investigation of the strength of seven portal frames." First Interim Report, Research Committee of the Institute of Welding, Trans, Inst. Weld., Vol. 1, No. 4.
158. Bindzi, I. and Sampson, M., Nov 1995, "New formula for influence of spiral grain on bending stiffness of wooden beams", Journal of Structural Engineering, A.S.C.E., Vol. 121, No. 11; pp. 1541-1546.
159. Illston, J. M., Dinwoodie, J.M. and Smith, A. A., 1979, "Concrete, Timber and Metals – The Nature and Behaviour of Structural Materials", Published by Van Nostrand Reinhold International, ISBN 0 442 30145 6.
160. Norén, B., 1968, "Nailed Joints – Their Strength and Rigidity Under Short Term and Long Term Loading", The National Swedish Institute for Building Research, Stockholm, Report No. 22.
161. Siimes, F.E., Johanson, P.E. and Niskansen, E., 1954, "Investigations on the Ultimate Embedding Stress and Nail Holding Power of Finnish Pine", The State Institute for Technical Research, Tiedoitus, Vol. 122. Helsinki.
162. Foschi, R.O., and Bonac, T., 1977, "Load-Slip Characteristics for Connections with Common Nails" Journal of the Institute of Wood Science, Vol. 9(3): pp. 118-123.
163. Smith, I., 1982, "Analysis of Mechanical Timber Joints with Dowel Type Connections subjected to Short Term Lateral Loading – by Finite Element Approximation", T.R.A.D.A., Research Publication No 12/82.
164. Pearson, R. G., Kloot, N.H. and Boyd, J.D., 1962, "Timber Engineering Design Handbook", Third Edition, Jacaranda Press, Brisbane, Australia.
165. Kuipers, J. and Vermeyden, P., 1965, "The Ratio between strength and Allowable Loads on Timber Joints", Procedings of the International Symposium on Joints, London 1965.
166. Foschi, R.O., 1991, "Material Characteristics and Reliability Design", Reliability Based Design of Engineered Wood Structures, Jozsef Bodig, Proceedings of the NATO Advanced

Research Workshop on Reliability-Based Design of Engineered Wood Structures, Florence, Italy.pp. 75-89.

167. Mettem, C.J., 1986, "Structural Timber Design and Technology", T.R.A.D.A., Longman Scientific and Technical Publication.
168. Norris, C.B., 1962, "Strength of orthotropic materials subjected to combined stresses", U.S. Forest Products Laboratory Report No. 1816.
169. BS CP 112 : Part 2 : 1971, "The Structural Use of Timber, Part 2"
170. Hollaway, L., 1989, "Design of Composites", Design with Advanced Materials, edited by L Philips, The Design Council, London.
171. A.S.C.E., 1996, "Mechanical Connections in Wood Structures", ASCE Manuals and Reports on Engineering Practice N0. 84, Published by ASCE.
172. McGowan, W.M., 1966, "A Nailed Plate Connector for Glued- Laminated Timbers", Journal of Materials, Vol. 1, Part 3; pp. 509-535.
173. Girhammer, U.A. and Andersson, H., 1988, "Effect of Loading Rate on Nailed Timber Joint Capacity", Journal of Structural Engineering, ASCE, Vol. 114, No. 11, November 1988.
174. Conseil International du Batiment, 1980, "CIB Structural Timber Design Code", CIB-W18 working group. Fifth Edition, August 1980.
175. Thomas, B. and Malhotra, S.K., May 1985, "Behaviour of Timber Joints with Multiple Nails", Journal of Structural Engineering, ASCE, Vol. 111, No. 5, pp. 973-991.
176. Smith, I. and Foliente, G., January 1992, "Load Resistance Factor Design of Timber Joints: International Practice and Future Direction", Journal of Structural Engineering, ASCE Vol.128:1(48), pp. 48-59.
177. Chui, Y.H., Ni, C. and Jiang, L., Jan. 1998, "Finite-Element Model for Nailed Wood Joints under Reversed Cyclic Load", Journal of Structural Engineering, ASCE, Vol. 124, No. 1; pp. 96-103.
178. Nishiyama, N. and Ando, N., 2002, "Analysis of load-slip characteristics of nailed wood-joints; application OF a two dimensional finite element method", The 7th World Conference on Timber Engineering, WCTE 2002, August 12-15 Vol.1 ; pp. 306-314.
179. Perkins, R.H., Suddarth, S.K. and Dale, A.C., 1962, "Rotational resistance of three member nailed joints subjected to bending moment. Purdue University, Wood Research Laboratory, Research Bulletin No. 753.
180. Reardon, G.F., 1971, "A Structural Analysis of Frames with Semi-rigid Joints (including a description of a computer program)", Division of Forest Products Technological Paper No. 59, CSIRO, Australia.
181. Harris, R., Kelly, O. and Dickson, M., 2003, "Downland gridshell-an innovation in timber design", Proceedings of the ICE, Civil Engineering, Vol. 156, Issue One, pp. 26-33.
182. BSI 4978: 1996, "Specification for softwood grades for structural timber".

APPENDIX A

PROCEDURES AND REQUIREMENTS TO SUPPORT

'TESTING PROGRAMME FOR NAILED JOINTS'

A Porteous

Issue	Date
Draft1	7 October 1999
Draft2	17 October 1999
Draft3	25 October 1999
Draft4	3 Nov 1999
Final	10 February 2000
Rev1	8 August 2002

CONTENTS

A.1.0 Timber and Plywood Selection Criteria

A.1.1 Timber

The timber will be delivered in planks, nominally 150mm by 50mm. Each plank will be visually inspected and only timber that does not contain cracks, fissures, knots, fungal decay, excessive width of annual growth rings, resin pockets and grain defects (including excessive grain slope) will be used for testing. To achieve a consistent standard of smoothness on the timber, the gusset plate faces of the planks will be lightly sanded in the power sander before joint assembly.

A.1.2 Plywood

Plywood will be delivered in sheets. Each sheet will be visually inspected and only plywood which does not exhibit areas of missing ply, areas of filling in the face veneers or other visual defects will be used for testing.

A.2.0 Material Reference System

A.2.1 General

2.1.1 To ensure that accurate records of tests will be maintained, all material used in tests will be given a reference number.

2.1.2 The reference system will identify the material to be used for Embedment Tests, Lateral Load Tests and Rotation Tests.

2.1.3 Timber Reference System

2.1.3.1 Each plank will be numbered sequentially and the sample to be used in a test will be referenced to denote the plank number it has been obtained from; incorporate the symbol E if it is to be used for an embedment test; the symbol S if it is to be used for a shear test; the symbol L or P to denote loading along or perpendicular to the grain direction; the symbol R if it is to be used for a rotation test.

2.1.3.2 The samples for embedment tests will be obtained by rip sawing the selected plank section along its length within its 50mm thickness to form four pieces 9mm thick. The cut pieces will be referenced E1, E2, E3 and E4 from face to face. The reference system used will be of the form XE/Y where X is the plank number, E is the cut piece reference and Y is the sample number of the plank, as follows:

Plank No 6 6E1/1; 6E3/1; 6E2/3 denotes cut pieces 1 and 3 obtained from sample 1 and cut piece 2 obtained from sample 3, all from plank 6.

2.1.3.3 The samples to be used for lateral shear tests loaded in the direction of the grain will be obtained by cutting three samples of equal width from plank sections cut to the required length. The cut samples will be referenced SXLA, SXLB, SXLC where X is the plank number, L denotes that the sample is to be loaded along the grain direction and A, B and C are the three cut pieces (with B being the central one). An example of the system is:

Plank No 9 S9L/1A; S9L/1B; S9L/1C denotes A, B and C cut pieces obtained from sample 1, all from plank 9.

2.1.3.4 Samples to be used for lateral shear tests loaded at right angles to the grain will be cut across the plank width and referenced SXP/Y, where X is the plank number, P denotes that the sample is to be loaded perpendicular to the grain, and Y is the sample number. An example of the system is:

Plank No 7 S7P/1; S7P/3; S7P/6 denotes samples 1, 3 and 6 cut from plank 7.

2.1.3.5 Samples to be used for rotation tests will be referenced RX/Y, where X is the plank number and Y is the sample number. An example of the system is:

Plank No 20 R20/1; R20/3; R20/6 denotes sample 1, 3 and 6 cut from plank 20.

2.1.4 Plywood Reference System

2.1.4.1 As for the timber, each sheet of plywood will be numbered sequentially and a record will be kept of the sheet thickness. Samples to be used in a test will be referenced to denote the plywood sheet; incorporate the symbol E if it is to be used for an embedment test; incorporate the symbol L if it is to be used for a lateral load test; incorporate the symbol R if it is to be used for a rotation test. Examples of the system are:

Plywood Sheet No 5 5E/1and 5E/2 denotes samples 1 and 2 obtained from Plywood sheet No5, to be used for Embedment tests.

Plywood Sheet No 2 2L/1and 2L/2; denotes samples 1 and 2 obtained from Plywood sheet No2 to be used for Lateral load tests.

Plywood Sheet No 9 9R/1and 9R/2; denotes samples 1 and 2 obtained from Plywood sheet No9, to be used for Rotation tests.

General - if 3 samples are to be used for Embedment tests, 2 to be used for Lateral load tests and 2 for Rotation tests from Plywood sheet 12, they will be referenced 12E/1; 12E/2; 12E/3; 12L/1; 12L/2; 12R/1 and 12R/2.

2.1.5 Records

2.1.5.1 Record of all relevant data will be kept in electronic format. The data will include:

Test Date; Sample and Joint Reference Number; Sample Sizes; Sample weight at test and when dry; Nail Manufacturer; Nail Diameter and Length; Prebore Drill size used; Nailing Pattern used; Shim sizes used; Rate of loading

A.3.0 Nail Strength and Stiffness Tests

A.3.1 Strength Testing

3.1.1 The objective of the test is to obtain the ultimate strength of the nail wire. The nail will be loaded to failure in tension using the Schenck-Trebel RM Testing Machine at a constant loading rate of 0.4mm/min.

3.1.2 The number of samples to be tested will be:

Nail Size	Length	Number of samples
2.65mm	60	5
3.00	60	5
3.35	60	5

A.4.0 Embedment Tests

A.4.1 Test Rig and Sample Sizes

4.1.1 The testing is to comply with the requirements of BS EN 383 (1993), using the rig shown in APPENDIX 1 and detailed in APPENDIX 2.

4.1.2 The rig will accommodate material up to 20mm thick and minimum nail lengths of 50mm.

4.1.3 When the samples are fitted into the rig a 0.25mm to 0.5mm gap will be left between each sample face and adjacent rig face to prevent friction pick up during the test.

4.1.4 To obtain data which will eliminate the stiffness effects of the rig from the test results, calibration tests will be undertaken as described in BS EN 383 (1993).

4.1.5 Sample Sizes

4.1.5.1 All samples will be made 40mm wide by 110mm long and the sample thicknesses will be:

Douglas Fir	9mm	
Plywood	(i)	Material Thickness
	(ii)	Plywood reduced to 9mm thick.

A.4.2 Test Samples

4.2.1 Timber Tests

4.2.1.1 Timber planks will be sawn along their lengths and reduced to four samples 9mm thick.

4.2.1.2 The 9mm thick timber strips will be cut into sections 40mm wide by 110mm long, the latter dimension being along the direction of the grain.

4.2.1.3 The number of tests to be done will be:

Nail Size	**Grain Direction For Test**	**Number of Tests**
2.65mm	Parallel	5
3.00mm	Parallel	5
3.35mm	Parallel	5

4.2.1.4 When preparing the sample for test, the nail is to be carefully driven through a predrilled hole in the centre of the sample, ensuring it is driven at right angles to the sample face. The nail point-side and head side must project the same distance from their respective faces.

4.2.1.5 The predrill drill sizes will be

Nail Diameter mm	Predrill Drill Size mm
2.65	2.1
3.00	2.5
3.35	2.8

4.2.1.6 The 'U' frame onto which the transducers will fit, is to be screwed onto the sample before the sample is secured in the test rig. An example of a sample fitted with the 'U' frame is shown in APPENDIX 3.

4.2.2 Plywood Tests

4.2.2.1 The test rig will be adjusted to suit the plywood thickness being used, ensuring there will be a 0.25mm gap between the sample and rig faces.

4.2.2.2 The section size to be used will be 40mm wide by 140mm long by the thickness of the plywood section or by samples reduced to 9mm thick.

4.2.2.3 The tests to be done will be:

Nail Dia. mm	**Face Grain Direction**	**Thickness of Test Sample**	**Number of Tests**
2.65mm	Parallel	19	5
2.65mm	Parallel	9	5
3.00mm	Parallel	9	5
3.35mm	Parallel	9	5

4.2.2.4 When preparing a sample for test, the nail is to be carefully driven at right angles to the sample face through a predrilled hole in the centre of the sample. The nail point-side and head side must project the same distance from their respective faces.

4.2.2.5 The predrill drill sizes will be as stated in paragraph 4.2.1.5.

4.2.2.6 The 'U' frame onto which the transducers will fit, is to be screwed onto the sample before the sample is fitted into the test rig as shown in APPENDIX 3.

A.4.3 Test Loading

4.3.1 The test rig will be centred in the Schenck-Trebel RM Testing Machine and the displacement transducers will be positioned to read on the U frame such that they are at equal distances from the nail centreline as shown in APPENDIX 3 and APPENDIX 4.

4.3.2 Test loading will in principle comply with the requirements of BS EN 26891 (1991) unless modified in the following paragraphs.

4.3.3 The load will be applied to the test sample through a spreader piece placed between the Testing Machine and the top face of the sample.

4.3.4 The load is to be applied at a constant rate of slip of 0.4mm/min up to 100N and reduced at the same rate to 10N. The sample will then be reloaded at the same rate to failure or until the displacement of the sample is at least 4.5mm. The loading regime is shown on APPENDIX 4.

4.3.5 The failure load will be the lesser of:

(a) the maximum load the sample can take - the load at which slip continues without any load increase or after which the load decreases.

(b) the load at which the nail slip is 4.5mm.

A.5.0 Joint Tests

A.5.1 Lateral Load Tests

5.1.1 Joint Sample

A typical joint set-up is shown in APPENDIX 5. The gusset plates will be 6mm steel, 9.5mm plywood, 12mm plywood or 19mm plywood.

5.1.2 Joint Assembly

5.1.2.1 To minimise the risk of inaccuracies and to maintain a high level of consistency and quality control in the assembly procedure, particularly in regard to the positioning of overlapping nails, the joints will be assembled using a jig

5.1.2.2 To reduce the effect of friction in the joint, when it is being assembled a 0.2mm spacer is to be positioned between the timber and adjacent gusset face. The spacers are to be removed when the test joint has been made.

5.1.2.3 All nails are to be driven into predrilled holes. The predrill drill diameter sizes will be:

Nail Diameter mm	Predrill Drill Diameter mm
2.65	2.1
3.00	2.5
3.35	2.8

5.1.2.4 Where steel gusset plates are being used, the plates will be predrilled using a drill which will not exceed 1.1 times the nail diameter, as follows:

Nail Diameter mm	Predrill Drill Diameter mm
2.65	2.8
3.00	3.2
3.35	3.5

5.1.2.5 To ensure overlapping nails will miss each other when being driven from both sides of the joint, the predrill holes on each side will be drilled at a slight offset (approximately the nail diameter) to each other.

5.1.2.6 For joints with steel gusset plates, an angle bracket to support the transducer arm will be screwed to each side of the central timber. The screw fixing for each bracket is to be centred just below the row of nails closest to the base of the joint.

5.1.2.7 For joints with plywood gussets, in addition to the angle brackets referenced in 5.1.2.6, similar brackets will be fitted to the plywood gussets. A bracket will be screwed to each gusset on the joint centreline and close to the joint base support.

5.1.3 Test Set-Up and Loading

5.1.3.1 The test joint will be centred in the Schenck-Trebel RM Testing Machine with the transducers positioned on the brackets at equal distances from joint centreline. Two transducers will be used for joints with steel gussets and four for joints with plywood gussets. A typical set-up is shown on APPENDIX 6.

5.1.3.2 Measurements will be taken of the applied load and associated displacement of the timber relative to the gussets. The displacement measurements will be taken at the position shown on APPENDIX 5.

5.1.3.3 Test loading will in principle comply with the requirements of BS EN 26891 (1991) unless modified in the following paragraphs.

5.1.3.4 The load will be applied to the test joint through a metal spreader block placed on top of the timber and any slight out of alignment between the loading head and the spreader block is to be taken up by inserting metal shims into the gap.

5.1.3.5 The load is to be applied at a constant rate of slip of 0.4mm/min up to 100N and reduced at the same rate to 10N. The sample will then be reloaded at the same rate to the failure load or until the joint slip is at least 4.5mm. The loading regime is shown on APPENDIX 4.

5.1.3.6 The failure load is to be taken as the lesser of:

a) The maximum load the sample can take - the load at which slip continues without any load increase.
b) The load at which the nail slip in the sample has reached 4.5mm.

A.5.2 Rotation Tests

5.2.1 Joint Sample

A typical joint set-up will be as shown in APPENDIX 5. The gusset plates being 6mm steel, 9.5mm plywood, 12mm plywood or 19mm plywood, as appropriate.

5.2.2 Joint Assembly

5.2.2.1 To minimise the risk of inaccuracies and to maintain a high level of consistency and quality control in the assembly procedure, particularly in regard to the positioning of overlapping nails, the joints will be assembled within a jig

5.2.2.2 To reduce the effect of friction in the joint, when it is being assembled a 0.2mm spacer is to be positioned between the timber and the adjacent gusset faces. The spacers are to be removed when the test joint has been made.

5.2.2.3 All nails are to be driven into predrilled holes and the predrill drill diameter sizes will be:

Nail Diameter mm	Predrill Drill Diameter mm
2.65	2.1
3.00	2.5
3.35	2.8

5.2.2.4 Where steel gusset plates are being used the plates will be predrill as stated in paragraph 5.1.2.4.

5.2.2.5 To ensure overlapping nails will miss each other when being driven from both sides of the joint, the predrill holes on each side will be drilled at a slight offset (approximately the nail diameter) to each other.

5.2.3 Test Set-Up and Loading

5.2.3.1 The test joint will be positioned in the Schenck-Trebel RM Testing Machine as shown in Figure F. Two transducers will be secured to one of the gusset plates to read on the top face of the timber cantilever and the centrelines of the transducers will align with the extreme nail positions in the joint as shown on Figure G.

5.2.3.2 Measurements will be taken of the applied load and associated displacement of the timber relative to the gusset plates. The horizontal distance between the Machine loading point on the joint cantilever and the centreline of the joint will also be taken.

5.2.3.3 Test loading will in principle comply with the requirements of BS EN 26891 (1991) unless modified in the following paragraphs.

5.2.3.4 The load will be applied to the test joint through a metal spreader block placed on top of the timber cantilever arm. To reduce the risk of the load point movement along the timber during the test, the load is to be applied through a spherically shaped loading head.

5.2.3.5 The load is to be applied at a constant rate of slip up to a load of 100N and then reduced at the same rate to 10N. The joint will then be reloaded at the same rate to failure or until the maximum joint slip at the extreme nail positions are at least 4.5mm. The loading regime is shown on APPENDIX 4.

5.2.3.6 The rate of loading at the machine loading head will be such that the rate of loading at the extreme nail positions will be approximately 0.4mm/min.

5.2.3.7 The failure load is to be taken as the lesser of

a) The maximum load the sample can take-the load at which slip continues without any load increase.
b) The load at which the nail slip in the most highest loaded pair of overlapping nails has reached 4.5mm

A.5.3 Rotation Tests – Combined Moment Joints

5.3.1 Joint Sample

A typical layout of a combined moment joint for a rotation test is shown in APPENDIX 8. The joint will comprise two plywood gusset plates connected to two sections of timber which are at right angles to each other. The timbers are positioned such that there will be a 20mm gap between them to prevent contact during the test.

5.3.2 Combined Moment Joint Assembly

5.3.2.1 To minimise the risk of inaccuracies and to maintain a high level of consistency and quality control in the assembly procedure, particularly in regard to the positioning of overlapping nails, the combined joints will be assembled within a jig

5.3.2.2 To reduce the effect of friction in the joint, when it is being assembled a 0.2mm spacer is to be positioned between the timber and the adjacent gusset faces. The spacers are to be removed when the test joint has been made.

5.3.2.3 All nails are to be driven into predrill holes and the predrill drill diameter sizes will be:

Nail Diameter mm	Predrill Drill Diameter mm
2.65	2.1
3.00	2.5
3.35	2.8

5.3.2.4 To ensure overlapping nails will miss each other when being driven from both sides of the joint, the predrill holes on each side will be drilled at a slight offset (approximately the nail diameter) to each other.

5.3.3 Test Set-Up and Loading

5.3.3.1 The test joint will be positioned in the Schenck-Trebel RM Testing Machine as shown in Figure I. A pair of transducers will be secured to one of the gusset plates at each joint to read on the face of the timber and the centrelines of the transducers will, where possible, align with the extreme nail positions of each joint as shown on Figure O.

5.3.3.2 Measurements will be taken of the applied load and associated displacement of the timber relative to the gusset plates. The horizontal distance between the Machine loading point on the joint cantilever and the centreline of the a joint will be noted as well as the positions of the joints relative to each other in the rig.

5.3.3.3 Test loading will in principle comply with the requirements of BS EN 26891 (1991) unless modified in the following paragraphs.

5.3.3.4 The load will be applied to the test joint through a metal spreader block placed on top of the timber cantilever arm. To reduce the risk of the load point movement along the timber during the test, the load is to be applied through a spherically shaped loading head.

5.3.3.5 The load is to be applied at a constant rate of slip up to a load of 100N and then reduced at the same rate to 10N. The joint will then be reloaded at the same rate to failure or until the maximum joint slip at the extreme nail positions are at least 4.5mm. The loading regime is shown on APPENDIX 4.

5.3.3.6 The rate of loading at the machine loading head will be such that the rate of loading at the extreme nail positions will be approximately 0.4mm/min.

5.3.3.7 The failure load is to be taken as the lesser of

5.1..7.1 The maximum load the sample can take-the load at which slip continues without any load increase.

5.1..7.2 The load at which the nail slip in the most highest loaded pair of overlapping nails has reached 4.5mm.

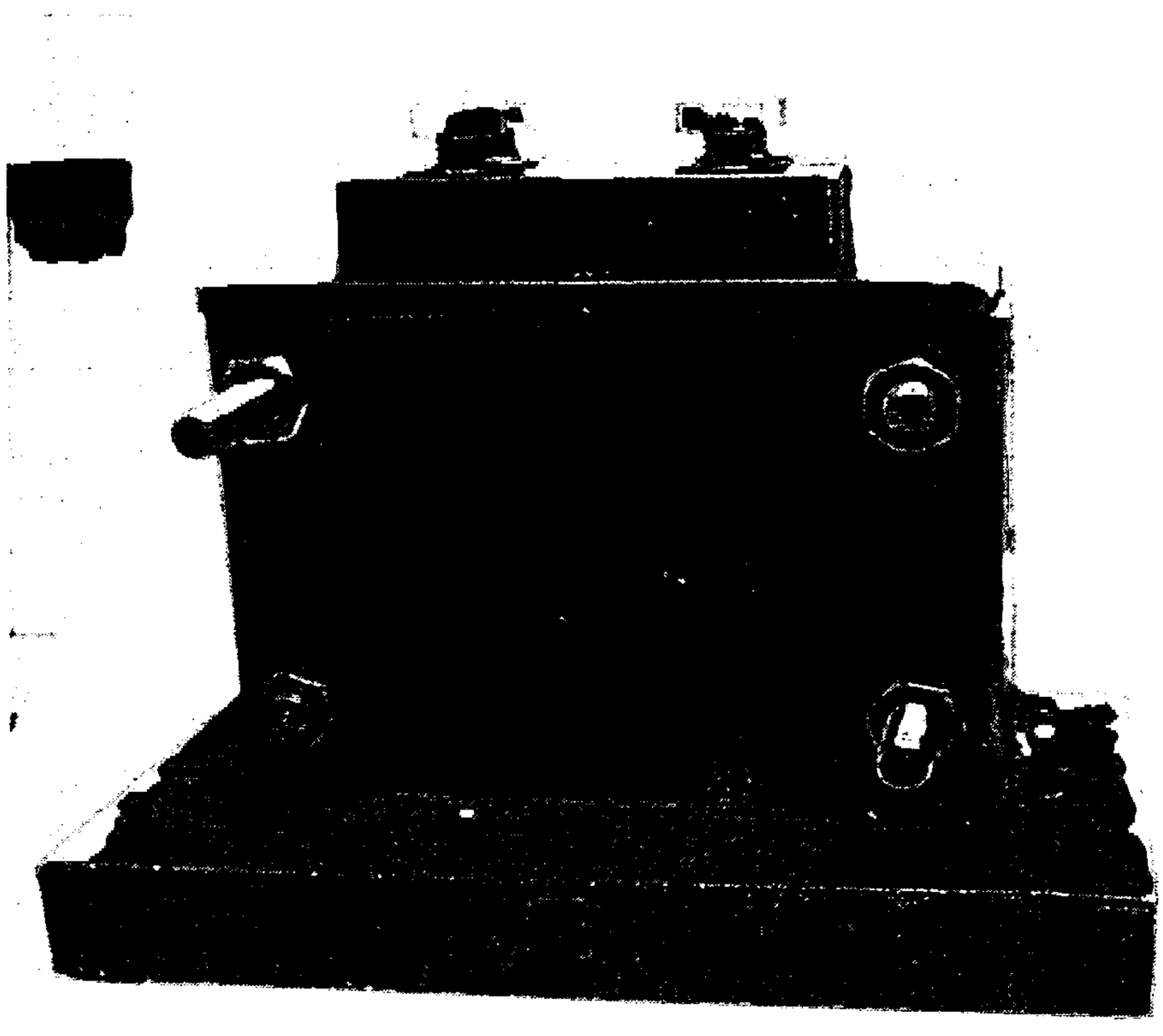

EMBEDMENT RIG – ELEVATION

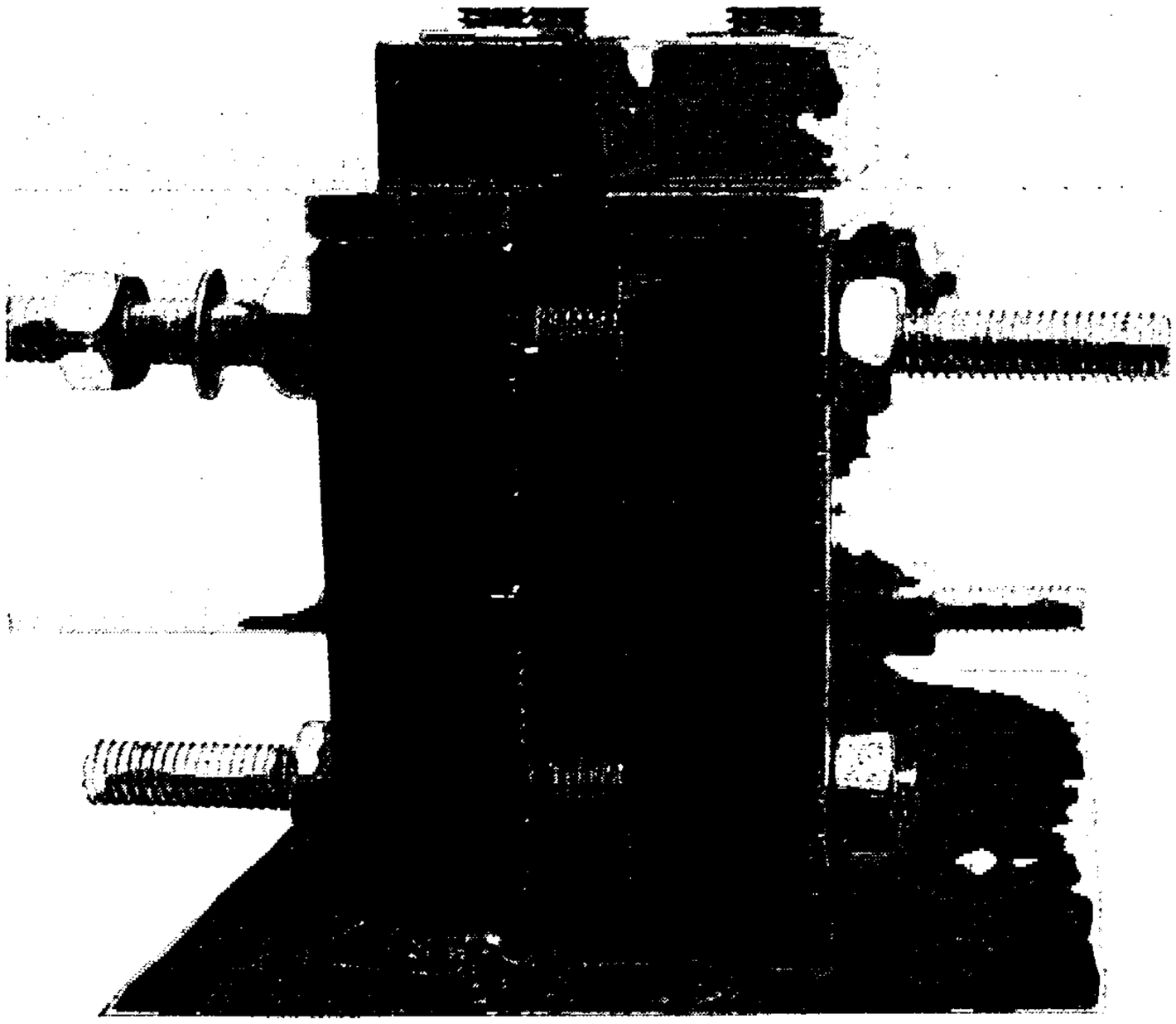

EMBEDMENT RIG – END ELEVATION

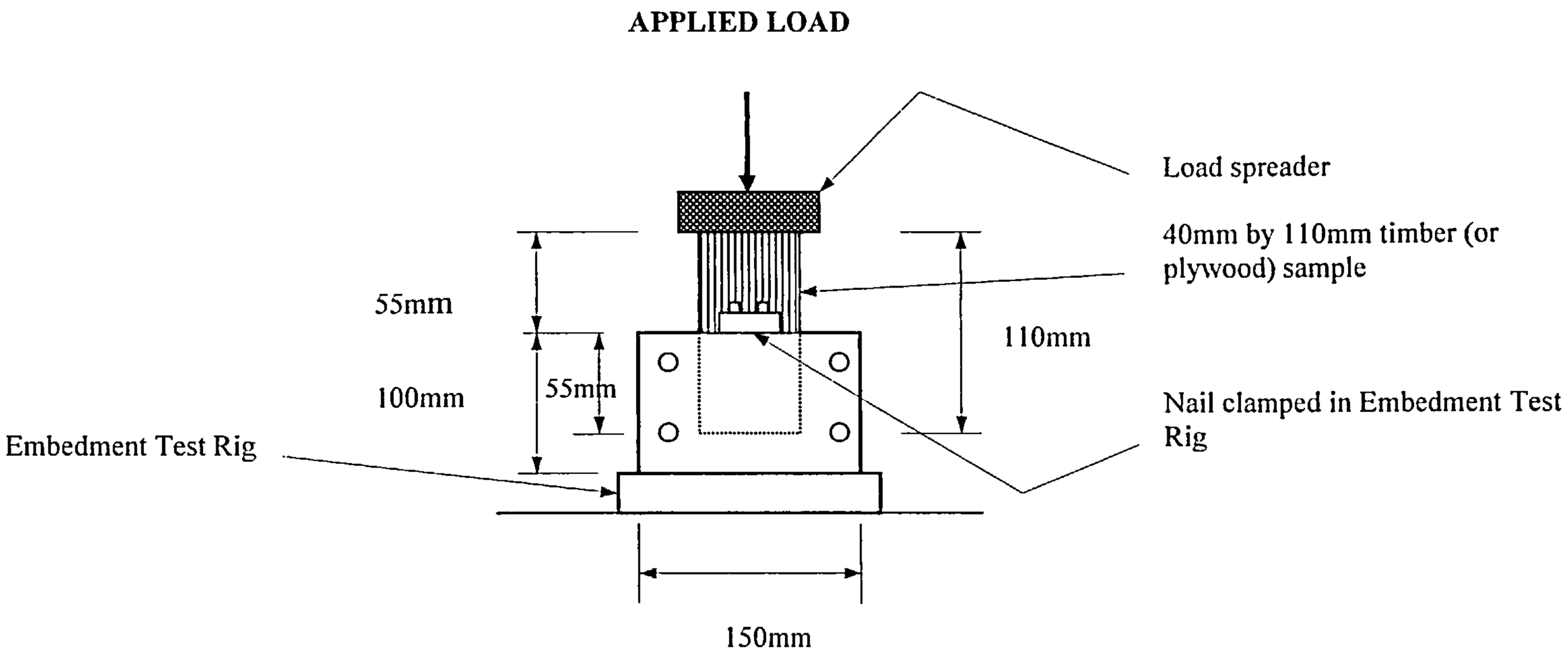

ELEVATION

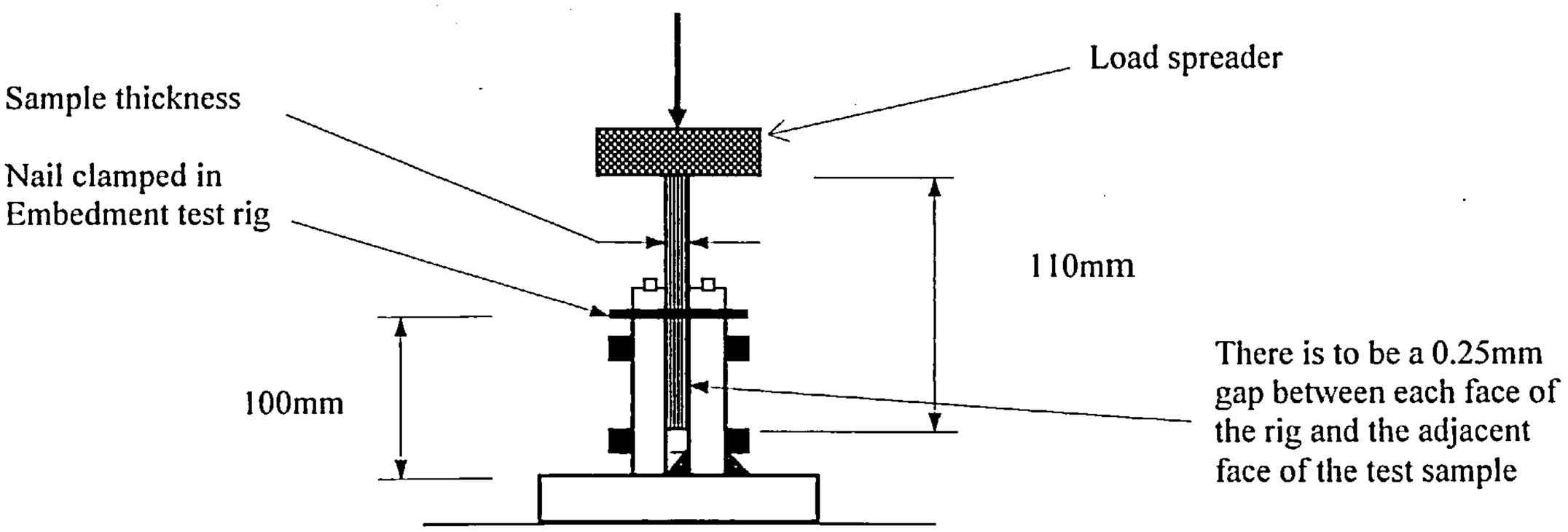

END
ELEVATION

EMBEDMENT TEST RIG

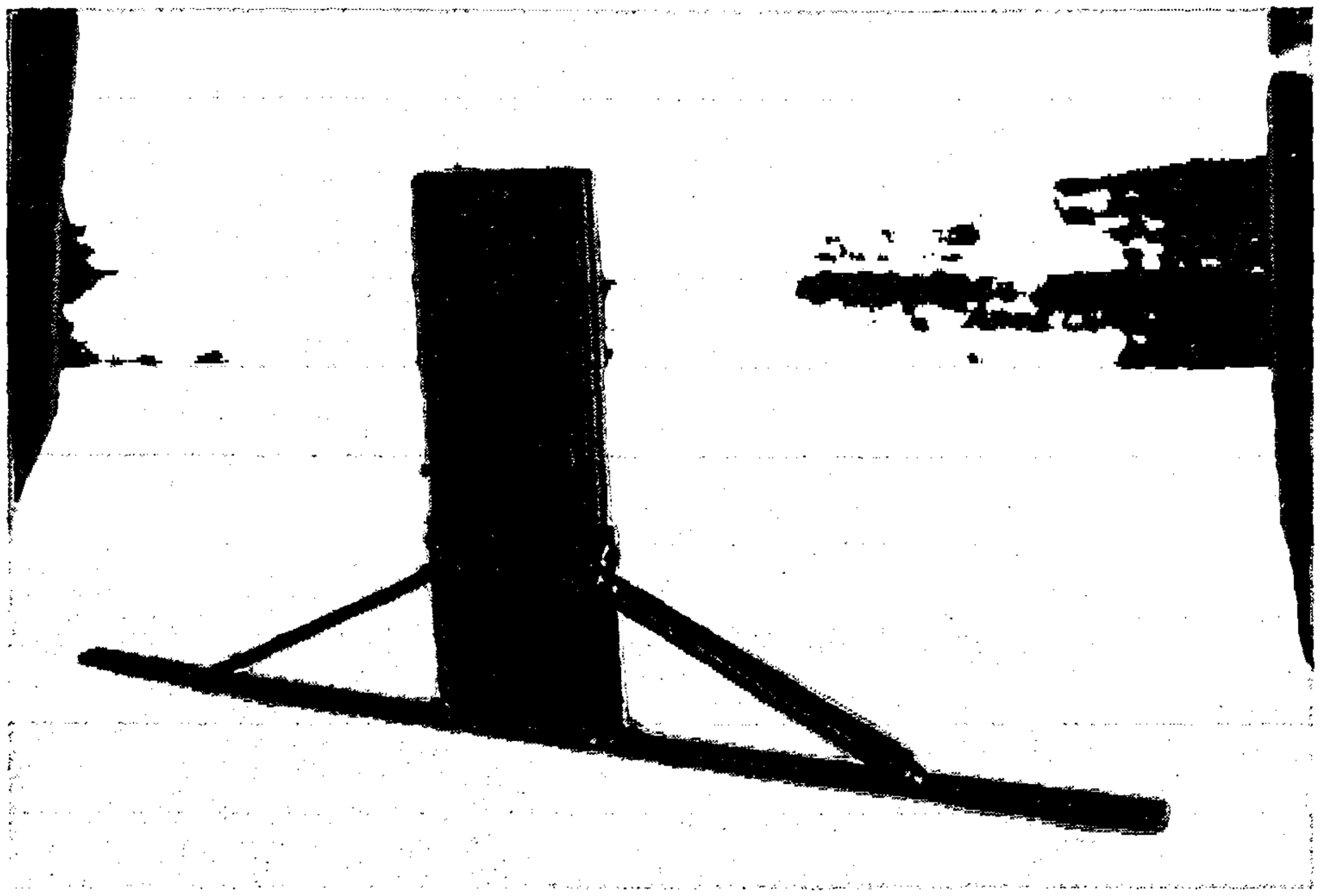

EMBEDMENT TEST SAMPLE IN 'U' FRAME

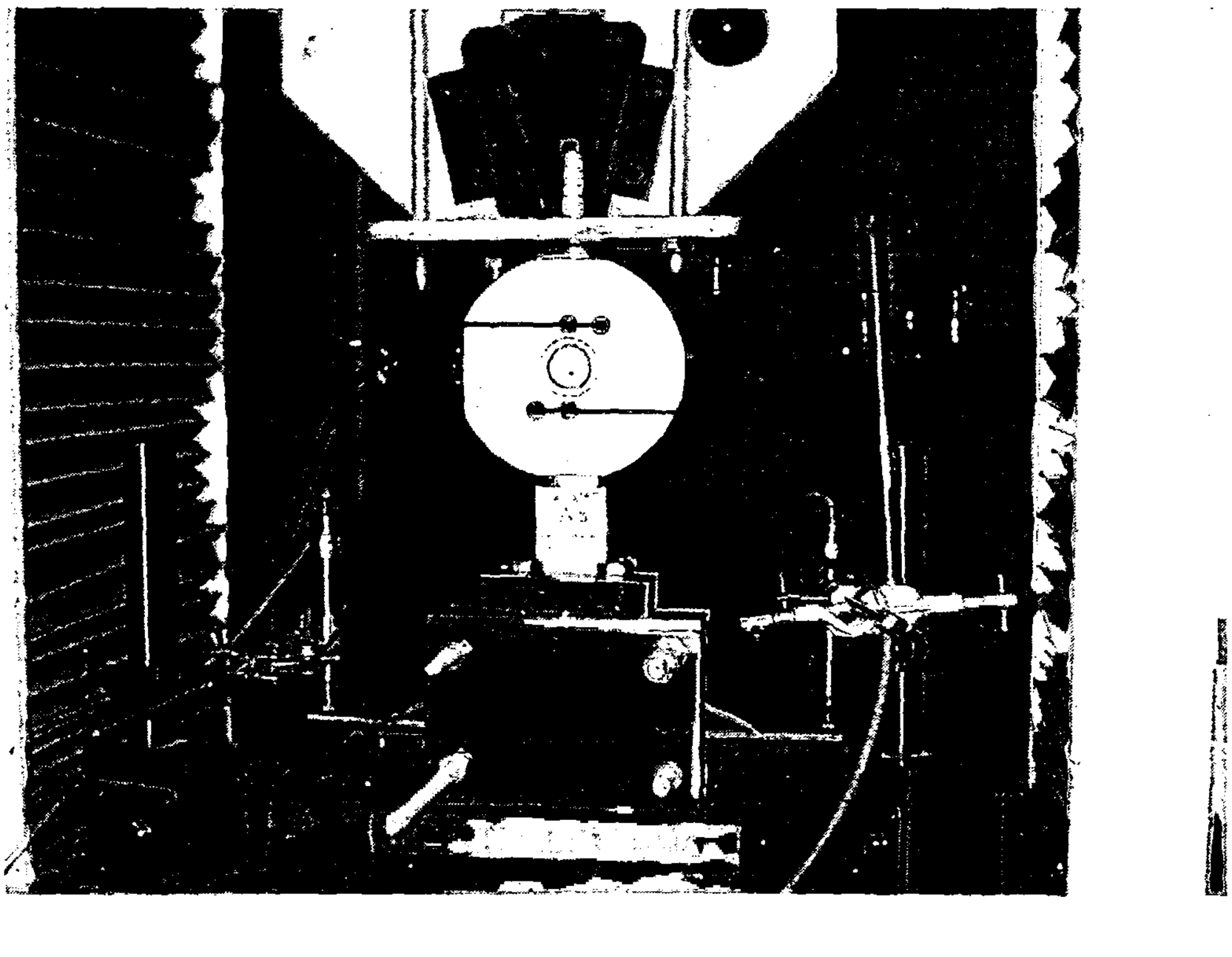

EMBEDMENT TEST RIG IN SCHENCK-TREBEL TESTING MACHINE

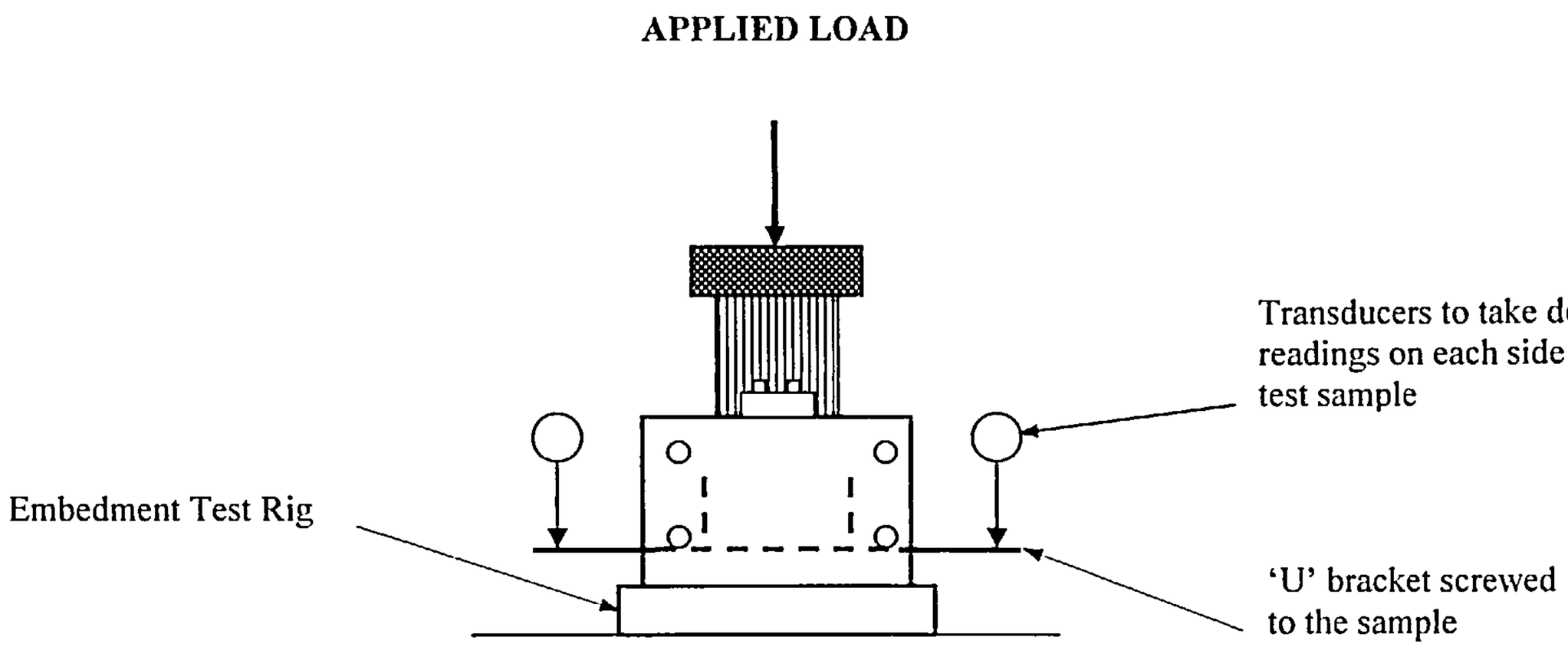

ELEVATION

EMBEDMENT TEST – DEFLECTION READINGS

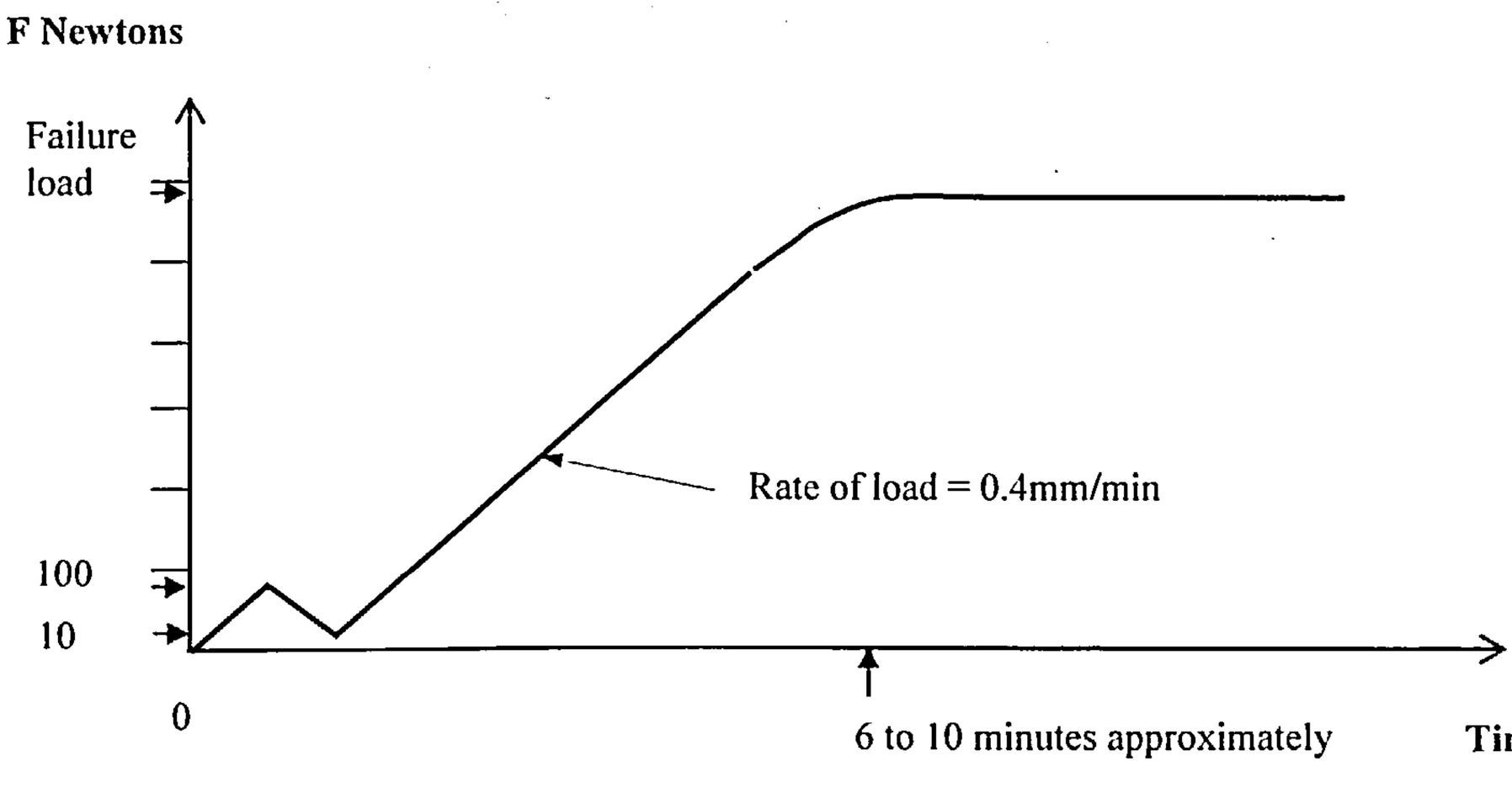

PROPOSED LOAD TEST REGIME

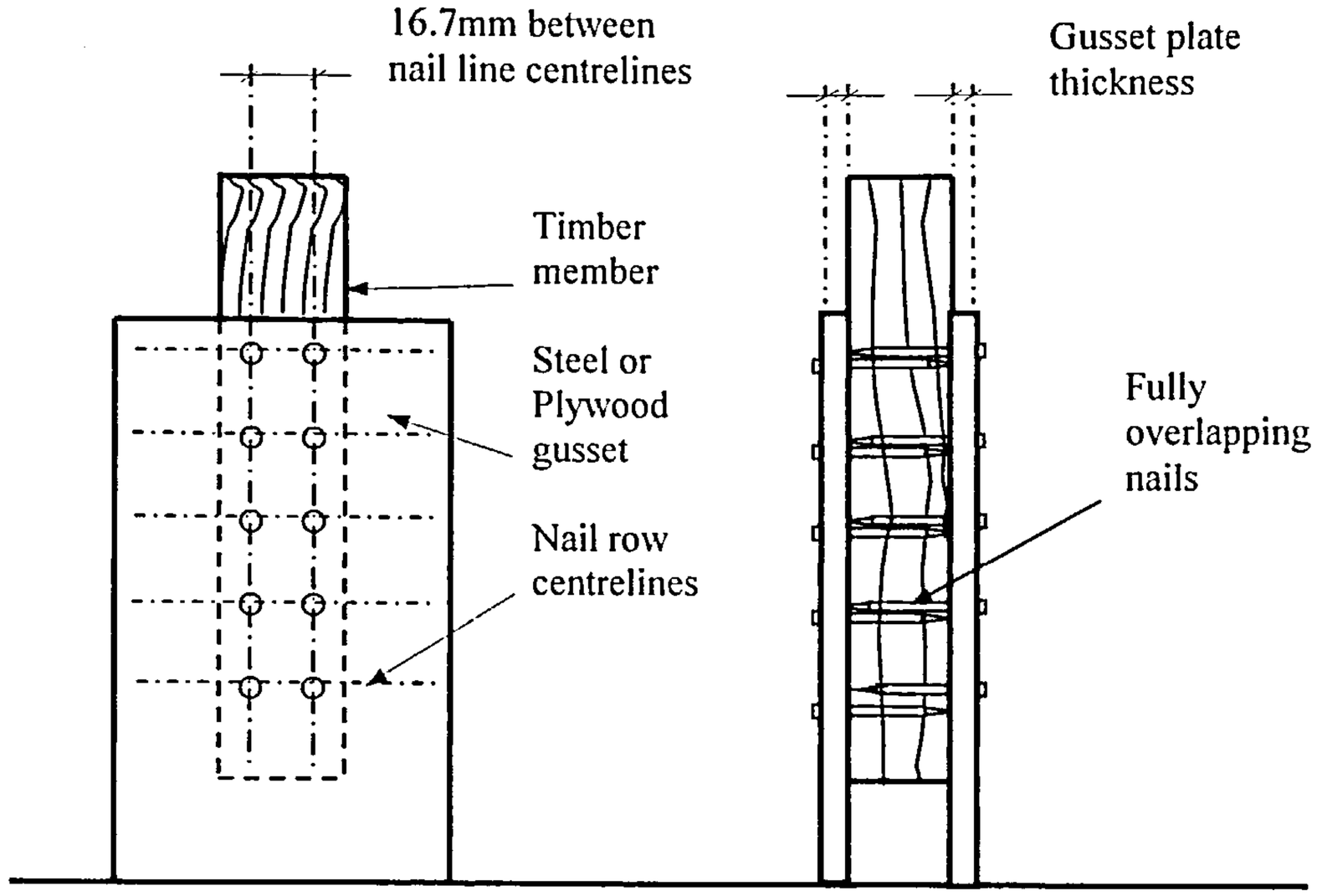

ELEVATION **END ELEVATION**

TYPICAL LATERAL LOAD TEST JOINT

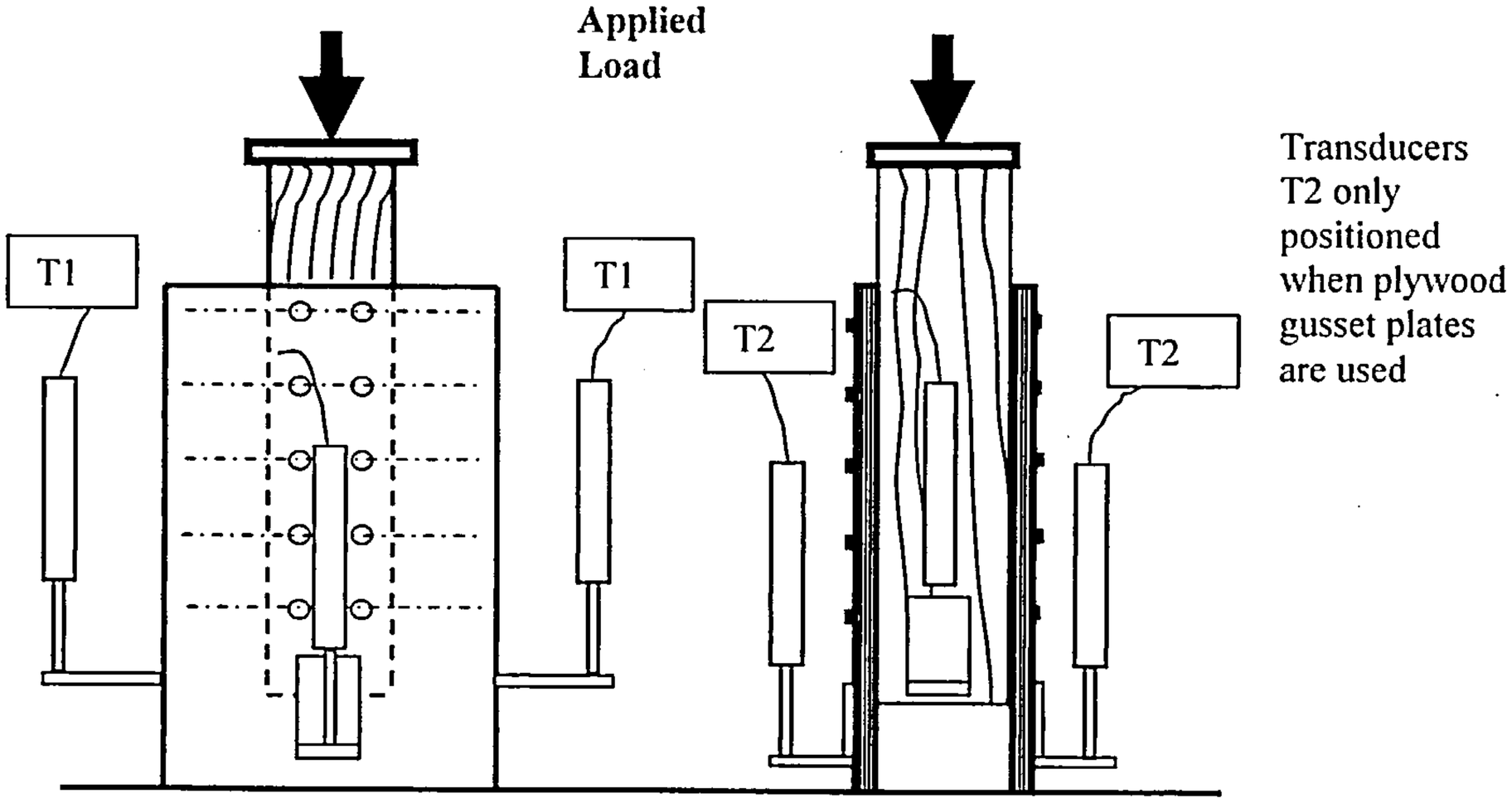

ELEVATION **END ELEVATION**

Note – The layout shows the 4 transducer positions (T1 and T2) when plywood gusset plates are used. When steel gusset plates are used, only the transducers T1 will be used.

TRANSDUCER POSITIONS FOR DIRECT SHEAR TESTS

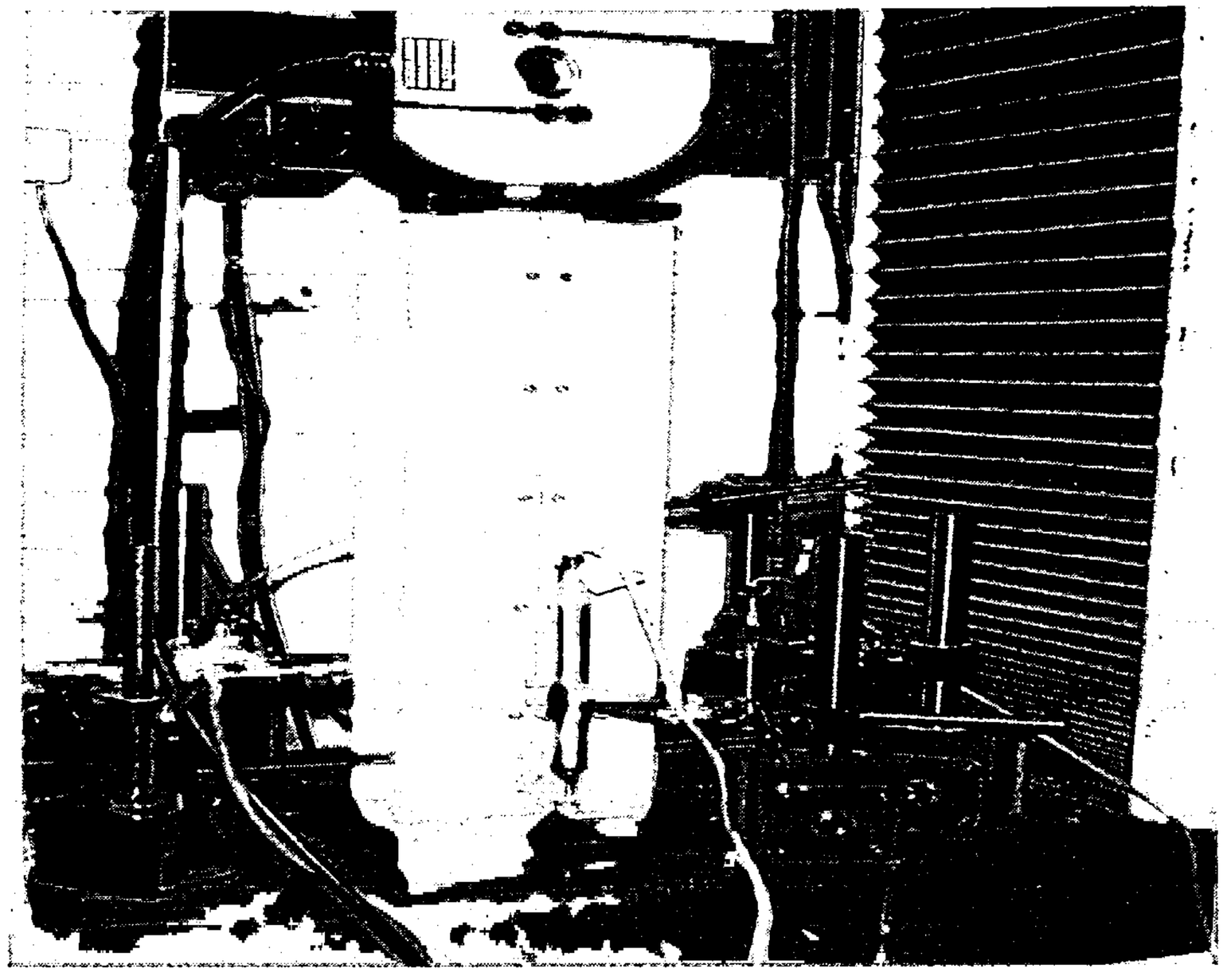

SHEAR TEST SAMPLE IN SCHENCK-TREBEL TESTING MACHINE

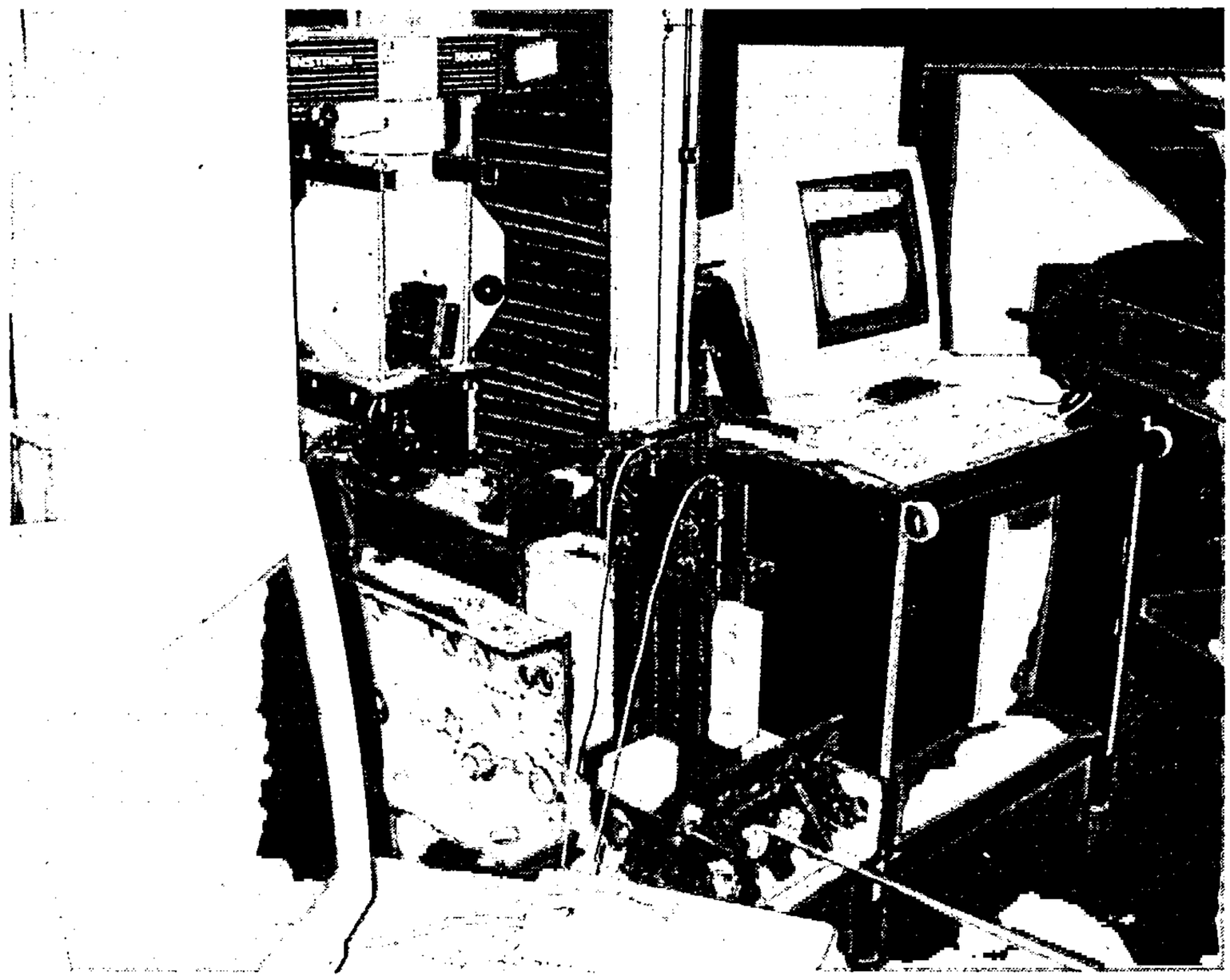

MOMENT JOINT IN TEST RIG

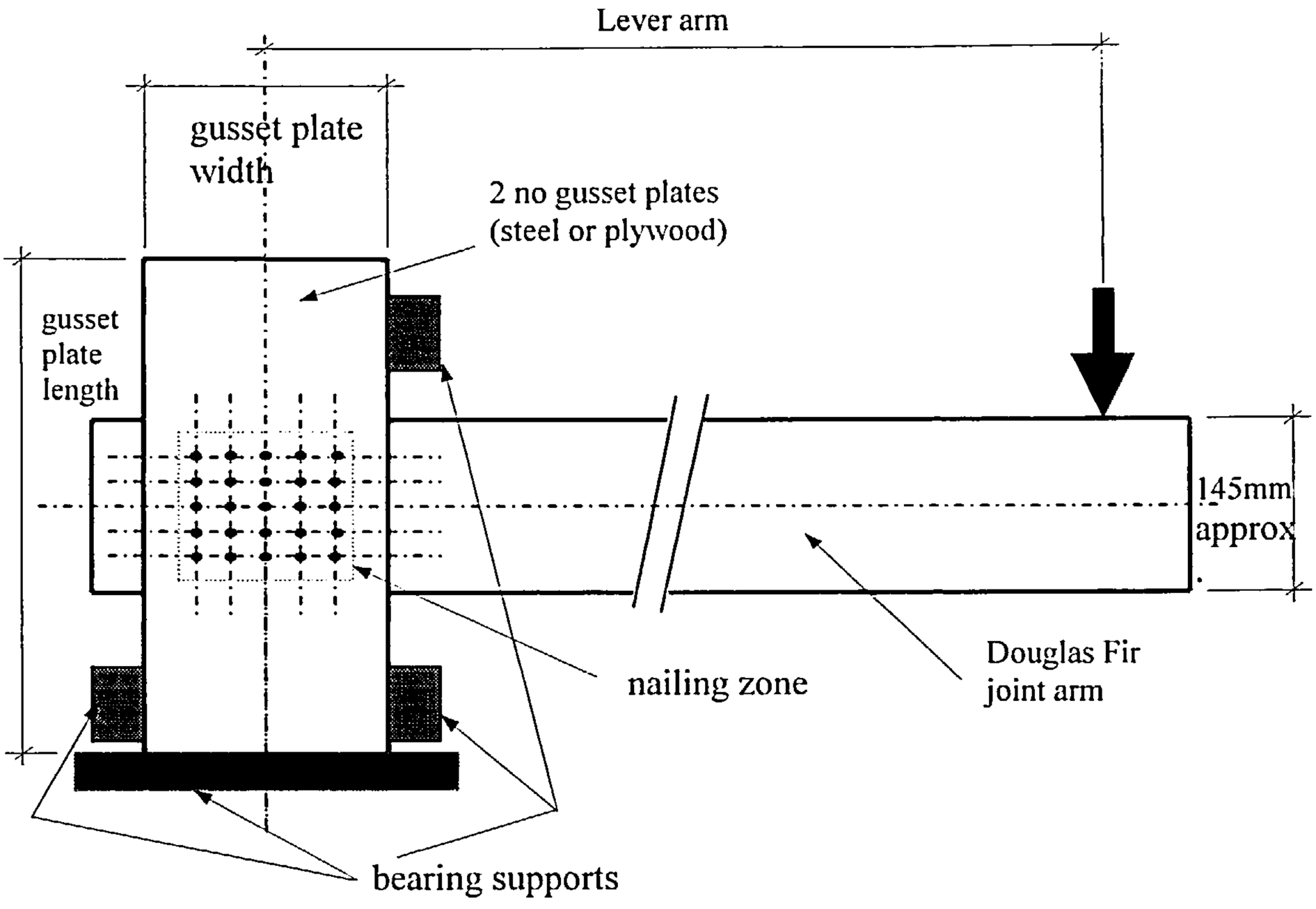

TYPICAL MOMENT JOINT

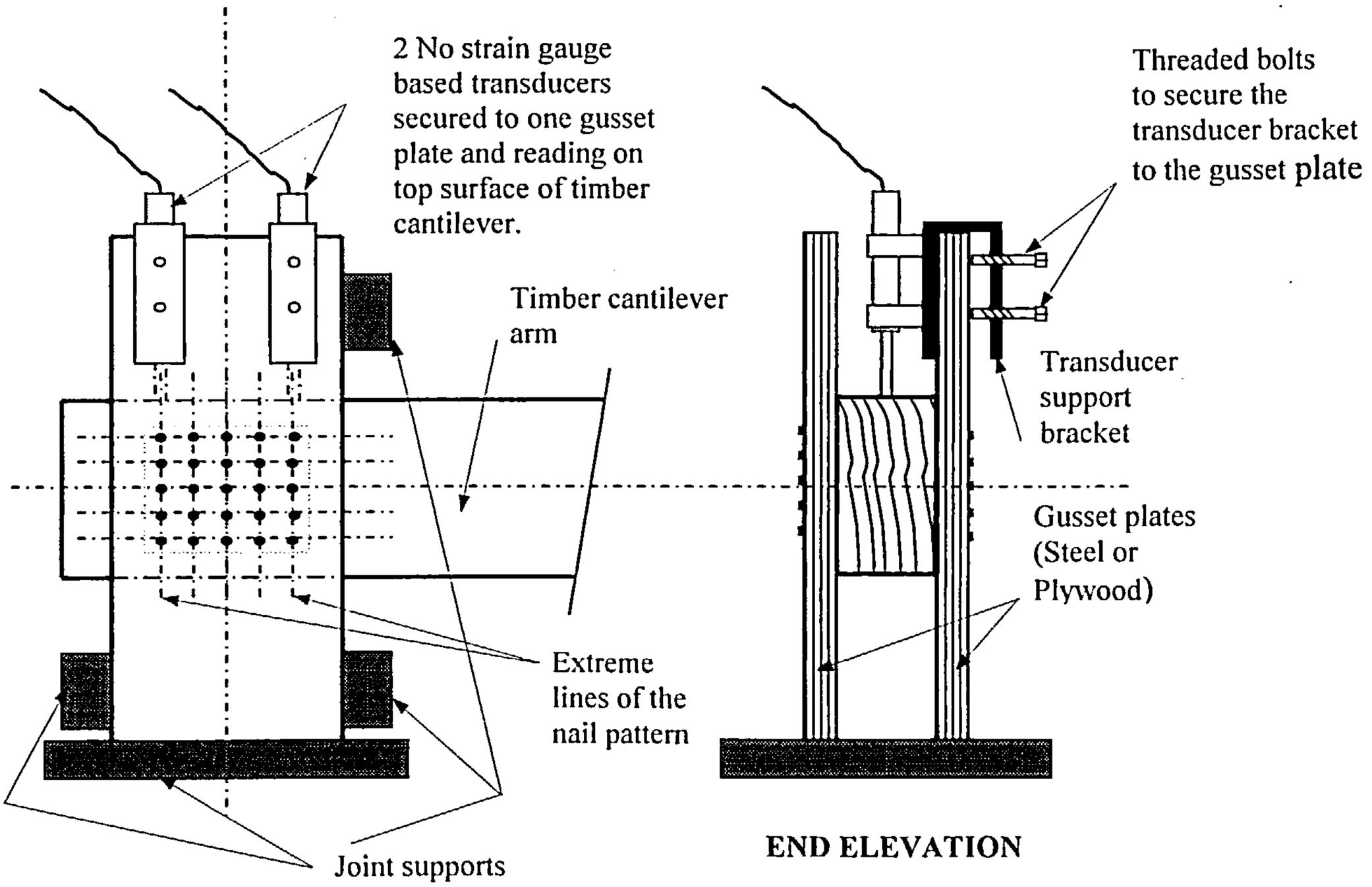

END ELEVATION

TRANSDUCER POSITIONS FOR MOMENT TESTS

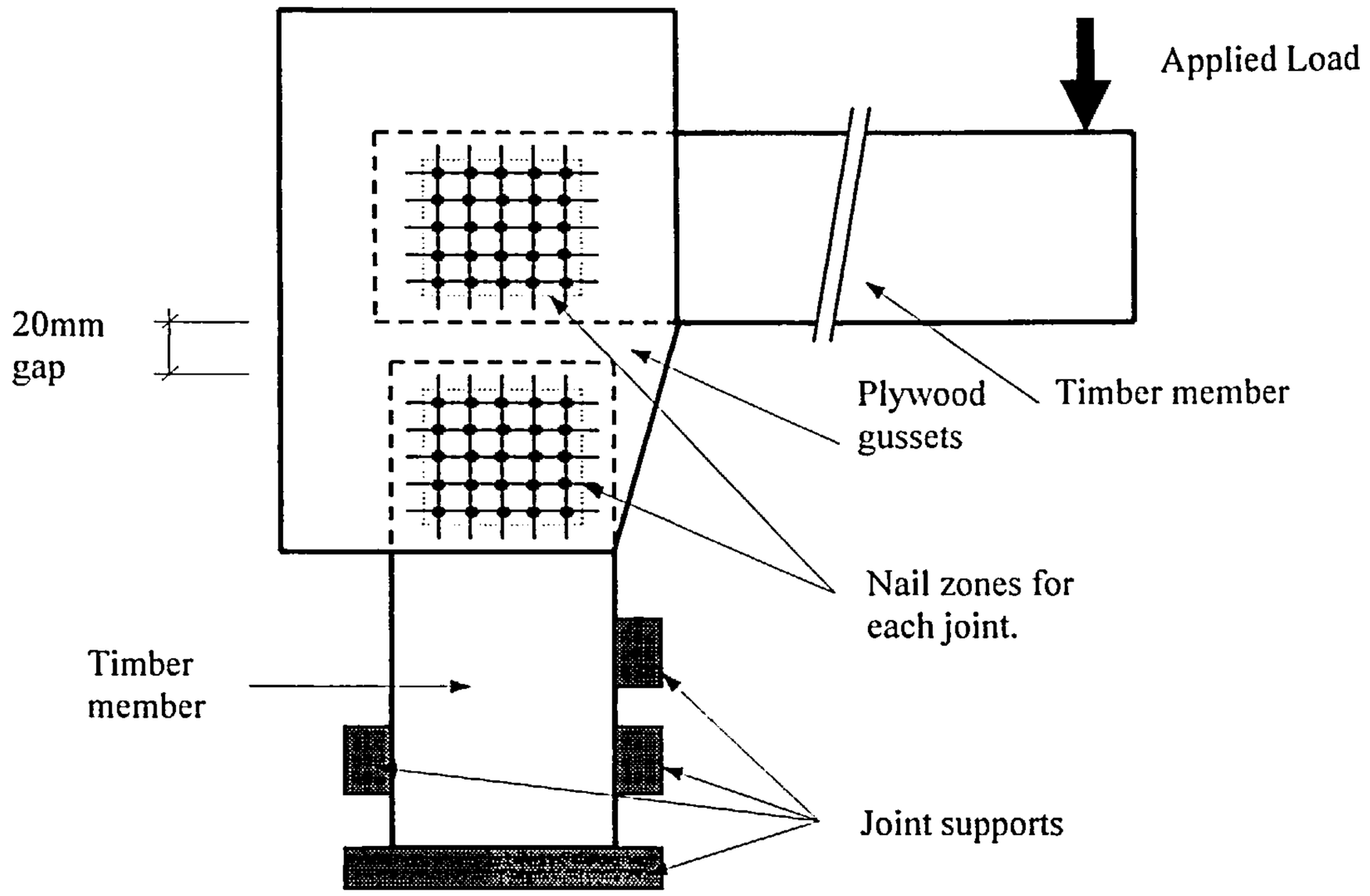

TYPICAL COMBINED JOINT

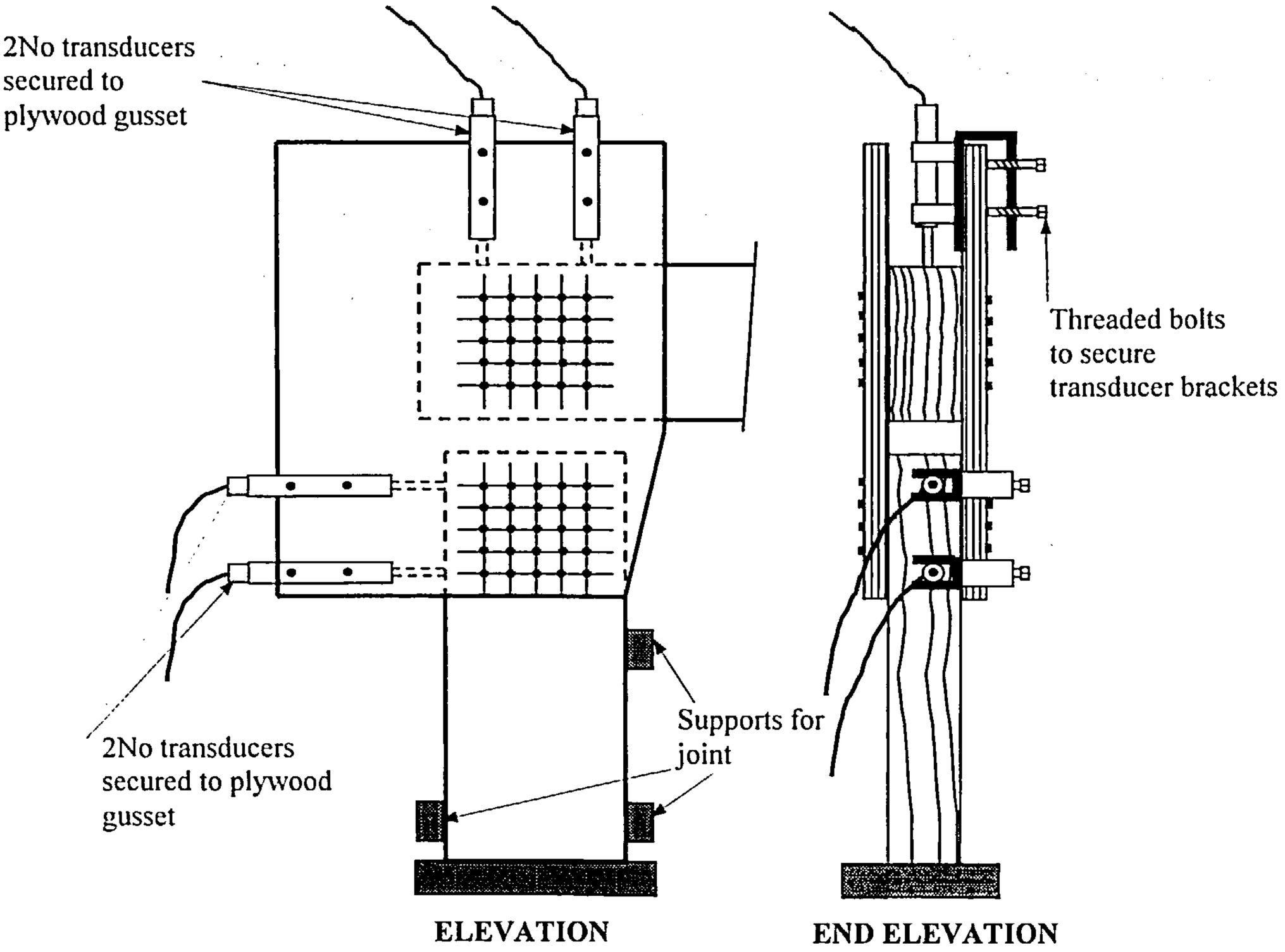

TRANSDUCER ARRANGEMENT FOR COMBINED JOINT

(Transducers only shown fitted to one of the gusset plates for clarity)

COMBINED JOINT IN TEST RIG

APPENDIX B

Material Properties

This appendix summarises the results of tests that were undertaken on the materials used in the research programme and provides information to supplement the joint testing results.

The tests provide information required for use in the modelling of the shear and moment joint test behaviour and the data required to make comparisons with equivalent strengths and stiffness criteria when using the recommendations in EC5 [11].

All of the testing was undertaken in accordance with the recommendations of the British Standards Institute [10, 31, 32, 33, 34, 35], and the European Standards approved by the European Committee for Standardisation [11, 26, 27, 28, 30, 36, 37, 38, 39].

Timber

The timber used for the testing programme was dressed British grown Douglas Fir, supplied by a local supplier in solid planks approximately 155 mm by 45 mm cross section, 6 m and 7 m long, all strength class C18 in accordance with BS 5268 Part 2 [10]. The material for each joint was visually inspected and the selection criteria used was that only timber that did not exhibit cracks, fissures, knots, fungal decay, excessive width of annual growth rings, resin pockets and grain defects (including excessive grain slope) was acceptable. All of the timber was stored in the same area for a period in excess of twelve months prior to the commencement of testing and the environmental conditions in the area maintained the moisture content (m.c.) within the range 11% to 15.5% over the testing period for the timber/steel gusset joints and 12.5% to 14% over the testing period of the timber/plywood gusset joints. Materials were generally cut by the in-house technician staff on the evening before or the day of assembly. The joints were assembled in the testing laboratory at normal room temperature and tested within 10 minutes of fabrication. Samples for material property testing were either cut from the joint material sample or from timber from the same plank as the test samples.

At the commencement of the joint testing programme moisture content tests were taken immediately before and after testing and this continued for a period of two months. Following a review of the results of these tests, as there was no significant difference in value between these stages, the protocol was changed and moisture content readings were only taken after the completion of each joint test.

The timber density varied from a minimum of 429.60 Kg/m^3 to a maximum of 743.33 Kg/m^3. For each set of 5 tests, the average and standard deviation was determined and the results of the maximum and minimum density test sets together with the associated standard deviation and coefficient of variation are given in Table B1. Similar information is also given in Table B1 for the results of moisture content

tests on the 5 tests with the lowest and the highest average moisture content and for the average moisture content for all of the samples tested. These tests show that within each test set the coefficient of variation is minimal and for the overall programme the dispersal of the samples is at an acceptable value of 0.1.

Samples were tested to obtain the modulus of elasticity of the timber parallel to the grain and the results, including the average density of the test samples used, are also given in the Table.

Property	Number of tests	Average Results	Standard deviation	Coefficient of variation
$Density_L$	5	441.81 kg/m^3	10.64 kg/m^3	0.024
$Density_H$	5	722.03 kg/m^3	30.13 kg/m^3	0.042
$Density_{AV}$	2011	562.22 kg/m^3	57.05 kg/m^3	0.101
$M.C._L$	5	11.0%	0%	0
$M.C._H$	5	15.5%	0%	0
$M.C._{AV}$	2011	13.69%	1.7%	0.095
$E_{comp,//}$	5	18375.33N/mm^2	1771.33N/mm^2	0.096
Density	5	565.58 kg/m^3	12.54 kg/m^3	0.022

Table B1 Properties of timber

where:

$Density_L$ = the lowest average density test set.

$Density_H$ = the highest average density test set.

$Density_{AV}$ = the average density of all samples tested

$M.C._L$ = the lowest average moisture content test set.

$M.C._H$ = the highest average moisture content test set.

$M.C._{AV}$ = the average moisture content of all samples tested.

$E_{comp,//}$ = modulus of elasticity parallel to the grain direction.

$E_{comp,\perp}$ = modulus of elasticity perpendicular to the grain direction.

Plywood

The plywood used for the testing programme was 19 mm thick 7-ply, 12 mm thick 5-ply and 9 mm thick 5-ply sheathing plywood formed using tropical hardwoods and dressed to nominal thicknesses of approximately 17 mm, 10 and 7mm respectively. It was imported from Indonesia and complied with the requirements of BSEN 314 [21] and BSEN 315 [22].

The plywood used for each test was visually inspected and only material that did not exhibit areas of missing ply, filled holes in the face veneers and any visual defects was used. All of the plywood was stored in the same area as the timber for a period in excess of twelve months prior to the commencement of testing. The environmental conditions in the area maintained the moisture content within the range 7% to 14%. Materials were generally cut by the in-house technician staff on the evening before or the day of assembly and the joints were assembled in the testing laboratory at normal room temperature and tested within 10 minutes of fabrication. Samples for material property testing were either cut from the joint test sample or from the plywood sheets used for the test samples.

At the commencement of the joint testing programme moisture content tests were taken immediately before and after testing and this continued for a period of two months. Following a review of the results of these tests, as for the timber samples, there was no significant difference in value between these stages and the protocol was changed to only take moisture content readings after the joint test was complete.

The plywood density varied from a minimum of 372.57 Kg/m^3 to a maximum of 749.10 Kg/m^3. For each set of 5 tests, an average and standard deviation was determined and the results of the maximum and minimum moisture content test sets together with the associated standard deviation and coefficient of variation are given in Table B2. Similar information is also given in Table B2 for the results of moisture content tests on the 5 tests with the lowest and the highest average moisture content and for the average moisture content for all of the samples tested. These tests show that within each test set the coefficient of variation is minimal and for the overall programme the dispersal of the samples is at 0.14.

Samples were tested to obtain the modulus of elasticity of the plywood parallel to the direction of the face grain and the results, including the average density of the test samples used, are given in the Table.

Property	Number of tests	Average results	Standard deviation	Coefficient of variation
$Density_L$	10	394.61 kg/m^3	20.56 kg/m^3	0.052
$Density_H$	10	714.46 kg/m^3	19.14 kg/m^3	0.027
$Density_{AV}$	1534	588.74 kg/m^3	82.34 kg/m^3	0.14
$M.C._L$	10	7.03%	0.06%	0.009
$M.C._H$	10	12.93%	0.67%	0.052
$M.C._{AV}$	1534	9.2%	2.43%	0.169
$E_{comp,//}$	5	7400.25N/mm^2	971.32 N/mm^2	0.131
Density	5	690.59 kg/m^3	15.18 kg/m^3	0.022

Table B2 Properties of Plywood

where:

$Density_L$ = the lowest average density test set.

$Density_H$ = the highest average density test set.

$Density_{AV}$ = the average density of all samples tested

$M.C._L$ = the lowest average moisture content test set.

$M.C._H$ = the highest average moisture content test set.

$M.C._{AV}$ = the average moisture content of all samples tested.

$E_{comp,//}$ = modulus of elasticity in compression parallel to the grain direction.

$E_{comp,\perp}$ = modulus of elasticity in compression perpendicular to the grain direction.

Nail Tests and Embedment tests

The testing programme was undertaken using three sizes of nail diameter with lengths selected to suit the joint configurations. At the outset of the programme nails manufactured by Rynail were used however, because of the extent of testing, additional nails were required and only Castlenails could be obtained. The programme was then structured such that Rynail nails were used for the timber/steel gusset tests, and Castlenail nails were used for the timber/plywood tests. The nails sizes were

2.35 mm diameter x 50mm long.
2.35 mm diameter x 60mm long.
3.00 mm diameter x 50mm long.
3.00 mm diameter x 60mm long.
3.35 mm diameter x 50mm long.
3.35 mm diameter x 60mm long.

The nails were checked for variations in diameter and length and it was found that the quality control of the length of the 2.65mm diameter Rynail nails was very poor and well outside the BS 1202 Part 1 [23] requirement of ± 0.8mm. To maintain control these nails were sized using a digital calliper. The remaining 3.00 and 3.35mm diameter Rynail nails and all sizes of the Castlenail nails were within the code length criteria. The nails were also checked for variation in nail diameter and both manufacturers were within the tolerance limit of ± 0.05 mm. In the analyses of all tests the actual nail sizes rather than the nominal sizes have been used and from control checks the average actual diameter of each nail size from each supplier was:

	Rynail	**Castlenail**
Nominal Diameter	**Actual Diameter**	**Actual Diameter**
mm	**mm**	**mm**
2.65	2.66	2.66
3.00	3.01	3.01
3.35	3.36	3.33

The nails were tested to obtain the tensile strength of the nail wire and the test results are summarised in Table B3. The results all exceed the 600 N/mm^2 value given in EC5 [11] and for all sets of tests the associated coefficient of variation was equal to or less than 0.04.

Tests were also carried out to obtain the modulus of elasticity of the nail wire in bending and the results are given in Table B3.

Nail size	Property	Number of tests	Average results	Standard deviation	Coefficient of variation
R2.65mm ø 60mm long	f_u	5	804.38 N/mm^2	12.98 N/mm^2	0.02
R3.00mm ø 60mm long	f_u	5	768.54 N/mm^2	15.29 N/mm^2	0.02
R3.35mm ø 60mm long	f_u	5	828.69 N/mm^2	24.36 N/mm^2	0.03
C2.65mm ø 60mm long	f_u	5	826.89 N/mm^2	8.06 N/mm^2	0.01
C3.00mm ø 60mm long	f_u	5	792.18 N/mm^2	32.78 N/mm^2	0.04
C3.35mm ø 60mm long	f_u	4	697.43 N/mm^2	18.42 N/mm^2	0.03
R2.65mm ø 60mm long	E_B	5	193453 N/mm^2	5139.61 N/mm^2	0.027

Table B3 Properties of nails

where:

Prefix R represents Rynail nails.

Prefix C represents Castlenail nails.

f_u = Tensile strength of the nail wire.

E_B = Modulus of Elasticity in Bending

Embedment tests were carried out in accordance with BS EN 383 [37]. The standard does not give details of the type of rig to be used and from a review of the testing rigs developed by Aune *et al* [17] and also Rodd *et al* [40] the rig shown in Appendix A was designed and fabricated.

The embedment strength divided by the associated density of the timber or plywood test sample is given in Table B4 for the three nail sizes together with the associated standard deviation and coefficient of variation. The average moisture content of the timber and plywood samples was 11.72% and 9.13%

respectively and as nail strength was not a factor in the embedment test, the tests were done using Rynail nails.

The BS EN sets an upper limit of four times the nail diameter as the maximum thickness of material to be used in an embedment test and the timber samples were sized in accordance with this requirement. For wood based products the code states that the test piece shall be the thickness of the panel as produced. Using 17mm plywood with 2.65mm nails gives an aspect ratio of 6.4, which well exceeds the limit of 4 given in the code and will lead to premature failure by bending in the nail rather than embedment failure of the plywood. Preliminary tests were undertaken using full thickness plywood and the nails did indeed fail by bending and the test results were unsatisfactory. The tests were redone using plywood reduced in thickness to approximate to four times the nail diameter and the results of these tests are given in the Table.

Nail diameter Material	Property	Number of tests	Average result	Standard deviation	Coefficient of variation
2.65mm ø in Timber	f_e	5	0.1052 N/mm^2/kg/m^3	0.0048 N/mm^2/kg/m^3	0.046
3.00mm ø in Timber	f_e	5	0.1261 N/mm^2/kg/m^3	0.0072 N/mm^2/kg/m^3	0.057
3.35mm ø in Timber	f_e	5	0.1027 N/mm^2/kg/m^3	0.0027 N/mm^2/kg/m^3	0.026
2.65mm ø in Plywood	f_e	5	0.1600 N/mm^2/kg/m^3	0.0105 N/mm^2/kg/m^3	0.066
3.00mm ø in Plywood	f_e	5	0.1480 N/mm^2/kg/m^3	0.0073 N/mm^2/kg/m^3	0.049
3.35mm ø in Plywood	f_e	5	0.1243 N/mm^2/kg/m^3	0.0050 N/mm^2/kg/m^3	0.040

Table B4 Embedment Test Results

where:

f_e = Embedment strength per unit density

APPENDIX C

JOINT TEST NAIL CONFIGURATIONS FOR SHEAR AND MOMENT TESTS

Legend:

Joint nailing configuration

- Denotes position of a pair of fully overlapping nails

  All dimensions are in millimetres

  The nailing configuration reference is given below the configuration diagram

  The number in the brackets below the reference is the number of pairs of fully overlapping nails in the joint

Lateral load tests

Direction of the lateral load applied to the joint

Moment tests

Direction of lateral load and moment applied to the joint

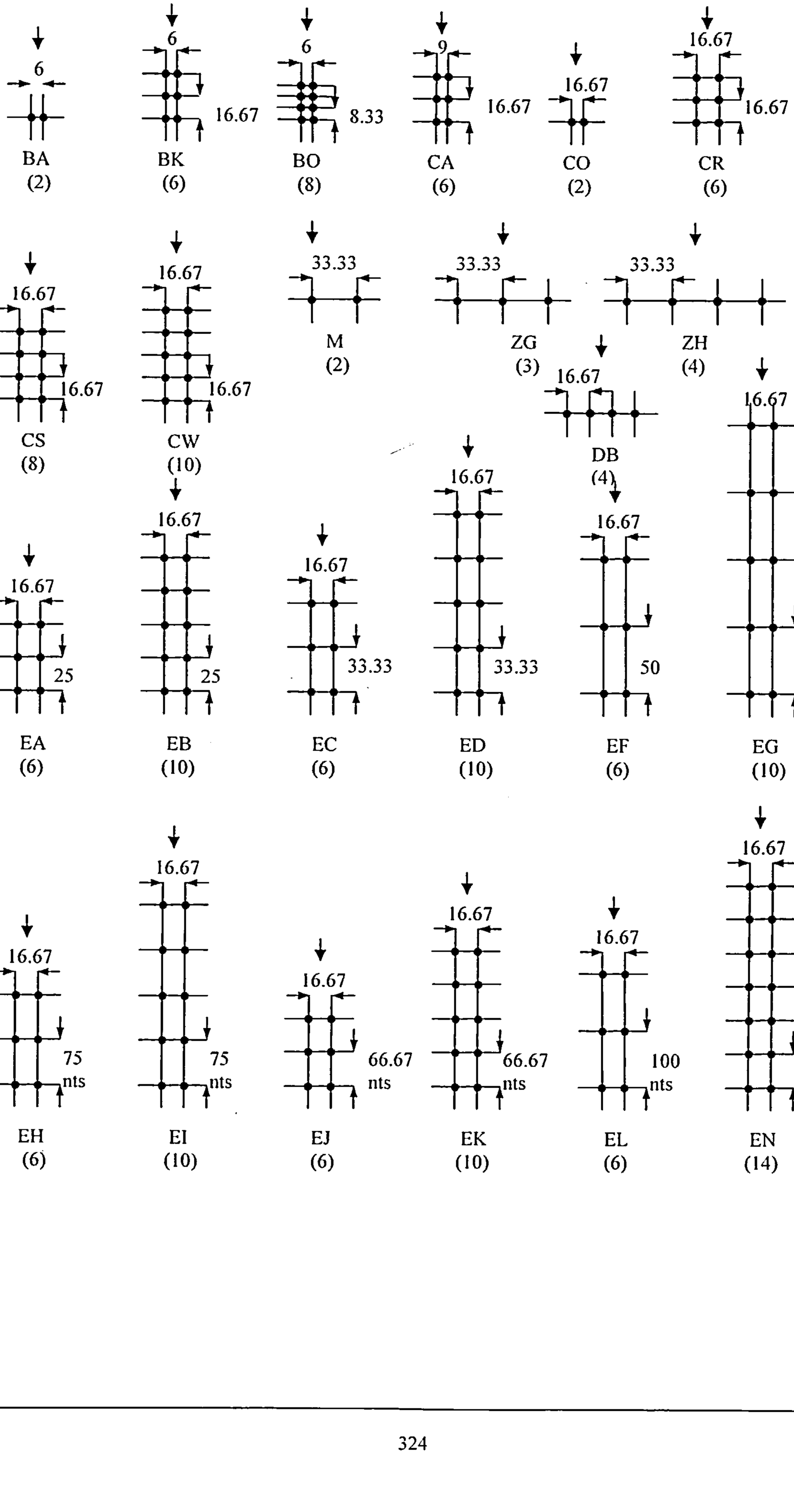
6
BA
(2)
6
16.67
BK
(6)
6
8.33
BO
(8)
9
16.67
CA
(6)
16.67
CO
(2)
16.67
16.67
CR
(6)
16.67
16.67
CS
(8)
16.67
16.67
CW
(10)
33.33
M
(2)
33.33
ZG
(3)
33.33
ZH
(4)
16.67
DB
(4)
16.67
25
16.67
25
16.67
33.33
16.67
33.33
16.67
50
16.67
50
EA
(6)
EB
(10)
EC
(6)
ED
(10)
EF
(6)
EG
(10)
16.67
75
nts
16.67
75
nts
16.67
66.67
nts
16.67
66.67
nts
16.67
100
nts
16.67
50
nts
EH
(6)
EI
(10)
EJ
(6)
EK
(10)
EL
(6)
EN
(14)

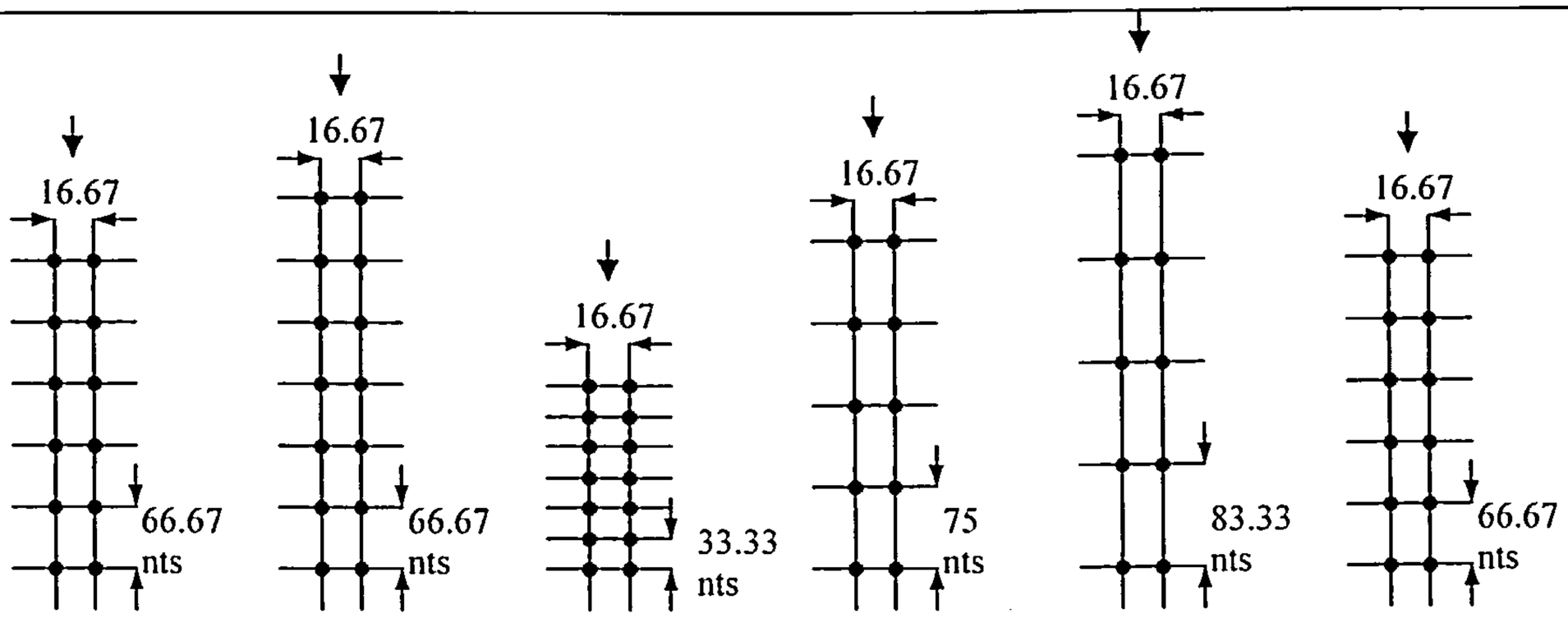
16.67
66.67
nts
EP
(12)
16.67
66.67
nts
EQ
(14)
16.67
33.33
nts
ER
(14)
16.67
75
nts
ES
(10)
16.67
83.33
nts
ET
(10)
16.67
66.67
nts
EU
(12)
16.67
33.33
nts
EV
(8)
16.67
23
nts
RT
(8)
16.67
26
nts
RU
(8)
16.67
28
nts
RV
(8)
16.67
66.67
nts
RY
(8)
16.67
75
nts
RZ
(8)
16.67
83.33
nts
RZA
(8)
16.67
33.33
nts
RZC
(12)
16.67
19
nts
RZD
(8)
16.67
38
nts
RZG
(6)
16.67
42
nts
RZH
(6)
16.67
33.33
nts
RZI
(8)
16.67
66.67
nts
RZJ
(8)

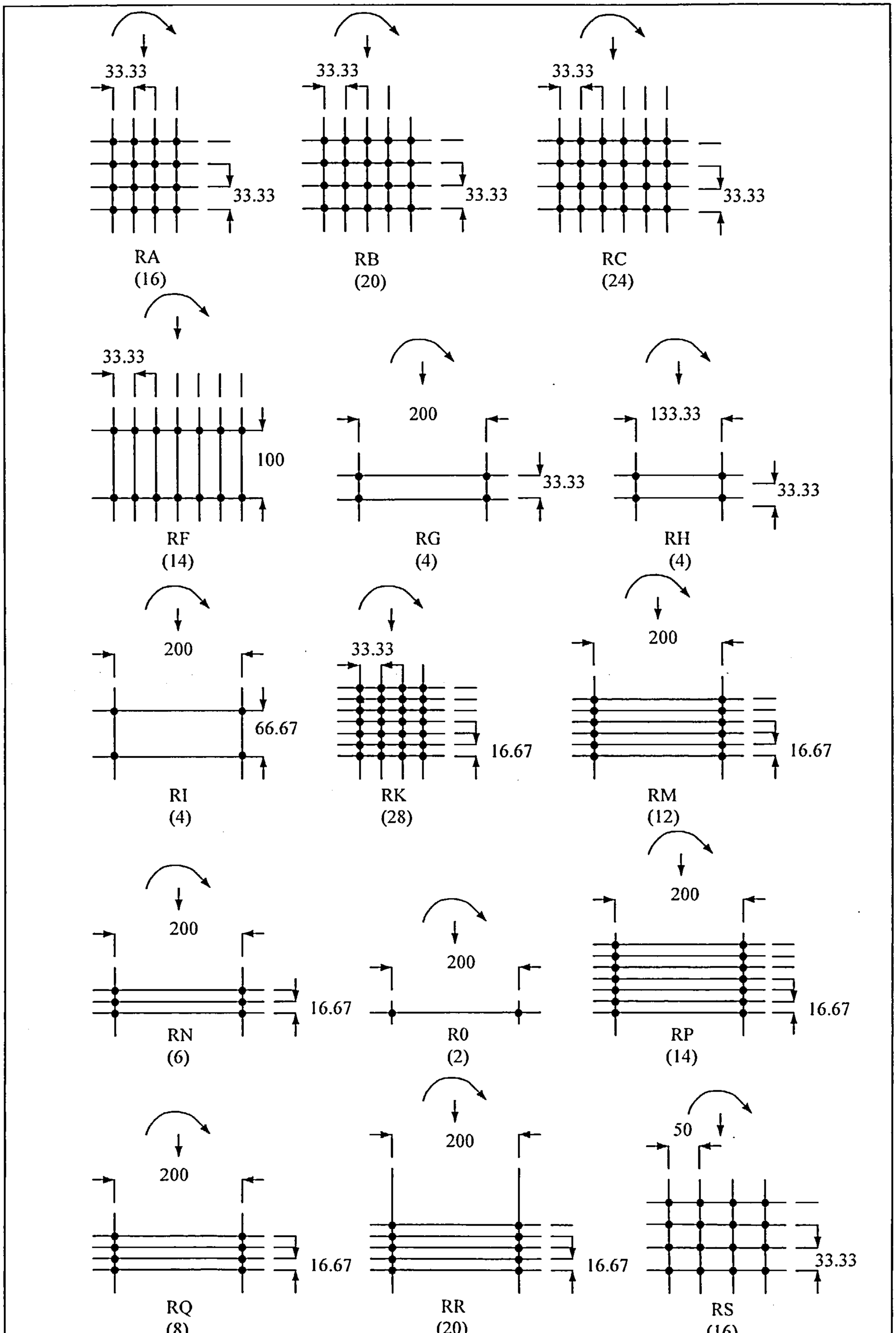
33.33
33.33
RA
(16)
33.33
33.33
RB
(20)
33.33
33.33
RC
(24)
33.33
100
RF
(14)
200
33.33
RG
(4)
133.33
33.33
RH
(4)
200
66.67
RI
(4)
33.33
16.67
RK
(28)
200
16.67
RM
(12)
200
16.67
RN
(6)
200
R0
(2)
200
16.67
RP
(14)
200
16.67
RQ
(8)
200
16.67
RR
(20)
50
33.33
RS
(16)

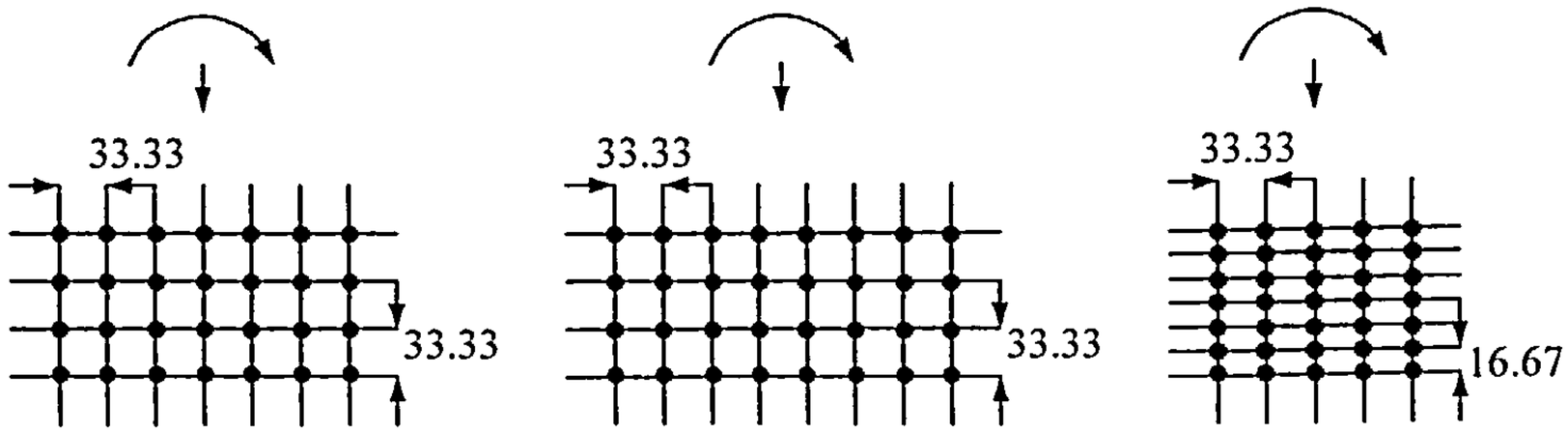
33.33
33.33
RD
(28)
33.33
33.33
RE
(32)
33.33
16.67
RL
(35)

APPENDIX D Data Acquisition System.

Measurements were taken by strain gauge based transducers positioned at predefined locations on the test samples and aligned to read in the required direction. The travel of the transducer spindle varied and gauges with 25mm travel and 50mm travel were used. Technical details of the transducers are given in Table D1.

Transducer	25mm spindle	50mm spindle
Average travel of spindle	25.9	50.2
Average non-linearity	± 0.1%	± 0.1%
Average strain sensitivity	1.24mv/mm	3.5mv/mm
Average volts sensitivity	6.4mv/v	6.4mv/v
Gauge factor	2.0	2.0

Table D1 Technical details of strain gauge based transducers

The load cell used was also strain gauge based, with a capacity of 50 kN.

The transducers and load cell were linked to System 5000, a data acquisition system manufactured by the Vishay Measurements Group, USA. The system comprised a scanner unit, Model 5100, fitted with 4 strain gauge based cards each having 5 channels for transducer and load cell connections. Because the scanner can accept data at a speed within 1 millisecond the system is able to accurately capture failure conditions under static loading. The maximum number of channels used for the test set up was nine and the data collected for each test was logged onto the system and transferred to disc for subsequent manual processing. For the test programme, transducer displacement and load cell readings were taken every 1 second. A visual output of the displacement curves was also used to provide assistance in monitoring the behaviour to failure or to the slip limit set for the test.

APPENDIX E *Moisture Content Function*

Over the period of the testing programme the moisture content of the timber used in the joints made with steel gusset plates ranged from 11% to 15.5% and strength tests were carried out to develop a moisture content factor which would take the effect of variation in moisture content on joint strength into account.

Sixteen clear samples were cut from adjacent sections of a timber plank. Eight were stored in the timber store area and eight in a laboratory for a period of seven weeks after which the average moisture content of the samples in the timber store area was 14.32% and in the laboratory area was 10.14%. Joints were then fabricated using steel gusset plates connected by 4 fully overlapping 3.35m diameter by 50mm long Rynail nails in nailing configuration CO and tested, all in one day.

The results of the tests on the two sets of joints are shown in Figure E1.

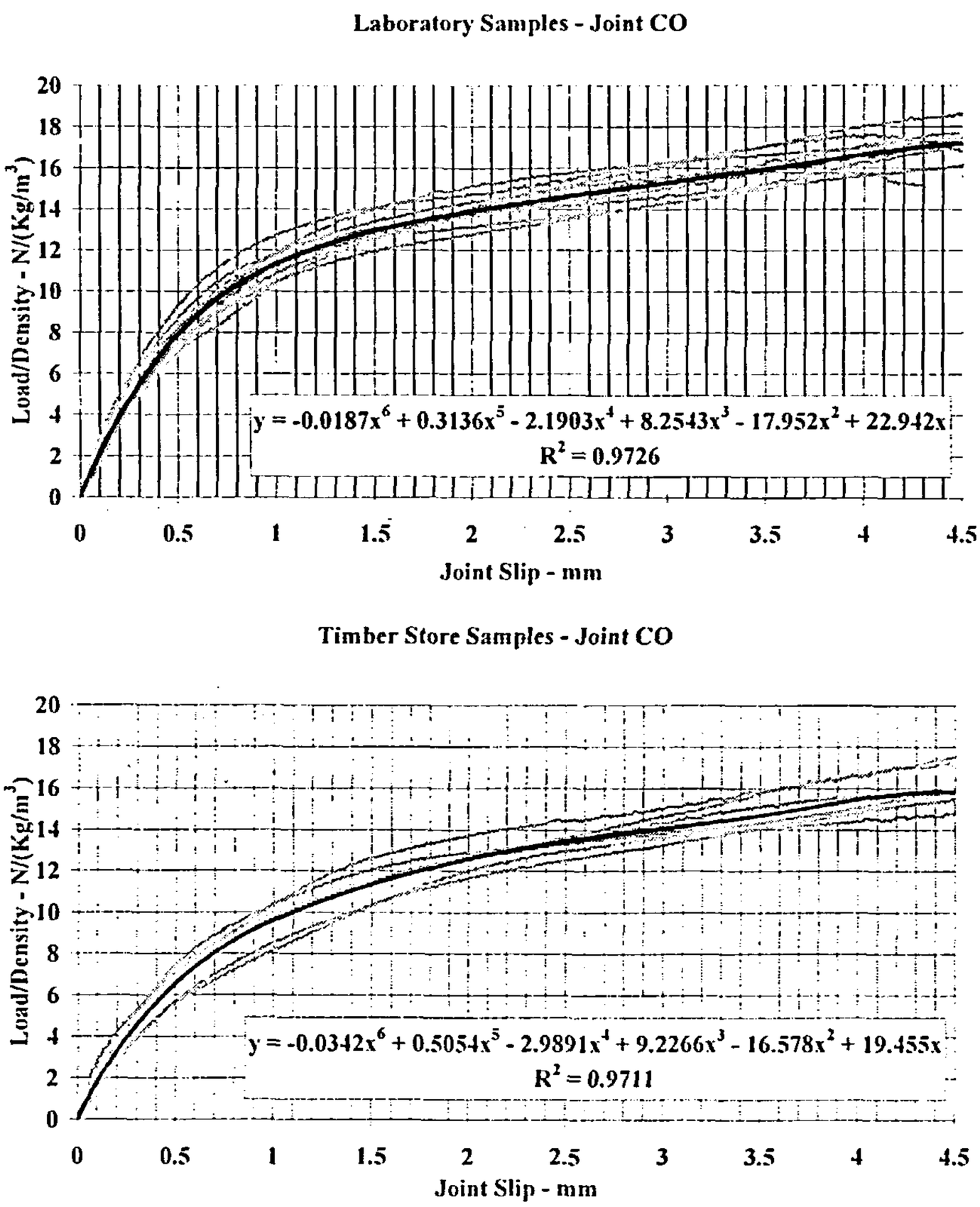

Figure E1 Results of moisture content tests on laboratory and timber Store samples

The coefficient of determination, R^2, for each set of tests was 0.97 and using a polynomial equation of the sixth order to give a close fit over the full range of joint slip with a linear least squares regression analysis, the best fit equations against the test data were:

Laboratory samples

$$f_L(x) = -0.0187x^6 + 0.3136x^5 - 2.1903x^4 + 8.2543x^3 - 17.592x^2 + 22.942x \quad \ldots(e1)$$

Timber Store samples

$$f_T(x) = -0.0342x^6 + 0.5954x^5 - 2.9891x^4 + 9.2266x^3 - 16.578x^2 + 19.455x \quad \text{...(e2)}$$

The regression graphs are superimposed on Figure E2 and from a comparison of the equations using a percentage mean deviation approach the relationship between the graphs is:

$$f_L(x) = 1.115\, f_T(x) \quad \text{....(e3)}$$

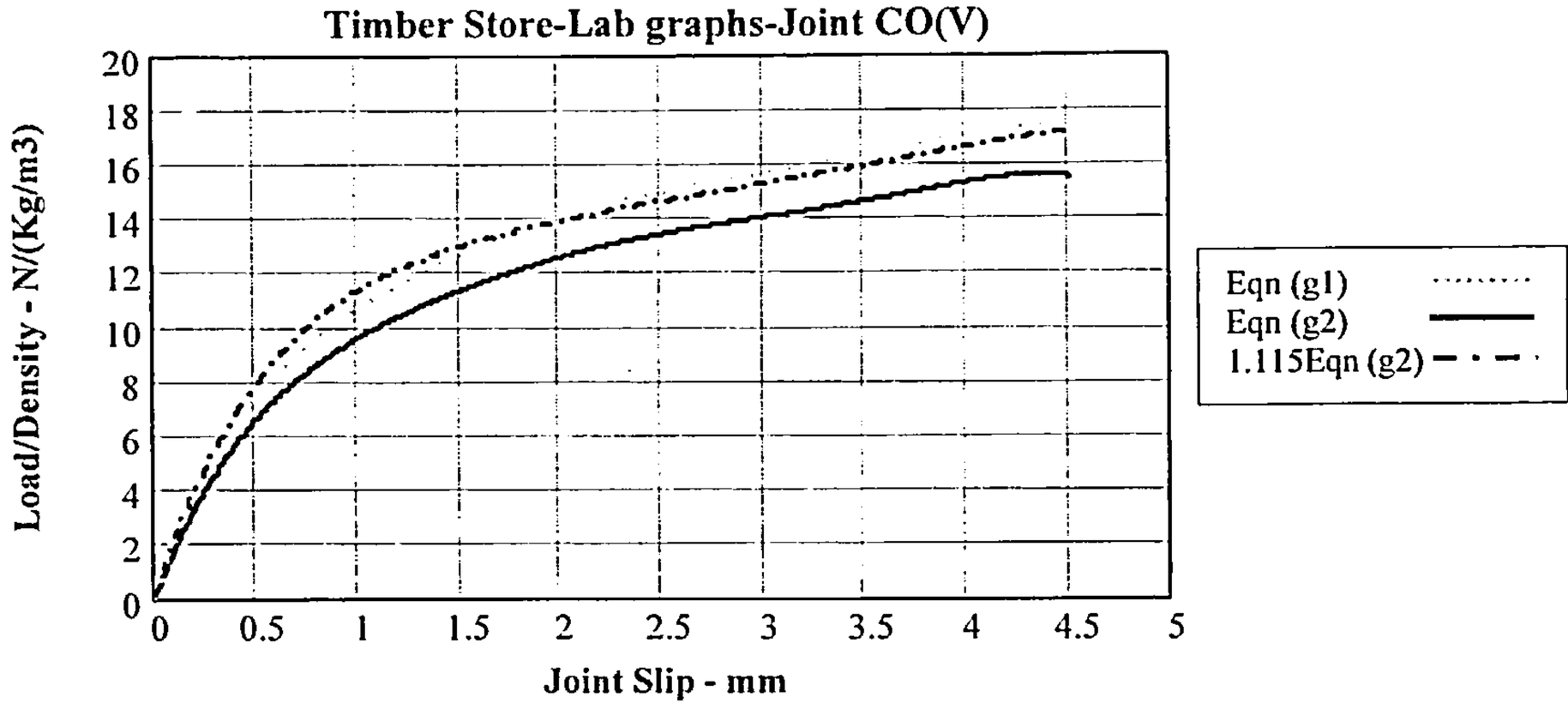

Figure E2 Comparison between Equations (g1) and (g2)

Equation (e3) is shown on Figure E2 by the dotted line graph.

Adopting a factor of unity for the joints with a moisture content of 14.32%, the factor for the joints with a moisture content of 10.14% will be 1.115 giving the relationship between strength and moisture content as stated in equation (e4) and shown graphically on Figure E3.

$$y(mc) = -0.0275(mc) + 1.394 \quad \text{....(e4)}$$

where $y(mc)$is the strength factor of the timber at a moisture content of mc.

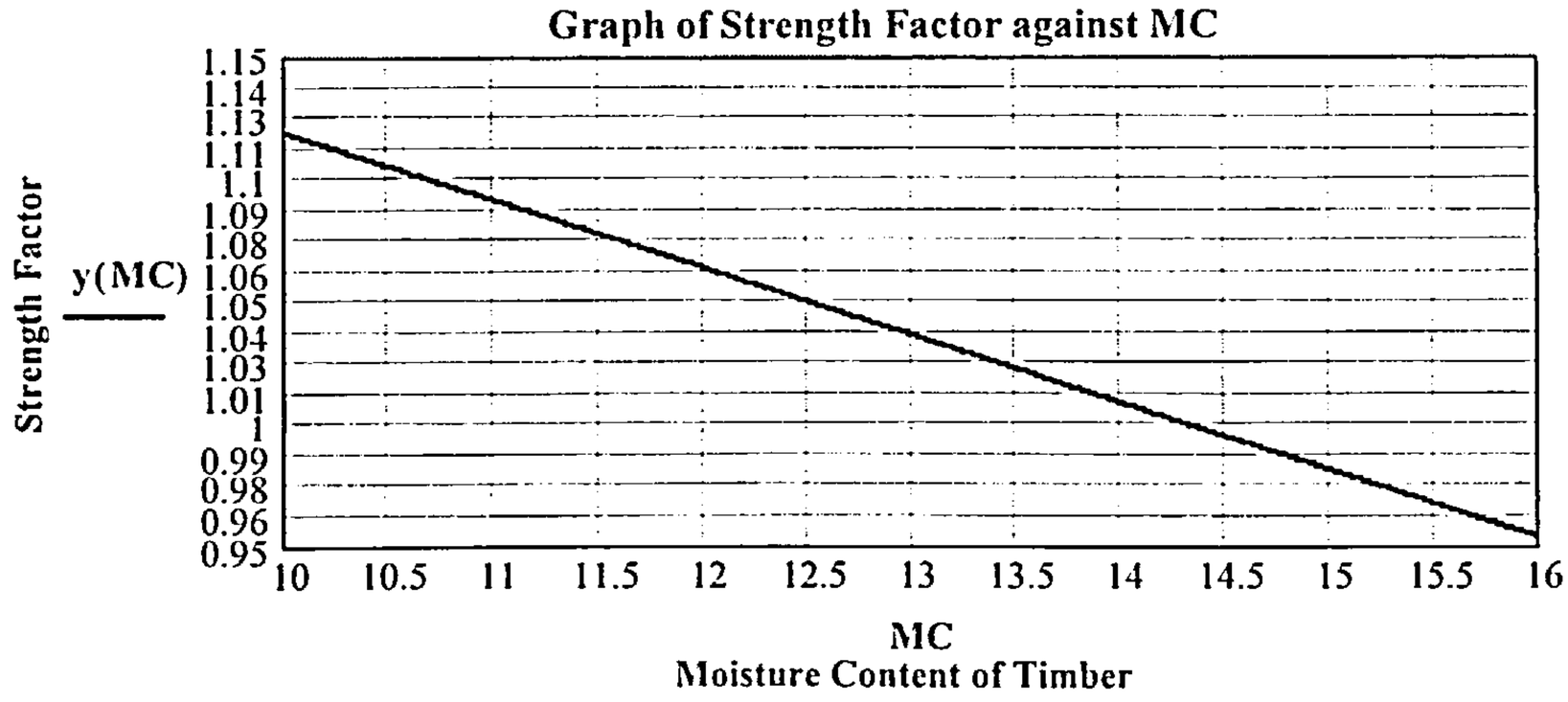

Figure E3 The relationship between Joint Strength and Moisture Content

For joints with a moisture content of 14.32% the factor is unity and for joints with a moisture content of 10.14% the factor is 1.115. To convert the strength of a joint using timber at any moisture content *mc* to

the strength it would have with timber at a moisture content of 12% is achieved by multiplying the joint strength by the following moisture content factor:

$$f(mc) = y(12)/y(mc) \qquad \text{.....(e5)}$$

For example, if the moisture content of the timber is 14%, to convert to the equivalent strength at 12% the factor to be applied to the joint strength equation is:

$$f(12)/f(14) = 1.0638/1.0088 = 1.0545$$

If the requirement is to convert from a joint strength at 12% to the strength at 14% the factor becomes:

$$f(14)/f(12) = 1.0088/1.0638 = 0.9483$$

APPENDIX F

A comparison of model, tests results and adjusted test results to take account of the effect of using average properties in joints with steel gusset plates.

The density and moisture content of each replicate in a set of samples for each joint nailing configuration will vary and comparing the joint strength derived from the semi-rigid model with results from the tests without making any adjustment to take account of the average properties of the test set, will introduce some error. The objective of this Appendix is to demonstrate that the effect of the error is small and can be ignored.

An example of the adjustment required to obtain a common baseline for joint nailing configuration EG connected by 3.35mm diameter nails is given using the tests results for samples S36L3A; 3B; 3C; 4B and 4C. The density, moisture content and $P_{3.2}$ value for each sample are given in Table F1 and the average density, moisture content and $P_{3.2}$ of the samples is 550.14 Kg/m^3, 13.11% and 38473.04 N, respectively.

Sample reference	Density kg/m^3	Moisture content %	$P_{3.2}$ N
S36L3A	531.27	13.35	38481.69
S36L3B	572.16	13.17	39370.00
S36L3C	537.84	13.01	39969.00
S36L4B	567.31	13.14	37662.52
S36L4C	542.14	12.87	36882.00
Average	**550.14**	**13.11**	**38473.04**

Table F1 Density and moisture content values of a set of samples used for joint configuration EG connected by 3.35mm diameter nails.

Without adjustment, using the average properties in the model results in the comparison of a graph based on an average density-moisture content of 550.14 kg/m^3-13.11% with 5 test results having density-moisture values of 531.27kg/m^3-13.35%; 572.16kg/m^3-13.17%; 537.84kg/m^3-13.01%; 567.31kg/m^3-13.14% and 542.14kg/m^3-12.87%.

From the analysis in Chapter 4 it has been shown that the joint strength is a linear function of the timber density and the moisture content and to achieve a true comparison each test result should be adjusted to give the strength at the average value of density and moisture content. This is done by multiplying the $P_{3.2}$ value of each test by the average density divided by the sample density then multiplying by the strength factor at the sample moisture content divided by the strength factor at the average moisture content. After modifying each replicate test result on this basis the adjusted results are given in Table F2.

$P_{3.2}$ at test N	$P_{3.2}$/Density N/(kg/m^3) (a)	(MC factor at test mc)/(MC factor at 13.11%) (b)	$P_{3.2}$/Density at average density and average mc. (c) = (a)×(b)	$P_{3.2}$ at average density and moisture content (c) × (550.14)	% Difference between the $P_{3.2}$ at test and the adjusted $P_{3.2}$ value
38461.69	72.4334	1.0267/1.0333	71.9677	39592.59	-2.89
39370.00	68.8094	1.0316/1.0333	68.6933	37791.2	+4.01
39969.00	74.3139	1.0360/1.0333	74.5049	40988.43	-2.55
37662.52	66.3879	1.0325/1.0333	66.3337	36493.07	+3.11
36882.00	68.0304	1.0399/1.0333	68.4620	37663.97	-2.12
38469.04	**Average**	**0.99999**	**69.9950**	**38507.18**	**-0.09**

Table F2 Adjustment of test results to obtain results based on average density and moisture content.

After adjusting the test results the average $P_{3.2}$ value of the test set is 38507.18 N, giving a marginally better fit than the test average of 38469.04 N against the model result of 38684.25 N.

This is a typical result and noting the negligible difference, the need to have to process the test results to equate to the average density and moisture content value can be ignored.

The graphs of the original test results and the adjusted results based on average density and moisture content plotted against the model (dotted line) are shown on Figure F1.

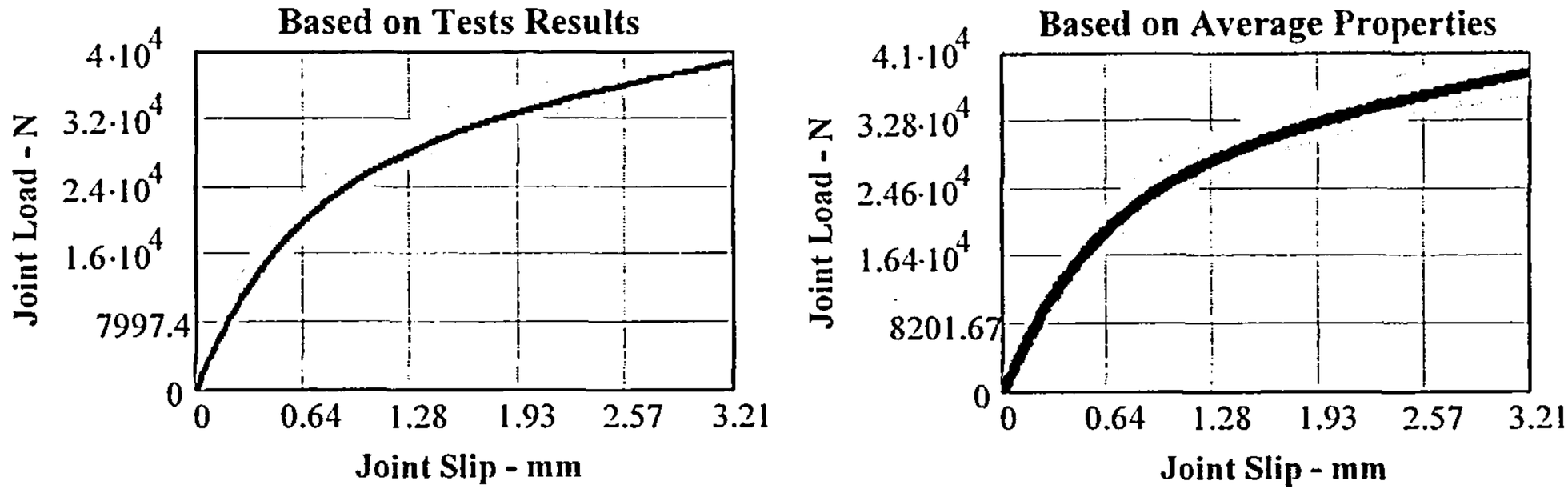

Figure F1 Plots of the Model graph against the Test results and the Average Properties results.

In this example converting to average properties results in a wider spread of the test graphs compared to the test results. This pattern will not be consistent across every test set and in other examples a closer fit will be obtained. However, as stated above, the average of the adjusted results will give a better fit.

APPENDIX G

The use of Mathcad to determine the centre of rotation when using a method based on the use of a variable centre of rotation.

Secant Stiffness Model 2

In this method the centre of joint rotation is adjusted to the position where the sum of the vertical forces is zero.The method also assumes the nail force is linearly proportional to the force in the maximum loaded nail. The method is applied to a joint with plywood gusset plates using nailing configuration RA. The simplified expression in equation (62) has been used in the example.

Joint - RA

The co-ordinates of the nails are:

$i := 1,2..16$

$x0_1 := -50$	$x0_2 := -16.67$	$x0_3 := 16.67$	$x0_4 := 50$
$y0_1 := 50$	$y0_2 := 50$	$y0_3 := 50$	$y0_4 := 50$
$x0_5 := -50$	$x0_6 := -16.67$	$x0_7 := 16.67$	$x0_8 := 50$
$y0_5 := 16.67$	$y0_6 := 16.67$	$y0_7 := 16.67$	$y0_8 := 16.67$
$x0_9 := -50$	$x0_{10} := -16.67$	$x0_{11} := 16.67$	$x0_{12} := 50$
$y0_9 := -16.67$	$y0_{10} := -16.67$	$y0_{11} := -16.67$	$y0_{12} := -16.67$
$x0_{13} := -50$	$x0_{14} := -16.67$	$x0_{15} := 16.67$	$x0_{16} := 50$
$y0_{13} := -50$	$y0_{14} := -50$	$y0_{15} := -50$	$y0_{16} := -50$

Check Calculation $\sum_{i=1}^{16} x0_i = 0$ $\sum_{i=1}^{16} y0_i = 0$

Generic Load - Displacement relationship for timber joints with plywood gusset plates

$d := 2.66$	Nail Dia - mm	$Yu := 827$	Ultimate Strength of Nail- N/mm2
$\delta max := 3.2$	Maximum movement of extreme nail - mm	$lever := 513$	mm
$Swe := 0.56796$	SG of timber	$Spe := 0.63519$	SG of Plywood
$t4 := 40.58$	Timberside Penetration - mm	$t3 := 11.52$	Nail penetration in gusset - mm
$n := 2$	Number of nails at a point	$Sp := 33.33$	Row Spacing - mm

$$G := 2\cdot\left[\left(0.000912\cdot Yu - 0.46409\right)\cdot\frac{t4}{(t4+t3)}\cdot Swe + \left(2.46409 - 0.000912\cdot Yu\right)\cdot\frac{t3}{(t4+t3)}\cdot Spe\right]$$

$m := 1,2..800$ mm Density function

$ro_m := \frac{-1}{10}\cdot m$ $r_{i,m} := \left[\left[\left(x0_i\right) - \left(ro_m\right)\right]^2 + \left(y0_i - \sum_{i=1}^{16} y0_i\right)^2\right]^{0.5}$

Value of the nail radius when the centre of rotation is at ro(m) mm.

The effect of spacing normal to the grain using the Hankinson expression:

$$Sp2_i := \frac{\left(0.009489 \cdot \frac{Sp}{d} + 0.839\right)}{\left(0.009489 \cdot \frac{Sp}{d} + 0.839\right) \cdot \left(\left|\sin\left(\text{angle}\left(x0_i, y0_i\right)\right)^2\right| + \left|\cos\left(\text{angle}\left(x0_i, y0_i\right)\right)^2\right|\right)}$$

$$C(G) := G \cdot 1000 \cdot \frac{Yu}{827} \cdot (1.148 \cdot 2) \cdot \left[0.1113 \cdot (d)^{2.236}\right]$$

The generic relationship for moment:

The moment on the joint M(m), is:

$$M_m := \frac{n}{2} \cdot \left[C(G) \cdot \left[\sum_{i=1}^{16} \left(1 - e^{-1.9 \cdot \delta max}\right)^{0.6} \cdot (0.1 \cdot \delta max + 0.68) \cdot \frac{\left(r_{i,m}\right)^2}{\max\left(r_{16,m}\right)} \cdot Sp2_i \right] \right]$$

$P_m := \frac{M_m}{(lever - ro_m)}$ N — Where P(m) is the force required on the beam at a lever arm of ro(m) mm to induce a moment M(m).

$$F_m := \frac{n}{2} \cdot \left[C(G) \cdot \left[\sum_{i=1}^{16} \left(1 - e^{-1.9 \cdot \delta max}\right)^{0.6} \cdot (0.1 \cdot \delta max + 0.68) \cdot \frac{\left(x0_i - ro_m\right)}{r_{i,m}} \cdot Sp2_i \right] \right]$$

Where F(m) is the sum of the vertical component of the shear force of all of the nails in the joint based on the maximum stressed nail being displaced by a maximum of 3.2mm.

$R_m := P_m - F_m$ N — This relationship is the basic equation for static equilibrium ie the sum of the vertical forces must equal ZERO. Equilibrium is achieved when R(m) is ZERO.

$$t(R, thres) := \left| \begin{array}{l} j \leftarrow 0 \\ \text{while } R_j \geq thres \\ \quad j \leftarrow j + 1 \\ j \end{array} \right.$$

$t(R, -0.01) = 60$ — The value of m at which the difference between P and F is negative.

$m := t(R, -0.01) - 1$ — The value of m just before P-F becomes negative

$ro_m = -5.9$ mm — The position of the centre of rotation relative to the geometric centre of the joint

$P_m = 1.897 \times 10^3$ N $\qquad F_m = 1.878 \times 10^3$ N

$M_m = 9.844 \times 10^5$ Nmm — Where M(m) is the value of the moment in the joint when the slip in the maximum loaded nail is 3.2mm

APPENDIX H

An example of the application of moment model Non- Linear 2.

Non-Linear Method 2

In this method the load-displacement relationship of each nail is modelled using the direct shear equations developed in Chapter 4. The slip in each nail is proportional to the slip of the nail with the maximum radius from the centre of rotation. The centre of rotation varies and its position is determined by the application of the equations of equilibrium. The simplified expression in equation (62) has been used in the example.

The method is applied to a joint with nailing configuration RN.

Joint - RN

$i := 1,2..6$

$x0_1 := -100$ $x0_2 := 100$ $x0_3 := -100$ $x0_4 := 100$ $x0_5 := -100$ $x0_6 := 100$

$y0_1 := 16.67$ $y0_2 := 16.67$ $y0_3 := 0$ $y0_4 := 0$ $y0_5 := -16.67$ $y0_6 := -16.67$

Check Calculation:

$$\sum_{i=1}^{6} x0_i = 0 \qquad \sum_{i=1}^{6} y0_i = 0$$

Generic Load - Displacement relationship for timber joints with plywood gusset plates

$d := 3.01$ Nail Dia - mm $Yu := 792$ Ultimate Strength of Nail- N/mm2

$\delta max := 3.2$ Maximum movement of extreme nail- mm $lever := 426.67$ mm

$S4 := 0.56864$ SG of wood $S3 := 0.61151$ SG of Plywood

$t4 := 41.35$ Woodside Penetration - mm $t3 := 17.67$ Nail penetration in plywood gusset - mm

$n := 2$ Number of nails at a point $Sp := 16.67$ Row Spacing - mm

$$G := 2\cdot\left[(0.000912\cdot Yu - 0.46409)\cdot\frac{t4}{(t4+t3)}\cdot S4 + (2.46409 - 0.000912\cdot Yu)\cdot\frac{t3}{(t4+t3)}\cdot S3\right]$$ Density Function

$m := 1,2..800$

$$ro_m := \frac{-1}{10}\cdot m \qquad \overline{r_{i,m}} := \left[\left[\left(x0_i\right) - \left(ro_m\right)\right]^2 + \left(y0_i - \sum_{i=1}^{6} y0_i\right)^2\right]^{0.5}$$

Value of the nail radius when the centre of rotation is at ro(m) mm.

The effect of spacing normal to the grain using the Hankinson expression:

$$Sp2_i := \frac{\left(0.009489\cdot\frac{Sp}{d} + 0.839\right)}{\left(0.009489\cdot\frac{Sp}{d} + 0.839\right)\cdot\left(\left|\sin\left(angle\left(x0_i, y0_i\right)\right)^2\right|\right) + \left|\cos\left(angle\left(x0_i, y0_i\right)\right)^2\right|}$$

To simplify the equations the constants can be represented as follows:

$$C := G\cdot 1000\cdot\frac{Yu}{827}\cdot\left(\frac{1.148}{1}\cdot 2\right)\cdot\left[0.1113\cdot(d)^{2.236}\right]\cdot\frac{n}{2}$$

Generic relationship for the moment in the joint M(m):

$$M_m := C\cdot\left[\sum_{i=1}^{6}\left(1-e^{-1.9\cdot\delta max\cdot\frac{r_{i,m}}{max\left(r_{6,m}\right)}}\right)^{0.6}\cdot\left(0.1\cdot\delta max\cdot\frac{r_{i,m}}{max\left(r_{6,m}\right)}+0.68\right)\cdot r_{i,m}\cdot Sp2_i\right]$$

$$P_m := \frac{M_m}{\left(lever - ro_m\right)} \quad N$$

P(m) is the force required on the beam at a lever arm of ro(m) mm to induce a moment M(m).

$$F_m := C\cdot\left[\sum_{i=1}^{6}\left(1-e^{-1.9\cdot\delta max\cdot\frac{r_{i,m}}{max\left(r_{6,m}\right)}}\right)^{0.6}\cdot\left(0.1\cdot\delta max\cdot\frac{r_{i,m}}{max\left(r_{6,m}\right)}+0.68\right)\cdot\frac{\left(x0_i - ro_m\right)}{r_{i,m}}Sp2_i\right]$$

F(m) is the sum of the vertical component of the shear force per nail in the joint and is based on the maximum loaded nail being displaced by 3.2mm.

$R_m := P_m - F_m$ N — This relationship is the basic equation for static equilibrium ie the sum of the vertical forces must equal ZERO. R(m) is the difference between F(m) and the cantilever force P(m).
Equilibrium is achieved when R(m) is ZERO, giving the position of the centre of rotation.

$t(R, thres) :=$
- $j \leftarrow 0$
- while $R_j \geq thres$
  - $j \leftarrow j + 1$
- j

$t(R,-0.01) = 629$ — The value of (m) at which the difference between P and F is negative.

$m := t(R,-0.01) - 1$ — The value of (m) just before P-F becomes negative

$ro_m = -62.8$ mm — The position of the centre of rotation relative to the geometric centre of the joint

$P_m = 2.506 \times 10^3$ N $\qquad F_m = 2.506 \times 10^3$ N

$M_m = 1.227 \times 10^6$ Nmm The value of the moment at 3.2mm slip in joint RN.

APPENDIX I

An example of the application of moment model Non- Linear 2 incorporating the grain direction factor.

Non-Linear 2 model - incorporating the grain direction factor

In this method the load-displacement of each nail is modelled using the direct shear equations developed in Chapter 4. The slip in each nail is proportional to the slip in the nail with the maximum radius from the centre of rotation. The centre of rotation varies and its position is determined by the equations of equilibrium. The grain direction factor is incorporated into the spacing factor Sp2i. The simlified expression in equation (62) has been used in the example.

Joint - RA

$i := 1, 2.. 16$

$x0_1 := -50$ $x0_2 := -16.67$ $x0_3 := 16.67$ $x0_4 := 50$

$y0_1 := 50$ $y0_2 := 50$ $y0_3 := 50$ $y0_4 := 50$

$x0_5 := -50$ $x0_6 := -16.67$ $x0_7 := 16.67$ $x0_8 := 50$

$y0_5 := 16.67$ $y0_6 := 16.67$ $y0_7 := 16.67$ $y0_8 := 16.67$

$x0_9 := -50$ $x0_{10} := -16.67$ $x0_{11} := 16.67$ $x0_{12} := 50$

$y0_9 := -16.67$ $y0_{10} := -16.67$ $y0_{11} := -16.67$ $y0_{12} := -16.67$

$x0_{13} := -50$ $x0_{14} := -16.67$ $x0_{15} := 16.67$ $x0_{16} := 50$

$y0_{13} := -50$ $y0_{14} := -50$ $y0_{15} := -50$ $y0_{16} := -50$

Check Calculation $\sum_{i=1}^{16} x0_i = 0$ $\sum_{i=1}^{16} y0_i = 0$

Generic load - displacement relationship for timber joints with plywood gusset plates

$d := 2.66$ Nail Dia - mm $Yu := 827$ Ultimate Strength of Nail- N/mm2

$\delta max := 3.2$ Maximum movement of extreme nail- mm $lever := 509$ mm

$S4 := 0.55477$ SG of wood $S3 := 0.64598$ SG of Plywood

$t4 := 41.65$ timberside penetration - mm $t3 := 17.61$ Nail penetration in gusset - mm

$n := 2$ Number of nails at a point $Sp := 33.33$ Row Spacing - mm

$$G := 2\cdot\left[(0.000912\cdot Yu - 0.46409)\cdot\frac{t4}{(t4+t3)}\cdot S4 + (2.46409 - 0.000912\cdot Yu)\cdot\frac{t3}{(t4+t3)}\cdot S3\right]$$ Density function

$m := 1, 2.. 200$ $ro_m := \frac{-1}{10}\cdot m$ mm The distance of the centre of rotation from the centoid of the nailing configuration

$$r_{i,m} := \left[\left[(x0_i) - (ro_m)\right]^2 + \left(y0_i - \sum_{i=1}^{16} y0_i\right)^2\right]^{0.5}$$ Value of the nail radius when the centre of rotation is at ro(m) mm.

$\beta := 90$ degrees The angle of plane of the grain of the timber relative

$$fTR := \frac{0.91}{\sin(\beta \cdot deg)^2 + 0.91 \cdot \cos(\beta \cdot deg)^2}$$ The grain direction factor

The effect of spacing normal to the grain using the Hankinson formula and including for the effect of the grain direction factor:

$$Sp2_i := \frac{\left(0.009489 \cdot \frac{Sp}{d} + 0.838684\right) \cdot fTR}{\left(0.009489 \cdot \frac{Sp}{d} + 0.838684\right) \cdot \left(\left|\sin\left(angle\left(x0_i, y0_i\right)\right)^2\right|\right) + \left|\cos\left(angle\left(x0_j, y0_j\right)\right)^2\right|}$$

To simplify the equations the constants can be represented as follows:

$$C := \frac{n}{2} \cdot G \cdot 1000 \cdot \frac{Yu}{827} \cdot (1.148 \cdot 2) \cdot \left[0.1113186 \cdot (d)^{2.2363}\right]$$

The Generic Relationship for Moment M(m) is:

$$M_m := C \cdot \left[\sum_{i=1}^{16} \left(1 - e^{-1.9 \cdot \delta max \cdot \frac{r_{i,m}}{\max\left(r_{16,m}\right)}}\right)^{0.6} \cdot \left(0.1 \cdot \delta max \cdot \frac{r_{i,m}}{\max\left(r_{16,m}\right)} + 0.68\right) \cdot r_{i,m} \cdot Sp2_i\right] \quad Nmm$$

$$P_m := \frac{M_m}{\left(lever - ro_m\right)} \quad N$$ Where Pm is the force required on the beam at a lever arm of (lever-ro(m)) mm to induce a moment M(m).

$$F_m := C \cdot \left[\sum_{i=1}^{16} \left(1 - e^{-1.9 \cdot \delta max \cdot \frac{r_{i,m}}{\max\left(r_{16,m}\right)}}\right)^{0.6} \cdot \left(0.1 \cdot \delta max \cdot \frac{r_{i,m}}{\max\left(r_{16,m}\right)} + 0.68\right) \cdot \frac{\left(x0_i - ro_m\right)}{r_{i,m}} \cdot Sp2_i\right]$$

Where F(m) is the sum of the vertical component of the shear force per nail for the joint and is based on the maximum loaded nail being displaced by 3.2mm.

$R_m := P_m - F_m$ N This relationship is the basic equation for static equilibrium ie the sum of the vertical forces must equal ZERO.
Where R(m) is the difference between F(m) and the cantilever force P(m).
Equilibrium is achieved when Rm is ZERO, givin the position of the point of rotation.

$$t(R, thres) := \begin{| j \leftarrow 0 \\ | \text{while } R_j \geq thres \\ | \quad j \leftarrow j + 1 \\ | j$$

$t(R, -0.01) = 69$ The value of m at which the difference between P and F is negative.

$m := t(R, -0.01) - 1$ The value of m just before P-F becomes negative

$ro_m = -6.8$ The position of the centre of rotation relative to the geometric centre of the joint

$P_m = 2.523 \times 10^3$ N $F_m = 2.509 \times 10^3$ N

$M_m = 1.301 \times 10^6$ Nmm The value of the moment at 3.2mm slip in joint RA.

MISSING
PAGE/
PAGES
HAS NO
CONTENT

APPENDIX J

The use of Mathcad to derive the rigidity factors for a joint with plywood gusset plates and fully overlapping nails.

The following is the non linear approach used to derive the fixity factors for plywood joints using fully overlapping nails, as referred to in Chapter 7. It is applied to the characteristic strength moment equation of the joint.

Joint RA This is the nailing configuration used in the analysis and the co-ordinates of each nail relative to the centroid of the nailing configuratio is given below

$i := 1,2..16$

$x0_1 := -50$ $x0_2 := -16.67$ $x0_3 := 16.67$ $x0_4 := 50$

$x0_5 := -50$ $x0_6 := -16.67$ $x0_7 := 16.67$ $x0_8 := 50$

$x0_9 := -50$ $x0_{10} := -16.67$ $x0_{11} := 16.67$ $x0_{12} := 50$

$x0_{13} := -50$ $x0_{14} := -16.67$ $x0_{15} := 16.67$ $x0_{16} := 50$

$y0_1 := 50$ $y0_2 := 50$ $y0_3 := 50$ $y0_4 := 50$

$y0_5 := 16.67$ $y0_6 := 16.67$ $y0_7 := 16.67$ $y0_8 := 16.67$

$y0_9 := -16.67$ $y0_{10} := -16.67$ $y0_{11} := -16.67$ $y0_{12} := -16.67$

$y0_{13} := -50$ $y0_{14} := -50$ $y0_{15} := -50$ $y0_{16} := -50$

$\sum_{i=1}^{16} x0_i = 0$ $\sum_{i=1}^{16} y0_i = 0$ Check calculation the summation of the coordinates equal zero

Data for timber joints with plywood gusset plates

$d := 2.66$ Nail Dia - mm $Yu := 827$ Ultimate strength of Nail- N/mm2

$n := 2$ Number of nails at a point $t4 := 41$ Timberside penetration - mm

$S4 := 0.45$ SG of timber $S3 := 0.4$ SG of Plywood

$t3 := 17.5$ Nail penetration in plywood gusset - mm $Sp := 33.33$ Row Spacing - mm

$span := 3000$ Beam span - mm

$$Sp2_i := \frac{\left(0.0095\cdot\frac{Sp}{d} + 0.839\right)}{\left(0.0095\cdot\frac{Sp}{d} + 0.839\right)\cdot\left(\left|\sin\left(angle\left(x0_i, y0_i\right)\right)^2\right|\right) + \left|\cos\left(angle\left(x0_i, y0_i\right)\right)^2\right|}$$ Spacing factor

$$G := 2\cdot\left[(0.000912\cdot Yu - 0.46409)\cdot\frac{t4}{(t4 + t3)}\cdot S4 + (2.46409 - 0.000912\cdot Yu)\cdot\frac{t3}{(t4 + t3)}\cdot S3\right]$$ Density function

$E := 9000$ E value of timber - N/mm2 $t := 43$ Timber thickness - mm

$depth := 143$ Timber depth - mm $I := \frac{t\cdot depth^3}{12}$ Second moment of area of timber - mm4

Analysis

$j := 1, 2 .. 2250$ The number of iterations to be used

$r_{j,i} := \left[\left(x0_i\right)^2 + \left(y0_i\right)^2 \right]^{0.5}$ The radius of each nail from the nailing group centroid

$\Delta_{j,i} := r_{j,i} \cdot \frac{\left(\frac{j}{500}\right)}{\max(r)}$ The value of nail displacement at each nail position at increment j.

$C := \left[G \cdot 1000 \cdot Yu \cdot \left(\frac{1.911}{10000}\right) \cdot (d)^{2.236} \right]$ Constant used to reduce the size of equation for Kj,i

The tangential stiffness of the M-Slip curve at nail position i at each increment j:

$$K_{j,i} := \frac{n}{2} \cdot C \cdot \left(Sp2_i\right) \cdot \left[1 - e^{-1.41 \cdot \left(\Delta_{j,i}\right)}\right]^{0.54} \cdot \left[\frac{0.7614 \cdot \left[0.121 \cdot \left(\Delta_{j,i}\right) + 1.0\right] \cdot e^{-1.41 \cdot \left(\Delta_{j,i}\right)}}{\left[1 - e^{-1.41 \cdot \left(\Delta_{j,i}\right)}\right]} + 0.121 \right]$$

$$Kr_j := \sum_{i=1}^{16} K_{j,i} \cdot \left(r_{j,i}\right)^2$$ The rotational stiffness of the full joint at each increment j.

$$\gamma_j := \frac{(1)}{(1) + \frac{3 \cdot E \cdot I}{Kr_j \cdot span}}$$ The rigidity factor for the joint $\gamma_1 := 0.828$

APPENDIX K

An example of the determination of the reduced end fixing moment and the secant rotation stiffness coefficient, using joints with steel gusset plates and fully overlapping nails at each end of a prismatic beam.

The following is the non linear approach used to derive the modified end fixing moment and the secant rotational stiffness coefficient for a point load at mid-span of a beam with semi-rigid joints of the same stiffness at each end. The joints are formed using steel gusset plates with a gap between the gusset plates and the timber. The characteristic value of the joint equation is used.

Joint RA

$i := 1,2..16$

$x0_1 := -50$ $x0_2 := -16.67$ $x0_3 := 16.67$ $x0_4 := 50$

$x0_5 := -50$ $x0_6 := -16.67$ $x0_7 := 16.67$ $x0_8 := 50$

$x0_9 := -50$ $x0_{10} := -16.67$ $x0_{11} := 16.67$ $x0_{12} := 50$

$x0_{13} := -50$ $x0_{14} := -16.67$ $x0_{15} := 16.67$ $x0_{16} := 50$

$y0_1 := 50$ $y0_2 := 50$ $y0_3 := 50$ $y0_4 := 50$

$y0_5 := 16.67$ $y0_6 := 16.67$ $y0_7 := 16.67$ $y0_8 := 16.67$

$y0_9 := -16.67$ $y0_{10} := -16.67$ $y0_{11} := -16.67$ $y0_{12} := -16.67$

$y0_{13} := -50$ $y0_{14} := -50$ $y0_{15} := -50$ $y0_{16} := -50$

$k_i := \left[\left(x0_i\right)^2 + \left(y0_i\right)^2\right]^{0.5}$ Check Calculation $\sum_{i=1}^{16} x0_i = 0$ $\sum_{i=1}^{16} y0_i = 0$

max(k) = 70.711

Data for Timber Joints with steel gusset plates

$d := 2.66$ Nail Dia - mm $Yu := 827$ Ultimate strength of Nail- N/mm2

$\delta max := 3.2$ Maximum movement of the extreme nail in the joint - mm $G := 0.450$ SG of timber

$t4 := 41$ Timberside Penetration - mm $n := 2$ Number of nails at a point

$Sp := 33.33$ Row Spacing - mm

$$Sp2_i := \frac{\left(0.013 \cdot \frac{Sp}{d} + 0.743\right)}{\left(0.013 \cdot \frac{Sp}{d} + 0.743\right) \cdot \left(\left|\sin\left(angle\left(x0_i, y0_i\right)\right)^2\right|\right) + \left|\cos\left(angle\left(x0_i, y0_i\right)\right)^2\right|}$$

Row spacing factor

$E := 9000$ E value of timber - N/mm2 $I := \frac{43 \cdot 143^3}{12}$ Second moment of area of timber - mm4

$L := 2000$ Span of beam - mm

Analysis

$i := 1,2..16$ $j := 1,2..1600$

The characteristic moment taken by the connection will be:

$$C := G\cdot 1000\cdot\frac{Yu}{1000}\cdot(1.373)\cdot\left[(d)^{1.45}\right]$$

$$Msr_i := \frac{n}{2}\cdot\left[C\cdot\left[\sum_{i=1}^{16}\left(1-e^{-1.71\cdot\frac{k_i}{\max(k)}\cdot\delta max}\right)^{0.93}\cdot\left[0.1\cdot\left(\frac{k_i}{\max(k)}\cdot\delta max\right)+0.68\right]\cdot k_i\cdot\left(Sp2_i\right)\right]\right]$$

$Msr_1 := 1.456\times 10^{6}$ Maximum moment in joint at the ULS in Nmm

$$r_{j,i} := \left[\left(x0_i\right)^2+\left(y0_i\right)^2\right]^{0.5} \qquad \Delta_{j,i} := r_{j,i}\cdot\frac{\left(\frac{j}{500}\right)}{\max(r)}$$

The tangential stiffness of the Moment-Rotation curve will be:

$$K1_{j,i} := \frac{n}{2}\cdot(C)\cdot\left(Sp2_i\right)\cdot\left(r_{j,i}\right)^2\cdot\left(1-e^{-1.71\cdot\Delta_{j,i}}\right)^{0.93}\cdot\left[\frac{1.5903\cdot\left(0.1\cdot\Delta_{j,i}+0.68\right)\cdot e^{-1.71\cdot\left(\Delta_{j,i}\right)}}{\left[1-e^{-1.71\cdot\left(\Delta_{j,i}\right)}\right]}+0.1\right]$$

The incremental moment taken by the joint will be the above stiffness times the increment of rotation of the joint. The increment of rotation is obtained by dividing the nail displacement at increment j by the nail radius:

$$m_{j,i} := \left[\frac{K1_{j,i}}{r_{j,i}}\cdot\left(\Delta_{j,i}-\Delta_{j-1,i}\right)\right] \qquad m5_{j,i} := \sum_{i=1}^{16} m_{j,i}$$

This is the increment of moment taken by the joint for each increment of rotation

$$K3_{j,i} := \sum_{i=1}^{16} K1_{j,i}$$

This is the tangential stiffness of the joint - taking all nails into account. It represents the tangential stiffness at each increment of displacement.

Based on the semi-rigid equation giving the relationship between the semi-rigid end fixing moment and the fully fixed end fixing moment with a point load at mid-span for a beam of span L, flexural rigidity EI, fixed by joints of equal rotational stiffness-as given above - the increment of load taken - p5 - by the beam will be:

$$p5_{j,i} := \frac{8}{L}\cdot\left(\left(\frac{m5_{j,i}\cdot L\cdot K3_{j,i}}{L\cdot K3_{j,i}}+m5_{j,i}\cdot E\cdot I\cdot\frac{2}{L\cdot K3_{j,i}}\right)\right) \qquad M5_{j,i} := \sum_{j=1}^{j} m5_{j,i}$$

This is the moment taken by the joint at each increment of slip j.

$$P5_{j,i} := \sum_{j=1}^{j} p5_{j,i}$$

This is the increment of load taking all nails into account for each increment of load j. To obtain the point load taken by the beam at any increment, substitute the value of the increment selected.

$$F1 := \frac{M5_{1600,1}}{L}\cdot 8$$

This is the point load at mid-span taken by the beam based on the maximum moment the beam will take with fully fixed ends

$$M7_{j,i} := \frac{F1\cdot L}{8}\cdot\left[\frac{L}{\left[L+2\cdot\frac{E\cdot I}{\frac{M5_{j,i}\cdot\max(r)}{\left(\frac{j}{500}\right)}}\right]}\right]$$

This is the moment taken by the joint due to a point load at mid-span when each end joint of the beam has semi-rigid behaviour

$\frac{M7_{299,1}}{M5_{1600,1}} = 0.453$ This is the ratio of the above moment to the fully fixed end moment case

$\frac{299}{500} = 0.598$ The joint slip at j

$F1 = 5.823 \times 10^3$ N

$P5_{299,1} = 5.829 \times 10^3$ This calculation is done to establish the displacement increment - j - for the beam with semi-rigid connections at which the point load is the same value as F.

$\beta_{j,i} := \frac{\frac{M7_{j,i} \cdot L}{j}}{\frac{j}{500} \cdot E \cdot I} \cdot \max(r)$ This is the secant rotational stiffness coefficient for the joint at the equilibrium position. The EC3 criteria for a pin joint is that the factor should not be less than 0.5.

$\beta_{299,1} := 1.563$ The secant stiffness coefficient at j